Convention on Long-range Transboundary Air Pollution

emep

Co-operative programme for monitoring and evaluation of the long-range transmission of air pollutants in Europe

STATUS REPORT 1/2019

Transboundary particulate matter, photo-oxidants, acidifying and eutrophying components

Status Report 1/2019

msc-w & ccc & ceip

Clean Air 40 YEARS

EMEP Report 1/2019
Date: September 4, 2019

METEOROLOGISK INSTITUTT
Norwegian Meteorological Institute

Transboundary particulate matter, photo-oxidants, acidifying and eutrophying components

EMEP/MSC-W:	Hilde Fagerli, Svetlana Tsyro, Jan Eiof Jonson, Ágnes Nyíri, Michael Gauss, David Simpson, Peter Wind, Anna Benedictow, Heiko Klein, Augustin Mortier
EMEP/CCC:	Wenche Aas, Anne-Gunn Hjellbrekke, Sverre Solberg, Stephen Matthew Platt, Karl Espen Yttri, Kjetil Tørseth
EMEP/CEIP:	Silke Gaisbauer, Katarina Mareckova, Bradley Matthews, Sabine Schindlbacher, Carlos Sosa, Melanie Tista, Bernhard Ullrich, Robert Wankmüller
CCE/UBA:	Thomas Scheuschner
Chalmers Univ. Tech.	Robert Bergström (on leave from SMHI)
FMI:	Lasse Johanson, Jukka-Pekka Jalkanen
ResearchConcepts:	Swen Metzger
TNO:	Hugo A.C. Denier van der Gon, Jeroen J.P. Kuenen, Antoon J.H. Visschedijk
Univ. of Gothenburg:	Lars Barregård, Peter Molnár, Leo Stockfelt

EMEP Status Report 2019; September 4, 2019

ISSN 1504-6109 (print)
ISSN 1504-6192 (on-line)

Executive Summary

This report presents the EMEP activities in 2018 and 2019 in relation to transboundary fluxes of particulate matter, photo-oxidants, acidifying and eutrophying components, with focus on results for 2017. It presents major results of the activities related to emission inventories, observations and modelling. The report also introduces specific relevant research activities addressing EMEP key challenges, as well as technical developments of the observation and modelling capacities.

Measurements and model results for 2017

In the first chapter, the status of air pollution in 2017 is presented, combining meteorological information and emissions with numerical simulations using the EMEP MSC-W model together with observed air concentration and deposition data.

Altogether 35 Parties reported measurement data for 2017, from 171 sites in total. Of these, 139 sites reported measurements of inorganic ions in precipitation and/or main components in air; 75 of these sites had co-located measurements in both air and precipitation. The ozone network consisted of 139 sites, particulate matter was measured at 69 sites, of which 50 performed measurements of both PM_{10} and $PM_{2.5}$. In addition, 45 sites reported at least one of the components required in the advanced EMEP measurement program (level 2). A complete aerosol program was implemented at 8 sites, while only a few sites provided the required oxidant precursor measurements.

The mean daily max O_3, SOMO35 and AOT40 all show a distinct gradient with levels increasing from north to south, a well established feature for ozone reflecting the dependency of ozone on the photochemical conditions. The geographical pattern in the measured values is fairly well reflected by the model results for all these three metrics. In particular, the modelled mean daily max for the summer half year agrees very well with the measured values except for an underestimation in a few regions, mainly in the Mediterranean. Particularly high levels are predicted by the model in the south-east, but due to the lack of monitoring sites these levels could not be validated.

The model results and the observations agree quite well on the geographical distribution of annual mean PM_{10} and $PM_{2.5}$, with concentrations below 2-5 μg m^{-3} in northern Europe, increasing to 5-15 μg m^{-3} in central Europe and further south. The regional background PM is fairly homogeneous over most of central and western Europe, with somewhat elevated PM_{10} and $PM_{2.5}$ levels of 15-20 μg m^{-3} modelled for the Po Valley, the Benelux countries, and also

observed in Poland, Czechia, Hungary and Spain. On average, the model underestimates the observed 2017 annual mean PM_{10} and $PM_{2.5}$ by 22% and 19% with annual mean spatial correlation coefficients of 0.76 and 0.81, respectively.

Due to meteorological conditions, the annual mean PM_{10} and $PM_{2.5}$ concentrations were 5 to 20% lower in 2017 compared to the 5-year (2012-2016) mean over central, eastern and south-eastern Europe, and the North Atlantic coast, with the largest negative anomalies of 20-30% seen over northern and north-western Europe. Due to the combined effect of meteorology and emission changes, annual mean PM_{10} and $PM_{2.5}$ in 2017 were considerably lower compared to the average levels in the 2000s, by 5-20% over Spain, Portugal and Italy and most of Russia, and by as much as 20-35% in many parts of northern, western and central Europe. In addition to emission reductions, 2017 was a meterologically favorable year in terms of air pollution removal by precipitation.

Exceedances and pollution episodes in 2017

In 2017, relatively few high ozone episodes were experienced in central and northern Europe whereas southern Europe, in particular the Po Valley and the Iberian Peninsula, experienced a number of episodes of smaller regional extent. An intense heat wave (named Lucifer) struck parts of southern Europe (south-east France, Italy, the Balkans) in early August, described as the worst heat wave since 2003 here. The highest ozone level observed, 119.5 ppb (239 μg m^{-3}), was just below EUs alert level of 240 μg m^{-3}, and was recorded at the rural background site Parco La Mandria in north-west Italy (data from the EEA data base). The EMEP MSC-W model reproduce the observed geographical extent of the episode very well, but underpredicts the peak values in many areas.

Model results and EMEP observational data show that in 2017, the annual mean PM_{10} and $PM_{2.5}$ concentrations were below the EU limit values for all of Europe. However, exceedences of the Air Quality Guideline (AQG) recommended by WHO (10 μg m^{-3}) in the annual mean of $PM_{2.5}$ were observed at ten sites.

Exceedance days for PM_{10} were observed at 35 out of 58 sites, but no violations of the PM_{10} EU limit value (more than 35 exceedance days) were registered. 18 sites had more than 3 exceedance days, the recommended AQG by WHO. $PM_{2.5}$ concentrations exceeded the WHO AQG value at 35 out of 46 stations in 2017 (on more than 3 days at 26 sites).

The largest PM pollution episodes occurred in January-February and affected air quality in many European countries. The timeseries of modelled and observed chemical composition of $PM_{2.5}$ at selected sites in France, Poland and Czechia (and also modelled PM_{10} chemical composition for several sites in central and eastern Europe), during the January-February 2017 episodes indicate a diversity of emission sources causing the episodes at different locations.

Critical loads (CL) for eutrophication were exceeded in virtually all countries in 2017, in about 63.9% of the ecosystem area, and the European average exceedance was about 277 eq ha^{-1}yr^{-1}. The highest exceedances are found in the Po Valley in Italy, the Dutch-German-Danish border areas and in north-east Spain. In contrast, critical loads of acidity were not exceeded in most of Europe. Hot spots of exceedances can be found in the Netherlands and its border areas to Germany and Belgium, and some smaller maximum in southern Germany and the Czechia. In Europe as a whole, acidity exceedances in 2017 occur in about 5.5% of the ecosystem area, and the European average exceedance is about 32.4 eq ha^{-1}yr^{-1}.

Status of emissions

In 2019, 45 out of 51 Parties (88%) submitted emission inventories to the EMEP Centre on Emission Inventories and Projections (CEIP). The quality of reported data differs significantly across countries, and the uncertainty of the data is considered to be relatively high.

Under the auspices of the *EU Action on Black Carbon in the Arctic* a technical report was recently compiled. The report reviewed, inter alia, the level of BC reporting under the LRTAP Convention. Despite a large number of Parties voluntarily reporting BC emissions, the review revealed a number of shortcomings. As of 2018, nine Parties had not yet submitted BC emissions inventories to the Convention. Furthermore, significant issues in terms of consistency, completeness and comparability were found in the reported emissions. For the majority of the Parties which reported emissions for 2017, BC emissions constitute between 10 and 20% of the respective total $PM_{2.5}$ emissions.

The condensable component of particulate matter is probably the largest single source of uncertainty in PM emissions. Currently the condensable component is not included or excluded consistently in PM emissions reported by Parties of the LRTAP Convention. Parties were asked to include a table with information on the inclusion of the condensable component in PM_{10} and $PM_{2.5}$ emission factors for the reporting under the CLRTAP convention in 2019. This table was added to the revised recommended structure for informative inventory reports. This year, 17 Parties provided information on the inclusion of the condensable component. However, the reporting in 2019 showed that in many cases Parties do not have information on whether or not the PM emissions of a specific source category include the condensable component. The status of inclusion or exclusion is best known for the emissions from road transport, whilst it is less clear for small-scale combustion sources.

2017 was the first year with reporting obligation of gridded emissions in $0.1^\circ \times 0.1^\circ$ longitude/latitude resolution. Until June 2019, thirty of the 48 countries which are considered to be part of the EMEP area reported sectoral gridded emissions in this resolution. For remaining areas missing emissions are gap-filled and spatially distributed using expert estimates. This year CEIP also performed gap-filling and gridding for the whole time series from 1990 to 2017 in $0.1^\circ \times 0.1^\circ$ longitude/latitude resolution on GNFR sector level for the main pollutants, and from 2000 to 2017 for PMs. Emissions from international shipping in different European seas were updated based on the CAMS global shipping emission dataset for the years 2000 to 2017, provided via ECCAD *CAMS_GLOB_SHIP*. Shipping emissions from 1990 to 1999 were estimated using CAMS global shipping emissions for 2000, adjusted with trends for global shipping from EDGAR v.4.3.2.

The 1999 Gothenburg Protocol lists emission reduction commitments of NO_x , SO_x, NH_3 and NMVOCs for most of the Parties to the LRTAP Convention for the year 2010. These commitments should not be exceeded in 2010 nor in subsequent years. When considering only reported data, approved adjustments and fuel use data of the respective countries, it can be seen that the Netherlands and USA had not reduce their NMVOC emissions according to the Gothenburg Protocol requirements, and that Croatia, Germany, Norway and Spain are above their Gothenburg Protocol ceilings for NH_3. In terms of NO_x emissions, Norway exceeded its ceilings.

Condensable organics; issues and implications for EMEP calculations and source-receptor matrices

Estimates of PM and NMVOC emissions as currently provided by Parties have a number of major uncertainties, and there is a clear need for clarification and standardisation of the meth-

ods used to define and report PM emissions, also concerning the fraction of PM that is primary organic aerosol (POA). For example, emissions from residential wood-burning in Europe represent around 50% of Europe's POA emissions, and they dominate wintertime POA sources, but several studies show that the definitions behind national emission estimates are inconsistent in their treatment of condensable organic compounds. A new bottom-up emissions inventory for OA was implemented for this study, taking account of condensable organics. For some countries (e.g. NO, DK) the bottom-up and EMEP estimates of $PM_{2.5}$ emissions are comparable, but for others (e.g. FI, SE) the expert estimates are far higher than the reported emissions. The new inventory gave improved model performance for organic aerosol and thus $PM_{2.5}$, especially in wintertime. We show that source-receptor calculations are also sensitive to these uncertainties, both for $PM_{2.5}$ and especially for organic aerosol contributions. Such inconsistencies pose grave problems for the modeling of $PM_{2.5}$ and for any analysis of emission control strategies or cost-benefit analysis. In the worst case these problems might lead to wrong priorities of measures. A review and harmonisation of methods for PM and POA emission inventories is recommended.

The EMEP Intensive Measurement Period (EIMP) 2017/18: Equivalent Black Carbon (EBC) from fossil fuel and biomass burning sources

In this report we present results from the ongoing analysis of data from the EMEP IMP 2017/18. We present source apportionment of equivalent black carbon into fossil and biomass fractions (EBC_{ff} and EBC_{bb}, respectively), using the aethalometer model and positive matrix factorization (PMF). According to the aethalometer model, EBC_{bb} represents between close to zero (e.g. Beirut, Lebanon) and just over 50 % (e.g. Beograd, Serbia) of background EBC. However, this model requires a priori knowledge of the aerosol Ångström exponent (AAE), and results from the aethalometer model vary widely depending on the input AAEs. Using a new application of PMF to aethalometer data, we were able to identify EBC_{ff} and EBC_{bb} results without input AAEs (rather AAEs are an output derived from factor profiles).

EMEP MSC-W model calculations were performed for the time period of the EMEP EIMP, using several sources of EC emission data, including the reported EMEP EC emissions. The resulting modelled EC concentrations and the share of EC concentrations from biomass burning (EC_{bb}) and fossil fuel (EC_{ff}) sources were compared to the preliminary data available from the EIMP (EBC and biomass burning fractions from PMF). The results suggest that the EC emissions are somewhat low (or the spatial distributions are erroneous) for this winter period, especially in the reported EMEP EC emission inventory. All the model results show reasonable agreement with observations at rural sites, whilst there is no correlation between model results and observations at urban sites (and even anti-correlation when reported EMEP EC emissions are used).

The fractions of EC emissions from biomass burning sources versus fossil fuel are very different in the reported EMEP emissions and in the emission data set developed by TNO (CAMS_2015_RWC), resulting in substantially different modelled EC_{bb}/EC_{ff} concentration fractions. Model calculations based on reported EMEP EC emissions are in reasonable agreement with the PMF values for biomass burning fractions, whilst model results based on CAMS_2015_RWC give consistently higher biomass burning fractions than PMF. Given that the reported EC emissions might be somewhat low, the proportion of different EC sources in the EMEP emission data could be approximately correct for the wrong reasons, as the emissions from different sources (with completely independent emission factors) would have to increase proportionally to keep the biomass burning fraction about the same.

Only a subset of the EIMP data has been used in this analyses, and measurement data will become available for more sites in the near future. Further investigations, including in depth analyses of model results at the different rural and urban EIMP sites and spatial distribution of emissions for different emission sectors, are needed to determine the validity and possible implications of these preliminary results.

The EMEP trend interface

A new trend interface is under development at MSC-W (available at `http://aerocom.met.no/trends/EMEP/`). The trend interface is designed for visualization of the long-term modelling results at all EMEP sites that have reported observations to EMEP/CCC. A range of new functionalities have been implemented in the interface since last year, the most important being inclusion of EMEP observations and model evaluation statistics. The interface has been extended to include more species, and now visualizes data for ozone, PM_{10} and $PM_{2.5}$. Furthermore, the impacts from different emission sectors on PM_{10} and $PM_{2.5}$ concentrations are vizualised and a number of other technical facilities have been introduced.

Evaluation of the gridded EMEP 0.1°×0.1° emissions using modelling

EMEP MSC-W model results using the EMEP $0.1°\times0.1°$ resolution emissions have been compared to model results using the older 50km × 50km resolution and to model results using CAMS-REG-AP - a widely used set of fine resolution emissions ($0.1° \times 0.05°$) developed by TNO. The three sets of model results have been compared to AirBase observations for each country individually, focusing on the spatial distribution of the results. The largest improvement in going from 50km × 50km resolution to $0.1°\times0.1°$ resolution is seen for NO_2, which can be explained by the high correlations between emissions and surface concentrations of NO_2. Interestingly, for NO_2 the model results using the EMEP $0.1°\times0.1°$ resolution emissions have higher (or similar) spatial correlation compared to observations for most countries than model results based on CAMS-REG-AP, suggesting that the gridding performed by the countries are superior to the gridding done for CAMS-REG-AP. This may not be surprising, as the gridding done by the countries in most cases are based on national data, that are probably better than the European-wide proxies used for CAMS-REG-AP. For some countries, the model runs with fine resolution EMEP emissions showed substantially worse correlation to observations than the CAMS-REG-AP fine resolution emissions. For these countries it would be worthwhile looking further into the methodology used for spatial distribution of the emissions.

Baltic Sea shipping

As part of the EU Interreg project EnviSum the effects of emissions from Baltic Sea shipping on air pollution and health have been calculated, and the results published in two journal papers. A resume of the papers is given in this report. We find that the implementation of the stricter SECA regulations from January 2015 has been successful in reducing sulphur emissions from shipping. As a result, $\mathrm{PM_{2.5}}$ concentrations, in particular in coastal zones, have been reduced. A large portion of the population in the Baltic Sea region lives in the coastal zones. The stricter SECA regulations have alleviated the health burden in the region by reducing the mortality and morbidity from Baltic Sea shipping by about one third. The main source of $\mathrm{PM_{2.5}}$ from the Emission Control Areas in the Baltic Sea (and the North Sea) is now $\mathrm{NO_x}$, and the resulting health effects are still significant. $\mathrm{NO_x}$ will be regulated from 2021 in the region, but only for new ships, resulting in only a gradual decrease in emissions.

Model improvements

The model version used for reporting this year has some significant changes since the rv4.17a documented last year. A new gas-phase chemical mechanism has been introduced (EmChem19), which is a substantial revision of the EmChem16 scheme used previously. The reaction rates in EmChem19 are updated to be consistent with the latest recommendations from the IUPAC. In addition to these updates some new gas-phase reactions have been added and a few new chemical species have been included in the chemical mechanism, in order to be more consistent with the Master Chemical Mechanism (MCM). An error in the calculations of photosynthetically active radiation (PAR) has been fixed, impacting mainly the ozone uptake for forests.

The latest version of the Equlibrium Simplified Aerosol Model V4 (EQSAM4clim), has been implemented in the EMEP MSC-W model as one of the alternative schemes to calculate gas/aerosol partitioning. First tests show that the results from EQSAM4clim are very similar, or slightly better, than those obtained with the MARS thermodynamic scheme. The advantage of EQSAM4clim is that the scheme allows completing the thermodynamic equilibrium with missing cations and anions from sea salt and mineral dust, which is anticipated to further improve EQSAM4clim performance.

In addition, a number of technical improvements with respect to flexibility and usability of the model have been made.

Development in the monitoring network and database infrastructure

The last chapter of the report presents the implementation of the EMEP monitoring strategy and general development in the monitoring programme including data submission. There are large differences between Parties in the level of implementation, as well as significant changes in the national activities during the period 2000-2017. With respect to the requirement for level 1 monitoring, 40% of the Parties have had an improvement since 2010, while 33% have reduced the level of monitoring. For level 2 monitoring there has been a general positive development in recent years. However, only few sites have a complete measurement program.

The complexity of data reporting has increased in recent years, and it is therefore now mandatory for the data providers to use the submission and validation tool when submitting data to EMEP to improve the quality and timeliness in the data flow. There is a need for improvements in the reporting, as only half of the data providers use the submission tool, and less than 60% report within the deadline of 31 July.

Acknowledgments

This work has been funded by the EMEP Trust Fund.

The development of the EMEP MSC-W model has also been supported by Copernicus Atmosphere Modelling Service (CAMS) projects, the Nordic Council of Ministers, the Norwegian Space Centre and the Norwegian Ministry of Climate and Environment. Development work has also been supported at Chalmers University of Technology in Sweden using funds from the Swedish Strategic Research project MERGE, the framework research program on 'Photochemical smog in China' financed by the Swedish Research Council (639-2013-6917), and FORMAS.

The work on condensable organics was partly funded by the Norwegian Ministry of Climate and Environment. The work of TNO was funded to a large extent by the Copernicus Atmosphere Monitoring Service (CAMS), in particular the Contracts on emissions (CAMS_81) and policy products (CAMS_71).

The work presented in this report has benefited largely from the work carried out under the four EMEP Task Forces and in particular under TFMM.

A large number of co-workers in participating countries have contributed in submitting quality assured data. The EMEP centers would like to express their gratitude for continued good co-operation and effort. The institutes and persons providing data are listed in the EMEP/CCC's data report and identified together with the data sets in the EBAS database.

For developing standardized methods, harmonization of measurements and improving the reporting guidelines and tools, the close co-operations with participants in the European Research Infrastructure for the observation of Aerosol, Clouds, and Trace gases (ACTRIS) as well as with the Scientific Advisory Groups (SAGs) in WMO/GAW are especially appreciated.

The Working Group on Effects and its ICPs and Task Forces are acknowledged for their assistance in determining the risk of damage from air pollution.

The computations were partly performed on resources provided by UNINETT Sigma2 - the National Infrastructure for High Performance Computing and Data Storage in Norway (grant NN2890k and NS9005k). IT infrastructure in general was available through the Norwegian Meteorological Institute (MET Norway). Furthermore, the CPU time granted on the

supercomputers owned by MET Norway has been of crucial importance for this year's source-receptor matrices and trend calculations. The CPU time made available by ECMWF to generate meteorology has been important for both the source-receptor and status calculations in this year's report.

Contents

CHAPTER 1

Introduction

1.1 Purpose and structure of this report

The mandate of the European Monitoring and Evaluation Programme (EMEP) is to provide sound scientific support to the Convention on Long-range Transboundary Air Pollution (LRTAP), particularly in the areas of atmospheric monitoring and modelling, emission inventories, emission projections and integrated assessment. Each year EMEP provides information on transboundary pollution fluxes inside the EMEP area, relying on information on emission sources and monitoring results provided by the Parties to the LRTAP Convention.

The purpose of the annual EMEP status reports is to provide an overview of the status of transboundary air pollution in Europe, tracing progress towards existing emission control Protocols and supporting the design of new protocols, when necessary. An additional purpose of these reports is to identify problem areas, new aspects and findings that are relevant to the Convention.

The present report is divided into four parts. Part I presents the status of transboundary air pollution with respect to acidification, eutrophication, ground level ozone and particulate matter in Europe in 2017. Part II summarizes research activities of relevance to the EMEP programme, while Part III deals with technical developments going on within the centres.

Appendix A in Part IV contains information on the national total emissions of main pollutants and primary particles for 2017, while Appendix B shows the emission trends for the period of 2000-2017. Country-to-country source-receptor matrices with calculations of the transboundary contributions to pollution in different countries for 2017 are presented in Appendix C.

Appendix D describes the country reports which are issued as a supplement to the EMEP status reports.

Appendix E introduces the model evaluation report for 2017 (Gauss et al. 2019c) which is available online and contains time series plots of acidifying and eutrophying components (Gauss et al. 2019b), ozone (Gauss et al. 2019a) and particulate matter (Tsyro et al. 2019). These plots are provided for all stations reporting to EMEP (with just a few exclusions due to data-capture or technical problems). This online information is complemented by numerical

fields and other information on the EMEP website. The reader is encouraged to visit the website, `http://www.emep.int`, to access this additional information.

1.2 Definitions, statistics used

For sulphur and nitrogen compounds, the basic units used throughout this report are μg (S or N)/m^3 for air concentrations and mg (S or N)/m^2 for depositions. Emission data, in particular in some of the Appendices, is given in Gg (SO_2) and Gg (NO_2) in order to keep consistency with reported values.

For ozone, the basic units used throughout this report are ppb (1 ppb = 1 part per billion by volume) or ppm (1 ppm = 1000 ppb). At 20°C and 1013 mb pressure, 1 ppb ozone is equivalent to 2.00 μg m^{-3} .

A number of statistics have been used to describe the distribution of ozone within each grid square:

Mean of Daily Max. Ozone - First we evaluate the maximum modelled concentration for each day, then we take either 6-monthly (1 April - 30 September) or annual averages of these values.

SOMO35 - The Sum of Ozone Means Over 35 ppb is the indicator for health impact assessment recommended by WHO. It is defined as the yearly sum of the daily maximum of 8-hour running average over 35 ppb. For each day the maximum of the running 8-hours average for O_3 is selected and the values over 35 ppb are summed over the whole year.

If we let A_8^d denote the maximum 8-hourly average ozone on day d, during a year with N_y days (N_y = 365 or 366), then SOMO35 can be defined as:

$SOMO35 = \sum_{d=1}^{d=N_y} \max\left(A_8^d - 35 \text{ ppb}, 0.0\right)$

where the `max` function evaluates $\max(A-B,0)$ to $A-B$ for $A > B$, or zero if $A \leq B$, ensuring that only A_8^d values exceeding 35 ppb are included. The corresponding unit is ppb.days.

POD$_Y$ - Phyto-toxic ozone dose, is the accumulated stomatal ozone flux over a threshold Y, i.e.:

$$\text{POD}_Y = \int \max(F_{st} - Y, 0)\, dt \tag{1.1}$$

where stomatal flux F_{st}, and threshold, Y, are in nmol m^{-2} s^{-1}. This integral is evaluated over time, from the start of the growing season (SGS), to the end (EGS).

For the generic crop and forest species, the suffix gen can be applied, e.g. POD$_{Y,gen}$ (or $AF_{st}1.6_{gen}$) is used for forests. POD was introduced in 2009 as an easier and more descriptive term for the accumulated ozone flux. The definitions of AFst and POD are identical however, and are discussed further in Mills and Simpson (2010). See also Mills et al. (2011a,b) and Mills et al. (2018).

AOT40 - is the accumulated amount of ozone over the threshold value of 40 ppb, i.e..

$$AOT40 = \int \max(O_3 - 40 \text{ ppb}, 0.0)\, dt$$

where the `max` function ensures that only ozone values exceeding 40 ppb are included. The integral is taken over time, namely the relevant growing season for the vegetation concerned. The corresponding unit are ppb.hours (abbreviated to ppb.h). The usage and definitions of AOT40 have changed over the years though, and also differ between UNECE and the EU. LRTAP (2009) give the latest definitions for UNECE work, and describes carefully how AOT40 values are best estimated for local conditions (using information on real growing seasons for example), and specific types of vegetation. Further, since O_3 concentrations can have strong vertical gradients, it is important to specify the height of the O_3 concentrations used. In previous EMEP work we have made use of modelled O_3 from 1 m or 3 m height, the former being assumed close to the top of the vegetation, and the latter being closer to the height of O_3 observations. In the Mapping Manual (LRTAP 2009) there is an increased emphasis on estimating AOT40 using ozone levels at the top of the vegetation canopy.

Although the EMEP MSC-W model now generates a number of AOT-related outputs, in accordance with the recommendations of LRTAP (2009) we will concentrate in this report on two definitions:

AOT40$^{\mathbf{uc}}_{f}$ - AOT40 calculated for forests using estimates of O_3 at forest-top (uc: upper-canopy). This AOT40 is that defined for forests by LRTAP (2009), but using a default growing season of April-September.

AOT40$^{\mathbf{uc}}_{c}$ - AOT40 calculated for agricultural crops using estimates of O_3 at the top of the crop. This AOT40 is close to that defined for agricultural crops by LRTAP (2009), but using a default growing season of May-July, and a default crop-height of 1 m.

In all cases only daylight hours are included, and for practical reasons we define daylight for the model outputs as the time when the solar zenith angle is equal to or less than 89°. (The proper UNECE definition uses clear-sky global radiation exceeding 50 W m^{-2} to define daylight, whereas the EU AOT definitions use day hours from 08:00-20:00.). In the comparison of modelled and observed AOT40$^{\text{uc}}_{f}$in chapter 2, we have used the EU AOT definitions of day hours from 08:00-20:00.

The AOT40 levels reflect interest in long-term ozone exposure which is considered important for vegetation - critical levels of 3 000 ppb.h have been suggested for agricultural crops and natural vegetation, and 5 000 ppb.h for forests (LRTAP 2009). Note that recent UNECE workshops have recommended that AOT40 concepts are replaced by ozone flux estimates for crops and forests. (See also Mills and Simpson 2010).

This report includes also concentrations of particulate matter (PM). The basic units throughout this report are μg m^{-3} for PM concentrations and the following acronyms are used for different components to PM:

SOA - secondary organic aerosol, defined as the aerosol mass arising from the oxidation products of gas-phase organic species.

SIA - secondary inorganic aerosols, defined as the sum of sulphate (SO_4^{2-}), nitrate (NO_3^-) and ammonium (NH_4^+). In the EMEP MSC-W model SIA is calculated as the sum: SIA= SO_4^{2-} + NO_3^-(fine) + NO_3^-(coarse) + NH_4^+.

SS - sea salt.

MinDust - mineral dust.

PPM - primary particulate matter, originating directly from anthropogenic emissions. One usually distinguishes between fine primary particulate matter, $PPM_{2.5}$, with aerosol diameters below 2.5 μm and coarse primary particulate matter, PPM_{coarse} with aerosol diameters between 2.5 μm and 10 μm.

$PM_{2.5}$ - particulate matter with aerodynamic diameter up to 2.5 μm. In the EMEP MSC-W model $PM_{2.5}$ is calculated as $PM_{2.5}$ = SO_4^{2-} + NO_3^-(fine) + NH_4^+ + SS(fine) + MinDust(fine) + SOA(fine) + $PPM_{2.5}$ + 0.27 NO_3^-(coarse) + PM25water. (PM25water = PM associated water).

PM_{coarse} - coarse particulate matter with aerodynamic diameter between 2.5μm and 10μm. In the EMEP MSC-W model PM_{coarse} is calculated as PM_{coarse} = 0.73 NO_3^-(coarse)+ SS(coarse) + MinDust(coarse) + PPM_{coarse}.

PM_{10} - particulate matter with aerodynamic diameter up to 10 μm. In the EMEP MSC-W model PM_{10} is calculated as PM_{10} = $PM_{2.5}$ + PM_{coarse}.

In addition to bias, correlation and root mean square the statistical parameter, index of agreement, are used to judge the model's agreement with measurements:

IOA - The index of agreement (IOA) is defined as follows (Willmott 1981, 1982):

$$IOA = 1 - \frac{\sum_{i=1}^{N}(m_i - o_i)^2}{\sum_{i=1}^{N}(|m_i - \bar{o}| + |o_i - \bar{o}|)^2} \tag{1.2}$$

where $\bar{o}$ is the average observed value. Similarly to correlation, IOA can be used to assess agreement either spatially or temporally. When IOA is used in a spatial sense, N denotes the number of stations with measurements at one specific point in time, and m_i and o_i are the modelled and observed values at station i. For temporal IOA, N denotes the number of time steps with measurements, while m_i and o_i are the modelled and observed value at time step i. IOA varies between 0 and 1. A value of 1 corresponds to perfect agreement between model and observations, and 0 is the theoretical minimum.

1.3 The EMEP grid

At the 36^{th} session of the EMEP Steering Body the EMEP Centres suggested to increase spatial resolution and projection of reported emissions from 50×50 km polar stereographic grid to 0.1°×0.1° longitude-latitude grid in a geographic coordinate system (WGS84). The EMEP domain shown in Figure 1.1 covers the geographic area between 30°N-82°N latitude

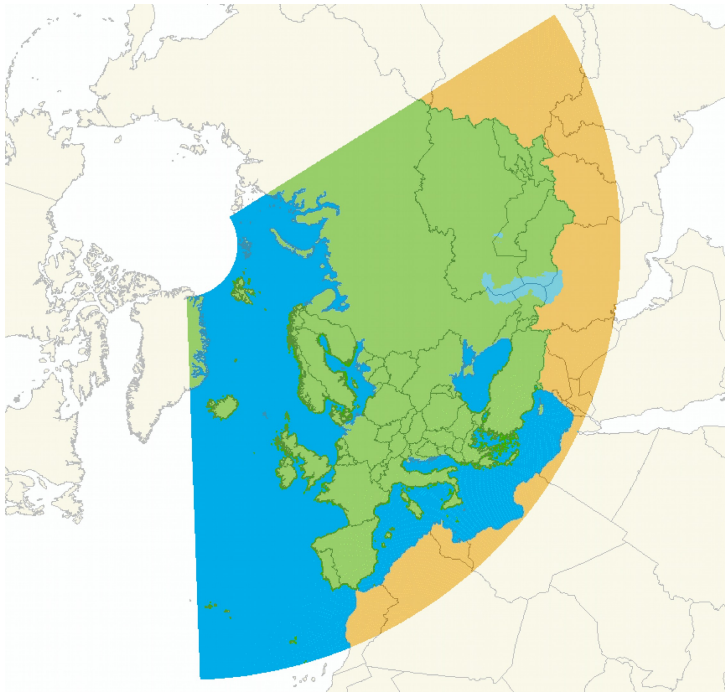

Figure 1.1: The EMEP domain covering the geographic area between 30°N-82°N latitude and 30°W-90°E longitude.

and 30°W-90°E longitude. This domain represents a balance between political needs, scientific needs and technical feasibility. Parties are obliged to report gridded emissions in this grid resolution from year 2017.

The higher resolution means an increase of grid cells from approximately 21500 cells in the 50×50 km^2 grid to 624000 cells in the $0.1°\times0.1°$ longitude-latitude grid.

1.3.1 The reduced grid: EMEP0302

For practical purposes, a coarser grid has also been defined. The EMEP0302 grid covers the same region as the $0.1°\times0.1°$ longitude-latitude EMEP domain (Figure 1.1), but the spatial resolution is 0.3° in the longitude direction and 0.2° in the latitude direction. Each gridcell from the EMEP0302 grid covers exactly 6 gridcells from the $0.1°\times0.1°$ official grid.

1.4 Country codes

Several tables and graphs in this report make use of codes to denote countries and regions in the EMEP area. Table 1.1 provides an overview of these codes and lists the countries and regions included.

All 51 Parties to the LRTAP Convention, except two, are included in the analysis presented in this report. The Parties that are excluded of the analysis are Canada and the United States of America, because they lie outside the EMEP domain.

Code	Country/Region/Source
AL	Albania
AM	Armenia
AST	Asian areas
AT	Austria
ATL	N.-E. Atlantic Ocean
AZ	Azerbaijan
BA	Bosnia and Herzegovina
BAS	Baltic Sea
BE	Belgium
BG	Bulgaria
BIC	Boundary/Initial Conditions
BLS	Black Sea
BY	Belarus
CH	Switzerland
CY	Cyprus
CZ	Czechia
DE	Germany
DK	Denmark
DMS	Dimethyl sulfate (marine)
EE	Estonia
ES	Spain
EU	European Union (EU28)
EXC	EMEP land areas
FI	Finland
FR	France
GB	United Kingdom
GE	Georgia
GL	Greenland
GR	Greece
HR	Croatia
HU	Hungary
IE	Ireland

Code	Country/Region/Source
IS	Iceland
IT	Italy
KG	Kyrgyzstan
KZ	Kazakhstan
LI	Liechtenstein
LT	Lithuania
LU	Luxembourg
LV	Latvia
MC	Monaco
MD	Moldova
ME	Montenegro
MED	Mediterranean Sea
MK	North Macedonia
MT	Malta
NL	Netherlands
NO	Norway
NOA	North Africa
NOS	North Sea
PL	Poland
PT	Portugal
RO	Romania
RS	Serbia
RU	Russian Federation
SE	Sweden
SI	Slovenia
SK	Slovakia
TJ	Tajikistan
TM	Turkmenistan
TR	Turkey
UA	Ukraine
UZ	Uzbekistan
VOL	Volcanic emissions

Table 1.1: Country/region codes used throughout this report.

1.5 Other publications

This report is complemented by a report on EMEP MSC-W model performance for acidifying and eutrophying components, photo-oxidants and particulate matter in 2017 (Gauss et al. 2019c), made available online, at `www.emep.int`.

A list of all associated technical reports and notes by the EMEP centres in 2019 (relevant for transboundary acidification, eutrophication, ozone and particulate matter) follows at the end of this section.

Peer-reviewed publications

The following scientific papers of relevance to transboundary acidification, eutrophication, ground level ozone and particulate matter, involving EMEP/MSC-W and EMEP/CCC staff, have become available in 2018:

Anenberg, S. C., Henze, D. K., Tinney, V., Kinney, P. L., Raich, W., Fann, N., Malley, C. S., Roman, H., Lamsal, L., Duncan, B., Martin, R. V., van Donkelaar, A., Brauer, M., Doherty, R., Jonson, J. E., Davila, Y., Sudo, K., Kuylenstierna, J. C. I. Estimates of the Global Burden of Ambient PM2.5, Ozone, and NO2 on Asthma Incidence and Emergency Room Visits. Environmental Health Perspectives, 126 (10), p. 107004-, 2018. DOI: 10.1289/EHP3766

Bartnicki, J., Semeena, V. S., Mazur, A., Zwozdziak, J. Contribution of Poland to Atmospheric Nitrogen Deposition to the Baltic Sea. Water, Air and Soil Pollution, 229 (353), p. 1-22, 2018. DOI: 10.1007/s11270-018-4009-5

Dong, X., Fu, J. S., Zhu, Q., Sun, J., Tan, J., Keating, T., Sekiya, T., Sudo, K., Emmons, L., Tilmes, S., Jonson, J. E., Schulz, M., Bian, H., Chin, M., Davila, Y., Henze, D., Takemura, T., Benedictow, A. M. K., and Huang, K. Long-range transport impacts on surface aerosol concentrations and the contributions to haze events in China: an HTAP2 multi-model study. Atmos. Chem. Phys., 18, p.15581-15600, 2018. DOI: 10.5194/acp-18-15581-2018

Evangeliou, N., Shevchenko, V. P., Yttri, K. E., Eckhardt, S., Sollum, E., Pokrovsky, O. S., Kobelev, V. O., Korobov, V. B., Lobanov, A. A., Starodymova, D. P., Vorobiev, S. N., Thompson, R. L., and Stohl, A. Origin of elemental carbon in snow from western Siberia and northwestern European Russia during winter-spring 2014, 2015 and 2016. Atmos. Chem. Phys., 18, 963-977, 2018. DOI: 10.5194/acp-18-963-2018

Fleming, Z. L., Doherty, R. M., von Schneidemesser, E., Malley, C. S., Cooper, O. R., Pinto, J. P., Colette, A., Xu, X., Simpson, D., Schultz, M. G., Lefohn, A. S., Hamad, S., Moolla, R., Solberg, S., Feng, Z. Tropospheric Ozone Assessment Report: Present-day ozone distribution and trends relevant to human health. Elementa: Science of the Anthropocene, 6 (12), p. 1-41, 2018. DOI: 10.1525/elementa.273

Galmarini, S., Kioutsioukis, I., Solazzo, E., Alyuz, U., Balzarini, A., Bellasio, R., Benedictow, A. M. K., Bianconi, R., Bieser, J., Brandt, J., Christensen, J. H., Colette, A., Curci, G., Davila, Y., Dong, X., Flemming, J., Francis, X., Fraser, A., Fu, J., Henze, D. K., Hogrefe, K., Im, U., Vivanco, M. G., Jiménez-Guerrero, P., Jonson, J. E., Kitwiroon, N., Manders, A., Mathur, R., Palacios-Peña, L., Pirovano, G., Pozzoli, L., Prank, M., Schultz, M. Sokhi, R. S., Sudo, K., Tuccella, P., Takemura, T., Sekiya, T. and Unal, A. Two-scale multi-model ensemble: is a hybrid ensemble of opportunity telling us more? Atmos. Chem. Phys., 18, p. 8727-8744, 2018. DOI: 10.5194/acp-18-8727-2018

Glasius, M., Hansen, A. M. K., Claeys, M., Henzing, J. S., Jedynska, A. D., Kasper-Giebl, A., Kistler, M., Kristensen, K., Martinsson, J., Maenhaut, W., Nøjgaard, J. K., Spindler, G., Stenström, K. E., Swietlicki, E., Szidat, S., Simpson, D., Yttri, K. E. Composition and sources of carbonaceous aerosols in Northern Europe during winter. Atmospheric Environment, 173, p. 127-141, 2018. DOI: 10.1016/j.atmosenv.2017.11.005

Jonson, J. E., Schulz, M., Emmons, L., Flemming, J., Henze, D., Sudo, K., Tronstad Lund, M., Lin, M., Benedictow, A., Koffi, B., Dentener, F., Keating, T. and Kivi, R. The effects of intercontinental emission sources on European air pollution levels. Atmos. Chem. Phys., 18 (18), p. 13655-13672, 2018. DOI: 10.5194/acp-18-13655-2018

Karset, I. H. H., Berntsen, T. K., Storelvmo, T., Alterskjær, K., Grini, A., Oliviè, D. J. L., Kirkevåg, A., Seland, Ø., Iversen, T., Schulz, M. Strong impacts on aerosol indirect effects from historical oxidant changes. Atmos. Chem. Phys., 18 (10), p. 7669-7690, 2018. DOI: 10.5194/acp-18-7669-2018

Kirkevåg, A., Grini, A., Oliviè, D. J. L., Seland, Ø., Alterskjær, K., Hummel, M., Karset, I. H. H., Lewinschal, A., Liu, X., Makkonen, R., Bethke, I., Griesfeller, J., Schulz, M., Iversen, T. A production-tagged aerosol module for earth system models, OsloAero5.3-extensions and updates for CAM5.3-Oslo. Geoscientific Model Development, 11 (10) p. 3945-3982, 2018. DOI: 10.5194/gmd-11-3945-2018

Le Breton, M., Hallquist, Å., Kant Pathak, R., Simpson, D., Wang, Y., Johansson, J., Zheng, J., Yang, Y., Shang, D., Wang, H., Liu, Q., Chan, C., Wang, T., Bannan, T. J., Priestley, M., Percival, C. J., Shallcross, D. E., Lu, K., Guo, S., Hu, M., Hallquist, M. Chlorine oxidation of VOCs at a semi-rural site in Beijing: significant chlorine liberation from ClNO2 and subsequent gas- and particle-phase Cl-VOC production. Atmos. Chem. Phys., 18 (17) p. 13013-13030, 2018. DOI: 10.5194/acp-18-13013-2018

Lefohn, A. S., Malley, C. S., Smith, L., Wells, B., Hazucha, M., Simon, H., Naik, V., Mills, G., Schultz, M. G., Paoletti, E., De Marco, A., Xu, X., Zhang, L., Wang, T., Neufeld, H. S., Musselman, R. C., Tarasick, D., Brauer, M., Feng, Z., Tang, H., Kobayashi, K., Sicard, P., Solberg, S. and Gerosa, G., Tropospheric ozone assessment report: Global ozone metrics for climate change, human health, and crop/ecosystem research. Elem. Sci. Anth., 6(1), p. 28, 2018. DOI: 10.1525/elementa.279

Liang, C.-K., West, J. J., Silva, R. A., Bian, H., Chin, M., Davila, Y., Dentener, F. J., Emmons, L., Flemming, J., Folberth, G., Henze, D., Im, U., Jonson, J. E., Keating, T. J., Kucsera, T., Lenzen, A., Lin, M., Lund, M. T., Pan, X., Park, R. J., Pierce, R. B., Sekiya, T., Sudo, K., Takemura, T. HTAP2 multi-model estimates of premature human mortality due to intercontinental transport of air pollution and emission sectors. Atmos. Chem. Phys., 18, p. 10497-10520, 2018. DOI: 10.5194/acp-18-10497-2018

Lund, M. T., Myhre, G., Haslerud, A. S., Skeie, R. B., Griesfeller, J., Platt, S. M., Kumar, R., Myhre, C. L., Schulz, M. Concentrations and radiative forcing of anthropogenic aerosols from 1750 to 2014 simulated with the Oslo CTM3 and CEDS emission inventory. Geoscientific Model Development, 11, p. 4909-4931, 2018. DOI: 10.5194/gmd-11-4909-2018

Mills, G., Sharps, K., Simpson, D., Pleijel, H., Broberg, M., Uddling, J., Jaramillo, F., Davies, W. J., Dentener, F., Van den Berg, M., Agrawal, M., Agrawal, S. B., Ainsworth, E. A., Buker, P., Emberson, L., Feng, Z., Harmens, H., Hayes, F., Kobayashi, K., Paoletti, E., Van Dingenen, R. Ozone pollution will compromise efforts to increase global wheat production. Global Change Biology, 24 (8), p. 3560-3574, 2018. DOI: 10.1111/gcb.14157

Mills, G., Pleijel, H., Malley, C. S., Sinha, B., Cooper, O. R., Schultz, M. G., Neufeld, H. S., Simpson, D., Sharps, K., Feng, Z., Gerosa, G., Harmens, H., Kobayashi, K., Saxena, P., Paoletti, E., Sinha, V., Xu, X. Tropospheric ozone assessment report: Present-day tropospheric ozone distribution and trends relevant to vegetation. Elementa: Science of the Anthropocene, 6: 47, p. 1-46, 2018. DOI: 10.1525/elementa.302

Mills, G., Sharps, K., Simpson, D., Pleijel, H., Frei, M., Burkey, K., Emberson, L., Uddling, J., Broberg, M., Feng, Z., Kobayashi, K., Agrawal, M. Closing the global ozone yield gap: Quantification and cobenefits for multistress tolerance. Global Change Biology, 24 (10), p. 4869-4893, 2018. DOI: 10.1111/gcb.14381

Muri, H., Tjiputra, J., Otterå, O. H., Adakudlu, M., Lauvset, S. K., Grini, A., Schulz, M., Niemeier, U., Kristjansson, J. E. Climate response to aerosol geoengineering: a multi-method comparison. Journal of Climate, 31 (16), p. 6319-6340, 2018. DOI: 10.1175/JCLI-D-17-0620.1

Nickel, S., Schröder, W., Schmalfuss, R., Saathoff, M., Harmens, H., Mills, G., Frontasyeva, M. V., Barandovski, L., Blum, O., Carballeira, A., De Temmerman, L., Dunaev, A. M., Ene, A., Fagerli, H., Godzik, B., Ilyin, I., Jonkers, S., Jeran, Z., Lazo, P., Leblond, S., Liiv, S., Mankovska, B., Nunez-Olivera, E., Piispanen, J., Poikolainen, J., Popescu, I. V., Qarri, F., Santamaria, J. M., Schaap, M., Skudnik, M., Spiric, Z., Stafilov, T., Steinnes, E., Stihi, C., Suchara, I., Uggerud, H. T., Zechmeister, H. G. Modelling spatial patterns of correlations between concentrations of heavy metals in mosses and atmospheric deposition in 2010 across Europe. Environmental Sciences Europe, 30, 2018. DOI: 10.1186/s12302-018-0183-8

Oliver, R. J., Mercado, L. M., Sitch, S., Simpson, D., Medlyn, B. E., Lin, Y.-S., Folberth, G. A. Large but decreasing effect of ozone on the European carbon sink. Biogeosciences, 15 (13), p. 4245-4269, 2018. DOI: 10.5194/bg-15-4245-2018

Otero, N., Sillmann, J., Mar, K., Rust, H. W., Solberg, S., Andersson, C., Engardt, M., Bergström, R., Bessagnet, B., Colette, A., Couvidat, F., Cuvelier, C., Tsyro, S., Fagerli, H., Schaap, M., Manders, A., Mircea, M., Briganti, G., Cappelletti, A., Adani, M., D'Isidoro, M., Pay, M. T., Theobald, M., Vivanco, M. G., Wind, P. A., Ojha, N., Raffort, V., Butler, T. A multi-model comparison of meteorological drivers of surface ozone over Europe. Atmos. Chem. Phys., 1 (16), p. 12269-12288, 2018. DOI: 10.5194/acp-18-12269-2018

Pandolfi, M., Alados-Arboledas, L., Alastuey, A., Andrade, M., Angelov, C., Artiñano, B., Backman, J., Baltensperger, U., Bonasoni, P., Bukowiecki, N., Collaud Coen, M., Conil, S., Coz, E., Crenn, V., Dudoitis, V., Ealo, M., Eleftheriadis, K., Favez, O., Fetfatzis, P., Fiebig, M., Flentje, H., Ginot, P., Gysel, M., Henzing, B., Hoffer, A., Holubova Smejkalova, A., Kalapov, I., Kalivitis, N., Kouvarakis, G., Kristensson, A., Kulmala, M., Lihavainen, H., Lunder, C., Luoma, K., Lyamani, H., Marinoni, A., Mihalopoulos, N., Moerman, M., Nicolas, J., O'Dowd, C., Petäjä, T., Petit, J.-E., Pichon, J. M., Prokopciuk, N., Putaud, J.-P., Rodróguez, S., Sciare, J., Sellegri, K., Swietlicki, E., Titos, G., Tuch, T., Tunved, P., Ulevicius, V., Vaishya, A., Vana, M., Virkkula, A., Vratolis, S., Weingartner, E., Wiedensohler, A., and Laj, P. A European aerosol phenomenology - 6: scattering properties of atmospheric aerosol particles from 28 ACTRIS sites. Atmos. Chem. Phys., 18, p. 7877-7911, 2018. DOI: 10.5194/acp-18-7877-2018

Pommier, M., Fagerli, H., Gauss, M., Simpson, D., Sharma, S., Sinha, V., Ghude, S., Landgren, O. A., Nyiri, A., Wind, P. A. Impact of regional climate change and future emission scenarios on surface O3 and PM2.5 over India. Atmos. Chem. Phys., 18 (1), p. 103-127, 2018. DOI: 10.5194/acp-18-103-2018

Popovici, I., Goloub, P., Podvin, T., Blarel, L., Loisil, R., Mortier, A., Deroo, C., Ducos, F., Victori, S., Torres, B. A mobile system combining lidar and sunphotometer on-road measurements: Description and first results. The European Physical Journal Conferences, 176, 2018. DOI: 10.1051/epjconf/201817608003

Popovici, I., Goloub, P., Podvin, T., Blarel, L., Loisil, R., Unga, F., Mortier, A., Deroo, C., Victori, S., Ducos, F., Torres, B., Delegove, C., Choel, M., Pujol-Sohne, N., Pietras, C. Description and applications of a mobile system performing on-road aerosol remote sensing and in situ measurements. Atmospheric Measurement Techniques, 11 (8), p. 4671-4691, 2018. DOI: 10.5194/amt-11-4671-2018

Samset, B. H., Stjern, C. W., Andrews, E., Kahn, R. A., Myhre, G., Schulz, M., Schuster, G. L. Aerosol Absorption: Progress Towards Global and Regional Constraints. Current Climate Change Reports, 4 (2), p. 65-83, 2018. DOI: 10.1007/s40641-018-0091-4

Schmeisser, L., Backman, J., Ogren, J. A., Andrews, E., Asmi, E., Starkweather, S., Uttal, T., Fiebig, M., Sharma, S., Eleftheriadis, K., Vratolis, S., Bergin, M., Tunved, P., and Jefferson, A. Seasonality of aerosol optical properties in the Arctic. Atmos. Chem. Phys., 18, p. 11599-11622, 2018. DOI: 10.5194/acp-18-11599-2018

Schwede, D. B., Simpson, D., Tan, J., Fu, J. S., Dentener, F., Du, E., deVries, W. Spatial variation of modelled total, dry and wet nitrogen deposition to forests at global scale. Environmental Pollution, 243, p. 1287-1301, 2018. DOI: 10.1016/j.envpol.2018.09.084

Stadtler, S., Simpson, D., Schroder, S., Taraborrelli, D., Bott, A., Schultz, M. Ozone impacts of gas-aerosol uptake in global chemistry transport models. Atmos. Chem. Phys., 18 (5), p. 3147-3171, 2018. DOI: 10.5194/acp-18-3147-2018

Tan, J., Fu, J. S., Dentener, F., Sun, J., Emmons, L., Tilmes, S., Sudo, K., Flemming, J., Jonson, J. E., Gravel, S., Bian, H., Davila, Y., Henze, D. K., Lund, M. T., Kucsera, T., Takemura, T., Keating, T. Multi-model study of HTAP II on sulfur and nitrogen deposition. Atmos. Chem. Phys., 18 (9), p. 6847-6866, 2018. DOI: 10.5194/acp-18-6847-2018

Turnock, S. T., Wild, O., Dentener, F. J., Davila, Y., Emmons, L. K., Flemming, J., Folberth, G. A., Henze, D. K., Jonson, J. E., Keating, T, J., Kengo, S., Lin, M., Lund, M., Tilmes, S., and O'Connor, F. M. The impact of future emission policies on tropospheric ozone using a parameterised approach. Atmos. Chem. Phys., 18, p. 8953-8978, 2018. DOI: 10.5194/acp-18-8953-2018

Vivanco, M. G., Theobald, M. R., García-Gómez, H., Garrido, J. L., Prank, M., Aas, W., Adani, M., Alyuz, U., Andersson, C., Bellasio, R., Bessagnet, B., Bianconi, R., Bieser, J., Brandt, J., Briganti, G., Cappelletti, A., Curci, G., Christensen, J. H., Colette, A., Couvidat, F., Cuvelier, C., D'Isidoro, M., Flemming, J., Fraser, A., Geels, C., Hansen, K. M., Hogrefe, C., Im, U., Jorba, O., Kitwiroon, N., Manders, A., Mircea, M., Otero, N., Pay, M.-T., Pozzoli, L., Solazzo, E., Tsyro, S., Unal, A., Wind, P., and Galmarini, S. Modeled deposition of nitrogen and sulfur in Europe estimated by 14 air quality model systems: evaluation, effects of changes in emissions and implications for habitat protection. Atmos. Chem. Phys., 18, p. 10199-10218, 2018. DOI: 10.5194/acp-18-10199-2018

Wang, R., Andrews, E., Balkanski, Y., Boucher, O., Myhre, G., Samset, B. H., Schulz, M., Schuster, G. L., Valari, M., Tao, S. Spatial Representativeness Error in the Ground-Level Observation Networks for Black Carbon Radiation Absorption. Geophysical Research Letters, 45 (4), p. 2106-2114, 2018. DOI: 10.1002/2017GL076817

Werner, M., Kryzaa, M., Wind, P. A. High resolution application of the EMEP MSC-W model over Eastern Europe - Analysis of the EMEP4PL results. Atmospheric research, 212, p. 6-22, 2018. DOI: 10.1016/j.atmosres.2018.04.025

Associated EMEP reports and notes in 2019

Joint reports

Transboundary particulate matter, photo-oxidants, acidification and eutrophication components. Joint MSC-W & CCC & CEIP Report. EMEP Status Report 1/2019

EMEP MSC-W model performance for acidifying and eutrophying components, photo-oxidants and particulate matter in 2017. Supplementary material to EMEP Status Report 1/2019

CCC Technical and Data reports

Anne-Gunn Hjellbrekke. Data Report 2017. Particulate matter, carbonaceous and inorganic compounds. EMEP/CCC-Report 1/2019

Anne-Gunn Hjellbrekke and Sverre Solberg. Ozone measurements 2017. EMEP/CCC-Report 2/2019

Wenche Aas, Knut Breivik and Pernilla Bohlin Nizzetto. Heavy metals and POP measurements 2017. EMEP/CCC-Report 3/2019

Sverre Solberg, Anja Claude and Stefan Reimann. VOC measurements 2017. EMEP/CCC-Report 4/2019

CEIP Technical and Data reports

Melanie Tista and Robert Wankmüller. Methodologies applied to the CEIP GNFR gap-filling 2019. Part Ia: BC, Part Ib: Main pollutants and Particulate Matter (NO_x, NMVOCs, SO_x, NH_3, CO, $PM_{2.5}$, PM_{10}, PM_{coarse}), Technical Report CEIP 1/2019

Melanie Tista and Robert Wankmüller. Methodologies applied to the CEIP GNFR gap-filling 2019. Part II: Heavy Metals (Pb, Cd, Hg), Technical Report CEIP 2/2019

Melanie Tista and Robert Wankmüller. Methodologies applied to the CEIP GNFR gap-filling 2019. Part III: Persistent organic pollutants (Benzo(a)pyrene, Benzo(b)fluoranthene, Benzo(k)fluoranthene, Indeno(1,2,3-cd)pyrene, Total polycyclic aromatic hydrocarbons, Dioxin and Furan, Hexachlorobenzene, Polychlorinated biphenyls), Technical Report CEIP 3/2019

Marion Pinterits, Bernhard Ullrich, Silke Gaisbauer (ETC-ACM), Katarina Mareckova and Robert Wankmüller (CEIP/ETC-ACM). Inventory review 2019. Review of emission data reported under the LRTAP Convention and NEC Directive. Stage 1 and 2 review. Status of gridded and LPS data. Annexes, Joint CEIP/EEA Report. Technical Report CEIP 4/2019

Katarina Mareckova, Robert Wankmüller, Marion Pinterits and Sabine Schindlbacher. Methodology report, Technical Report CEIP 5/2019

Robert Wankmüller. Documentation of the new EMEP gridding System for the spatial disaggregation of emission data with resolution of $0.1^\circ \times 0.1^\circ$ (long-lat), Technical Report CEIP 6/2019

Sabine Schindlbacher and Robert Wankmüller. Uncertainty and recalculations of emission inventories, Technical Report CEIP 7/2019

Sabine Schindlbacher. The condensable component of particulate matter - summary of the information on the inclusion of the condensable component in PM_{10} and $PM_{2.5}$ emission factors provided by Parties, Technical Report CEIP 7/2019

MSC-W Technical and Data reports

Heiko Klein, Michael Gauss, Ágnes Nyíri and Svetlana Tsyro. Transboundary air pollution by main pollutants (S, N, O_3) and PM in 2017, Country Reports. EMEP/MSC-W Data Note 1/2019

References

Gauss, M., Hjellbrekke, A.-G., Aas, W., and Solberg, S.: Ozone, Supplementary material to EMEP Status Report 1/2019, available online at www.emep.int, The Norwegian Meteorological Institute, Oslo, Norway, 2019a.

Gauss, M., Tsyro, S., Fagerli, H., Hjellbrekke, A.-G., and Aas, W.: Acidifying and eutrophying components, Supplementary material to EMEP Status Report 1/2019, available online at www.emep.int, The Norwegian Meteorological Institute, Oslo, Norway, 2019b.

Gauss, M., Tsyro, S., Fagerli, H., Hjellbrekke, A.-G., Aas, W., and Solberg, S.: EMEP MSC-W model performance for acidifying and eutrophying components, photo-oxidants and particulate matter in 2017., Supplementary material to EMEP Status Report 1/2019, available online at www.emep.int, The Norwegian Meteorological Institute, Oslo, Norway, 2019c.

LRTAP: Mapping critical levels for vegetation, in: Manual on Methodologies and Criteria for Mapping Critical Loads and Levels and Air Pollution Effects, Risks and Trends. Revision of 2009, edited by Mills, G., UNECE Convention on Long-range Transboundary Air Pollution. International Cooperative Programme on Effects of Air Pollution on Natural Vegetation and Crops, updated version available at www.icpmapping.com/, 2009.

Mills, G. and Simpson, D.: New flux-based critical levels for ozone-efefcts on vegetation, in: Transboundary acidification, eutrophication and ground level ozone in Europe. EMEP Status Report 1/2010, pp. 123–126, The Norwegian Meteorological Institute, Oslo, Norway, 2010.

Mills, G., Hayes, F., Simpson, D., Emberson, L., Norris, D., Harmens, H., and Büker, P.: Evidence of widespread effects of ozone on crops and (semi-)natural vegetation in Europe (1990-2006) in relation to AOT40- and flux-based risk maps, Global Change Biology, 17, 592–613, doi:10.1111/j.1365-2486.2010.02217.x, 2011a.

Mills, G., Pleijel, H., Braun, S., Büker, P., Bermejo, V., Calvo, E., Danielsson, H., Emberson, L., Grünhage, L., Fernández, I. G., Harmens, H., Hayes, F., Karlsson, P.-E., and Simpson, D.: New stomatal flux-based critical levels for ozone effects on vegetation, Atmos. Environ., 45, 5064 – 5068, doi:10.1016/j.atmosenv.2011.06.009, 2011b.

Mills, G., Sharps, K., Simpson, D., Pleijel, H., Broberg, M., Uddling, J., Jaramillo, F., Davies, William, J., Dentener, F., Berg, M., Agrawal, M., Agrawal, S., Ainsworth, E. A., Büker, P., Emberson, L., Feng, Z., Harmens, H., Hayes, F., Kobayashi, K., Paoletti, E., and Dingenen, R.: Ozone pollution will compromise efforts to increase global wheat production, Global Change Biol., 24, 3560–3574, doi:10.1111/gcb.14157, URL https://onlinelibrary.wiley.com/doi/abs/10.1111/gcb.14157, 2018.

Tsyro, S., Gauss, M., Hjellbrekke, A.-G., and Aas, W.: PM10, PM2.5 and individual aerosol components, Supplementary material to EMEP Status Report 1/2019, available online at www.emep.int, The Norwegian Meteorological Institute, Oslo, Norway, 2019.

Willmott, C. J.: On the validation of models, Physical Geography, 2, 184–194, 1981.

Willmott, C. J.: Some Comments on the Evaluation of Model Performance, Bulletin American Meteorological Society, 63, 1309–1313, doi:10.1175/1520-0477(1982)063<1309:SCOTEO>2.0.CO;2, 1982.

Part I

Status of air pollution

CHAPTER 2

Status of transboundary air pollution in 2017

Svetlana Tsyro, Wenche Aas, Sverre Solberg, Anna Benedictow, Hilde Fagerli and Thomas Scheuschner

This chapter describes the status of transboundary air pollution in 2017. A short summary of the meteorological conditions for 2017 is presented and the EMEP network of measurements in 2017 is briefly described. Thereafter, the status of air pollution and exceedances in 2017 is discussed.

2.1 Meteorological conditions in 2017

Air pollution is significantly influenced by both emissions and weather conditions. Temperature and precipitation are important factors and therefore a short summary describing the situation in 2017 as reported by the meteorological institutes in European and EECCA countries is given first.

The meteorological data to drive the EMEP MSC-W air quality model have been generated by the Integrated Forecast System model (IFS) of the European Centre for Medium-Range Weather Forecasts (ECMWF), hereafter referred to as the ECMWF-IFS model. In the meteorological community the ECMWF-IFS model is considered as state-of-the-art, and MSC-W has been using this model in hindcast mode to generate meteorological reanalyses for the year to be studied (Cycle 40r1 is the model version used for the year 2017 model run). Next section show temperature and precipitation in 2017 compared to the 2000-2016 average based on the same ECMWF-IFS model hindcast setup.

2.1.1 Temperature and precipitation

The mean temperature in 2017 was reported by the World Meteorological Organisation (WMO 2018) as one of the three highest on record globally, the fifth highest in Europe. According to

the Arctic Report Card 2017 (Overland et al. 2017) October 2016 to September 2017 was the second warmest on record since 1900 in the Arctic.

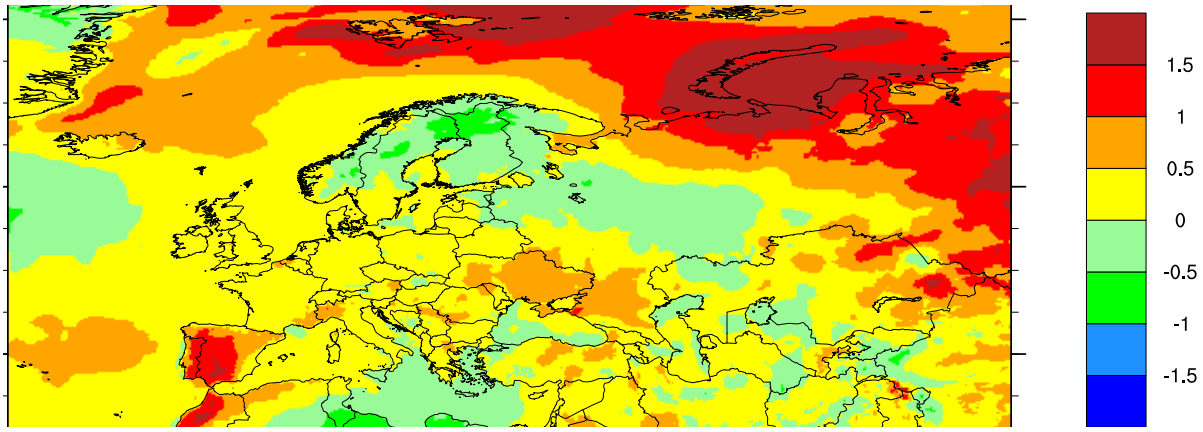

(a) Δtemperature at 2m (2017-climavg)

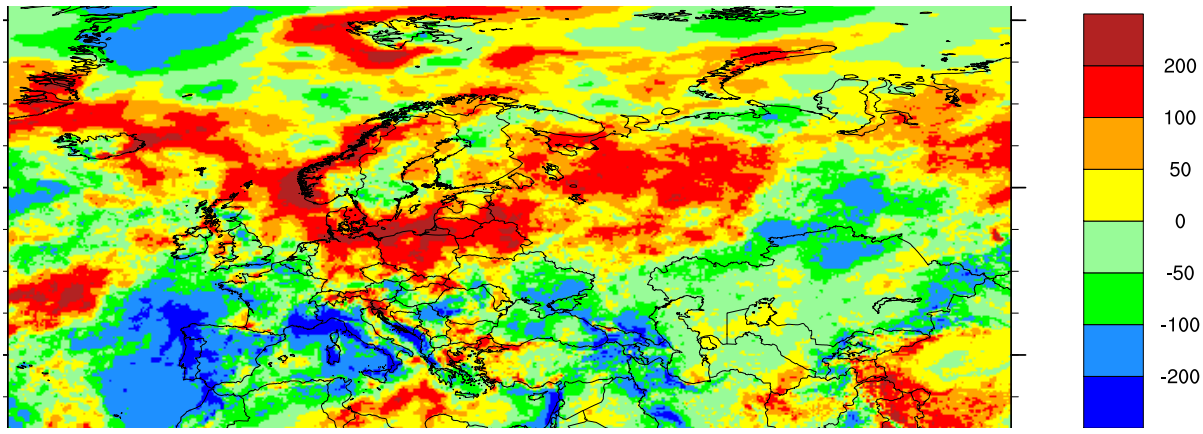

(b) Δprecipitation (2017-climavg)

Figure 2.1: Meteorological conditions in 2017 compared to the 2000-2016 average (climavg) for: a) Annual mean temperature at 2m [K] and b) Annual precipitation [mm]. The meteorological data have been calculated with the ECMWF-IFS model.

Compared to the 2000-2016 average, higher temperatures in 2017 are clearly seen in Figure 2.1 a) over the Arctic, the south-western and eastern Europe, and lower temperatures over northern and north-eastern Europe. Particularly, the Iberian peninsula was abnormally warm throughout the year. Despite a cold start and end, Portugal recorded its fifth warmest April and third warmest May, and second warmest year. In Spain, spring was observed as the warmest since 1965, summer the second warmest and October the warmest, and as a result 2017 was the warmest year on record. Ukraine reported above average temperatures for all seasons and had its third hottest year since 1961. Slovenia and Serbia reported their second warmest summer. Over north-eastern Europe, a cold wave in May, led to record low temperatures in Finland and Latvia. The summer was rather cold in the Nordic and Baltic countries, with Sweden having its coolest summer since 1922 and June was ranked as the eight coldest on record in the European part of Russia.

Especially, the warm winter temperatures shown in Figure 2.2 b) in the Arctic, western and north-eastern Europe, the cold summer temperatures (Figure 2.2 a)) in Scandinavia, the

Baltic states and European Russia and warm summer temperatures on the Iberian Peninsula was characteristic of the year 2017 (Figure 2.1 a)).

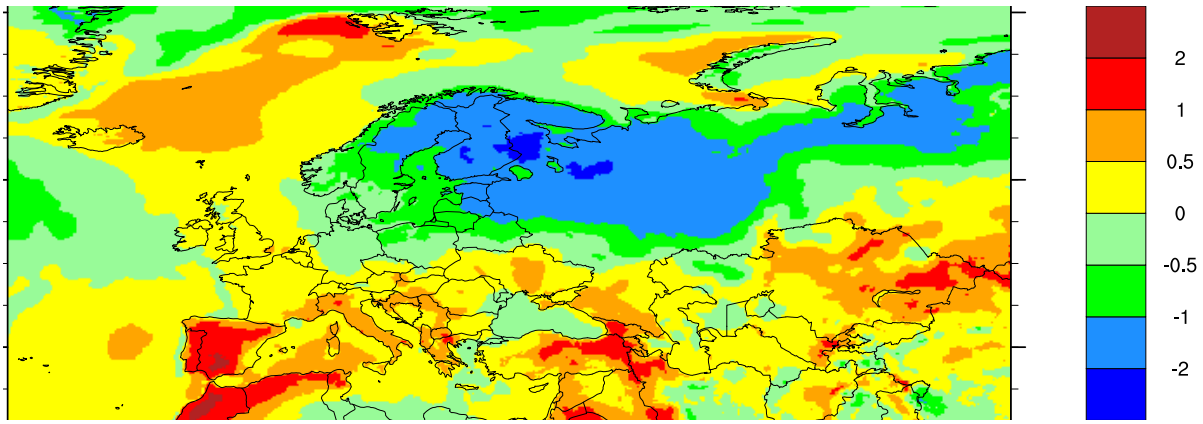

(a) Δtemperature at 2m (AprSep 2017-climavg)

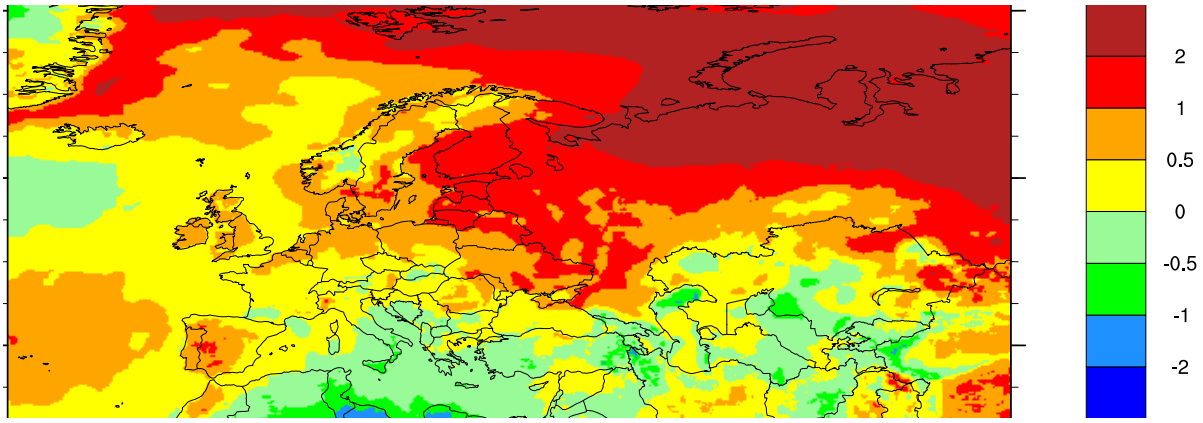

(b) Δtemperature at 2m (OctMar 2017-climavg)

Figure 2.2: Meteorological conditions in 2017 compared to the 2000-2016 average (climavg) for: a) Summer (April-September) temperature [K], b) Winter (January-March and October-December) temperature [K]. The meteorological data have been calculated with the ECMWF-IFS model.

Globally areas affected by precipitation anomalies were fewer due to low El Niño activity in 2017. Nevertheless WMO reported yearly rainfall above the 90 percentile in northern Europe, an area extending from European Russia, through Germany to South Norway, while the Mediterranean area experience dry conditions with rainfall below the 10th percentile.

The precipitation in 2017 compared to the 2000-2016 average is shown in Figure 2.1 b) with rainfall surplus in northern and central Europe and a deficit in south-western Europe. The large amounts of precipitation throughout the year 2017 resulted in the second wettest on record in the European part of Russia, and in Norway the sixth wettest year. In the first half of the year, most Baltic states and Nordic countries received less than normal precipitation, with Latvia having its sixth driest May. However in summer Lithuania and Denmark received large amount of precipitation and Norway recorded its third wettest summer since 1900. Estonia and Lithuania reported their wettest autumn on record and Latvia reported its second wettest autumn in 94 years. A precipitation deficit was especially prevailed in south-western Europe, from Italy to Portugal, as Italy reported its driest, Spain its second driest (since 1965) and Portugal its third driest year on record.

In the summer months (April-September) compared to the 2000-2016 average, visualised in Figure 2.3 a), the area extending from European Russia, through Germany to South Norway and Iceland is wet, while southern Europe is dry. Figure 2.3 b) show that for the 2017 winter months (January-March and October-December) precipitation was higher than normal in northern and south-eastern Europe and lower than normal in south-western Europe.

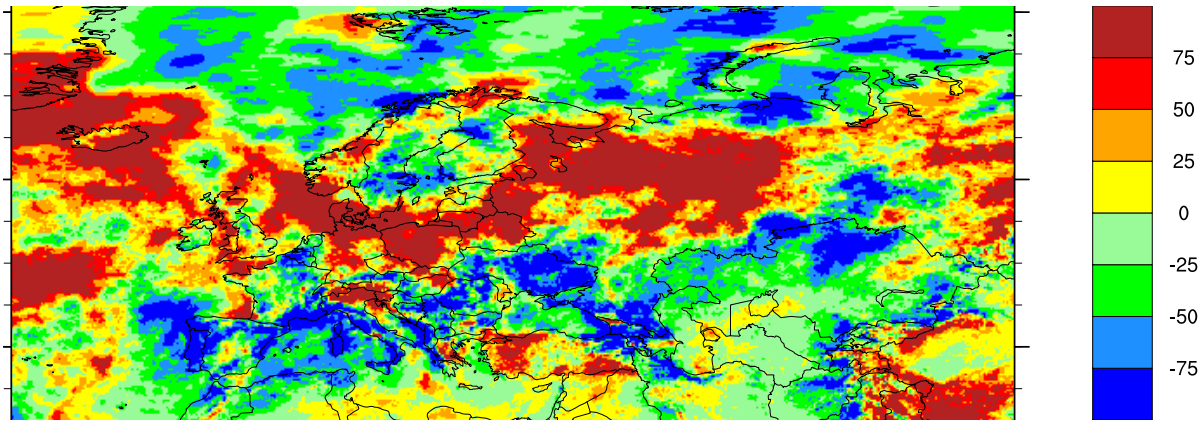

(a) Δprecipitation (AprSep 2017-climavg)

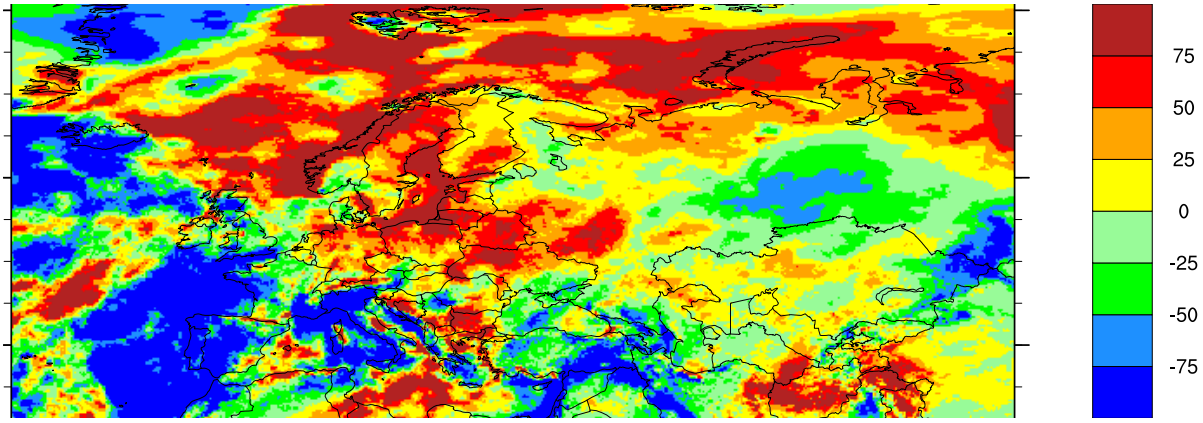

(b) Δprecipitation (OctMar 2017-climavg)

Figure 2.3: Meteorological conditions in 2017 compared to the 2000-2016 average (climavg) for: a) Summer (April-September) precipitation [mm], b) Winter (January-March and October-December) precipitation [mm]. The meteorological data have been calculated with the ECMWF-IFS model.

2.2 Measurement network 2017

In 2017, a total of 35 Parties reported measurement data of inorganic components, particulate matter and/or ozone to EMEP from altogether 171 sites, which is the relevant components for level 1 sites (UNECE 2009). All the data are available from the EBAS database (`http://ebas.nilu.no/`) and are also reported separately in technical reports by EMEP/CCC (Hjellbrekke 2019, Hjellbrekke and Solberg 2019). Figure 2.4 shows an overview of the spatial distribution of the sites reporting data for inorganic ions in air and precipitation, particulate matter and ozone in 2017.

139 sites reported measurements of inorganic ions in precipitation and/or main components in air; however not all of these measurements were co-located as illustrated in Fig-

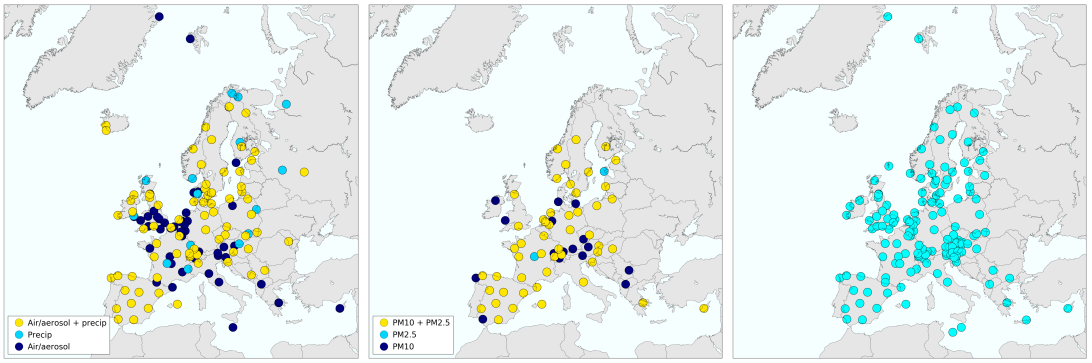

(a) Inorganic compunds (b) PM mass concentration (c) Ozone

Figure 2.4: EMEP measurement network for level 1 components in 2017

ure 2.4. There were 75 sites with measurements in both air and precipitation. Ozone was measured at 139 EMEP sites.

There were 69 sites measuring either PM_{10} or $PM_{2.5}$ mass. 50 of these sites measured both size fractions, as recommended in the EMEP Monitoring strategy (UNECE 2009). The stations measuring EMEP level 2 variables are shown in Figure 11.2. Compliance with the monitoring obligations, and the development of the programme the last decade is discussed in Chapter 11.1.

2.3 Setup for EMEP MSC-W model runs

The EMEP MSC-W model version rv4.33 has been used for the 2017 model runs. The horizontal resolution is $0.1^\circ \times 0.1^\circ$, with 20 vertical layers (the lowest with a height of approximately 50 meters).

Meteorology, emissions, boundary conditions and forest fires for 2017 have been used as input (for description of these input data see Simpson et al. 2012). The meteorological input has been derived from ECMWF-IFS(cy40r1) simulations (2.1). The land-based emissions have been derived from the 2019 official data submissions to UNECE CLRTAP (Pinterits et al. 2019), as documented in Chapter 3. Emissions from international shipping within the EMEP domain are derived from the CAMS global shipping emissions (Granier et al. 2019), developed by the Finish Meteorological Institute (FMI). The forest fires emissions are taken The Fire INventory from NCAR (FINN) (Finnigan et al. 1990), version 5. For more details on the emissions for 2017 model run see Chapter 3 and Appendix A.

Preliminary simulations for 2018 have been performed with the same EMEP MSC-W model version (rv4.33), driven with 2018 meteorological input (also derived from ECMWF-IFS cy40r1), and used the same emissions (anthropogenic and forest fires) as in the 2017 run. Climatological means were used for boundary conditions. No evaluation of the 2018 results have been made as EMEP observational data for 2018 were not available. The model results for 2018 can be downloaded from the EMEP webpage (`http://www.emep.int`).

Trend runs with the EMEP MSC-W model have been performed for the period of 2000–2016, using meteorological data and emissions for the respective years. The land-based emissions for 2000–2016 were derived from the 2019 official data submissions to UNECE CLRTAP (Pinterits et al. 2019), and the international shipping emissions were derived from

the CAMS global shipping emission dataset (Granier et al. 2019, ECCAD 2019), produced by FMI using AIS (Automatic Identification System) tracking data (see also Appendix B). FINNv5 forest fire emissions have been used for corresponding years in the runs for 2002-2016, whereas for 2000 and 2001 average emissions over the 2005-2015 period have been used. Note that the SO_x emissions from the eruption of the Grimsvotn volcano in 2011 have deliberately been excluded, since the model cannot accurately simulate their dispersion as their intrusion occurred above the model's top layer.

2.4 Air pollution in 2017

2.4.1 Ozone

The ozone observed at a surface station is the net result of various physio-chemical processes; surface dry deposition and uptake in vegetation, titration by nearby NO_x emissions, regional photochemical ozone formation and atmospheric transport of baseline ozone levels, each of which may have seasonal and diurnal systematic variations. Episodes with elevated levels of ozone are observed during the summer half year when certain meteorological situations (dry, sunny, cyclonic stable weather) promotes the formation of ozone over the European continent.

Figure 2.5 shows various modelled ozone metrics for 2017 with the corresponding measured metrics based on the EMEP measurement sites plotted on top of the maps. Figure 2.6 show similar plots with data from Airbase measurement sites. Note that most of the EMEP sites are also classified as Airbase sites and thus included in Figure 2.6 as well. Only stations located below 500 metres above sea level were used in this comparison to avoid uncertainties related to the extraction of model data in regions with complex topography. The maps show a) the mean of the daily max concentration for the 6-months period April-September, b) SOMO35 (= Sum of Ozone Means Over 35 ppb), c) AOT40 for forests (= Accumulated Ozone exposure over a Threshold of 40 ppb) for the 6-months period April-September using the hours between 08 and 20 and d) POD_1 for forests (= Phytotoxic Ozone Dose above a threshold 1 mmol m^{-2}) (only for Figure 2.5). POD_1 could not be calculated from the ozone monitoring data directly and are thus not given in plot d).

The mean daily max O_3, SOMO35 and AOT40 all show a distinct gradient with levels increasing from north to south, a well established feature for ozone in general reflecting the dependency of ozone on the photochemical conditions. Ozone formation is promoted by solar radiation and high temperatures. The highest levels of these ozone metrics are predicted over the Mediterranean Ocean and in the southeast corner of the model grid. The measurement network are limited to the continental western part of the model domain with no valid data in Belarus, Ukraine, Turkey or the area further east.

For the region covered by the monitoring sites, the pattern with increased levels to the south with maximum levels near the Mediterranean is seen in the measurement data as well as the model. The geographical pattern in the measured values are fairly well reflected by the model results for all these three metrics. In particular, the modelled mean daily max for the summer half year agrees very well with the measured values. Particularly high levels are predicted by the model in the southeast, but due to the lack of monitoring sites these levels could not be validated.

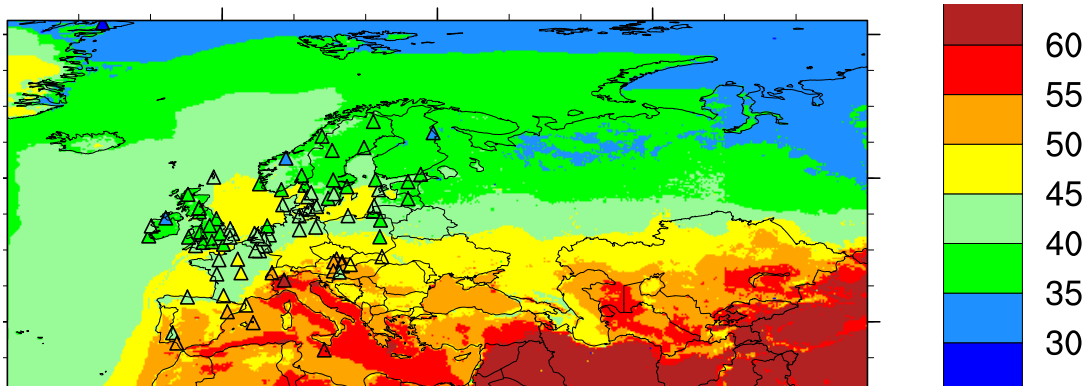

(a) Max. O_3

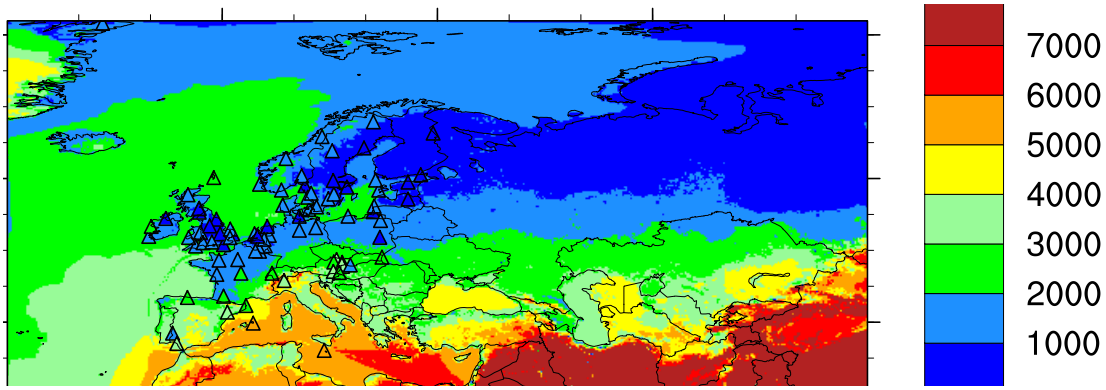

(b) SOMO35

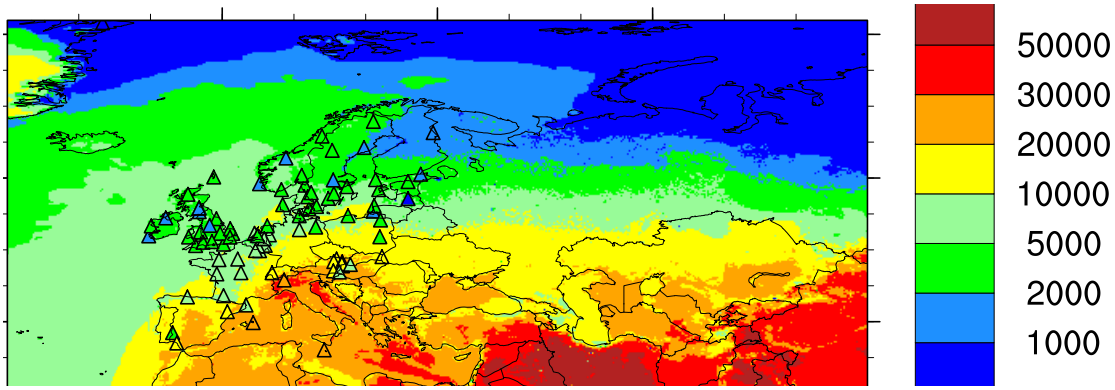

(c) AOT40

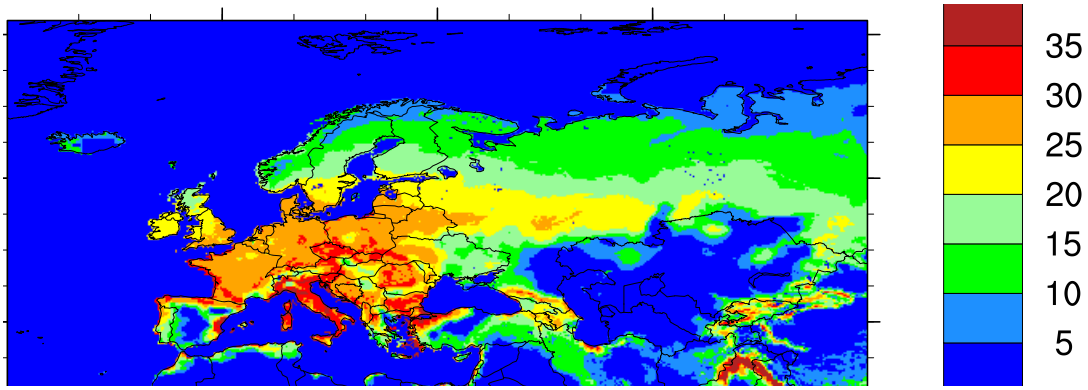

(d) POD1

Figure 2.5: Model results and observations at EMEP stations (triangles) for mean of daily maximum ozone concentrations (ppb, April-September), SOMO35 [ppd.days], AOT40 for forests [ppb.hours] and POD_1 for forests [mmol m^{-2}] in 2017. Only data from measurement sites below 500 m a.s.l. are shown.

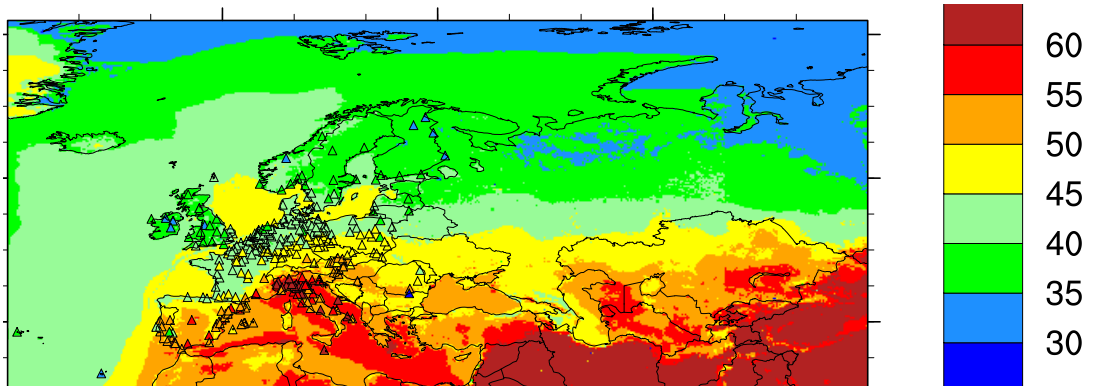

(a) Max. O_3

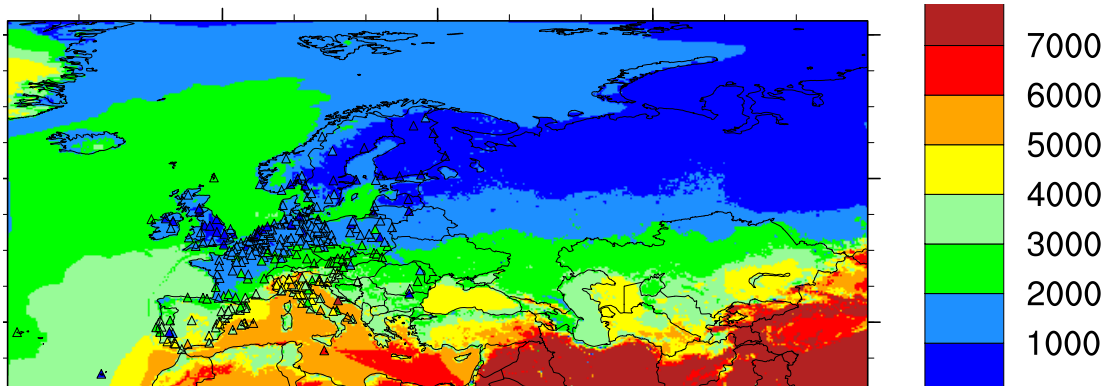

(b) SOMO35

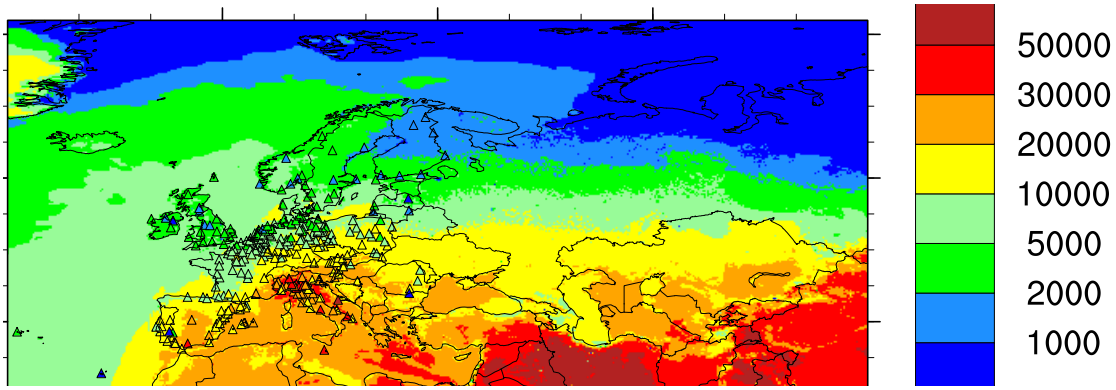

(c) AOT40

Figure 2.6: Model results and observations at Airbase stations (triangles) for mean of daily maximum ozone concentrations (ppb, April-September), SOMO35 [ppd.days], AOT40 for forests [ppb.hours] in 2017. Only data from measurement sites below 500 m a.s.l. are shown.

A good agreement between modelled and observed levels of SOMO35 and AOT40 is also seen from Figure 2.5 and Figure 2.6. It should be noted that the O_3 metrics such as AOT40 are very sensitive to the calculation of vertical O_3 gradients between the middle of the surface layer and the 3m height used for comparison with measurements (Tuovinen et al. 2007) and thus more difficult to compare with measurement data than e.g. the mean daily maximum. Indeed, the formulation we use (Simpson et al. 2012) is probably better suited to a first model layer of 90m height (since we equate the centre of this, ca. 45m, with a 'blending-height') than to a first level of 50m height (as used throughout this report).

The modelled POD_1 pattern differs from the other metrics reflecting the influence of additional parameters such as plant physiology, soil moisture etc., and is a metric more indicative of the direct impact of ozone on vegetation than e.g. AOT40. The POD_1 field could however not be validated by the EMEP ozone measurement data alone.

SOMO35 is an indicator for health impact assessment recommended by WHO, and the results given in Figure 2.5 and Figure 2.6 indicates that the health risk associated with surface ozone increased towards southern Europe in 2017. SOMO35 is a health risk indicator without any specific threshold or limit value.

AOT40 and POD_1 are indicators for effects on vegetation. UN-ECE's critical level for forests is 5000 ppb hours, and the measurements given in Figure 2.5 and Figure 2.6 indicate that this level was exceeded in most of the European continent in 2017 whereas it was not exceeded in most of Scandinavia and the British Isles. As mentioned, the model predicts larger areas with exceedances than the measurements. For POD_1 the limit value depends on the species and Mills et al (2011) give a value of 4 mmol m^{-2} for birch and beech and 8 mmol m^{-2} for Norway spruce. The results in Figure 2.5 indicate that both these limit values were exceeded in most of Europe. The modelled levels of POD_1 could, however, not be validated by observations.

A more detailed comparison between model and measurements for ozone for the year 2017 can be found in Gauss et al. (2019).

Ozone episodes in 2017

The surface ozone levels are closely connected to the weather conditions and in particular to the temperature. As shown in Figure 2.2 a) the 2m summer temperatures were lower than normal in Germany, Poland and Scandinavia in 2017 and slightly above the normal in the UK and France. As discussed above, a stronger positive temperature anomaly was seen in the Mediterranean, in particular in Spain and Portugal.

This is reflected in the occurrence of ozone episodes. Relatively few marked episodes was experienced in central and northern Europe whereas in the south, the Po Valley and the Iberian peninsula experienced a number of episodes of smaller regional extent. In the following, three episodes affecting larger parts of the European continent are presented briefly - one in the end of May, one in the last part of June and the last one in the beginning of August.

28 - 29 May

This episode was linked to a high pressure located over central Europe and low pressures west of Spain/France setting up a southerly flow of warm air into central Europe. The episode lasted only a couple of days and affected mainly the Netherlands, Germany and northern Italy. The episode peaked on 29 May when several sites crossed EU's information threshold of 180 μg m^{-3} and two sites experienced ozone levels above 200 μg m^{-3}. On 30 May the warm air mass had moved to the east with lower ozone levels. As shown in Figure 2.7 and Figure 2.8 the model captures the area of elevated ozone very well but apparently underpredicts the daily maximum ozone in some areas, particularly Belgium and the Netherlands.

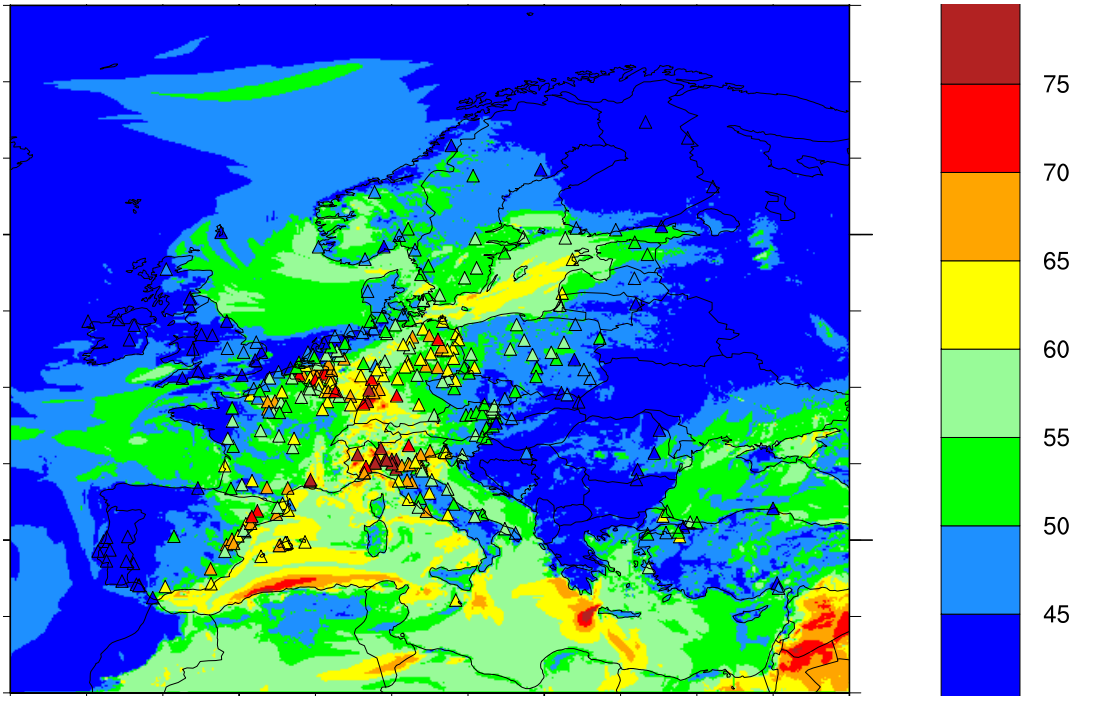

Figure 2.7: Modelled and measured daily max ozone [ppb] 28 May 2017. Data from EMEP and Airbase sites below 500 m asl are shown.

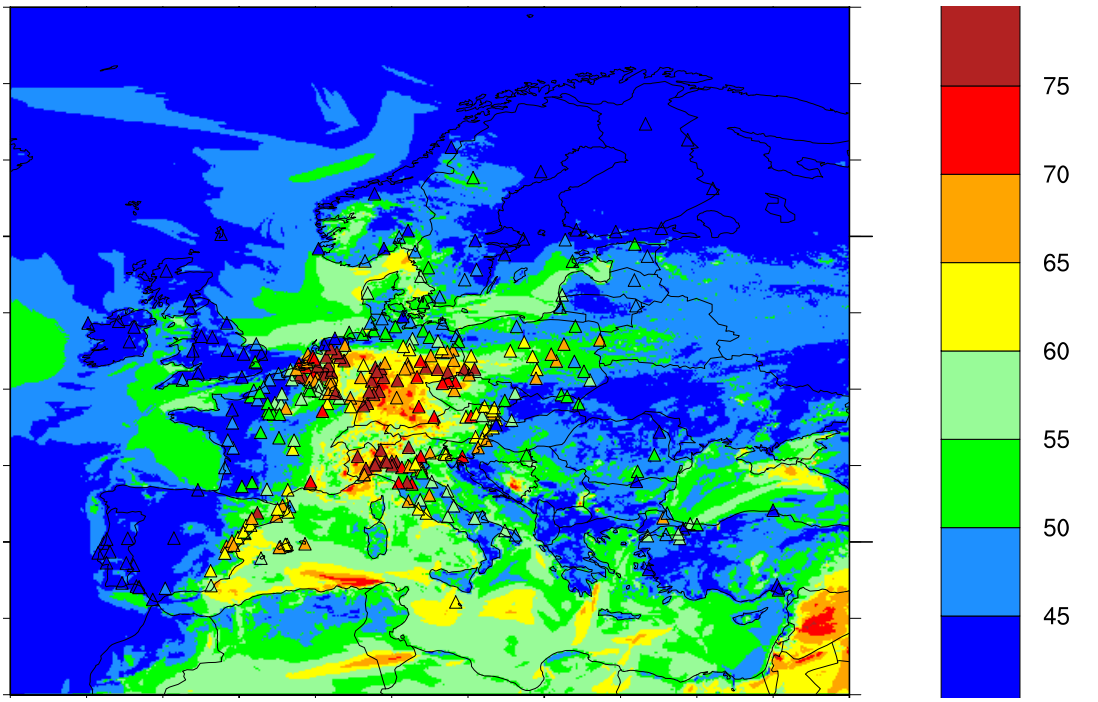

Figure 2.8: Modelled and measured daily max ozone [ppb] 29 May 2017. Data from EMEP and Airbase sites below 500 m asl are shown.

20 - 21 June

June 2017 was characterized by high temperatures in western Europe leading to monthly mean temperatures 3 °C above the normal. In the period 18-22 June a strong heatwave hit western and central Europe peaking on the 21st when the warm air masses extended north to the UK, and at London Heathrow temperatures reached 34.5 °C, the hottest day since 1976. Elevated ozone levels were measured over large areas from the 19 June and peaked on 21 and 22 June when exceedances of EU's information threshold was seen over a large region, including sites in Italy, France, Austria, Germany, Belgium, the Netherlands and the UK. On 21 June one Italian site even hit the alert threshold of 240 μg m^{-3}. The following days the warm air moved to the south and the ozone levels in central Europe dropped to the normal while it stayed high in northern Italy and parts of Austria. Figure 2.9 and Figure 2.10 show that also for this episode the geographical extent of the episode is very well reflected in the model although it underpredicts the daily maximum levels in many areas.

3 - 4 August

An intense heat wave struck southern Europe (southeast France, Italy, the Balkans) in early August that was named Lucifer, referring to the 3-days period 3 - 5 August 2017. Temperatures soared 40 °C and several records were broken. The heat wave was accompanied by high levels of humidity, making the human-felt heat particularly strong, and the episode was described as the worst heat wave since 2003 in the southern countries. Ozone formation is promoted both by heat and absolute humidity, and thus it is not surprising that the surface ozone levels also peaked during Lucifer. The highest ozone level observed, 119.5 ppb (239 μg m^{-3}), was just below EUs alert level of 240 μg m^{-3}, and was recorded at EEAs rural background site Parco La Mandria approximately 15 km northwest of the city centre of Turin in north-western Italy.

The map of modelled and measured daily maximum ozone levels on 3 and 4 August (Figure 2.11 and Figure 2.12) show a band of very high ozone levels stretching from the south-eastern tip of France, across northern Italy and Slovenia to the border area between Austria and Hungary. The difference compared to the low ozone levels further north is very marked and presumably reflects that the heat wave was confined to these areas in the south. The modelled ozone fields these days match the station data very well although the peak values are clearly underestimated by the model as also seen by Gauss et al. (2019). The heat wave was linked to a tongue of very hot air masses transported northwards from Africa, and more precisely from Tunisia as seen by the modelled ozone fields, into France/Italy and then further to the east the next days. An analysis of the Lucifer episode concluded that human caused climate change made this episode at least four times more likely to occur (Kew et al. 2019).

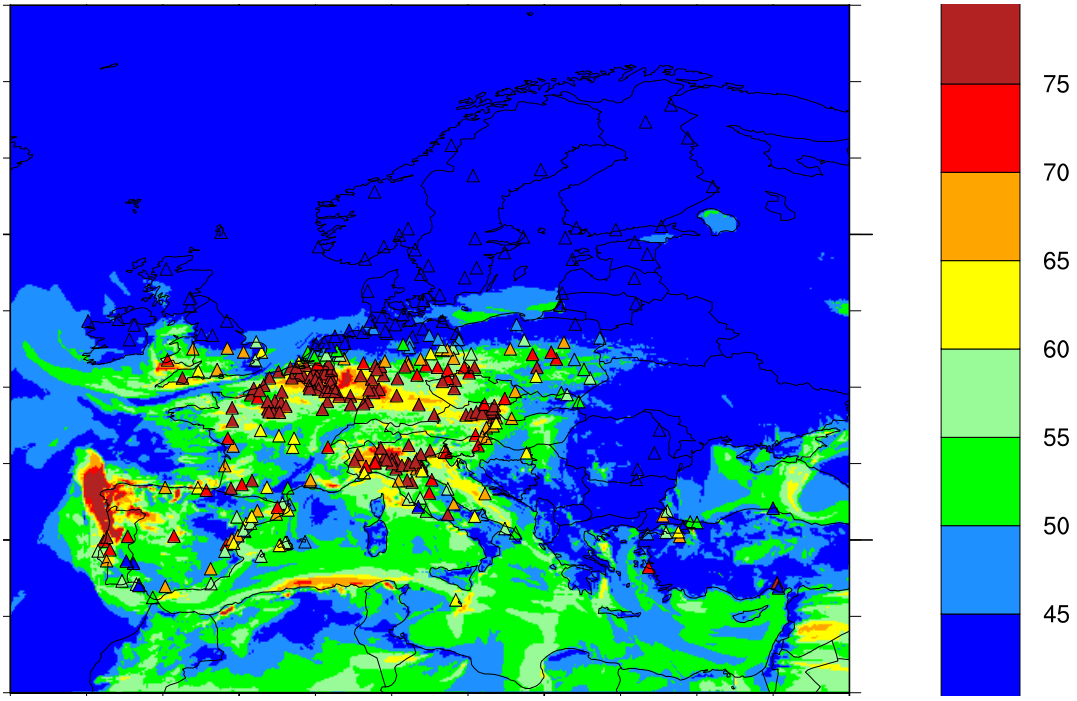

Figure 2.9: Modelled and measured daily max ozone [ppb] 20 June 2017. Data from EMEP and Airbase sites below 500 m asl are shown.

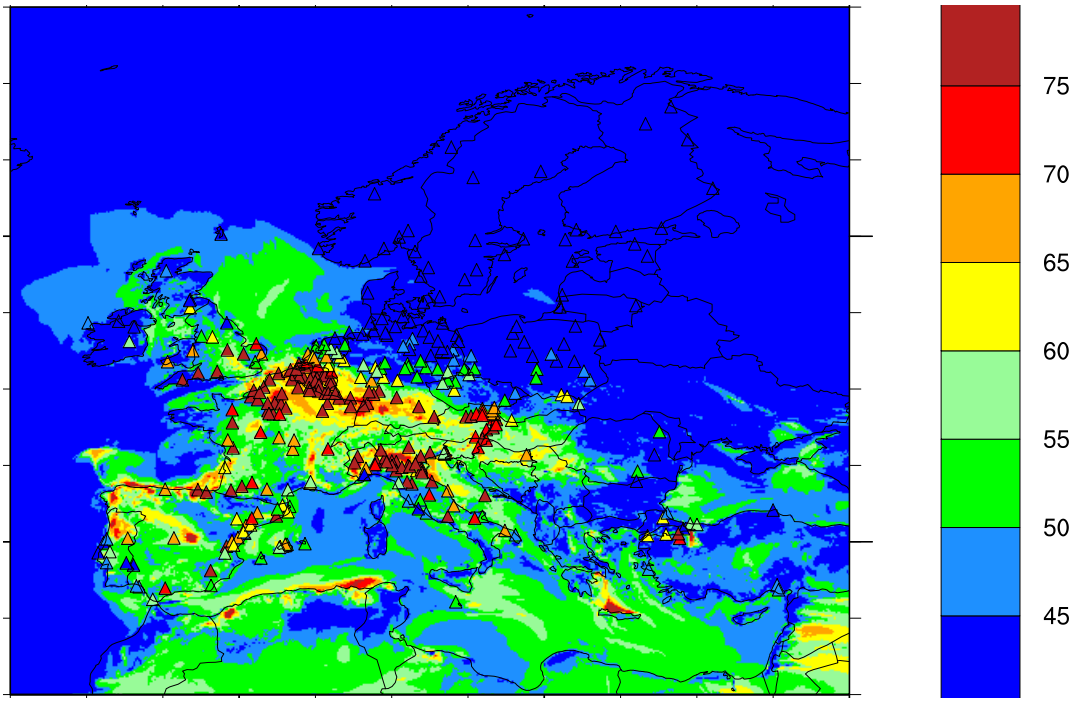

Figure 2.10: Modelled and measured daily max ozone [ppb] 21 June 2017. Data from EMEP and Airbase sites below 500 m asl are shown.

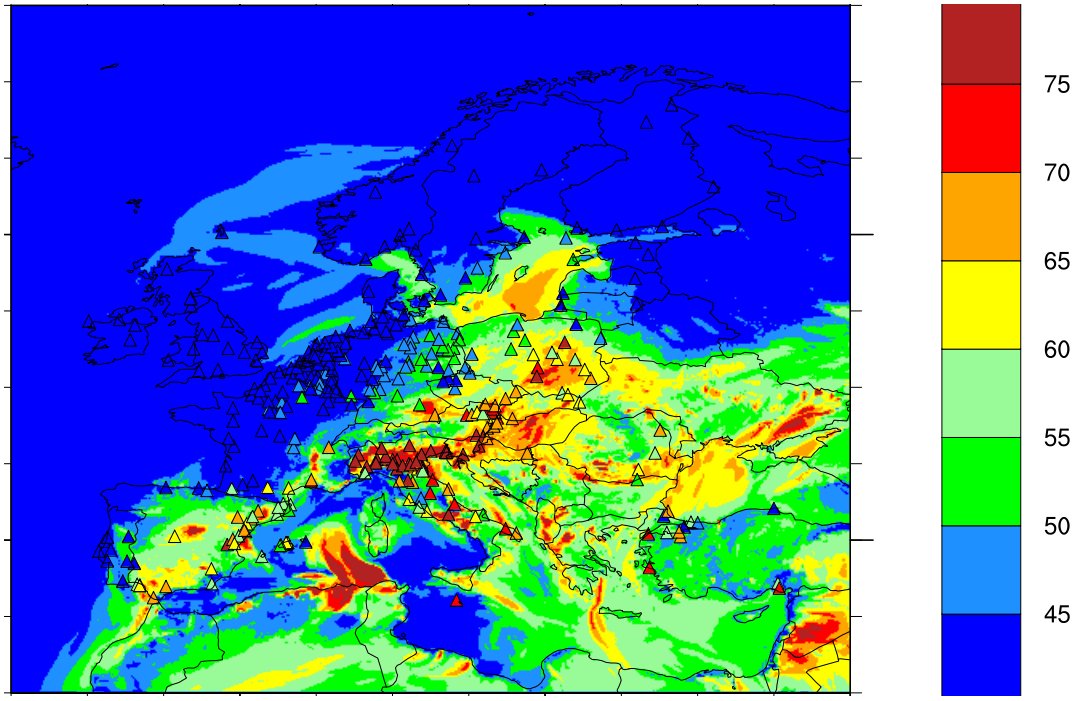

Figure 2.11: Modelled and measured daily max ozone [ppb] 3 August 2017. Data from EMEP and Airbase sites below 500 m asl are shown.

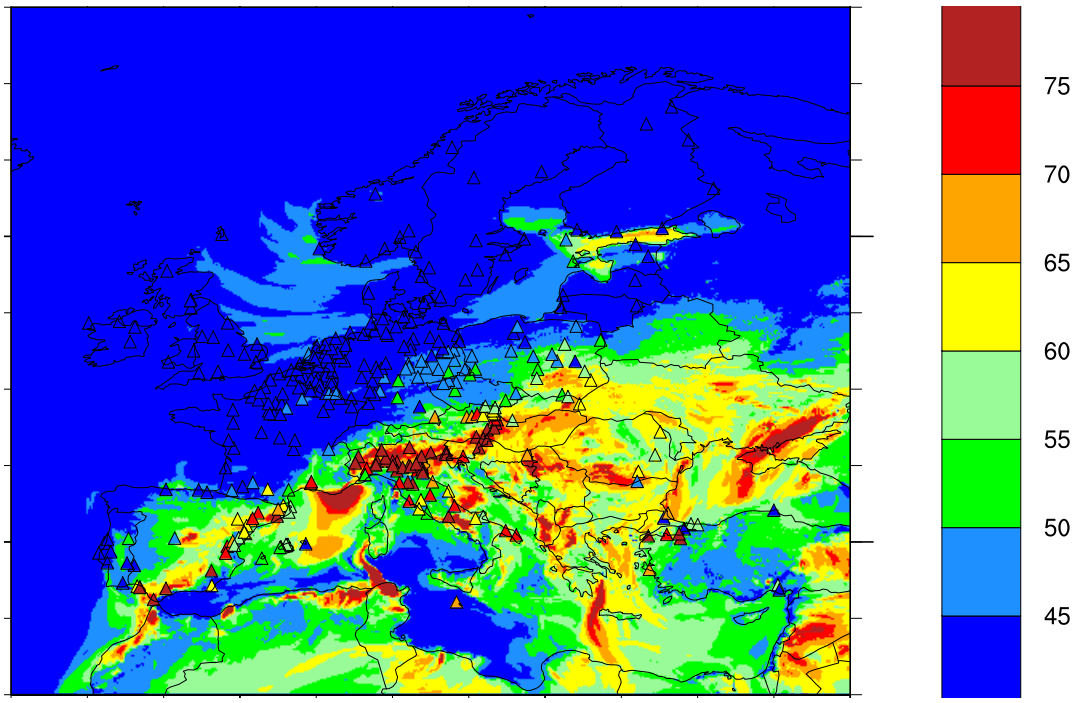

Figure 2.12: Modelled and measured daily max ozone [ppb] 4 August 2017. Data from EMEP and Airbase sites below 500 m asl are shown.

2.4.2 Particulate matter

Maps of annual mean concentrations of PM_{10} and $PM_{2.5}$ in 2017, calculated by the EMEP MSC-W model are presented in Figure 2.13. The figures also show annual mean PM_{10} and $PM_{2.5}$ concentrations observed at EMEP monitoring network, represented by colour triangles overlaying the contours of the modelled concentration fields.

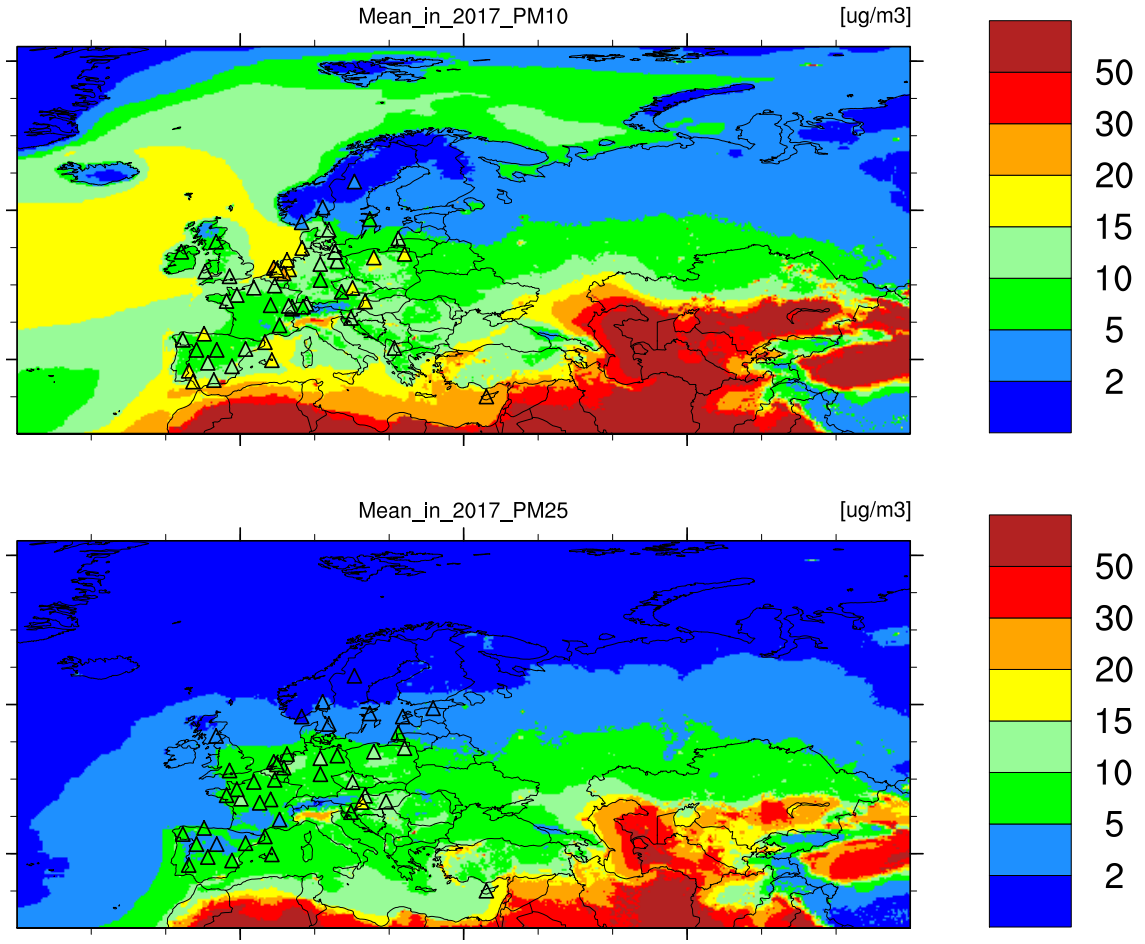

Figure 2.13: Annual mean concentrations of PM_{10} and $PM_{2.5}$ in 2017: calculated with the EMEP MSC-W model (colour contours) and observed at EMEP monitoring network (colour triangles). *Note: Observations include hourly, daily and weekly data.*

The modelling results and the observations are well in agreement regarding the geographical distribution of the annual mean levels of PM_{10} and $PM_{2.5}$, showing their general decrease over land from north to south. The concentrations are below 2-5 μg m^{-3} in northern Europe, increasing to 5-15 μg m^{-3} in the mid-latitude and further south, with $PM_{2.5}$ levels being somewhat lower than those of PM_{10}. Figure 2.13 displays fairly homogeneous levels of regional background PM over most of central and western Europe, with somewhat elevated PM_{10} levels of 15-20 μg m^{-3} in the Po Valley, the Benelux countries, and as well observed levels in Poland, Czech Republic, Hungary and Spain. Elevated $PM_{2.5}$ levels are also calculated by the model for the regions east from the Caspian Sea (parts of Kazakhstan, Uzbekistan, Turkmenistan) and in southern Mediterranean, with the annual mean PM levels being in excess of 50 μg m^{-3}. As explained in earlier EMEP reports, these high PM concentrations are due to

windblown dust from the arid soils and deserts of the Central Asia, though the accurateness of the calculated values still cannot presently be verified due to the lack of observations in these regions.

There is a good agreement between the modelled and observed distribution of annual mean PM_{10} and $PM_{2.5}$, with correlation coefficients of 0.76 and 0.81 respectively. Overall, the model underestimates the observed annual mean of PM_{10} by 22% and $PM_{2.5}$ by 19%. A comprehensive model evaluation is provided in Tsyro et al. (2019).

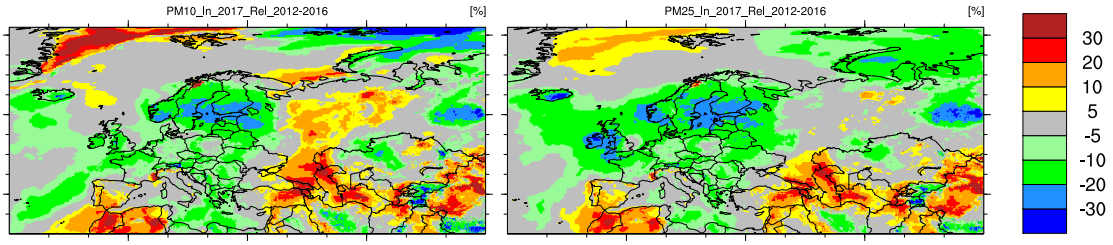

Figure 2.14: Relative anomaly of mean PM_{10} and $PM_{2.5}$ in 2017 from the 2012-2016 mean.

Figure 2.14 shows the maps of the relative anomaly of PM_{10} and $PM_{2.5}$ concentration levels in 2017 with respect to the mean values in the preceding 5-year period (2012-2016). As emission changes during 2012-2016 were rather moderate (Figure 3.7), at least not in western Europe (Figure 3.8), the PM anomalies in 2017 can be considered to be mainly due to meteorological conditions (see 2.1). The annual amount of precipitation in 2017 were relatively large over pollution main source areas in central, eastern/south-eastern Europe (especially in the Benelux countries, Germany, Poland, Belarus, Austria, and the Balkan countries), European and north-eastern parts of Russia, and also over the North-East Atlantic, including along the Norwegian coast. Due to the enhanced wet removal of aerosols and their gaseous precursors, the annual mean PM_{10} and $PM_{2.5}$ concentrations in 2017 were 5 to 20% lower than the 5-year mean over the mentioned regions. The PM largest negative anomalies of 20-30% occurred over northern/north-western Europe (which was 'isolated' from the continental transboundary pollution by the belt of enhanced precipitation), and also in the north-eastern Russia and the Balkans. Positive PM_{10} and $PM_{2.5}$ anomalies of 10-30% are calculated for arid/desert regions in the south-west/south-east of the domain. This is probably due to warmer and drier weather during the March-September period, when most of the dust storms typically occur.

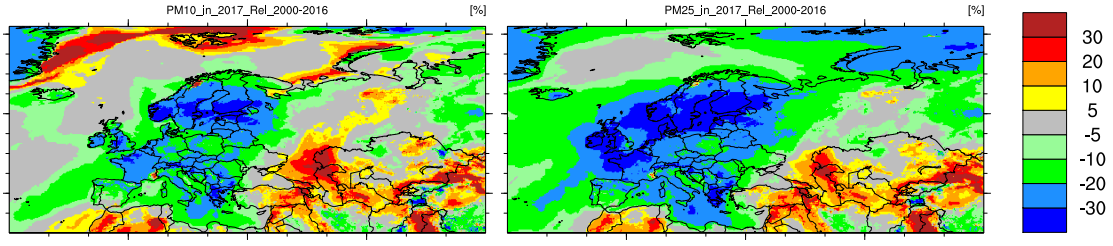

Figure 2.15: Relative anomaly of mean PM_{10} and $PM_{2.5}$ in 2017 from the 2000-2016 mean.

Figure 2.15 presents the relative anomaly of PM_{10} and $PM_{2.5}$ concentration levels in 2017 compared to the corresponding averages over the 2000-2016 period. Compared to the 2000s average levels, the annual mean concentrations of PM_{10} and $PM_{2.5}$ were considerably lower over the European part of the EMEP grid. Annual mean PM_{10} was 5-20 % lower over most

of European Russia, Spain, Portugal and Italy, and as much as 20-35% lower in many parts of northern, western and central Europe. Similar is seen for $PM_{2.5}$, except that the annual mean levels are everywhere even lower in 2017 compared to the 2000-2016 period. In addition to that 2017 was a meteorological favorable year in terms of air pollution removal by precipitation, the reason for those negative PM anomalies were emission reductions during the 2000s in the EMEP West (Figures 3.7 and 3.8). Though in the EMEP East, the gaseous (except SO_2) and particulate emissions somewhat increased from 2000 to 2017, the combination of the weather conditions and reduced transboundary pollution from the West, resulted in the negative PM anomalies also on those areas in 2017.

Exceedances of EU limit values and WHO Air Quality Guidelines in 2017

This section compares the exceedances by PM_{10} and $PM_{2.5}$ concentrations of EU critical limits and WHO recommended Air Quality Guidelines (WHO 2005) calculated with the EMEP MSC-W model and measured at EMEP sites. The EU limit values for PM_{10} (Council Directive 1999/30/EC) are 40 μg m^{-3} for the annual mean and 50 μg m^{-3} for the daily mean concentrations, with the daily limit not to be exceeded more than 35 times per calendar year (EU 2008). For $PM_{2.5}$, the annual mean limit value of 25 μg m^{-3} entered into force 01.01.2015.

The Air Quality Guidelines (AQG) recommended by WHO (WHO 2005) are:

- for PM_{10}: 20 μg m^{-3} annual mean, 50 μg m^{-3} 24-hourly (99th perc. or 3 days per year)
- for $PM_{2.5}$: 10 μg m^{-3} annual mean, 25 μg m^{-3} 24-hourly (99th perc. or 3 days per year)

The EU limit values for protection of human health from particulate matter pollution and the WHO AQG for PM should apply to concentrations for so-called zones, or agglomerations, in rural and urban areas, which are representative for exposure of the general population. PM_{10} and $PM_{2.5}$ concentrations calculated with the EMEP MSC-W model on the $0.1^\circ \times 0.1^\circ$ grid cannot reproduce urban hotspot levels, but give a reasonable representation of PM levels occurring in rural and to some extend in urban background areas.

Model results and EMEP observational data show that the annual mean PM_{10} concentrations were below the EU limit value of 40 μg m^{-3} for all of Europe in 2017 (Figure 2.13). The model calculates annual mean PM_{10} above the WHO recommended AQG of 20 μg m^{-3} in only small regions of the Po Valley and western Turkey. The highest observed annual mean PM_{10} concentrations were seen in Greece (GR0001, but only 61% data coverage) with 31 μg m^{-3}, in Cyprus (CY0002) with 22 μg m^{-3}, and in the Netherland (NL0010) with 19 μg m^{-3}, closely followed by NL0007 (18 μg m^{-3}), ES0017, AT0002(18 μg m^{-3}), and ES0011 (17 μg m^{-3}).

Further, the observations and model calculations show that in 2017, $PM_{2.5}$ pollution (Figure 2.13) did not exceed the EU limit value of 25 μg m^{-3} for annual mean level (except in the Po Valley according to the model). However, there were observed cases of exceedance of the WHO AQG value of 10 μg m^{-3} by observed annual mean $PM_{2.5}$ at ten sites, with the highest values in Hungary (HU0003 with 16 μg m^{-3} and HU0002 with 15 μg m^{-3}) and in Austria (AT0002) with 13 μg m^{-3}.

The maps in Figure 2.16 show the number of days with exceedances of 50 μg m^{-3} for PM_{10} and 25 μg m^{-3} for $PM_{2.5}$ in 2017: model calculated as colour contours and observed as triangles.

Out of the 58 sites with daily or hourly PM_{10} measurements and data coverage above 75%, exceedance days were observed at 35 sites. No violations of the PM_{10} EU limit value (more

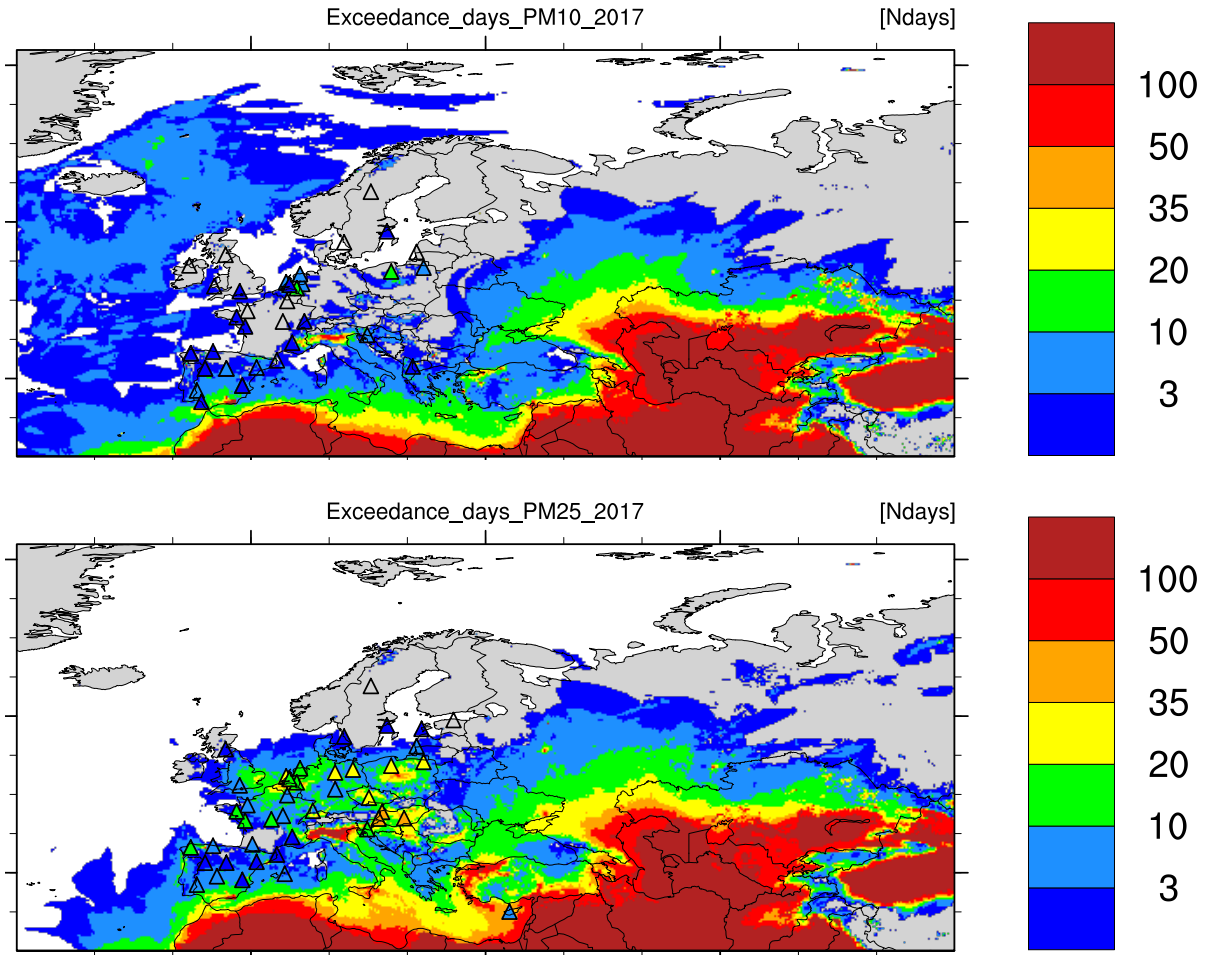

Figure 2.16: Calculated (with 0.1 °resolution) and observed (triangles) number of days with exceedances in 2017: PM_{10} exceeding 50 μg m^{-3} (upper) and $PM_{2.5}$ exceeding 25 μg m^{-3} (lower). *Note: EU Directive requires no more than 35 days with exceedances for PM_{10}, whereas WHO recommends no more than 3 days with exceedances for PM_{10} and $PM_{2.5}$ per a calendar year.*

than 35 exceedance days) were observed, still 18 sites had more than 3 exceedance days (according to WHO AQG recommendations). The highest numbers of days with observed exceedances of PM_{10} were 19 at CY0002 and 18 at AT0002.

$PM_{2.5}$ concentrations exceeded the WHO AQG value at 35 out of 46 stations in 2017. Among those, at 26 sites the number of exceedance days were more than 3 (the recommended limit according to WHO AQG). The highest number of exceedance days are observed in Hungary (HU0003 (43) and HU0002 (41)), AT0002 (38) and in Poland (PL0009 (28) and PL0005 (27))

The model calculated exceedance days in 2017 are in generally good agreement with the observations, which is better for PM_{10} than for $PM_{2.5}$. The model underestimates the occurrence of PM exceedances in central Europe, for instance at AT0002 (2 exceedance days versus 18 observed) and PL0009 (1 exceedance day versus 13 observed), also based on hourly obsevations at GR0001 (5 versus 23) for PM_{10}; and for $PM_{2.5}$ at HU0002 (19 modelled vs 41 observed), AT0002 (16 modelled vs 38 observed), PL0005, PL0009, DE0002, DE0007, and some others. Compared to daily averaged hourly $PM_{2.5}$ measurements, the model exceedance days correspond well with observations at five of the French sites, but underestimate those at

FR0018, FR0024 and FR0025. Also for the Dutch sites, the model underestimates observed $PM_{2.5}$ exceedance days at NL0009 and NL0091, whereas it overestimates those at NL0010 and NL0644.

On the other hand, some overestimation of the occurrence of exceedance days by the model is found at ES0007 and ES0017 for PM_{10} and at ES0008 and CY0002 for $PM_{2.5}$, which is probably due to inaccuracies in windblown dust calculations.

PM pollution episodes in 2017

Winter episodes of particulate pollution in central Europe were already discussed in a number of earlier EMEP Status Reports (i.e. 4/2013, 1/2014, 1/2016-2018). The meteorological situations favouring them are typically characterized by low temperatures and stagnant air conditions, and in addition the enhanced use of wood burning and coal burning for residential heating in the cold weather leads to considerable increase of local PM emissions.

Several PM pollution episodes were recorded in different parts of Europe in 2017. Among the major PM episodes, identified in the CAMS Interim Annual Assessment Report on European air quality for 2017 (Tarrason et al. 2018), the two largest PM_{10} and PM_{25} episodes occurred in the periods of 20-30 January and 9-17 February. Both the January and February episodes affected a large area, stretching from the Atlantic coast to over central and eastern Europe, with minor impacts in southern and northern Europe.

These episodes are also simulated by the EMEP model and registered by observations at several EMEP sites. Some examples of the January-February episodes are given in Figure 2.17, where details on PM chemistry are included to better describe the possible origins of the air pollution. Due to the lack of observations of chemical composition of coarse fraction and PM_{10}, we look here at $PM_{2.5}$ only. Note some inconsistencies in those observations. At the French sites, chemical composition measurements in $PM_{2.5}$ have reduced sampling frequency, with one 24-hour sample per week. At PL0009, the inorganic components were measured in a filterpack system on a weekly sampling interval, while EC/OC were collected at 24-hours samples every 2nd day in $PM_{2.5}$. The filterpack sampler has no size cut-off, and the sum of gas and aerosols are measured for the nitrogen compounds, thus these estimates indicate a higher limit of the possible concentrations of the aerosols in $PM_{2.5}$.

The occurrence time of the winter episodes at the four sites shown in Figure 2.17 somewhat deviates from the dates indicated in the CAMS report (Tarrason et al. 2018). There are two distinct episodes at the sites in France and Poland, with the first episode being the largest at all sites and both episodes occurring some days earlier at the French sites. Namely at FR0024 and FR0025, the first episode started on 16 January and lasted for two weeks, while at PL0009 the first episode started on 25 January and lasted till 5 February. The second, less intense episode took place a few days later and had a shorter duration. On the other hand at CZ0003, the observed $PM_{2.5}$ episode lasted continuously for a month from 17 January. The model tends to underestimate the peak levels of $PM_{2.5}$ during the episodes at the French and Polish sites. As to the Czech site, the model simulates elevated $PM_{2.5}$ concentrations for the January weeks, but fails to reproduce the second half of the episode.

The measurements of $PM_{2.5}$ chemical composition during the January-February episodes indicate rather moderate changes in the relative contribution of SIA and organic mass, which suggests that the episodes were of mixed origin, i.e. from agriculture, traffic and residential heating. Still at FR0024 and FR0025, enhancement of the relative levels of NO_3^- and NH_4 were observed during the episodes. At CZ0003, SO_4^{2-} and organic mass appear to increase

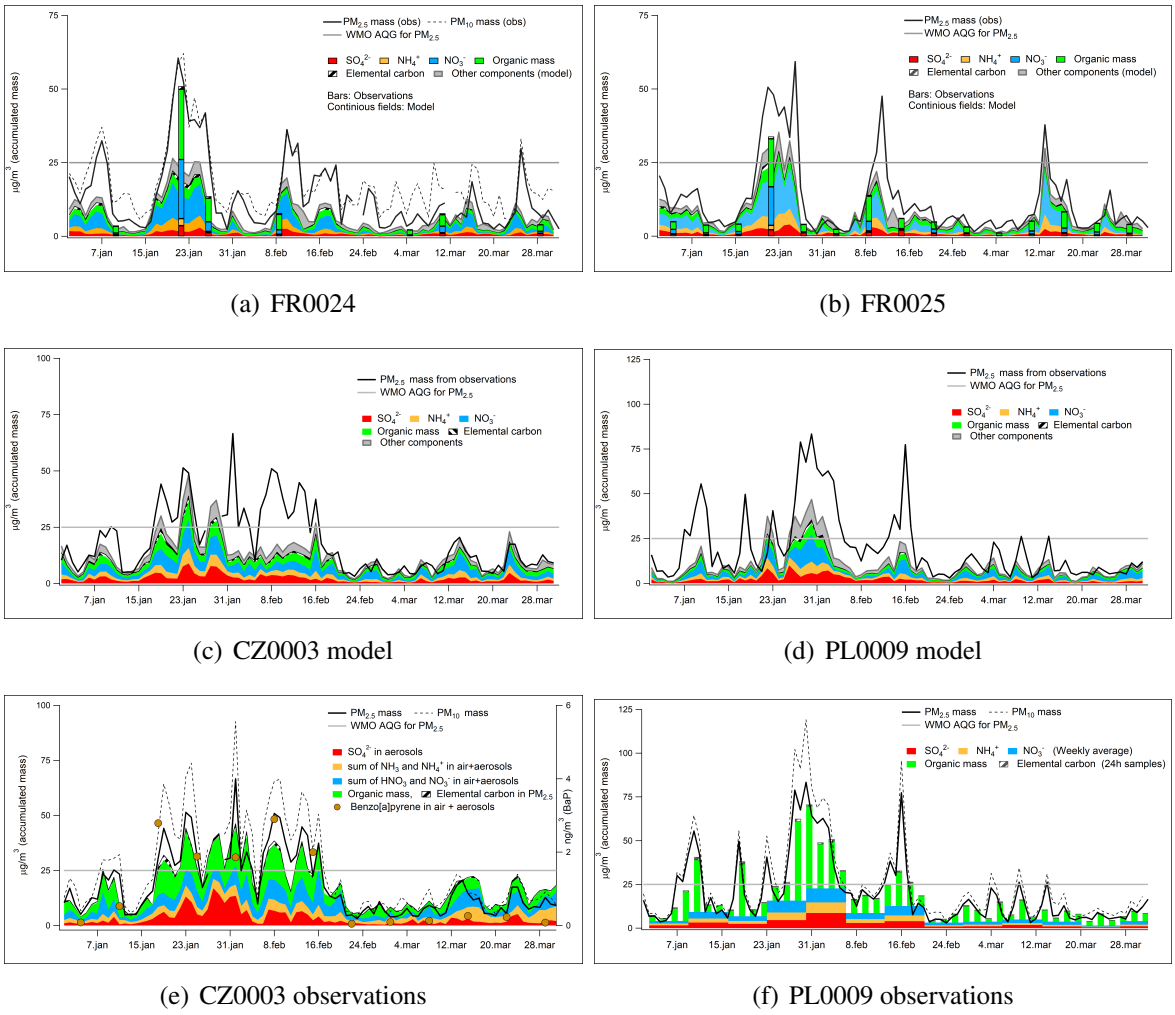

(a) FR0024

(b) FR0025

(c) CZ0003 model

(d) PL0009 model

(e) CZ0003 observations

(f) PL0009 observations

Figure 2.17: Chemical composition of $PM_{2.5}$ in January-March 2017 at selected sites. At FR0024 (a) and FR0025 (b), the model and observations data are combined in the same figures, while for CZ0003 (c and e) and PL0009 (d and f) these are separated. Note that for PL0009, the SIA components and Benzo[a]pyrene] are in air+aersosols and are therefore positively biased to what is expected in $PM_{2.5}$. Organic mass in the observations are calculated multiplying the observed OC with 1.5.

more than the other components. The levels of PAH compound Benzo[a]pyrene, also measured at CZ0003, were as well enhanced during the episode, pointing to wood burning as an important source of $PM_{2.5}$. Also at the Polish site PL0009, the relative contribution of organic aerosol seems to get increased during the episodes, but an accurate estimate is difficult to establish since the SIA components are weekly averages.

For those sites, the model calculated SIA components in $PM_{2.5}$ are quite close to the observed, thus reproducing fairly well the contribution of long-range transported aerosols to the $PM_{2.5}$ episodes (with the exception of the February episode at CZ0003). However, the model failed to accurately represent the enhanced concentrations of organic aerosol during the episodes. As reported before, the main reason for that is partly related to problems with the current emission inventories for primary organic aerosol. As concluded in Denier van der Gon et al. (2015), the current emission inventories have major issues, especially with regard to the inclusion or exclusion of condensable organics.

The rather severe January-February PM episodes were also registered at a number of other sites over central and eastern Europe, e.g. in the Netherlands, Hungary and Slovenia. At those sites, daily PM_{10} in exceedance of 70-80 μg m^{-3} were observed. The episodes are also seen in the model results (Figure 2.18), though the PM_{10} peak values are considerably underestimated. Unfortunately, no measurements of PM chemistry were carried out at those sites, instead the model calculated concentrations of the individual PM_{10} components are presented as a stacked graph in Figure 2.18. The graphs show a particular large increase in NO_3^- levels at the Dutch sites, whereas at the Hungarian (HU0003) and Slovenian (SI0008) sites the concentrations of all PM_{10} components were elevated during the episodes.

Also during the autumn months, shorter periods with elevated PM_{10} and $PM_{2.5}$ concentrations were observed and modelled at a number of sites in Germany, the Netherlands and Hungary.

In the Mediterranean region, several Saharan dust episodes took place in 2019. One of the most pronounced dust episodes occurred in the end of February, and another one mid-April, which were registered at several Spanish sites. Also during summer, especially in June-July, a number of days with elevated PM_{10} due to dust impact were observed and modelled in Spain. Also Ayia Marina (CY0002), experienced a number of dust events through February to mid-May, with the most severe episodes on 22 December and 15-16 November (the last ones were not reproduced by the model).

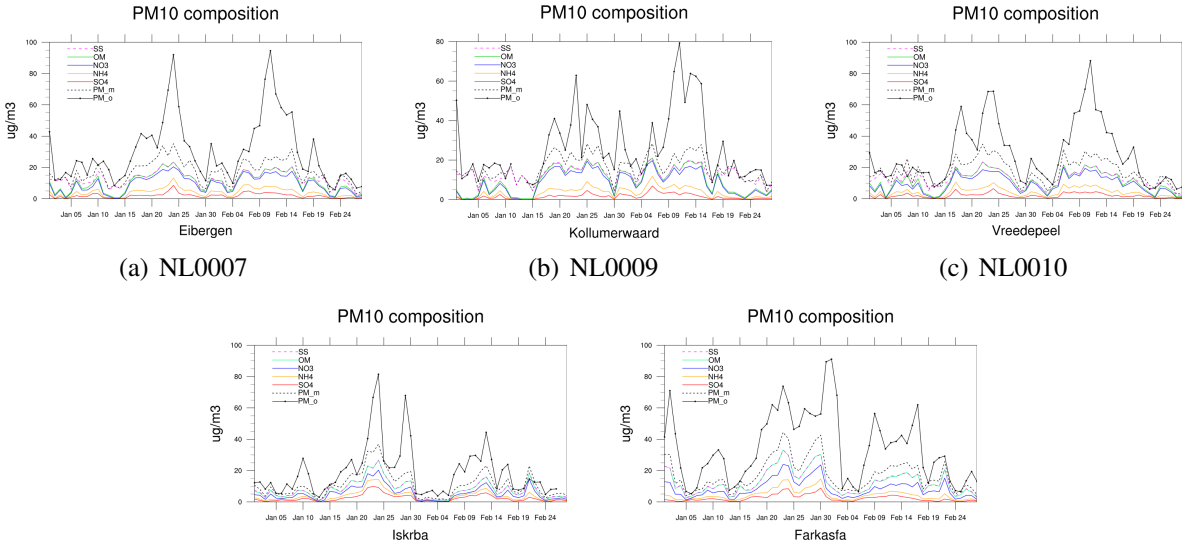

(a) NL0007 (b) NL0009 (c) NL0010

(d) HU0008 (e) SI0008

Figure 2.18: Observed and modelled PM_{10}, supplemented with stacked concentrations of PM_{10} components from the model, in January-February 2017 at selected EMEP sites.

2.4.3 Deposition of sulphur and nitrogen

Modelled total depositions of sulphur and oxidised and reduced nitrogen are presented in Figure 2.19. For sulphur, many hot spot areas are found in the south-eastern part of the domain. In addition, volcanic emissions of SO_2 leads to high depositions in and around Sicily.

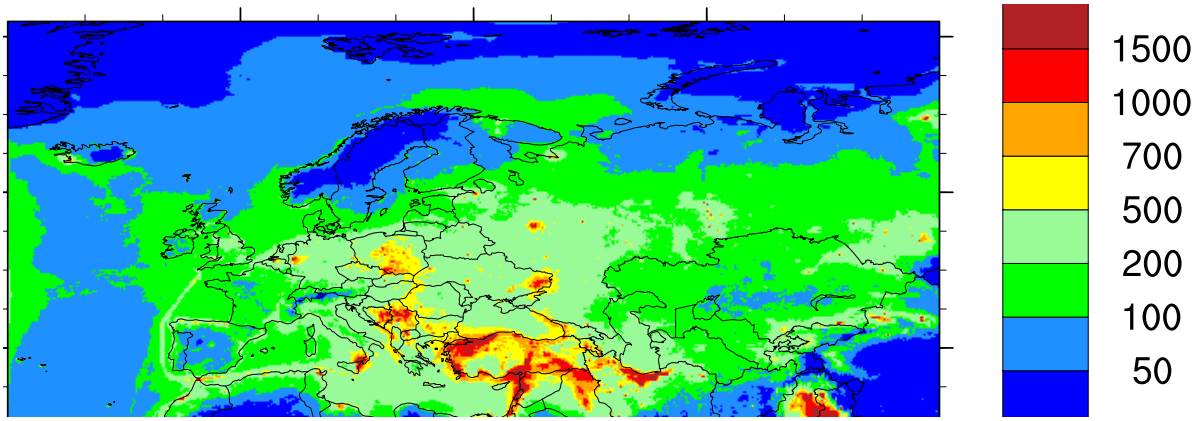

(a) oxidized S

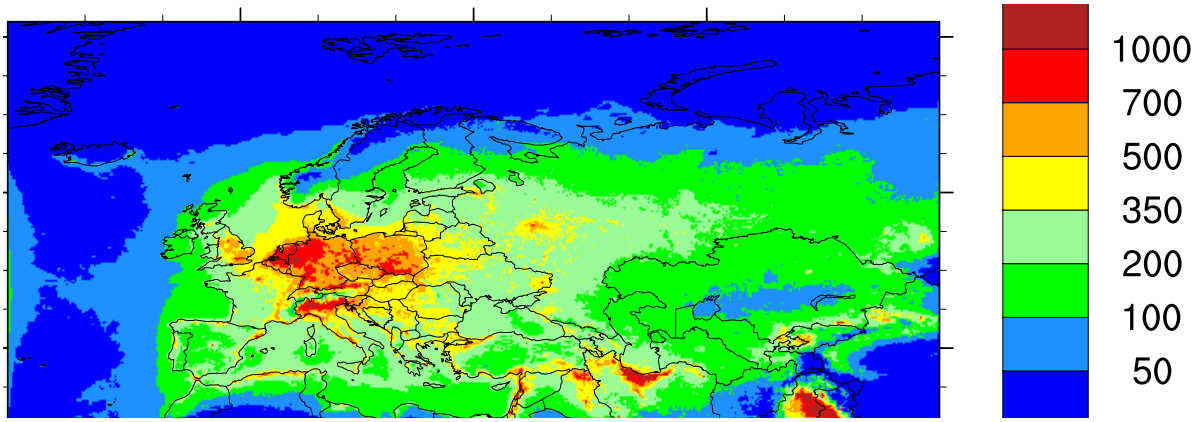

(b) oxidized N

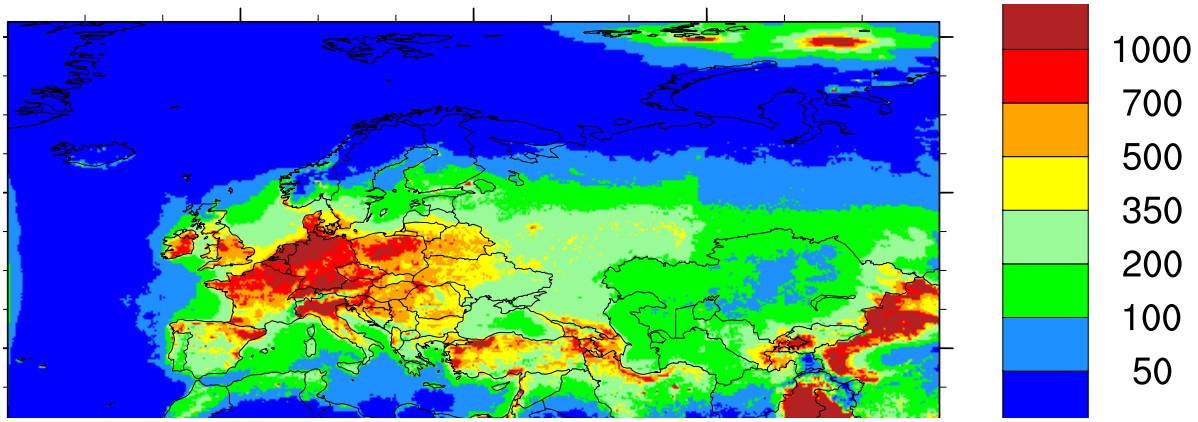

(c) Reduced N

Figure 2.19: Deposition of sulphur and nitrogen [mgS(N)m^{-2}] in 2017.

Oxidised nitrogen depositions are highest in northern Germany, the Netherlands, Belgium, Poland and northern Italy. These countries also have high depositions of reduced nitrogen, as

do parts of the United Kingdom, France, Belgium in western Europe, and Turkey, Georgia, Armenia, Azerbaijan, Kyrgyzstan, Uzbekistan and Tajikistan in the east.

In Figure 2.20 wet depositions of nitrogen and sulphur compounds are compared to measurements at EMEP sites for 2017. Overall, the bias between model and measurements are around -27% to +17%, but higher for individual sites. A more detailed comparison between model and measurements for the year 2017 can be found in Gauss et al. (2019).

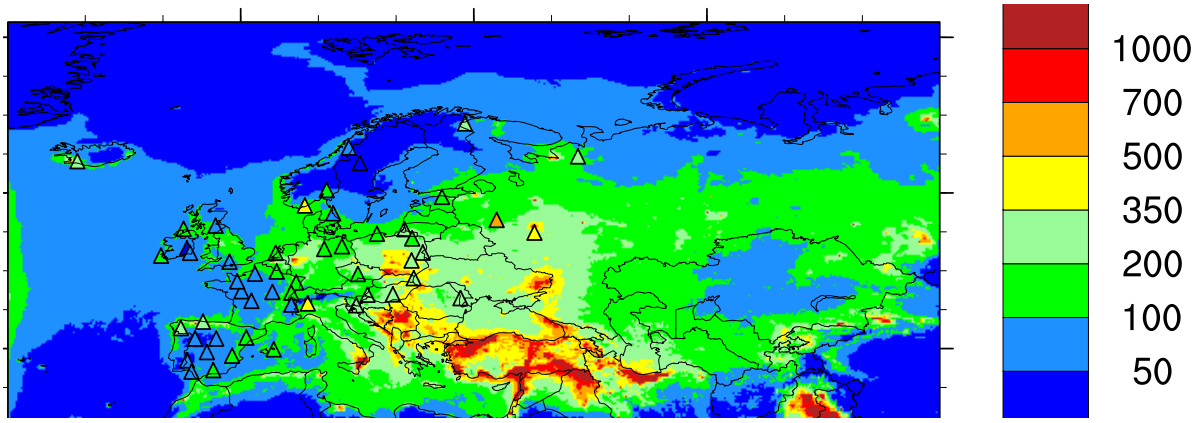

(a) oxidized S

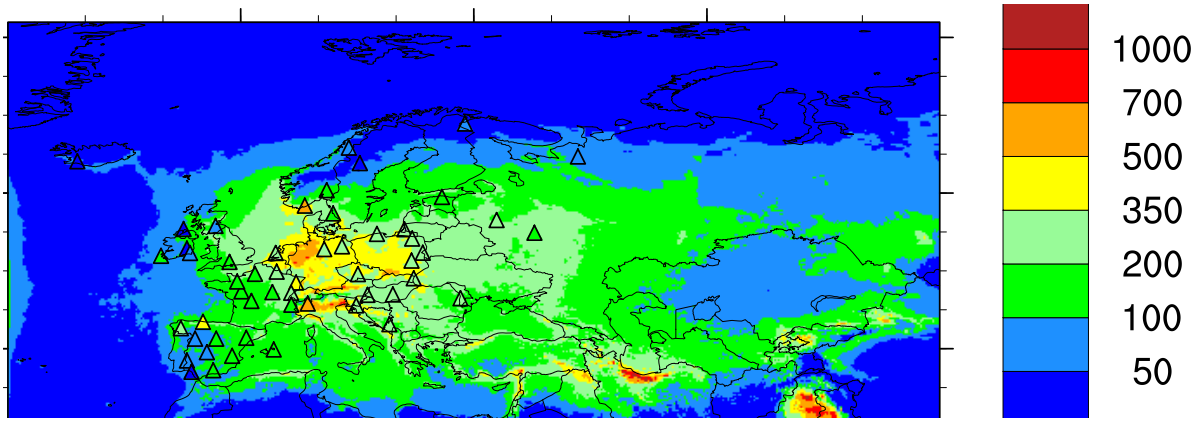

(b) oxidized N

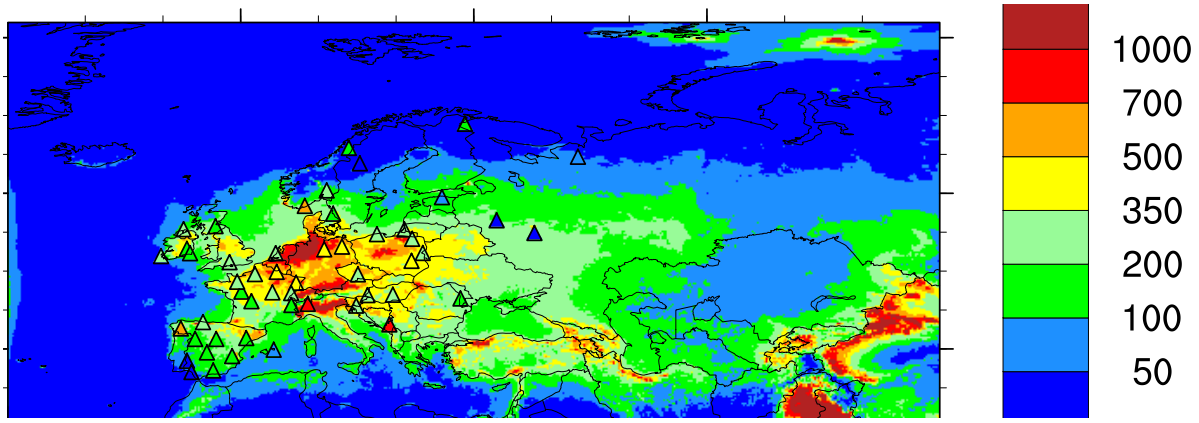

(c) Reduced N

Figure 2.20: Wet deposition of sulphur and nitrogen [mgS(N)m^{-2}] in 2017. EMEP observations on top (triangles).

Exceedances of critical loads of acidification and eutrophication

The exceedances of European critical loads (CLs) are computed for the total nitrogen (N) and sulphur (S) depositions modelled on the 0.1°x 0.1°longitude-latitude grid (approx. 11 x 5.5 km^2 at 60°N). Exceedances are calculated for the European critical loads data documented in Hettelingh et al. (2017), whereas a description of the methodologies can be found in De Vries et al. (2015). The critical loads data for eutrophication by N (CLeutN) and for acidification by N and S are also used by the CIAM (located at IIASA) in integrated assessment modelling. The exceedance in a grid cell is the so-called 'average accumulated exceedance' (AAE), computed as the area-weighted mean of the exceedances of the critical loads of all ecosystems in that grid cell. The units for critical loads and their exceedances are equivalents (eq; same as moles of charge, molc) per area and time, making S and N depositions comparable on their impacts (important for acidity CLs). Critical loads are available for about 4 million ecosystems in Europe covering an area of about 3 million km^2 (west of 42°E). The exceedances (AAE) of those critical loads are computed on a 0.1°x 0.1°longitude-latitude grid, and maps thereof are shown in Figures 2.21 and 2.22. As it can be seen from the maps, critical loads for eutrophication are exceeded in virtually all countries in 2017, in about 63.9% of the ecosystem area and the European average exceedance is about 277 eq $ha^{-1}yr^{-1}$. The highest exceedances are found in the Po Valley in Italy, the Dutch-German-Danish border areas and in north-eastern of Spain. In contrast, critical loads of acidity are exceeded in a much smaller area. Hot spots of exceedances can be found in the Netherlands and its border areas to Germany and Belgium, and some smaller maxima in southern Germany and the Czech Republic, whereas most of Europe is not exceeded (grey areas). In Europe as a whole, acidity exceedances in 2017 occur in about 5.5% of the ecosystem area and the European average AAE is about 32.4 eq $ha^{-1}yr^{-1}$.

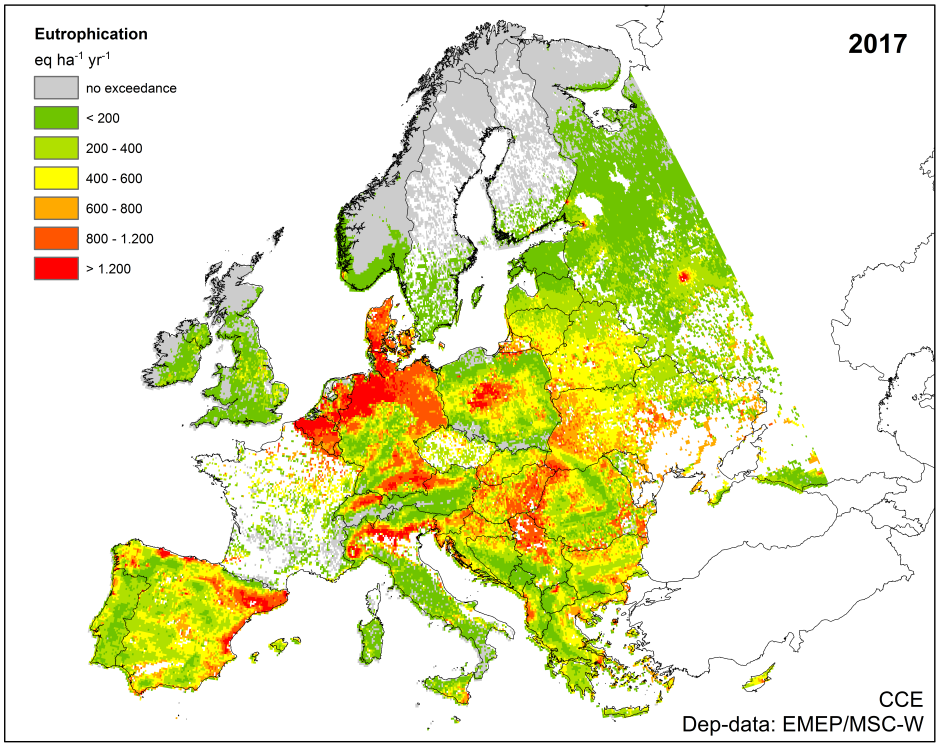

Figure 2.21: Exceedances of critical loads for eutrophication [eq $ha^{-1}yr^{-1}$] in 2017 simulated with the EMEP MSC-W model on a $0.1\times0.1°$longitude-latitude grid and mapped on a $0.5°\times0.25°$grid.

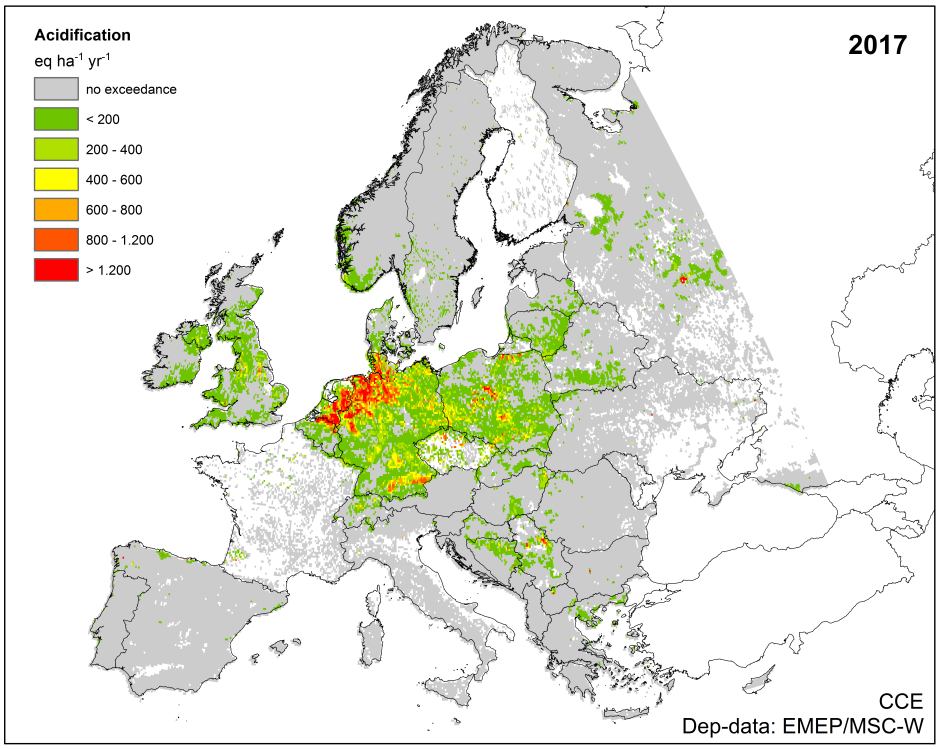

Figure 2.22: Exceedances of critical loads for acidification [eq $ha^{-1}yr^{-1}$] in 2017.

References

De Vries, W., Hettelingh, J.-P., and Posch, M.: Critical Loads and Dynamic Risk Assessments: Nitrogen, Acidity and Metals in Terrestrial and Aquatic Ecosystems, doi:10.1007/978-94-017-9508-1, Environmental Pollution Series Vol. 25, Springer, Dordrecht, xxviii+662 pp.; ISBN 978-94-017-9507-4, 2015.

Denier van der Gon, H. A. C., Bergström, R., Fountoukis, C., Johansson, C., Pandis, S. N., Simpson, D., and Visschedijk, A. J. H.: Particulate emissions from residential wood combustion in Europe - revised estimates and an evaluation, Atmos. Chem. Physics, pp. 6503–6519, doi:doi:10.5194/acp-15-6503-2015, URL http://www.atmos-chem-phys.net/15/6503/2015/, 2015.

ECCAD: Emissions of atmospheric Compounds and Compilation of Ancillary Data, URL https://eccad.aeris-data.fr, 2019.

EU: Directive 2008/50/EC of the European Parliament and of the Council on ambient air quality and cleaner air for Europe., Official Journal of the European Union L 152, 11 June 2008, pp. 1-44., L 152, 1–44, URL http://faolex.fao.org/docs/pdf/eur80016.pdf, 2008.

Finnigan, J. J., Raupach, M. R., Bradley, E. F., and Aldis, G. K.: A Wind-Tunnel Study Of Turbulent-Flow Over A 2-Dimensional Ridge, Boundary-Layer Meteorology, 50, 277–317, 1990.

Gauss, M., Tsyro, S., Fagerli, H., Hjellbrekke, A.-G., Aas, W., and Solberg, S.: EMEP MSC-W model performance for acidifying and eutrophying components, photo-oxidants and particulate matter in 2017., Supplementary material to EMEP Status Report 1/2019, available online at www.emep.int, The Norwegian Meteorological Institute, Oslo, Norway, 2019.

Granier, C., Darras, S., Denier van der Gon, H., Doubalova, J., Elguindi, N., Galle, B., Gauss, M., Guevara, M., Jalkanen, J.-P., Kuenen, J., Liousse, C., Quack, B., Simpson, D., and Sindelarova, K.: The Copernicus Atmosphere Monitoring Service global and regional emissions (April 2019 version), doi:10.24380/d0bn-kx16, URL https://atmosphere.copernicus.eu/sites/default/files/2019-06/cams_emissions_general_document_apr2019_v7.pdf, 2019.

Hettelingh, J.-P., Posch, M., and Slootweg, J.: European critical loads: database, biodiversity and ecosystems at risk., doi:10.21945/RIVM-2017-0155, CCE Final Report 2017. RIVM Report 2017-0155, 2017.

Hjellbrekke, A.-G.: Data Report 2017 Particulate matter, carbonaceous and inorganic compounds, Tech. Rep. EMEP/CCC Report 1/2019, Norwegian Institute for Air Research, Kjeller, Norway, 2019.

Hjellbrekke, A.-G. and Solberg, S.: Ozone measurements 2017, Tech. Rep. EMEP/CCC Report 2/2019, Norwegian Institute for Air Research, Kjeller, Norway, 2019.

Kew, S. F., Philip, S. Y., van Oldenborgh, G. J., Otto, F. E. L., Vautard, R., and van der Schrier, G.: Attribution study of the exceptional summer heatwave in southern Europe 2017 [in

"Explaining Extremes of 2017 from a Climate Perspective"], bull. Amer. Meteor. Soc., 100 (1), S49S53, https://doi.org/10.1175/BAMS-D-18-0109.1., 2019.

Overland, J., Hanna, E., Hanssen-Bauer, I., Kim, S.-J., Walsh, J., Walsh, J. E., Wang, M., Bhatt, U. S., and Thoman, R. L.: Surface Air Temperature, in Arctic Report Card 2017, NOAA, http://www.arctic.noaa.gov/Report-Card/Report-Card-Archive, 2017.

Pinterits, M., Ullrich, B., Gaisbauer, S., Mareckova, K., and Wankmüller, R.: Inventory review 2019. Review of emission data reported under the LRTAP Convention and NEC Directive. Stage 1 and 2 review. Status of gridded and LPS data, EMEP/CEIP 4/2019, CEIP/EEA Vienna, 2019.

Simpson, D., Benedictow, A., Berge, H., Bergström, R., Emberson, L. D., Fagerli, H., Hayman, G. D., Gauss, M., Jonson, J. E., Jenkin, M. E., Nyíri, A., Richter, C., Semeena, V. S., Tsyro, S., Tuovinen, J.-P., Valdebenito, A., and Wind, P.: The EMEP MSC-W chemical transport model – technical description, Atmos. Chem. Physics, 12, 7825–7865, doi:10.5194/acp-12-7825-2012, 2012.

Tarrason, L., Hamer, P., Meleux, F., and Rouil, L.: Interim Annual Assessment Report. European air quality in 2017, Tech. Rep. CAMS71_2018SC3_D71.1.1.10_IAAR2017_final, URL https://policy.atmosphere.copernicus.eu/reports/CAMS71_D71.1.1.10_201807_IAAR2017_final.pdf, 2018.

Tsyro, S., Gauss, M., Hjellbrekke, A.-G., and Aas, W.: PM10, PM2.5 and individual aerosol components, Supplementary material to EMEP Status Report 1/2019, available online at www.emep.int, The Norwegian Meteorological Institute, Oslo, Norway, 2019.

Tuovinen, J.-P., Simpson, D., Ashmore, M., Emberson, L., and Gerosa, G.: Robustness of modelled ozone exposures and doses, Environ. Poll., 146, 578–586, 2007.

UNECE: Progress in activities in 2009 and future work. Measurements and modelling (acidification, eutrophication, photooxidants, heavy metals, particulate matter and persistent organic pollutants). Draft revised monitoring strategy., Tech. Rep. ECE/EB.AIR/GE.1/2009/15, UNECE, URL http://www.unece.org/env/documents/2009/EB/ge1/ece.eb.air.ge.1.2009.15.e.pdf, 2009.

WHO: Air quality guidelines. Global update 2005. Particulate matter, ozone, nitrogen dioxide and sulfur dioxide, URL http://www.who.int/phe/health_topics/outdoorair/outdoorair_aqg/en/, World Health Organisation, European Centre for Environment and Health Bonn Office, ISBN 92 890 2192, 2005.

WMO: WMO Statement on the State of the Global Climate in 2017, WMO-No. 1212, https://public.wmo.int/en/resources/library, ISBN 978-92-63-11212-5, 2018.

CHAPTER 3

Emissions for 2017

Silke Gaisbauer, Robert Wankmüller, Bradley Matthews, Katarina Mareckova, Sabine Schindlbacher, Carlos Sosa, Melanie Tista and Bernhard Ullrich

In addition to meteorological variability, changes in the emissions affect the inter-annual variability and trends of air pollution, deposition and transboundary transport. The main changes in emissions in 2017 with respect to previous years are documented in the following sections.

The EMEP Reporting guidelines (UNECE 2014) requests all Parties to the LRTAP Convention to report annually emissions and activity data of air pollutants (SO_x[1], NO_2[2], NMVOCs[3], NH_3, CO, HMs, POPs, PM[4] and voluntary BC). Further, every four years, projection data, gridded data and information on large point sources (LPS) have to be reported to the EMEP Centre on Emission Inventories and Projections (CEIP).

3.1 Reporting of emission inventories in 2019

Completeness and consistency of submitted data have improved significantly since EMEP started collecting information on emissions. Data of at least 45 Parties each year were submit-

[1]"Sulphur oxides (SO_x)" means all sulphur compounds, expressed as sulphur dioxide (SO_2), including sulphur trioxide (SO_3), sulphuric acid (H_2SO_4), and reduced sulphur compounds, such as hydrogen sulphide (H_2S), mercaptans and dimethyl sulphides, etc.

[2]"Nitrogen oxides (NO_x)" means nitric oxide and nitrogen dioxide, expressed as nitrogen dioxide (NO_2).

[3]"Non-methane volatile organic compounds" (NMVOCs) means all organic compounds of an anthropogenic nature, other than methane, that are capable of producing photochemical oxidants by reaction with nitrogen oxides in the presence of sunlight.

[4]"Particulate matter" (PM) is an air pollutant consisting of a mixture of particles suspended in the air. These particles differ in their physical properties (such as size and shape) and chemical composition. Particulate matter refers to:
(i) "$PM_{2.5}$", or particles with an aerodynamic diameter equal to or less than 2.5 micrometers (μm);
(ii) "PM_{10}", or particles with an aerodynamic diameter equal to or less than 10 (μm).

ted to CEIP for the last seven years (see Figure 3.1). 45 Parties (88%) submitted inventories[5] in 2019; six Parties[6] did not submit any data and 39 Parties reported black carbon (BC) emissions (see section 3.2). Although 2019 was no reporting year for large point sources (LPS), gridded emissions and projections, three Parties reported information on LPS, five Parties reported gridded data in new resolution, and twenty-five Parties reported projection data (Pinterits et al. 2019).

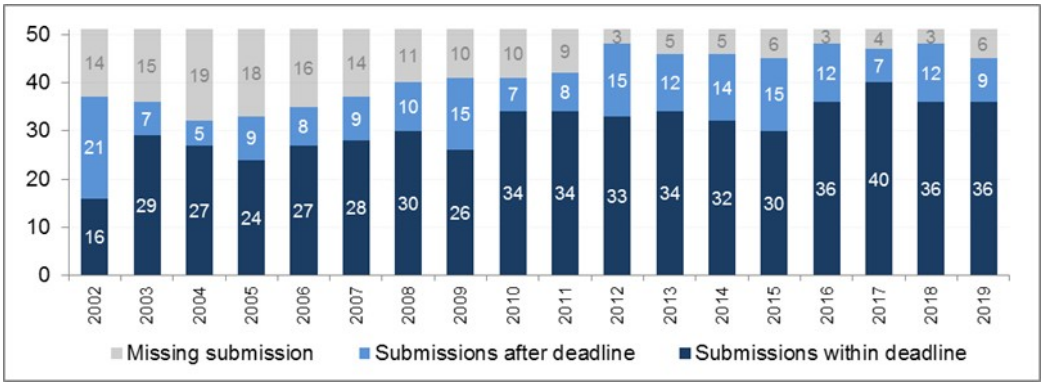

Figure 3.1: Parties reporting emission data to EMEP since 2002, as of 4 June 2019.

The quality of the submitted data across countries differs quite significantly. By compiling the inventories, countries have to use the newest available version of the EMEP/EEA air pollutant emission inventory guidebook, which is the version of 2016 (EMEP/EEA 2016). However, many countries still use the 2013 Guidebook (EMEP/EEA 2013) or older versions. Uncertainty of the reported data (national totals, sectoral data) is considered relatively high, the completeness of reported data has not turned out satisfactory for all pollutants and sectors either.

Detailed information on recalculations, completeness and key categories, plus additional review findings can be found in the annual EEA & CEIP technical inventory review reports (Pinterits et al. 2019) and its Annexes[7].

3.2 Black Carbon (BC) emissions

Over the last decade, black carbon (BC) has emerged as one of the most important anthropogenic air pollutants. Due to its distinct physical properties and its potential toxicity (Janssen et al. (2012)) BC is a significant air pollutant in terms of both climate change and air quality. Given its absorption spectrum in the visible range, BC warms the atmosphere directly by absorbing solar radiation and, indirectly, by accelerating snow-/ice melt when deposited (Bond et al. (2013)). According to recent estimates, the direct radiative forcing effect of black carbon emissions during the first part of the industrial era may have been of the same magnitude as methane (CH_4) emissions (Bond et al. (2013), Wang et al. (2016)). Meanwhile, in terms of human health, epidemiological studies suggest that certain pulmonary and cardiovascular

[5]The original submissions from the Parties can be accessed via the CEIP homepage on `http://www.ceip.at/status_reporting/2019_submissions`.

[6]Greece, Bosnia and Herzegovina, Kazakhstan, Liechtenstein, the Republic of Moldova, and Montenegro

[7]`http://www.ceip.at/review_proces_intro/review_reports`

conditions are more strongly associated with exposure to BC rather than aggregate PM (e.g. Baumgartner et al. (2014)).

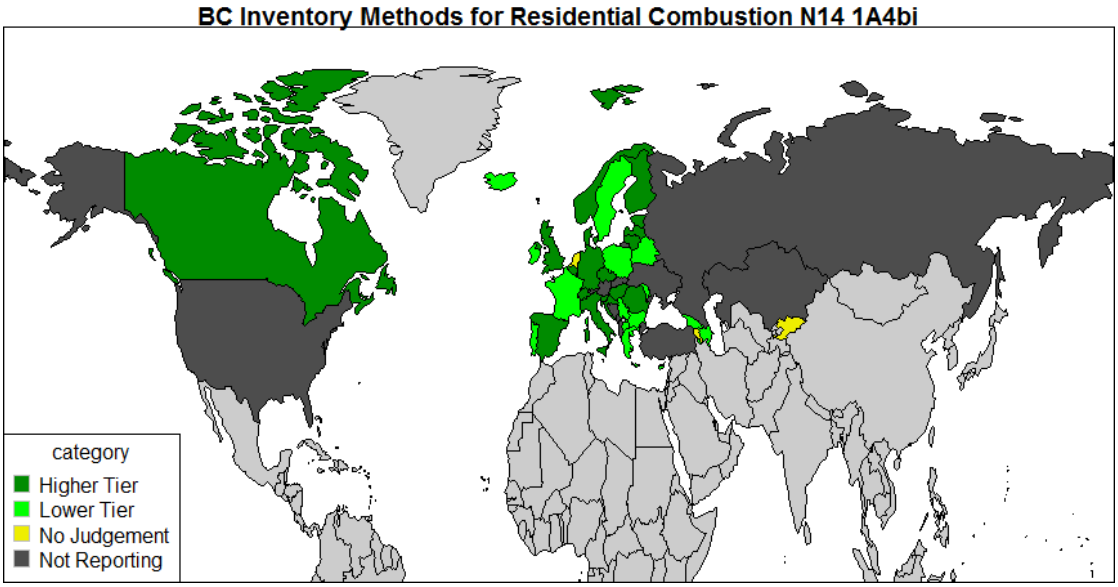

Figure 3.2: Varying level of reporting and Tiers applied by the CLRTAP Parties for BC emissions from the sector "Residential combustion" (N14 1A4bi).

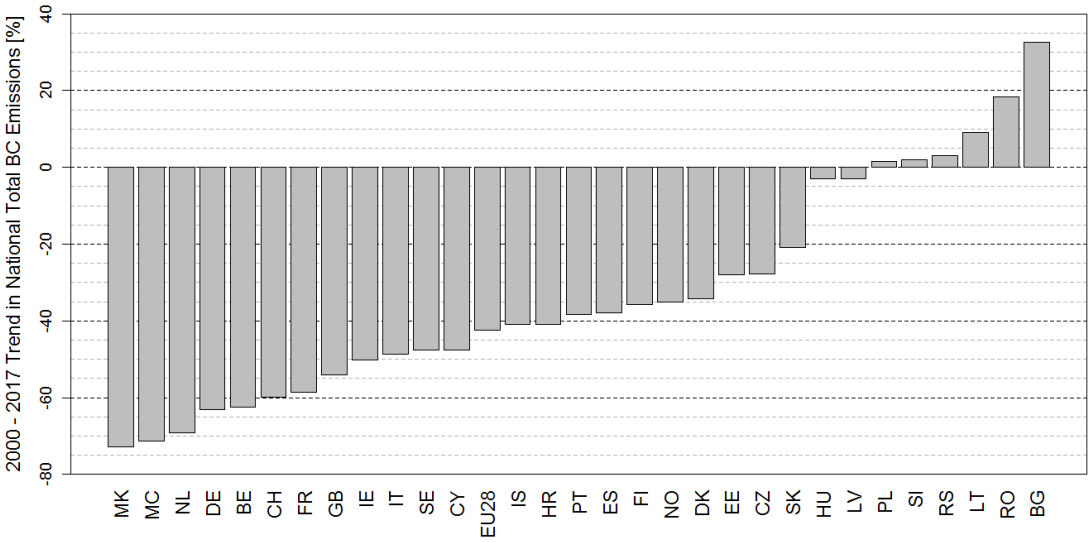

Figure 3.3: Black carbon emissions trends of Parties reporting 2000 and 2017 emissions estimates.

The emerging significance of BC is mirrored in developments in the international policy arena. Since the Executive Body Decision 2013/04, Parties to the LRTAP Convention have been formally encouraged to submit inventory estimates of their national BC emissions, and in 2015 the reporting templates were updated to include BC data emissions. In addition to reporting under CLRTAP, EU member states are also encouraged to submit BC emissions estimates as part of their emissions reporting under the National Emissions Ceilings (NEC) Directive (2016/2284/EU). Furthermore, in the context of the particularly acute impacts of

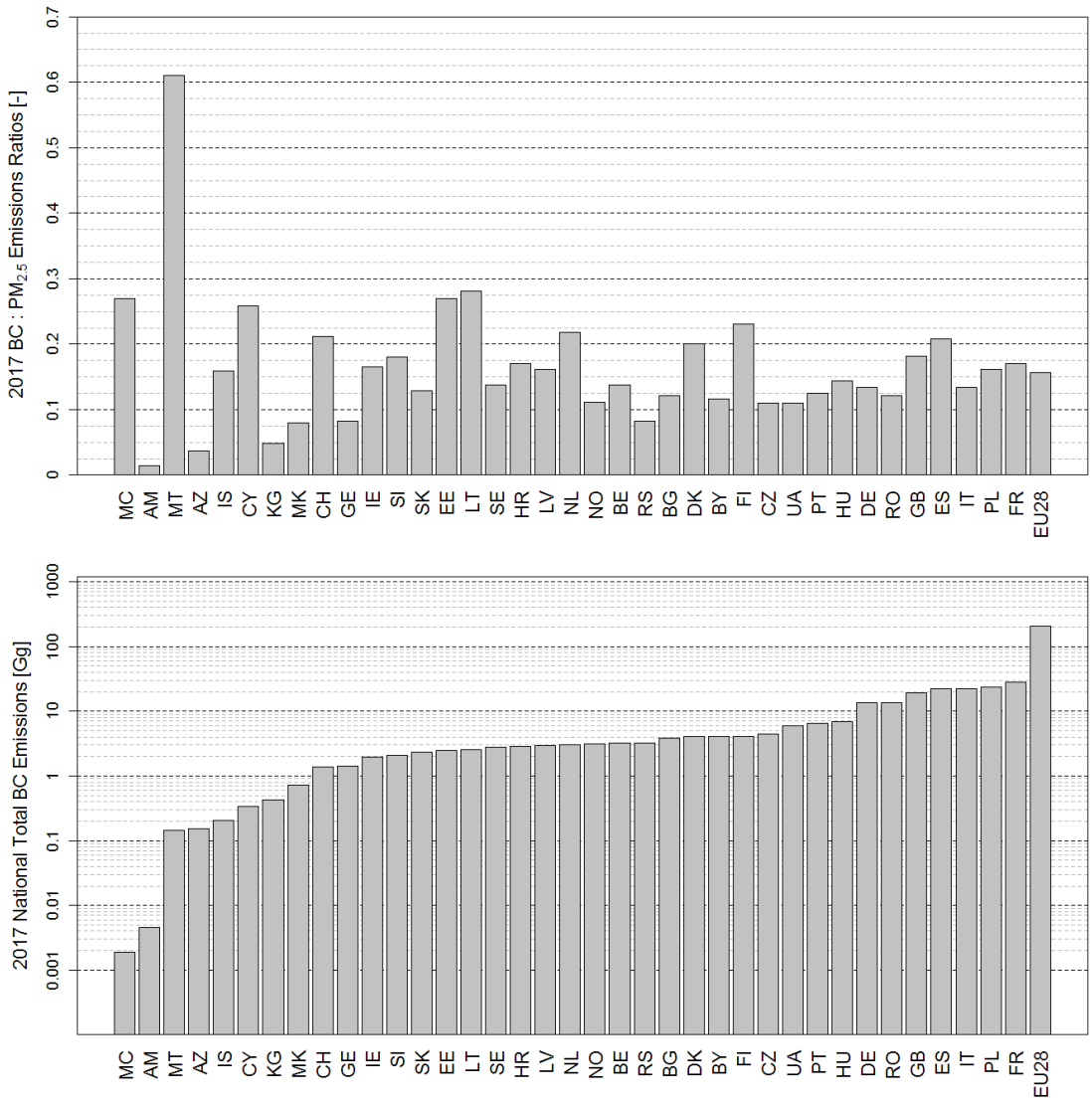

Figure 3.4: Black carbon emissions of the year 2017 as absolute emissions values (below) and as fractions of $PM_{2.5}$ emissions (above).

BC in accelerating climate change in the Arctic (Sand et al. (2016)), ministers of the Arctic Council adopted the *Enhanced Black Carbon and Methane Emissions Reductions: An Arctic Council Framework Action* which committed the Arctic States (Canada, Denmark, Finland, Iceland, Norway, Russia, Sweden and United States of America) to develop and submit emissions inventories for BC and CH_4 to the Council.

Under the auspices of the *EU Action on Black Carbon in the Arctic* (EUA-BCA) a technical report, *Review of Reporting Systems for National Black Carbon Emissions Inventories*, was recently compiled. The report, which was co-led by CEIP and will soon be published on the Action's website[8], reviewed, *inter alia*, the level of BC reporting under the LRTAP Convention. Despite a large number of Parties voluntarily reporting BC emissions, the review revealed a number of shortcomings. As of 2018, nine Parties had not yet submitted BC emissions inventories to the Convention. Furthermore, analysis of the emissions estimates which were reported revealed significant issues in terms of consistency, completeness and compara-

[8] https://eua-bca.amap.no/

bility. As an example, Figure 3.2 illustrates the varying level of reporting of BC emissions for the sector *Residential combustion* N14 1A4bi. The review thus highlights that caution should be taken when utilizing and/or analyzing BC emissions reported by the CLRTAP Parties.

Beyond this report CEIP continues to monitor and review the level of BC reporting by the Convention's Parties. Below a brief overview of BC emissions estimates submitted by EMEP countries in 2019 is given.

Twenty-one countries (out of 39) submitted a complete time series of national total BC emissions (1990-2017), 31 submitted a complete time series from 2000 onwards. Figure 3.3 shows the 2000-2017 BC emissions trends for those 31 Parties. Most Parties (24) report a negative trend, with the emissions of 22 Parties decreasing by 20% or more. Six Parties report an increase in emissions when comparing the 2017 and 2000 estimates.

Figure 3.4 gives an overview on the BC emissions reported for the year 2017. Thirty-eight of 39 reporting Parties reported emissions for 2017. The United States reported BC emissions data in 2019, however, the most recent estimate is for the year 2014. As the upper part of the graph illustrates, for the majority of these Parties, 2017 BC emissions constitute between 10 and 20% of the respective total $PM_{2.5}$ emissions. Indeed the median BC fraction based on reported BC and $PM_{2.5}$ emissions lies at 15.01%.

For more detailed information on BC consult the annual EEA & CEIP technical inventory review report (Pinterits et al. 2019).

3.3 Inclusion of the condensable component in PM emissions

The condensable component of particulate matter is probably the biggest single source of uncertainty in PM emissions. Currently the condensable component is not included or excluded consistently in PM emissions reported by Parties of the LRTAP Convention. Also in the EMEP/EEA Guidebook (EMEP/EEA 2016) the condensable fraction is not consistently included or excluded in the emission factors, but improvements are planned for the 2019 update of the EMEP/EEA Guidebook. However, PM emissions reported by Parties to the LRTAP Convention are not directly comparable at the moment with implications on the modeling of overall exposure to PM compliance with $PM_{2.5}$ emissions reduction commitments.

Parties were asked to include a table with information on the inclusion of the condensable component in PM_{10} and $PM_{2.5}$ emission factors for the reporting under the CLRTAP convention in 2019. This table has been added to the revised recommended structure for IIRs[9]. Seventeen Parties provided information on the inclusion of the condensable component in PM_{10} and $PM_{2.5}$ emission factors (Austria, Belgium, Croatia, Estonia, Germany, Finland, France, Latvia, the Netherlands, Portugal, Romania, Slovakia, Slovenia, Spain, Sweden, Switzerland and United Kingdom)[10]. Eleven of these Parties provided the information in the recommended format. Some Parties chose to report the information on an aggregated level. This reporting is a first step towards a better understanding of the reported PM data. However, the reporting in 2019 showed that in many cases Parties do not have the information if the PM emissions of a specific source category include the condensable component. For the majority of the source

[9] https://www.ceip.at/ms/ceip_home1/ceip_home/reporting_instructions/annexes_to_guidelines/

[10] Status 30 April 2019

Table 3.1: Information on the inclusion of the condensable component in PM_{10} and $PM_{2.5}$ emission factors

Party	NFR category	Source/sector name (according to Annex I, Reporting Guidelines, modified in selected cases)	PM emissions: the condensable component is included	PM emissions: the condensable component is excluded
Austria	1A4bi	Residential: Stationary	x	x
Belgium	1A4bi	Residential: Stationary	p	p
Belgium	1A4bi	Residential: Stationary (wood)	x	
Belgium	1A4bi	Residential: Stationary (natural gas)	u	u
Belgium	1A4bi	Residential: Stationary (gasoil)		x
Belgium	1A4bi	Residential: Stationary (coal)	u	u
Estonia	1A4bi	Residential: Stationary		x
Croatia	1A4bi	Residential: Stationary	u	u
France	1A4bi	Residential: Stationary		x
Germany	1A4bi	Residential: Stationary		x
Latvia	1A4bi	Residential: Stationary	u	u
Portugal	1A4bi	Residential: Stationary	x	
Romania	1A4bi	Residential: Stationary	x	
Slovakia	1A4bi	Residential: Stationary	u	u
Slovenia	1A4bi	Residential: Stationary	p	
Spain	1A4bi	Residential: Stationary Solid biomass (excluding Wood and similar wood waste)	x	
Spain	1A4bi	Residential: Stationary Wood and similar wood waste	x	
Spain	1A4bi	Residential: Stationary Steam coal		x
Switzerland	1A4bi	Charcoal use Bonfire	x	
United Kingdom	1A4bi	Residential: Stationary	x	

p = partially included; u = unclear status of inclusion

categories of PM emission Parties either indicated that it is "unknown" if the condensable component is included in the PM emissions, or they provided no information or the provided information was not clear. The status of inclusion or exclusion is best known for the emissions from road transport. For example for "1A3bi Road transport passenger cars" ten of the twelve Parties that provided information for this source category report emissions to be included and only two Parties state that the status of inclusion is unknown.

Small-scale combustion sources make a notable contribution to total PM emissions. For all Parties that reported $PM_{2.5}$ emissions for "1A4bi Residential: Stationary" for the year 2017[11]

[11] Status 2 May 2019

emissions from this source category contributed 44% to the national total $PM_{2.5}$ emissions. Small-scale combustion is one of the sources where the inclusion of the condensable component has the largest impact on the emission factor. For example, for conventional woodstoves, one of the most important categories in Europe, the emission factors excluding and including the condensable fractions may differ by up to a factor of five (Denier van der Gon et al. 2015). Here the status of the inclusion was less clear. Of the thirteen Parties that provided information for "1A4bi Residential: Stationary" three parties reported the condensable component to be included and three Parties to be excluded. The other Parties reported "unknown", "partially included" or provided information on a more detailed level with different status of inclusion (see Table 3.1).

As 2019 was the first year in which Parties were asked to provide information on the inclusion of the condensable component, it is expected that the reporting will improve over the coming years, with more parties reporting the information and with a higher quality of the reported information.

3.4 Comparison of 2016 data (reported in 2018) and 2017 data (reported in 2019)

The comparison of 2016 emissions (reported in 2018) and 2017 emissions (reported in 2019) showed, that for 21 countries data changed by more than 10% for one or several pollutants (see Figure 3.5 and Table 3.2-3.3). These changes can be caused by real emission reductions or increases, or recalculations made by the respective country.

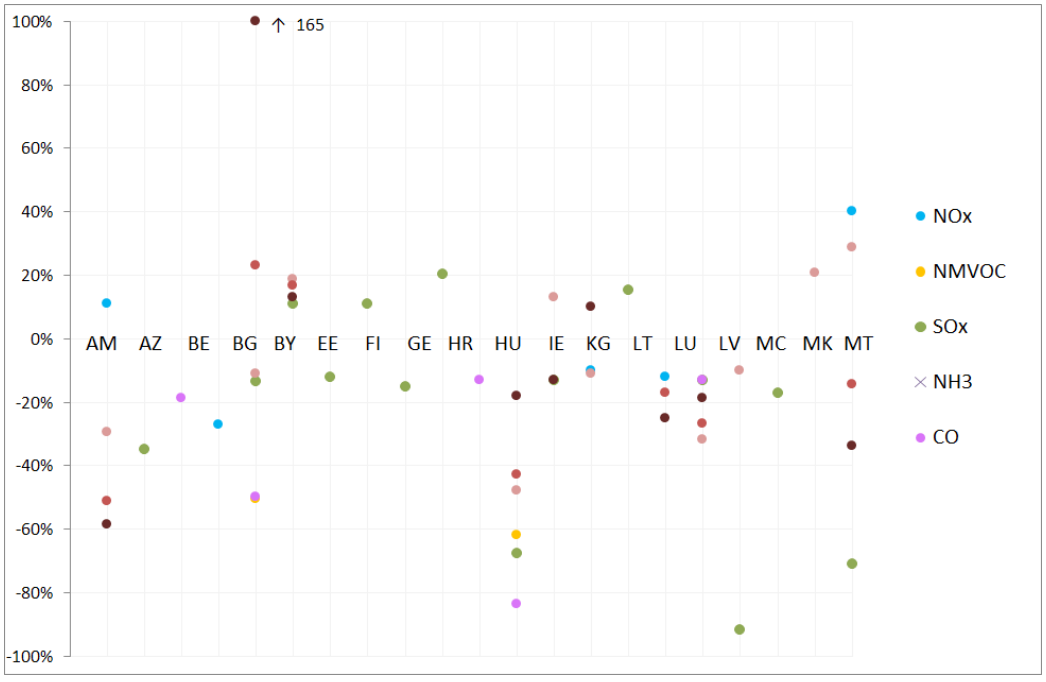

Figure 3.5: Emission changes between 2016 and 2017 in reported data (only changes larger than 10% are shown).

In five countries, both NO_x and CO emissions changed by more than 10%. For NMVOCs, emissions changed in two countries by more than 10%. For SO_x, emissions changed by more

Table 3.2: Reported emission changes between 2016 (reported in 2018) and 2017 (reported in 2019) over 10% for main pollutants.

Pollutant	Country	2016 emissions (kt)	2017 emissions (kt)	Difference (kt)	Difference (%)
NO_x	AM	18.168	20.181	2.013	11%
NO_x	BG	141.328	102.813	-38.515	-27%
NO_x	LU	20.350	18.314	-2.036	-10%
NO_x	MC	0.174	0.154	-0.020	-12%
NO_x	UA	417.479	584.957	167.478	40%
NMVOC	BY	290.672	143.296	-147.376	-51%
NMVOC	KG	88.555	33.722	-54.834	-62%
SO_x	AZ	17.677	11.510	-6.167	-35%
SO_x	BY	55.859	48.271	-7.588	-14%
SO_x	EE	34.947	38.653	3.706	11%
SO_x	FI	39.804	35.020	-4.783	-12%
SO_x	GE	9.526	10.544	1.018	11%
SO_x	HR	14.804	12.557	-2.247	-15%
SO_x	HU	23.012	27.722	4.710	20%
SO_x	KG	46.929	15.277	-31.652	-67%
SO_x	LT	15.107	13.177	-1.930	-13%
SO_x	LV	3.470	3.996	0.526	15%
SO_x	MK	64.746	56.064	-8.682	-13%
SO_x	MT	1.785	0.151	-1.634	-92%
SO_x	RU	1165.416	967.862	-197.555	-17%
SO_x	UA	947.527	274.257	-673.270	-71%
CO	BE	360.942	293.338	-67.604	-19%
CO	BY	760.174	381.192	-378.982	-50%
CO	IE	101.960	88.423	-13.537	-13%
CO	KG	498.964	81.053	-417.910	-84%
CO	MK	65.435	56.913	-8.521	-13%

than 10% in 14 countries, while for NH_3 the change of emission levels were less than 10% in each country. Of the PMs, emissions changed by more than 10% in ten countries for $PM_{2.5}$, in seven countries for PM_{10} and in nine countries for PM_{coarse}[12] (see Figure 3.5 and Table 3.2-3.3). The largest changes occurred in Belarus, Kyrgyzstan, Malta and Ukraine.

In Belarus PM_{coarse} emissions increased significantly (+165%), mostly due to the sector '1A4bi – Residential: Stationary'.

For Kyrgyzstan a significant reduction in CO emissions (-84%) were detected, which originates mostly in the NFR sector '1A4bi – Residential: Stationary'. These changes may be

[12] PM_{coarse} emissions are not reported by Parties but calculated as difference between PM_{10} and $PM_{2.5}$ emissions.

Table 3.3: Reported emission changes between 2016 (reported in 2018) and 2017 (reported in 2019) over 10% for PM.

Pollutant	Country	2016 emissions (kt)	2017 emissions (kt)	Difference (kt)	Difference (%)
$PM_{2.5}$	AM	0.462	0.325	-0.137	-30%
$PM_{2.5}$	BY	38.991	34.802	-4.189	-11%
$PM_{2.5}$	EE	7.770	9.222	1.452	19%
$PM_{2.5}$	KG	16.751	8.743	-8.008	-48%
$PM_{2.5}$	LT	8.017	9.081	1.064	13%
$PM_{2.5}$	LU	1.509	1.345	-0.164	-11%
$PM_{2.5}$	MK	13.465	9.197	-4.269	-32%
$PM_{2.5}$	MT	0.265	0.238	-0.027	-10%
$PM_{2.5}$	TR	13.874	16.761	2.887	21%
$PM_{2.5}$	UA	41.803	53.774	11.971	29%
PM_{10}	AM	1.824	0.891	-0.933	-51%
PM_{10}	BY	48.190	59.216	11.026	23%
PM_{10}	EE	11.920	13.911	1.992	17%
PM_{10}	KG	20.056	11.449	-8.607	-43%
PM_{10}	MC	0.016	0.013	-0.003	-17%
PM_{10}	MK	21.973	16.120	-5.853	-27%
PM_{10}	UA	133.590	114.367	-19.223	-14%
PM_{coarse}	AM	1.362	0.565	-0.797	-58%
PM_{coarse}	BY	9.199	24.414	15.215	165%
PM_{coarse}	EE	4.150	4.689	0.539	13%
PM_{coarse}	KG	3.305	2.706	-0.599	-18%
PM_{coarse}	LT	5.873	5.115	-0.758	-13%
PM_{coarse}	LU	0.599	0.660	0.061	10%
PM_{coarse}	MC	0.008	0.006	-0.002	-25%
PM_{coarse}	MK	8.508	6.923	-1.585	-19%
PM_{coarse}	UA	91.787	60.593	-31.194	-34%

caused by recalculations of the time series made by Kyrgyzstan.

For Malta a huge change of SO_x emissions (-92%) occurs, which mainly originates in the NFR category '1A1a – Public electricity and heat production'. Malta explained in its IIR[13], that the decline in SO_x emissions mirrors the decrease in electricity generated from fuel combustion.

In Ukraine there are significant changes in the emissions of SO_x (-71%), NO_x (+40%) and $PM_{2.5}$ (+29%) between 2016 and 2017. The decrease in SO_x emissions and the increase in NO_x and $PM_{2.5}$ emissions are mainly caused by the NFR sector '1A1a – Public electricity and

[13] https://webdab01.umweltbundesamt.at/download/submissions2018/MT_IIR2018.zip?cgiproxy_skip=1

heat production'.

3.5 Gothenburg Protocol targets

The 1999 Gothenburg Protocol (GP) lists emission reduction commitments of NO_x, SO_x, NMVOCs and NH_3 for most of the Parties to the LRTAP Convention for the year 2010 (UNECE (1999)). These commitments should not be exceeded in 2010 and in subsequent years either.

In 2012, the Executive Body of the LRTAP Convention decided that adjustments to inventories may be applied in some circumstances (UNECE (2012)). From 2014 to 2018, adjustment applications of nine countries (Belgium, Denmark, Finland, France, Hungary, Germany, Luxembourg, Spain and the United Kingdom) have been accepted and therefore these approved adjustments have to be subtracted for the respective countries when compared to the targets. In April 2019, the Netherlands submitted a new adjustment application, which will be approved most likely later this year.

Further, the reporting guidelines (UNECE (2014)) specify that some Parties within the EMEP region (i.e. Austria, Belgium, Ireland, Lithuania, Luxembourg, the Netherlands, Switzerland and the United Kingdom of Great Britain and Northern Ireland) may choose to use the national emission total calculated on the basis of fuels used in the geographic area of the Party as a basis for compliance with their respective emission ceilings. However, when considering only reported data, approved adjustments and fuel used data of the respective countries, Figure 3.6 indicates that the Netherlands and the United States of America could not reduce their NMVOC emissions with regard to the Gothenburg Protocol requirements, and that Croatia, Germany, Norway and Spain are above their Gothenburg Protocol ceilings for NH_3. In terms of NO_x emissions, Norway exceeded their ceilings.

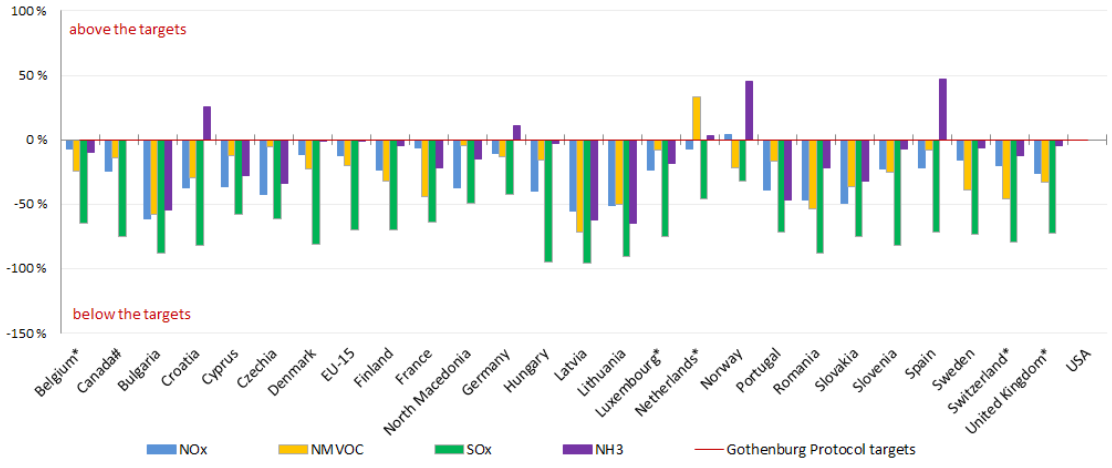

Figure 3.6: Distance to Gothenburg Protocol targets in 2019 (based on reported data). Only Parties that ratified the Gothenburg Protocol are included. * Emission data based on fuels used for road transport. Approved adjustments are considered for Denmark (NMVOCs, NH_3), Finland (NH_3), Germany (NO_x, NMVOCs, NH_3), Hungary (NMVOCs), Luxembourg (NO_x, NMVOCs) and Spain (NO_x).

3.6 Emission trends in the EMEP area

To provide a picture as complete as possible of the emission trends in the EMEP area[14], data as used for EMEP models (i.e. gap-filled data) were used for the calculations (see Section 3.8). The trend indicates that in the EMEP area total emissions of three of the reported pollutants have decreased overall since 2000 (Figure 3.7). The presented emission trends are based on gap-filled data as used in the EMEP models, therefore there is a certain uncertainty in the magnitude of this development. The observed decrease is significant for SO_x, CO and NO_x, while PM, NMVOC and NH_3 emissions increase, whereas PM_{coarse} and NH_3 increased most (33% and 31%, respectively) since the year 2000.

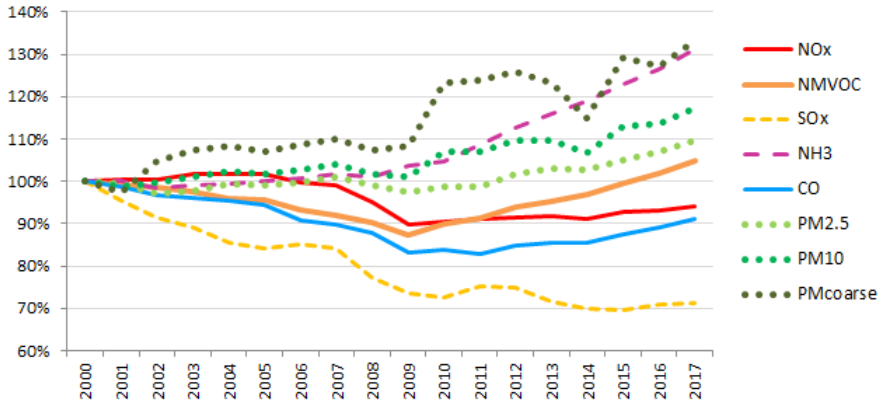

Figure 3.7: Emission trends 2000–2017 in the EMEP area (based on gap–filled data as used in EMEP models)

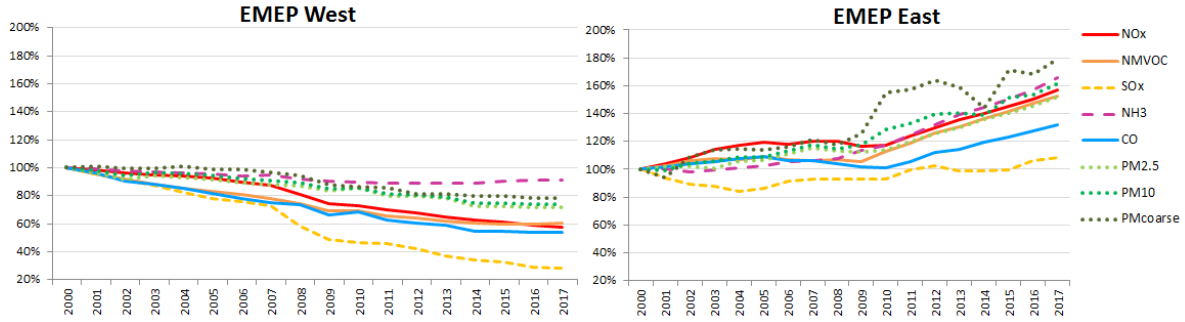

Figure 3.8: Emission trends 2000-2017 in the EMEP area (based on gap-filled data as used in EMEP models) divided in 2 areas 'EMEP West' (left), 'EMEP East' (right).

A more detailed assessment shows that emission developments in the eastern and western part of the EMEP area seem to follow strongly different patterns (see Figure 3.8)[15].

While emissions of all pollutants in the western part of the EMEP domain are slowly decreasing, emissions of all pollutants in the eastern part of the EMEP domain have increased since the year 2000. The emissions in the western parts of the EMEP area are mostly based

[14]The EMEP domain covers the geographic area between 30° N-82° N latitude and 30° W-90° E longitude.

[15]The split between the EMEP West region and the EMEP East region according to `http://www.ceip.at/emep_countries`. 'North Africa' and sea areas are not included and 'Asian Areas' are included in the EMEP East region.

on reported data; the emissions in eastern parts are often expert estimates so the uncertainty is rather high. The significant increase in emissions (of all pollutants) in the 'EMEP east' area is mainly influenced by emission estimates made for the remaining Asian Areas in the EMEP domain. The expert estimates for this area are based on gridded emissions from EDGAR (JRC/PBL 2016) for 2000, 2005 and 2010, extrapolated with the GDP trend for China.

3.6.1 Trend analysis

Emission levels in the EMEP domain for 2017 of individual countries and areas are compared to 2000 emission levels for NO_x, NMVOCs, SO_x, NH_3, CO and PMs (see Tables 3.4-3.4 continued). For this comparison, gap-filled data as used in the EMEP models were used (see Section 3.8). Overview tables with reported emission trends for individual countries have been published on the CEIP website at `http://www.ceip.at/status_reporting/2019_submissions`. Detailed information on the sectoral level can also be accessed in WebDab[16].

The assessment of emission levels in individual countries and areas show an increase of emissions in 2017 compared to 2000 emission levels in several countries or areas. In case of PM emissions, 28 countries/areas have higher PM_{coarse} emissions in 2017 then in 2000, while PM_{10} and $PM_{2.5}$ emissions increased in 23 and 19 countries/areas, respectively. In case of NO_x, there are 16 countries/areas, NMVOCs 15, SO_x 14, NH_3 21 and CO 14 countries/areas with higher emissions in 2017 than in year 2000. Detailed explanatory information on emission trends should be provided in the informative inventory reports (IIRs).

NO_x emissions

Emissions decreased in 45 countries or areas and increased in 15 countries or areas (see Table 3.4) between 2000 and 2017. For the whole EMEP domain, emissions decreased by 6%. The strongest increase is shown for Georgia (+239%).

NMVOC emissions

Emissions in the EMEP domain have decreased by 5% compared with 2000 levels. Compared with 2000, NMVOC emissions have decreased in 46 countries or areas and increased in 14 (see Table 3.4). The strongest NMVOC increases can be observed in Kyrgyzstan (+383%).

SO_x emissions

SO_x emissions decreased by 29% between 2000 and 2017 within the EMEP domain. Compared with 2000, SO_x emissions have decreased in 47 countries or areas and increased in 13 (see Table 3.4), among them Armenia (+358%), Montenegro (+248%) and Tajikistan (+289%).

[16] `http://www.ceip.at/webdab_emepdatabase/reported_emissiondata` and/or `http://www.ceip.at/webdab_emepdatabase/emissions_emepmodels`

Table 3.4: Differences between emissions for 2000 and 2017 (based on gap–filled data as used in EMEP models). Negative values mean that 2017 emissions were lower than 2000 emissions. Orange/red coloured data means that 2017 emissions were higher than 2000 emissions.

	NO_x	NMVOC	SO_x	NH_3	CO	$PM_{2.5}$	PM_{10}	PM_{coarse}
Albania	40 %	65 %	-61 %	-15 %	93 %	70 %	53 %	10 %
Armenia	102 %	123 %	358 %	34 %	2 %	2 %	6 %	19 %
Asian Areas	146 %	103 %	109 %	107 %	89 %	115 %	114 %	114 %
Atlantic Ocean	-33 %	-21 %	-31 %		-21 %	-26 %	-26 %	0 %
Austria	-32 %	-33 %	-60 %	8 %	-28 %	-37 %	-27 %	-11 %
Azerbaijan	68 %	26 %	-41 %	70 %	19 %	-15 %	12 %	34 %
Baltic Sea	-30 %	-19 %	-96 %		-20 %	-71 %	-71 %	0 %
Belarus	6 %	-36 %	-69 %	-3 %	-47 %	38 %	62 %	116 %
Belgium	-49 %	-49 %	-78 %	-27 %	-68 %	-43 %	-40 %	-30 %
Black Sea	-26 %	-14 %	-24 %		-13 %	-18 %	-18 %	0 %
Bosnia and Herzegovina	-12 %	-36 %	41 %	26 %	-47 %	-13 %	-17 %	-21 %
Bulgaria	-33 %	-28 %	-88 %	-9 %	-30 %	24 %	1 %	-28 %
Caspian Sea	193 %	193 %	193 %		193 %	193 %	193 %	193 %
Croatia	-38 %	-39 %	-79 %	-17 %	-56 %	-50 %	-39 %	8 %
Cyprus	-31 %	-33 %	-66 %	-12 %	-54 %	-50 %	-57 %	-65 %
Czechia	-42 %	-28 %	-53 %	-23 %	-24 %	-19 %	-22 %	-32 %
Denmark	-51 %	-40 %	-68 %	-21 %	-48 %	-15 %	-14 %	-10 %
Estonia	-26 %	-40 %	-60 %	17 %	-30 %	-40 %	-57 %	-72 %
Finland	-46 %	-50 %	-57 %	-9 %	-40 %	-31 %	-27 %	-20 %
France	-50 %	-63 %	-77 %	-6 %	-59 %	-50 %	-42 %	-19 %
Georgia	239 %	3 %	-14 %	-8 %	35 %	-39 %	-34 %	-8 %
Germany	-39 %	-35 %	-51 %	2 %	-41 %	-41 %	-30 %	-15 %
Greece	-38 %	-37 %	-89 %	-16 %	-63 %	-51 %	-51 %	-51 %
Hungary	-36 %	-28 %	-94 %	-6 %	-49 %	0 %	-5 %	-14 %
Iceland	-32 %	-35 %	28 %	-1 %	110 %	-5 %	1 %	31 %
Ireland	-38 %	-7 %	-91 %	3 %	-64 %	-41 %	-29 %	-17 %
Italy	-52 %	-42 %	-85 %	-16 %	-52 %	-16 %	-20 %	-37 %
Kazakhstan	106 %	73 %	53 %	56 %	109 %	235 %	274 %	458 %
Kyrgyzstan	159 %	383 %	96 %	124 %	509 %	142 %	93 %	-10 %
Latvia	-6 %	-22 %	-77 %	17 %	-52 %	-17 %	-1 %	95 %
Liechtenstein	-24 %	-46 %	-64 %	-4 %	-26 %	-10 %	-14 %	-34 %
Lithuania	-5 %	-36 %	-65 %	9 %	-24 %	-3 %	8 %	22 %
Luxembourg	-55 %	-23 %	-69 %	-14 %	-48 %	-44 %	-31 %	23 %
North Macedonia	-42 %	-40 %	-47 %	-24 %	-61 %	-69 %	-63 %	-49 %
Malta	-39 %	-41 %	-93 %	-39 %	-61 %	-53 %	-67 %	-78 %
Republic of Moldova	123 %	73 %	135 %	-3 %	206 %	185 %	96 %	18 %

Table 3.4 continued. Differences between emissions for 2000 and 2017 (based on gap–filled data as used in EMEP models).

Mediterranean Sea	-31 %	-19 %	-33 %		-19 %	-26 %	-26 %	0 %
Monaco	-66 %	-35 %	-81 %	-85 %	-45 %	-59 %	-47 %	-21 %
Montenegro	58 %	-16 %	248 %	-63 %	-35 %	9 %	48 %	89 %
Netherlands	-46 %	-24 %	-65 %	-25 %	-26 %	-53 %	-39 %	-9 %
North Africa	81 %	30 %	66 %	72 %	5 %	61 %	63 %	66 %
North Sea	-33 %	-21 %	-94 %		-21 %	-67 %	-67 %	0 %
Norway	-27 %	-62 %	-44 %	3 %	-36 %	-35 %	-28 %	10 %
Poland	-6 %	-6 %	-59 %	-7 %	-24 %	-8 %	-10 %	-13 %
Portugal	-44 %	-33 %	-84 %	-25 %	-53 %	-31 %	-33 %	-39 %
Romania	-17 %	-10 %	-78 %	-12 %	4 %	8 %	6 %	0 %
Russian Federation (European part)	-1 %	10 %	-52 %	35 %	-4 %	-28 %	18 %	128 %
Russian Federation (Asian part)	-10 %	6 %	-21 %	4 %	-21 %	-15 %	-5 %	12 %
Serbia	0 %	-14 %	-9 %	-15 %	-33 %	-4 %	-1 %	7 %
Slovakia	-39 %	-47 %	-77 %	-37 %	-33 %	-56 %	-55 %	-46 %
Slovenia	-41 %	-43 %	-95 %	-14 %	-44 %	6 %	2 %	-18 %
Spain	-45 %	-34 %	-84 %	-7 %	-43 %	-25 %	-27 %	-31 %
Sweden	-42 %	-35 %	-59 %	-11 %	-42 %	-39 %	-22 %	6 %
Switzerland	-42 %	-47 %	-67 %	-8 %	-60 %	-38 %	-19 %	6 %
Tajikistan	104 %	187 %	289 %	132 %	130 %	217 %	254 %	364 %
Turkey	58 %	8 %	5 %	33 %	-22 %	1 %	7 %	13 %
Turkmenistan	62 %	-9 %	43 %	178 %	-14 %	136 %	141 %	174 %
Ukraine	-23 %	-6 %	-64 %	-20 %	-2 %	19 %	28 %	49 %
United Kingdom	-56 %	-51 %	-87 %	-7 %	-65 %	-28 %	-28 %	-22 %
Uzbekistan	-22 %	-41 %	-84 %	69 %	-38 %	53 %	69 %	119 %
Increase (number of countries)	**15**	**14**	**13**	**20**	**13**	**18**	**22**	**27**
Decrease (number of countries)	**45**	**46**	**47**	**34**	**47**	**42**	**38**	**28**

NH_3 emissions

NH_3 emissions have increased in the EMEP domain[17] by 31% compared with 2000 levels. Emissions have decreased in 34 countries or areas and increased in 20 (see Table 3.4). The strongest increases are shown for Turkmenistan (+178%) and Tajikistan (+132%).

CO emissions

The total decrease in emissions in the EMEP domain from 2000 to 2017 amounted to 9%. Compared with 2000 CO emissions have decreased in 47 countries or areas and increased in 13 (see Table 3.4), particularly in Kyrgyzstan (+509%).

[17] There is no NH_3 emissions for sea areas.

$PM_{2.5}$ emissions

$PM_{2.5}$ emissions in the EMEP domain increased by 10% compared with 2000 levels. Compared with the year 2000, $PM_{2.5}$ emissions have decreased in 42 countries or areas and increased in 18 countries or areas (see Table 3.4). The largest increase is seen in Kazakhstan (+235%), followed by Tajikistan (+217%).

PM_{10} emissions

The total emission increase of PM_{10} emissions from 2000 to 2017 in the EMEP domain is 17%. Compared with 2000, PM_{10} emissions decreased in 38 countries or areas and increased in 22 (see Table 3.4). As for $PM_{2.5}$, the strongest increase can be observed in Kazakhstan (+274%), followed by Tajikistan (+254%).

PM_{coarse} emissions

PM_{coarse} emissions are not reported by Parties but calculated as difference between PM_{10} and $PM_{2.5}$ emissions. PM_{coarse} emissions in the EMEP domain increased by 33% compared with 2000 levels. PM_{coarse} emissions decreased in 28 countries or areas and increased in 27 (see Table 3.4). The largest increases occur in Kazakhstan (+458%) and Tajikistan (+364%).

3.7 Contribution of individual sectors to total EMEP emissions

Figure 3.9 shows the contribution of each GNFR sector to the total emissions of individual air pollutants (SO_x, NO_x, CO, NMVOC, NH_3, $PM_{2.5}$ and PM_{coarse}). To provide a picture as complete as possible of the situation of the individual sectors to total EMEP emissions, data as used for the EMEP models (i.e. gap-filled data) were used for the calculations (see Section 3.8). Sea regions, North Africa and the remaining Asian areas were excluded for this analysis, as sectoral distributions are better reflected when only using country data.

It is evident that the combustion of fossil fuels is responsible for a significant part of all emissions. 47% of NO_x emissions are produced by transport (F, G, H, I) but 22% of NO_x also comes from large power plants (A).

NMVOC sources are distributed more evenly among the different sectors, such as 'E – Emissions from solvents' (25%), 'F – Road transport' (20%), 'D – Fugitive Emissions' (12%), 'B – Industry combustion' (11%), 'K – Manure management' (12%) and 'C – Other stationary combustion' (11%).

The main source of SO_x emissions are large point sources from combustion in energy and transformation industries (79%).

Ammonia arises mainly from agricultural activities (K and L), about 93%, while CO emissions originate primarily from 'F – Road transport' (37%) and 'C – Other stationary combustion' (29%).

The main sources of primary PM emissions are industry and other stationary combustion processes (up to 62%) and agriculture with a share of 12% to 38%.

Figure 3.10 illustrates the sector contribution for the sum of total emissions in the EMEP West region and the EMEP East region. The split between the EMEP West and EMEP East

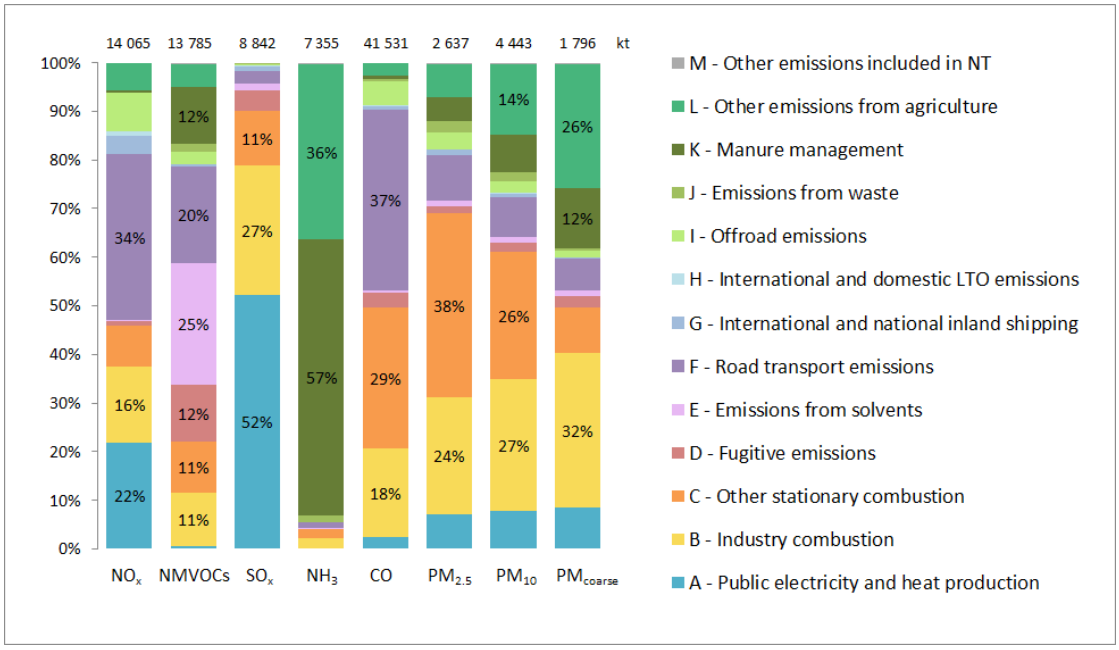

Figure 3.9: GNFR sector contribution to national total emissions in 2017 for the EMEP domain without sea regions, North Africa and remaining Asian areas (only percentages above 10% are shown).

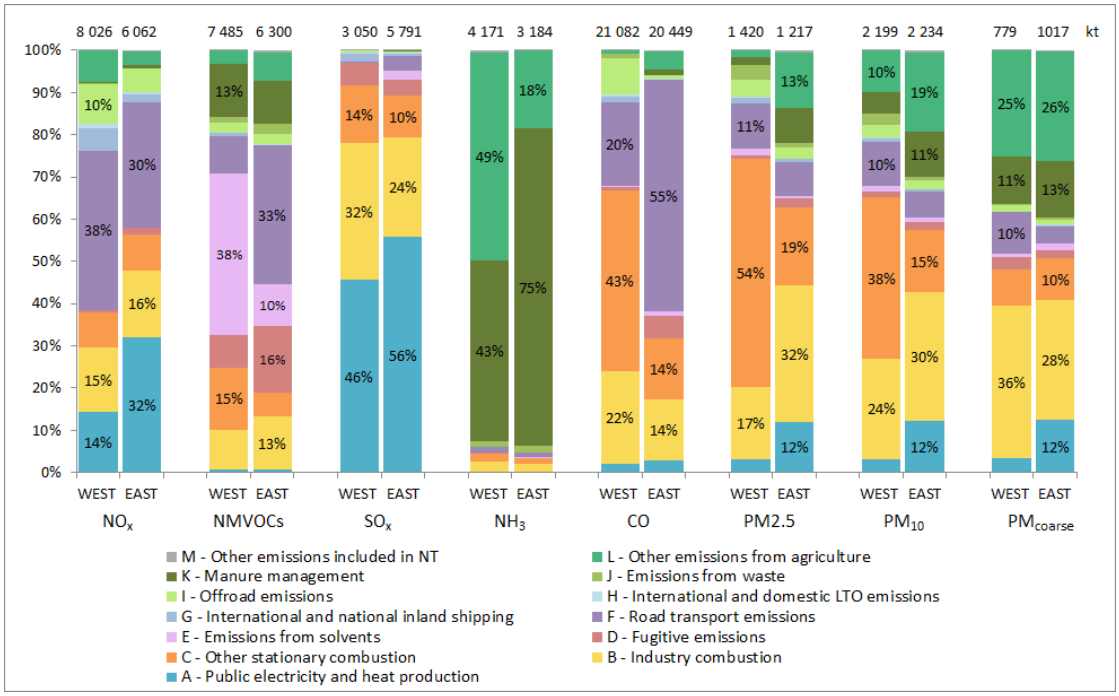

Figure 3.10: GNFR sector contribution to national total emissions in 2017 for the EMEP West and EMEP East areas (only percentages above 10% are visible).

regions is according to `http://www.ceip.at/emep_countries` (sea regions, North Africa and the remaining Asian areas are excluded). The comparison of both graphs highlights some significant differences between West and East.

For NO_x in the EMEP West region the most important sector is 'F – Road transport emissions' (38%), whereas in the EMEP East region the sector 'A – Public electricity and heat production' is of higher importance (32%).

For NMVOC in the EMEP West region the most relevant sector is 'E – Emissions from solvents' with a share of 38%. In the EMEP East region the same sector has a considerable lower share (10%), whilst the sector 'F – Road transport emissions' is of high importance (33%).

The main source of SO_x are 'A – Public electricity and heat production' and and 'B – Industry combustion'. These two sectors together contribute to 78% of SO_x emissions within the EMEP West and EMEP East areas.

The main source of NH_3 emissions for both EMEP West and EMEP East is the agricultural sectors (K and L) with 92% and 94%, respectively.

CO emissions arise mainly from 'F – Road transport emissions' (55%) in EMEP East. In the EMEP West region the main sector is 'C – Other stationary combustion' (43%).

For $PM_{2.5}$ and PM_{10} 'C – Other stationary combustion' holds a significant share of the total emissions in the EMEP West area (up to 54%), while for the EMEP East area the sector 'B – Industry combustion' is of higher importance.

3.8 Data sets for modelers 2019

Data used by CEIP were reported by the Parties to the LRTAP Convention as sectoral emissions (NFR14) and National Total emissions according to the UNECE guidelines for reporting emissions and projections data under the LRTAP Convention, Annex I (UNECE (2014)).

The sector data were aggregated to 13 GNFR sectors. In several cases, no data were submitted by the countries, or the reporting is not complete or contains errors. Before these emission data can be used by modelers, missing or erroneous information have to be filled in. To gap-fill those missing data, CEIP typically applies different gap-filling methods. The gap-filling procedure in 2019 is fully documented in a technical report (Technical report CEIP 01/2019), which can be downloaded from the CEIP website[18].

The countries where data were (partly) replaced in 2019 are Albania, Armenia, Azerbaijan, Belarus, Bosnia and Herzegovina, Bulgaria, Georgia, Kazakhstan, Kyrgyzstan, Lithuania, Malta, Monaco, the Republic of Moldova, the Russian Federation, Slovakia, North Macedonia, Turkey and the Ukraine.

After the gap-filling, sector emissions are spatially distributed over the EMEP grid. In 2019, data series for the years 1990 to 2017 were provided for the pollutants NO_x, NMVOCs, SO_x, NH_3, CO, $PM_{2.5}$, PM_{10} and PM_{coarse}[19].

In cases, where data are in all probability erroneous, these data are replaced. If data in such cases will not be replaced, it is likely to get a wrong picture in the gridded maps. In 2019, data of 18 countries were (partly) replaced, including replacements of $PM_{2.5}$ and PM_{10} because of negative values for PM_{coarse}. Data for PM_{coarse} are calculated as the difference between PM_{10} and $PM_{2.5}$. In all cases, in a later step the National Totals were corrected (e.g. by the sum of the sectors).

[18] http://www.ceip.at/ceip_reports/

[19] http://www.ceip.at/ms/ceip_home1/ceip_home/webdab_emepdatabase/emissions_emepmodels/

3.8.1 Reporting of gridded data

2017 was the first year with reporting obligation of gridded emissions in the grid resolution of 0.1°×0.1° longitude/latitude. Until June 2019, thirty of the 48 countries which are considered to be part of the EMEP area reported sectoral gridded emissions in this resolution. One country reported only gridded national total values (instead of sectoral data).

The majority of gridded sectoral emissions in 0.1°×0.1° longitude/latitude resolution have been reported for the year 2015 (29 countries). For the year 2017, gridded sectoral emissions have been reported by four countries.

Thirteen countries reported gridded emissions additionally for previous years (one country for the whole time series from 1980 to 2017; one country for the whole time series from 1990 to 2017; four countries for the years 1990, 1995, 2000, 2005 and 2010; one country for the years 1990, 2000, 2005 and 2010; one country for the years 2005 and 2010; one country for the year 2005; one country for the year 2010; and three countries for the year 2014).

Reported gridded sectoral data in 0.1°×0.1° longitude/latitude resolution, which can be used for the preparation of gridded emissions for modelers, covers less than 20% of the cells within the geographic EMEP area. For the remaining areas missing emissions are gap-filled and spatially distributed by expert estimates. Reported grid data can be downloaded from the CEIP website[20].

An overview of reported gridded data available in the years 2017 and 2019 is provided in Table 3.5, while an example map of the gap-filled and gridded NO_x emissions in 2017 in 0.1°×0.1° longitude-latitude resolution is shown in Figure 3.11.

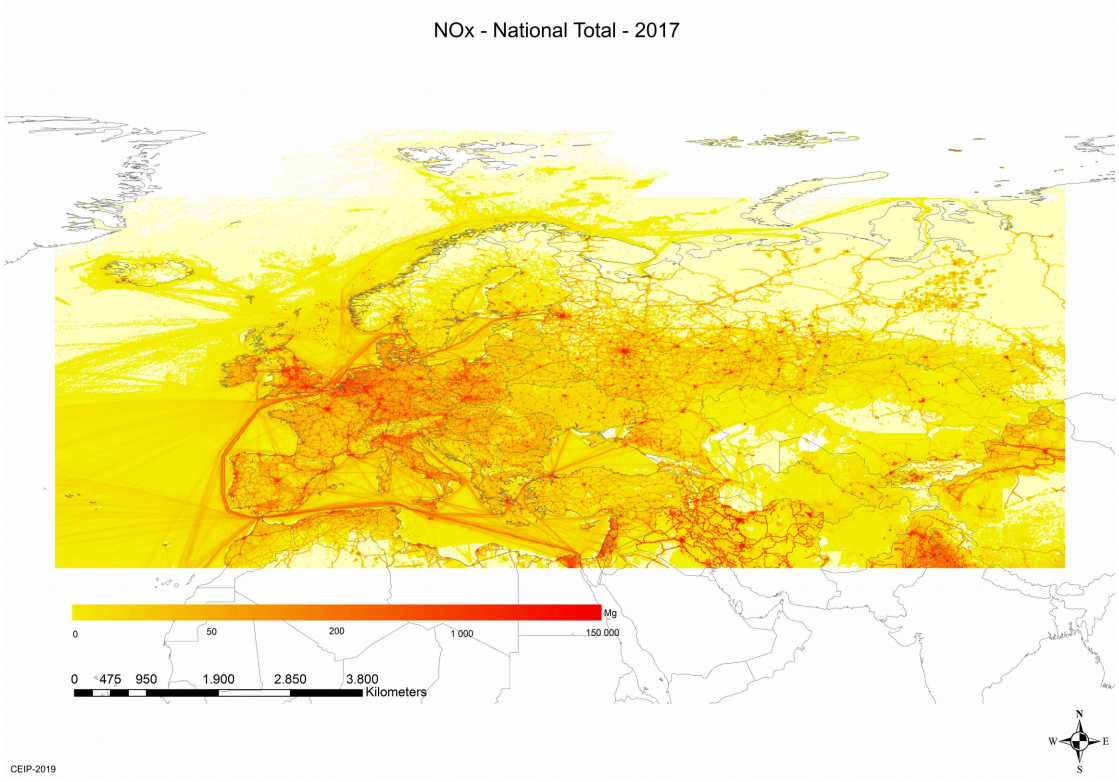

Figure 3.11: Visualized gap-filled and gridded NO_x emissions in 0.1°×0.1° long-lat resolution.

[20] http://www.ceip.at/status_reporting

Table 3.5: Reported gridded emissions available in the years 2017 and 2019.

Country	2017	2019	Comments
Austria	2015	2015	
Belgium	2015	2015	
Bulgaria	2015	2015	
Croatia	1990, 1995, 2000, 2005, 2010, 2015	1990, 1995, 2000, 2005, 2010, 2015	
Czechia	2015	2015	
Denmark	2015	2015	
Finland	2014, 2015	2014, 2015, 2016, 2017[a]	[a] Gridded data for 2014 and 2015 could not be used for the preparation of spatial distributed emission data.
France		2015	
North Macedonia		2015	
Georgia		2015	
Germany	1990, 1995, 2000, 2005, 2010, 2015	1990, 1995, 2000, 2005, 2010, 2015, 2017	
Greece		2015	
Hungary	2015[b]	2015	[b] The submission of gridded emissions from Hungary was too late to be considered for the preparation of gridded data for modelers in 2017
Ireland	2015	2015	
Italy		2015[c]	[c] Reported gridded data from Italy had to be completely replaced by CAMS and EDGAR proxies
Latvia	2015	2015	
Lithuania	2015[d]	2015[d]	[d] Lithuania reported gridded emissions only on national total level, which could not be used for the gridding, which is done on sectoral level
Luxembourg	2005, 2010, 2015	2005, 2010, 2015	
Malta		2016	
Monaco	2014, 2015	2014, 2015, 2016	
Netherlands		1990, 1995, 2000, 2005, 2010, 2015	
Norway	1990, 1995, 2000, 2005, 2010, 2015	1990, 1995, 2000, 2005, 2010, 2015	
Poland	2014, 2015	2014, 2015[e]	[e] For Poland, the spatial disaggregation of sector 'F – Road Transport' had to be replaced by CAMS proxies
Portugal	2015	2015[f]	[f] For Portugal, the spatial disaggregation of sector 'F – Road Transport' had to be replaced by CAMS proxies
Romania	2005	2005, 2015	
Slovakia	2015	2015	
Slovenia	2015	2015	
Spain	1990-2015	1990-2017[g]	[g] For Spain, the spatial disaggregation of sector 'F – Road Transport' had to be replaced by CAMS proxies
Sweden		1990, 2000, 2005, 2010, 2015	
Switzerland	1980-2015	1980-2017	
United Kingdom	2010, 2015	2010, 2015	

3.8.2 Time series from 1990 to 2017 in 0.1°×0.1° longitude/latitude resolution

For this year it was agreed with the modelers to perform gap-filling and gridding for the whole time series from 1990 to 2017 (for all main pollutants and PMs) in 0.1°×0.1° longitude/latitude resolution on GNFR sector level. In addition, gap-filling and gridding for BC was done

for the first time, but only for the year 2017 and not the whole time series.

The $0.1° \times 0.1°$ GNFR grids of NO_x, NMVOCs, SO_x, NH_3, CO, $PM_{2.5}$, PM_{10} and PM_{coarse} were gridded based on the gridding system developed by CEIP. The system is module based and uses as a first step reported gridded emission data for each country and sector where it is available and usable. If no reported gridded data in the $0.1° \times 0.1°$ longitude/latitude resolution is available, data from the Copernicus Atmospheric Monitoring Service (CAMS-81, CAMS-REG-AP-v2.2) and the Emission Database for Global Atmospheric Research (EDGAR) is used as proxy for spatial disaggregation, upgraded by point source information available under the European Pollutant Release and Transfer Register (E-PRTR). The system also uses data from FMI which is based on AIS tracking data for the spatial disaggregation of international shipping emissions.

Reported gridded data in $0.1° \times 0.1°$ longitude/latitude resolution was used from Austria, Belgium, Bulgaria, Croatia, Czech Republic, Denmark, France, Georgia, Germany, Greece, Hungary, Ireland, Latvia, Luxembourg, Malta, Monaco, Netherlands, North Macedonia, Norway, Poland, Portugal, Romania, Slovakia, Slovenia, Spain, Sweden, Switzerland and United Kingdom.

For Poland, Portugal and Spain the spatial disaggregation of sector 'F – Road Transport' had to be replaced by CAMS proxies. Reported gridded data from Italy had to be completely replaced by CAMS and EDGAR proxies.

3.8.3 International shipping

Under this category emissions from international shipping occurring in different European seas are accounted (European part of the North Atlantic, Baltic Sea, Black Sea, Mediterranean Sea and North Sea). International shipping emissions are not reported by Parties. Gridded emissions for the sea regions were calculated using the CAMS global shipping emission dataset (Granier et al. 2019) for the years 2000 to 2017 (Figure 3.12), developed by the Finish Meteorological Institute (FMI), and provided via ECCAD *CAMS_GLOB_SHIP* (ECCAD 2019). Shipping emissions from 1990 to 1999 were estimated using CAMS global shipping emissions for 2000 adjusted with trends for global shipping from EDGAR v.4.3.2 (JRC/PBL 2016).

Due to the selective implementation of the Sulphur Emission Control Areas (SECAs) on the North Sea and Baltic Sea only, the emission trends differ between those seas and the other seas.

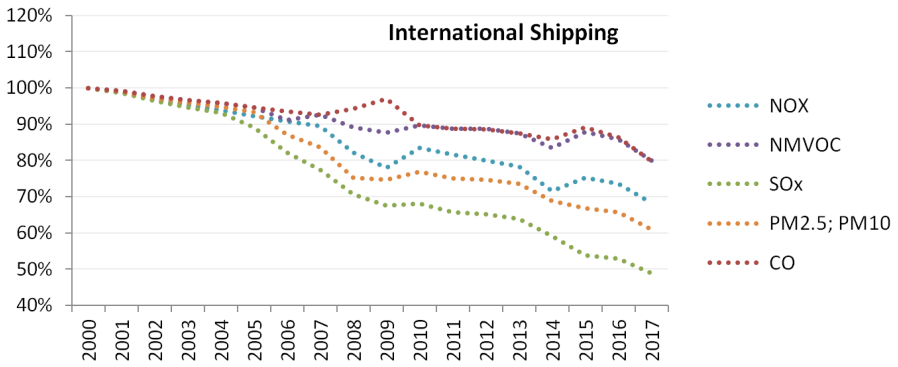

Figure 3.12: International shipping emission trends in the EMEP area, extracted from the CAMS global ship dataset developed by FMI, and provided via ECCAD (CAMS_GLOB_SHIP).

References

Baumgartner, J., Zhang, Y., Schauer, J. J., Huang, W., Wang, Y., and Ezzati, M.: Highway proximity and black carbon from cookstoves as a risk factor for higher blood pressure in rural China, PNAS 111, 36, 13 229–13 234, doi:doi:10.1073/pnas.1317176111, 2014.

Bond, T. C., Doherty, S. J., Fahey, D. W., Forster, P. M., Berntsen, T., DeAngelo, B. J., Flanner, M. G., Ghan, S., Kärcher, B., Koch, D., Kinne, S., Kondo, Y., Quinn, P. K., Sarofim, M. C., Schultz, M. G., Schulz, M., Venkataraman, C., Zhang, H., Zhang, S., Bellouin, N., Guttikunda, S. K., Hopke, P. K., Jacobson, M. Z., Kaiser, J. W., Klimont, Z., Lohmann, U., Schwarz, J. P., Shindell, D., Storelvmo, T., Warren, S. G., and Zender, C. S.: Bounding the role of black carbon in the climate system: A scientific assessment, J. Geophys. Res., 118, 5380–5552, doi:10.1002/jgrd.50171, 2013.

Denier van der Gon, H. A. C., Bergström, R., Fountoukis, C., Johansson, C., Pandis, S. N., Simpson, D., and Visschedijk, A. J. H.: Particulate emissions from residential wood combustion in Europe - revised estimates and an evaluation, Atmos. Chem. Physics, pp. 6503–6519, doi:doi:10.5194/acp-15-6503-2015, URL http://www.atmos-chem-phys.net/15/6503/2015/, 2015.

ECCAD: Emissions of atmospheric Compounds and Compilation of Ancillary Data, URL https://eccad.aeris-data.fr, 2019.

EMEP/EEA: EMEP/EEA air pollutant emission inventory guidebook - 2013, 12/2013, European Environment Agency, EEA, URL http://www.eea.europa.eu/publications/emep-eea-guidebook-2013, 2013.

EMEP/EEA: EMEP/EEA air pollutant emission inventory guidebook - 2016, 21/2016, European Environment Agency, EEA, URL http://www.eea.europa.eu/publications/emep-eea-guidebook-2016, 2016.

Granier, C., Darras, S., Denier van der Gon, H., Doubalova, J., Elguindi, N., Galle, B., Gauss, M., Guevara, M., Jalkanen, J.-P., Kuenen, J., Liousse, C., Quack, B., Simpson, D., and Sindelarova, K.: The Copernicus Atmosphere Monitoring Service global and regional emissions (April 2019 version), doi:10.24380/d0bn-kx16, URL https://atmosphere.copernicus.eu/sites/default/files/2019-06/cams_emissions_general_document_apr2019_v7.pdf, 2019.

Janssen, N. A. H., Gerlofs-Nijla, M. E., Lanki, T., Salonen, R. O., Cassee, F., Hoek, G., Fischer, P., Brunekreef, B., and Krzyzanowsi, M.: Health effects of black carbon, World Health Organization, pp. 1–96, URL http://www.euro.who.int/__data/assets/pdf_file/0004/162535/e96541.pdf, 2012.

JRC/PBL: Emission Database for Global Atmospheric Research (EDGAR), Global Emissions EDGAR v4.3.1., European Commission, Joint Research Centre (JRC)/Netherlands Environmental Assessment Agency (PBL), URL http://edgar.jrc.ec.europa.eu, 2016.

Pinterits, M., Ullrich, B., Gaisbauer, S., Mareckova, K., and Wankmüller, R.: Inventory review 2019. Review of emission data reported under the LRTAP Convention and NEC Directive.

Stage 1 and 2 review. Status of gridded and LPS data, EMEP/CEIP 4/2019, CEIP/EEA Vienna, 2019.

Sand, M., Berntsen, T. K., von Salzen, K., Flanner, M. G., Langner, J., and Victor, D. G.: Response of Arctic temperature to changes in emissions of short-lived climate forcers, Nat. Clim. Change, 6, 286–290, doi:10.1038/nclimate2880, 2016.

UNECE: Protocol to the 1979 Conventionon on long-range transboundary air pollution to abate acidification, eutrophication and ground-level ozone, Tech. rep., UNECE, URL http://www.unece.org/fileadmin/DAM/env/lrtap/fulltext/1999Multi.E.Amended.2005.pdf, 1999.

UNECE: Decision 2012/3: Adjustments under the Gothenburg Protocol to emission reduction commitments or to inventories for the purposes of comparing total national emissions with them, Tech. Rep. ECE/EB.AIR/111, UNECE, URL http://www.unece.org/fileadmin/DAM/env/documents/2013/air/ECE_EB.AIR_111_Add.1__ENG_DECISION_3.pdf, 2012.

UNECE: Guidelines for reporting emission data under the Convention on Long-range Transboundary Air Pollution, Tech. Rep. ECE/EB.AIR/130, UNECE, URL http://www.ceip.at/fileadmin/inhalte/emep/2014_Guidelines/ece.eb.air.125_ADVANCE_VERSION_reporting_guidelines_2013.pdf, 2014.

Wang, R., Balkanski, Y., Boucher, O., Ciais, P., Schuster, G. L., Chevallier, F., Samset, B. H., Liu, J., Piao, S., Valari, M., and Tao, S.: Estimation of global black carbon direct radiative forcing and its uncertainty constrained by observations., J. Geophys. Res. Atmos., 121, 5948–5971, doi:10.1002/2015JD024326, URL https://agupubs.onlinelibrary.wiley.com/doi/epdf/10.1002/2015JD024326, 2016.

CHAPTER 4

The EMEP interface for visualization of trends

Augustin Mortier, Svetlana Tsyro and Hilde Fagerli

In EMEP Status Report 1/2018 (2018), we introduced a new trend interface under development at MSC-W. The trend interface is designed for visualization of the long-term modelling results at all EMEP sites that have ever reported observations to CCC.

In this chapter, we describe further developments of the interface since last year. The most important new functionalities are the inclusion of EMEP observations and model evaluation statistics against the observations. The interface has been extended to include more species (i.e. ozone). Furthermore, the impacts from different emission sectors on PM_{10} and $PM_{2.5}$ concentrations are vizualised and a number of other technical facilities for data representation and analysis are introduced.

4.1 Data used in the EMEP trends interface

4.1.1 EMEP MSC-W model calculations

The EMEP MSC-W model data for 2000-2016 is documented in EMEP Status Report 1/2018 (2018). The calculations were performed with the model version v4.17a (applied for 2018 reporting) and used a consistent set of $0.1^\circ \times 0.1^\circ$ EMEP emissions.

The impacts of different emission sectors on PM_{10} and $PM_{2.5}$ concentrations for the period 2000-2016 were derived from a series of model runs, in which sector emissions were individually reduced by 15%. The following sectors are considered: traffic, industry, residential heating and agriculture. In addition, the contributions to PM_{10} and $PM_{2.5}$ from natural sources (i.e. sea spray and windblown dust) are distinguished.

4.1.2 EMEP observations

The EMEP observations included in the EMEP trends interface is a direct extract from the NILU/CCC EBAS system, and no further quality control of the data has been performed.

4.2 EMEP trends interface

In EMEP Status Report 1/2018 (2018) an interface dedicated to the visualization of the EMEP trends computation was presented. Together with the more general trends interface on which it is based (`http://aerocom-trends.met.no`), this interface has been developed during the past year. It is now available at the following address: `http://aerocom.met.no/trends/EMEP/`.

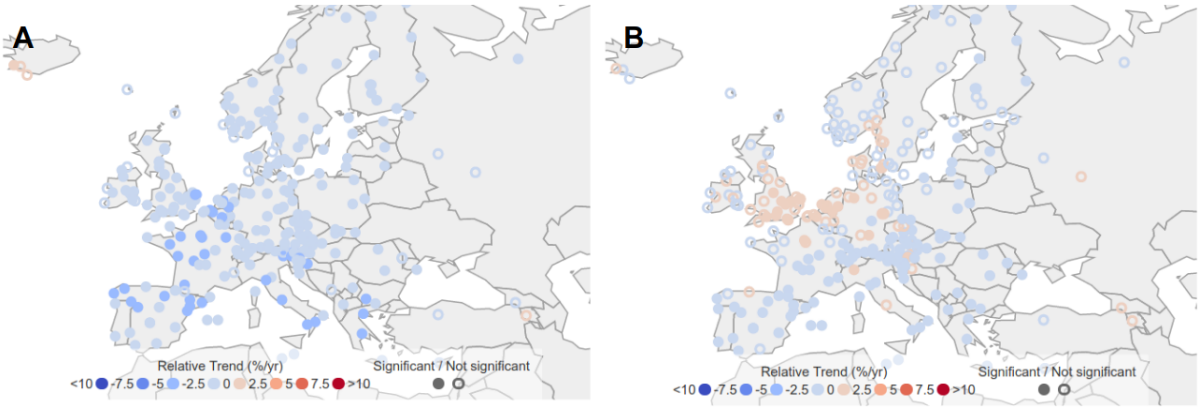

Figure 4.1: European PM_{10} (A) and O_3 (B) trends at EMEP stations between 2000 and 2016.

The new version of the overall map, as illustrated in Figure 4.1, provides a better visualization of the trends computed at each EMEP station. The combination of the different markers style together with the gradual color-scale allows to distinguish significant/non-significant, positive/negative, and strong/weak trends. The trends computation remains similar. First, the significance of the linear trend is determined with the Mann-Kendall test. The trends associated with a p-value smaller than 0.1 are considered as significant. The slope is then computed with the Theil-Sen slope, which is less sensitive to the outliers than the classic linear regression method. The trend is provided as a relative trend (in percent per year) with respect to the first year of the series. In addition to PM_{10}, the trends are now available for $PM_{2.5}$ and O_3.

The time series for PM_{10}, $PM_{2.5}$ and O_3 are available for each of the individual stations. An example for PM10 at Birkenes is shown in Figure 4.2. The dynamic charts allow the exploration of daily and monthly data (upper graph in Figure 4.2) and also provide the yearly averages (lower graph in Figure 4.2).

For PM_{10} and $PM_{2.5}$ the tab navigation system allows accessing the bar-graphs showing the chemical composition (example for PM_{10} at Birkenes in Figure 4.3) and the source attribution (Figure 4.4). The latter shows the relative contribution both from anthropogenic sources (presently from agriculture, residential heating, industry and traffic) and from the natural sources (marine sea salt and mineral dust).

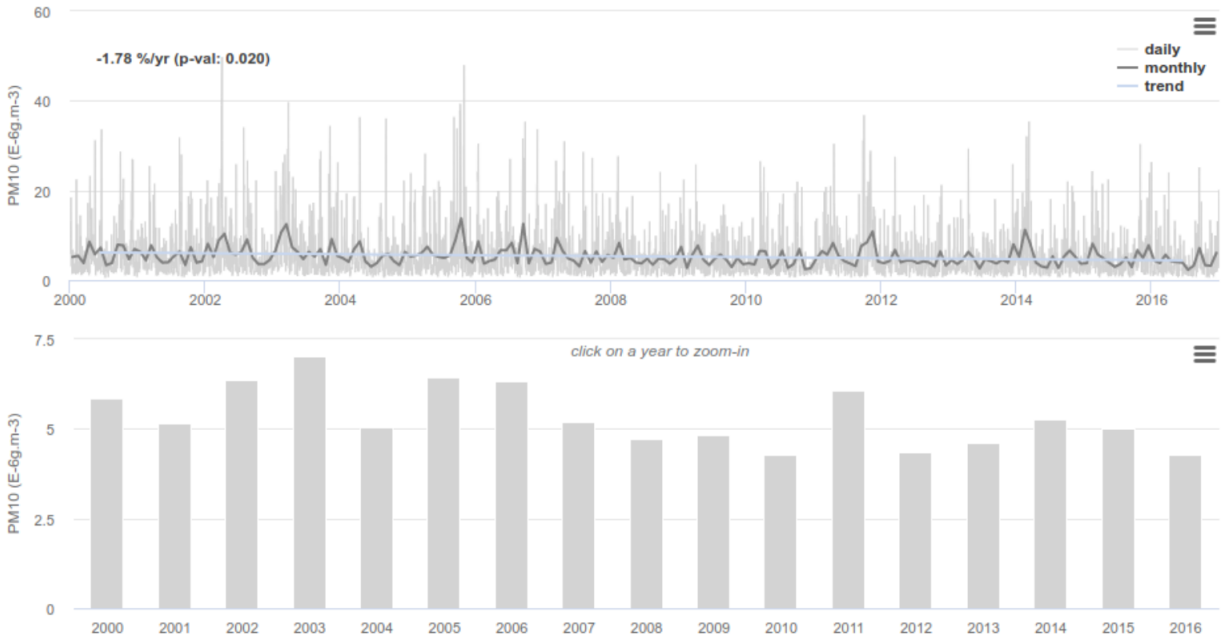

Figure 4.2: Daily and monthly total PM_{10} concentration at Birkenes (South of Norway) between 2000 and 2016.

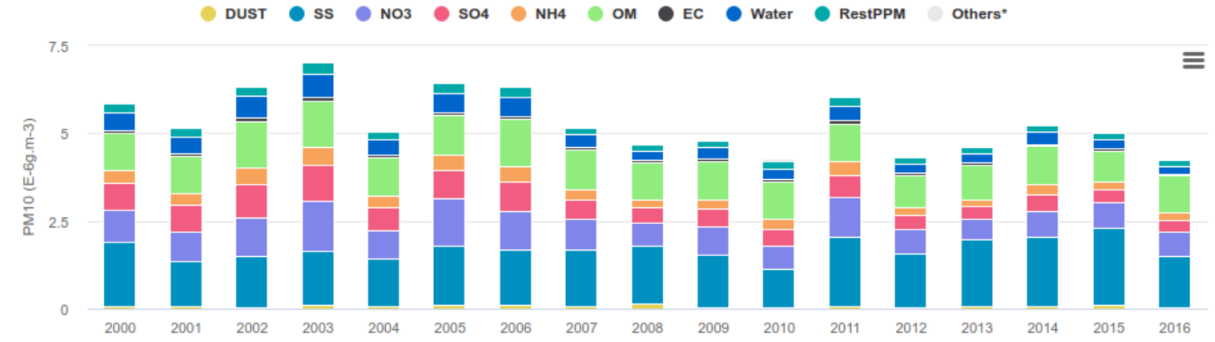

Figure 4.3: Chemical species contributing to total PM_{10} at Birkenes (yearly averages) from 2000 to 2016.

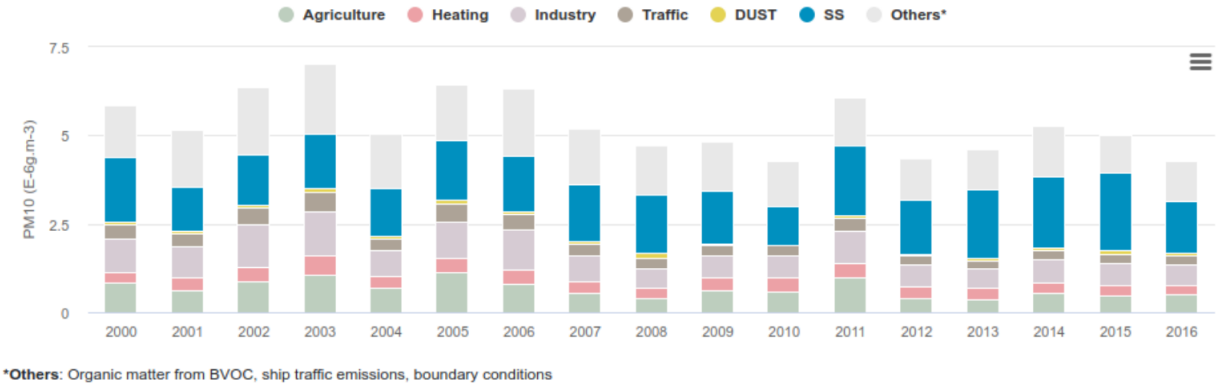

Figure 4.4: Sectors contributing to total PM_{10} at Birkenes (yearly averages) from 2000 to 2016.

For each of the parameters currently available in the interface (PM_{10}, $PM_{2.5}$ and O_3), all available observations are provided at EMEP stations. Pressing "Observations" button allows displaying model calculated and observed time series as shown for PM_{10} at Birkenes in Figure 4.5. A scatter plot is also computed online with some basic statistics, such as the regression line and the correlation coefficient (Figure 4.5 B).

Furthermore in the time series plots, it is possible to 'click' on and off the legends, e.g. choosing only daily or monthly comparisons, or the individual species or sectors. The modelled annual mean trend at the selected site is written in the upper left corner. Zooming into a chosen timeperiods in the time series plot facilates investigating, e.g. the correspondence between model and observations at different time scales. Also hovering (moving the mouse) over time series plots and bar charts give detailed information per day/month/year.

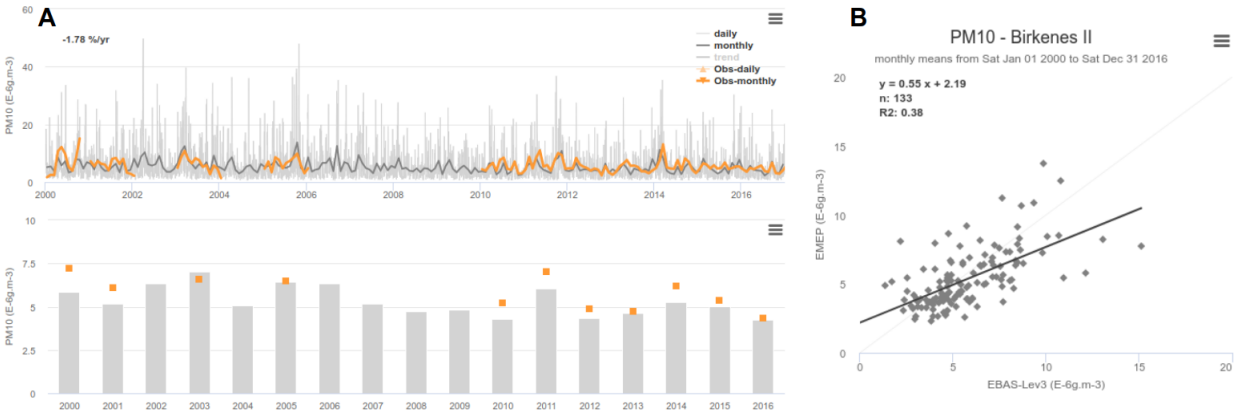

Figure 4.5: Time series of model (gray) and observation (orange) PM_{10} concentration at different time scales (A) at Birkenes. Scatterplot of monthly modelled vs observed PM_{10} concentration at Birkenes between 2000 and 2016 (B).

References

EMEP Status Report 1/2018: Transboundary particulate matter, photo-oxidants, acidifying and eutrophying components, EMEP MSC-W & CCC & CEIP, Norwegian Meteorological Institute (EMEP/MSC-W), Oslo, Norway, 2018.

Part II

Research Activities

CHAPTER 5

Condensable organics; issues and implications for EMEP calculations and source-receptor matrices

David Simpson, Robert Bergström, Hugo A.C. Denier van der Gon, Jeroen J.P. Kuenen, Sabine Schindlbacher and Antoon J.H. Visschedijk

5.1 Introduction

Condensable, or low and semi-volatile organic compounds (loosely denoted SVOC hereafter, see Table 5.1) are a class of compounds of low volatility that may exist in equilibrium between the gas ($SVOC_{(g)}$) and particle (condensed, $SVOC_{(pm)}$) phase. Such compounds may or may not be included in current emission inventories for fine particulate matter ($PM_{2.5}$), and PM_{10}, with their treatment varying from country to country and from one emissions source to another. The treatment of these compounds, first highlighted by Robinson et al. (2007), and for the EMEP situation in Bergström et al. (2012), Denier van der Gon et al. (2015) and Simpson and Denier van der Gon (2015), has significant implications for the modelling of organic aerosol and therefore PM levels in the ambient atmosphere. These problems with the organic carbon (OC) fraction of PM inventories are interlinked with those of elemental carbon (EC) through the common use of OC/EC ratios to derive one component from the other, and to non-methane volatile organic compounds (NMVOC) as discussed further below.

As an example, the emission factors (EFs) used for national estimates of wood-burning in Norwegian emission estimates are many times those used by Sweden, even for the same type of wood and burner (Sternhufvud et al. 2004, Genberg et al. 2013). Differences are mainly caused by the handling of condensable compounds (loosely referred to hereafter as condensables). Also in the EMEP/EEA Guidebook the condensable fraction is not consistently included or excluded in the emission factors.

Over the last years, scientific studies using modelled OC, EC and PM concentrations and comparing those with measured values (Simpson et al. 2007, Bergström et al. 2012, Denier van der Gon et al. 2015, Genberg et al. 2011, 2013) have shown rather strong discrepancies,

Table 5.1: Acronyms

OA, OM	Organic aerosol, organic matter. Used interchangably here for any condensed organic matter.
OC	Organic carbon, usually refers only to the condensed phase
BC, EC	Black, elemental carbon
VOC	Volatile organic compound
NMVOC	non-methane VOC
C_i^*	Effective saturation concentration at 298K. A measure of volatilty.
SVOC	Semi-volatile organic compounds. Here we use the term to cover any compound that can condense into OA in conditions ranging from exhaust plume to ambient. In terms of C_i^*, we include compounds here with C_i^* up to 320 μg m^{-3} .
IVOC	Intermediate-volatilty compounds. These are gas-phase upon emission, but are readily oxidised with the potential to form SOA. C_i^* between 320 – 3.2$\times 10^6$ μg m^{-3} .
POA, POM	Primary emissions of OA, OM
NVPOA	non-volatile POA
SVOA	Semi-volatile OA; the condensed part of SVOC
SOA	Secondary OA, formed from oxidation of NMVOC
$SVOC_{(g)}$, $SVOC_{(pm)}$	gas and particle phases of SVOC
EF	Emission factor

suggesting that some emission sources could be missing from the existing inventories. Condensables are one of the key factors in this story. Modelling and use of expert-emissions strongly suggests that PM emissions in Europe are currently underestimated, and condensables from the residential combustion sector, in particular wood burning, are a key source for these missing emissions.

A note prepared by TFEIP/TFMM (2018) on this issue asked countries to start reporting their procedures regarding condensables. Therefore, Parties were asked to include a table with information on the inclusion of the condensable component in PM_{10} and $PM_{2.5}$ emission factors for their reporting under the CLRTAP convention in 2019. The results are presented in Sect. 3.3, but we can summarise here to say that the results are very mixed. For example, of the thirteen Parties that provided information for the '1A4bi Residential: Stationary' sector by the end of April 2019, three parties reported the condensable component to be included and three Parties to be excluded. The other Parties reported 'unknown' or 'partially included'.

As 2019 was the first year in which Parties were asked to provide such information it is expected that the reporting will improve over the coming years, with more parties reporting, and with a higher quality of the reported information.

We can identify several main problems:

1. As noted above, the emission factors used for POA are estimated in very different ways

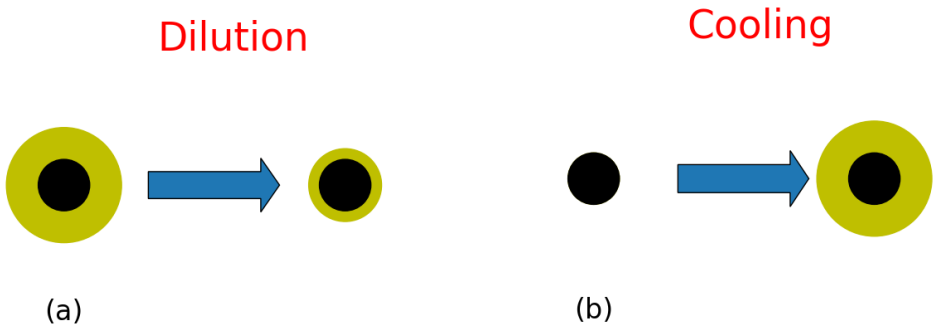

Figure 5.1: Sketch (very simplified!) of condensable issues, in which POM measured in or near the source can either lose or gain mass, depending on the importance of dilution or cooling. Case (a) illustrates the case where high gaseous loading of SVOC in the measurement device promotes condensation to form a substantial liquid phase SVOC (green) around the more solid core (black). When such an exhaust plume is diluted to ambient conditions, much of this condensed SVOC will evaporate, leaving a smaller mass of SVOC in the particle phase. Case (b) on the other hand represents a situation with very high temperatures at the point of measurement, in which essentially only the solid core is present. Upon cooling SVOC from the surrounding exhaust gases condense onto this core.

between countries, and across emission sectors. These problems can be illustrated with a simple sketch, Fig. 5.1, showing two simplified examples for (a) the evaporation issue, and (b) the condensation issue. Countries may report just the solid cores of (a) or (b) as PM emissions, or they may report the mixture of condensed SVOC and solid core of (a) as PM emissions. Actually even within one country, different methods may be used for e.g. residential wood combustion or traffic emissions.

These problems arise from the fact that measurement devices sample PM emissions at very different conditions to those applicable once the plume has diluted into ambient air (Donahue et al. 2006, Nussbaumer et al. 2008). Measured EFs may be an overestimate or underestimate of particulate matter emissions to the environment. The magnitude and even sign of the error depends on the measurement methodology used. Such methodologies are not prescribed in current inventories.

2. As noted by Donahue et al. (2006), Robinson et al. (2007) and Grieshop et al. (2009) for the US, where POA emission factors already include condensables, a large fraction of these (more than half) may evaporate after dilution to atmospheric conditions (cf Fig. 5.1, case (a)). The initial effect of this evaporation is to lower the ambient PM levels below those that would be obtained if the POA was inert. The gaseous SVOC may however partition to aerosol, especially after one or more oxidation reactions.

   Although such 'evaporation+SVOC oxidation' effects, based upon the US studies, have been included in many OA modelling studies (e.g. Robinson et al. 2007, Lane et al. 2008, Bergström et al. 2012), it should be noted that their importance in Europe is unclear. In the US, diesel vehicle emissions are mainly from heavy duty vehicles and using low dilutions (by a factor 10) to measure emissions. European studies tend to use different measurement protocols for emissions to the US, and Europe also has different type vehicles. Of the 49 parties (includes EU-28) that lie within the EMEP region 42

have submitted an inventory and an inventory report. Of these 42 parties 26 parties use or mainly use the COPERT model (https://www.emisia.com/utilities/copert/, Ntziachristos and Samaras 2018) for the calculation of their road transport emissions. In this model, PM mass emission factors correspond to primary emissions from road traffic and not formation of secondary aerosol from chemical reactions in the atmosphere minutes or hours after release. The measurement procedure regulated for vehicle exhaust PM mass characterisation requires that samples are taken at a temperature lower than 52°C. At this temperature, PM contains a large fraction of condensable species, although the COPERT documentation does not specify any particular dilution conditions. In any case, PM mass emission factors in COPERT are considered to include both filterable and condensable material.

Procedures for other emitters vary widely. For example, industrial PM emission methodologies often explicitly exclude condensable PM and require measurements in the stack, often at temperatures of 300 °C, whereas road transport exhaust measurements often involve cooling to ca. 50 °C. Murphy et al. (2014) discusses various approaches and problems associated with the methods used to report PM and NMVOC in the United States. Of course, countries may follow their own protocols, and methods may differ from source to source. While each of these protocols may have particular merits it is clear that countries report very different type of quantity (apples and oranges!) under the umbrella name of $PM_{2.5}$.

3. The source-receptor (SR) matrices which are an important output of the EMEP model (e.g. Fagerli et al. 2018) treat all PM emissions equally, and indeed currently assume that all official $PM_{2.5}$ emissions are inert. This is equivalent to assuming that all emissions are basically representing the solid phase of Fig. 5.1, or that any included condensables are inert.

   If allowance is made for SVOC (and/or IVOC, see below) the changes calculated for $PM_{2.5}$ might differ substantially, and hence the impact of emission control measures might also differ significantly from today's calculations. Examples of this issue are presented later in this chapter.

4. Until recently, countries only reported total $PM_{2.5}$ and PM_{10} to EMEP, which left it up to expert estimates such as those made at TNO to establish the relative fractions of elemental carbon (EC), POA, and other primary emissions within these PM totals. Often one associates certain POA/EC ratios with specific sources. However, since we don't know how POA is defined, use of these ratios can result in EC as well as POA being set incorrectly in the modelling inventory. Although a start has been made on collecting specific information on national BC emissions through the EMEP system (c.f. Chap. 3, Sect. 6.6), these data are not yet fully evaluated or understood (c.f. Sect.6.6).

5. Robinson et al. (2007) also noted that inventories miss a class of 'intermediate'-volatility compounds (IVOC), which consist of compounds (e.g. C15 alkanes, heavy aromatics) that are too volatile to be included as POA, but which are not usually measured or included among the NMVOC compounds reported in national inventories. They estimated that for North America, the sum of NVPOA, SVOC and IVOC should be about 2.5 times the official POA emission estimate. As pointed out by Ots et al. (2016) though, the assumption of the factor 2.5 is derived from American work from the 1990s, and

is in many ways highly uncertain. For example, measurements made in London found IVOC emissions from vehicles to be ten(!) times higher than NMVOC emissions from vehicles, with significant implications for the sources of $PM_{2.5}$ in London (Ots et al. 2016). In general, it is possible that even if the amount of IVOC is low compared to total NMVOC, IVOC oxidation might be a significant source of $PM_{2.5}$.

6. Although the question is often phrased: 'are condensables included or not', the answer if 'yes' tells nothing about how the amount or type of condensables was derived or defined. Further, although the TFEIP/TFMM (2018) note further suggested that the EMEP/EEA Guidebook should be updated in 2019 to include condensables for wood and coal combustion, no suggestions were made with regard to other potentially important sources such as vehicles, and no definition of the amount of condensables to be included was offered either.

The background to these statements follows from the large (and continuing) reassessment of the composition of POA emissions and the role of associated NMVOC for SOA modelling which followed the work of especially Robinson et al. (2007) and Donahue et al. (2006), as well as recent European work exploring the uncertainty of emissions from residential wood combustion (Denier van der Gon et al. 2015, Genberg et al. 2013) and road traffic (Kim et al. 2016, Ots et al. 2016). Here we focus mainly on the 'condensables' (rather than IVOC) and PM problems, which encompasses items (1)–(3) above, and also (4) to some extent.

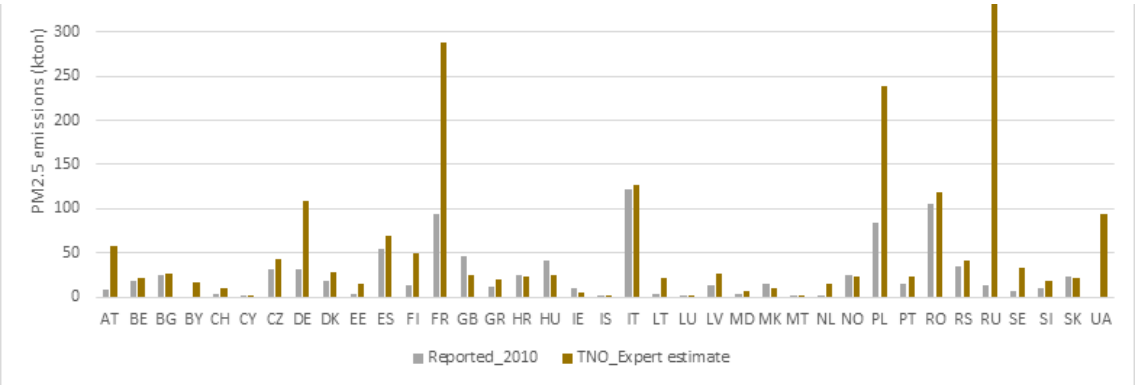

Figure 5.2: Reported $PM_{2.5}$ emissions from small-scale combustion for 2010 compared to TNO expert estimate. Updated from TFEIP/TFMM (2018).

Figure 5.2 illustrates the differences between officially reported emissions of $PM_{2.5}$ from small-scale combustion for 2010, and expert estimates made by TNO which include condensables in a consistent way across all countries. As can be seen, for some countries (e.g. NO, DK) the two estimates are comparable, but for others (e.g. FI, SE) the expert estimate is far higher than the reported emissions. Such inconsistencies pose grave problems for the modeling of $PM_{2.5}$ and for any analysis of emission control strategies or cost-benefit analysis. In the worst case these problems might lead to wrong priorities of measures.

5.1.1 Implications for EMEP modelling

The complex emissions processing discussed above presents a dilemma for EMEP modelling. On the one hand, the EMEP model should use 'official' estimates as far as possible, with

Parties to the Convention defining PM versus NMVOC emissions as they see fit. On the other hand, the science issues suggest that these official emissions, and their use in models, are likely wrong (Robinson et al. 2007, Denier van der Gon et al. 2015). Further approaches such as those suggested by Robinson et al. (2007), Jathar et al. (2014), Ots et al. (2016) add NMVOC compounds (IVOC, SVOC) which are likely not captured by either the official PM or NMVOC emissions, and which are essentially a (well motivated!) 'invention' of new sources of carbon and hence PM.

At the time of writing, and for EMEP model runs designed to support policy, we currently accept national $PM_{2.5}$ and NMVOC estimates as reported by the countries, and treat the POA fraction of $PM_{2.5}$ as inert (non-volatile). There are two main reasons for this choice: (i) the volatility distribution of POA and associated SVOC and IVOC compounds is poorly known; the amount of SVOC+IVOC emissions is probably substantial, but so far we have only a very limited number of (mainly American) studies with which to estimate this contribution (e.g. Shrivastava et al. 2008, Grieshop et al. 2009, Presto et al. 2012, Ciarelli et al. 2017); (ii) official European emission inventories used for policy modelling consist of PM compounds which are assumed to be inert, as well as NMVOC emissions. No consideration of volatility is made in either the PM or NMVOC inventories.

In research applications of the EMEP model (Bergström et al. 2012, Bergström et al. 2014, Denier van der Gon et al. 2015) we have used volatile POA and added IVOC emissions, and the two approaches have been compared in Bergström et al. (2012) and Simpson et al. (2012) (Supplementary). Briefly, considering some of the POA to be semi-volatile results in lower concentrations of OA near the source (since some POA is allowed to evaporate), and 10-20% higher levels of OM in other European areas, as a result of the assumed SVOC compounds being oxidised to ASOA.

5.2 Methods

In this work we have made use of both new emission inventories from TNO (Sect. 5.2.1) and new schemes (Sect. 5.2.2) for treating POM and secondary organic aerosol (SOA) in the EMEP model. The new model version is still under-development, but is believed to have a more robust treatment of organic aerosol than earlier EMEP efforts.

5.2.1 Emissions

Table 5.2 summarises the two emission inventories used in this work, and here we briefly outline their background. The CAMS-REG-AP_2015 v1.1 for 2015, which we refer hereafter to as 'Ref1', is based upon data reported to EMEP, and thus represents the emission inventory normally used in EMEP modelling. As part of other research projects including CAMS-71, TNO has produced a 'Ref2' inventory, with a best-estimate for each country of the POM when condensable SVOC are included. It should be noted that here we make use only of the SNAP-2 changes in POM/SVOC (from residential wood combustion and coal), not changes in other compounds or sectors.

An illustration of the differences between Ref1 and Ref2 for the selected countries is shown in Fig. 5.3. This figure also makes it clear that Ref1 and Ref2 differ in all components, not just OM. The reason behind this is different assumptions in the split of PM for different

Table 5.2: Notation for emissions scenarios used in this report, and link to CAMS/TNO nomenclature

Scenario (this report)	Source
Ref1	CAMS-REG-AP_2015 v1.1; Emissions are based on national reported emissions to EMEP as of 2017. The data set is made by TNO in the framework of the Copernicus Atmospheric Monitoring Service (CAMS) and released early 2018. Data provided by TNO.
Ref2	Based on the Ref1 year 2015 emissions but the PM emissions from the Residential combustion sector (SNAP2) are replaced by a bottom-up TNO estimate using emission factors including condensable PM as defined in Denier van der Gon et al. (2015). Data provided by TNO.

sources. For example, EC/OM ratios vary markedly from appliance to appliance, and differences in how countries define POM (e.g. with or without condensables) can affect assumed EC emissions since usually the same ratio is applied across all countries for the same appliance type. Since the reported data do not contain information on the appliance types nor on the definition of POM used, only a generic PM split could be applied which is based on the situation with solid PM only. In this Norwegian case, different assumptions on the appliance-type composition were made in Ref1 and Ref2. Thus, for Norway, one can see that despite

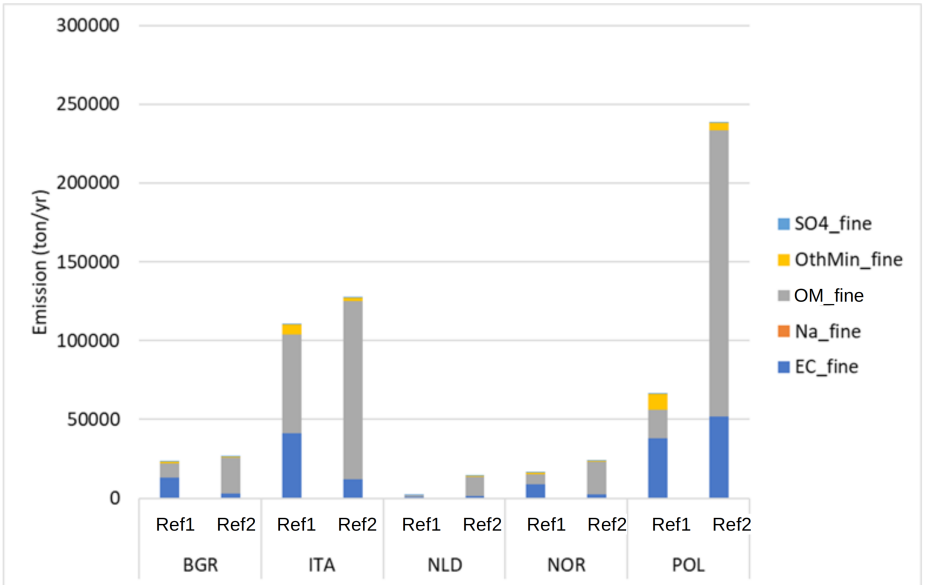

Figure 5.3: $PM_{2.5}$ emissions in 2015 for residential combustion (SNAP2) under the Ref1 and Ref2 scenarios for selected countries broken down by its components using a generic European PM split for Ref1 and source and appliance specific PM split for Ref2.

rather similar emission levels of $PM_{2.5}$, the EC/OM ratios in Ref1 are far higher than in Ref2. Conversely, POM emissions from Ref2 are far higher than from Ref1.

5.2.2 Model setup

Previous research work with S/IVOC in the EMEP and several other models (e.g. Bergström et al., 2012) has been based upon these well-used American estimates of the relation between primary organic matter emissions (POM) and S/IVOC, together with assumptions concerning the distribution of S/IVOC in terms of volatility (in the so-called volatility-basis-set, or VBS framework).

We implemented four 'scenarios' in the EMEP model and emissions for testing:

a) Ref1-NVPOA – uses POA emissions as inert species, with SOA formation from anthropogenic and biogenic VOC using the VBS scheme following standard EMEP model practice (Simpson et al. 2012). This scenario is the one that most closely matches current EMEP emissions and assumptions.

b) Ref1-SVPOA – as (a), but POA is now treated as a mixture of solids and SVOC, with the latter able to evaporate/condense and to age, following the 1.5D VBS framework (see below). This scenario, allowing some POA emissions to be volatile, would be plausible if the emissions reported by countries now already included condensables.

c) Ref2-NVPOA - now uses the bottom-up estimate of POA emissions, which we treat as inert. This scenario presents some kind of upper-limit, in that we treat all POA as non-volatile even though we know that the POA emissions contain SVOC.

d) Ref2-SVPOA – as (c), but now the SVPOA is able to evaporate/condense and to age, also following the 1.5D VBS framework as in Ref1-SVPOA. This scenario represents one of the two best-estimates, in that we have a consistent inclusion of SVOC across all countries, and the model handles these as a mixture of NVPOA and SVOC.

The primary organic aerosol (POA) emissions were treated either as inert NVPOA (runs Ref1-NVPOA, Ref2-NVPOA), or as semi-volatile, and subject to evaporation and oxidation (in the gas phase). A new scheme was introduced into the EMEP model for handling these emissions: the "1.5-dimensional" volatility basis set (VBS), based on Koo et al. (2014), slightly extended to include semi-volatile organic compound (SVOC) emissions in the C_i^* $= 10^4$ μg m^{-3} bin. The 1.5D VBS scheme includes two different basis sets for primary emission – one hydrocarbon like, for fossil fuel based emissions, and a more oxidised set for emissions from biomass burning.

The assumed volatility distribution of POA from biomass combustion (both residential biofuel combustion and vegetation fires) was taken from May et al. (2013). The volatility distribution for all other anthropogenic POA emissions was based on the SVOC volatility distribution suggested by Robinson et al. (2007), adapted to the 1.5D VBS scheme. For all POA the VBS-bins with $C^* < 1$ μg m^{-3} were treated as non-volatile in the model.

We also tested adding additional SVOC compounds. For residential biomass combustion the SVOC emissions were scaled by a factor 1.4 compared to POM (loosely based on an assumed dilution tunnel temperature of 35 °C and OA concentration of 5 mg m^{-3}). All other emission sectors were scaled by the factor 1.6 (as by Hodzic et al. 2016, based on Jathar et al. 2014).

For secondary organic aerosol (SOA) formed in the atmosphere by oxidation of volatile organic compounds (VOC), we have also introduced a new scheme into the EMEP model. The 6-bin VBS-scheme suggested by Hodzic et al. (2016) was used for SOA formation from biogenic VOC (monoterpenes and isoprene), aromatic VOC (from anthropogenic and open vegetation fire emissions). For the monoterpenes we assume that the SOA yield is the same from oxidation by ozone and nitrate radicals as for OH radicals. SOA from biogenic emissions of sesquiterpenes were treated as non-volatile in the model.

5.2.3 Source-receptor calculations

Similar to Fagerli et al. (2018) we performed model runs in which all emissions from five example countries were reduced by 15% in turn, and the model used to calculate the differences in pollutant concentrations arising from these reductions. In this report we will focus only on the changes in $PM_{2.5}$ concentrations, since these are most directly affected by the condensables issues. The five example emitter countries are Bulgaria (BG), Italy (IT), The Netherlands (NL), Norway (NO) and Poland (PL). These countries provide a variation in terms of geographical location and emission characteristics.

5.3 Results

5.3.1 Comparison with observations

In order to both evaluate the model and to illustrate the impacts of the emissions changes, we have compared modelled OC concentrations against observations from the EMEP EC/OC network (ebas.nilu.no). Figures 5.4-5.5 illustrate results from the Ref1-NVPOA and Ref2-SVPOA cases for six sites. In all cases the Ref2-SVPOA runs has significantly higher OC concentrations, and for most sites this produces much better results in terms of bias than the Ref1-NVPOA runs. The unfortunate exceptions to this are the Norwegian sites, Birkenes and Hurdal, where the Ref2-SVPOA case over-estimates the observed OC. The reason for this difference is not known, but the Norwegian sites have much lower OC concentrations, and also rather different seasonal patterns to other sites in that they display no increase in OC concentrations during winter time. (The lack of seasonal cycle is likely due to counterbalancing contributions from wintertime residential and summertime biomass-burning and biogenic SOA: pers.comm., Karl Espen Yttri, NILU). The most polluted sites, Ispra (Italy) and Diablo Gora (Poland), show substantial improvements in bias with the Ref2-SVPOA results, and the latter site also shows a very strong increase in correlation (from 0.44 to 0.81).

Figure 5.6 shows the scatter plots for modelled versus observed OC from all EMEP EC/OC sites with data for this period, but now for four model-emission cases. Overall, the Ref2 simulations (either with NVPOA or SVPOA) show substantial improvements (in terms of slope and correlation) compared to the Ref1 cases. The Ref2-SVPOA case provides best overall correlation, though the Ref2-NVPOA case has better slope and some sites (e.g. NO56, CH02) are better captured.

These results confirm and complement those found for OC in Denier van der Gon et al. (2015), essentially that OC emissions from most countries seem to be underestimated, and assumptions concerning the condensable OM have a large impact on the emission estimate and modelling result. In a related study for EC, Genberg et al. (2013) also found large dif-

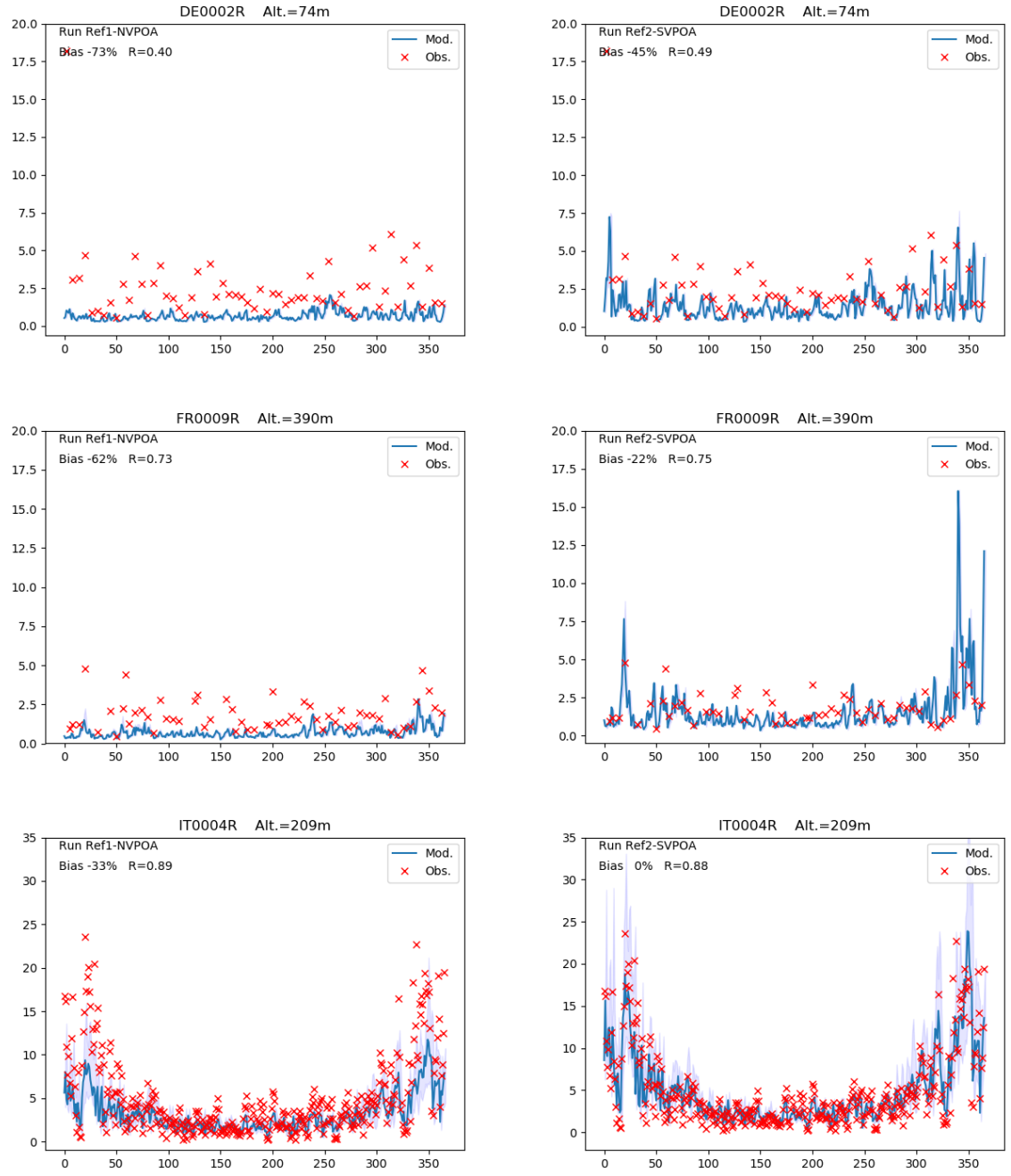

Figure 5.4: Comparison of modelled versus observed OC for 2016 at sites in Germany (DE0002, Waldhof), France (FR0009, Revin), and Italy (IT0004, Ispra). Two model-emission versions are used, Ref-NVPOA (left) and Ref2-SVPOA (right). Units: μg m^{-3}

ferences between different inventory estimates (also for Norwegian emissions rates compared to Swedish rates for example), and that the new bottom-up inventory for residential wood combustion improved model results compared to using the earlier EUCAARI inventory (cf Fig. 5.3).

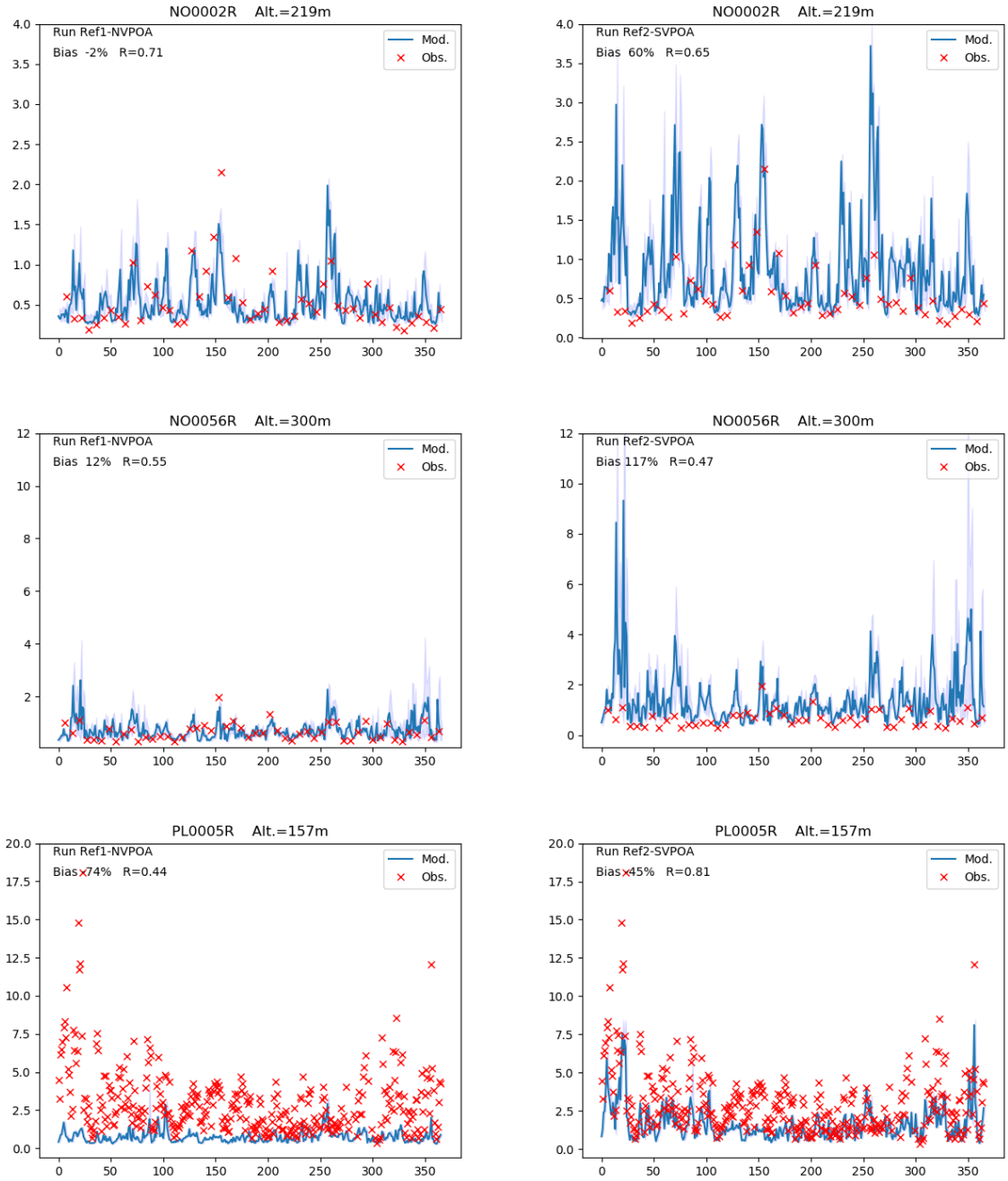

Figure 5.5: Comparison of modelled versus observed OC for 2016 at sites in Norway (NO0002, Birkenes, NO0056, Hurdal) and Poland (PL0005, Diabla Gora). Two model-emission versions are used, Ref-NVPOA (left) and Ref2-SVPOA (right). Units: μg m^{-3}

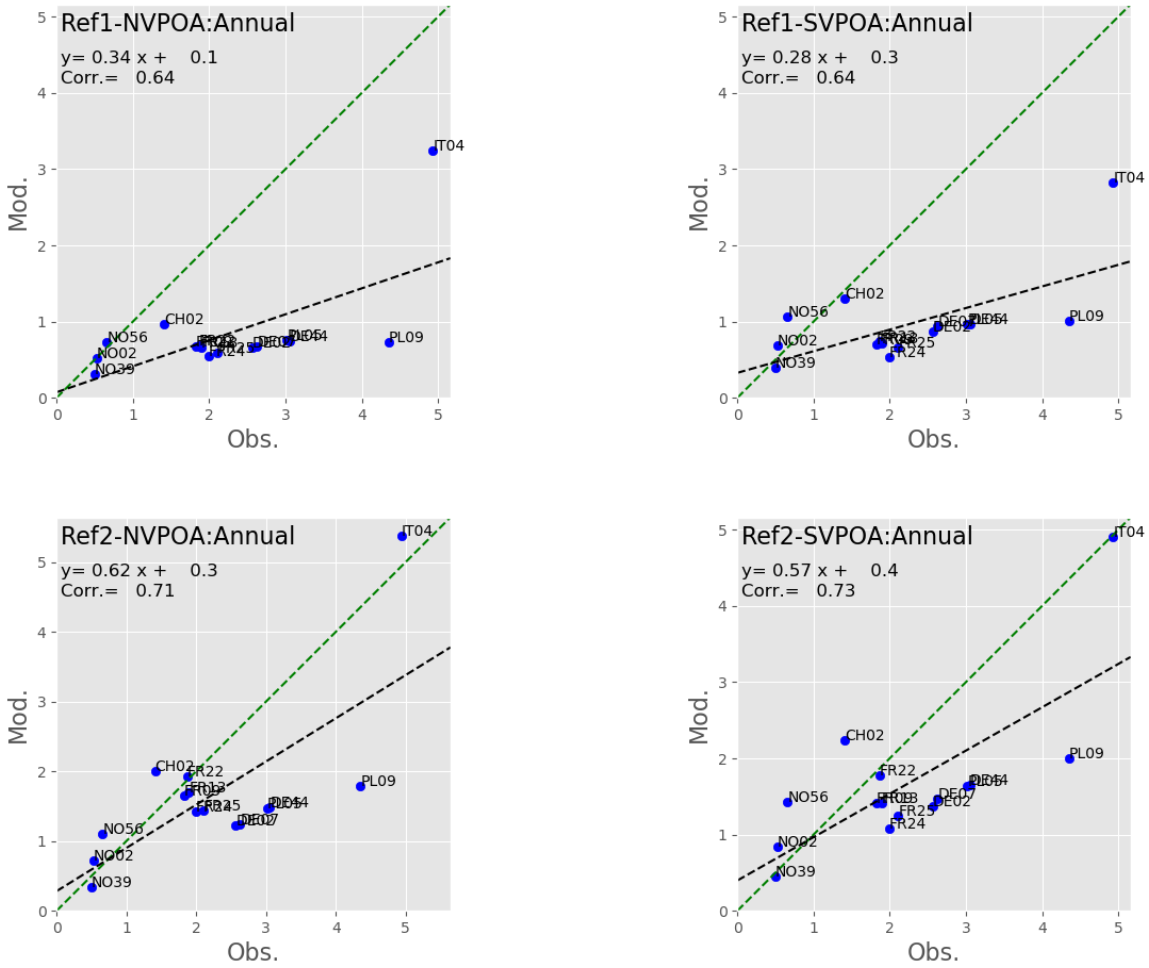

Figure 5.6: Comparison of modelled versus observed OC (μg m^{-3}, in $PM_{2.5}$) for 2016, using four model-emissions setups. Observations from EMEP EC/OC network, ebas.nilu.no.

5.3.2 Impacts on source receptor calculations

The largest impact of the SR calculations was in all cases to the emitter country itself, and so we present results of the country-to-self calculations for the 5 example emitter countries. Taking the Bulgarian case as an example, Fig. 5.7(a) shows the simple difference between the base-case (scenario Ref1-NVPOA) and the run with 15% reductions of Bulgarian emissions. In this case we see that these 'own' contributions to $PM_{2.5}$ are not very sensitive to the base-case used, whether Ref1-NVPOA, Ref2-NVPOA or Ref2-SVPOA. Changes in the own-contribution to fine-OM are however significant, with the Ref2-NVPOA showing twice the change of Ref1-NVPOA. The difference in magnitude between $PM_{2.5}$ and OM is not surprising given the PM emission composition as shown in Fig. 5.3. but given that both the POM fraction and total $PM_{2.5}$ emission are uncertain, the differences caused by POM alone are a cause for concern.

Figs 5.7(b)–(e) present similar plots for Italy, Netherlands, Norway and Poland, with generally similar features, but some differences. For Poland the results for $PM_{2.5}$ do differ significantly among the cases, and differences for OM are very large. The Netherlands also shows

very large differences for the OM components.

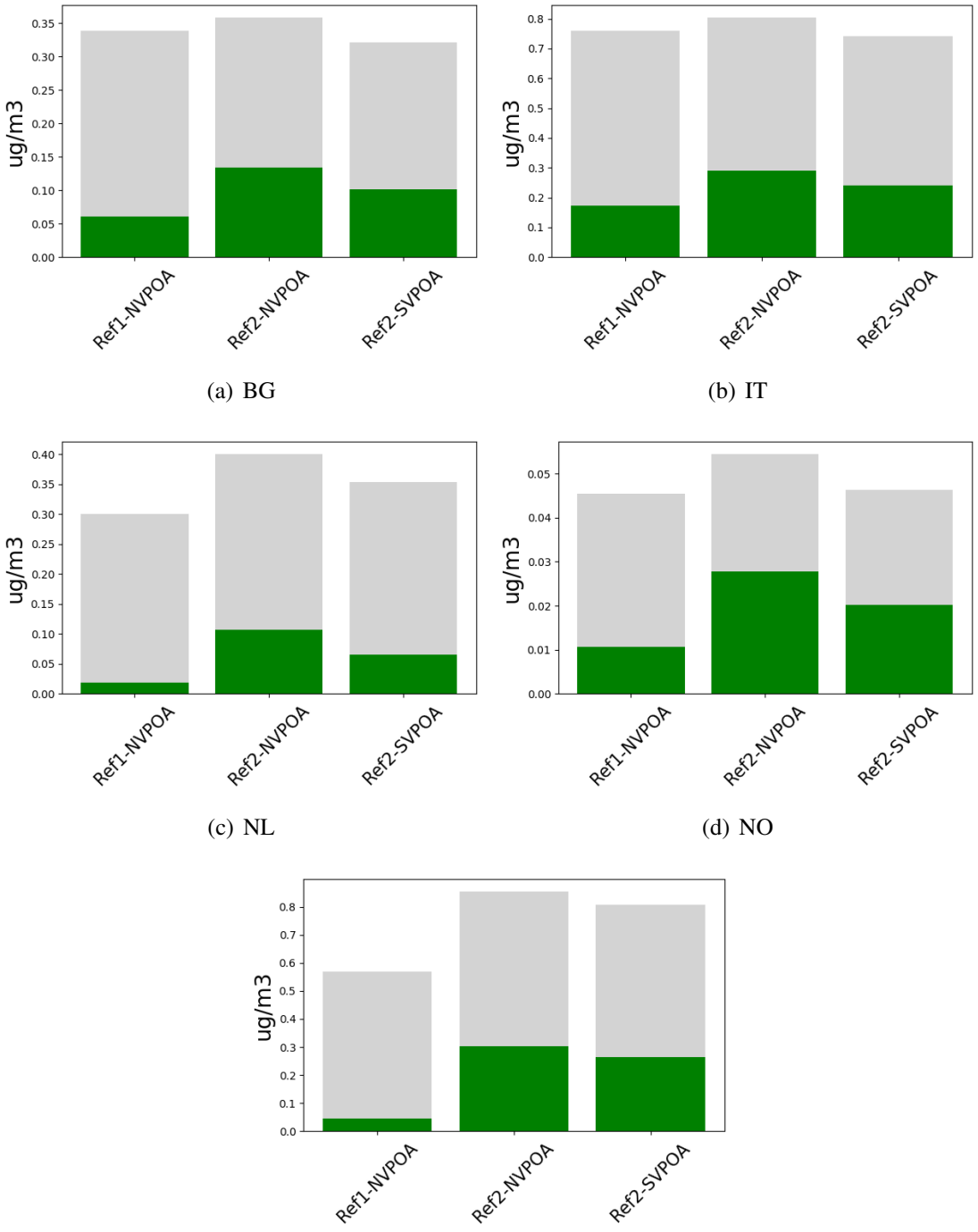

(a) BG (b) IT

(c) NL (d) NO

(e) PL

Figure 5.7: Source-receptor calculations for five example countries: (a) impact of 15% emissions reductions (of all pollutants) on own-country $PM_{2.5}$, for the OM component (green) and total $PM_{2.5}$ (grey). See text for further details.

5.4 Discussion and Conclusions

Estimates of PM and NMVOC as currently provided by Parties have a number of major uncertainties, and there is a clear need for clarification and standardisation of the methods used to define and report PM emissions, and concerning the fraction of PM that is OA. For example, emissions from residential wood-burning in Europe represent around 50% of Europe's OA emissions, and dominate wintertime OA sources, but the study of Denier van der Gon et al. (2015) clearly showed that the definitions behind national emission estimates are inconsistent in their treatment of condensable VOCs. The use of top-down versus bottom-up inventories had dramatic effects on the modelled concentrations of OA and hence PM. Similarly, implementation of a new bottom-up emissions inventory for OA in this study, taking account of SVOC, gave improved model performance for organic aerosol and thus $PM_{2.5}$, especially in wintertime. The improvement was seen at almost all sites, although as expected the extent of the change depends on location (and the methods used to define POA emissions in nearby countries). Although there is good evidence for the basic concepts which are applied here, many of the assumptions are very uncertain, even by the standards of organic aerosol modelling in general.

For some countries (e.g. NO, DK) the bottom-up and EMEP estimates of $PM_{2.5}$ emissions are comparable, but for others (e.g. FI, SE) the expert estimate is far higher than the reported emissions. In order to estimate the impact of such problems on source-receptor matrices we have presented model experiments which explored the changes in $PM_{2.5}$ and OM resulting from the contributions of five example countries to local (i.e. 'own') concentrations, calculated for three emission setups. The changes in $PM_{2.5}$ and especially OM were quite sensitive to the assumed emission setup.

We have noted that some of the problems with specifying OM and EC emissions arise from the coupling of such emissions to EC through OM/EC ratios, and assumptions concerning total $PM_{2.5}$ emissions. Since 2015 the EMEP reporting templates for emissions have been updated to include national BC emissions (Tista et al. 2018), which should be a good start on improving inventories, but reporting of BC is still not mandatory, and many undertainties remain (c.f. Chap. 3, Sect. 6.6). In connection with condensables, a particular problem arises if countries derive these EC emissions by simple application of OC/EC ratios without consideration of the status of condensables in the OC fraction.

All such inconsistencies pose grave problems for the modeling of $PM_{2.5}$ and for any analysis of emission control strategies or cost-benefit analysis. In the worst case these problems might lead to wrong priorities of measures.

As recommended in Simpson and Denier van der Gon (2015) and TFEIP/TFMM (2018) the most important improvement at this stage would be to ensure that reporting is consistent across all countries for PM. Particular attention needs to be paid to condensables from residential combustion, since they are such a large share of the emissions.

We cannot give here a recommendation on 'how-to-define' POA emissions as the issues are just too complex, and EMEP must find a system that can be accepted and applied across Europe and North America. We recommend however that these issues are brought into the open, a new system devised that provides more reliable data for modelling, and which ensures transparency in the methodologies and assumptions used to tackle the grey zone that exists between particle and vapour phases of organic compounds, and their classification as either $PM_{2.5}$ or NMVOC.

References

Bergström, R., Denier van der Gon, H., Prevot, A., Yttri, K., and Simpson, D.: Modelling of organic aerosols over Europe (2002-2007) using a volatility basis set (VBS) framework with application of different assumptions regarding the formation of secondary organic aerosol, Atmos. Chem. Physics, 12, 5425–5485, 2012.

Bergström, R., Hallquist, M., Simpson, D., Wildt, J., and Mentel, T. F.: Biotic stress: a significant contributor to organic aerosol in Europe?, Atmos. Chem. Physics, 14, 13 643–13 660, doi:10.5194/acp-14-13643-2014, URL http://www.atmos-chem-phys.net/14/13643/2014/, 2014.

Ciarelli, G., El Haddad, I., Bruns, E., Aksoyoglu, S., Möhler, O., Baltensperger, U., and Prévôt, A. S. H.: Constraining a hybrid volatility basis-set model for aging of wood-burning emissions using smog chamber experiments: a box-model study based on the VBS scheme of the CAMx model (v5.40), Geoscientific Model Development, 10, 2303–2320, doi:10.5194/gmd-10-2303-2017, URL https://www.geosci-model-dev.net/10/2303/2017/, 2017.

Denier van der Gon, H. A. C., Bergström, R., Fountoukis, C., Johansson, C., Pandis, S. N., Simpson, D., and Visschedijk, A. J. H.: Particulate emissions from residential wood combustion in Europe - revised estimates and an evaluation, Atmos. Chem. Physics, pp. 6503–6519, doi:doi:10.5194/acp-15-6503-2015, URL http://www.atmos-chem-phys.net/15/6503/2015/, 2015.

Donahue, N., Robinson, A., Stanier, C., and Pandis, S.: Coupled Partitioning, Dilution, and Chemical Aging of Semivolatile Organics, Environ. Sci. Technol., 40, 2635–2643, URL http://pubs3.acs.org/acs/journals/doilookup?in_doi=10.1021/es052297c, 2006.

Fagerli, H., Tsyro, S., Benedictow, A., Klein, H., Nyíri, A., , and Valdebenito, Á.: Source receptor matrices in the new EMEP grid, in: Transboundary particulate matter, photo-oxidants, acidifying and eutrophying components. EMEP Status Report 1/2018, pp. 75–81, The Norwegian Meteorological Institute, Oslo, Norway, 2018.

Genberg, J., Hyder, M., Stenström, K., Bergström, R., Simpson, D., Fors, E., Jönsson, J. Å., and Swietlicki, E.: Source apportionment of carbonaceous aerosol in southern Sweden, Atmos. Chem. Physics, 11, 11 387 – 11 400, doi:10.5194/acp-11-11387-2011, URL http://www.atmos-chem-phys-discuss.net/11/13575/2011/, 2011.

Genberg, J., Denier van der Gon, H. A. C., Simpson, D., Swietlicki, E., Areskoug, H., Beddows, D., Ceburnis, D., Fiebig, M., Hansson, H. C., Harrison, R. M., Jennings, S. G., Saarikoski, S., Spindler, G., Visschedijk, A. J. H., Wiedensohler, A., Yttri, K. E., and Bergström, R.: Light-absorbing carbon in Europe - measurement and modelling, with a focus on residential wood combustion emissions, Atmospheric Chemistry and Physics, 13, 8719–8738, doi:10.5194/acp-13-8719-2013, URL http://www.atmos-chem-phys.net/13/8719/2013/, 2013.

Grieshop, A. P., Miracolo, M. A., Donahue, N. M., and Robinson, A. L.: Constraining the Volatility Distribution and Gas-Particle Partitioning of Combustion Aerosols Using Isothermal Dilution and Thermodenuder Measurements, Environ. Sci. Technol., 43, 4750–4756, doi:10.1021/es8032378, 2009.

Hodzic, A., Kasibhatla, P. S., Jo, D. S., Cappa, C. D., Jimenez, J. L., Madronich, S., and Park, R. J.: Rethinking the global secondary organic aerosol (SOA) budget: stronger production, faster removal, shorter lifetime, Atmos. Chem. Physics, 16, 7917–7941, doi:10.5194/acp-16-7917-2016, URL http://www.atmos-chem-phys.net/16/7917/2016/, 2016.

Jathar, S. H., Gordon, T. D., Hennigan, C. J., Pye, H. O. T., Pouliot, G., Adams, P. J., Donahue, N. M., and Robinson, A. L.: Unspeciated organic emissions from combustion sources and their influence on the secondary organic aerosol budget in the United States, Proceedings of the National Academy of Sciences of the United States of America, 111, 10 473–10 478, doi:10.1073/pnas.1323740111, 2014.

Kim, Y., Sartelet, K., Seigneur, C., Charron, A., Besombes, J.-L., Jaffrezo, J.-L., Marchand, N., and Polo, L.: Effect of measurement protocol on organic aerosol measurements of exhaust emissions from gasoline and diesel vehicles, Atmos. Environ., 140, 176 – 187, doi:https://doi.org/10.1016/j.atmosenv.2016.05.045, URL http://www.sciencedirect.com/science/article/pii/S1352231016303922, 2016.

Koo, B., Knipping, E., and Yarwood, G.: 1.5-Dimensional volatility basis set approach for modeling organic aerosol in {CAMx} and {CMAQ}, Atmospheric Environment, 95, 158 – 164, doi:http://dx.doi.org/10.1016/j.atmosenv.2014.06.031, 2014.

Lane, T. E., Donahue, N. M., and Pandis, S. N.: Simulating secondary organic aerosol formation using the volatility basis-set approach in a chemical transport model, Atmos. Environ., 42, 7439–7451, doi:10.1016/j.atmosenv.2008.06.026, 2008.

May, A. A., Levin, E. J. T., Hennigan, C. J., Riipinen, I., Lee, T., Collett, Jeffrey L., J., Jimenez, J. L., Kreidenweis, S. M., and Robinson, A. L.: Gas-particle partitioning of primary organic aerosol emissions: 3. Biomass burning, Journal of Geophysical Research-atmospheres, 118, 11 327–11 338, doi:10.1002/jgrd.50828, 2013.

Murphy, B. N., Donahue, N. M., Robinson, A. L., and Pandis, S. N.: A naming convention for atmospheric organic aerosol, Atmos. Chem. Physics, 14, 5825–5839, doi:10.5194/acp-14-5825-2014, URL http://www.atmos-chem-phys.net/14/5825/2014/, 2014.

Ntziachristos, L. and Samaras, Z.: Methodology for the calculation of exhaust emissions - SNAPs 070100-070500, NFRs 1A3bi-iv, Tech. rep., EEA (European Environment Agency), URL https://www.emisia.com/utilities/copert/documentation/, (co-authors: Kouridis, C., Hassel, D., McCrae, I., Hickman, J., Zierock, K.-H., Keller, M., Andre, M., Gorissen, N., Boulter, P., Joumard, R., Rijkeboer, R., Geivanidis, S., Hausberger, S.), 2018.

Nussbaumer, T., Czasch, C., Klippel, N., Johansson, L., and Tullin, C.: Particulate Emissions from Biomass Combustion in IEA Countries, Survey on Measurements and Emission Factors, Bioenergy task 32, In- ternational Energy Agency (IEA), Zurich, 2008.

Ots, R., Young, D. E., Vieno, M., Xu, L., Dunmore, R. E., Allan, J. D., Coe, H., Williams, L. R., Herndon, S. C., Ng, N. L., Hamilton, J. F., Bergström, R., Di Marco, C., Nemitz, E., Mackenzie, I. A., Kuenen, J. J. P., Green, D. C., Reis, S., and Heal, M. R.: Simulating secondary organic aerosol from missing diesel-related intermediate-volatility organic compound emissions during the Clean Air for London (ClearfLo) campaign, Atmos. Chem. Physics, 16, 6453–6473, doi:10.5194/acp-16-6453-2016, URL http://www.atmos-chem-phys.net/16/6453/2016/, 2016.

Presto, A. A., Hennigan, C. J., Nguyen, N. T., and Robinson, A. L.: Determination of Volatility Distributions of Primary Organic Aerosol Emissions from Internal Combustion Engines Using Thermal Desorption Gas Chromatography Mass Spectrometry, Aerosol Science and Technology, 46, 1129–1139, doi:10.1080/02786826.2012.700430, 2012.

Robinson, A. L., Donahue, N. M., Shrivastava, M. K., Weitkamp, E. A., Sage, A. M., Grieshop, A. P., Lane, T. E., Pierce, J. R., and Pandis, S. N.: Rethinking Organic Aerosols: Semivolatile Emissions and Photochemical Aging, Science, 315, 1259–1262, doi:10.1126/science.1133061, 2007.

Shrivastava, M. K., Lane, T. E., Donahue, N. M., Pandis, S. N., and Robinson, A. L.: Effects of gas particle partitioning and aging of primary emissions on urban and regional organic aerosol concentrations, J. Geophys. Res., 113, doi:10.1029/2007JD009735, 2008.

Simpson, D. and Denier van der Gon, H.: Problematic emissions - particles or gases?, in: Transboundary particulate matter, photo-oxidants, acidifying and eutrophying components. EMEP Status Report 1/2015, pp. 87–96, The Norwegian Meteorological Institute, Oslo, Norway, 2015.

Simpson, D., Yttri, K., Klimont, Z., Kupiainen, K., Caseiro, A., Gelencsér, A., Pio, C., and Legrand, M.: Modeling Carbonaceous Aerosol over Europe. Analysis of the CARBOSOL and EMEP EC/OC campaigns, J. Geophys. Res., 112, D23S14, doi:10.1029/2006JD008158, 2007.

Simpson, D., Benedictow, A., Berge, H., Bergström, R., Emberson, L. D., Fagerli, H., Hayman, G. D., Gauss, M., Jonson, J. E., Jenkin, M. E., Nyíri, A., Richter, C., Semeena, V. S., Tsyro, S., Tuovinen, J.-P., Valdebenito, A., and Wind, P.: The EMEP MSC-W chemical transport model – technical description, Atmos. Chem. Physics, 12, 7825–7865, doi:10.5194/acp-12-7825-2012, 2012.

Sternhufvud, C., Karvosenoja, N., Illerup, J., Kindbom, K., Lükewille, A., Johansson, M., and Jensen, D.: Particulate matter emissions and abatement options in residential wood burning in the Nordic countries, Report anp 2004:735, Nordic Council of Ministers, Copenhagen, URL http://www.norden.org/en/publications/publikationer/2004-735/atdownload/publicationfile, 2004.

TFEIP/TFMM (2018): Improving Emissions of Condensable Particulate Matter in the Context of the LRTAP Convention, URL http://www.unece.org/fileadmin/DAM/env/documents/2018/Air/EB/TFEIP-TFMM_proposal_condensables_for_EMEP_Steering_Body_v6.pdf, EMEP TFEIP/TFMM note submitted to 2019 Executive Body as informal document, 2018.

Tista, M., Wankmüller, R., Matthews, B., Mareckova, K., Fagerli, H., , and Nyíri, A.: Emissions for 2016, in: Transboundary particulate matter, photo-oxidants, acidifying and eutrophying components. EMEP Status Report 1/2018, pp. 41–64, The Norwegian Meteorological Institute, Oslo, Norway, 2018.

CHAPTER 6

The winter 2018 intensive measurement period. A brief update

Stephen Matthew Platt, Karl Espen Yttri, Wenche Aas, Sverre Solberg, Hilde Fagerli, Ágnes Nyíri, Svetlana Tsyro, Anna Benedictow, Hugo A.C. Denier van der Gon, Robert Bergström and David Simpson

6.1 Background

Carbonaceous aerosol is a major fraction of the ambient aerosol in Europe. It influences the atmospheric radiative balance and contributes to adverse health effects. Consequently, carbonaceous aerosol is a key species measured regularly in monitoring networks, such as EMEP. There are numerous anthropogenic and natural sources of carbonaceous aerosol, and it is important to identify and quantify these to develop efficient abatement strategies. Particularly, there is an interest to distinguish between combustion sources using fossil fuels and biomass, which is possible by multi-wavelength measurements of the absorption coefficient (Sandradewi et al. 2008), an on-line feature of the aethalometer manufactured by Magee Scientific. Being robust, easy to operate, available at relatively low cost, and widespread across Europe, this instrument holds the potential to be an important tool for source apportionment (SA) of carbonaceous aerosol.

In a study presented in last year's EMEP Status report (1/2018), we made a brief update of ongoing work on the EMEP intensive measurement period (IMP) in winter 2017-2018. We separated equivalent black carbon (EBC), which is the black carbon mass derived from measurements of absorption into a fossil fuel (EBC_{ff}) fraction and a biomass burning (EBC_{bb}) fraction using the aethalometer model described by Sandradewi et al. (2008). Furthermore, we presented preliminary results using a new application of positive matrix factorization (PMF) to apportion EBC. The multi wavelength aethalometer approach for separating EBC into EBC_{bb} and EBC_{ff} is based on the assumption that aerosol particles emitted from wood burning absorbs relatively more in the near UV than in the IR, compared to those from combustion

of fossil fuels, which show no wavelength dependence. Unlike the aethalometer model, the PMF approach requires no a priori knowledge of the aerosol Ångström exponents (AAEs) for EBC_{ff} and EBC_{bb} (rather, these may be derived as an output from PMF), and 3 factor source apportionment might be possible. Here we present results from ongoing work on the EMEP IMP dataset using the aethalometer model and including results from PMF at several sites. We compare the aethalometer model and PMF-derived EBC factors to the source apportioned EC obtained from a series of EMEP model runs using four different emission datasets.

More information on the IMP Winter 2018 can be found here:

- EMEP/ACTRIS intensive measurement period - winter 2018
  `https://www.nilu.no/projects/ccc/tfmm/Winter%20intensive%20measurement%20period.pdf`.
- On aerosol filter sample collection routine for the EMEP/ACTRIS/COLOSSAL IMP Winter 2018
  `https://www.nilu.no/projects/ccc/tfmm/Guidlines_Filter_sampling.pdf`.
- Laboratories offering analysis of OC/EC and levoglucosan for the EMEP/ACTRIS/COLOSSAL IMP winter 2018
  `https://www.nilu.no/projects/ccc/tfmm/Labs_offering_centralized_analysis.pdf`.

6.2 Aim

The IMP Winter 2018 aims to use the PMF approach to separate EBC into EBC_{ff} and EBC_{bb} in the European rural background environment, including low loading areas in Scandinavia and more polluted regions in Central Europe, and in areas likely differing in source composition, preferably also with an influence of coal combustion. Further, it should compare EBC_{ff} and EBC_{bb} apportioned by the PMF approach to filter based measurements of the biomass burning tracer levoglucosan for validation purposes, and to elemental carbon (EC) to derive site-specific Mass Absorption Coefficients (MAC) values. A desired outcome of the IMP is a harmonised European-wide data set with carbonaceous aerosol apportioned into EBC_{ff} and EBC_{bb}, which also is applicable for model validation. Finally, the IMP should encourage initiation of regular monitoring of EBC_{ff} and EBC_{bb}, and reporting of such data to EBAS, which then will pursue the EMEP monitoring strategy, as well as deliverables of ACTRIS.

6.3 Participation and partnership and co-benefit

All EMEP/ACTRIS sites performing absorption coefficient measurements with a multi-wavelength aethalometer were invited to participate in the EMEP/ACTRIS/COLOSSAL intensive measurement period. Participation also required off-line analysis of levoglucosan and OC/EC/TC on filter samples from a co-located filter sampler. A successful outcome of the IMP Winter 2018 depends on participants following the IMP guidelines (`https://www.nilu.no/projects/ccc/tfmm/Guidlines_Filter_sampling.pdf`). It also relies on the existing infrastructure of EMEP and ACTRIS, such as protocols for sampling and

analysis, calibrated instruments and inter laboratory compared analytical methods. In addition, the IMP Winter 2018 greatly benefits from cooperation with the recently established COST action COLOSSAL (Chemical On-Line cOmpoSition and Source Apportionment of fine aerosoL).

IMP winter 2018 was presented in various fora before the start up in December 2017, and we experienced a substantial interest in the initiative and requests to participate also outside EMEP/ACTRIS/COLOSSAL associated partners. Thus, urban background sites were included as well, as long as they fulfilled the measurement guidelines of participation. Inclusion of additional site categories adds value to the study in several ways, e.g. twin sites allow the study of incremental changes in pollution at urban locations or investigation of the influence of local sources at rural background sites.

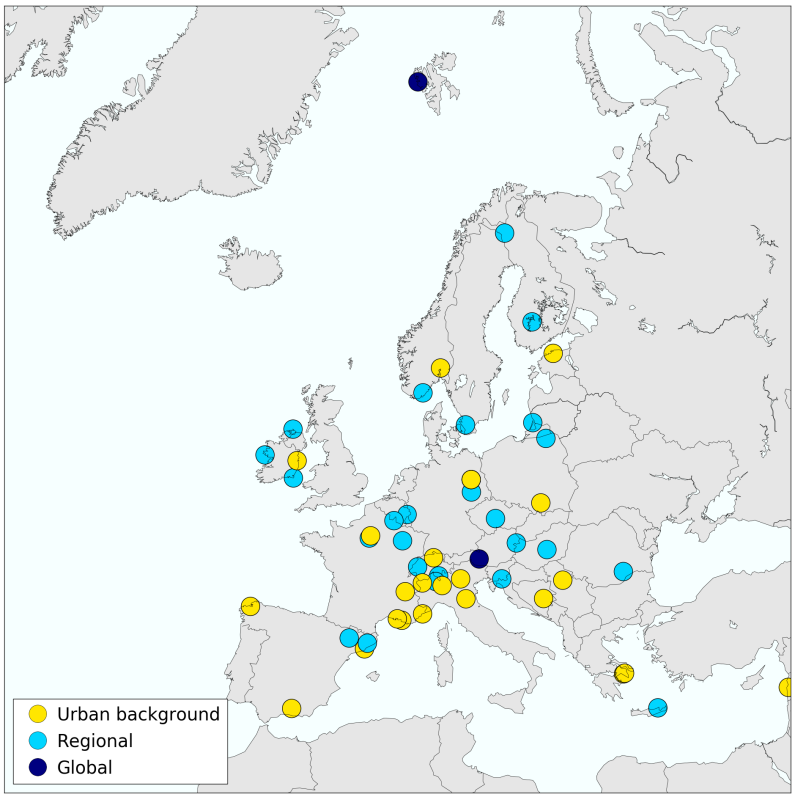

Figure 6.1: Location and category of sites participating in IMP Winter 2018

Figure 6.1 shows the location of the 52 sites that participated in the IMP Winter 2018, and their site category. This includes 2 global sites, 25 regional background sites and 25 urban background sites in 22 different countries. The northernmost regional/global site is the Zeppelin Observatory at Svalbard (Norway), whereas Beirut Mansourieh (Lebanon) in the Eastern Mediterranean Sea is both the southern- and easternmost site. Mace Head at the Western coast of Ireland is situated furthest to the west. The sites that participated in IMP Winter 2018 cover a wider area than those sites regularly addressing carbonaceous aerosol by OC/EC measurements within EMEP. This extension is particularly pronounced to the east, including several sites along a north to south transect from northern parts of Finland to Lebanon, and to the north-west by inclusion of sites in Ireland.

Numerous variables relevant for air-quality and climate issues were measured at most of the sites participating in IMP Winter 2018, which also support our interpretation of the core

variables, EBC_{ff} and EBC_{bb}. This includes on- and off-line variables monitored as part of long-term obligations within EMEP, but not exclusively; e.g. novel instrumentation such as the Total Carbon Analyzer (TCA-08) was tested at a selection of sites.

6.4 Data submission and quality control

The core variables (EBC, OC/EC and levoglucosan) asked for in IMP winter 2018 were to be reported by 1st June 2018, a deadline most participants failed to meet. This deadline has been moved several times and the final deadline is now August 2019, after which data will not be analysed as a part of the EMEP IMP or used in subsequent reports and publications. Data asked for in IMP Winter 2018 are reported to EBAS via the EBAS submission tool, using predefined templates with substantial requirements for metadata and data quality control via flagging, thus that ensuring all information required for complete data analysis is available to users in consistent way, which is also harmonised with the broader atmospheric dataset on EBAS. Even for an experienced user and submitter of aethalometer data, the level of sophistication asked for and needed for the analysis is challenging, and several rounds of iteration have been necessary for some of the data to obtain the requested quality. Note that the following information is required for the PMF analysis of these data: instrument flows, intensities, reference zero intensities, instrument status data, loading compensation parameters and time data. Metadata should include information on invalid data, the multiple scattering parameter, and in particular, the zero readings needed for the PMF analysis. The multiple scattering parameter depending on the tape used in the instrument can take the value 1.39, 1.57, or 4.00 for the dual-spot aethalometer (AE33), and the calculated absorption/mass will scale linearly with this parameter. Not all sites have reported the multiple scattering correction used, and we have low confidence that all sites which have reported it have done so correctly, since the most recent tape type takes the value 4, and it is possible that not all participants updated their previous reporting templates. Furthermore, not all sites have reported/collected zero data. Due to these challenges we have accepted data from a number of sites which are not in the NASA-Ames format required for EBAS. Nevertheless, we aim for all data collected as part of this campaign to be uploaded to EBAS.

A total of 42 sites (most of those submitted) have so far been analysed for absorption (Figure 6.2). Levoglusocan and elemental carbon (EC), where reported, have also been analysed for these sites. We have excluded user-flagged data, including zero data, from the analyses. Additionally, we have also excluded data where large variation in instrument flows was observed, even when not flagged by the data submitter, since this produces spikes in the data. Data coverage is not complete for a lot of sites, and some lack levoglucosan and/or EC. Furthermore, levoglucosan is reported for discrete sampling intervals at some sites which further reduces coverage.

6.5 Data analysis

We calculated absorption coefficients using an attenuation step at a fixed signal to noise interval (rather than a fixed time step) according to the methodology of Backman et al. (2017) We determined the signal to noise using the measurements of zero air, where submitted, for each site. Where zero data were not submitted, we used the average zero value from sites which

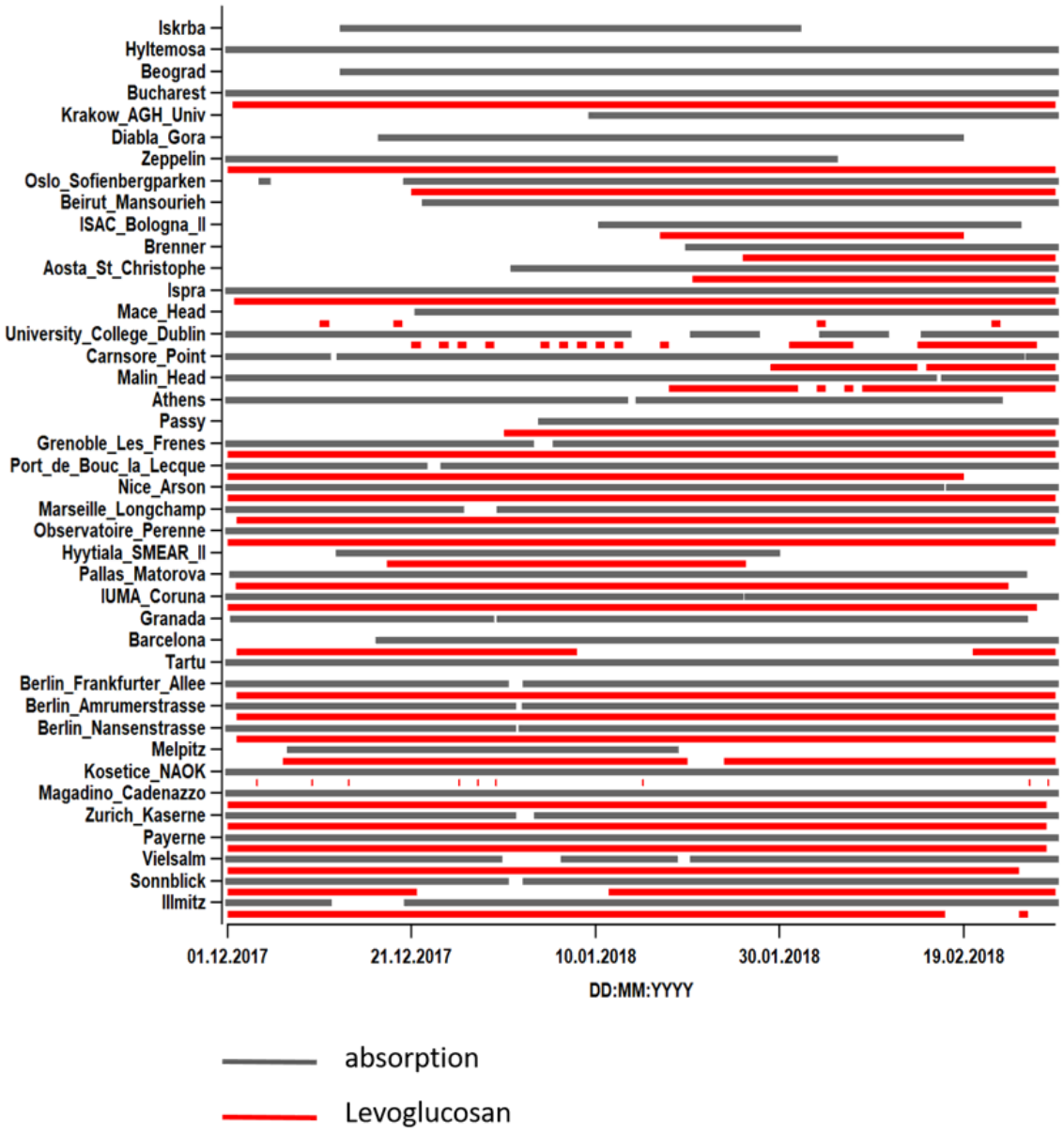

Figure 6.2: Coverage of analysed data from the EMEP intensive measurement period in winter 2017/2018, absorption data in grey, levoglucosan in red. Note that there are some sites, for which data have been submitted, but which have not yet been analysed.

did submit these data. We also used the zero data to calculate the error matrix required for PMF.

We observed overcompensation of the loading effect for several sites operating the AE33 aethalometer (clear jumps in the absorption after each tape advance). To correct for this effect, we scaled the loading compensation parameter for each tape advance such that the average of the last two absorption coefficients at tape advance count number n was equal to the average of the first two absorption coefficients at tape advance count $\mathrm{n}+1$. For consistency, and because error in the loading compensation parameter might be present but not easily observed, we corrected all AE33 data in this way. For the AE31 and AE42 we used Virkkula et al. (2007) compensation equation.

We performed repeated PMF runs ($n = 4000$) on bootstrapped absorption (B_{abs}) / error matrix data to yield 2 factor profiles and time series from each site. An effective AAE was calculated using the PMF-derived factor profiles. This factor derived AAE was used to map the solutions such that factor 1 is defined as the profile with the lowest AAE (note that PMF yields factors in random order such that comparison of two or more solutions requires that profiles must be matched or 'mapped' to each other in order to calculate average results). By binning the runs by the PMF-derived AAE (bin width 0.01) we could determine the modal AAEs (e.g. Figure 6.3). The final PMF time series were calculated from the average of the run results in this modal bin at wavelength 880nm. For the AE33 we included the absorption coefficient calculated from the lower flow/higher noise spot 2 (yielding a matrix of 14 columns). Note that the data from spot 2 were not used to bin the solutions or to calculate AAEs and time series.

To calculate EBC we used an effective mass absorption cross section (MAC) determined from the ratio of absorption to elemental carbon (EC). Since there is considerable uncertainty due to missing information about the tape types used, the resulting MAC is not a true MAC value since it also compensates for this uncertainty. For sites which did not submit EC we used the standard MAC for each instrument type. Note that uncertainty in total concentrations does not influence the source apportionment, either by PMF or by the aethalometer model.

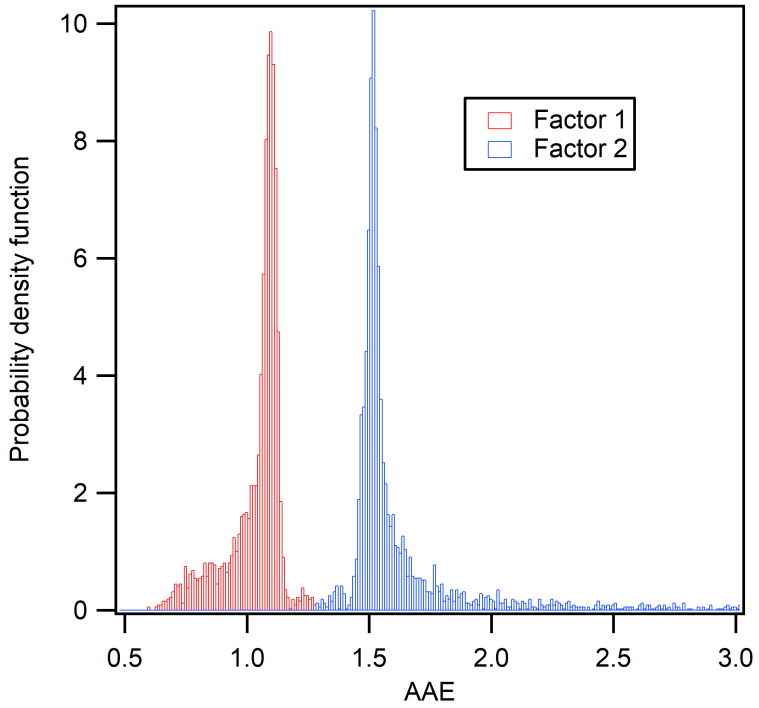

Figure 6.3: Positive matrix factorisation (2 factor solution) bootstrap runs ($n = 4000$) binned by factor-derived aerosol Ångström exponent (AAE) for the Brenner site.

6.6 Set-up of EMEP MSC-W model simulation

Simulations of elemental carbon have been performed with the EMEP MSC-W model (rv4.33) for the period 15 November 2017 to 31 March 2018. The model setup and input data is the

Scenario	EC emissions per country and sector	Spatial distribution	EC_{ff}/EC_{bb} ratio
TNOS5	TNOS5	TNOS5 PM	TNOS5
EC_splitTNO	EC reported to EMEP	EMEP PM	TNOS5
PM_splitIIASA	Derived from EMEP PM using EC/PM fractions from IIASA	EMEP PM	IIASA
EC_splitIIASA	EC reported to EMEP	EMEP PM	IIASA

Table 6.1: Overview of the emission data used in the four different model runs and their notations.

same as for the status runs in this report (described in Chapter 2), except for the emission input data. In the standard setup, the model uses emissions of $PM_{2.5}$ and coarse PM, which are split into organic and elemental carbon from fossil fuel and biomass burning, and remaining inorganic PM, using so-called emission split files (containing fractions per country and emission sectors). Four different sets of emissions have been used, with two different spatial distributions, summarized in Table 6.1.

The TNOS5 data set (also referred to as CAMS_2015_RWC, similar to 'Ref2' in Chapter 5) is developed by TNO as part of other research projects, including CAMS, and includes a best-estimate of PM/POM (Primary Organic Matter) for each country when condensable SVOC are included for the residential sector. We apply the TNOS5 data set in two model runs, where the full emission data set is used directly in one model run (e.g. the $PM_{2.5}$ and PM_{coarse} emissions with corresponding split files). In the second model run (EC_splitTNO), reported EMEP emissions of EC have been combined with EC_{bb}/EC_{ff} fractions per country and sector from TNOS5.

Emission split factors for EC/PM and EC_{bb}/EC_{ff} per country and sector are also available from IIASA (personal communication, 2018). In the model run 'PM_splitIIASA', EC_{bb} and EC_{ff} emissions are derived from reported primary PM emissions using these split factors. This corresponds to the standard setup in the EMEP MSC-W model. The fourth model run, 'EC_splitIIASA', combine reported EC emissions with EC_{bb}/EC_{ff} fractions from IIASA. For all model runs, the spatial distributions of EC emissions are identical per country and sector to those for $PM_{2.5}$ emissions from the corresponding data set.

6.7 Meteorology during IMP Winter 2018

The core sampling time of IMP Winter 2018 was 1 December 2017 - 1 March 2018. For certain sites, typically Scandinavia, northern Europe and European high altitude sites, there was an option to extend sampling to reflect the period when EBC was elevated, as well as to handle low ambient levels, which requires prolonged sampling time to cope with instrumental detection limits and the criteria of 25-30 filter samples for OC/EC and levoglucosan analysis.

Overall, the winter 2017-2018 was characterised by windy, wet and rather mild conditions most of the time followed by a period at the end with extremely low temperatures associated with eastern air masses. In December 2017, low pressure activity led to windy conditions with frequent precipitation and west and north-westerly winds over northern and central Europe. Although there were periods of cold Arctic air mass inflow, the mean temperatures were above normal in most of northern Europe, and precipitation was significantly above normal (180-200% of the normal in some areas). An anticyclone located over southwestern Europe led to

drier and colder conditions in that area.

January 2018 started with strong westerly and north-westerly winds over central Europe, leading to precipitation and low temperatures, and continued with a period of cold winds from the north and northeast. By the middle of the month, the weather returned to the conditions with strong westerly winds and frequent low-pressure passages. Monthly mean temperatures were 2-3 degrees above normal in many areas and the precipitation was higher than normal in most areas. Paris received more than twice the normal precipitation and experienced severe flooding in the river Seine. A location in Switzerland received two meter snowfall during 24 hours.

February continued with westerly winds and precipitation in the first part. From the middle of the month a weak anticyclone was developing in central Europe that was gradually drifting to the northeast and intensifying. By the 24th an extensive high-pressure system was established over north-western Russia, sending very cold air masses westwards over most of Europe leading to snowfall in the Mediterranean and freezing temperatures over large areas. This was named "the beast from the east" (or "the Siberian bear" in the Netherlands). The cold outbreak lasted until the 9th or 10th of March when milder air masses were entering from the south and west. Thus, IMP Winter 2018 provides an excellent opportunity to study changes in the relative share of biomass and fossil fuel to EBC under various winter time meteorological situations, in particular as a function of a wide range in the ambient temperature.

6.8 Results from the aethalometer model and positive matrix factorisation

So far, we have run the aethalometer model on 42 sites and PMF on 25 sites (Figure 6.4). According to the aethalometer model, the sites with the highest biomass burning fraction tend to be regional. Beirut is the site with the lowest EBC_{bb}, consistent with warmer conditions expected for the country compared to many northern and eastern European sites.

Note that the site ranking in Figure 6.4 is valid for any AAE pair, but might be different if, as expected, the true AAE varies. Meanwhile, a large range in the fraction is possible for reasonable input AAEs for the fossil and biomass burning fractions, though a setting of AAE_{ff} =1 and AAE_{bb} =2 tends to yield a biomass burning fraction at the lower part of the range. Furthermore, many AAE input settings generate negative values in either the EBC_{ff} or EBC_{bb} time series. In extreme cases the negative values can dominate the time series such that the net average biomass burning fraction is lower than zero or above one. However, negative concentrations are also present in time series where the net average is positive. Such negative values, together with the wide range of possible results indicated by the width of the bars are a motivation to investigate new source apportionment techniques for EBC.

So far we have run PMF with 2 factors for all sites analysed. This has consistently produced 2 factors with clear profiles (as defined by the factor-derived AAEs, see e.g. Figure 6.3). The mapped solutions yield a factor 1 with an AAE around 1 and an AAE around 1.5-2.0 (Table 6.2) which is close to what is expected to correspond to AAE_{ff} and AAE_{bb} (Zotter et al. 2017). We therefore assume that factor 1 corresponds to B_{abs} from fossil fuel and factor 2 B_{abs} from biomass burning, i.e. EBC_{ff} and EBC_{bb}, respectively. PMF tends to produce a lower EBC_{bb} fraction compared to the aethalometer model, although all results are within the range indicated. However, since the site ranking shown in Figure 6.4 is only valid for any fixed input pair, this result might be an artefact of ranking the aethalometer data in this way.

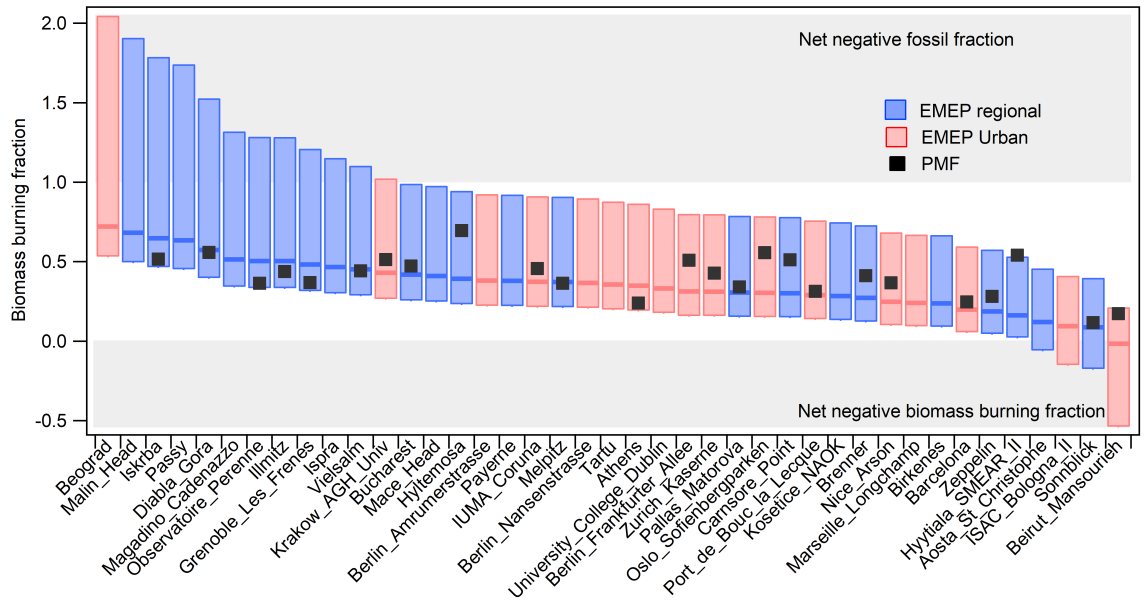

Figure 6.4: Averaged biomass burning fractions of EBC at the EMEP intensive measurement period sites, according to the aethalometer model (blue for regional sites, red for urban sites) and positive matrix factorisation (black squares). The sites are ranked according to highest biomass burning fraction from the aethalometer model and the bars show the range of results possible by varying the aethalometer model input aerosol Ångström exponents (AAE) from 0.9 - 1.2 for fossil (AAE_{ff}) and 1.5 - 2.0 for biomass burning (AAE_{bb}). The dark horizontal center line shows the result using a setting of AAE_{ff} = 1.0 and AAEbb = 2.0. Note that for a number of settings, the biomass burning fraction is below zero, i.e. the model yields a net negative biomass contribution, or above one implying a net negative fossil contribution. These results are not physically reasonable (indicated by the grey background).

6.9 Comparison with EMEP MSC-W model results

As shown in Figure 6.5 and 6.6, there is reasonable agreement between modelled EC and EBC derived from observations, especially for the model run that use TNOS5 as input data. Note that not all of the sites in Figure 6.5 had paralell EC measurements, and thus not site specific MAC values. For the sites without site specific MAC values, EBC and EC cannot be expected to compare well. For all the other figures, we only use EBC from sites that had site specific MAC values, and only for the time periods where there were paralell EC measurements. The model data was averaged to the corresponding EC measurement periods.

Only one of the model runs that use reported EC emissions is shown in these figures ('EC_splitIIASA'), as the total EC emissions by country and sector are the same in 'EC_splitIIASA' and 'EC_splitTNOS5' - they differ only in their split of EC into EC_{ff} and EC_{bb}. Note that the modelled EC results are for the fine fraction ($PM_{2.5}$), whilst the EC from observations represent a mix of EC in $PM_{2.5}$ and PM_{10}, with most sites providing only one size fraction. However, since most EC is in the fine fraction, we assume that the error made by comparing to fine EC is small.

The overall EC concentrations are somewhat low in the model run that uses reported EC emissions. The correlations between model results and observations are fairly low, but highest for TNOS5 (r^2=0.17). This 'scenario' gives substantially higher EC concentrations for large

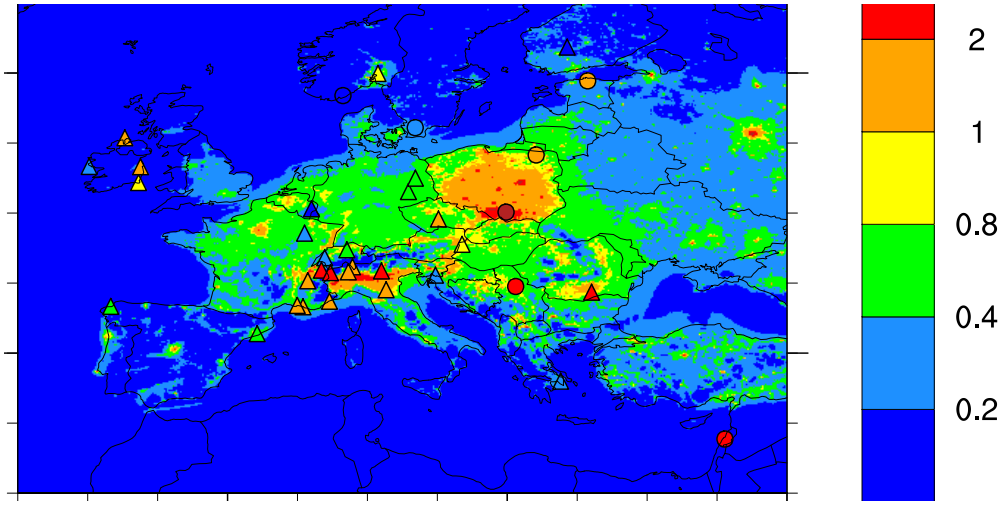

(a) TNOS5

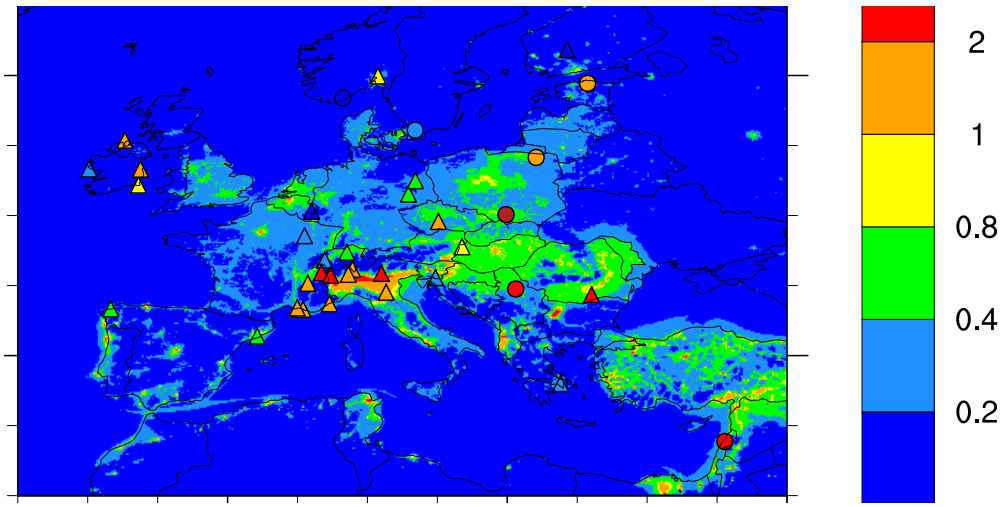

(b) EC_splitIIASA

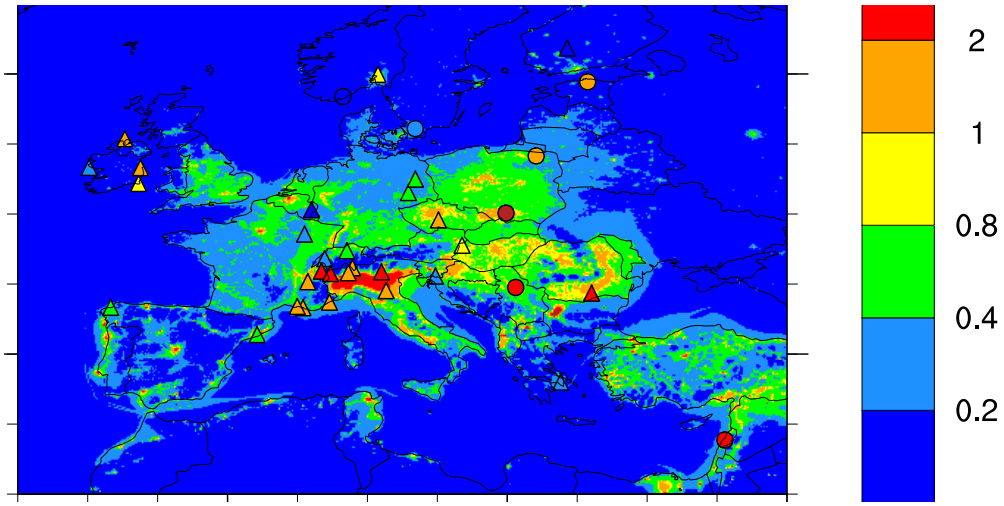

(c) PM_splitIIASA

Figure 6.5: Model results (background) of fine EC with EBC derived from observations with paralell EC measurements (triangles) and EBC derived from observations without paralell EC measurements (circles) for December 2017-February 2018 (units: μg m^{-3}). Only data from measurement sites below 1000 meter above sea level are shown.

Table 6.2: Positive matrix factorisation factor-derived Aerosol Ångström exponents (AAE) for fossil fuel (ff) and biomass burning (bb) for the sites analysed so far from the EMEP intensive measurement period winter 2017/2018.

	AAEff	AAEbb
Illmitz	1.39	1.76
Sonnblick	0.9	1.64
Vielsalm	1.01	1.8
Zurich_Kaserne	0.95	1.62
Melpitz	1.1	1.64
Berlin_Frankfurter_Allee	0.87	1.65
Barcelona	0.99	1.57
IUMA_Coruna	0.85	1.72
Pallas_Matorova	1.15	1.48
Hyytiala_SMEAR_II	1.04	1.29
Observatoire_Perenne	1.06	1.93
Nice_Arson	0.92	1.63
Port_de_Bouc_la_Lecque	0.9	1.91
Grenoble_Les_Frenes	1.02	1.89
Athens	1.05	2.22
Carnsore_Point	0.84	1.74
Aosta_St_Christophe	0.88	1.39
Brenner	1.09	1.51
Beirut_Mansourieh	0.82	1.79
Oslo_Sofienbergparken	0.91	1.51
Zeppelin	0.59	0.93
Diabla_Gora	1.18	1.78
Krakow_AGH_Univ	0.92	1.75
Bucharest	1.01	1.72
Hyltemosa	0.85	1.6
Iskrba	1.07	1.87

areas of Europe, which can be explained by the higher EC emissions in TNOS5 for countries such as France, Poland and Germany (see Figure 6.8). For the model runs that use reported EC emissions, the correlation to the observations is almost none.

In Figure 6.7 the biomass burning fractions of fine EC in model results have been compared to the biomass burning fractions derived from PMF (and the aethalometer model). Whilst the model runs based on reported EC emissions (EC_splitTNOS5 and EC_splitIIASA) are in reasonable agreement with the PMF values, the model results based on the TNOS5 emissions are consistently higher than the biomass burning fractions from PMF, with a few exceptions. PM_splitIIASA also tend to overestimate the biomass burning fraction, but to a lesser extent than TNOS5. During winter time, wood burning is a major source of EC from

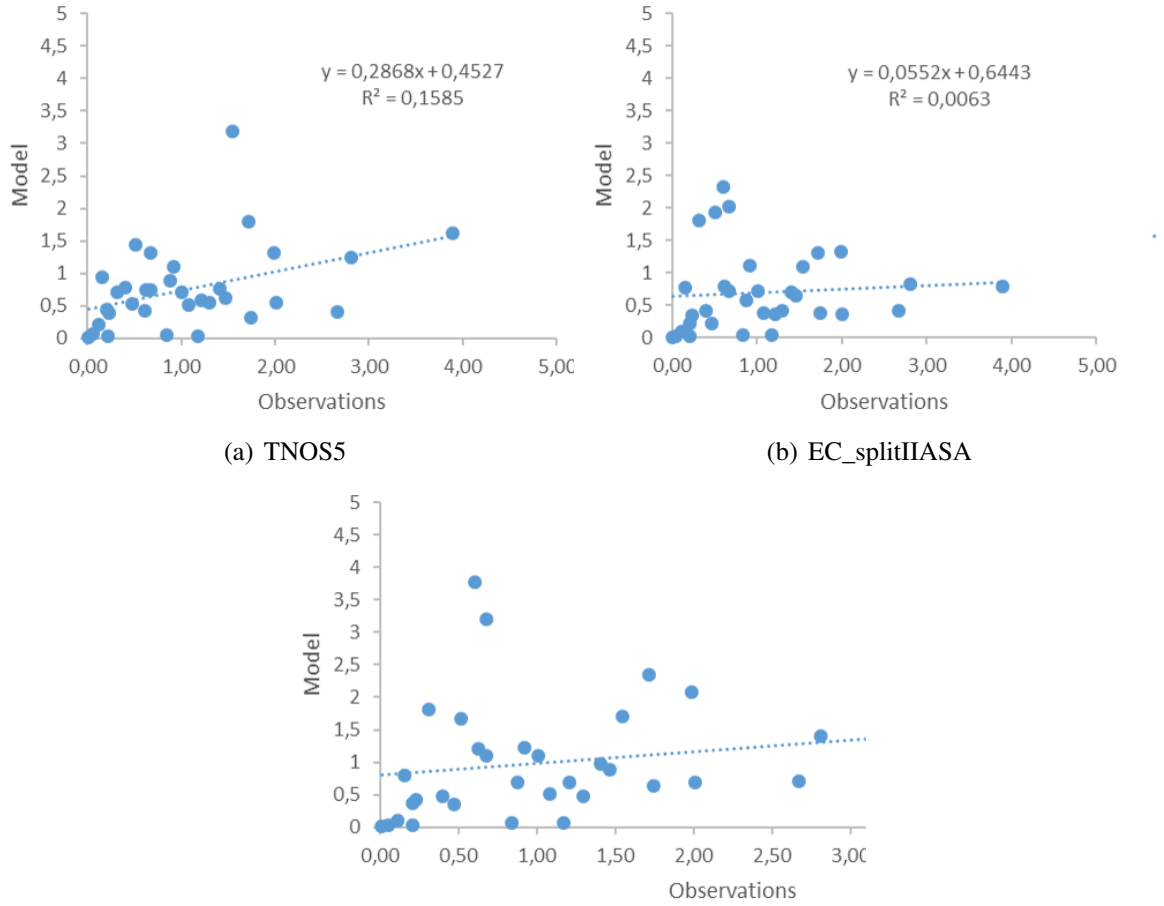

(a) TNOS5

(b) EC_splitIIASA

(c) PM_splitIIASA

Figure 6.6: Comparison of model results of fine EC with EBC derived from observation (for measurement sites that also have EC measurements/site specific MAC values).

biomass burning, while traffic emissions constitute the largest source of EC from fossil fuel. The differences in the biomass burning fractions in the modelled EC results are results of the different shares of sources in the emissions data. As it can be seen from Figure 6.8, the emissions from residential heating are for most countries higher in TNOS5 than in the reported EC emissions, while it is opposite for traffic emissions.

These preliminary model results suggest that the share of EC emissions from fossil fuel and biomass burning emissions are about right in the reported EMEP EC emissions, whilst the total EC emissions appear to be biased low. However, the proportion of different EC sources in the EMEP emission data could be about right for the wrong reasons, considering that the emissions from different sources (with completely independent emission factors) would have to increase proportionally to keep the biomass burning fraction about the same.

Further, although the modelled EC results using TNOS5 emissions overall are in better agreement with EBC derived from observations (Figure 6.5), the proportion of sources from biomass burning in TNOS5 seems to be too high. Possibly this means that some fossil fuel sources are missing in the TNOS5 data set. Some support for this hypothesis can be find in Figure 6.9, where TNOS5 and EC_splitIIASA are compared to observations at urban and rural sites individually. Whilst there is excellent correlation between the observations and the measurements at rural sites (r^2=0.47), there is no correlation for urban sites - and very low

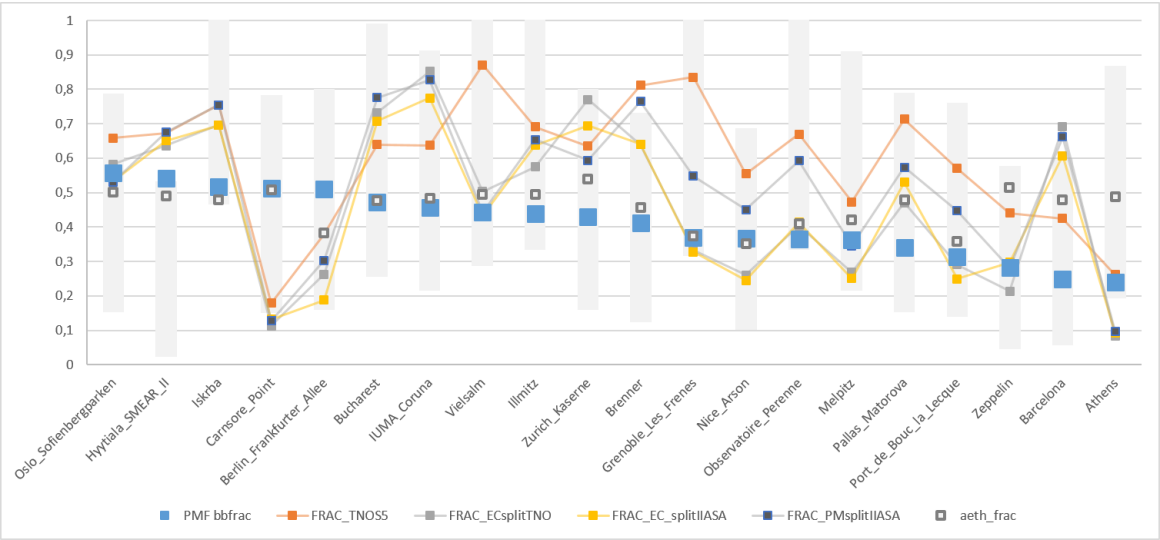

Figure 6.7: Biomass burning fractions from model results compared to results from PMF and the aethalometer model (aeth_frac). The shaded area show the range of results possible by varying the aethalometer model input aerosol Ångström exponents (see Figure 6.4 and text for explanations) but we show only the physically reasonable range here. The sites are ranked according to the highest biomass burning fraction from PMF.

Figure 6.8: Comparison of EC emissions from TNOS5 and EC emissions reported to EMEP (Note: it is not clear whether the emissions reported to EMEP are EC or BC). Not all countries reported EC to EMEP, see chapter 3.

modelled EC values.

The spatial correlation between modelled EC and observations for the model runs that use reported EC emissions (EC_splitIIASA is shown in Figure 6.9) is also rather good for rural sites (r^2=0.31), but for urban sites the observations and model results are anti-correlated. Further investigations are need to understand why, but probably this could at least partly be related to the spatial distributions of emissions.

It is not clear how the reported EMEP emissions ($PM_{2.5}$ and thus EC distributed according

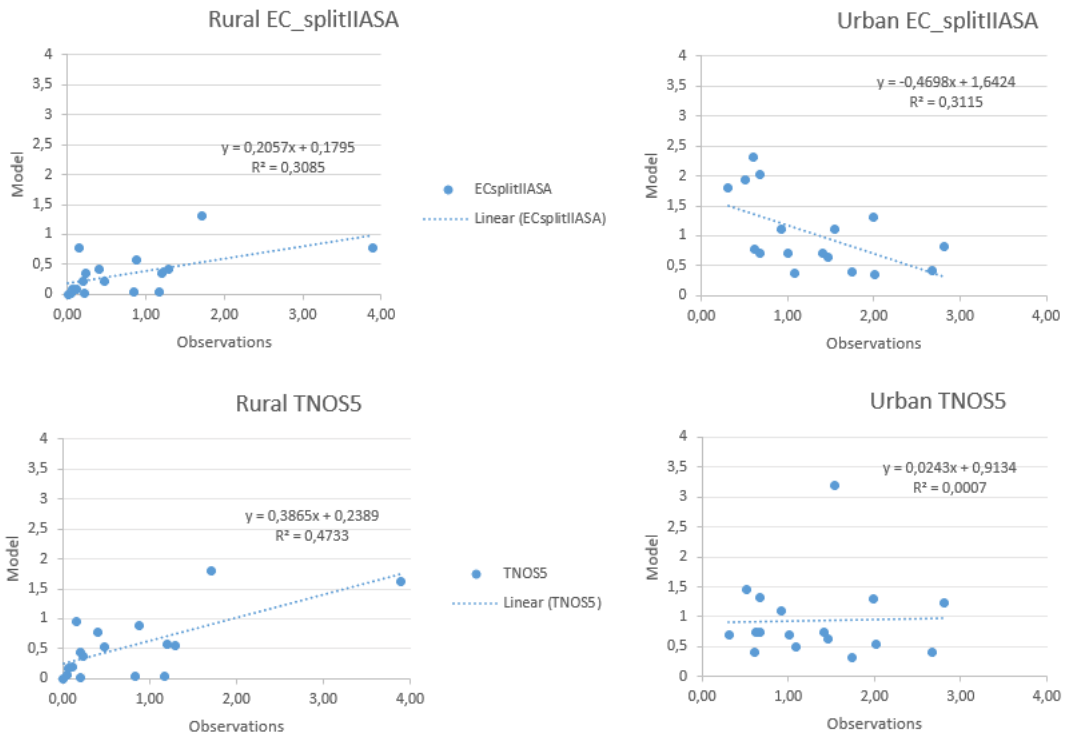

Figure 6.9: Comparison of model results of fine EC with EBC derived from observation at urban and rural sites separately (using only measurements that have paralell EC measurements/site specific MAC values).

to $PM_{2.5}$) for the residential combustion sector are spatially distributed, but some countries do have very good data available, while others might simply use population for distributing these emissions. In the latter case, the share of wood burning emissions in urban areas compared to rural areas would be substantially overestimated. The TNOS5 emissions for the residential sector are distributed based on a weighting of urban to rural population which favours the rural population. In addition, an 'access to wood factor' based on landuse maps are used, so that rural areas with a lot of forest get higher weighting. Given the potentially very different spatial distribution of emissions in the residential combustion sector, it is not surprising that the results from TNOS5 and the model results using reported EC emissions show very different correlation to the observations.

Only a subset of the EIMP data has been used in this analyses, and measurement data will become available for more sites in the near future. Further investigations, including in depth analyses of model results at the different rural and urban EIMP sites, and spatial distribution of emissions for different emission sectors and different size fractions of EC observations are needed to understand the validity and possible implications of these preliminary results.

6.10 Continuation/Work ahead

The results presented provide only a snapshot of what is possible with the core data collected in the IMP Winter 2018. In future, other issues will be addressed as well.

The results should be considered preliminary, as adjustments to the PMF approach and the

data treatment are still possible, but the PMF-approach as used here is close to a final version, and will be presented in a forthcoming paper (Platt et al., in prep.). Data will be analysed according to the PMF-approach as soon as possible after they are submitted to EBAS and found to have a sufficient data and metadata quality.

Future work will focus on investigation of 3 factor solutions. The aethalometer model can only resolve two fractions (usually defined as fossil and biomass), however there are multiple combustion sources contributing to ambient EC, e.g. coal combustion, waste burning etc. Furthermore, other sources can influence absorption (EBC) measurements to some extent, e.g. mineral dust and secondary organic aerosol (SOA). Therefore, for some locations an understanding of several sources may be important to understand the total EC/EBC, i.e. it might be reasonable to split fossil and biomass into further fractions.

So far we performed test runs of three factor PMF solutions for most of the 25 sites presented in this chapter. In these test runs we did a smaller number of runs ($n = 750$) to save on computation time. In most cases, there was no clear separation of the factor profiles as was seen for 2 factor solution (e.g. Figure 6.3). However, for the Brenner site we did find a 3 factor solution with clear separation (Figure 6.10). More work is needed to investigate whether this is repeated at other sites, and to establish the sources for each of the factors.

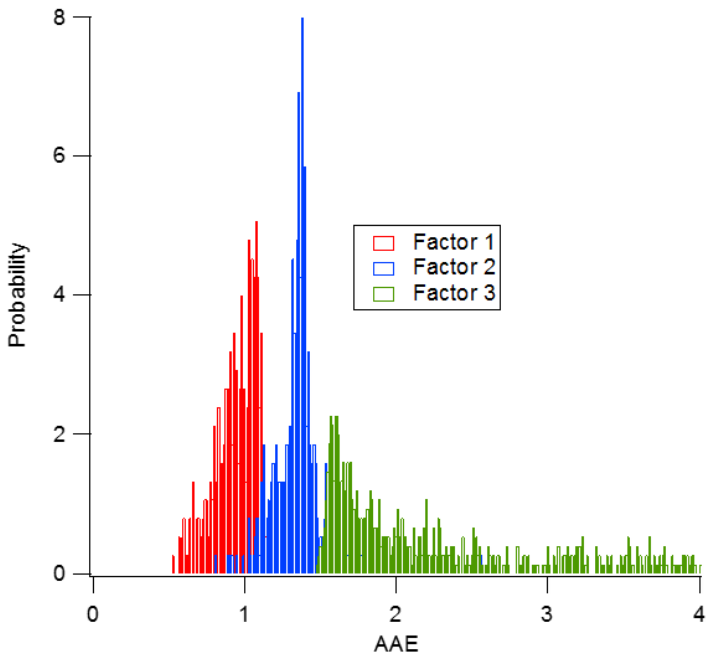

Figure 6.10: Positive matrix factorisation (3 factor solution) bootstrap runs (n=750) binned by factor-derived aerosol Ångström exponent (AAE) for the Brenner site.

The chemical transport modelling results presented in this chapter are examples of what will be possible to investigate with the EIMP data, but further investigations, including in depth analyses of model results at the different rural and urban EIMP sites, spatial distribution of emissions for different emission sectors are needed to understand the validity and possible implications of these preliminary results.

It should be noted that there are a number of important caveats with this type of exercise. An earlier study of light-absorbing carbon in Europe (Genberg et al. 2013) showed that the difference between EC and EBC can be substantial. The correlation between simultaneous

measurements of EC and EBC was found to be low at many sites in Europe, and this limits the possibility to accurately model EBC using a simple EC model (based on EC emissions and not taking into account other light-absorbing components or differences in optical properties of different BC-containing particles). Further, as noted in Genberg et al. (2013), there is an extensive and sometimes contradictory nomenclature for various forms of light-absorbing carbon (e.g. Bond and Bergström 2006), and so far we have ignored differences between the terms 'EC' and 'BC'. The EMEP model is designed for EC. The reported emissions are said to be BC, but the exact meaning is unclear.

Within the Task Force on Measurement and Modelling (TFMM), a model intercomparison excercise focused on EC is planned. This exercise will make extensive use of the EIMP data for EC and its sources.

References

Backman, J., Schmeisser, L., Virkkula, A., Ogren, J. A., Asmi, E., Starkweather, S., Sharma, S., Eleftheriadis, K., Uttal, T., Jefferson, A., Bergin, M., Makshtas, A., Tunved, P., and Fiebig, M.: On Aethalometer measurement uncertainties and an instrument correction factor for the Arctic, Atmospheric Measurement Techniques, 10, 5039–5062, doi:10.5194/amt-10-5039-2017, URL https://www.atmos-meas-tech.net/10/5039/2017/, 2017.

Bond, T. C. and Bergström, R. W.: Light Absorption by Carbonaceous Particles: An Investigative Review, Aer. Sci. Technol., 40, 27–67, doi:10.1080/02786820500421521, 2006.

Genberg, J., Denier van der Gon, H. A. C., Simpson, D., Swietlicki, E., Areskoug, H., Beddows, D., Ceburnis, D., Fiebig, M., Hansson, H. C., Harrison, R. M., Jennings, S. G., Saarikoski, S., Spindler, G., Visschedijk, A. J. H., Wiedensohler, A., Yttri, K. E., and Bergström, R.: Light-absorbing carbon in Europe - measurement and modelling, with a focus on residential wood combustion emissions, Atmospheric Chemistry and Physics, 13, 8719–8738, doi:10.5194/acp-13-8719-2013, URL http://www.atmos-chem-phys.net/13/8719/2013/, 2013.

Sandradewi, J., Prevot, A. S. H., Szidat, S., Perron, N., Alfarra, M. R., Lanz, V. A., Weingartner, E., and Baltensperger, U.: Using aerosol light absorption measurements for the quantitative determination of wood burning and traffic emission contributions to particulate matter, Environ. Sci. Technol., 42, 3316–3323, doi:10.1021/es702253m, 2008.

Virkkula, A., Mäkelä, T., Hillamo, R., Yli-Tuomi, T., Hirsikko, A., Hämeri, K., and Koponen, I. K.: A Simple Procedure for Correcting Loading Effects of Aethalometer Data, Journal of the Air & Waste Management Association, 57, 1214–1222, doi:10.3155/1047-3289.57.10.1214, URL https://doi.org/10.3155/1047-3289.57.10.1214, 2007.

Zotter, P., Herich, H., Gysel, M., El-Haddad, I., Zhang, Y., Močnik, G., Hüglin, C., Baltensperger, U., Szidat, S., and Prévôt, A. S. H.: Evaluation of the absorption Ångström exponents for traffic and wood burning in the Aethalometer-based source apportionment using radiocarbon measurements of ambient aerosol, Atmospheric Chemistry and Physics, 17, 4229–4249, doi:10.5194/acp-17-4229-2017, URL https://www.atmos-chem-phys.net/17/4229/2017/, 2017.

CHAPTER 7

Evaluation of the gridded EMEP emissions using modelling

Hilde Fagerli and Ágnes Nyíri

Since 2017, Parties to CLRTAP have been reporting gridded emissions in $0.1^\circ \times 0.1^\circ$ resolution, whilst emissions were reported in 50km $\times$ 50km resolution before. In this chapter we compare the EMEP MSC-W model results using these fine resolution emissions to model results using the older 50km $\times$ 50km resolution and to model results using CAMS-REG-AP - a widely used set of fine resolution emissions. The aim of this work is to investigate whether the model results improve compared to observations when using the finer resolution emissions reported to EMEP and if the model results can tell us something about the quality of the fine resolution emissions reported to EMEP compared to another fine resolution emission inventory available, i.e. CAMS-REG-AP.

Because the fine resolution emission inventories reported to EMEP in 2019 (for 2017) were only available in June, the work here was performed with the emission inventory reported last year (for 2016). In those inventories, fine resolution gridded emissions reported by Parties to CLRTAP were available from 27 countries. In this years inventory (for 2017), additional reported fine resolution data are available for Sweden and Malta.

All the model runs are performed for the year 2016 and compared to observations for NO_2, O_3, $PM_{2.5}$, PM_{10} and SO_2 available from AirBase.

7.1 Setup of experiments

The model runs are performed for the year 2016, using EMEP/MSC-W model version rv4.32. The horizontal resolution is $0.1^\circ \times 0.1^\circ$, with 20 vertical layers (the lowest with a height of approximately 50 meters). Meteorology, emissions, boundary conditions and forest fires for 2016 have been used as input (for a description of these input data see Simpson et al. 2012). DMS emissions are created 'on-the-fly', e.g. they are dependent on meteorology, as described in Chapter 9 in EMEP Status Report 1/2016. International shipping emission data within the

model domain are derived from FMI global shipping emissions (based on AIS tracking data). Three sets of emission data have been used:

- EMEP $0.1^\circ \times 0.1^\circ$emissions for 2016 (as reported in 2018) in GNFR categories
- CAMS-REG-AP-v3.1 $0.1^\circ \times 0.05^\circ$ emissions for 2016 in GNFR categories
- EMEP 50km $\times$ 50km emissions for 2015 (as reported in 2017) in SNAP sectors

The EMEP emissions for 2016 are described in EMEP Status Report 1/2018, Chapter 3. Reported gridded emission data (in $0.1^\circ \times 0.1^\circ$) were available for 27 countries in this data set, which is 6 more than for the previous year (emissions for 2015, reported in 2017). The remaining areas are gap filled and spatially distributed by CEIP. The 50km $\times$ 50km emission data set for 2015 is documented in EMEP Status Report 1/2017, Chapter 3. The CAMS-REG-AP-v3.1 emissions are documented in Granier et al. (2019). Overall the absolute emissions are similar to the reported emissions, but the spatial disaggregation is different. Whilst the EMEP emissions are gridded by the countries themselves (using the best available data within the country), the CAMS-REG-AP-v3.1 emissions are spatially distributed using proxy data available on the European scale.

Name	Emissions	Emission year	Meteorology	Resolution
EMEP_{01}	EMEP $0.1^\circ \times 0.1^\circ$in GNFR	2016	2016	$0.1^\circ \times 0.1^\circ$
CAMS_TNO	CAMS-REG-AP $0.1^\circ \times 0.05^\circ$ in GNFR	2016	2016	$0.1^\circ \times 0.1^\circ$
EMEP_{50km}	EMEP 50km $\times$ 50km in SNAP	2015	2016	$0.1^\circ \times 0.1^\circ$

Table 7.1: Overview of model runs.

An overview of the model runs can be found in Table 7.1. Ideally, the EMEP 50km $\times$ 50km emissions should have been representative for 2016. However, a scaling of the 2015 emissions to 2016 is not straightforward, as the 2 emission data sets vary in their sector definitions (SNAP versus GNFR). A scaling of the absolute emissions per country is possible, but will not influence the spatial distribution, and thus only to a minor extent affect the results we are interested in here. We therefore chose to keep the 2015 emissions as in the original emission data set, except the international shipping emissions which are the same as in the 2016 EMEP emissions.

Observations

The AirBase data for NO_2, O_3, SO_2, $PM_{2.5}$ and PM_{10} for 2016 has been used (as downloaded in 2018). We have chosen to exclude traffic stations from our comparison, since it is not meaningful to compare the somewhat coarse model data to observational data from curb sites.

7.2 Results

NO_2

The main source of NO_x is traffic, which is a low level source, and one would therefore expect high correlations between emissions and surface concentrations of NO_2. Thus one

would expect that improved spatial distribution of NO_x emissions should result in improved spatial distribution of NO_2 concentrations.

Spatial correlation between model runs of $EMEP_{50km}$, $EMEP_{0.1}$ and CAMS_TNO and observations for each country is presented in Figure 7.1. For NO_2, there is a clear improvement with higher resolution of the emissions for almost all countries (e.g. both in $EMEP_{0.1}$ and CAMS_TNO). There are only a few exceptions; for Bulgaria the correlation is lower in CAMS_TNO than in $EMEP_{50km}$, but highest in $EMEP_{0.1}$ (but the correlation is in general low for Bulgaria). For Slovenia, $EMEP_{50km}$ has the highest spatial correlation compared to the observations. Finally, for Montenegro the correlation is negative for the model results with fine resolution emissions (but there are only 2 measurement sites, so these results should not be put much weight on). For all other countries, $EMEP_{0.1}$ and CAMS_TNO compare better with observations than $EMEP_{50km}$ in terms of spatial correlation.

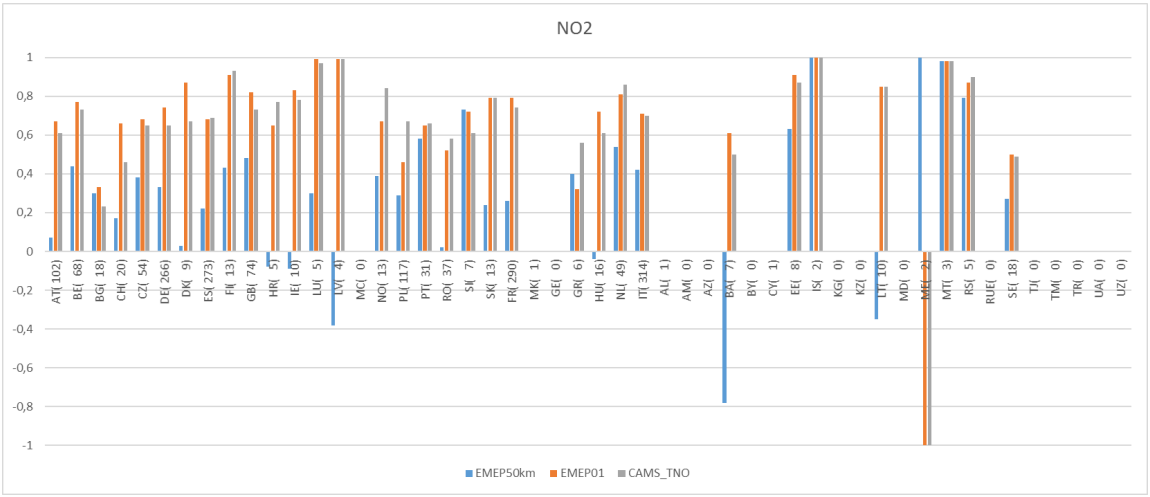

Figure 7.1: Spatial correlation coefficient for annual averages of model results (see table 7.1 for the definition) versus AirBase observations for NO_2. The number of stations used in the comparison for each country is given in parentheses. The countries AT to NL reported fine resolution emissions to EMEP, the other countries were gridded by CEIP.

Interestingly, $EMEP_{0.1}$ has higher (or similar) spatial correlation compared to observations than CAMS_TNO in most cases - suggesting that the gridding performed by the countries are superior to the gridding done for CAMS-REG-AP. This may not be surprising, as the gridding done by the countries in most cases are based on national data, that are probably better than the European-wide proxies used for CAMS-REG-AP. There are some exceptions though; for Norway, Poland and Greece the CAMS-REG-AP emissions yields better results than the $EMEP_{0.1}$ emissions - indicating the need to revisit the gridding performed by these countries.

In Figure 7.2 for Denmark and Great Britain respectively, scatter plots of the 3 different model runs against observations are presented, showing excellent comparison of the $EMEP_{0.1}$ model run both in terms of spatial correlation and bias. On the contrary, the scatterplots for Poland and Norway in Figure 7.3 show that using the CAMS-REG-AP emissions gives better results than using $EMEP_{0.1}$ emissions.

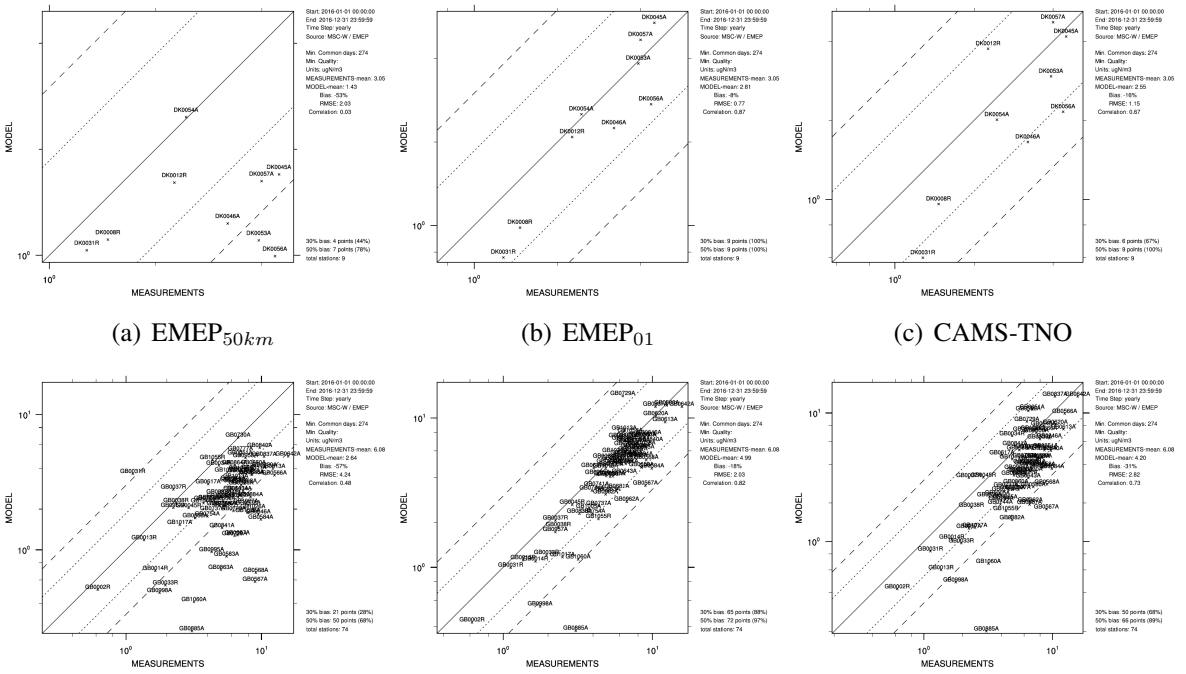

(a) EMEP_{50km} (b) EMEP_{01} (c) CAMS-TNO

(d) EMEP_{50km} (e) EMEP_{01} (f) CAMS-TNO

Figure 7.2: Comparison of model and observations (annual average) for Denmark (a), b) and c)) and Great Britain (d), e) and f)) for NO_2 (see table 7.1 for the definition).

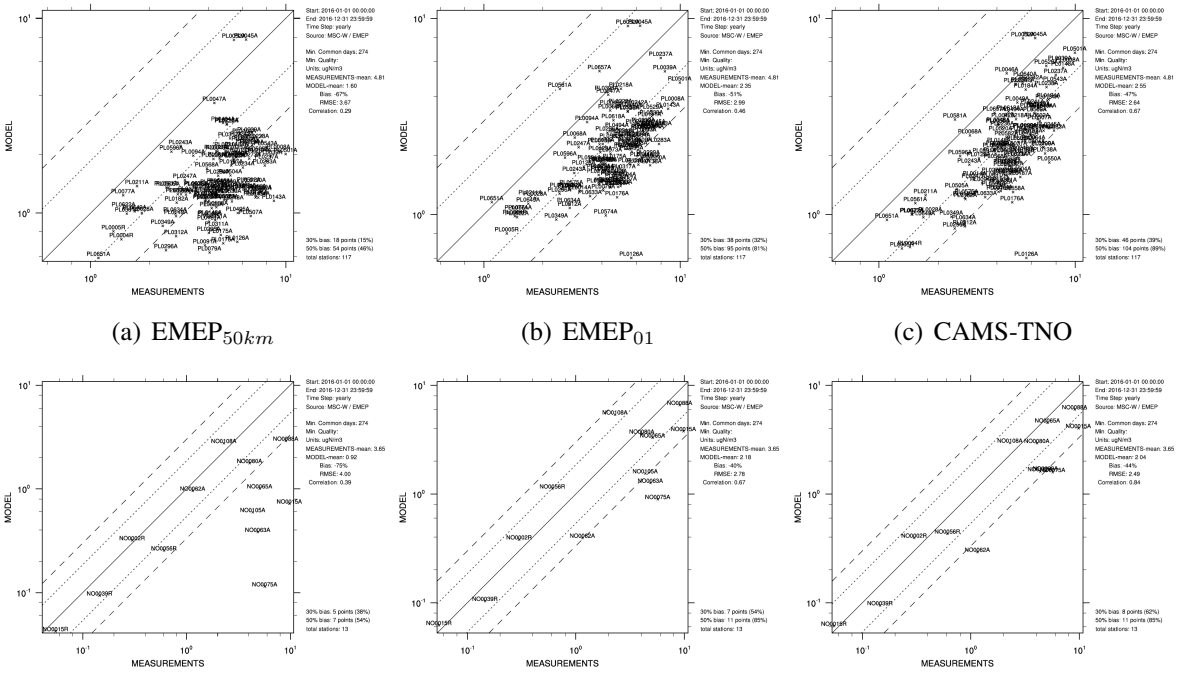

(a) EMEP_{50km} (b) EMEP_{01} (c) CAMS-TNO

(d) EMEP_{50km} (e) EMEP_{01} (f) CAMS-TNO

Figure 7.3: Comparison of model and observations (annual average) for Poland (a), b) and c)) and Norway (d), e) and f)) for NO_2 (see table 7.1 for the definition).

SO_2

Because the emission sources of SO_2 to a large extent are higher level sources, the correlation of emissions and surface concentrations is less evident than for NO_2. Despite this, the spatial correlations for most countries are better in $EMEP_{0.1}$ than in $EMEP_{50km}$, as shown in Figure 7.4, although the improvements are not as large as for NO_2. For some countries, like Finland, Great Britain, the Netherlands, Germany, Norway and Czech Republic, the correlations improve a lot. For other countries, like Bulgaria and Poland, the correlations decrease somewhat.

As expected, the improvements in spatial correlation for SO_2 are not as large as for NO_2 when using finer resolution emissions. Moreover, the performance of $EMEP_{01}$ and CAMS-TNO are rather similar.

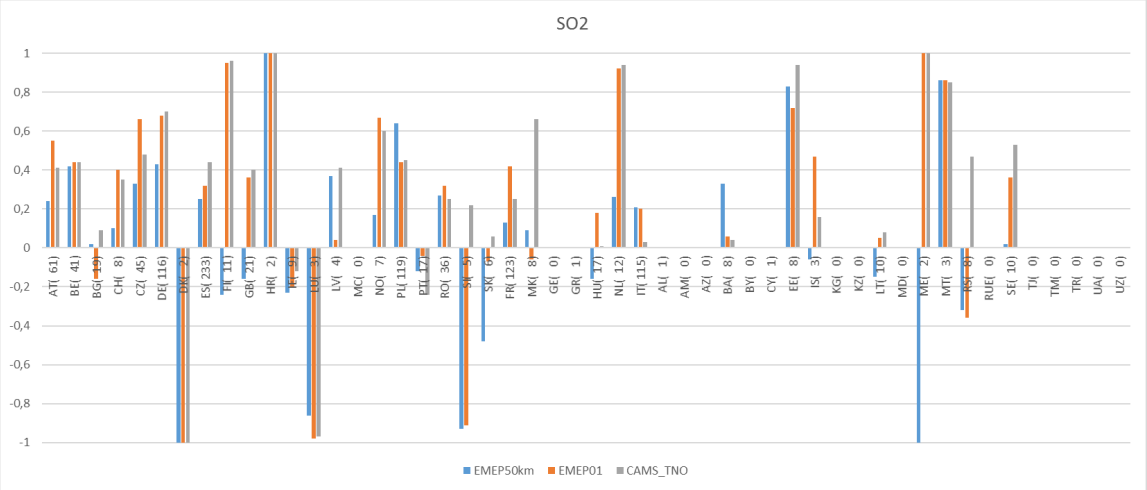

Figure 7.4: Spatial correlation coefficient for annual averages of model results (see table 7.1 for the definition) versus AirBase observations for SO_2. The number of stations used in the comparison for each country is given in parentheses. The countries AT to NL reported fine resolution emissions to EMEP, the other countries were gridded by CEIP.

O_3

As shown in Figure 7.5, there is systematically better agreement in terms of spatial correlation between observations and modelled annual mean concentrations of O_3 for the model runs using fine resolution emissions. Annual mean ozone concentrations are closely linked to the annual mean NO_2 concentrations through local titration effects, thus it is expected that improved spatial correlation of NO_2 would lead to improved spatial correlation of O_3. However, while $EMEP_{0.1}$ correlated better to observations than CAMS-TNO for NO_2, the overall results for ozone annual averages are rather similar.

$PM_{2.5}$ and PM_{10}

For the majority of countries, spatial correlations between modelled PM concentrations and observed PM concentrations, shown in Figures 7.6 and 7.7, improve using the fine resolution emissions. For some countries this is not the case, e.g. Bulgaria, Poland, Slovenia and Slovakia show worse results for PM_{10} for $EMEP_{0.1}$ than for $EMEP_{50km}$.

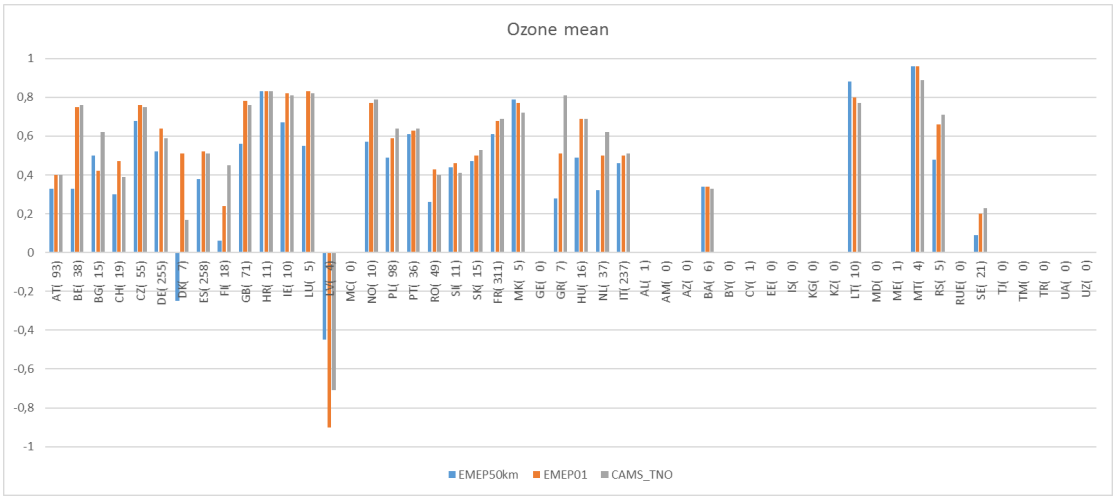

Figure 7.5: Spatial correlation coefficient for annual averages of model results (see table 7.1 for the definition) versus AirBase observations for O_3. The number of stations used in the comparison for each country is given in parentheses. The countries AT to NL reported fine resolution emissions to EMEP, the other countries were gridded by CEIP.

There is no systematic difference between the $EMEP_{0.1}$ and CAMS-TNO model runs, but as these components are secondary species with precursors from numerous sources, this is not expected.

7.3 Conclusions

In this chapter we have investigated the spatial distribution of EMEP MSC-W model runs with 3 different sets of emissions; 1) with EMEP 50km $\times$ 50km resolution, 2) with EMEP $0.1^\circ \times 0.1^\circ$ resolution and 3) with CAMS-REG-AP $0.1^\circ \times 0.05^\circ$ resolution. The model has been run with $0.1^\circ \times 0.1^\circ$ resolution meteorology for 2016 for all cases. The model results have been compared to AirBase observations for 2016 for each country individually.

The largest improvement in going from 50km $\times$ 50km resolution is seen for NO_2, which can be explained by the high correlations between emissions and surface concentrations of NO_2. Interestingly, $EMEP_{0.1}$ has higher (or similar) spatial correlation compared to observations than CAMS_TNO for NO_2 for most countries - suggesting that the gridding performed by the countries are superior to the gridding done for CAMS-REG-AP. This may not be surprising, as the gridding done by the countries in most cases are based on national data, that are probably better than the European-wide proxies used for CAMS-REG-AP.

The spatial correlations between model results and observations improve with the resolution of emissions (for most countries) for all the other components investigated as well, but not as much as for NO_2. This can be explained by the weaker correlation of surface concentrations and emissions for those components, and that there are many precursors for secondary components from different sources.

For some countries, the model runs with fine resolution EMEP emissions showed worse correlation to observation than the CAMS-REG-AP fine resolution emissions. For NO_2 this concerns especially Norway and Poland, for which it would be worthwhile looking further into the spatial distribution of the emissions.

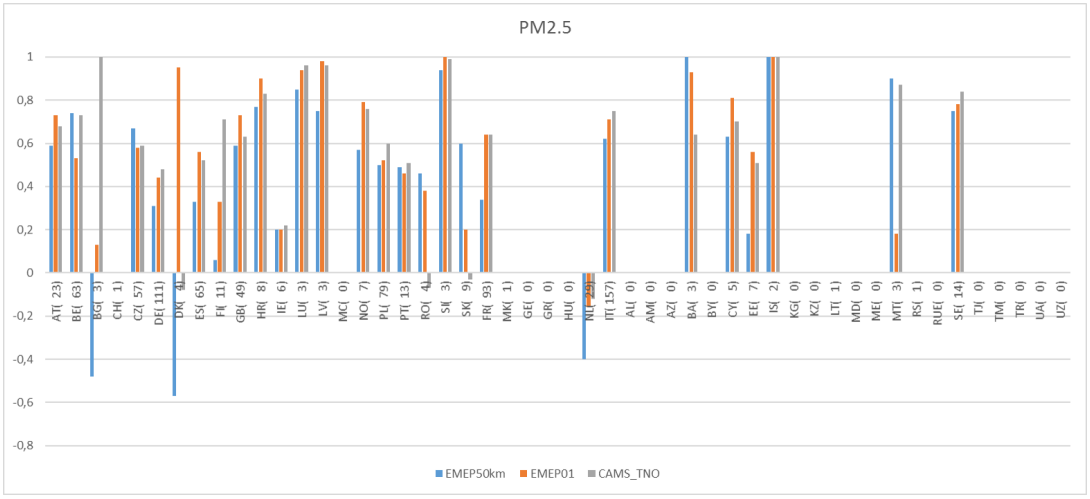

Figure 7.6: Spatial correlation coefficient for annual averages of model results (see table 7.1 for the definition) versus AirBase observations for $PM_{2.5}$. The number of stations used in the comparison for each country is given in parentheses. The countries AT to NL reported fine resolution emissions to EMEP, the other countries were gridded by CEIP.

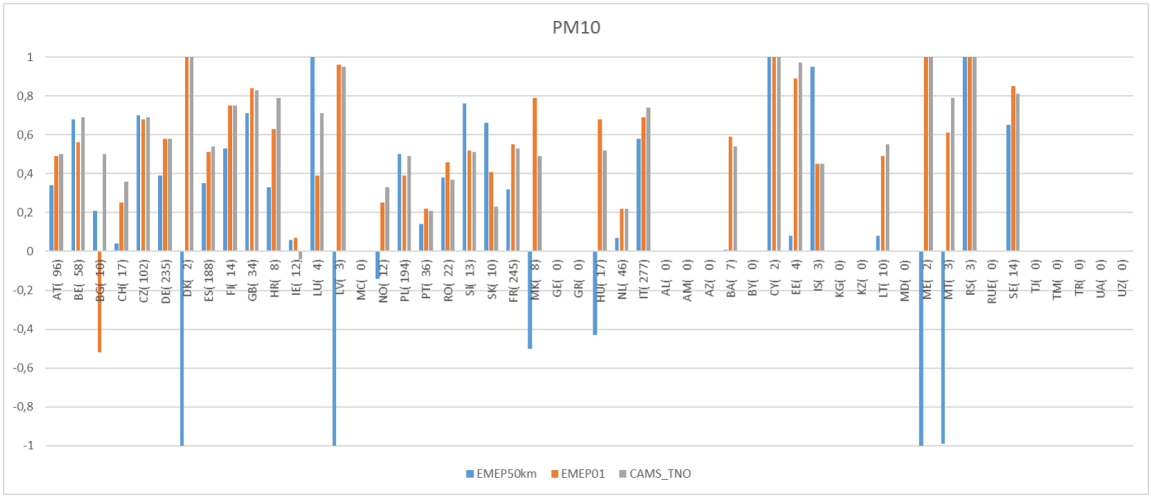

Figure 7.7: Spatial correlation coefficient for annual averages of model results (see table 7.1 for the definition) versus AirBase observations for PM_{10}. The number of stations used in the comparison for each country is given in parentheses. The countries AT to NL reported fine resolution emissions to EMEP, the other countries were gridded by CEIP.

References

Granier, C., Darras, S., Denier van der Gon, H., Doubalova, J., Elguindi, N., Galle, B., Gauss, M., Guevara, M., Jalkanen, J.-P., Kuenen, J., Liousse, C., Quack, B., Simpson, D., and Sindelarova, K.: The Copernicus Atmosphere Monitoring Service global and regional emissions (April 2019 version), doi:10.24380/d0bn-kx16, URL https://atmosphere.copernicus.eu/sites/default/files/2019-06/cams_emissions_general_document_apr2019_v7.pdf, 2019.

Simpson, D., Benedictow, A., Berge, H., Bergström, R., Emberson, L. D., Fagerli, H., Hayman, G. D., Gauss, M., Jonson, J. E., Jenkin, M. E., Nyíri, A., Richter, C., Semeena, V. S., Tsyro, S., Tuovinen, J.-P., Valdebenito, A., and Wind, P.: The EMEP MSC-W chemical transport model – technical description, Atmos. Chem. Physics, 12, 7825–7865, doi:10.5194/acp-12-7825-2012, 2012.

CHAPTER 8

Baltic Sea shipping: Effects of the 2015 SECA regulations and perspectives for the future

Jan Eiof Jonson, Lars Barregård, Peter Molnár, Jukka-Pekka Jalkanen, Leo Stockfelt and Lasse Johansson

8.1 Background

Both the North Sea and the BAS (Baltic Sea) have been accepted by the IMO (International Maritime Organisation) as SECA (Sulphur Emission Control Areas) regions. From 1 January 2015 the maximum allowed sulphur content in marine fuels was reduced from 1% to 0.1%. Fuels with higher sulphur content may be used in combination with technology reducing sulphur emission to levels corresponding to the use of low sulphur fuels. The two sea areas are also designated as NECAs (NO_x Emission Control Areas) from 2021. Only gradual reductions of NO_x emissions are expected as the NECA regulation only applies to new ships or major modifications of existing ships.

In this chapter we present some of the results from the EU InterReg project EnviSum (`https://projects.interreg-baltic.eu/projects/envisum-16.html`) where The Norwegian Meteorological Institute has been a partner. The goals for the EnviSum project have been to provide policy makers and authorities with tools and recommendations for the development of future environmental regulations, and the shipping sector with guidance to support future investment decisions. In the project we addressed measurement and modelling strategies to assess present and future cost and the health and environmental effects of ship emissions. In particular we have studied the effects of the stricter SECA regulations that entered into force in 2015 in the BAS (and in the North Sea). Furthermore we have also looked into the effects of future (2030) emission reductions. Parts of the results from the EnviSum project are now published as two companion papers. In the first paper (Jonson et al. 2019) we present regional model calculations of the effects of emissions from BAS shipping on air pollutants and deposition in the region before and after 1 January 2015. Furthermore

we also include calculations with projections for land based and ship emissions for year 2030. In the second paper (Barregård et al. 2019) the results from the first paper are used to estimate the health benefits from the implementation of the 2015 SECA regulations. A resume of these two papers are given here.

8.2 Paper 1: Effects of strengthening the Baltic Sea ECA regulations

In this paper we have calculated the effects of ship emissions in the BAS on air pollution and depositions of oxidised sulphur and nitrogen in adjacent countries. Calculations have been made applying BAS emissions prior to (2014) and after (2016) the implementation of the stricter SECA regulations, which went into force on 1 January 2015. Furthermore, model calculations have been made with future (2030) land-based emissions and ship emissions. For a more detailed description of the model results, including also depositions of oxidised nitrogen and sulphur, we refer to the original publication (Jonson et al. 2019).

8.2.1 Emissions

Land-based emissions used in this study are from the European FP7 project ECLIPSE. In this study we use version 5a (hereafter 'ECLIPSEv5a'), a global emission data set on 0.5 x 0.5 degree resolution, which has been widely used in recent years by the scientific community (`http://www.iiasa.ac.at/web/home/research/researchPrograms/air/ECLIPSEv5.html`).

The emissions from shipping have been calculated with the Ship Traffic Emission Assessment Model (STEAM) based on ship movements from the automatic identification system (AIS) providing real time information on ship positions. The model requires as input detailed technical specifications of all onboard fuel-consuming systems and other relevant technical details for all ships considered. The data from IHS Global (2017) constituted the most significant source for this information. The STEAM model is described in Jalkanen et al. (2009, 2012, 2016) and Johansson et al. (2013, 2017). Hourly emissions for BAS ship emissions were produced based on vessel-specific modelling, considering the changes in fuel sulphur content that occurred between 2014 and 2016. For other sea areas, emissions from 2015 was used. Also these emissions were calculated with the STEAM model. These 2015 emissions were also used in the 2018 EMEP main report (Jonson et al. 2018a).

From 2021 onward, NO_x emissions for new ships have to comply with IMO Tier 3 regulations in both the BAS and the North Sea. These regulations were taken into account when modelling the emissions, as well as other factors such as fleet size increase and energy efficiency improvements.

As the ship emission data are used for multiple meteorological years, we did not retain the high (hourly) temporal resolution in the data but rather aggregated them to monthly resolution before use in the chemistry transport model.

8.2.2 EMEP Model setup

Concentrations of air pollutants and depositions of sulphur and nitrogen have been calculated with the EMEP MSC-W model (hereafter 'EMEP model'), version rv4.14, on a 0.1 x 0.1

degrees resolution for the domain between 30 degrees W and 45 degrees E and between 30 and 75 degrees N. All model scenarios have been run for the three meteorological years 2014, 2015 and 2016, and then averaged, in order to cancel out meteorological variability. The simulations are:

- Present_Base: Base case with ship emissions of 2016. Land-based emissions for 2015 (from ECLIPSEv5);
- Present_NoShip: As Present_Base, but without ship emissions in the BAS;
- Present_HiSulphur: As Present_Base, but with ship emissions of 2014 (i.e high sulphur content) in the BAS;
- Future_Base: Ship emissions of 2030 (assuming NECA and business as usual development) and land-based emissions of 2030 (from ECLIPSEv5);
- Future_NoShip: As Future_Base, but without ship emissions in the BAS.

8.2.3 Model results

For all model scenarios results are shown as averages for the three meteorological years, focusing on the BAS region. Below we discuss the effects on air pollution. The effects on depositions of oxidised nitrogen and sulphur shown in Jonson et al. (2019) are not included in this resume.

Air pollution due to Baltic Sea shipping

Concentrations of NO_2 for Present_Base are shown in Figure 8.1a. The concentrations largely reflect the locations of the main source areas. Concentrations of NO_2 are high in Central Europe and in and around the English Channel with markedly lower concentrations north and east of the BAS region. The major ship tracks are clearly visible. Figure 8.1c shows the percentage difference between the Present_Base and the Present_NoShip scenarios. The calculations show that ship emissions account for more than 50% of NO_2 in central parts of the BAS area and for a substantial percentage also in coastal zones, in particular in Denmark, southern parts of Sweden, Finland and the Baltic states (Estonia, Latvia and Lithuania). This is also reflected in the measurements. In Table 8.1 measured NO_2 at sites located in Baltic coastal regions are compared to the Present_Base, Present_NoShip and Present_HiSulphur model calculations calculated with 2016 meteorology. The corresponding time series plots for NO_2 are shown in Jonson et al. (2019). In the Present_NoShip case NO_2 levels are clearly underestimated and correlations and RMS errors deteriorated compared to the Present_Base calculation, in particular for those sites located close to major shipping routes. The comparisons with measurements convincingly show that these measurements can only be reproduced with BAS ship emissions included.

Measured SO_2 levels (Table 8.1) for 2016 are relatively well reproduced by the model for the Present_Base calculation. The corresponding time series plots for SO_2 are shown in Jonson et al. (2019). The effects of excluding the Baltic Sea ship emissions in the Present_NoShip scenario have only minor effects on the SO_2 levels. Replacing 2016 BAS emissions with 2014 (Present_HiSulphur) has much larger effects, resulting in an overestimation of SO_2 levels at most of the sites listed in Table 8.1, and in particular so for Anholt and Råö, located very close

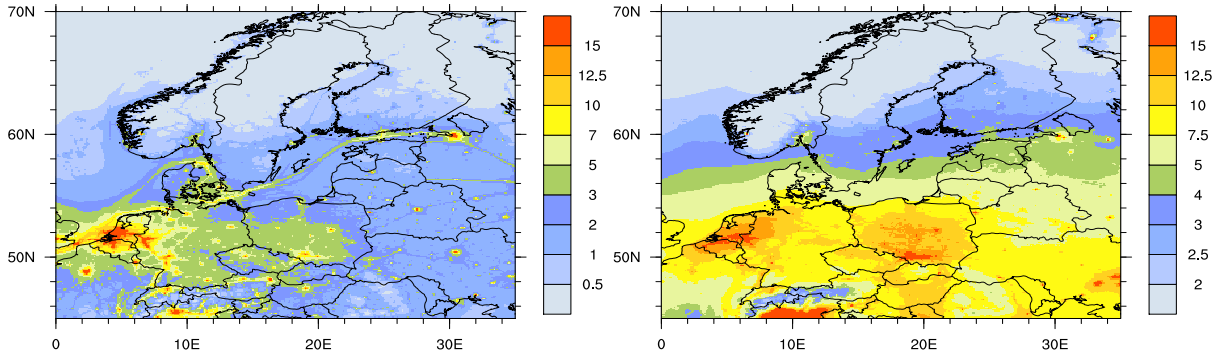

a) Present_Base NO_2 concentrations in μgm^{-3} **b)** Present_Base $PM_{2.5}$ concentrations in μgm^{-3}

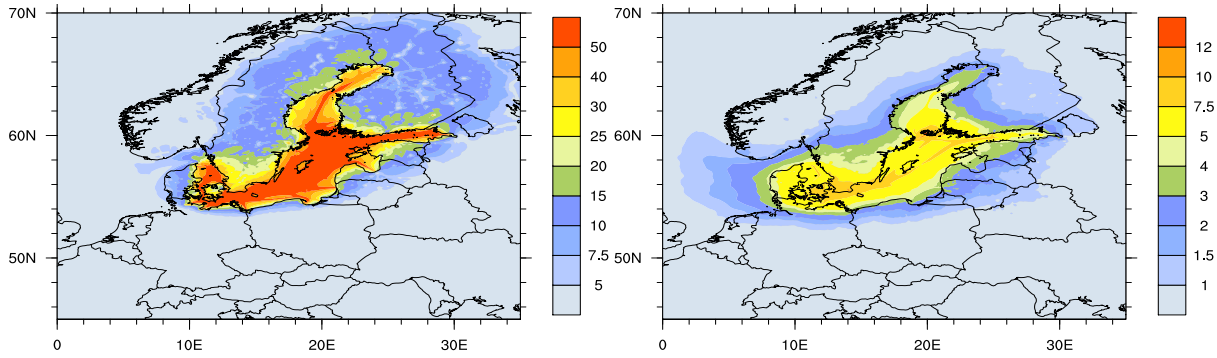

c) NO_2 Present_Base – Present_NoShip in % **d)** $PM_{2.5}$ Present_Base – Present_NoShip in %

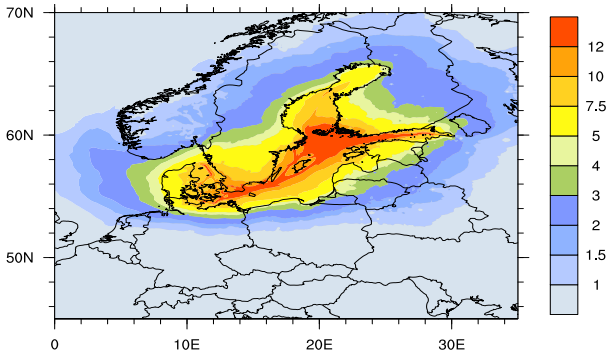

e) $PM_{2.5}$ Present_HiSulphur – Present_NoShip in %

Figure 8.1: Top panels: concentrations of NO_2 and $PM_{2.5}$ in the Present_Base case. Middle panels: present percentage contribution from BAS ship emissions to NO_2 and $PM_{2.5}$ after the new sulphur regulations. Bottom panel: percentage contribution to $PM_{2.5}$ concentrations before the new sulphur regulations. Figure adapted from Jonson et al. (2019).

to major shipping routes. This clearly illustrates the effects of the stricter SECA regulations. With the high ship emissions of 2014, the measurements for 2016 can not be reproduced. This is also a strong indication that the ships are largely in compliance with the SECA regulations.

$PM_{2.5}$ in the atmosphere is a mixture of many chemical species of both natural and anthropogenic origins. It is emitted both as a primary pollutant and formed as a secondary pollutant in the atmosphere. As a result $PM_{2.5}$ concentrations are more spread out compared to NO_2. As shown in Figure 8.1b concentrations decrease from south to north from a maximum in central Europe. As shown in Figure 8.1d the percentage contributions from BAS shipping,

Table 8.1: Annual average measured (Obs) and model calculated concentrations (Calc) of NO_2 and SO_2 for the present (2016) Base, NoShip, HiSulphur scenarios. Also listed are normalized mean bias (NMB), the daily correlations (Corr) and RMS errors (RMS) between model and measurements. The timeseries plots for the same sites are shown in Jonson et al. (2019). Km is a classification of the distance in kilometres between the stations and the Baltic Sea coast. The distance is equal to or smaller than distance listed. Table adapted from Jonson et al. (2019).

NO_2

			Base				HiSulphur				NoShip			
Station	Km	Obs	Calc	NMB	Corr.	RMS	Calc.	NMB	Corr	RMS	Calc	NMB	Corr.	RMS
Aspvreten	10	0.44	0.44	0.00	0.50	0.28	0.44	0.00	0.48	0.28	0.31	-0.25	0.48	0.31
Råö	10	1.09	1.06	-0.03	0.58	0.73	0.99	-0.09	0.60	0.70	0.46	-0.48	0.60	0.91
Hallahus	50	0.96	0.85	-0.11	0.71	0.52	0.84	- 0.12	0.71	0.52	0.58	-0.40	0.70	0.64
Anholt	10	1.48	0.98	- 0.34	0.73	0.96	0.92	-0.38	0.76	0.99	0.35	-0.76	0.66	1.55
Keldsnor	10	2.47	1.89	-0.23	0.69	1.52	1.78	-0.28	0.72	1.55	0.58	-0.77	0.58	2.52
Rucava	100	0.75	0.38	-0.49	0.63	0.56	0.38	-0.49	0.63	0.56	0.30	-0.60	0.57	0.63
Zingst	10	2.10	0.96	-0.46	0.65	1.48	0.96	-0.46	0.65	1.48	0.52	-0.75	0.53	1.89
Utö	10	0.95	-0.40	0.57	0.76	0.58	0.59	-0.38	0.76	0.56	0.17	-0.82	0.25	1.00

SO_2

			Base				HiSulphur				NoShip			
Station	Km	Obs	Calc	NMB	Corr.	RMS	Calc.	NMB	Corr	RMS	Calc	NMB	Corr.	RMS
Aspvreten	10	0.10	1.50	0.25	0.11	0.34	0.30	2.00	0.13	0.38	0.25	1.50	0.11	0.34
Råö	10	0.12	0.09	-0.25	0.29	0.12	0.22	0.83	0.31	0.21	0.07	-0.42	0.26	0.13
Hallahus	50	0.13	0.08	0.14	0.58	0.16	0.21	0.62	0.55	0.19	0.13	0.00	0.61	0.15
Utö	10	0.15	-0.40	0.09	0.23	0.27	0.23	0.53	0.12	0.30	0.08	-0.47	0.24	0.28
Anholt	10	0.10	0.10	0.00	0.72	0.08	0.28	1.80	0.61	0.30	0.07	-0.30	0.66	0.08
Risø	10	0.13	0.19	0.37	0.59	0.18	0.26	1.00	0.64	0.23	0.17	0.13	0.59	0.17
Vilsandi	10	0.30	0.11	-0.63	0.37	0.43	0.18	-0.40	0.28	0.42	0.10	-0.67	0.38	0.43
Zingst	10	0.29	0.27	-0.07	0.74	0.30	0.40	0.38	0.71	0.33	0.25	-0.14	0.74	0.31
Rucava	100	0.20	0.18	-0.10	0.48	0.30	0.21	0.05	0.48	0.30	0.18	-0.10	0.48	0.30

calculated as Present_Base – Present_NoShip, are much smaller for $PM_{2.5}$ than for NO_2 but with noticeable contributions in coastal zones, in particular in parts of Denmark, Sweden and Finland. Figure 8.1e shows higher contributions when assuming BAS shipping at 2014 levels (Present_HiSulphur), prior to the implementation of the stricter SECA regulations. In Jonson et al. (2019) these results are also illustrated in the comparisons of model scenario calculations at the measurement sites located in Baltic Sea coastal regions. For $PM_{2.5}$ differences between the Present_Base and the Present_NoShip cases are much smaller than for NO_2. Likewise, differences are smaller than for SO_2 between Present_Base and Present_HiSulphur. In Jonson et al. (2019) we show that both the measured and model calculated fraction of SO_4 in $PM_{2.5}$ is about 0.15, and this fraction increase only marginally with the Present_HiSulphur scenario.

The model results underestimate the measurements of $PM_{2.5}$ at most of the sites listed. Based only on the comparisons between measurements and the different model scenarios for $PM_{2.5}$ one can not conclude that the Present_Base scenario is more realistic than the other two.

Contributions to individual countries from BAS shipping.

Figure 8.2 shows the concentrations of NO_2, SO_2 and $PM_{2.5}$ averaged over individual countries bordering the BAS. The black (Present) and green (Future) bars represent contributions from all other sources (both anthropogenic and natural) than BAS shipping. The blue part of the bars represents the (present and future) contributions from BAS shipping calculated as Base – NoShip where Base can be either Present_Base or Future_Base and NoShip can be either Present_NoShip or Future_NoShip. The red part is the additional BAS contributions

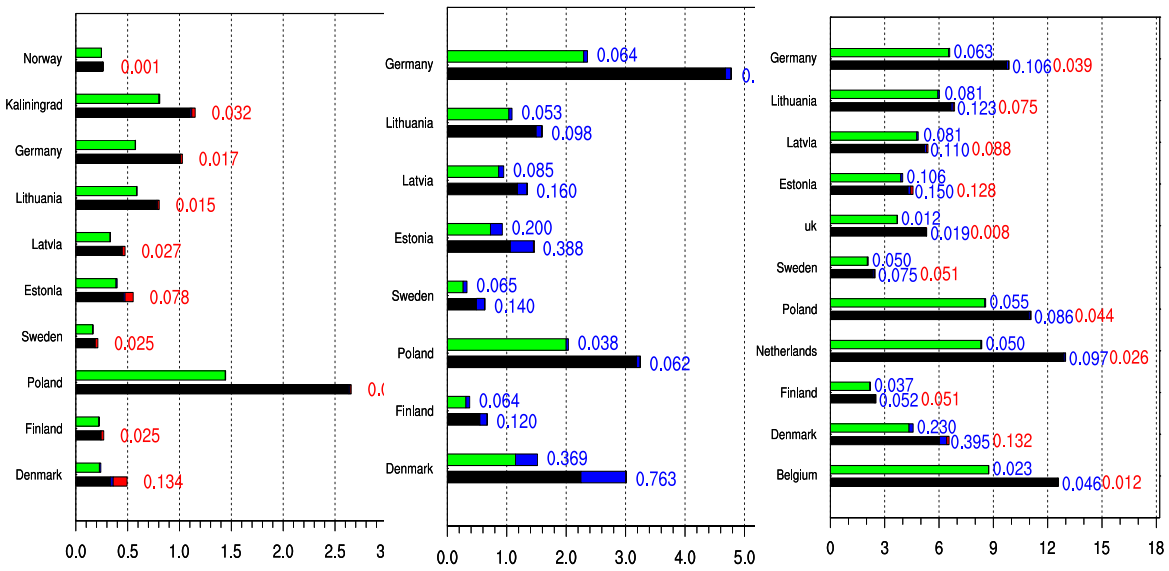

a) SO_2 in μgS/m ^{3} **b)** NO_2 in μgN/m ^{3} **c)** $PM_{2.5}$ in μg/m ^{3}

Figure 8.2: For each country, the upper bar shows the future (2030) case and the lower bar the present case country average concentration of a) SO_2, b) NO_2 and c) $PM_{2.5}$. The black and green bars represent the Present_NoShip and Future_NoShip calculations respectively. The additional contributions from BAS (Add Baltic) are shown in blue and the additional effect assuming high sulphur fuel emissions (Add Baltic 2014) in red (These are also given as numbers. Numeric values for NO_2 Add Baltic and for SO_2 Add Baltic 2014 not given as they are very small).

assuming BAS ship emissions at 2014 levels calculated as Present_HiSulphur – Present_Base. The full length of the bars then represent the total average concentration burden for the countries. The calculations are made assuming linearity. Previous calculations, adding up contributions from different sources, have shown that this assumption is reasonable (Jonson et al. 2017, 2018b). Irrespective of species and depositions, the largest contributions are seen for smaller countries with long coastlines exposed to the Baltic Sea as Denmark and the Baltic States, and the least for large countries as Germany and Poland with major parts of their areas located far inland from the shipping routes.

Following the expected reductions between 2016 and 2030 in both land-based and ship emissions, calculated concentrations and depositions (see Jonson et al. (2019) for deposition results) are reduced over the 2016 to 2030 time-span. For SO_2 and depositions of sulphur, BAS shipping is already an insignificant source in 2016 and the differences between 2030 and 2016 are almost entirely caused by changes in land-based emissions. For NO_2 concentrations and depositions of oxidised nitrogen, reductions of land-based and BAS ship emissions both contribute to the improvements in pollution levels. In the BAS region the fractional reductions of future concentrations attributed to (mainly) land-based, and to BAS ship emissions are roughly in the same range.

The largest contributions from BAS shipping is seen for NO_2 (Figure 8.2b) and partially also for SO_2 (Figure 8.2a) when assuming 2014 emissions (Present_HISulphur). However, for SO_2 calculated contributions are insignificant following the implementation of the stricter SECA in 2015. $PM_{2.5}$ contributions from BAS shipping are markedly smaller than for NO_2 even though contributions are higher when assuming Present_HiSulphur emissions. After the implementation of stricter SECA regulations in 2015, $PM_{2.5}$ from shipping mainly originates

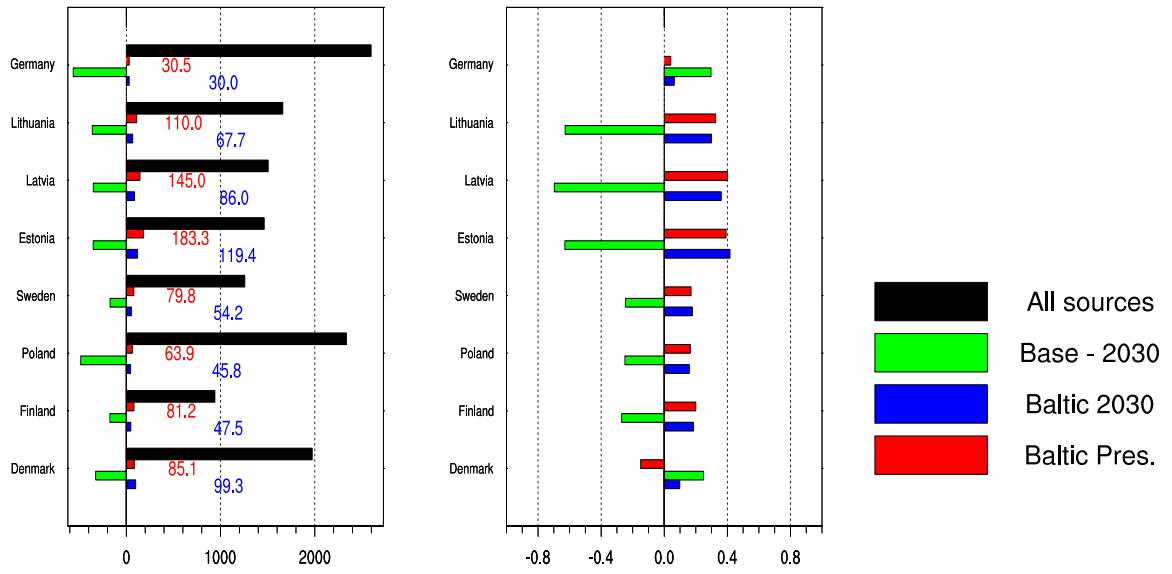

a) SOMO35 in ppb days **b)** ozone differences in ppb

Figure 8.3: Left, SOMO35 in ppb days where black bars represent Present_Base levels. Right, changes in annual ozone in ppb (annual average ozone is in the 30 - 35 ppb range in all countries). For both SOMO35 and annual ozone blue bars represent changes in levels from 2016 to 2030 (Present_Base – Future_Base), red bars: contributions from BAS (Present_Base – Present_NoShip) , green bars: contributions from BAS in 2030 (Future_Base – Future_NoShip) Figure adapted from Jonson et al. (2019).

from NO_2 and, in part, primary PM emissions. As shown in Figure 8.1d,e elevated $PM_{2.5}$ concentrations from BAS shipping are mainly seen in coastal zones close to shipping lanes.

Figure 8.3 (left) shows calculated SOMO35[1] as an average for countries around the BAS and the effect of BAS shipping. The effects on annual average ozone are shown in the same figure (right). For all countries annual averaged ozone is in the 33 - 37 ppb range. For most countries both SOMO35 and annually averaged ozone increase only slightly as a result of BAS shipping, and relatively more so for SOMO35 than for annually averaged ozone. However, in Denmark emissions from BAS shipping result in a decrease in annually averaged ozone with present emissions.

Changes in ozone are caused by a combination of ozone production, mainly in the summer months, and ozone titration by NO, mainly in winter. In winter reductions in NO_x emissions (including reductions in emissions from ships) result in a decrease in ozone titration. As a result calculated ozone winter levels in 2030 are higher than in 2016 throughout northern and central Europe. Ozone production dominates in the summer months and with the exception of a region around the English channel, the expected reductions in the emissions of ozone precursors result in lower ozone levels in 2030. For SOMO35 the relative increase in winter is much smaller as ozone is largely below the 35 ppb threshold. In summer the increase caused by titration around the English channel is confined to a much smaller area. As a result annually average ozone production and titration in the Baltic Sea region partially cancel out, and for some regions and countries titration dominates the annual values. As shown in Figure 8.3 the expected emission reductions (land based and from ships) from year 2016 to 2030 result

[1]SOMO35 is the indicator for health impacts recommended by WHO calculated as the daily maximum of 8-hour running ozone maximum over 35 ppb, defined in chapter 1.2 (Definitions, statistics used)

in overall reductions in ozone levels (both annually averaged ozone and SOMO35) for all countries except Germany and Denmark, where calculated average ozone levels are higher in 2030 (but SOMO35 is reduced). In 2030 the additional emissions from BAS shipping result in increased SOMO35 and annually average ozone in all countries except Denmark. Here average ozone decreases (in contrast to the case in 2016, where SOMO35 increases when adding the emissions from BAS shipping). These results are in good agreement with detailed model calculations with projected emission changes, demonstrating a future transition from NMVOC[2]-limited to NO_x-limited regimes in large parts of Europe north of the Alps (Beekmann and Vautard 2010).

It has to be noted that in our model calculations the ship emissions are instantly diluted throughout the model grid cell where the emissions occur. Previous studies (Vinken et al. 2011, Huszar et al. 2010) have shown that this could lead to an overestimation of ozone formation. However, Vinken et al. (2011) found that the overestimation caused by instant dilution was small in polluted regions, such as the central parts of the Baltic Sea area.

8.3 Paper 2: Impact on Population Health of Baltic Shipping Emissions

The results in this paper builds on the results from paper 1 described above. The study is based on model calculations based on "real life" changes of emissions before and after the application of the stricter SECA regulation in the Baltic Sea validated with measurements of relevant air pollutants. The aim of the present study was to assess the long-term effects on mortality and morbidity from exposure to particulate air pollution from shipping in countries bordering the Baltic Sea. Moreover, the possible health effects of the sulphur regulations for marine fuels enforced in January 2015 in the Baltic SECA area were estimated. In this chapter we show the main results. For more details we refer to the original paper (Barregård et al. 2019). This paper fills a gap in our knowledge about the health effects of the stricter SECA regulations in the Baltic Sea region.

8.3.1 Models for health impacts

Gridded population (1 x 1 km) density by country was obtained from Eurostat for 2011 (Eurostat 2019) and used to calculate population-weighted exposure to $PM_{2.5}$ (in $\mu g/m^3$ x number of persons) from Baltic shipping based on output from the EMEP modelling. The data were extrapolated to 2015 with population sizes for that year. Gridded population data with a similar resolution was not available for Russia. Instead, for 72 million people, residing in relevant parts of European Russia, population-weighted exposure was estimated from Administrative Unit Center Points from NASA SEDAC (Socioeconomic Data and Applications Center) in 2010 (NASA CADAC 2018). Population-weighted exposure from Baltic shipping was also averaged by country. Age-specific mortality rates for 2015 were obtained from Eurostat (Eurostat 2018). For the present study, we used listed total mortality from $\geq$25 years of age, which represents 98-99% of total mortality. Natural mortality was approximated as 95% of total mortality, which is the typical fraction for Northern Europe. We used two alternative exposure-response (ER) functions for natural mortality based on long-term effects

[2]NMVOC - Non Methane Volatile Organic Compounds

of particulate air pollution. The first one was the WHO HRAPIE recommendation regarding concentration-response functions related to air pollutants for the metrics ("Group A") for which enough data were considered available to enable quantification of effects. The HRAPIE review was based on a meta-analysis of 11 epidemiological studies by Hoek et al. (2013) and has been widely used in health impact assessments (Héroux et al. 2015). For annual mean $\mathrm{PM}_{2.5}$, they recommended a relative risk of 1.0062 (95% CI 1.004 –1.008) per μg/m^3 for natural mortality. Recommendations are given also for some specific causes of death (e.g., lung cancer), and for mortality related to daily mean $\mathrm{PM}_{2.5}$, but these outcomes are included in the relative risk for natural mortality. WHO HRAPIE also suggests some concentrations-response functions for hospital admissions related to daily mean $\mathrm{PM}_{2.5}$. The disease burden is, however, dominated by natural mortality as a long-term effect. The second ER function was based on the large European multi-center ESCAPE project (Beelen et al. 2014). The confounder-adjusted relative risk (hazard ratio) was 1.014 per μg/m^3 (95% CI 1.004–1.026). This was based on a meta-analysis of 19 cohorts from 13 countries, among them Sweden, Finland, Denmark, and Germany. The population attributable fraction of disease (PAF; in this case natural mortality) was calculated from the relative risk (RR) at the specific exposure level as $(RR1)/((RR-1)+1)$. The PAF was then applied to the background of natural mortality per country to calculate the extra mortality attributed to air pollution from shipping. The years of life lost (YLL) were estimated from life tables obtained from the national statistics units and Eurostat assuming increased mortality from Baltic shipping as indicated above. For estimates of morbidity, we used data on baseline incidence of ischemic heart disease (IHD) and stroke from the Global Burden of Disease (GBD) database (Global Burden of Disease Database 2017), and exposure response-functions from the ESCAPE study for acute coronary events (Cesaroni et al. 2014) and stroke (Stafoggia et al. 2014). The relative risks were 1.026 (95% CI 1.00 – 1.06) per μg/m^3 of annual mean $\mathrm{PM}_{2.5}$ for IHD and 1.038 (95% CI 0.98 – 1.12) per μg/m^3 for stroke. To avoid double counting with mortality estimates we subtracted the numbers of deaths, due to ischemic heart disease and stroke from the incidence, again using the GBD database and assuming that half the deaths were from new (incident) cases of IHD/stroke.

8.3.2 Health results

The contribution of Baltic shipping to population exposure to $\mathrm{PM}_{2.5}$ depends on the relationship between population density and air pollution levels. In this paper the population weighted exposure is derived from the $\mathrm{PM}_{2.5}$ concentrations calculated in paper 1. As the population density in general is higher along the coast, the population weighted concentrations are higher than the country averaged contributions shown in Figure 8.2c. The contribution of Baltic shipping to population exposure was about 10% of total levels of $\mathrm{PM}_{2.5}$ in coastal areas of the Baltic SECA area, but <1% in remote areas. The mean exposure was highest in Denmark (about 0.5 μg/m^3), followed by Sweden, Estonia, Finland, Latvia, and Lithuania, while the highest total population exposure (in μg/m^3 x persons) was highest in Germany and Poland, due to their large population (see Table 1 in the original publication (Barregård et al. 2019)). The stricter SECA regulations from 2015 resulted in a clear reduction in population weighted exposure from 2014 to 2016. Using the mean meteorology of 2014–2016, the reduction was 34%.

Total natural mortality and estimated number of premature deaths, due to $\mathrm{PM}_{2.5}$ emissions from Baltic shipping in 2014 and 2016, are shown in Table 8.2 using the two alternative

ER functions described above. The numbers were largest in Germany and Poland in line with their large populations. The total number of estimated premature deaths, due to Baltic shipping, decreased from about 1,500–3,400 in 2014 to about 1,000–2,260 in 2016 where the high and low end of the range is calculated based on the HRAPIE review and ESCAPE respectively. The estimated numbers for premature deaths in Table 8.2 are annual numbers, so these numbers are (approximately) valid also for the years before 2014, and after 2016, respectively.

The number of years of life lost decreased from about 17,000–38,000 with 2014 emissions to about 11,000–25,000 with 2016 emissions. The number of YLL per premature death varied slightly between countries, due to differences in age-specific death rates. Estimated morbidity from non-fatal IHD and stroke, caused by $\mathrm{PM}_{2.5}$ emissions, from Baltic shipping in 2014 and 2016 has also been calculated and are included in the original Barregård et al. (2019) paper.

The present study suggests that the stricter SECA regulations on fuel sulphur for the Baltic have indeed been successful in reducing adverse health effects due to air pollution from shipping, reducing its impact on mortality, YLL, and morbidity by at least one third. A positive impact of SECA on health was predicted in some previous forecasts (Winebrake et al. 2009, Brandt et al. 2013), but this is the first study using actual empirical data on emissions before (2014) and after (2016) implementation of the stricter SECA regulations. Our results showed a larger impact on mortality after the decrease in fuel sulphur than predicted by Winebrake et al. (2009). However, the number of YLL in Denmark, due to Baltic shipping, in the present study when the HRAPIE ER function was used (1900 in 2014 and 1400 in 2016) are consistent with the estimates by Brandt et al. (2011), who used the same ER function and estimated about 4100 YLL pre-SECA (in 2011) and 3600 post-SECA (in 2020). They considered not only the Baltic Sea, but also shipping emissions in the North Sea. The study by Winebrake et al. (2009) used a much lower resolution (1 x 1 degree) for air pollution modelling, while the grid size used by Brandt et al. (2011) for air pollution and population density was consistent with the present study. Emissions were calculated assuming 100% compliance with the SECA regulations after 1 January 2015. Separate studies have indicated that compliance is indeed high, varying from 89 to 99% in fairways examined (Mellqvist et al. 2019). Even though the present study had a grid size of 0.1 x 0.1 degrees for air pollution modelling, this resolution will probably underestimate population exposure to shipping pollution and thereby adverse health effects. The reason for this is that population density usually is higher very close to the coastline where the contribution of air pollution from shipping is highest. The extent of such underestimation of exposure can be evaluated using high resolution air pollution modelling.

The exposure-response functions for $\mathrm{PM}_{2.5}$ versus mortality used in the present study were based on two alternative recent sources, The HRAPIE review and ESCAPE. The ER function from the ESCAPE study is about twice as steep as the one reported in the HRAPIE review. This may be due to the fact that the ESCAPE studies were based on within-city estimates, while the studies used in the HRAPIE review also included between-city estimates. A recent meta-regression using estimates from 53 different studies found a relative risk of 1.013 per μg/m^3 of $\mathrm{PM}_{2.5}$ when air concentrations were around 10 μg/m^3 of $\mathrm{PM}_{2.5}$ (Vodonos et al. 2018). Therefore, we consider our results based on the ER function from the ESCAPE study (Table 8.2) somewhat more likely than the estimate based on the HRAPIE review. The estimates for both mortality and morbidity were based on studies of long-term exposure mainly using annual exposures to PM. Long-term studies of PM air pollution generally find higher risk estimates than short-term studies, but using ten years of exposure rather than one only increases the risk marginally more. Population exposure to total $\mathrm{PM}_{2.5}$ from shipping is a

Table 8.2: Estimated number of premature deaths (natural mortality), due to $PM_{2.5}$ emissions from Baltic Sea shipping in 2014 and 2016 according to two alternative exposure response functions. The left one of the two numbers given refers to the ER function suggested in the HRAPIE report (Héroux et al. 2015) and the right one the ER function found in the ESCAPE study (Global Burden of Disease Database 2017). Table adapted from Barregård et al. (2019).

Country	Mortality at Age > 25 2015 (n/year)	Premature Deaths per year 2014	Years of life Lost in 2014	Premature deaths per year 2016	Years of life lost in 2016	Change (%)
Sweden	90,103	187-421	1812–4092	120–272	1167–2635	-35
Norway	40,312	12–28	127–287	8–17	78–176	-39
Denmark	52,111	173–390	1901–4293	130–294	1431–3231	-25
Finland	53,536	75–169	775–1750	40–90	414–935	-47
Germany	919,548	471–1063	4940–11155	342–773	3634–8206	-27
Poland	390,815	236–532	2868–6476	158–358	1922–4340	-33
Estonia	15,121	30–68	346–781	17–38	191–431	-45
Latvia	28,237	37–83	414–935	22–50	249–562	-40
Lithuania	41,339	47–105	514–1161	30–68	330–745	-36
Russia[a]	958,514	245–553	2977–6722	134–302	1625–3670	-45
Sum	2621,754	1,511–3,413	16,674–37,651	1,001–2,261	11,041–24,932	37

mixture of primary PM compounds emitted (elemental carbon, organic and inorganic PM) and secondary inorganic particles (SIA - Secondary Inorganic Aerosols; sulphates, nitrates, and ammonium) produced by chemical reactions over hours and days. It has been estimated that in the long range transported PM reaching populated areas, SIA accounts for about 80% of total PM exposure (Andersson et al. 2009). There are some indications that primary combustion PM has stronger effects on mortality than SIA and some researchers, therefore, applied different ER functions to assumed fractions of total PM (Andersson et al. 2009). However, in the large U.S. studies, SIA constituted a major fraction of total PM, and showed the same ER function as the one used in the HRAPIE review (Pope III et al. 2002). In that study, associations between mortality and sulphate particles were consistent with associations between mortality and total PM. We chose to apply a single ER function to the total $PM_{2.5}$ contribution from shipping in line with the health impact assessment by Brandt et al. (2013) and Sofiev et al. (2018). The exposure-responses for $PM_{2.5}$ and IHD and stroke were selected from the ESCAPE study, since it includes multiple cohorts from the relevant countries. Obviously, the contributions from Baltic shipping to total PM exposure are highest in coastal areas (see paper 1 above). In these areas, Baltic shipping contributes about 10% of the total adverse health effects from particulate air pollution, which is not negligible. This is the first study using empirical data on emissions and meteorology to model the effects on air pollution of the SECA regulations and estimate the beneficial health effects of lowering fuel sulphur. Another strength is the use of relatively detailed modeling of air pollution and estimates of populations. As mentioned above, a limitation of this study is the fact that high resolution (less than 1 x 1 km) data on air pollution and populations were not available. Moreover, the three years modelled (2014 – 2016) may not have captured all variability in meteorology. There is also some uncertainty regarding the exposure–response functions used, since they are based on air pollution contrasts, due to mixtures of emissions, often dominated by road traffic.

8.4 Conclusions and outlook

Our calculations in paper 1 clearly show that, following the stricter SECA regulations from 1 January 2015, sulphur emissions from BAS shipping now contribute little to depositions of oxidised sulphur and $PM_{2.5}$ concentrations in air. This is in contrast to pre-2015 conditions when less stringent sulphur regulations were in place, and even more compared to pre-2011 conditions when up to 1.5% sulphur were allowed in marine fuels in the SECAs.

Furthermore, the second paper shows that lowering fuel sulphur have had substantial effects on population exposure to $PM_{2.5}$ in coastal areas, thereby reducing premature deaths, ischemic hearts disease, stroke and years of life lost from shipping emissions. For example, the number of estimated extra premature deaths decreased by about one third from 2014 to 2016 (after SECA), a reduction of >1000 cases. This is an example of how environmental policy development on air pollution can directly improve the health of the population.

Still, emissions of NO_x and particles from BAS shipping continue to be high, causing health problems and other detrimental impacts on the environment in the BAS region. At present emission levels, particles originating from BAS shipping are mainly formed from NO_x emissions and partially by primary particles other than SO_4.

Our source-receptor calculations show that, for many countries in the BAS region emissions from BAS shipping (and also North Sea shipping) are among the 5 to 6 largest regions/countries contributing to SIA in 2016, which is a major constituent of $PM_{2.5}$ (see EMEP reports for the individual countries for year 2016 (Klein et al. 2018)).

BAS ship emissions also affect the formation of ground level ozone. In much of the BAS region NO_2 levels are already influenced by large land-based sources, and additional contributions from BAS shipping to ozone and ozone metrics, exemplified by SOMO35, is moderate, and for several regions even negative. In this paper we have shown that for most countries future ozone and ozone metrics are expected to decrease from their present levels.

A significant portion of the depositions of oxidised nitrogen is due to BAS shipping. This is also corroborated by the source-receptor calculations for the individual countries in Europe for 2016, see Klein et al. (2018) where they calculate that BAS shipping is the largest contributor to oxidised nitrogen deposition in Estonia (with 14%), and among the 3 to 5 largest contributors in several other countries in the region. As discussed above, these depositions are projected to be gradually reduced following the implementation of the NECA regulations, with relative reductions largely comparable to the decrease from other anthropogenic sources.

In the North Sea and the Baltic Sea the NECA regulation will enter into force in 2021. As for depositions on oxidised nitrogen this regulation is expected to result in gradual reductions in $PM_{2.5}$ from BAS shipping, as shown in our calculations for future versus present conditions. The relative reductions are largely comparable to the decrease from other anthropogenic sources in the region.

Presently there are no further emission mitigation regulations targeted specifically for other European waters. A global cap on sulphur content in marine fuels of 0.5% will enter into force in 2020 emissions that will alleviate the burden in regions not benefiting from the SECA regulations. Even so, emissions from shipping, in particular outside the ECA, regions will remain high. In a recent study Cofala et al. (2018) showed that with an extension of the SECA regulations to all European waters sulphur emissions here can be reduced by more than 90%. With the projected decrease of land based NO_x emissions and no further control at sea, ship emissions could exceed European land based emissions after 2030. According to the same study a designation of the Mediterranean Sea as an ECA could result in more than

4000 avoided premature deaths by 2030 and more than 10000 by 2050. Even with the most conservative assumptions for health valuation, they found that the monetised benefits would on average be 4.4 times higher than the costs in 2030 and 7.5 times higher in 2050.

The IMO has recently set a target for future CO_2 emissions from shipping: "Under the identified levels of ambition, the initial GHG strategy envisages, in particular, a reduction in carbon intensity of international shipping to reduce CO_2 emissions per transport work, as an average across international shipping, by at least 40% by 2030, pursuing efforts towards 70% by 2050, compared to 2008); and that total annual GHG emissions from international shipping should be reduced by at least 50% by 2050 compared to 2008" (IMO 2018). It seems unlikely that this goal can be reached without substantial penetration of zero emission ships resulting in reductions of all air pollutants well beyond the projected future emission reductions assumed in this chapter.

References

Andersson, C., Bergstrom, R., and Johansson, C.: Population exposure and mortality due to regional background PM in Europe - Long-term simulations of source region and shipping contributions, Atmos. Environ., 43, 3614–3620, doi:10.1016/j.atmosenv.2009.03.040, 2009.

Barregård, L., Molnár, P., Jonson, J. E., and Stockfelt, L.: Impact on Population Health of Baltic Shipping Emissions, International Journal of Environmental Research and Public Health, 16, doi:10.3390/ijerph16111954, URL https://www.mdpi.com/1660-4601/16/11/1954, 2019.

Beekmann, M. and Vautard, R.: A modelling study of photochemical regimes over Europe: robustness and variability, Atmos. Chem. Physics, 10, 10 067–10 084, 2010.

Beelen, R., Raaschou-Nielsen, O., Stafoggia, M., Andersen, Z. J., Weinmayr, G., Hoffmann, B., Wolf, K., Samoli, E., Fischer, P., Nieuwenhuijsen, M., Vineis, P., Xun, W. W., Katsouyanni, K., Dimakopoulou, K., Oudin, A., Forsberg, B., Modig, L., Havulinna, A. S., Lanki, T., Turunen, A., Oftedal, B., Nystad, W., Nafstad, P., Faire, U. D., Pedersen, N. L., Östenson, C.-G., Fratiglioni, L., Penell, J., Korek, M., Pershagen, G., Eriksen, K. T., Overvad, K., Ellermann, T., Eeftens, M., Peeters, P. H., Meliefste, K., Wang, M., de Mesquita, B. B., Sugiri, D., Krämer, U., Heinrich, J., de Hoogh, K., Key, T., Peters, A., Hampel, R., Concin, H., Nagel, G., Ineichen, A., Schaffner, E., Probst-Hensch, N., KÃijnzli, N., Schindler, C., Schikowski, T., Adam, M., Phuleria, H., Vilier, A., Clavel-Chapelon, F., Declercq, C., Grioni, S., Krogh, V., Tsai, M.-Y., Ricceri, F., Sacerdote, C., Galassi, C., Migliore, E., Ranzi, A., Cesaroni, G., Badaloni, C., Forastiere, F., Tamayo, I., Amiano, P., Dorronsoro, M., Katsoulis, M., Trichopoulou, A., Brunekreef, B., and Hoek, G.: Effects of long-term exposure to air pollution on natural-cause mortality: an analysis of 22 European cohorts within the multicentre ESCAPE project, The Lancet, 383, 785 – 795, doi:https://doi.org/10.1016/S0140-6736(13)62158-3, URL http://www.sciencedirect.com/science/article/pii/S0140673613621583, 2014.

Brandt, J., Silver, J. D., Christensen, J. H., Andersen, M. S., Geels, C., Gross, A., Hansen, A. B., Hansen, K. M., Hedegaard, G. B., and Skjøth, C.: Assessment of Health-Cost Externalities of Air Pollution at the National Level using the EVA Model System, URL http://www.ceeh.dk/CEEH_Reports/Report_3/CEEH_Scientific_Report3.pdf, CEEH Scientific Report No 3. Roskilde, Denmark., 2011.

Brandt, J., Silver, J. D., Christensen, J. H., Andersen, M. S., Bønløkke, J. H., Sigsgaard, T., Geels, C., Gross, A., Hansen, A. B., Hansen, K. M., Hedegaard, G. B., Kaas, E., and Frohn, L. M.: Assessment of past, present and future health-cost externalities of air pollution in Europe and the contribution from international ship traffic using the EVA model system, Atmospheric Chemistry and Physics, 13, 7747–7764, doi:10.5194/acp-13-7747-2013, URL https://www.atmos-chem-phys.net/13/7747/2013/, 2013.

Cesaroni, G., Forastiere, F., Stafoggia, M., Andersen, Z. J., Badaloni, C., Beelen, R., Caracciolo, B., de Faire, U., Erbel, R., Eriksen, K. T., Fratiglioni, L., Galassi, C., Hampel, R., Heier, M., Hennig, F., Hilding, A., Hoffmann, B., Houthuijs, D., Jöckel, K.-H., Korek, M., Lanki, T., Leander, K., Magnusson, P. K. E., Migliore, E., Ostenson, C.-G., Overvad, K.,

Pedersen, N. L., J, J. P., Penell, J., Pershagen, G., Pyko, A., Raaschou-Nielsen, O., Ranzi, A., Ricceri, F., Sacerdote, C., Salomaa, V., Swart, W., Turunen, A. W., Vineis, P., Weinmayr, G., Wolf, K., de Hoogh, K., Hoek, G., Brunekreef, B., and Peters, A.: Long term exposure to ambient air pollution and incidence of acute coronary events: prospective cohort study and meta-analysis in 11 European cohorts from the ESCAPE Project, BMJ, 348, doi:10.1136/bmj.f7412, URL https://www.bmj.com/content/348/bmj.f7412, 2014.

Cofala, J., Amann, M., Borken-Kleefeld, J., Gomez-Sanabria, A., Heyes, C., Kiesewetter, G., Sander, R., Schoepp, W., Holland, M., Fagerli, H., and Nyíri, A.: The potential for cost-effective air emission reductions from international shipping through designation of further Emission Control Areas in EU waters with focus on the Mediterranean Sea, Tech. Rep. RR-18-002, CIAM, URL http://pure.iiasa.ac.at/id/eprint/15729/, 2018.

Eurostat: Causes of death, URL http://ec.europa.eu/eurostat/web/gisco/geodata/reference-data/population-distribution-demography/geostat, 2018.

Eurostat: EU population data, URL http://ec.europa.eu/eurostat/web/gisco/geodata/reference-data/population-distribution-demography/geostat, 2019.

Global Burden of Disease Database: Data Resources, URL http://ghdx.healthdata.org/gbd-2017, 2017.

Héroux, M., Atkinson, R., Brunekreef, B., Cohen, A., Forastiere, F., Hurley, F., Katsouyanni, K., Krewski, D., Krzyzanowski, M., KÃijnzli, N., Mills, I., Querol, X., Ostro, B., and Walton, H.: Quantifying the health impacts of ambient air pollutants: recommendations of a WHO/Europe project, Int J Public Health, 60, 619–627, doi:10.1007/s00038-015-0690-y, 2015.

Hoek, G., Krishnan, R. M., Beelen, R., Peters, A., Ostro, B., Brunekreef, B., and Kaufman, J. D.: Long-term air pollution exposure and cardio- respiratory mortality: a review, Environmental Health, 12, 43, doi:10.1186/1476-069X-12-43, URL https://doi.org/10.1186/1476-069X-12-43, 2013.

Huszar, P., Cariolle, D., Paoli, R., Halenka, T., Belda, M., Schlager, H., Miksovsky, J., and Pisoft, P.: Modeling the regional impact of ship emissions on NO_x and ozone levels over the Eastern Atlantic and Western Europe using ship plume parameterization, Atmospheric Chemistry and Physics, 10, 6645–6660, doi:10.5194/acp-10-6645-2010, URL https://www.atmos-chem-phys.net/10/6645/2010/, 2010.

IHS Global: SeaWeb database of the global ship fleet, Commercial content, IHS Global, Chemin de la Mairie, Perly, Geneva), URL https://maritime.ihs.com/, 2017.

IMO: Adoption of the initial IMO strategy on reduction of GHG emissions from ships and existing IMO activity related to reducing GHG emissions in the shipping sector., Available at https://unfccc.int/sites/default/files/resource/250_IMO%20submission_Talanoa%20Dialogue_April%202018.pdf, IMO (International Maritime Organization), 2018.

Jalkanen, J. P., Brink, A., Kalli, J., Pettersson, H., Kukkonen, J., and Stipa, T.: A modelling system for the exhaust emissions of marine traffic and its application in the Baltic Sea area, Atmos. Chem. Physics, 9, 9209–9223, 2009.

Jalkanen, J.-P., Johansson, L., Kukkonen, J., Brink, A., Kalli, J., and Stipa, T.: Extension of an assessment model of ship traffic exhaust emissions for particulate matter and carbon monoxide, Atmos. Chem. Physics, 12, 2641–2659, doi:10.5194/acp-12-2641-2012, URL http://www.atmos-chem-phys.net/12/2641/2012/acp-12-2641-2012.pdf, 2012.

Jalkanen, J.-P., Johansson, L., and Kukkonen, J.: A comprehensive inventory of ship traffic exhaust emissions in the European sea areas in 2011, Atmos. Chem. Physics, 16, 71–84, doi:10.5194/acp-16-71-2016, URL http://www.atmos-chem-phys.net/16/71/2016/acp-16-71-2016.pdf, 2016.

Johansson, L., Jalkanen, J.-P., Kalli, J., and Kukkonen, J.: The evolution of shipping emissions and the costs of regulation changes in the northern EU area, ACP, 13, 11 375–11 389, doi:10.5194/acp-13-11375-2013, URL https://www.atmos-chem-phys.net/13/11375/2013/, 2013.

Johansson, L., Jalkanen, J.-P., and Kukkonen, J.: Global assessment of shipping emissions in 2015 on a high spatial and temporal resolution, Atmos. Environ., in review, 2017.

Jonson, J., Borken-Kleefeld, J., Nyíri, A., Posch, M., and Heyes, C.: Impact of excess NO_x emissions from diesel cars on air quality, public health and eutrophication in Europe, Env. Res. Lett., 12, doi:10.1088/1748-9326/aa8850, 2017.

Jonson, J., , Gauss, M., Schulz, and Nyíri, A.: Effects of international shipping, in: Transboundary particulate matter, photo-oxidants, acidifying and eutrophying components. EMEP Status Report 1/2018, The Norwegian Meteorological Institute, Oslo, Norway, 2018a.

Jonson, J. E., Schulz, M., Emmons, L., Flemming, J., Henze, D., Sudo, K., Tronstad Lund, M., Lin, M., Benedictow, A., Koffi, B., Dentener, F., Keating, T., Kivi, R., and Davila, Y.: The effects of intercontinental emission sources on European air pollution levels, Atmospheric Chemistry and Physics, 18, 13 655–13 672, doi:10.5194/acp-18-13655-2018, URL https://www.atmos-chem-phys.net/18/13655/2018/, 2018b.

Jonson, J. E., Gauss, M., Jalkanen, J.-P., and Johansson, L.: Effects of strengthening the Baltic Sea ECA regulations, Atmospheric Chemistry and Physics Discussions, 2019, 1–23, doi:10.5194/acp-2019-51, URL https://www.atmos-chem-phys-discuss.net/acp-2019-51/, 2019.

Klein, H., Gauss, M., Nyiri, A., and Benedictow, A. C.: Transboundary Data by Main Pollutants (S,N,O3) and PM Country Reports, Tech. Rep. EMEP MSC-W Note 1/2018 Individual Country Reports, The Norwegian Meteorological Institute, Oslo, Norway, available for 49 countries, at www.emep.int, 2018.

Mellqvist, J., Conde, V., and Ekholm, J.: Surveillance of Sulfur Emissions from Ships in Danish Waters., Report to the Danish Environmental Protecion Agency, available online at http://dx.doi.org/10.17196/DEPA.001, 2019.

NASA CADAC: Center for International Earth Science Information Network, CIESIN Columbia University, Gridded Population of the World, Version 4 (GPWv4): Administrative Unit Center Points with Population Estimates, Revision 11; NASA Socioeconomic Data and Applications Center (SEDAC): Palisades, NY, USA, URL http://sedac.ciesin.columbia.edu/data/collection/gpw-v, 2018.

Pope III, C. A., Burnett, R. T., Thun, M. J., Calle, E. E., Krewski, D., Ito, K., and Thurston, G. D.: Lung Cancer, Cardiopulmonary Mortality, and Long-term Exposure to Fine Particulate Air Pollution, JAMA, 287, 1132–1141, doi:10.1001/jama.287.9.1132, URL https://doi.org/10.1001/jama.287.9.1132, 2002.

Sofiev, M., Winebrake, J. J., Johansson, L., Carr, E. W., Prank, M., Soares, J., Vira, J., Kouznetsov, R., Jalkanen, J.-P., and Corbett, J. J.: Cleaner fuels for ships provide public health benefits with climate tradeoffs, Nature, 9, doi:10.1038/s41467-017-02774-9, 2018.

Stafoggia, M., Cesaroni, G., Peters, A., Andersen, Z. J., Badaloni, C., Beelen, R., Caracciolo, B., Cyrys, J., de Faire, U., de Hoogh, K., Eriksen, K. T., Fratiglioni, L., Galassi, C., Gigante, B., Havulinna, A. S., Hennig, F., Hilding, A., Hoek, G., Hoffmann, B., Houthuijs, D., Korek, M., Lanki, T., Leander, K., Magnusson, P. K., Meisinger, C., Migliore, E., Overvad, K., ÃŰstenson, C.-G., Pedersen, N. L., Pekkanen, J., Penell, J., Pershagen, G., Pundt, N., Pyko, A., Raaschou-Nielsen, O., Ranzi, A., Ricceri, F., Sacerdote, C., Swart, W. J., Turunen, A. W., Vineis, P., Weimar, C., Weinmayr, G., Wolf, K., Brunekreef, B., and Forastiere, F.: Long-Term Exposure to Ambient Air Pollution and Incidence of Cerebrovascular Events: Results from 11 European Cohorts within the ESCAPE Project, Environmental Health Perspectives, 122, 919–925, doi:10.1289/ehp.1307301, URL https://ehp.niehs.nih.gov/doi/abs/10.1289/ehp.1307301, 2014.

Vinken, G. C. M., Boersma, K. F., Jacob, D. J., and Meijer, E. W.: Accounting for non-linear chemistry of ship plumes in the GEOS-Chem global chemistry transport model, Atmospheric Chemistry and Physics, 11, 11 707–11 722, doi:10.5194/acp-11-11707-2011, URL http://www.atmos-chem-phys.net/11/11707/2011/, 2011.

Vodonos, A., Awad, Y. A., and Schwartz, J.: The concentration-response between long-term PM2.5 exposure and mortality; A meta-regression approach, Environmental Research, 166, 677 – 689, doi:https://doi.org/10.1016/j.envres.2018.06.021, URL http://www.sciencedirect.com/science/article/pii/S0013935118303256, 2018.

Winebrake, J. J., Corbett, J. J., Green, E. H., Lauer, A., and Eyring, V.: Mitigating the Health Impacts of Pollution from Oceangoing Shipping: An Assessment of Low-Sulfur Fuel Mandates, Environmental Science & Technology, 43, 4776–4782, doi:10.1021/es803224q, URL https://doi.org/10.1021/es803224q, pMID: 19673264, 2009.

CHAPTER 9

EQSAM4clim

Svetlana Tsyro and Swen Metzger

The latest version of the Equilibrium Simplified Aerosol Model V4 (EQSAM4clim) has been implemented in the EMEP MSC-W model as an option to calculate gas/aerosol partitioning. EQSAM4clim, designed to combine computational efficiency with accuracy and flexibility, is comprehensively described in Metzger et al. (2016) and Metzger et al. (2018). Its framework is based on a unique analytical representation of the multi-component and multi-phase partitioning of salt solutes by only using a single solute-specific coefficient Metzger et al. (2012). This approach not only allows to efficiently parameterise the aerosol water uptake for mixtures of semi-volatile and non-volatile electrolyte compounds, but dividing the relative humidity (RH) and composition space into subdomains, it further helps to minimize the number of equations to be solved. Thus, the gas-liquid-solid aerosol partitioning can be solved computationally efficient at regional and global scales. This chapter presents the results of a first comparison of EQSAM4clim against observations and with the MARS equilibrium model (Binkowski and Shankar 1995), which is presently in operational use in the EMEP MSC-W model.

The EMEP MSC-W model applies a thermodynamic equilibrium approach for modelling the partitioning of semi-volatile inorganic components. While the MARS model calculates the composition of metastable aqueous aerosols of the inorganic system SO_4^{2-} - NO_3^- - NH_4^+ - HNO_3 - NH_3 - water, EQSAM4clim also allows to consider a full gas-liquid-solid partitioning by accounting for additional major cations (e.g. Na^+, K^+, Ca^{2+}, Mg^{2+}) and anions (Cl^-). As the EMEP MSC-W model does not presently distinguish the individual base cations, only Na^+ and Cl^- from sea salt were included for EQSAM4clim for all simulations.

Note that testing of EQSAM4clim was performed with a EMEP MSC-W model version two-month older than the reporting version rv4.33. The calculations have been performed for the year 2016 (the latest year with available EMEP observations at the time of the testing) and also for June 2006 and January 2007, when EMEP Intensive Measurement Periods (EIMP) took place. During EIMP2006 and EIMP2007, simultaneous measurements of gases and

aerosols were carried out at several sites Aas et al. (2012). The hourly averages of those observational data facilitates the evaluation of modelled diurnal variations and gas/aerosol partitioning of nitrogen compounds.

Here, the base setup of EQSAM4clim (eq4cl) is using the assumption about metastable aqueous aerosols, i.e. equilibrium between gas and liquid phases. In addition, a series of sensitivity tests have been performed to investigate the effect of different setups of EQSAM4clim.

9.1 Evaluation and comparison with MARS for 2016

Table 9.1 compares the statistical evaluation with 2016 observations of model results obtained with MARS and EQSAM4clim. The evaluation is presented for the aerosols species NO_3^- and NH_4^+, the gases HNO_3 and NH_3, as well as PM_{10} and $PM_{2.5}$. The number of the sites is the same as used in Gauss et al. (2018). The base setup of EQSAM4clim appears to slightly shift the equilibrium to favour the gas phase, so that less ammonium nitrate is formed compared to MARS, though the differences are very small.

Looking at the individual sites, the results from MARS and EQSAM4clim are also quite similar. For a number of sites, the correspondence between EQSAM4clim produced NO_3^- and NH_4^+ with observations is in fact somewhat better than for MARS, both in terms of bias and correlation (for instance at DE0001, DE0002, DE0008, FR0009, FR0024, IT0004, SI0008 and others).

Table 9.1: Statistics of model evaluation against EMEP observations in 2016 for runs with the two equilibrium models MARS and EQSAM4clim. Here: Bias-y is the yearly mean bias (%), Corr-yd and IOA-yd are the spatio-temporal correlation and Index Of Agreement.

Model	NO_3^-			NH_4^+			HNO_3	NH_3	PM_{10}	$PM_{2.5}$
	Bias-y	Corr-yd	IOA-yd	Bias-y	Corr-yd	IOA-yd	Bias-y			
MARS	9	0.83	0.90	-11	0.65	0.80	68	-31	-22	-22
EQSAM	5	0.83	0.90	-14	0.64	0.79	73	-30	-24	-20

9.2 Testing different setups for EQSAM4clim

EQSAM4clim allows a variable degree of complexity and flexibility with respect to the processes and gas/aerosol components included in equilibrium modelling. In principle, the scheme including all relevant processes should be yielding the best results, providing all main cations and anions are included. Otherwise, the results may depend on assumption artefacts, e.g., ammonia may buffer inorganic acids in absence of mineral cations and organic acids, yielding a good agreement with ammonium observations but wrong aerosol composition (Metzger et al. 2006). As noted above, the present version of the EMEP MSC-W model does not include base cations from mineral dust (i.e. K^+, Ca^{2+}, Mg^{2+} etc.) and neither organic acids.

In order to investigate the effect of different assumptions within EQSAM4clim on model results, a series of sensitivity tests have been carried out. The tested setups are:

- **eq4cl** – metastable aqueous aerosols, i.e., gas/aerosol partitioning (same as in MARS).

- **mixs** – equilibrium dissociation constant Kp for NH_4NO_3 depending not only on the relative humidity and temperature, but also on the composition (Kp decreases with increasing $(NH_4)_2SO_4$ content).
- **g/a/s** – full gas/aerosol/solid equilibrium.

The results are summarised in Figure 9.1, presenting the graphs with verification statistics against observations in 2016. The results with the metastable assumption and with the full gas/aerosol/solid partitioning are overall quite similar in terms of all three statistical indicators. The plausible reason for that is that some base cations are missing in aerosol composition simulated by the EMEP MSC-W model. Without inclusion of the major mineral cations and organic acids, the gas-aerosol and liquid-solid partitioning is controlled by ammonium salts. Among those, ammonium bi-sulphate $(NH_4)HSO_4$ due to its low deliquescence RH (of 40% at room temperature, see e.g., Table 1 of Metzger et al. (2016)) often controls the water uptake in cation deficient cases, regardless whether the full gas/aerosol/solid equilibrium or the metastable aqueous aerosols assumption is used in thermodynamic modelling.

The resulting PM_{10} and $PM_{2.5}$ are slightly less underestimated in the base set up (likely due to larger aerosol water content) which renders better IOA compared to the 'g/a/s' run. The results using the 'mixs' assumption deviate from the other two runs, in particularly for NO_3 (relatively large overestimation) and HNO_3 (relatively large underestimation and low correlation). EMEP model not accounting for K^+, Ca^{2+}, Mg^{2+} and organic acids is a probable reason for that. Interestingly, the 'mixs' run produces the best results w.r.t. PM_{10} and $PM_{2.5}$ observations, which is aparently due to 'wrong reasons' (i.e. error compesations).

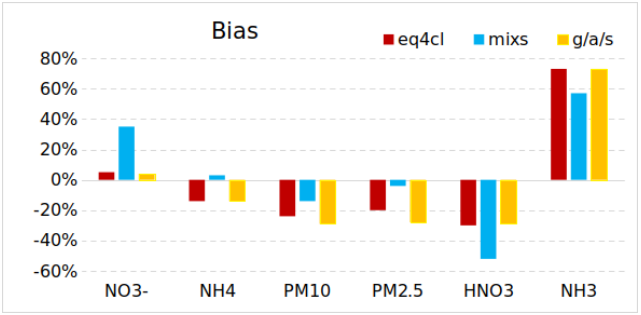

(a)

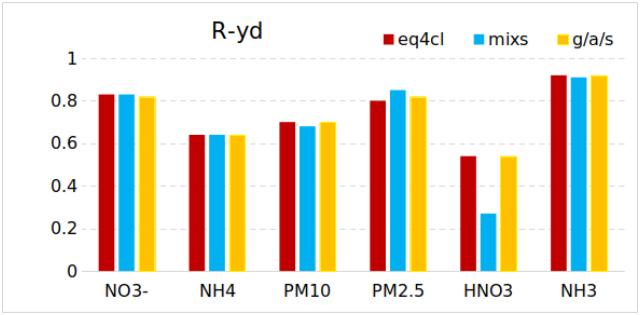

(b)

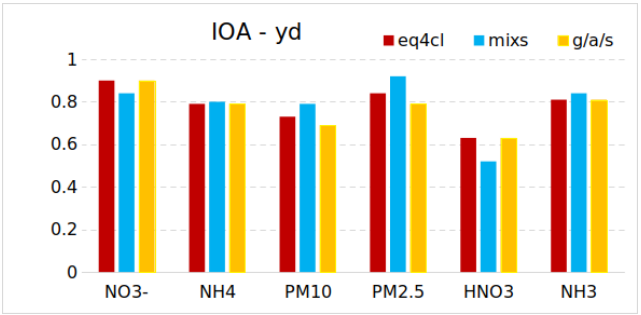

(c)

Figure 9.1: Statistics of model evaluation against EMEP observations in 2016 for the runs with different EQSAM4clim setups (see setups' description in the text): Bias is the yearly mean bias (%), R-yd and IOA-yd are the spatio-temporal correlation and Index Of Agreement.

9.3 Evaluation of diurnal variation and gas/aerosol partitioning with EIMP data

For evaluation of the diurnal variation and gas/aerosol partitioning of nitrogen compounds, three sites with most complete observational data have been selected. The sites are located in the Netherlands (Cabauw), northern Italy (Ispra) and the UK (Harwell, Auchencorth Moss), thus representing the regions with rather different meteorological conditions and emissions.

Figures 9.2–9.7 show that the concentrations of gaseous HNO_3 and NH_3 and aerosols NO_3^- and NH_4^+ and their diurnal variation from the runs with EQSAM4clim (eq4cl) and MARS (mars) are nearly identical in the most of cases, with slightly lower aerosol concentrations for eq4cl. The only considerable differences between EQSAM4clim and MARS are seen for Ispra and Auchencorth Moss in January 2017, with EQSAM4clim calculating significantly lower concentrations of NH_4^+ in the base setup (9.5 (d, h) and 9.7 (d, h)). Note that this result somewhat depends on the EQSAM4clim setup as shown above (Figure 9.1).

In summary, our preliminary tests of EQSAM4clim within the EMEP MSC-W model shows that for most of the case studies (components, periods, sites), the results are very similar to those obtained using the current MARS thermodynamic scheme. Implementation in the EMEP MSC-W of the missing mineral cations of Ca^{2+}, Mg^{2+}, K^+ and Na^+ (and maybe also organic acids) is anticipated to further improve EQSAM4clim performance (Metzger et al. 2006). Given that, the EQSAM4clim scheme is considered to be a good candidate for future use in the EMEP MSC-W model. Further testing of EQSAM4clim is still needed before it can be employed in EMEP status and source-receptor calculations.

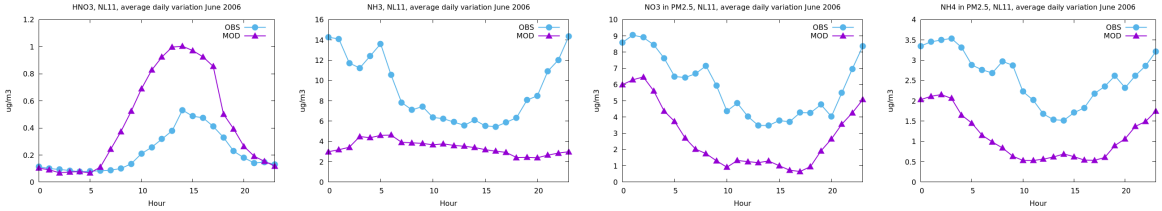

(a) eq4cl HNO_3 (b) eq4cl NH_3 (c) eq4cl NO_3^- (d) eq4cl NH_4^+

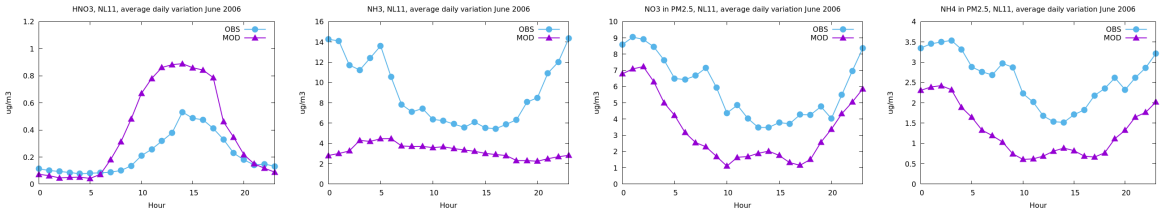

(e) mars HNO_3 (f) mars NH_3 (g) mars NO_3^- (h) mars NH_4^+

Figure 9.2: Diurnal variations of gaseous HNO_3 and NH_3, and fine aerosols NO_3^- and NH_4^+ at Cabauw (NL0011) during EIMP in June 2006.

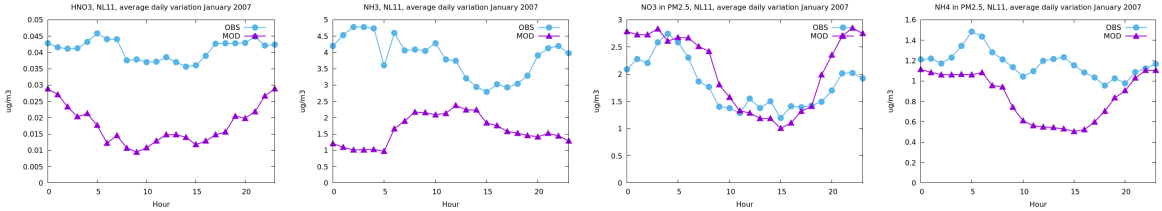

(a) eq4cl HNO_3 (b) eq4cl NH_3 (c) eq4cl NO_3^- (d) eq4cl NH_4^+

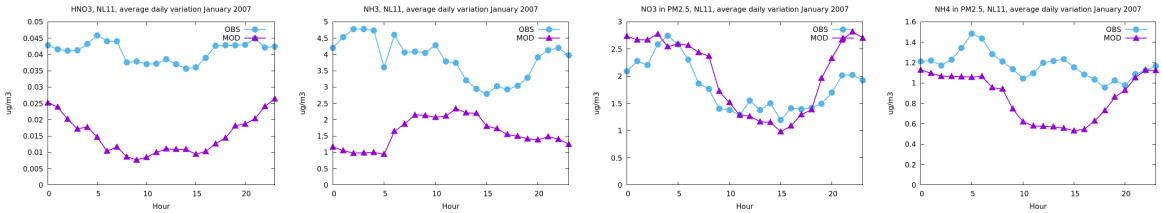

(e) mars HNO_3 (f) mars NH_3 (g) mars NO_3^- (h) mars NH_4^+

Figure 9.3: Diurnal variations of gaseous HNO_3 and NH_3, and fine aerosols NO_3^- and NH_4^+ at Cabauw (NL0011) during EIMP in January 2007.

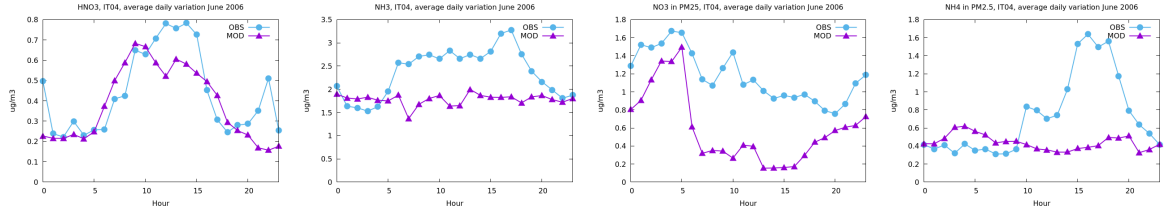

(a) eq4cl HNO_3 (b) eq4cl NH_3 (c) eq4cl NO_3^- (d) eq4cl NH_4^+

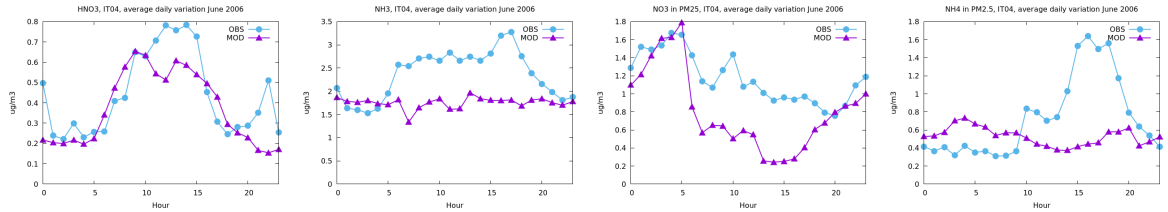

(e) mars HNO_3 (f) mars NH_3 (g) mars NO_3^- (h) mars NH_4^+

Figure 9.4: Diurnal variations of gaseous HNO_3 and NH_3, and fine aerosols NO_3^- and NH_4^+ at Ispra (IT0004) during EIMP in June 2006.

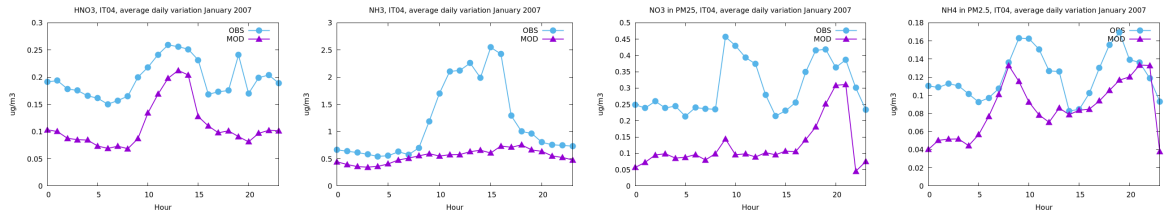

(a) eq4cl HNO_3 (b) eq4cl NH_3 (c) eq4cl NO_3^- (d) eq4cl NH_4^+

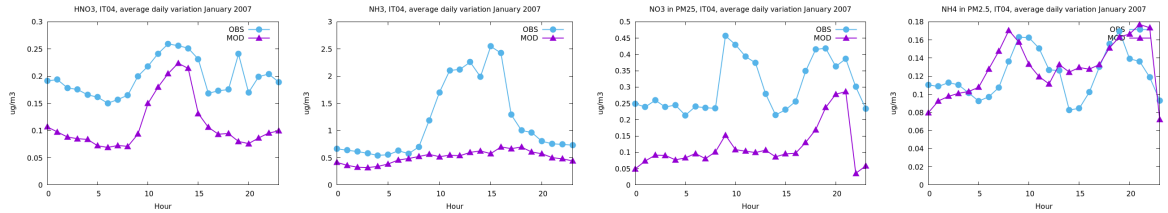

(e) mars HNO_3 (f) mars NH_3 (g) mars NO_3^- (h) mars NH_4^+

Figure 9.5: Diurnal variations of gaseous HNO_3 and NH_3, and fine aerosols NO_3^- and NH_4^+ at Ispra (IT0004) during EIMP in January 2007.

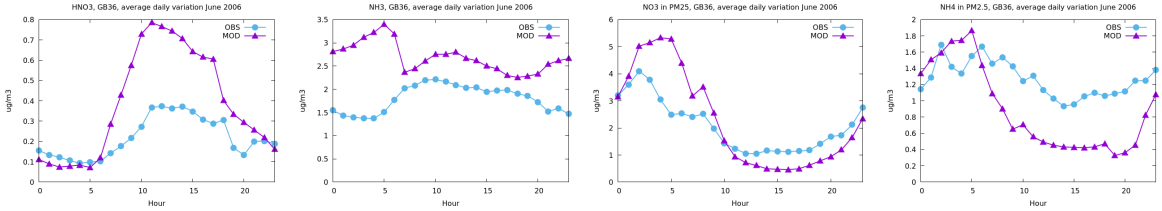

(a) eq4cl HNO_3 (b) eq4cl NH_3 (c) eq4cl NO_3^- (d) eq4cl NH_4^+

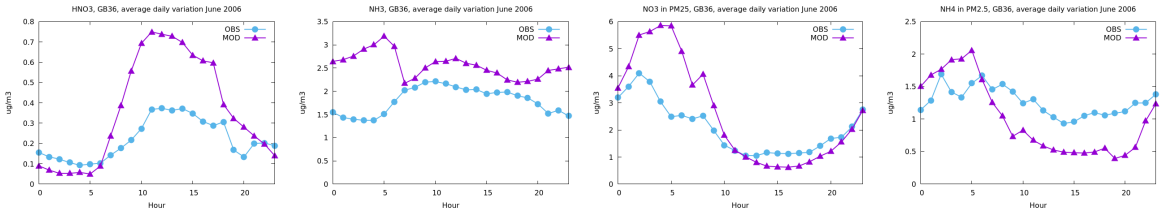

(e) mars HNO_3 (f) mars NH_3 (g) mars NO_3^- (h) mars NH_4^+

Figure 9.6: Diurnal variations of gaseous HNO_3 and NH_3, and fine aerosols NO_3^- and NH_4^+ at Harwell (GB0036) during EIMP in June 2006.

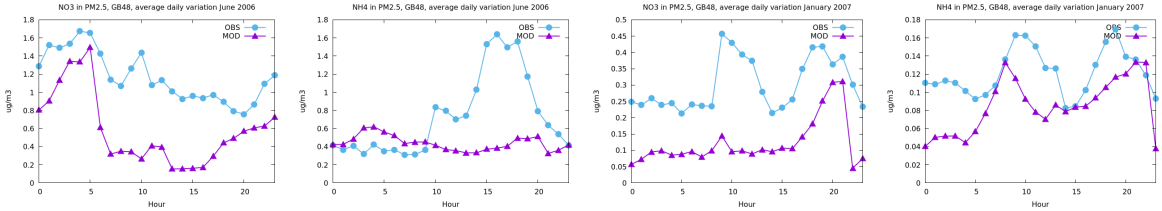

(a) eq4cl HNO_3 (b) eq4cl NH_3 (c) eq4cl NO_3^- (d) eq4cl NH_4^+

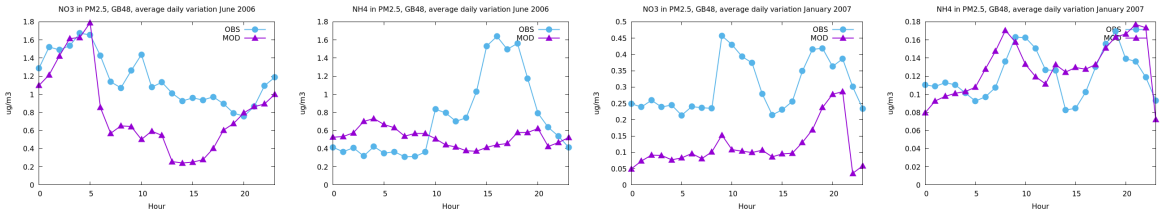

(e) mars HNO_3 (f) mars NH_3 (g) mars NO_3^- (h) mars NH_4^+

Figure 9.7: Diurnal variations of fine aerosols NO_3^- and NH_4^+ at Auchencorth Moss (GB0048) during EIMPs in June 2006 and January 2007.

References

Aas, W., Tsyro, S., Bieber, E., Bergström, R., Ceburnis, D., Ellermann, T., Fagerli, H., Frölich, M., Gehrig, R., Makkonen, U., Nemitz, E., Otjes, R., Perez, N., Perrino, C., Prévôt, A. S. H., Putaud, J.-P., Simpson, D., Spindler, G., Vana, M., and Yttri, K. E.: Lessons learnt from the first EMEP intensive measurement periods, Atmos. Chem. Physics, 12, 8073–8094, doi:10.5194/acp-12-8073-2012, 2012.

Binkowski, F. and Shankar, U.: The Regional Particulate Matter Model .1. Model description and preliminary results, J. Geophys. Res., 100, 26 191–26 209, 1995.

Gauss, M., Tsyro, S., Fagerli, H., Hjellbrekke, A.-G., Aas, W., and Solberg, S.: EMEP MSC-W model performance for acidifying and eutrophying components, photo-oxidants and particulate matter in 2016., Supplementary material to EMEP Status Report 1/2018, available online at www.emep.int, The Norwegian Meteorological Institute, Oslo, Norway, 2018.

Metzger, S., Mihalopoulos, N., and Lelieveld, J.: Importance of mineral cations and organics in gas-aerosol partitioning of reactive nitrogen compounds: case study based on MINOS results, Atmos. Chem. Physics, 6, 2549–2567, 2006.

Metzger, S., Steil, B., Xu, L., Penner, J. E., and Lelieveld, J.: New representation of water activity based on a single solute specific constant to parameterize the hygroscopic growth of aerosols in atmospheric models, Atmospheric Chemistry and Physics, 12, 5429–5446, doi:10.5194/acp-12-5429-2012, URL https://www.atmos-chem-phys.net/12/5429/2012/, 2012.

Metzger, S., Steil, B., Abdelkader, M., Klingmüller, K., Xu, L., Penner, J. E., Fountoukis, C., Nenes, A., and Lelieveld, J.: Aerosol water parameterisation: a single parameter framework, Atmospheric Chemistry and Physics, 16, 7213–7237, doi:10.5194/acp-16-7213-2016, URL https://www.atmos-chem-phys.net/16/7213/2016/, 2016.

Metzger, S., Abdelkader, M., Steil, B., and Klingmüller, K.: Aerosol water parameterization: long-term evaluation and importance for climate studies, Atmospheric Chemistry and Physics, 18, 16 747–16 774, doi:10.5194/acp-18-16747-2018, URL https://www.atmos-chem-phys.net/18/16747/2018/, 2018.

Part III

Technical EMEP Developments

CHAPTER 10

Updates to the EMEP MSC-W model, 2018-2019

David Simpson, Robert Bergström, Svetlana Tsyro and Peter Wind

This chapter summarises the changes made to the EMEP MSC-W model since Simpson et al. (2018), and along with changes discussed in Simpson et al. (2013), Tsyro et al. (2014), Simpson et al. (2015, 2016, 2017), updates the standard description given in Simpson et al. (2012). The model version used for reporting this year is denoted rv4.33, which has some significant changes since the rv4.17a documented last year. Table 10.3 summarises the changes made in the EMEP model since the version documented in Simpson et al. (2012).

10.1 Overview of changes

- EmChem19 – a new gas-phase chemical mechanism has been introduced (Bergström et al., 2019), updating the EmChem16x scheme used previously. See Sect. 10.2.

- CRI v2.2a-emep – the Common Reactive Intermediates (CRI) mechanism (Jenkin et al. 2008) used in research versions of the EMEP model has been updated and a new isoprene scheme for the CRI scheme has been implemented in the model (Jenkin et al. 2019, McFiggans et al. 2019).

- The carbon-bond scheme used in research versions of the EMEP model has been updated from CB05 (Yarwood et al. 2005) to CB6r2 (Luecken et al. 2019).

- Two new schemes for handling secondary organic aerosol (SOA) have been added to the model – a new volatility basis set (VBS) scheme from Hodzic et al. (2016), that takes into account recent findings regarding high formation rates for SOA, and an alternative "1.5-dimensional" volatility basis set (VBS) scheme, based on Koo et al. (2014), which handles both oxygenation and fragmentation of primary and secondary OA by atmospheric oxidation (chemical aging), in a simplified way.

- The EMEP 3D model and chemical pre-processing systems (GenChem) were re-harmonised, making use of a new python-based system. See Sect. 10.3.
- We have added 'EQSAM4clim' as an option for aerosol thermodynamics. See Sect. 10.4.
- A bug-fix for radiation (PAR) was also needed, with significant impact on POD calculations for forests. See Sect. 10.5.
- New methods to specify emissions inputs were added, which allow more flexible input of data from external sources. See Sect. 10.6.
- The vertical profiles of emission releases were modified, reflecting the transition to a finer resolution of the modelling grid and as a part of the general model development towards a flexible code
- The use of configuration files was again expanded, replacing some of the earlier hard-coded methods to specify model setups. See Sect. 10.8.

10.2 EmChem19 chemical mechanism

The new gas-phase chemistry scheme – EmChem19 – is a substantial revision of the EmChem16 scheme (Simpson et al. 2017). The reaction rates in EmChem19 are updated to be consistent with the latest recommendations from the IUPAC (IUPAC 2019, Atkinson et al. 2004, 2006), and evaluated against the latest Master Chemical Mechanism (MCM v3.3.1, Jenkin et al. 2015, and refs therein). In addition to these updates (and bug fixes) some new gas-phase reactions have been added and a few new chemical species have been included in the chemical mechanism. Major changes compared to EmChem16 include:

- The addition of benzene and toluene as emitted species.
- A revised (very simplified) aromatic chemistry – tuned to give reasonably good agreement with the Master Chemical Mechanism (MCM, see Jenkin et al. 2015) in box model simulations.
- Addition of more than 20 new reactions – including a number of reactions between peroxy and nitrate radicals and a new treatment of peroxy - peroxy radical reactions, using the total RO_2 pool as a reactant.
- Changes of the rates and/or products of ca 45 reactions.
- Revised SOA formation from sesquiterpenes (SQT) – in EmChem19 SQT emissions are assumed to be equal to 5% (by mass) of the monoterpene emissions; in the model the emitted SQT is assumed to immediately form non-volatile BSOA, with 17% yield (mass based).
- A few reactions were removed or simplified compared to EmChem16 – this includes a simplification of the minimal scheme for monoterpene chemistry (based on Lamarque et al. 2012), which was introduced in EmChem16; in the standard EmChem19 scheme monoterpenes are modelled using a single surrogate MT (APINENE) instead of the three used in EmChem16.

A detailed description of the EmChem19 scheme, including evaluation against ambient measurements and comparison to the MCM and other chemical mechanisms in box model simulations, will be given by Bergström et al., 2019.

10.3 Revised GenChem system

.

The chemical mechanism files used in the EMEP CTM have for many years been generated with a chemical pre-processor. Originally written in perl, GenChem.pl, and now in python, GenChem.py, this pre-processor reads files which describe the chemical mechanism using chemical notation (e.g. krate OH + NO2 = HNO3), and produces differential equations in fortran, ready for import into the EMEP source code as the CM_ files (e.g. CM_ChemSpecs_mod.f90). GenChem.pl used to be a part of the emepctm package as used at MSC-W, but now GenChem.py is part of a separate system which allows testing of chemical mechanisms with either a box-model (BoxChem) or the 1-D Ecosystem Surface Exchange model (ESX, Simpson and Tuovinen 2014). With this system the EMEP model chemistry can be evaluated against more advanced and well-evaluated schemes such as the Master Chemical Mechanism (MCM, e.g. Jenkin et al. 2015, Saunders et al. 2003, CRI (Jenkin et al. 2019) or carbon-bond (Yarwood et al. 2005, Luecken et al. 2019).

10.4 EQSAM4clim

Three thermodynamic equilibrium models are currently implemented in the EMEP MSC-W model to calculate gas/aerosol partitioning of inorganic semi-volatile species. The alternative models are: Ammonium (EMEP simplified equilibrium scheme, Hov et al. 1988), MARS (Binkowski and Shankar 1995), and EQSAM (Metzger and Lelieveld 2007). The MARS scheme, presently used in the standard model, has some limitations, the major one being the number of chemical species included in the thermodynamic equlibrium, but also the assumption of metastable aqueous aerosols. This year, a new version of EQSAM - EQSAM4clim (Metzger et al. 2016) - has been implemented as an optional thermodynamic scheme. The advantage of the scheme is that it considers a full gas-liquid-solid partitioning and can account for more cations (e.g. Na^+, Ca^{2+}, Mg^{2+}) and anions (Cl^-). Preliminary testing of EQSAM4clim has been carried out, and the results are presented in Chapter 9. Further evaluation of the scheme with more observations, as well as its testing in source-receptor calculations are needed before the EQSAM4clim can be considered for use in EMEP MSC-W reporting runs.

10.5 Radiation issues

As noted in Simpson et al. (2018), the radiation scheme of Weiss and Norman (1985) was introduced in order to give better estimates of diffuse versus direct photosynthetically active radiation (PAR), and to fix a bug in the calculations of these variables which had been identified in previous model versions. PAR is used in modelling both stomatal uptake and biogenic VOC emissions. Unfortunately this bug-fix contained itself a bug in the units used in the stomatal uptake (DO3SE) module, so that calculated PAR levels were too low. This has now

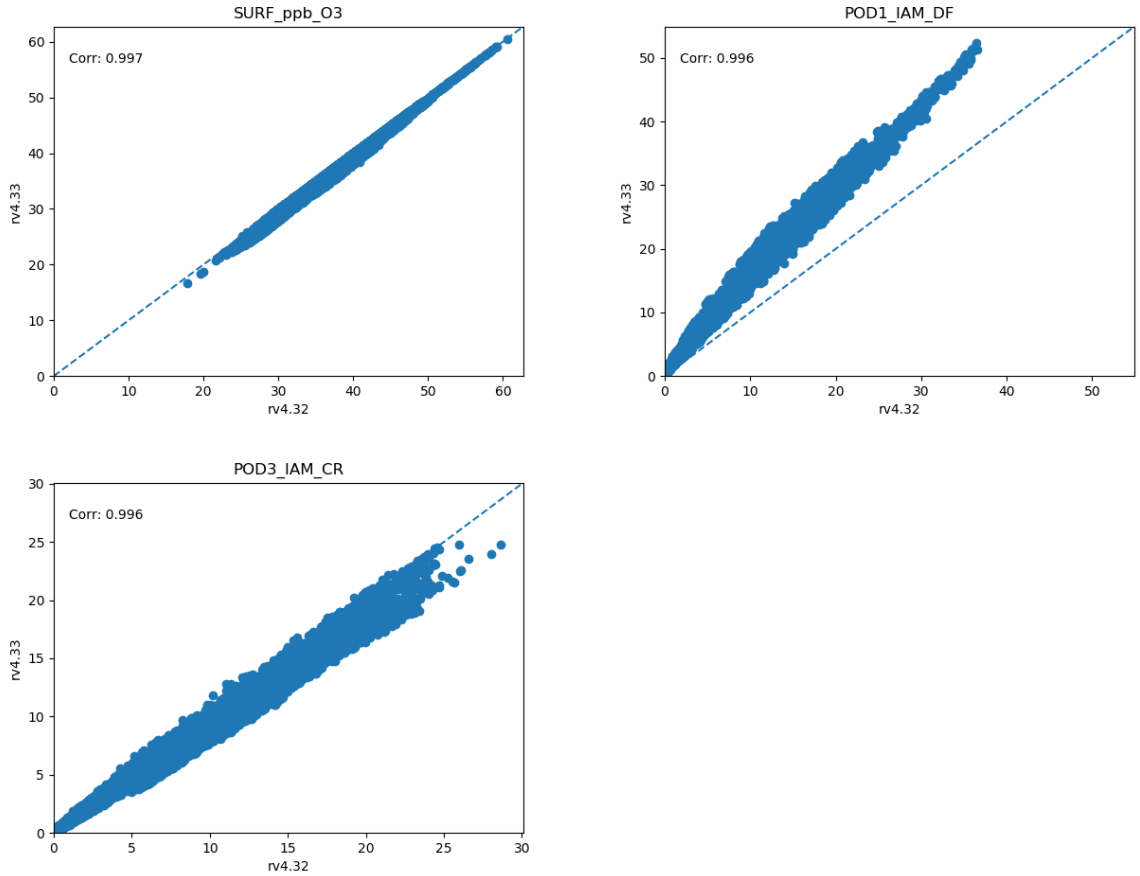

Figure 10.1: Comparison of model versions rv4.33 and rv4.32 for mean ozone (top-left), POD1 for IAM deciduous forests (top-right) and POD_3IAM for crops (bottom). The dashed line represents the 1:1 line. Calculations are for the year 2012, using the 50km version of the model.

been corrected. As found and explained in Simpson et al. (2018), and illustrated in Fig. 10.1, the impact of the change is mainly apparent for forests. The net result of fixing this bug is to restore POD levels to very similar levels to those seen in the rv4.15 version discussed in Simpson et al. (2018). As before, the correlation coefficient between new and old versions is very high ($\geq$0.996).

10.6 Emission inputs

A new system for reading emissions has been implemented. The new system allows to read emissions in NetCDF, without the need of heavy preprocessing of these inputs. Any 2-dimensional emission field can be directly used by the model, provided the longitude and latitude data is provided. The metadata, such as species, units, names, sectors, etc. can be provided separately in the configuration file, if they are not found in the emission file. The new system is at present implemented in addition to the previous one, and emissions in both formats can be used at the same time.

An emission mask can be defined using any field in a NetCDF file. This mask can then be used to reduce emission over the region covered by the mask.

10.7 Emission heights

As documented in EMEP Status Report 1/2016 (2016), the release heights of GNFR sectoral emissions are assigned based on those previously developed for the SNAP system. The heights of emission release are now expressed in pressure levels, as documented in Table 10.1. Here, the P-levels indicate air pressure at the top of the layer, within which the given fraction of emissions is released. The lowest layer (second column) is confined between 101325.0 Pa (the surface) and 101084.9 Pa (appr. 20m), etc. The vertical profiles of emission releases have been slightly modified, using the experiences of EMEP (Simpson et al. 2012) and EuroDelta (Bessagnet et al. 2014).

Table 10.1: Definition used for the fractions of emissions, released within a given vertical layer, defined by pressure (P) levels. The P-levels are pressure (Pa) at the top of corresponding layer (P Surface = 101325.0 Pa). The approximate heights (ΔZ, m) of the layer boundaries are also included.

P-level	101084.9	100229.1	99133.2	97489.35	95206.225	92283.825	88722.15
ΔZ (m)	0 - 20	20 - 92	92 - 184	184 - 324	324 - 522	522-781	781-1106
GNFR 1	0.0	0.00	0.0025	0.1475	0.40	0.30	0.15
GNFR 2	0.06	0.16	0.75	0.03	0.00	0.00	0.0
GNFR 3	1.0	0.00	0.00	0.00	0.00	0.00	0.0
GNFR 4	0.05	0.15	0.70	0.10	0.00	0.00	0.0
GNFR 5	1.0	0.00	0.00	0.00	0.00	0.00	0.0
GNFR 6	1.0	0.00	0.00	0.00	0.00	0.00	0.0
GNFR 7	1.0	0.00	0.00	0.00	0.00	0.00	0.0
GNFR 8	1.0	0.00	0.00	0.00	0.00	0.00	0.0
GNFR 9	1.0	0.00	0.00	0.00	0.00	0.00	0.0
GNFR 10	0.0	0.00	0.41	0.57	0.02	0.00	0.0
GNFR 11	1.0	0.00	0.00	0.00	0.00	0.00	0.0
GNFR 12	1.0	0.00	0.00	0.00	0.00	0.00	0.0
GNFR 13	0.02	0.08	0.60	0.30	0.00	0.00	0.0

Table 10.2: The fractions of emissions, released within the actual model layers, for which the approximate heights (ΔZ, m) of their boundaries are also shown.

ΔZ (m)	0 - 50	50 - 94	94 - 155	155 - 237	237 - 341	341 - 623	623 - 1015	1015 -1522
GNFR 1	0.000	0.000	0.002	0.056	0.125	0.485	0.290	0.042
GNFR 2	0.127	0.111	0.498	0.245	0.019	0.000	0.000	0.000
GNFR 3	1.000	0.000	0.000	0.000	0.000	0.000	0.000	0.000
GNFR 4	0.113	0.104	0.465	0.256	0.062	0.000	0.000	0.000
GNFR 5	1.000	0.000	0.000	0.000	0.000	0.000	0.000	0.000
GNFR 6	1.000	0.000	0.000	0.000	0.000	0.000	0.000	0.000
GNFR 7	1.000	0.000	0.000	0.000	0.000	0.000	0.000	0.000
GNFR 8	1.000	0.000	0.000	0.000	0.000	0.000	0.000	0.000
GNFR 9	1.000	0.000	0.000	0.000	0.000	0.000	0.000	0.000
GNFR 10	0.000	0.010	0.272	0.342	0.357	0.018	0.000	0.000
GNFR 11	1.000	0.000	0.000	0.000	0.000	0.000	0.000	0.000
GNFR 12	1.000	0.000	0.000	0.000	0.000	0.000	0.000	0.000
GNFR 13	0.054	0.061	0.398	0.300	0.187	0.000	0.000	0.000

These emission vertical profiles are defined independently of the model's actual vertical layers. Thus, the emissions layers do not necesserily match model layers, and the emissions

are then redistributed into actual model layers. For the model levels used in the runs for this report, the final emission release vertical profiles are shown in Table 10.2. Note that compared to earlier runs, the thickness of the lowest layer is now decreased from 92 m to about 50 m.

10.8 Configuration

The configuration parameters of the model run is entirely steered through a fortran namelist. The file can easily be edited, to provide alternative parameters and paths to the input data. Some key changes are:

- Many small changes to make model configuration easier and more flexible; see the User Guide for further explanation of some new methods and possibilities.
- The 'femis' file used to control emission changes per country and sector was developed further, and can now use country codes (e.g. 'SE') rather than numbers (e.g. 18) to specify the source to be modified.
- The configuration file is now organized in one large namelist instead of several ones. This will reduce the chances for syntactic errors.

10.9 Nesting

A full snapshot of the model concentrations can be saved at specific given dates, in addition to the standard modes for periodically saving boundary conditions. Typically those can be used to be used as initial conditions for a new run in a finer grid.

10.10 Biomass burning emissions

It is easy now to switch between different schemes for forest fires emissions by simply specifying the source in the configuration file (FINN, GFAS or GFED). No need to recompile the code. The vertical distribution of those emission takes into account the layer thickness.

10.11 WRF

When WRF meteorological input is used, the model height of the surface is read from the parameter 'HGT', instead of an ad hoc separate file (topography.nc).

The model will now treat correctly the singularity at the Poles in the 'lon lat' projection.

10.12 Outputs

The time stamp of the NetCDF output is now defined in the middle of the period, instead of the end.

Table 10.3: Summary of major EMEP MSC-W model versions from 2012–2017. Extends Table S1 of Simpson et al. 2012

Version	Update	Ref[(a)]
rv4.33	Public domain (June 2019) EmChem19, PAR bug-fix, EQSAM4clim	This report
rv4.32	Used for EMEP course, April 2019	
rv4.30	Moved to new GenChem-based system	
rv4.17a	Used for R2018. Small updates	R2018
rv4.17	Public domain (Feb. 2018)	R2018
	Corrections in global land-cover/deserts; added 'LOTOS' option for European NH_3 emissions; corrections to snow cover	R2018
rv4.16	New radiation scheme (Weiss&Norman); Added dry and wet deposition for N_2O_5; (Used for Stadtler et al. 2018, Mills et al. 2018b)	R2018
rv4.15	EmChem16 scheme	R2017
rv4.14	Updated chemical scheme	R2017
rv4.12	New global land-cover and BVOC	R2017
rv4.10	Public domain (Oct. 2016) (Used for Mills et al. 2018a)	R2016
rv4.9	Updates for GNFR sectors, DMS, sea-salt, dust, S_A and γ, N_2O_5	
rv4.8	Public domain (Oct. 2015) ShipNOx introduced. Used for EMEP HTAP2 model calculations, see see acp special issue: `https://www.atmos-chem-phys.net/special_issue390.html`). Also for Jonson et al. (2017).	R2015
rv4.7	Used for reporting, summer 2015 : New calculations of aerosol surface area; ; New gas-aerosol uptake and N_2O_5 hydrolysis rates ; Added 3-D calculations pf aerosol extinction and AODs; ; Emissions - new flexible mechanisms for interpolation and merging sources ; Global - monthly emissions from ECLIPSE project ; Global - LAI changes from LPJ-GUESS model ; WRF meteorology (Skamarock and Klemp 2008) can now be used directly in EMEP model.	R2015
rv4.6	Used for Euro-Delta SOA runs Revised boundary condition treatments ; ISORROPIA capability added	R2015
rv4.5	Sixth open-source (Sep 2014) Improved dust, sea-salt, SOA modelling ; AOD and extinction coefficient calculations updated ; Data assimilation system added ; Hybrid vertical coordinates replace earlier sigma ; Flexibility of grid projection increased.	R2014
rv4.4	Fifth open-source (Sep 2013) ; Improved dust and sea-salt modelling ; AOD and extinction coefficient calculations added ; gfortran compatibility improved	R2014, R2013
rv4.3	Fourth public domain (Mar. 2013) ; Initial use of namelists ; Smoothing of MARS results ; Emergency module for volcanic ash and other events; Dust and road-dust options added as defaults ; Advection algorithm changed	R2013
rv4.0	Third public domain (Sep. 2012) As documented in Simpson et al. (2012)	R2013

Notes: (a) R2018 refers to EMEP Status report 1/2018, etc.

References

Atkinson, R., Baulch, D. L., Cox, R. A., Crowley, J. N., Hampson, R. F., Hynes, R. G., Jenkin, M. E., Rossi, M. J., and Troe, J.: Evaluated kinetic and photochemical data for atmospheric chemistry: Volume I - gas phase reactions of O_x, HO_x, NO_x and SO_x species, Atmos. Chem. Physics, 4, 1461–1738, URL http://www.atmos-chem-phys.net/4/1461/2004/, 2004.

Atkinson, R., Baulch, D. L., Cox, R. A., Crowley, J. N., Hampson, R. F., Hynes, R. G., Jenkin, M. E., Rossi, M. J., Troe, J., and Subcommittee, I.: Evaluated kinetic and photochemical data for atmospheric chemistry: Volume II – gas phase reactions of organic species, Atmos. Chem. Physics, 6, 3625–4055, URL http://www.atmos-chem-phys.net/6/3625/2006/, 2006.

Bergström, R. et al.: Updating the chemical schemes of the EMEP MSC-W model; EmChem19, CRI v2.2a-emep, CB6r2-emep, In preperation, pp. –, 2019.

Bessagnet, B., Colette, A., Meleux, F., Rouïl, L., Ung, A., Favez, O., Cuvelier, C., Thunis, P., Tsyro, S., Stern, R., Manders, A., Kranenburg, R., Aulinger, A., Bieser, J., Mircea, M., Briganti, G., Cappelletti, A., Calori, G., Finardi, S., Silibello, C., Ciarelli, G., Aksoyoglu, S., Prévot, A., Pay, M.-T., Baldasano, J. M., Vivanco, M. G., Garrido, J. L., Palomino, I., Martín, F., Pirovano, G., Roberts, P., Gonzalez, L., White, L., Menut, L., Dupont, J.-C., Carnevale, C., and Pederzoli, A.: The EURODELTA III exercise – Model evaluation with observations issued from the 2009 EMEP intensive period and standard measurements in Feb/Mar 2009. TFMM & MSC-W 1/2014, Tech. rep., ., 2014.

Binkowski, F. and Shankar, U.: The Regional Particulate Matter Model .1. Model description and preliminary results, J. Geophys. Res., 100, 26 191–26 209, 1995.

EMEP Status Report 1/2016: Transboundary particulate matter, photo-oxidants, acidifying and eutrophying components, EMEP MSC-W & CCC & CEIP, Norwegian Meteorological Institute (EMEP/MSC-W), Oslo, Norway, 2016.

Hodzic, A., Kasibhatla, P. S., Jo, D. S., Cappa, C. D., Jimenez, J. L., Madronich, S., and Park, R. J.: Rethinking the global secondary organic aerosol (SOA) budget: stronger production, faster removal, shorter lifetime, Atmos. Chem. Physics, 16, 7917–7941, doi:10.5194/acp-16-7917-2016, URL http://www.atmos-chem-phys.net/16/7917/2016/, 2016.

Hov, Ø., Eliassen, A., and Simpson, D.: Calculation of the distribution of NO_x compounds in Europe., in: Troposheric ozone. Regional and global scale interactions, edited by Isaksen, I., pp. 239–262, D. Reidel, Dordrecht, 1988.

IUPAC: IUPAC Task Group on Atmospheric Chemical Kinetic Data Evaluation, URL http://iupac.pole-ether.fr, accessed: 2019-06-13, 2019.

Jenkin, M., Khan, M., Shallcross, D., Bergström, R., Simpson, D., Murphy, K., and Rickard, A.: The CRI v2.2 reduced degradation scheme for isoprene, Atmos. Environ., 212, 172 – 182, doi:https://doi.org/10.1016/j.atmosenv.2019.05.055, URL http://www.sciencedirect.com/science/article/pii/S1352231019303607, 2019.

Jenkin, M. E., Watson, L. A., Utembe, S. R., and Shallcross, D. E.: A Common Representative Intermediates (CRI) mechanism for VOC degradation. Part 1: Gas phase mechanism development, Atmos. Environ., 42, 7185–7195, doi:10.1016/j.atmosenv.2008.07.028, 2008.

Jenkin, M. E., Young, J. C., and Rickard, A. R.: The MCM v3.3.1 degradation scheme for isoprene, Atmos. Chem. Physics, 15, 11 433–11 459, doi:10.5194/acp-15-11433-2015, 2015.

Jonson, J. E., Borken-Kleefeld, J., Simpson, D., Nyíri, A., Posch, M., and Heyes, C.: Impact of excess NOx emissions from diesel cars on air quality, public health and eutrophication in Europe, Environ. Res. Lett., 12, 094 017, URL http://stacks.iop.org/1748-9326/12/i=9/a=094017, 2017.

Koo, B., Knipping, E., and Yarwood, G.: 1.5-Dimensional volatility basis set approach for modeling organic aerosol in {CAMx} and {CMAQ}, Atmospheric Environment, 95, 158 – 164, doi:http://dx.doi.org/10.1016/j.atmosenv.2014.06.031, 2014.

Lamarque, J. F., Emmons, L. K., Hess, P. G., Kinnison, D. E., Tilmes, S., Vitt, F., Heald, C. L., Holland, E. A., Lauritzen, P. H., Neu, J., Orlando, J. J., Rasch, P. J., and Tyndall, G. K.: CAM-chem: description and evaluation of interactive atmospheric chemistry in the Community Earth System Model, Geoscientific Model Dev., 5, 369–411, doi:10.5194/gmd-5-369-2012, 2012.

Luecken, D., Yarwood, G., and Hutzell, W.: Multipollutant modeling of ozone, reactive nitrogen and HAPs across the continental US with CMAQ-CB6, Atmos. Environ., 201, 62 – 72, doi:https://doi.org/10.1016/j.atmosenv.2018.11.060, URL http://www.sciencedirect.com/science/article/pii/S1352231018308434, 2019.

McFiggans, G., Mentel, T. F., Wildt, J., Pullinen, I., Kang, S., Kleist, E., Schmitt, S., Springer, M., Tillmann, R., Wu, C., Zhao, D., Hallquist, M., Faxon, C., Le Breton, M., Hallquist, A. M., Simpson, D., Bergström, R., Jenkin, M. E., Ehn, M., Thornton, J. A., Alfarra, M. R., Bannan, T. J., Percival, C. J., Priestley, M., Topping, D., and Kiendler-Scharr, A.: Secondary organic aerosol reduced by mixture of atmospheric vapours, Nature, 565, 587–593, 2019.

Metzger, S. and Lelieveld, J.: Reformulating atmospheric aerosol thermodynamics and hygroscopic growth into fog, haze and clouds, Atmos. Chem. Physics, 7, 3163–3193, 2007.

Metzger, S., Steil, B., Abdelkader, M., Klingmüller, K., Xu, L., Penner, J. E., Fountoukis, C., Nenes, A., and Lelieveld, J.: Aerosol water parameterisation: a single parameter framework, Atmospheric Chemistry and Physics, 16, 7213–7237, doi:10.5194/acp-16-7213-2016, URL https://www.atmos-chem-phys.net/16/7213/2016/, 2016.

Mills, G., Sharps, K., Simpson, D., Pleijel, H., Broberg, M., Uddling, J., Jaramillo, F., Davies, William, J., Dentener, F., Berg, M., Agrawal, M., Agrawal, S., Ainsworth, E. A., Büker, P., Emberson, L., Feng, Z., Harmens, H., Hayes, F., Kobayashi, K., Paoletti, E., and Dingenen, R.: Ozone pollution will compromise efforts to increase global wheat production, Global Change Biol., 24, 3560–3574, doi:10.1111/gcb.14157, URL https://onlinelibrary.wiley.com/doi/abs/10.1111/gcb.14157, 2018a.

Mills, G., Sharps, K., Simpson, D., Pleijel, H., Frei, M., Burkey, K., Emberson, L., Uddling, J., Broberg, M., Feng, Z., Kobayashi, K., and Agrawal, M.: Closing the global ozone yield gap: Quantification and cobenefits for multistress tolerance, Global Change Biology, 0, doi:10.1111/gcb.14381, URL https://onlinelibrary.wiley.com/doi/abs/10.1111/gcb.14381, 2018b.

Saunders, S. M., Jenkin, M. E., Derwent, R. G., and Pilling, M. J.: Protocol for the development of the Master Chemical Mechanism, MCM v3 (Part A): tropospheric degradation of non-aromatic volatile organic compounds, Atmos. Chem. Physics, 3, 161–180, URL http://www.atmos-chem-phys.net/3/161/2003/, 2003.

Simpson, D. and Tuovinen, J.-P.: ECLAIRE Ecosystem Surface Exchange model (ESX), in: Transboundary particulate matter, photo-oxidants, acidifying and eutrophying components. Status Report 1/2014, pp. 147–154, The Norwegian Meteorological Institute, Oslo, Norway, 2014.

Simpson, D., Benedictow, A., Berge, H., Bergström, R., Emberson, L. D., Fagerli, H., Hayman, G. D., Gauss, M., Jonson, J. E., Jenkin, M. E., Nyíri, A., Richter, C., Semeena, V. S., Tsyro, S., Tuovinen, J.-P., Valdebenito, A., and Wind, P.: The EMEP MSC-W chemical transport model – technical description, Atmos. Chem. Physics, 12, 7825–7865, doi:10.5194/acp-12-7825-2012, 2012.

Simpson, D., Tsyro, S., Wind, P., and Steensen, B. M.: EMEP model development, in: Transboundary acidification, eutrophication and ground level ozone in Europe in 2011. EMEP Status Report 1/2013, The Norwegian Meteorological Institute, Oslo, Norway, 2013.

Simpson, D., Tsyro, S., and Wind, P.: Updates to the EMEP/MSC-W model, in: Transboundary particulate matter, photo-oxidants, acidifying and eutrophying components. EMEP Status Report 1/2015, pp. 129–138, The Norwegian Meteorological Institute, Oslo, Norway, 2015.

Simpson, D., Nyíri, A., Tsyro, S., Valdebenito, Á., and Wind, P.: Updates to the EMEP/MSC-W model, in: Transboundary particulate matter, photo-oxidants, acidifying and eutrophying components. EMEP Status Report 1/2016, The Norwegian Meteorological Institute, Oslo, Norway, 2016.

Simpson, D., Bergström, R., Imhof, H., and Wind, P.: Updates to the EMEP MSC-W model, 2016-2017, in: Transboundary particulate matter, photo-oxidants, acidifying and eutrophying components. EMEP Status Report 1/2017, The Norwegian Meteorological Institute, Oslo, Norway, 2017.

Simpson, D., Bergström, R., , Gauss, M., Tsyro, S., Wind, P., and Valdebenito, Á.: Updates to the EMEP MSC-W model, 2017-2018, in: Transboundary particulate matter, photo-oxidants, acidifying and eutrophying components. EMEP Status Report 1/2018, The Norwegian Meteorological Institute, Oslo, Norway, 2018.

Skamarock, W. C. and Klemp, J. B.: A time-split nonhydrostatic atmospheric model for weather research and forecasting applications, J. Comp. Phys., 227, 3465–3485, doi:10.1016/j.jcp.2007.01.037, 2008.

Stadtler, S., Simpson, D., Schröder, S., Taraborrelli, D., Bott, A., and Schultz, M.: Ozone impacts of gas–aerosol uptake in global chemistry-transport models, Atmos. Chem. Physics, 18, 3147–3171, doi:10.5194/acp-18-3147-2018, URL https://www.atmos-chem-phys.net/18/3147/2018/, 2018.

Tsyro, S., Karl, M., Simpson, D., Valdebenito, A., and Wind, P.: Updates to the EMEP/MSC-W model, in: Transboundary particulate matter, photo-oxidants, acidifying and eutrophying components. EMEP Status Report 1/2014, pp. 143–146, The Norwegian Meteorological Institute, Oslo, Norway, 2014.

Weiss, A. and Norman, J. M.: Partitioning Solar-radiation into Direct and Diffuse, Visible and Near-infrared Components, Agricultural and Forest Meteorology, 34, 205–213, doi:10.1016/0168-1923(85)90020-6, 1985.

Yarwood, G., Rao, S., Yocke, M., and Whitten, G.: Updates to the Carbon Bond chemical mechanism: CB05, Final report to the US EPA, RT-0400675, December 8, 2005, Yocke and Company, URL www.camx.com/publ/pdfs/CB05_Final_Report_120805.pdfS, 2005.

CHAPTER 11

Developments in the monitoring network, data quality and database infrastructure

Wenche Aas, Anne Hjellbrekke and Kjetil Tørseth

11.1 Compliance with the EMEP monitoring strategy

The monitoring obligations in EMEP are defined by the Monitoring Strategy for 2010-2019 (UNECE (2009), Tørseth et al. (2012)). The complexity in the monitoring program with respect to the number of variables and sites, whether parameters are a level 1 or level 2, and the required time resolution (hourly, daily, weekly), makes it challenging to assess whether a country is in compliance. CCC has developed an index to illustrate to what extent the Parties comply, how implementation compares with other countries, and how activities evolve with time.

For the level 1 parameters an index is defined, calculated based on what has been reported compared to what is expected. EMEP recommends one site pr 50.000 km^2, but this target number is adjusted for very large countries (i.e. KZ, RU, TR and UA). The components and number of variables to be measured in accordance to the strategy are as follows: major inorganic ions in precipitation (10 variables), major inorganic components in air (13 variables), ozone (1 variable), PM mass (2 variables) and heavy metals in precipitation (7 variables). For heavy metals, the sampling frequency is weekly, and for the other components it is daily or hourly (ozone). Based on the relative implementation of the different variables, the index has been given the following relative weights: Inorganics in precipitation: 30%, inorganics in air: 30%, ozone: 20%, PM mass: 10%, heavy metals: 10%.

Figure 11.1 summarises implementation in 2017 compared to 2000, 2005 and 2010. The countries are sorted from left to right with increasing index for 2017. Slovenia has a full score as they measure all the required parameters with satisfactory sampling frequency. Estonia, The Netherlands, Slovakia, Denmark, and Switzerland have almost complete program with an

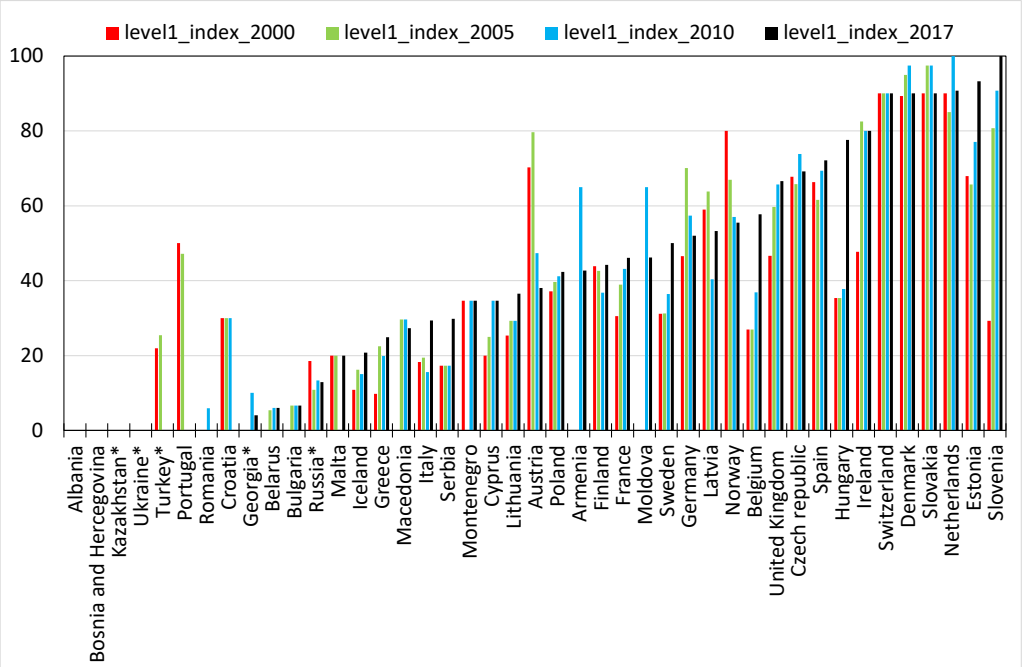

Figure 11.1: Index for implementation of the EMEP monitoring strategy, level 1 based on what has been reported for 2000, 2005, 2010 and 2016. * means adjusted land area.

index of 90% or higher. Small countries with requirements of less number of level 1 sites seem to comply easier than large countries. Since 2010, 40% of the Parties have improved their monitoring programme, while 33% have a decrease. Improvements are seen in e.g. Germany and Latvia. One Party, Malta, has reported data in 2017 and not in 2010, while Croatia and Romania have stopped reporting/measuring. In Figure 2.4 in Chapter 2.2, the geographical distribution of level 1 sites is shown for 2017. In large parts of Europe, implementation of the EMEP monitoring strategy is far from satisfactory.

For the level 2 parameters, an index based system has not been defined, but mapping the site distribution illustrate the compliance to the monitoring strategy. 45 sites from 18 different Parties reported at least one of the required EMEP level 2 parameters relevant to this report (aerosols (36 sites), photo-oxidants (19 sites) and trace gases (9 sites)). The sites with measurements of POPs and heavy metals are covered in the EMEP status report published by MSC-E. Figure 11.2 shows that level 2 measurements of aerosols have better spatial coverage than oxidant precursors (VOC + methane) and trace gases. Few sites have a complete measurement program, and only 8 sites have a complete aerosol program. Nevertheless, regarding the aerosol monitoring, there have been large improvements in the spatial coverage and the data quality over the last decade. Standardization and reference methodologies have been developed, and the reporting has improved significantly with much more metadata information available. For oxidant precursors and trace gases, there are ongoing improvement in the measurement capabilities resulting from development in ACTRIS (Aerosols, Clouds, and Trace gases Research InfraStructure Network) and in co-operation with the WMO Global

Atmospheric Watch Programme (GAW).

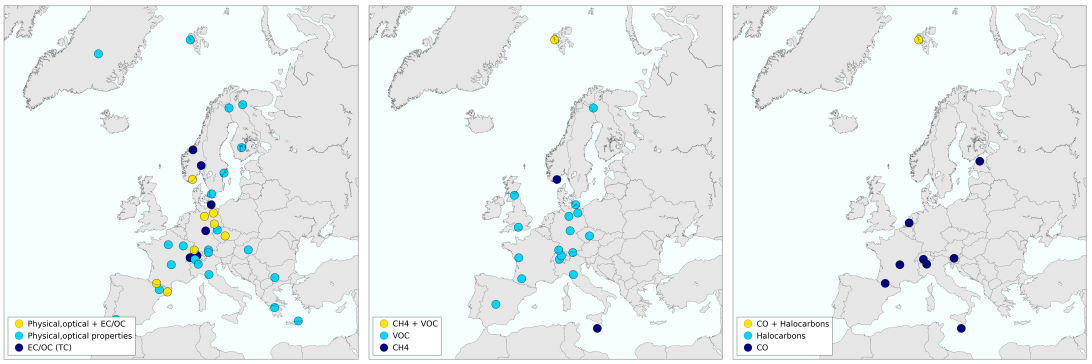

(a) Particulate matter (b) Oxidant precursors (c) Trace gases

Figure 11.2: Sites measuring and reporting EMEP level 2 parameters for the year 2017.

11.2 Updates in reporting templates and guidelines

In addition to the requirement that variables has to be measured as defined in the EMEP monitoring strategy discussed above, it is important that the data are reported in time to ensure that they can be quality assured and included in the database. This allows them to be included in the annual model validation, interpretations for the EMEP status reports, as well as other regional assessments and studies carried out beyond EMEP.

Figure 11.3 shows the status of the submission of data for 2017 and to what extent the data were reported in time. It is obvious that large volumes of data are reported late and some not at all. Of the 32 Parties reporting either level 1 or level 2 data, less than 60% reported within the deadline of 31 July 2018.

An online data submission and validation tool (`http://ebas-submit-tool.niluu.no`) was developed in 2016 improve the timelines and quality of the data reporting. The tool is designed to give the data submitters direct feedback on the formatted NASA Ames files, and suggestions on how to correct the files. The format checker is directly linked to all (approx. 40) data format templates located at `http://ebas-submit.nilu.no/`, and it is continuously being improved and updated, after feedback from the users or when new templates are developed. The requirement of checking the data files using the submission tool has significantly improved the correctness in the data files submitted, but still there are only 40% of the data, which are reported using the submission tool (or ftp), the rest is reported by e-mails. EMEP/CCC strongly encourage all the Parties to use the submission tool, which in fact is mandatory for submitting all the data to EMEP, unless otherwise have been agreed upon.

In the coming years there will be more focus on developing additional software tools for automatic creation of NASA Ames files directly from the output from various instruments for either regular annual reporting or Near-Real Time data submission, in addition to tools for checking the data based on requirements of consistency, completeness, data quality etc. defined by the different stakeholders i.e. EMEP, ACTRIS and WMO/GAW.

The EMEP data are extensively used. In 2009, a user statistic was implemented for the EBAS database infrastructure. The statistic counts how much data are downloaded, displayed

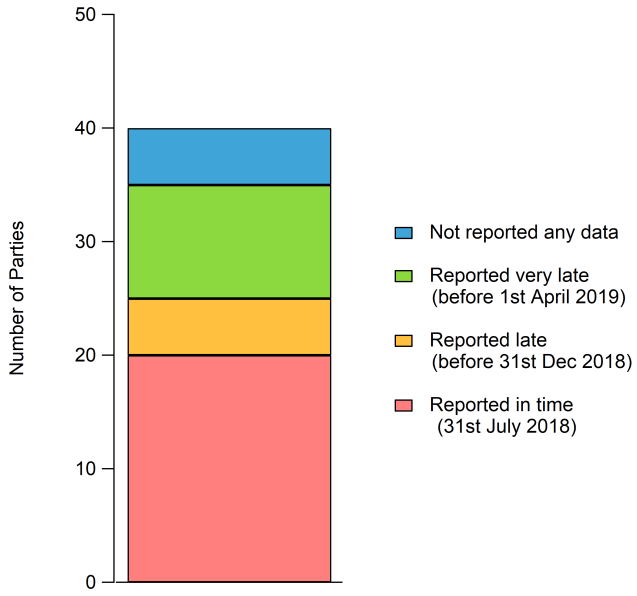

Figure 11.3: Submission of 2017 data to EMEP/CCC.

or plotted. Data are either downloaded directly from the web interface `http://ebas.nilu.no/`, or a system is setup for direct transfer to specific users in need of large data sets. Figure 11.4 shows the access requests for EMEP data per year (about 300 thousand annual datasets). There was a big jump in 2013. This was the year when an automatic system for distributing all the data in EBAS to specific users was implemented.

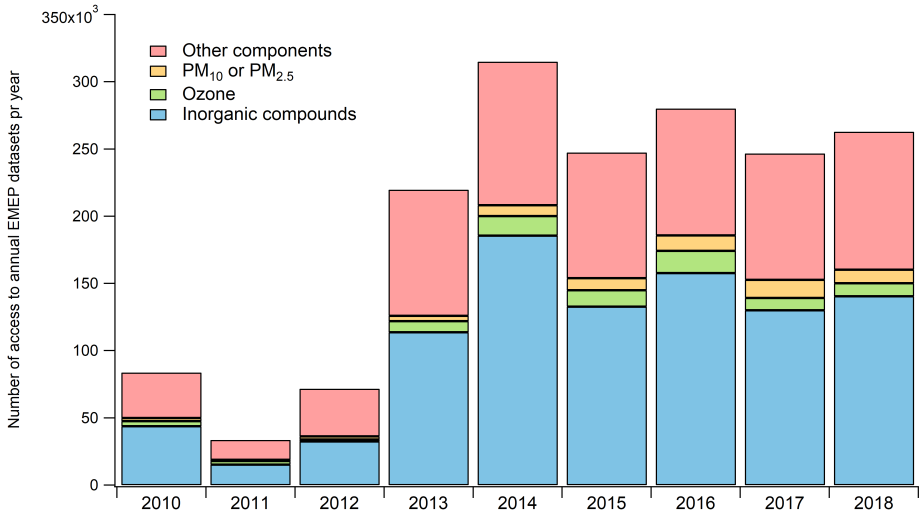

Figure 11.4: Access of EMEP data, number of annual dataset (compounds) per year.

References

Tørseth, K., Aas, W., Breivik, K., Fjæraa, A. M., Fiebig, M., Hjellbrekke, A. G., Lund Myhre, C., Solberg, S., and Yttri, K. E.: Introduction to the European Monitoring and Evaluation Programme (EMEP) and observed atmospheric composition change during 1972–2009, Atmos. Chem. Physics, 12, 5447–5481, doi:10.5194/acp-12-5447-2012, URL http://www.atmos-chem-phys.net/12/5447/2012/, 2012.

UNECE: Progress in activities in 2009 and future work. Measurements and modelling (acidification, eutrophication, photooxidants, heavy metals, particulate matter and persistent organic pollutants). Draft revised monitoring strategy., Tech. Rep. ECE/EB.AIR/GE.1/2009/15, UNECE, URL http://www.unece.org/env/documents/2009/EB/ge1/ece.eb.air.ge.1.2009.15.e.pdf, 2009.

Part IV

Appendices

APPENDIX A

National emissions for 2017 in the EMEP domain

This appendix contains the national emission data for 2017 used throughout this report for main pollutants and primary particle emissions in the new EMEP domain, which covers the geographic area between 30°N-82°N latitude and 30°W-90°E longitude.

These are the emissions that are used as basis for the 2017 source-receptor calculations. Results of these source-receptor calculations are presented in Appendix C.

The land-based emissions for 2017 have been derived from the 2019 official data submissions to UNECE CLRTAP (Pinterits et al. 2019).

Emissions from international shipping occurring in different European seas within the EMEP domain are not reported to UNECE CLRTAP, but derived from other sources. This year's update uses the CAMS global shipping emissions (Granier et al. 2019) developed by FMI (Finish Meteorological Institute).

Natural marine emissions of dimethyl sulphid (DMS) are calculated dynamically during the model run and vary with current meteorological conditions.

SO_x emissions from passive degassing of Italian volcanoes (Etna, Stromboli and Vulcano) are reported by Italy.

Note that emissions in this appendix are given in different units than used elsewhere in this report in order to keep consistency with the reported data.

References

Granier, C., Darras, S., Denier van der Gon, H., Doubalova, J., Elguindi, N., Galle, B., Gauss, M., Guevara, M., Jalkanen, J.-P., Kuenen, J., Liousse, C., Quack, B., Simpson, D., and Sindelarova, K.: The Copernicus Atmosphere Monitoring Service global and regional emissions (April 2019 version), doi:10.24380/d0bn-kx16, URL https://atmosphere.copernicus.eu/sites/default/files/2019-06/cams_emissions_general_document_apr2019_v7.pdf, 2019.

Pinterits, M., Ullrich, B., Gaisbauer, S., Mareckova, K., and Wankmüller, R.: Inventory review 2019. Review of emission data reported under the LRTAP Convention and NEC Directive. Stage 1 and 2 review. Status of gridded and LPS data, EMEP/CEIP 4/2019, CEIP/EEA Vienna, 2019.

Table A:1: National total emissions for 2017 in the EMEP domain. Unit: Gg. (Emissions of SO_x and NO_x are given as Gg(SO_2) and Gg(NO_2), respectively.)

Area/Pollutant	SO_x	NO_x	NH_3	NMVOC	CO	$PM_{2.5}$	PM_{co}	PM_{10}
Albania	13	25	24	39	177	15	4	19
Armenia	39	20	19	36	112	4	2	6
Austria	13	145	69	120	529	16	12	28
Azerbaijan	12	79	85	85	124	4	8	13
Belarus	48	143	138	143	381	35	24	59
Belgium	38	176	67	109	293	23	10	33
Bosnia and Herzegovina	170	31	21	33	96	14	12	26
Bulgaria	103	103	49	77	242	32	15	47
Croatia	13	55	38	63	197	17	9	25
Cyprus	16	15	6	12	14	1	1	2
Czechia	110	163	67	207	819	40	11	51
Denmark	10	112	76	102	241	20	11	31
Estonia	39	33	10	22	138	9	5	14
Finland	35	130	31	88	359	18	11	29
France	144	807	606	612	2695	164	90	254
Georgia	11	38	31	41	177	17	5	22
Germany	315	1188	673	1069	2832	99	107	206
Greece	57	255	56	199	323	26	30	56
Hungary	28	119	88	142	423	48	21	69
Iceland	50	23	5	6	113	1	0	2
Ireland	13	110	118	113	88	12	15	27
Italy	115	709	384	935	2331	165	31	196
Kazakhstan	698	756	234	294	1304	180	64	244
Kyrgyzstan	48	55	57	95	546	18	3	21
Latvia	4	37	17	38	125	18	7	25
Liechtenstein	0	0	0	0	1	0	0	0
Lithuania	13	53	30	46	140	7	7	14
Luxembourg	1	18	6	12	22	1	1	2
Malta	1	5	1	3	6	0	0	0
Moldova	9	28	23	51	85	11	5	17
Monaco	0	0	0	0	1	0	0	0
Montenegro	47	14	2	8	26	5	8	12
Netherlands	27	252	132	252	564	14	13	27
North Macedonia	56	24	10	29	57	9	7	16
Norway	15	163	33	153	437	28	9	37
Poland	583	804	308	691	2543	147	99	246
Portugal	48	159	58	168	325	51	22	73
Romania	107	232	164	240	783	112	31	143
Russian Federation	1663	3239	1204	3734	12369	369	441	809
Serbia	420	148	65	125	268	39	14	53
Slovakia	27	66	27	89	365	18	5	23
Slovenia	5	35	19	30	105	11	2	13
Spain	220	739	518	618	1309	105	67	172
Sweden	18	124	53	147	384	20	20	40
Switzerland	5	61	55	78	155	7	8	15
Tajikistan	19	10	53	19	116	5	2	7
Turkey	2350	785	740	1099	2033	388	377	765
Turkmenistan	27	99	61	75	259	19	3	22
Ukraine	839	637	286	519	2481	145	71	216
United Kingdom	173	893	283	809	1555	107	64	171
Uzbekistan	28	174	254	109	462	23	11	33
Asian areas	6665	7450	4890	10555	25595	1801	992	2793
North Africa	1627	1452	627	1374	2819	150	125	275
Baltic Sea	9	287	0	2	19	9	0	9
Black Sea	40	90	0	1	7	6	0	6
Mediterranean Sea	603	1171	0	9	79	86	0	86
North Sea	29	609	0	5	45	20	0	20
North-East Atlantic Ocean	403	773	0	6	54	57	0	57
Natural marine emissions	2394	0	0	0	0	0	0	0
Volcanic emissions	943	0	0	0	0	0	0	0
TOTAL	21554	25921	12872	25737	70148	4765	2914	7679

APPENDIX B

National emission trends

This appendix contains trends of national emission data for main pollutants and primary particle emissions for the years 2000–2017 in the EMEP domain, which covers the geographic area between 30°N-82°N latitude and 30°W-90°E longitude.

The land-based emissions for 2000–2017 have been derived from the 2019 official data submissions to UNECE CLRTAP (Pinterits et al. 2019).

Emissions from international shipping occurring in different European seas within the EMEP domain are not reported to UNECE CLRTAP, but derived from other sources. This year, emissions for the sea regions are based on the CAMS global shipping emission dataset (Granier et al. 2019, ECCAD 2019) for the years 2000 to 2017, developed by the Finish Meteorological Institute using AIS (Automatic Identification System) tracking data.

Natural marine emissions of dimethyl sulphid (DMS) are calculated dynamically during the model run and vary with current meteorological conditions.

SO_x emissions from passive degassing of Italian volcanoes (Etna, Stromboli and Vulcano) are those reported by Italy. SO_x and PM emissions from volcanic eruptions of Icelandic volcanoes in the period 2000–2017 (Eyjafjallajökull in 2010 and Barðarbunga in 2014-2015) are reported by Iceland. Emissions from the eruption of Grímsvötn volcano in May 2011 are not included in the table, as the eruption event has not been included in the model simulations.

Note that emissions in this appendix are given in different units than used elsewhere in this report in order to keep consistency with the reported data.

References

ECCAD: Emissions of atmospheric Compounds and Compilation of Ancillary Data, URL https://eccad.aeris-data.fr, 2019.

Granier, C., Darras, S., Denier van der Gon, H., Doubalova, J., Elguindi, N., Galle, B., Gauss, M., Guevara, M., Jalkanen, J.-P., Kuenen, J., Liousse, C., Quack, B., Simpson, D., and Sindelarova, K.: The Copernicus Atmosphere Monitoring Service global and regional emissions (April 2019 version), doi:10.24380/d0bn-kx16, URL https://atmosphere.copernicus.eu/sites/default/files/2019-06/cams_emissions_general_document_apr2019_v7.pdf, 2019.

Pinterits, M., Ullrich, B., Gaisbauer, S., Mareckova, K., and Wankmüller, R.: Inventory review 2019. Review of emission data reported under the LRTAP Convention and NEC Directive. Stage 1 and 2 review. Status of gridded and LPS data, EMEP/CEIP 4/2019, CEIP/EEA Vienna, 2019.

Table B:1: National total emission trends of sulphur (2000-2008), as used for modelling at the MSC-W (Gg of SO_2 per year).

Area/Year	2000	2001	2002	2003	2004	2005	2006	2007	2008
Albania	34	34	36	40	41	34	34	37	29
Armenia	8	4	8	10	14	18	22	26	27
Austria	32	33	32	31	27	25	26	23	20
Azerbaijan	20	18	18	17	17	18	17	17	17
Belarus	157	151	143	131	95	79	94	100	84
Belgium	172	167	157	152	155	143	134	124	96
Bosnia and Herzegovina	121	119	131	134	134	139	155	161	179
Bulgaria	863	829	759	826	791	779	766	825	576
Croatia	59	59	63	64	52	59	55	60	54
Cyprus	48	45	45	47	40	38	31	29	22
Czechia	233	229	223	218	215	208	207	212	170
Denmark	32	30	28	35	29	26	30	27	21
Estonia	97	91	87	100	88	76	70	88	69
Finland	82	96	90	101	84	70	83	81	67
France	626	565	524	499	481	460	431	414	353
Georgia	12	4	4	4	4	5	3	5	8
Germany	646	625	561	534	492	472	472	455	451
Greece	532	537	525	532	528	549	505	491	423
Hungary	427	346	272	246	152	43	39	36	36
Iceland	39	42	45	42	37	43	42	61	78
Ireland	144	142	107	83	73	73	61	55	45
Italy	756	704	623	524	487	409	387	345	290
Kazakhstan	457	477	503	542	574	634	640	668	680
Kyrgyzstan	25	25	25	25	25	25	27	30	33
Latvia	18	14	13	11	9	8	8	8	7
Lithuania	37	41	37	27	27	28	26	22	20
Luxembourg	3	4	3	3	2	2	3	2	2
Malta	10	11	10	11	11	12	12	12	10
Moldova	4	4	5	6	5	5	5	3	8
Montenegro	14	11	15	15	14	13	14	12	15
Netherlands	78	79	71	66	69	67	67	63	53
North Macedonia	106	108	97	95	96	97	94	99	101
Norway	27	25	23	23	25	24	21	19	20
Poland	1411	1386	1298	1268	1211	1172	1237	1174	947
Portugal	301	280	276	185	188	189	165	157	108
Romania	490	506	508	587	560	606	649	520	525
Russian Federation	2875	2918	2961	2931	2755	2608	2609	2270	2064
Serbia	464	459	484	509	520	446	463	472	481
Slovakia	117	123	99	102	93	86	85	69	68
Slovenia	94	63	63	60	51	40	17	16	15
Spain	1389	1328	1470	1217	1249	1205	1074	1044	382
Sweden	43	41	41	42	37	36	35	31	28
Switzerland	16	17	15	15	15	14	13	12	12
Tajikistan	5	7	8	7	9	8	10	13	13
Turkey	2242	1982	1872	1791	1779	2003	2160	2522	2558
Turkmenistan	19	17	18	19	19	19	19	20	21
Ukraine	2310	1844	1329	1252	1048	1192	1446	1363	1386
United Kingdom	1286	1198	1077	1052	894	773	728	632	529
Uzbekistan	176	175	173	162	155	135	130	107	93
Asian areas	3193	3191	3188	3186	3183	3181	3345	3509	3674
North Africa	982	1019	1056	1092	1129	1166	1187	1208	1229
Baltic Sea	225	220	218	216	212	206	138	109	100
Black Sea	52	52	51	51	50	49	48	47	44
Mediterranean Sea	902	891	870	855	839	823	809	795	721
North Sea	450	443	432	421	415	363	300	248	231
North-East Atlantic Ocean	586	581	564	554	547	534	527	517	471
Natural marine emissions	2364	2318	2380	2232	2298	2338	2376	2352	2386
Volcanic emissions	5746	4279	5300	3556	2701	1205	1308	840	973
TOTAL	33657	31006	31037	28558	26852	25077	25461	24660	23121

Table B:2: National total emission trends of sulphur (2009-2017), as used for modelling at the MSC-W (Gg of SO_2 per year).

Area/Year	2009	2010	2011	2012	2013	2014	2015	2016	2017
Albania	29	27	25	23	21	19	17	15	13
Armenia	27	28	29	30	31	32	35	39	39
Austria	15	16	15	15	14	15	14	14	13
Azerbaijan	15	16	15	16	15	15	14	18	12
Belarus	80	59	63	68	55	53	57	56	48
Belgium	74	61	53	48	43	40	41	39	38
Bosnia and Herzegovina	180	180	178	176	174	172	171	170	170
Bulgaria	442	387	514	328	194	187	143	105	103
Croatia	56	35	29	25	17	14	16	15	13
Cyprus	18	22	21	16	14	17	13	16	16
Czechia	169	164	168	160	145	134	129	115	110
Denmark	16	15	14	13	13	11	10	10	10
Estonia	55	83	73	43	42	47	36	35	39
Finland	59	66	60	50	48	44	41	40	35
France	297	278	254	236	213	173	163	144	144
Georgia	9	11	15	14	3	6	7	10	11
Germany	395	409	395	375	366	346	343	320	315
Greece	352	205	146	120	106	89	84	72	57
Hungary	30	30	34	31	29	26	24	23	28
Iceland	73	77	84	86	72	66	61	52	50
Ireland	32	26	25	23	23	17	15	14	13
Italy	237	218	196	178	146	131	124	117	115
Kazakhstan	693	732	884	835	785	758	744	714	698
Kyrgyzstan	35	38	39	41	42	44	45	47	48
Latvia	6	4	4	4	4	4	4	3	4
Lithuania	19	18	20	17	15	14	15	15	13
Luxembourg	2	2	1	1	2	2	1	1	1
Malta	7	8	8	8	5	5	2	2	1
Moldova	10	10	9	8	10	9	9	9	9
Montenegro	8	28	40	41	42	43	45	46	47
Netherlands	39	35	34	34	30	30	31	29	27
North Macedonia	96	91	102	96	83	83	77	65	56
Norway	15	19	19	17	17	17	17	15	15
Poland	811	875	836	803	768	724	711	591	583
Portugal	75	65	59	54	48	44	46	46	48
Romania	445	356	325	261	208	181	157	110	107
Russian Federation	1927	1903	1915	1857	1828	1819	1795	1850	1663
Serbia	433	403	458	421	436	343	416	423	420
Slovakia	63	68	67	57	52	44	67	26	27
Slovenia	12	11	13	12	14	10	5	5	5
Spain	284	244	280	279	221	243	260	217	220
Sweden	27	28	26	25	22	20	18	18	18
Switzerland	10	11	9	9	8	8	6	5	5
Tajikistan	13	13	14	15	16	17	18	18	19
Turkey	2662	2557	2637	2703	1940	2149	1948	2250	2350
Turkmenistan	21	22	23	26	26	26	26	26	27
Ukraine	1290	1241	1346	1366	1449	922	854	948	839
United Kingdom	432	450	415	460	397	322	250	176	173
Uzbekistan	84	84	75	66	56	47	38	29	28
Asian areas	3838	4002	4383	4728	5094	5466	5843	6235	6665
North Africa	1250	1271	1338	1378	1441	1479	1546	1564	1627
Baltic Sea	96	89	75	75	74	73	9	9	9
Black Sea	42	45	44	44	43	43	42	41	40
Mediterranean Sea	686	696	689	682	669	614	661	648	603
North Sea	224	204	178	178	175	168	31	31	29
North-East Atlantic Ocean	450	473	469	464	455	413	449	441	403
Natural marine emissions	2356	2314	2446	2368	2434	2250	2454	2390	2394
Volcanic emissions	950	1070	943	943	943	11823	2070	943	943
TOTAL	22069	21892	22632	22447	21638	31911	22267	21424	21554

Table B:3: National total emission trends of nitrogen oxides (2000-2008), as used for modelling at the MSC-W (Gg of NO_2 per year).

Area/Year	2000	2001	2002	2003	2004	2005	2006	2007	2008
Albania	18	19	20	21	25	25	24	22	22
Armenia	10	13	13	15	17	19	21	24	23
Austria	214	224	230	239	236	238	225	214	199
Azerbaijan	47	56	54	55	57	56	61	74	86
Belarus	135	135	137	140	148	171	187	181	189
Belgium	344	334	322	320	332	318	304	295	269
Bosnia and Herzegovina	35	34	34	34	33	33	33	33	33
Bulgaria	154	159	180	184	183	191	187	172	173
Croatia	88	88	91	90	89	87	87	89	84
Cyprus	21	21	21	22	21	21	21	21	20
Czechia	280	284	278	280	281	276	271	269	253
Denmark	227	225	222	230	214	206	205	190	174
Estonia	45	47	47	48	45	42	41	45	42
Finland	241	244	242	248	237	208	224	211	194
France	1618	1582	1546	1501	1465	1420	1336	1275	1178
Georgia	11	14	15	16	20	26	28	32	32
Germany	1945	1868	1792	1736	1658	1584	1574	1504	1429
Greece	412	439	436	447	451	470	474	470	447
Hungary	185	185	178	181	179	176	169	165	159
Iceland	33	30	32	31	32	29	28	31	29
Ireland	177	175	168	167	168	170	165	162	147
Italy	1487	1458	1398	1380	1335	1280	1211	1155	1069
Kazakhstan	366	436	448	470	515	548	581	612	625
Kyrgyzstan	21	22	23	24	25	26	30	33	36
Latvia	40	43	42	44	43	42	43	44	41
Lithuania	56	58	59	59	61	62	65	62	63
Luxembourg	41	43	43	45	54	55	48	43	39
Malta	9	9	9	10	10	10	10	10	10
Moldova	13	16	15	20	20	21	19	20	22
Montenegro	9	7	7	7	8	8	8	8	9
Netherlands	465	453	436	431	416	408	399	381	372
North Macedonia	43	40	38	34	36	37	37	40	39
Norway	224	222	217	217	215	217	216	217	211
Poland	852	829	798	818	840	869	890	893	863
Portugal	285	280	286	261	262	268	248	238	221
Romania	280	285	294	302	307	326	324	306	301
Russian Federation	3361	3455	3549	3801	3783	3745	3386	3304	3215
Serbia	148	153	164	167	183	167	169	173	172
Slovakia	107	108	102	100	100	103	97	96	96
Slovenia	59	58	58	55	54	55	56	54	58
Spain	1356	1324	1360	1351	1383	1364	1315	1306	1098
Sweden	216	206	198	194	188	184	179	172	164
Switzerland	105	102	96	94	92	92	89	86	85
Tajikistan	5	5	5	5	6	6	7	8	8
Turkey	495	473	560	542	633	671	689	741	732
Turkmenistan	61	62	65	72	73	75	77	84	87
Ukraine	828	835	851	954	874	883	892	913	893
United Kingdom	2051	2000	1893	1849	1791	1777	1705	1637	1466
Uzbekistan	223	222	225	221	210	200	204	202	199
Asian areas	3029	3193	3358	3522	3686	3850	3975	4100	4225
North Africa	803	827	852	876	901	926	967	1009	1051
Baltic Sea	408	400	397	392	385	378	372	369	339
Black Sea	122	121	120	119	118	115	113	112	104
Mediterranean Sea	1706	1682	1647	1625	1601	1573	1548	1524	1391
North Sea	907	895	877	860	849	835	823	807	753
North-East Atlantic Ocean	1147	1133	1108	1090	1077	1057	1040	1023	936
Natural marine emissions	0	0	0	0	0	0	0	0	0
Volcanic emissions	0	0	0	0	0	0	0	0	0
TOTAL	27566	27633	27654	28020	28027	28001	27499	27266	26171

Table B:4: National total emission trends of nitrogen oxides (2009-2017), as used for modelling at the MSC-W (Gg of NO_2 per year).

Area/Year	2009	2010	2011	2012	2013	2014	2015	2016	2017
Albania	22	22	23	23	23	24	24	25	25
Armenia	23	23	23	22	22	22	20	18	20
Austria	184	183	173	168	169	160	156	151	145
Azerbaijan	69	74	80	87	81	83	82	79	79
Belarus	189	170	171	175	166	159	145	143	143
Belgium	241	246	229	215	208	198	198	186	176
Bosnia and Herzegovina	33	32	32	32	32	31	31	31	31
Bulgaria	157	148	165	152	137	146	147	141	103
Croatia	79	71	67	62	61	57	57	56	55
Cyprus	20	19	21	22	16	17	15	15	15
Czechia	239	232	220	207	191	184	176	167	163
Denmark	155	150	141	130	125	116	114	115	112
Estonia	37	43	41	38	37	37	33	32	33
Finland	176	187	171	161	158	151	139	134	130
France	1095	1077	1020	991	980	909	884	843	807
Georgia	31	33	37	39	35	36	37	37	38
Germany	1331	1356	1340	1307	1309	1273	1250	1224	1188
Greece	436	361	325	286	271	266	263	260	255
Hungary	148	145	135	127	125	123	124	117	119
Iceland	28	27	24	24	23	23	24	22	23
Ireland	123	117	105	108	109	109	112	112	110
Italy	984	967	929	871	818	800	775	751	709
Kazakhstan	622	642	648	727	738	737	773	760	756
Kyrgyzstan	39	43	44	46	48	50	51	53	55
Latvia	38	41	38	38	38	38	38	37	37
Lithuania	57	59	56	58	57	57	58	58	53
Luxembourg	34	34	34	31	28	26	22	20	18
Malta	9	9	8	9	7	7	6	6	5
Moldova	22	25	25	24	24	26	26	27	28
Montenegro	7	10	13	13	13	13	14	14	14
Netherlands	338	333	317	302	292	272	273	258	252
North Macedonia	39	38	41	40	38	29	27	27	24
Norway	201	206	207	203	196	189	178	170	163
Poland	856	888	872	836	796	747	725	742	804
Portugal	209	192	176	164	161	158	162	156	159
Romania	254	241	252	250	229	225	225	221	232
Russian Federation	2953	2930	3023	3120	3172	3193	3153	3185	3239
Serbia	161	150	163	151	153	129	146	149	148
Slovakia	87	85	77	75	73	73	72	67	66
Slovenia	50	48	48	46	44	39	35	36	35
Spain	978	921	904	870	757	774	777	741	739
Sweden	153	157	149	141	138	137	132	128	124
Switzerland	79	78	73	73	73	69	65	63	61
Tajikistan	8	8	8	8	9	9	9	10	10
Turkey	713	707	745	656	710	705	713	722	785
Turkmenistan	85	83	86	88	90	92	94	97	99
Ukraine	731	716	704	693	682	671	659	648	637
United Kingdom	1273	1250	1161	1185	1125	1054	1018	928	893
Uzbekistan	195	194	191	188	185	182	179	177	174
Asian areas	4349	4474	4901	5286	5695	6111	6532	6969	7450
North Africa	1092	1134	1194	1229	1285	1320	1379	1395	1452
Baltic Sea	323	346	335	306	320	303	299	300	287
Black Sea	99	105	103	101	99	98	97	94	90
Mediterranean Sea	1315	1420	1392	1377	1339	1210	1294	1258	1171
North Sea	722	755	736	719	709	661	675	662	609
North-East Atlantic Ocean	885	953	934	928	891	799	863	840	773
Natural marine emissions	0	0	0	0	0	0	0	0	0
Volcanic emissions	0	0	0	0	0	0	0	0	0
TOTAL	24778	24956	25127	25230	25313	25127	25577	25675	25921

Table B:5: National total emission trends of ammonia (2000-2008), as used for modelling at the MSC-W (Gg of NH_3 per year).

Area/Year	2000	2001	2002	2003	2004	2005	2006	2007	2008
Albania	29	29	28	28	27	27	26	24	24
Armenia	14	13	12	15	15	16	16	17	17
Austria	64	64	63	63	63	63	63	65	64
Azerbaijan	50	51	54	58	61	63	66	66	81
Belarus	142	137	128	120	121	135	134	144	147
Belgium	92	88	85	81	77	75	75	71	71
Bosnia and Herzegovina	17	17	17	18	18	18	18	19	19
Bulgaria	54	51	50	52	53	52	51	52	49
Croatia	45	48	46	46	49	48	45	45	42
Cyprus	7	8	8	8	8	7	8	8	7
Czechia	87	87	85	83	79	77	77	78	77
Denmark	97	95	94	93	92	89	85	84	83
Estonia	9	10	9	10	10	10	10	10	11
Finland	34	34	35	36	37	37	36	36	35
France	646	639	625	617	610	605	594	601	609
Georgia	34	34	35	37	36	35	30	32	33
Germany	662	669	654	651	640	640	642	646	649
Greece	66	65	65	64	67	65	63	65	62
Hungary	93	92	93	94	91	86	86	86	79
Iceland	5	5	5	5	5	5	5	5	5
Ireland	115	115	115	114	113	113	112	108	110
Italy	459	462	449	448	443	427	422	425	415
Kazakhstan	150	150	160	170	178	195	194	200	205
Kyrgyzstan	26	26	27	27	27	28	29	29	30
Latvia	14	15	15	15	14	15	15	16	15
Lithuania	27	27	29	30	30	31	32	31	30
Luxembourg	7	7	6	6	6	6	6	6	6
Malta	2	2	2	2	2	1	1	2	1
Moldova	23	24	25	24	23	24	24	19	19
Montenegro	6	5	6	6	5	4	3	3	3
Netherlands	176	170	163	160	158	155	158	154	140
North Macedonia	13	13	12	12	12	12	12	12	12
Norway	33	33	33	34	34	34	34	34	34
Poland	331	336	334	318	308	324	337	336	324
Portugal	77	73	71	64	64	63	61	62	60
Romania	186	182	187	190	203	206	205	201	198
Russian Federation	967	936	905	899	901	818	879	860	859
Serbia	76	74	80	75	81	81	80	82	73
Slovakia	42	43	43	41	38	38	36	36	33
Slovenia	22	21	23	21	20	20	20	21	20
Spain	556	552	540	556	551	522	508	511	472
Sweden	60	59	59	59	59	58	57	57	57
Switzerland	60	59	58	57	57	58	58	59	59
Tajikistan	23	21	27	28	29	31	32	33	37
Turkey	557	521	479	526	518	554	566	580	541
Turkmenistan	22	28	26	31	34	47	54	54	56
Ukraine	358	378	270	242	225	260	227	213	206
United Kingdom	306	298	294	287	294	285	278	274	259
Uzbekistan	151	147	148	160	169	175	183	186	193
Asian areas	2361	2416	2471	2525	2580	2635	2695	2755	2815
North Africa	365	380	394	409	423	438	448	458	469
Baltic Sea	0	0	0	0	0	0	0	0	0
Black Sea	0	0	0	0	0	0	0	0	0
Mediterranean Sea	0	0	0	0	0	0	0	0	0
North Sea	0	0	0	0	0	0	0	0	0
North-East Atlantic Ocean	0	0	0	0	0	0	0	0	0
Natural marine emissions	0	0	0	0	0	0	0	0	0
Volcanic emissions	0	0	0	0	0	0	0	0	0
TOTAL	9817	9811	9645	9714	9761	9810	9897	9969	9914

Table B:6: National total emission trends of ammonia (2009-2017), as used for modelling at the MSC-W (Gg of NH_3 per year).

Area/Year	2009	2010	2011	2012	2013	2014	2015	2016	2017
Albania	24	24	24	24	25	25	25	24	24
Armenia	17	18	18	18	18	19	20	21	19
Austria	66	66	65	66	66	67	67	68	69
Azerbaijan	81	80	83	83	84	85	85	85	85
Belarus	150	151	154	157	149	141	143	136	138
Belgium	71	71	70	70	71	68	68	68	67
Bosnia and Herzegovina	19	19	19	19	20	20	20	21	21
Bulgaria	46	47	45	45	46	49	50	51	49
Croatia	41	41	42	42	36	34	39	37	38
Cyprus	7	7	7	7	6	6	6	6	6
Czechia	72	71	69	69	71	71	72	72	67
Denmark	79	80	78	77	74	75	75	75	76
Estonia	10	10	10	10	10	10	10	10	10
Finland	35	36	35	34	33	34	32	32	31
France	599	604	594	596	594	600	608	609	606
Georgia	33	33	33	36	41	35	34	33	31
Germany	661	641	671	659	677	679	689	681	673
Greece	61	64	64	62	62	60	57	57	56
Hungary	77	78	79	79	82	82	87	87	88
Iceland	5	5	5	5	5	5	5	5	5
Ireland	110	108	104	106	108	108	111	116	118
Italy	400	390	392	403	387	376	377	392	384
Kazakhstan	211	216	207	211	213	222	229	238	234
Kyrgyzstan	31	31	35	39	43	46	50	54	57
Latvia	16	16	16	16	16	17	16	16	17
Lithuania	32	31	31	31	30	31	31	30	30
Luxembourg	6	6	6	5	5	6	6	6	6
Malta	1	1	1	1	1	1	1	1	1
Moldova	21	22	21	20	19	23	23	23	23
Montenegro	3	3	3	3	3	3	2	2	2
Netherlands	138	134	131	125	124	128	129	128	132
North Macedonia	11	11	12	10	10	10	10	10	10
Norway	34	33	33	33	33	33	33	33	33
Poland	309	303	304	294	294	289	285	292	308
Portugal	57	57	57	55	53	56	57	57	58
Romania	191	175	173	172	172	169	172	168	164
Russian Federation	1082	1053	1087	1120	1123	1137	1167	1180	1204
Serbia	78	69	71	76	71	66	65	66	65
Slovakia	33	33	31	32	32	32	32	28	27
Slovenia	20	20	19	19	18	18	19	19	19
Spain	470	459	449	445	451	472	490	498	518
Sweden	54	55	54	53	54	54	54	53	53
Switzerland	58	58	57	56	56	56	56	55	55
Tajikistan	39	40	42	44	46	47	49	51	53
Turkey	571	606	643	713	755	704	673	683	740
Turkmenistan	56	56	56	57	57	57	57	59	61
Ukraine	187	251	256	261	266	271	276	281	286
United Kingdom	260	264	266	262	258	271	276	281	283
Uzbekistan	203	212	218	224	230	236	242	248	254
Asian areas	2876	2936	3216	3468	3737	4010	4287	4574	4890
North Africa	479	490	515	531	555	570	596	602	627
Baltic Sea	0	0	0	0	0	0	0	0	0
Black Sea	0	0	0	0	0	0	0	0	0
Mediterranean Sea	0	0	0	0	0	0	0	0	0
North Sea	0	0	0	0	0	0	0	0	0
North-East Atlantic Ocean	0	0	0	0	0	0	0	0	0
Natural marine emissions	0	0	0	0	0	0	0	0	0
Volcanic emissions	0	0	0	0	0	0	0	0	0
TOTAL	10190	10284	10670	11043	11393	11685	12063	12422	12872

Table B:7: National total emission trends of non-methane volatile organic compounds (2000-2008), as used for modelling at the MSC-W (Gg of NMVOC per year).

Area/Year	2000	2001	2002	2003	2004	2005	2006	2007	2008
Albania	23	25	26	29	32	33	33	33	33
Armenia	16	28	14	28	30	32	33	35	35
Austria	180	175	170	168	156	156	159	154	149
Azerbaijan	68	70	71	74	76	80	89	79	83
Belarus	225	215	229	308	324	349	358	367	387
Belgium	212	208	194	186	176	172	167	158	150
Bosnia and Herzegovina	52	50	49	48	46	45	44	42	41
Bulgaria	107	94	102	107	94	94	97	90	90
Croatia	104	103	106	109	114	116	116	112	109
Cyprus	18	19	18	20	22	22	21	21	21
Czechia	287	279	277	272	263	252	254	247	243
Denmark	169	161	156	151	147	143	140	137	133
Estonia	37	36	36	34	34	32	31	28	26
Finland	177	174	166	162	157	145	141	136	122
France	1644	1557	1432	1356	1268	1175	1065	966	891
Georgia	40	46	45	45	42	35	34	37	37
Germany	1638	1534	1467	1395	1402	1349	1369	1302	1242
Greece	317	312	333	315	320	306	304	302	270
Hungary	197	199	185	188	182	172	159	155	150
Iceland	9	8	8	8	8	7	7	7	7
Ireland	122	122	122	120	120	120	120	120	116
Italy	1602	1537	1447	1427	1331	1348	1310	1294	1266
Kazakhstan	170	175	177	187	194	205	223	245	254
Kyrgyzstan	20	21	23	25	26	28	32	36	39
Latvia	49	51	50	50	49	48	48	47	42
Lithuania	72	69	67	64	63	62	61	60	59
Luxembourg	16	15	15	14	16	15	13	12	14
Malta	5	5	5	5	5	4	4	4	4
Moldova	29	35	33	34	38	47	50	53	65
Montenegro	10	9	8	9	10	8	9	10	10
Netherlands	333	304	289	281	261	266	260	263	257
North Macedonia	48	40	39	39	39	37	39	39	43
Norway	406	416	370	326	293	243	214	210	176
Poland	732	705	723	702	708	721	761	733	748
Portugal	249	245	239	228	221	210	204	199	188
Romania	266	255	259	271	279	320	314	310	310
Russian Federation	3420	3590	3761	3635	3525	3572	3126	2948	2829
Serbia	146	144	145	148	150	146	143	147	142
Slovakia	168	166	149	148	148	151	148	145	141
Slovenia	52	52	50	50	48	45	45	43	42
Spain	942	913	885	846	831	802	775	765	698
Sweden	224	218	216	217	210	209	204	198	187
Switzerland	147	140	128	119	110	107	104	101	99
Tajikistan	6	8	9	9	10	9	11	13	13
Turkey	1016	930	986	1009	1013	998	995	988	1002
Turkmenistan	82	84	86	93	88	84	80	82	87
Ukraine	555	609	632	632	611	631	664	680	682
United Kingdom	1635	1558	1468	1351	1262	1179	1130	1089	1010
Uzbekistan	183	180	174	181	148	144	141	138	138
Asian areas	5200	5327	5454	5581	5708	5835	5936	6036	6136
North Africa	1059	1058	1057	1057	1056	1055	1058	1062	1066
Baltic Sea	3	3	3	3	3	3	3	3	3
Black Sea	1	1	1	1	1	1	1	1	1
Mediterranean Sea	11	11	11	11	11	11	11	10	10
North Sea	7	6	6	6	6	6	5	6	6
North-East Atlantic Ocean	8	8	7	7	7	7	7	7	7
Natural marine emissions	0	0	0	0	0	0	0	0	0
Volcanic emissions	0	0	0	0	0	0	0	0	0
TOTAL	24516	24302	24179	23890	23490	23396	22869	22507	22113

Table B:8: National total emission trends of non-methane volatile organic compounds (2009-2017), as used for modelling at the MSC-W (Gg of NMVOC per year).

Area/Year	2009	2010	2011	2012	2013	2014	2015	2016	2017
Albania	33	34	35	35	36	37	37	38	39
Armenia	35	34	34	34	34	34	35	36	36
Austria	136	137	131	129	133	120	124	122	120
Azerbaijan	85	89	93	95	89	90	90	89	85
Belarus	362	308	346	347	334	330	310	291	143
Belgium	138	138	126	123	120	114	111	111	109
Bosnia and Herzegovina	40	39	38	37	36	35	35	34	33
Bulgaria	86	87	87	85	78	77	79	80	77
Croatia	94	90	84	78	73	67	68	68	63
Cyprus	19	20	14	14	13	12	12	12	12
Czechia	243	241	230	224	221	214	212	207	207
Denmark	124	122	115	112	112	104	107	103	102
Estonia	24	23	23	23	22	22	22	22	22
Finland	112	114	105	102	97	94	89	90	88
France	801	817	736	700	685	661	632	619	612
Georgia	37	38	38	37	44	42	41	41	41
Germany	1136	1257	1148	1146	1102	1069	1042	1043	1069
Greece	257	255	243	223	206	204	208	204	199
Hungary	150	146	150	152	151	141	144	142	142
Iceland	6	6	6	5	5	5	6	6	6
Ireland	113	110	107	108	111	107	107	109	113
Italy	1188	1124	1033	1024	996	932	915	899	935
Kazakhstan	267	277	259	290	280	312	300	297	294
Kyrgyzstan	43	47	54	61	68	75	82	89	95
Latvia	42	40	41	42	41	42	40	38	38
Lithuania	55	55	53	53	50	49	47	46	46
Luxembourg	12	11	11	12	12	11	11	12	12
Malta	4	3	3	3	3	3	3	3	3
Moldova	60	42	44	46	43	48	48	50	51
Montenegro	10	8	9	8	8	8	8	8	8
Netherlands	258	268	265	261	257	245	253	251	252
North Macedonia	43	36	39	34	34	28	30	30	29
Norway	160	161	154	154	156	166	164	157	153
Poland	748	712	694	676	633	631	641	674	691
Portugal	176	178	169	166	165	170	170	167	168
Romania	267	261	257	255	246	242	237	237	240
Russian Federation	2715	3424	3519	3624	3642	3646	3640	3665	3734
Serbia	141	134	133	128	127	116	123	127	125
Slovakia	131	133	127	125	107	89	97	95	89
Slovenia	39	37	35	33	33	30	30	30	30
Spain	638	630	606	583	564	569	588	603	618
Sweden	182	181	174	164	160	156	154	145	147
Switzerland	96	93	90	88	86	83	80	78	78
Tajikistan	13	14	14	15	16	16	17	18	19
Turkey	1027	1049	1034	1094	1039	1039	1077	1062	1099
Turkmenistan	80	78	77	77	77	76	76	75	75
Ukraine	559	534	532	530	528	525	523	521	519
United Kingdom	906	880	861	845	818	813	815	801	809
Uzbekistan	141	139	134	130	125	121	116	112	109
Asian areas	6237	6337	6941	7487	8068	8656	9254	9874	10555
North Africa	1069	1073	1129	1163	1216	1249	1305	1320	1374
Baltic Sea	3	3	3	3	2	2	2	2	2
Black Sea	1	1	1	1	1	1	1	1	1
Mediterranean Sea	10	10	10	10	10	9	10	10	9
North Sea	6	6	6	6	6	5	6	6	5
North-East Atlantic Ocean	7	7	7	7	7	6	7	7	6
Natural marine emissions	0	0	0	0	0	0	0	0	0
Volcanic emissions	0	0	0	0	0	0	0	0	0
TOTAL	21365	22090	22405	23006	23326	23751	24379	24975	25737

Table B:9: National total emission trends of carbon monoxide (2000-2008), as used for modelling at the MSC-W (Gg of CO per year).

Area/Year	2000	2001	2002	2003	2004	2005	2006	2007	2008
Albania	92	97	109	125	154	151	158	145	148
Armenia	110	104	106	120	118	116	114	112	111
Austria	730	710	685	693	683	618	610	579	558
Azerbaijan	104	112	109	112	112	118	128	130	147
Belarus	718	711	712	733	749	969	1070	1033	1063
Belgium	927	879	864	838	800	753	699	654	655
Bosnia and Herzegovina	181	167	153	92	96	94	93	90	86
Bulgaria	347	301	347	353	313	298	310	277	274
Croatia	451	435	417	439	416	419	391	376	324
Cyprus	30	29	28	29	28	27	25	24	22
Czechia	1075	1058	1018	1033	1020	934	939	939	886
Denmark	465	456	432	434	418	418	405	408	387
Estonia	199	200	190	183	174	155	142	158	157
Finland	595	595	579	556	541	509	500	481	463
France	6506	6146	5926	5635	5736	5240	4662	4496	4282
Georgia	131	170	173	167	187	221	225	178	178
Germany	4833	4657	4382	4202	3964	3756	3660	3543	3434
Greece	879	878	817	779	773	718	739	673	629
Hungary	830	839	691	817	750	682	582	540	481
Iceland	54	53	54	52	52	51	56	71	108
Ireland	246	242	230	221	216	215	198	185	177
Italy	4898	4575	3986	4038	3478	3510	3363	3423	3549
Kazakhstan	625	631	616	663	671	720	853	1009	1082
Kyrgyzstan	90	97	105	113	120	128	146	163	180
Latvia	261	267	254	253	241	221	218	197	180
Lithuania	183	182	184	178	174	176	187	192	182
Luxembourg	43	44	41	40	43	38	36	39	34
Malta	16	16	15	15	14	13	12	12	14
Moldova	28	29	34	50	48	49	50	44	47
Montenegro	40	37	34	40	40	37	36	37	35
Netherlands	762	760	750	744	754	735	746	734	738
North Macedonia	145	113	115	116	121	115	118	113	125
Norway	683	666	658	635	606	610	587	571	557
Poland	3356	3198	3194	3086	3090	3089	3228	2995	3009
Portugal	690	625	600	576	546	510	479	455	417
Romania	750	675	703	774	864	1063	966	957	1008
Russian Federation	13299	13643	13988	14065	14586	14722	13201	13079	11736
Serbia	401	403	404	419	436	404	359	403	367
Slovakia	546	563	483	509	514	557	510	506	470
Slovenia	188	182	178	177	166	163	154	147	143
Spain	2297	2102	1992	1891	1840	1757	1637	1604	1499
Sweden	662	624	589	578	541	528	502	497	480
Switzerland	384	365	340	332	316	302	280	265	255
Tajikistan	50	56	65	67	77	78	87	98	88
Turkey	2605	2357	2420	2376	2376	2318	2350	2399	2722
Turkmenistan	301	297	305	337	317	310	322	294	296
Ukraine	2531	2864	2888	2796	2955	2980	2841	2849	2940
United Kingdom	4446	4468	3983	3628	3411	3163	2967	2754	2600
Uzbekistan	740	724	704	740	594	594	580	573	568
Asian areas	13567	13828	14089	14349	14610	14871	14970	15069	15169
North Africa	2677	2600	2524	2447	2370	2294	2275	2257	2239
Baltic Sea	24	23	23	23	22	22	22	22	22
Black Sea	8	8	8	8	8	7	7	7	7
Mediterranean Sea	98	97	95	94	94	93	92	91	91
North Sea	57	56	56	55	54	54	53	53	54
North-East Atlantic Ocean	68	68	67	66	66	65	64	63	65
Natural marine emissions	0	0	0	0	0	0	0	0	0
Volcanic emissions	0	0	0	0	0	0	0	0	0
TOTAL	77023	76087	74517	73897	73465	72760	70003	69063	67535

Table B:10: National total emission trends of carbon monoxide (2009-2017), as used for modelling at the MSC-W (Gg of CO per year).

Area/Year	2009	2010	2011	2012	2013	2014	2015	2016	2017
Albania	146	150	154	158	162	165	169	173	177
Armenia	110	109	108	107	106	105	106	108	112
Austria	538	553	525	526	566	522	540	535	529
Azerbaijan	152	161	174	183	132	134	135	127	124
Belarus	990	870	880	878	848	843	767	760	381
Belgium	428	497	395	345	519	319	372	361	293
Bosnia and Herzegovina	94	94	94	94	95	95	95	95	96
Bulgaria	257	278	276	272	250	243	240	245	242
Croatia	316	300	272	254	239	205	219	205	197
Cyprus	20	19	17	16	15	15	14	14	14
Czechia	903	927	897	883	883	843	825	820	819
Denmark	354	346	305	287	273	250	254	244	241
Estonia	156	157	132	142	134	129	129	140	138
Finland	440	454	414	407	389	383	361	368	359
France	3816	4211	3535	3195	3259	2732	2688	2738	2695
Georgia	172	173	171	158	184	183	169	177	177
Germany	2983	3350	3262	2890	2862	2761	2868	2805	2832
Greece	576	522	478	504	418	417	397	352	323
Hungary	521	523	530	546	538	460	445	437	423
Iceland	111	109	107	107	109	108	111	109	113
Ireland	156	143	131	124	118	111	108	102	88
Italy	3155	3121	2477	2704	2535	2299	2344	2269	2331
Kazakhstan	1149	1252	1097	1361	1196	1520	1354	1313	1304
Kyrgyzstan	198	215	262	310	357	404	452	499	546
Latvia	189	153	158	161	147	141	119	116	125
Lithuania	174	156	172	167	159	151	145	143	140
Luxembourg	30	29	26	27	26	25	21	22	22
Malta	11	11	10	7	7	7	6	6	6
Moldova	46	50	52	51	52	78	78	82	85
Montenegro	29	30	33	32	31	30	28	27	26
Netherlands	687	685	660	627	597	574	576	564	564
North Macedonia	134	115	120	89	90	62	65	65	57
Norway	508	520	493	485	453	433	438	434	437
Poland	2939	3077	2782	2787	2658	2387	2343	2456	2543
Portugal	395	395	363	349	329	312	320	308	325
Romania	906	897	828	835	794	796	774	779	783
Russian Federation	10929	10783	11201	11705	11952	12012	11999	12172	12369
Serbia	360	349	346	308	284	268	270	277	268
Slovakia	412	452	420	428	399	359	370	377	365
Slovenia	132	130	128	123	122	102	107	110	105
Spain	1353	1421	1382	1317	1298	1313	1298	1292	1309
Sweden	466	454	441	417	411	397	384	385	384
Switzerland	238	229	208	200	193	174	165	162	155
Tajikistan	92	89	93	97	100	104	108	112	116
Turkey	2933	2900	2597	2827	2044	1961	2185	2050	2033
Turkmenistan	290	276	274	272	269	267	264	262	259
Ukraine	2614	2502	2499	2496	2493	2490	2487	2484	2481
United Kingdom	2128	2040	1855	1838	1837	1747	1707	1573	1555
Uzbekistan	594	576	560	544	527	511	494	478	462
Asian areas	15268	15367	16833	18155	19564	20991	22440	23943	25595
North Africa	2220	2202	2318	2387	2496	2562	2678	2709	2819
Baltic Sea	22	21	20	20	20	19	20	20	19
Black Sea	8	7	7	7	7	7	7	7	7
Mediterranean Sea	95	88	87	87	86	85	89	85	79
North Sea	54	51	50	50	50	48	50	49	45
North-East Atlantic Ocean	67	61	61	61	60	59	61	59	54
Natural marine emissions	0	0	0	0	0	0	0	0	0
Volcanic emissions	0	0	0	0	0	0	0	0	0
TOTAL	64068	64651	63772	65408	65744	65720	67263	68606	70148

Table B:11: National total emission trends of fine particulate matter (2000-2008), as used for modelling at the MSC-W (Gg of $PM_{2.5}$ per year).

Area/Year	2000	2001	2002	2003	2004	2005	2006	2007	2008
Albania	9	9	10	13	14	13	14	13	13
Armenia	4	4	4	4	4	4	4	4	4
Austria	25	25	24	24	24	22	21	20	20
Azerbaijan	5	5	5	5	5	5	5	7	6
Belarus	25	25	26	28	37	46	52	52	54
Belgium	41	39	37	37	37	35	36	34	34
Bosnia and Herzegovina	16	17	18	19	20	20	19	18	17
Bulgaria	26	24	29	31	31	31	33	31	31
Croatia	33	36	36	40	39	41	37	34	32
Cyprus	3	2	2	2	2	2	2	2	2
Czechia	49	50	47	47	46	43	44	42	41
Denmark	24	24	23	25	25	26	26	29	27
Estonia	15	16	17	14	15	14	10	13	12
Finland	26	27	27	27	26	25	25	24	23
France	328	316	294	294	280	260	235	222	216
Georgia	28	26	25	23	21	19	19	19	19
Germany	167	162	155	151	146	139	135	129	122
Greece	53	56	52	50	52	50	50	49	50
Hungary	48	52	37	46	43	40	40	40	36
Iceland	1	1	1	1	2	1	2	2	2
Ireland	20	20	19	19	19	19	19	18	18
Italy	196	189	159	177	152	175	179	203	217
Kazakhstan	54	71	60	66	73	81	68	125	143
Kyrgyzstan	7	8	8	8	8	8	9	9	9
Latvia	22	22	22	23	25	23	23	22	21
Lithuania	7	7	8	7	8	8	9	9	9
Luxembourg	2	3	2	3	3	2	2	2	2
Malta	1	1	1	1	1	1	1	1	1
Moldova	4	4	4	5	4	4	5	4	4
Montenegro	4	4	5	5	5	5	5	5	6
Netherlands	30	28	27	26	25	24	24	23	21
North Macedonia	30	18	19	29	31	28	27	21	25
Norway	43	42	43	40	39	39	37	37	36
Poland	159	159	159	157	161	160	164	158	155
Portugal	74	71	71	67	68	67	63	62	59
Romania	103	84	87	103	116	120	115	114	133
Russian Federation	492	483	475	438	478	442	517	530	423
Serbia	40	40	41	42	42	40	37	41	37
Slovakia	41	41	30	30	28	34	30	27	24
Slovenia	11	11	12	12	13	13	13	13	14
Spain	140	130	131	133	132	132	128	128	117
Sweden	33	32	31	32	31	31	29	29	27
Switzerland	11	10	10	10	10	9	9	9	9
Tajikistan	2	1	2	2	2	3	3	3	3
Turkey	384	372	359	348	351	354	357	360	362
Turkmenistan	8	8	10	12	12	12	15	12	12
Ukraine	121	138	140	137	152	153	147	146	162
United Kingdom	148	147	131	132	128	126	124	117	116
Uzbekistan	15	15	17	15	16	16	17	18	17
Asian areas	839	864	889	914	939	964	988	1011	1034
North Africa	93	95	98	100	102	104	107	109	112
Baltic Sea	29	29	28	28	28	27	21	18	17
Black Sea	7	7	7	7	7	7	7	7	6
Mediterranean Sea	117	116	113	112	111	109	108	106	96
North Sea	61	60	59	58	57	57	47	42	39
North-East Atlantic Ocean	76	76	74	73	73	72	71	70	60
Natural marine emissions	0	0	0	0	0	0	0	0	0
Volcanic emissions	0	0	0	0	0	0	0	0	0
TOTAL	4350	4321	4219	4253	4317	4308	4331	4393	4310

Table B:12: National total emission trends of fine particulate matter (2009-2017), as used for modelling at the MSC-W (Gg of $PM_{2.5}$ per year).

Area/Year	2009	2010	2011	2012	2013	2014	2015	2016	2017
Albania	14	14	14	14	15	15	15	15	15
Armenia	4	4	4	4	4	4	4	4	4
Austria	19	19	18	18	18	16	16	16	16
Azerbaijan	6	6	6	7	6	6	6	4	4
Belarus	52	46	50	52	44	44	40	39	35
Belgium	30	33	26	27	29	22	24	25	23
Bosnia and Herzegovina	16	15	15	15	15	14	14	14	14
Bulgaria	29	31	34	34	32	31	32	32	32
Croatia	31	31	28	26	24	20	21	18	17
Cyprus	2	2	2	1	1	1	1	1	1
Czechia	42	45	43	43	44	41	40	39	40
Denmark	25	25	23	21	21	19	21	21	20
Estonia	10	14	18	9	12	9	10	8	9
Finland	22	24	21	21	20	19	18	18	18
France	206	215	189	192	194	168	170	170	164
Georgia	20	20	20	20	19	19	17	18	17
Germany	115	122	117	110	109	104	104	101	99
Greece	49	40	34	34	30	30	28	27	26
Hungary	47	49	55	58	59	49	52	50	48
Iceland	2	2	1	2	1	2	1	1	1
Ireland	17	16	15	14	15	14	14	13	12
Italy	202	196	150	177	172	155	161	157	165
Kazakhstan	133	122	131	139	147	155	163	172	180
Kyrgyzstan	10	10	11	12	13	15	16	17	18
Latvia	23	19	19	20	19	18	16	16	18
Lithuania	8	8	8	8	8	8	7	7	7
Luxembourg	2	2	2	2	2	2	1	2	1
Malta	0	0	0	0	0	0	0	0	0
Moldova	4	4	5	5	5	11	11	11	11
Montenegro	4	4	5	5	5	5	5	5	5
Netherlands	19	19	18	16	16	15	15	14	14
North Macedonia	19	24	29	22	24	17	16	13	9
Norway	35	38	35	36	31	28	28	27	28
Poland	148	157	150	149	144	136	136	142	147
Portugal	56	56	57	54	52	51	51	51	51
Romania	126	129	119	122	114	115	110	110	112
Russian Federation	412	427	424	429	416	413	390	369	369
Serbia	43	43	42	42	37	37	38	41	39
Slovakia	22	25	23	24	22	17	18	19	18
Slovenia	13	13	13	13	13	11	12	12	11
Spain	118	114	114	110	106	105	105	103	105
Sweden	26	26	26	24	24	21	20	20	20
Switzerland	8	8	8	8	8	7	7	7	7
Tajikistan	4	3	4	4	4	4	4	5	5
Turkey	365	368	371	374	377	379	382	385	388
Turkmenistan	15	14	15	16	16	17	18	18	19
Ukraine	139	135	136	138	139	141	142	143	145
United Kingdom	111	119	107	113	114	108	109	107	107
Uzbekistan	19	19	20	20	21	21	22	22	23
Asian areas	1058	1081	1184	1277	1376	1477	1579	1685	1801
North Africa	115	117	123	127	133	136	143	144	150
Baltic Sea	16	16	15	15	15	14	9	9	9
Black Sea	6	7	7	6	6	6	6	6	6
Mediterranean Sea	94	97	96	96	94	87	94	92	86
North Sea	39	38	35	35	35	34	22	22	20
North-East Atlantic Ocean	62	65	65	64	63	58	63	62	57
Natural marine emissions	0	0	0	0	0	0	0	0	0
Volcanic emissions	0	1673	0	0	0	0	0	0	0
TOTAL	4230	5972	4300	4425	4483	4473	4566	4650	4765

Table B:13: National total emission trends of coarse particulate matter (2000-2008), as used for modelling at the MSC-W (Gg of PM_{coarse} per year).

Area/Year	2000	2001	2002	2003	2004	2005	2006	2007	2008
Albania	4	4	4	4	4	4	4	4	4
Armenia	1	1	1	1	1	1	1	1	1
Austria	14	14	13	13	13	13	13	12	13
Azerbaijan	6	6	7	7	7	9	9	10	8
Belarus	11	11	10	10	11	8	9	12	12
Belgium	15	15	14	14	14	12	12	11	11
Bosnia and Herzegovina	15	15	16	16	16	17	16	15	14
Bulgaria	21	21	19	22	23	26	27	31	27
Croatia	8	8	10	11	12	11	11	11	12
Cyprus	2	2	2	2	2	2	2	2	2
Czechia	17	16	15	14	14	15	15	15	14
Denmark	12	12	11	11	12	12	12	12	12
Estonia	17	16	11	10	9	8	7	10	7
Finland	14	15	15	16	15	14	15	14	14
France	110	108	105	106	106	101	99	97	95
Georgia	5	5	5	4	4	4	4	4	4
Germany	126	117	118	112	111	107	108	105	106
Greece	62	63	65	61	66	57	61	57	67
Hungary	24	27	24	27	32	32	24	22	29
Iceland	0	0	0	0	0	0	0	1	0
Ireland	18	20	19	21	22	22	23	23	21
Italy	49	51	49	48	47	45	43	41	40
Kazakhstan	12	16	13	14	17	18	16	40	43
Kyrgyzstan	4	4	3	3	3	3	4	4	4
Latvia	4	4	4	4	11	7	8	9	9
Lithuania	6	6	6	6	6	7	7	7	7
Luxembourg	1	1	1	1	1	1	1	1	1
Malta	1	1	1	1	1	0	0	0	0
Moldova	5	5	2	5	5	5	5	5	5
Montenegro	4	3	5	5	4	3	4	3	4
Netherlands	14	14	14	13	13	13	13	13	13
North Macedonia	14	9	9	13	14	13	12	10	11
Norway	8	8	8	8	8	9	9	9	8
Poland	114	119	121	118	119	124	130	121	119
Portugal	36	50	54	41	41	41	45	36	38
Romania	31	32	32	36	39	37	37	40	37
Russian Federation	225	236	247	295	323	300	258	266	214
Serbia	13	13	14	13	14	14	14	14	14
Slovakia	8	8	8	7	7	6	6	5	5
Slovenia	2	2	2	2	2	2	2	2	2
Spain	97	97	100	102	104	104	106	104	90
Sweden	19	19	19	19	20	20	20	20	19
Switzerland	8	8	8	8	8	8	8	8	8
Tajikistan	1	1	1	1	1	1	1	1	1
Turkey	334	238	385	374	339	340	392	394	386
Turkmenistan	1	1	1	2	2	2	2	2	2
Ukraine	48	47	49	53	51	53	59	60	61
United Kingdom	88	95	82	94	82	77	74	70	63
Uzbekistan	5	5	5	6	6	6	6	7	7
Asian areas	463	476	488	500	512	524	538	553	567
North Africa	75	77	79	80	82	84	87	89	92
Baltic Sea	0	0	0	0	0	0	0	0	0
Black Sea	0	0	0	0	0	0	0	0	0
Mediterranean Sea	0	0	0	0	0	0	0	0	0
North Sea	0	0	0	0	0	0	0	0	0
North-East Atlantic Ocean	0	0	0	0	0	0	0	0	0
Natural marine emissions	0	0	0	0	0	0	0	0	0
Volcanic emissions	0	0	0	0	0	0	0	0	0
TOTAL	2192	2139	2294	2357	2377	2343	2377	2405	2344

Table B:14: National total emission trends of coarse particulate matter (2009-2017), as used for modelling at the MSC-W (Gg of PM_{coarse} per year).

Area/Year	2009	2010	2011	2012	2013	2014	2015	2016	2017
Albania	4	4	4	4	4	4	4	4	4
Armenia	1	1	1	1	2	2	2	2	2
Austria	12	12	12	12	12	12	12	12	12
Azerbaijan	11	9	8	8	10	10	9	9	8
Belarus	12	13	13	15	12	11	11	9	24
Belgium	9	10	9	9	10	9	10	10	10
Bosnia and Herzegovina	13	12	12	12	12	12	12	12	12
Bulgaria	22	22	23	22	20	21	24	16	15
Croatia	11	9	9	9	8	8	9	8	9
Cyprus	2	2	1	1	1	1	1	1	1
Czechia	13	13	12	12	12	12	12	11	11
Denmark	11	11	11	11	11	11	11	11	11
Estonia	6	9	16	5	8	6	5	4	5
Finland	13	14	14	13	12	12	12	12	11
France	90	91	92	91	91	88	88	88	90
Georgia	4	4	4	4	4	4	4	4	5
Germany	101	107	111	110	113	113	111	103	107
Greece	59	44	31	28	29	31	28	30	30
Hungary	29	22	19	15	19	23	22	21	21
Iceland	0	0	0	0	0	0	0	0	0
Ireland	21	19	15	15	15	14	15	15	15
Italy	35	34	34	32	32	31	31	31	31
Kazakhstan	38	38	41	45	49	53	57	61	64
Kyrgyzstan	4	4	4	4	4	4	3	3	3
Latvia	7	7	9	8	8	8	9	8	7
Lithuania	7	7	7	7	7	7	7	7	7
Luxembourg	1	1	1	1	1	1	1	1	1
Malta	0	0	0	0	0	0	0	0	0
Moldova	5	5	5	5	5	5	5	5	5
Montenegro	3	4	7	7	7	7	7	8	8
Netherlands	13	13	13	13	13	13	13	13	13
North Macedonia	9	10	13	12	13	10	9	9	7
Norway	8	8	8	9	8	8	8	8	9
Poland	113	118	107	106	101	96	96	99	99
Portugal	39	32	37	31	22	17	18	20	22
Romania	34	35	36	36	35	36	35	33	31
Russian Federation	226	454	456	462	456	457	447	440	441
Serbia	13	13	14	13	13	13	14	15	14
Slovakia	5	5	5	5	5	5	5	5	5
Slovenia	2	2	2	2	2	1	1	1	2
Spain	81	77	75	71	67	68	69	70	67
Sweden	18	19	20	18	20	19	19	20	20
Switzerland	8	8	8	8	8	8	8	8	8
Tajikistan	2	2	2	2	2	2	2	2	2
Turkey	452	539	499	515	403	171	424	336	377
Turkmenistan	2	2	3	3	3	3	3	3	3
Ukraine	60	61	63	64	65	67	68	70	71
United Kingdom	58	64	60	57	63	60	61	62	64
Uzbekistan	8	8	9	9	9	10	10	10	11
Asian areas	581	596	652	704	758	814	870	928	992
North Africa	95	98	103	106	111	114	119	120	125
Baltic Sea	0	0	0	0	0	0	0	0	0
Black Sea	0	0	0	0	0	0	0	0	0
Mediterranean Sea	0	0	0	0	0	0	0	0	0
North Sea	0	0	0	0	0	0	0	0	0
North-East Atlantic Ocean	0	0	0	0	0	0	0	0	0
Natural marine emissions	0	0	0	0	0	0	0	0	0
Volcanic emissions	0	4297	0	0	0	0	0	0	0
TOTAL	2370	6989	2710	2752	2693	2513	2821	2779	2914

Table B:15: National total emission trends of particulate matter (2000-2008), as used for modelling at the MSC-W (Gg of PM_{10} per year).

Area/Year	2000	2001	2002	2003	2004	2005	2006	2007	2008
Albania	12	13	14	17	18	17	18	17	17
Armenia	5	5	5	5	5	5	5	5	5
Austria	38	38	37	37	37	35	34	33	32
Azerbaijan	11	11	12	12	13	14	14	16	14
Belarus	37	36	36	38	48	54	61	63	66
Belgium	55	53	51	52	51	47	48	45	44
Bosnia and Herzegovina	31	32	34	35	36	37	35	33	31
Bulgaria	47	44	48	54	54	57	59	62	58
Croatia	41	44	45	52	51	52	48	46	44
Cyprus	5	4	4	4	4	4	4	4	4
Czechia	66	66	61	61	61	58	59	57	55
Denmark	36	36	34	36	36	37	38	41	39
Estonia	32	32	28	24	25	22	16	23	19
Finland	40	41	42	43	42	39	41	38	37
France	438	424	400	400	386	361	334	319	311
Georgia	33	31	29	27	25	23	23	23	23
Germany	294	279	273	263	257	246	243	234	228
Greece	115	120	117	111	118	107	111	106	117
Hungary	72	79	61	73	75	72	64	62	65
Iceland	2	2	2	2	2	2	2	3	2
Ireland	39	40	39	40	40	41	42	41	39
Italy	246	239	208	225	200	219	222	245	256
Kazakhstan	65	86	73	80	90	100	84	164	187
Kyrgyzstan	11	11	11	11	12	12	12	13	13
Latvia	25	26	26	28	36	30	30	32	30
Lithuania	13	13	14	14	14	15	16	15	16
Luxembourg	3	3	3	4	3	3	3	3	3
Malta	1	1	1	1	1	1	1	1	1
Moldova	9	9	6	9	9	10	10	9	9
Montenegro	8	7	9	10	10	8	9	8	10
Netherlands	44	42	41	39	38	37	36	36	34
North Macedonia	43	28	28	42	46	41	39	31	36
Norway	51	51	51	49	47	48	46	47	45
Poland	274	278	280	275	279	284	295	279	274
Portugal	109	121	125	108	109	108	108	97	97
Romania	135	116	119	139	155	157	153	154	170
Russian Federation	717	719	721	733	801	743	775	797	637
Serbia	53	53	55	55	56	54	51	55	51
Slovakia	50	49	38	37	34	40	36	32	29
Slovenia	13	13	14	14	15	15	15	15	16
Spain	237	226	232	235	236	235	234	232	207
Sweden	52	51	50	51	51	51	49	49	47
Switzerland	18	18	18	17	17	17	17	17	17
Tajikistan	2	2	3	3	3	4	4	4	5
Turkey	718	610	744	722	690	694	749	754	749
Turkmenistan	9	9	11	13	14	14	17	14	14
Ukraine	169	185	189	190	203	207	205	206	223
United Kingdom	236	242	213	226	210	203	197	188	178
Uzbekistan	20	20	22	21	22	22	23	25	24
Asian areas	1302	1339	1377	1414	1451	1488	1526	1564	1601
North Africa	169	172	176	180	184	188	193	199	204
Baltic Sea	29	29	28	28	28	27	21	18	17
Black Sea	7	7	7	7	7	7	7	7	6
Mediterranean Sea	117	116	113	112	111	109	108	106	96
North Sea	61	60	59	58	57	57	47	42	39
North-East Atlantic Ocean	76	76	74	73	73	72	71	70	60
Natural marine emissions	0	0	0	0	0	0	0	0	0
Volcanic emissions	0	0	0	0	0	0	0	0	0
TOTAL	6542	6461	6513	6609	6694	6651	6708	6798	6654

Table B:16: National total emission trends of particulate matter (2009-2017), as used for modelling at the MSC-W (Gg of PM_{10} per year).

Area/Year	2009	2010	2011	2012	2013	2014	2015	2016	2017
Albania	18	18	18	18	19	19	19	19	19
Armenia	5	5	5	5	6	6	6	6	6
Austria	31	31	30	30	30	29	28	28	28
Azerbaijan	16	16	14	15	16	15	15	13	13
Belarus	65	58	63	68	55	55	51	48	59
Belgium	39	42	35	37	38	32	34	35	33
Bosnia and Herzegovina	29	27	27	27	26	26	26	26	26
Bulgaria	51	53	57	56	52	52	55	48	47
Croatia	42	40	37	35	32	28	29	27	25
Cyprus	3	3	3	2	2	2	2	2	2
Czechia	55	57	55	55	55	52	52	50	51
Denmark	36	36	34	32	32	30	31	31	31
Estonia	16	23	34	14	20	15	15	12	14
Finland	36	38	35	33	32	31	29	30	29
France	296	306	281	284	284	256	258	258	254
Georgia	24	24	24	24	23	23	22	22	22
Germany	215	229	228	220	222	217	214	203	206
Greece	108	85	65	62	59	61	56	57	56
Hungary	76	72	74	73	78	73	74	71	69
Iceland	2	2	2	2	2	2	2	2	2
Ireland	38	35	29	29	29	28	28	28	27
Italy	237	231	184	209	204	187	193	189	196
Kazakhstan	171	160	172	184	196	208	220	232	244
Kyrgyzstan	14	14	15	16	17	18	19	20	21
Latvia	29	25	28	28	26	26	26	24	25
Lithuania	15	15	15	15	15	15	14	14	14
Luxembourg	3	2	2	2	2	2	2	2	2
Malta	0	1	1	1	1	1	0	0	0
Moldova	9	10	10	10	10	16	16	16	17
Montenegro	7	8	12	12	12	12	12	12	12
Netherlands	32	31	31	29	29	28	28	27	27
North Macedonia	28	34	41	35	37	28	25	22	16
Norway	43	46	43	45	39	36	36	36	37
Poland	261	275	257	255	245	232	232	241	246
Portugal	94	88	93	85	74	68	69	71	73
Romania	159	164	155	158	149	150	145	144	143
Russian Federation	638	881	880	891	872	870	837	809	809
Serbia	56	56	56	55	51	50	52	55	53
Slovakia	27	29	27	28	26	21	23	24	23
Slovenia	15	15	15	14	14	12	13	13	13
Spain	199	191	189	181	174	173	174	173	172
Sweden	45	45	46	42	44	40	39	40	40
Switzerland	17	17	16	16	16	15	15	15	15
Tajikistan	5	5	5	6	6	6	7	7	7
Turkey	818	907	870	889	779	551	807	721	765
Turkmenistan	17	17	18	18	19	20	21	21	22
Ukraine	199	196	199	202	205	207	210	213	216
United Kingdom	169	183	167	169	177	168	169	169	171
Uzbekistan	27	28	28	29	30	31	32	32	33
Asian areas	1639	1677	1837	1981	2135	2291	2449	2613	2793
North Africa	210	215	226	233	244	250	262	265	275
Baltic Sea	16	16	15	15	15	14	9	9	9
Black Sea	6	7	7	6	6	6	6	6	6
Mediterranean Sea	94	97	96	96	94	87	94	92	86
North Sea	39	38	35	35	35	34	22	22	20
North-East Atlantic Ocean	62	65	65	64	63	58	63	62	57
Natural marine emissions	0	0	0	0	0	0	0	0	0
Volcanic emissions	0	5970	0	0	0	0	0	0	0
TOTAL	6601	12961	7010	7177	7176	6986	7387	7429	7679

APPENDIX C

Source-receptor tables for 2017

The source-receptor tables in this appendix are calculated for the meteorological and chemical conditions of 2017. The EMEP MSC-W model version rv4.33 has been used for the 2017 source-receptor model runs. The emissions used are the latest reported emissions for 2017 as shown in Appendix A.

It can be noted that there also have been changes in chemistry and the vertical profiles of emission release in the current rv4.33 setup compared to the rv4.17 source-receptor matrix calculations performed in EMEP Status Report 1/2018. For more details about the changes see Chapter 10.

The tables are calculated for the EMEP domain covering the geographic area between 30°N-82°N latitude and 30°W-90°E longitude, and are based on model runs driven by ECMWF-IFS meteorology in $0.3° \times 0.2°$ longitude-latitude projection.

The source-receptor (SR) relationships give the change in air concentrations or depositions resulting from a change in emissions from each emitter country.

For each country, reductions in five different pollutants have been calculated separately, with an emission reduction of 15% for SO_x, NO_x, NH_3, NMVOC or PPM, respectively. Here reduction in PPM means that PPM_{fine} and PPM_{coarse} are reduced together in one simulation. For year 2017, reductions in volcanic emissions are done for passive SO_2 degassing of Italian volcanoes (Etna, Stromboli and Vulcano). The boundary conditions for all gaseous and aerosol species were given as 5-year monthly average concentrations, derived from EMEP MSC-W global runs, kept invariable over the calculation period.

The deposition tables show the contribution from one country to another. They have been calculated adding the differences obtained by a 15% reduction for all emissions in one country multiplied by a factor of 100/15, in order to arrive at total estimates.

For the concentrations and indicator tables, the differences obtained by the 15% emission

reduction of the relevant pollutants are given directly. Thus, the tables should be interpreted as estimates of this reduction scenario from the chemical conditions in 2017.

The SR tables in the following aim to respond to two fundamental questions about transboundary air pollution:

1. Where do the pollutants emitted by a country or region end up?
2. Where do the pollutants in a given country or region come from?

Each column answers the first question. The numbers within a column give the change in the value of each pollutant (or indicator) for each receiver country caused by the emissions in the country given at the top of the column.

Each row answers the second question. The numbers given in each row show which emitter countries were responsible for the change in pollutants in the country given at the beginning of each row.

Note that more information on aerosol components and SR tables in electronic format are available from the EMEP website `www.emep.int`.

Acidification and eutrophication

- Deposition of OXS (oxidised sulphur). The contribution from SO_x, NO_x, NH_3, PPM and VOC emissions have been summed up and scaled to a 100% reduction. Units: 100 Mg of S.
- Deposition of OXN (oxidised nitrogen). The contribution from SO_x, NO_x, NH_3, PPM and VOC emissions have been summed up and scaled to a 100% reduction. Units: 100 Mg of N.
- Deposition of RDN (reduced nitrogen). The contribution from SO_x, NO_x, NH_3, PPM and VOC emissions have been summed up and scaled to a 100% reduction. Units: 100 Mg of N.

Ground Level Ozone

- $AOT40_f^{uc}$. Effect of a 15% reduction in NO_x emissions. Units: ppb.h
- $AOT40_f^{uc}$. Effect of a 15% reduction in VOC emissions. Units: ppb.h
- SOMO35. Effect of a 15% reduction in NO_x emissions. Units: ppb.d
- SOMO35. Effect of a 15% reduction in VOC emissions. Units: ppb.d

Particulate Matter

- $PM_{2.5}$. Effect of a 15% reduction in PPM emissions. Units: ng/m^3
- $PM_{2.5}$. Effect of a 15% reduction in SO_x emissions. Units: ng/m^3
- $PM_{2.5}$. Effect of a 15% reduction in NO_x emissions. Units: ng/m^3
- $PM_{2.5}$. Effect of a 15% reduction in NH_3 emissions. Units: ng/m^3
- $PM_{2.5}$. Effect of a 15% reduction in VOC emissions. Units: ng/m^3
- $PM_{2.5}$. Effect of a 15% reduction in all emissions. The contribution from a 15% reduction in PPM, SO_x, NO_x, NH_3 and VOC emissions have been summed up. Units: ng/m^3

Fine Elemental Carbon

- Fine EC. Effect of a 15% reduction in PPM emissions. Units: 0.1 ng/m^3

Coarse Elemental Carbon

- Coarse EC. Effect of a 15% reduction in PPM emissions. Units: 0.1 ng/m^3

Table C.1: 2017 country-to-country blame matrices for **oxidised sulphur** deposition.
Units: 100 Mg of S. **Emitters →, Receptors ↓.**

	AL	AM	AT	AZ	BA	BE	BG	BY	CH	CY	CZ	DE	DK	EE	ES	FI	FR	GB	GE	GR	HR	HU	IE	IS	IT	KG	KZ	LT	LU	LV	MD	ME	
AL	27	0	0	0	6	0	1	0	0	0	0	1	0	0	1	0	0	0	0	3	0	0	0	0	4	0	0	0	0	0	0	5	AL
AM	0	63	0	1	0	0	0	0	0	0	0	0	0	0	0	0	0	0	1	0	0	0	0	0	0	0	0	0	-0	0	0	0	AM
AT	0	0	25	-0	4	1	1	0	2	0	13	35	0	0	3	0	6	2	0	0	1	1	0	0	4	-0	0	0	0	0	0	1	AT
AZ	0	16	0	15	0	0	0	0	0	0	0	0	0	0	0	0	0	0	4	0	0	0	0	0	0	0	3	0	0	0	0	0	AZ
BA	1	0	1	0	231	0	1	0	0	0	6	5	0	0	1	0	1	0	0	0	4	4	0	0	6	0	0	0	0	0	0	10	BA
BE	0	0	0	-0	0	42	0	0	0	0	0	10	0	0	2	0	16	8	-0	0	0	0	0	0	0	-0	0	0	0	-0	0	0	BE
BG	1	0	1	0	12	0	177	1	0	0	3	4	0	0	1	0	1	0	0	12	1	2	0	0	2	0	1	0	0	0	1	5	BG
BY	0	0	0	0	11	1	6	91	0	0	13	21	1	3	1	1	2	3	0	2	0	2	0	0	1	0	2	5	0	1	2	3	BY
CH	0	0	0	0	0	0	0	0	11	0	0	5	0	0	3	0	9	1	0	0	0	0	0	0	3	0	0	0	0	0	0	0	CH
CY	0	0	0	0	0	0	0	0	0	6	0	0	0	0	0	0	0	0	0	0	0	0	0	0	0	0	0	0	0	0	0	0	CY
CZ	0	0	3	-0	5	2	1	0	0	0	143	49	0	0	2	0	5	3	0	0	1	2	0	0	1	0	0	0	0	0	0	1	CZ
DE	0	0	5	-0	2	37	1	0	5	0	43	650	1	0	15	0	62	46	0	0	0	1	2	0	3	-0	0	0	2	0	0	0	DE
DK	0	0	0	0	0	2	0	0	0	0	2	16	9	0	1	0	2	7	0	0	0	0	0	0	0	0	0	0	0	0	0	0	DK
EE	0	0	0	0	1	0	0	1	0	0	1	4	0	15	0	3	1	1	0	0	0	0	0	0	0	0	0	2	0	1	0	0	EE
ES	0	0	0	0	1	0	0	0	0	0	1	2	0	0	349	0	7	1	0	0	0	0	0	0	3	0	0	0	0	0	0	0	ES
FI	0	0	0	0	2	1	1	3	0	0	5	12	1	18	1	62	2	4	0	0	0	1	0	0	0	0	0	2	0	1	0	0	FI
FR	0	0	1	-0	3	11	0	0	2	0	4	32	0	0	95	0	303	33	-0	0	1	0	2	0	10	0	0	0	1	0	0	1	FR
GB	0	0	0	-0	0	3	0	0	0	0	1	11	0	0	8	0	12	263	0	0	0	0	8	1	0	0	0	0	0	0	0	0	GB
GE	0	16	0	3	0	0	1	0	0	0	0	0	0	0	0	0	0	0	24	0	0	0	0	0	0	0	1	0	0	0	0	0	GE
GL	0	0	0	0	0	0	0	0	0	0	0	0	0	0	0	0	0	0	0	0	0	0	0	0	0	0	0	0	0	0	0	0	GL
GR	3	0	0	0	9	0	24	0	0	0	2	2	0	0	1	0	1	0	0	76	0	1	0	0	6	0	0	0	0	0	0	4	GR
HR	0	0	2	0	43	0	1	0	0	0	5	6	0	0	3	0	3	0	0	0	20	3	0	0	9	0	0	0	0	0	0	3	HR
HU	0	0	3	0	39	0	4	0	0	0	12	11	0	0	2	0	2	1	0	1	3	49	0	0	4	0	0	0	0	0	0	6	HU
IE	0	0	0	-0	0	0	0	0	0	0	0	1	0	0	2	0	1	5	0	0	0	0	21	0	0	0	0	0	0	0	0	0	IE
IS	0	0	0	-0	0	0	0	0	0	0	0	1	0	0	0	0	0	1	0	0	0	0	0	56	0	-0	0	0	0	0	0	0	IS
IT	1	0	2	0	22	0	2	0	1	0	5	7	0	0	21	0	23	1	0	1	5	1	0	0	201	0	0	0	0	0	0	4	IT
KG	0	1	0	0	0	0	0	0	-0	0	0	0	0	0	-0	0	0	0	0	0	-0	0	0	-0	0	117	47	0	0	0	0	0	KG
KZ	0	23	0	5	3	0	4	4	0	1	3	5	0	2	1	1	1	0	3	1	0	1	0	0	1	72	1435	1	0	0	1	2	KZ
LT	0	0	0	0	2	1	0	6	0	0	4	9	1	1	1	1	1	2	0	0	0	1	0	0	0	0	0	17	0	1	0	1	LT
LU	0	0	0	0	0	0	0	0	0	0	0	1	0	0	0	0	1	0	0	0	0	0	0	0	0	0	0	0	1	0	0	0	LU
LV	0	0	0	0	2	0	0	4	0	0	3	7	1	2	1	1	1	2	0	0	0	1	0	0	0	0	0	8	0	7	0	0	LV
MD	0	0	0	0	2	0	3	1	0	0	1	1	0	0	0	0	0	0	0	1	0	0	0	0	0	0	0	0	0	0	9	1	MD
ME	1	0	0	0	16	0	0	0	0	0	0	0	0	0	0	0	0	0	0	0	0	0	0	0	2	0	0	0	0	0	0	33	ME
MK	2	0	0	0	4	0	3	0	0	0	1	1	0	0	0	0	0	0	0	9	0	0	0	0	1	0	0	0	0	0	0	2	MK
MT	0	-0	0	-0	0	0	0	0	0	0	0	0	0	0	0	0	0	0	-0	0	0	0	0	0	0	-0	0	0	0	0	0	0	MT
NL	0	0	0	-0	0	22	0	0	0	0	1	20	0	0	2	0	10	14	-0	0	0	0	0	0	0	-0	0	0	0	0	0	0	NL
NO	0	0	0	0	0	1	0	1	0	0	3	11	1	1	2	2	2	11	0	0	0	0	0	2	0	0	0	0	0	0	0	0	NO
PL	0	0	3	0	17	6	2	7	0	0	84	174	3	1	4	1	10	14	0	0	2	7	1	0	2	0	1	1	0	0	0	3	PL
PT	0	-0	0	-0	0	0	0	0	0	-0	0	0	0	0	14	0	0	0	-0	0	0	0	0	0	0	-0	-0	0	0	0	0	0	PT
RO	2	0	2	0	41	1	46	2	0	0	10	14	0	0	2	0	2	1	0	9	2	11	0	0	6	0	2	0	0	0	4	16	RO
RS	2	0	1	0	67	0	10	0	0	0	6	7	0	0	1	0	1	1	0	5	2	8	0	0	4	0	0	0	0	0	0	29	RS
RU	2	28	2	10	44	4	36	73	1	2	40	69	3	103	7	48	9	15	8	12	2	8	1	1	6	9	1143	13	0	5	8	15	RU
SE	0	0	0	0	1	2	0	2	0	0	6	28	6	4	3	10	4	12	0	0	0	1	0	0	0	0	0	2	0	0	0	0	SE
SI	0	0	2	0	2	0	0	0	0	0	1	2	0	0	1	0	1	0	0	0	4	1	0	0	4	0	0	0	0	0	0	0	SI
SK	0	0	2	0	13	0	1	0	0	0	16	10	0	0	1	0	2	1	0	0	1	8	0	0	2	-0	0	0	0	0	0	2	SK
TJ	0	0	0	0	0	0	0	0	-0	0	0	0	0	0	-0	0	0	0	0	0	0	0	0	0	0	5	8	0	0	0	0	0	TJ
TM	0	4	0	2	0	0	0	0	-0	0	0	0	0	0	0	0	0	0	1	0	0	0	-0	0	0	1	20	0	0	0	0	0	TM
TR	1	18	0	1	7	0	23	1	0	13	2	3	0	0	2	0	1	0	2	12	0	1	0	0	6	0	2	0	0	0	1	3	TR
UA	1	2	2	1	36	2	29	24	0	0	26	37	1	2	3	1	4	5	1	8	2	10	0	0	5	0	8	2	0	0	12	11	UA
UZ	0	4	0	1	0	0	0	0	-0	0	0	0	0	0	0	0	0	0	0	0	0	0	-0	0	0	18	41	0	0	0	0	0	UZ
ATL	0	0	1	0	3	10	2	3	0	0	16	58	2	9	249	13	48	127	0	1	0	1	23	160	3	0	18	1	0	0	0	1	ATL
BAS	0	0	1	0	5	5	1	5	0	0	21	81	13	22	4	28	8	19	0	0	0	2	1	0	1	0	0	7	0	2	0	1	BAS
BLS	1	4	1	1	16	0	39	3	0	1	6	9	0	0	1	0	1	1	7	9	0	2	0	0	3	0	5	0	0	0	6	5	BLS
MED	17	0	4	0	142	3	54	1	2	27	22	29	0	1	160	0	86	7	0	63	12	5	0	0	220	0	1	0	0	0	1	41	MED
NOS	0	0	1	0	1	26	1	1	0	0	14	100	6	1	21	1	58	243	0	0	0	1	6	5	1	0	0	1	0	0	0	0	NOS
AST	0	24	0	19	2	0	2	1	0	9	1	1	0	0	1	0	0	0	3	2	0	0	0	0	1	21	214	0	0	0	0	1	AST
NOA	1	0	1	0	9	0	3	0	0	0	2	4	0	0	36	0	8	1	0	3	1	0	0	0	16	-0	0	0	0	0	0	3	NOA
SUM	65	206	66	59	827	188	481	238	28	61	549	1568	51	189	1030	173	721	859	55	236	65	139	65	228	545	244	2955	65	5	20	46	215	SUM
EXC	46	178	58	39	651	144	380	224	25	23	467	1286	30	155	558	131	511	462	44	158	51	126	36	63	300	222	2716	55	4	17	38	163	EXC
EU	9	1	50	0	221	134	263	28	13	6	366	1118	23	43	534	79	478	424	0	103	41	91	35	3	261	0	5	33	4	10	7	48	EU
emis	67	193	64	58	848	188	515	241	27	82	550	1577	51	193	1102	175	719	864	53	283	63	139	66	249	576	242	3489	66	5	20	47	236	emis
	AL	AM	AT	AZ	BA	BE	BG	BY	CH	CY	CZ	DE	DK	EE	ES	FI	FR	GB	GE	GR	HR	HU	IE	IS	IT	KG	KZ	LT	LU	LV	MD	ME	

Table C.1 Cont.: 2017 country-to-country blame matrices for **oxidised sulphur** deposition.
Units: 100 Mg of S. **Emitters →, Receptors ↓.**

	MK	MT	NL	NO	PL	PT	RO	RS	RU	SE	SI	SK	TJ	TM	TR	UA	UZ	ATL	BAS	BLS	MED	NOS	AST	NOA	BIC	DMS	VOL	SUM	EXC	EU	
AL	10	0	0	0	1	0	1	14	0	0	0	0	0	0	3	1	-0	0	0	0	8	0	0	11	4	2	39	145	80	13	AL
AM	0	0	0	0	0	0	0	0	0	0	0	0	0	0	37	1	0	0	0	0	1	0	95	2	5	0	5	212	104	1	AM
AT	0	0	1	0	11	0	1	8	0	0	2	1	-0	0	0	1	-0	1	0	0	4	0	0	5	11	2	3	149	123	107	AT
AZ	0	0	0	0	0	0	0	0	6	0	0	0	0	0	39	4	0	0	0	0	1	0	204	2	8	0	6	312	90	1	AZ
BA	1	0	0	0	12	0	3	49	0	0	0	2	0	0	1	2	0	0	-0	0	8	-0	0	12	7	2	21	396	345	49	BA
BE	0	0	4	0	1	0	0	0	0	0	0	0	-0	-0	0	0	-0	2	0	0	0	2	0	1	4	2	0	96	85	84	BE
BG	13	0	0	0	10	0	28	104	8	0	0	1	0	0	96	35	0	0	0	4	9	0	3	12	11	2	49	613	522	245	BG
BY	3	0	1	0	155	0	12	39	32	1	0	4	0	0	30	104	0	1	1	1	4	1	2	4	18	5	12	602	555	236	BY
CH	0	0	0	0	0	0	0	0	0	0	0	0	0	0	0	0	-0	1	0	0	3	0	0	3	7	1	1	51	36	24	CH
CY	0	0	0	0	0	0	0	0	0	0	0	0	0	0	16	0	0	0	0	0	2	0	7	3	1	1	2	38	23	6	CY
CZ	0	0	1	0	45	0	1	15	0	0	1	3	0	0	0	2	-0	1	-0	0	2	0	0	3	10	2	2	308	289	265	CZ
DE	0	0	29	0	52	1	1	6	2	0	0	1	-0	0	1	5	-0	10	1	0	6	8	0	10	50	21	3	1084	975	954	DE
DK	0	0	2	0	9	0	0	1	1	0	0	0	-0	0	0	1	-0	1	1	0	0	1	0	1	6	8	0	73	55	51	DK
EE	0	0	0	0	14	0	1	3	7	1	0	0	-0	0	1	4	-0	0	1	0	0	0	0	0	3	3	1	71	63	45	EE
ES	0	0	0	0	1	15	0	1	0	0	0	0	0	0	0	0	0	40	0	0	68	0	0	106	63	24	7	690	382	379	ES
FI	1	0	1	2	40	0	1	5	59	7	0	1	0	0	4	10	-0	2	2	0	1	1	0	1	21	19	3	295	246	160	FI
FR	0	0	3	0	6	4	0	4	0	0	0	0	0	-0	1	1	-0	43	0	0	47	8	0	49	75	42	18	802	520	507	FR
GB	0	0	3	0	5	1	0	1	0	0	0	0	0	0	0	1	-0	36	0	0	2	5	0	4	41	41	1	450	320	316	GB
GE	0	0	0	0	1	0	0	2	5	0	0	0	0	0	131	7	0	0	0	2	1	0	121	4	9	1	9	341	193	4	GE
GL	0	0	0	0	0	0	0	0	1	0	0	0	0	0	0	0	-0	0	0	0	0	0	0	0	41	5	0	49	3	1	GL
GR	23	0	0	0	6	0	5	47	3	0	0	1	0	0	97	12	0	0	0	1	42	0	2	35	16	10	85	517	326	125	GR
HR	1	0	0	0	11	0	3	38	0	0	2	2	0	0	1	2	0	1	0	0	16	0	0	15	8	4	21	227	161	73	HR
HU	3	0	0	0	33	0	16	114	1	0	1	14	0	0	4	6	-0	0	0	0	6	0	0	9	8	2	14	372	332	157	HU
IE	0	0	0	0	1	0	0	0	0	0	0	0	-0	-0	0	0	-0	9	0	0	1	0	0	2	14	20	0	79	33	32	IE
IS	0	-0	0	0	0	0	0	0	0	0	0	0	-0	0	0	0	-0	3	0	0	0	0	0	0	22	17	0	102	60	3	IS
IT	3	0	0	0	11	1	2	26	1	0	2	1	0	0	4	4	-0	3	0	0	105	0	0	89	39	20	217	828	354	288	IT
KG	0	0	0	0	0	0	0	0	3	0	0	0	12	1	11	2	27	0	0	0	0	0	152	1	25	0	5	405	221	0	KG
KZ	2	0	0	0	25	0	5	12	415	0	0	1	9	23	239	246	34	0	0	3	5	0	1432	12	137	3	53	4230	2585	55	KZ
LT	0	0	1	0	56	0	2	10	7	1	0	1	0	0	1	8	-0	1	1	0	1	0	0	1	6	3	2	149	135	99	LT
LU	0	0	0	0	0	0	0	0	0	0	0	0	0	0	0	0	0	0	0	0	0	0	0	0	0	0	0	5	4	4	LU
LV	0	0	0	0	32	0	1	7	8	1	0	1	0	0	1	8	0	0	1	0	1	0	0	1	6	4	1	117	103	71	LV
MD	1	0	0	0	8	0	5	7	4	0	0	0	0	0	21	26	0	0	0	1	1	0	2	3	3	0	6	109	93	22	MD
ME	1	0	0	0	1	0	0	10	0	0	0	0	0	0	1	0	0	0	0	0	4	0	0	5	2	1	13	95	69	7	ME
MK	56	0	0	0	2	0	1	27	0	0	0	0	0	0	8	1	0	0	0	0	2	0	0	3	3	0	15	145	121	19	MK
MT	0	0	0	0	0	0	0	0	0	0	0	0	-0	-0	0	0	-0	0	0	0	0	0	0	0	0	0	0	1	0	0	MT
NL	0	0	32	0	2	0	0	0	0	0	0	0	-0	0	0	0	-0	2	0	0	0	5	0	0	5	5	0	122	104	103	NL
NO	0	0	1	24	14	0	0	2	14	3	0	0	0	0	1	5	0	15	1	0	0	6	0	1	45	54	1	225	102	54	NO
PL	1	0	5	0	1118	0	11	66	11	1	1	15	0	0	3	43	-0	3	1	0	4	1	0	5	33	13	9	1688	1619	1466	PL
PT	0	0	0	0	0	49	0	0	0	0	0	0	-0	-0	0	0	-0	20	0	0	4	0	0	11	13	9	0	122	65	65	PT
RO	18	0	0	0	53	0	220	214	14	0	1	7	0	0	83	75	0	1	0	5	11	0	5	24	23	3	64	999	862	389	RO
RS	23	0	0	0	19	0	17	447	2	0	0	3	0	0	13	7	0	0	-0	0	6	-0	0	10	9	2	30	736	678	87	RS
RU	19	0	3	4	344	1	46	134	5874	11	1	12	2	12	1065	1713	6	15	6	24	29	3	742	36	557	138	197	12720	10973	802	RU
SE	0	0	2	6	42	0	1	4	22	32	0	1	0	0	1	6	0	5	4	0	1	3	0	1	33	23	1	275	204	160	SE
SI	0	0	0	0	2	0	1	6	0	0	7	0	0	0	0	0	0	0	0	0	5	0	0	3	3	1	3	52	38	28	SI
SK	1	0	0	0	43	0	5	39	1	0	1	32	-0	0	1	4	-0	0	0	0	3	0	0	3	5	1	5	202	185	124	SK
TJ	0	0	0	0	0	0	0	0	1	0	0	0	51	2	7	1	7	0	0	0	0	0	142	1	19	0	3	248	83	0	TJ
TM	0	0	0	0	1	0	0	1	11	0	0	0	2	37	39	10	5	0	0	0	1	0	712	4	29	0	10	890	134	2	TM
TR	6	0	0	0	11	0	12	44	21	0	0	1	0	0	4447	56	0	1	0	16	84	0	1453	110	101	16	188	6667	4699	89	TR
UA	12	0	1	0	256	0	55	139	111	1	1	12	0	1	349	1101	0	2	0	14	17	1	44	26	50	7	76	2509	2273	465	UA
UZ	0	0	0	0	1	0	0	1	12	0	0	0	14	12	37	10	46	0	0	0	1	0	507	3	28	0	10	748	199	2	UZ
ATL	1	0	6	23	62	98	3	10	411	7	0	2	0	0	24	47	-0	1391	2	0	61	20	9	254	2855	3917	23	9977	1445	743	ATL
BAS	1	0	5	3	170	0	3	15	44	18	0	3	0	0	3	18	-0	4	20	0	2	4	0	3	31	45	3	622	510	415	BAS
BLS	8	0	0	0	50	0	43	88	86	0	0	3	0	0	1246	299	0	0	0	110	28	0	155	27	35	4	81	2388	1947	172	BLS
MED	40	2	1	0	64	5	20	163	12	0	3	6	0	0	1477	52	-0	23	0	9	1841	1	697	1445	250	497	1360	8868	2743	795	MED
NOS	0	0	30	11	57	2	2	5	9	2	0	1	0	0	1	12	-0	55	2	0	5	69	0	8	121	233	3	1119	623	576	NOS
AST	1	0	0	0	5	0	2	6	68	0	0	0	13	20	601	71	12	0	0	2	27	0	11638	94	752	9	93	13718	1103	27	AST
NOA	2	0	0	0	4	5	1	12	1	0	0	0	-0	0	38	4	0	25	0	0	106	0	22	1374	214	32	109	2038	156	86	NOA
SUM	255	3	136	75	2872	188	532	1945	7292	88	25	136	102	111	10184	4027	138	1719	44	193	2585	142	18150	3852	5894	5276	2885	81087			SUM
EXC	201	1	92	39	2459	76	459	1646	6661	60	21	120	89	90	6794	3525	126	220	20	72	516	47	5628	646	1636	539	1212		31821	8239	EXC
EU	67	0	85	10	1606	74	300	718	147	44	18	83	0	0	316	228	-0	183	11	10	342	36	19	394	508	282	512		8126	6305	EU
emis	280	4	134	75	2913	238	535	2101	8317	88	24	135	96	135	11750	4194	142	2013	44	200	3013	143	33323	8137	0	11970	4715	107766	44208	11370	emis
	MK	MT	NL	NO	PL	PT	RO	RS	RU	SE	SI	SK	TJ	TM	TR	UA	UZ	ATL	BAS	BLS	MED	NOS	AST	NOA	BIC	DMS	VOL	SUM	EXC	EU	

Table C.2: 2017 country-to-country blame matrices for **oxidised nitrogen** deposition.
Units: 100 Mg of N. **Emitters →, Receptors ↓.**

	AL	AM	AT	AZ	BA	BE	BG	BY	CH	CY	CZ	DE	DK	EE	ES	FI	FR	GB	GE	GR	HR	HU	IE	IS	IT	KG	KZ	LT	LU	LV	MD	ME	
AL	17	0	1	0	1	0	1	0	0	0	0	2	0	0	1	0	2	0	0	7	1	1	0	0	11	0	0	0	0	0	0	2	AL
AM	0	14	0	6	0	0	0	0	0	0	0	0	0	0	0	0	0	0	2	0	0	0	0	0	0	0	0	0	0	0	0	0	AM
AT	0	0	96	0	0	6	0	0	13	0	13	101	0	0	5	0	29	10	0	0	3	4	1	0	33	0	0	0	1	0	0	0	AT
AZ	0	5	0	60	0	0	0	0	0	0	0	0	0	0	0	0	0	0	9	0	0	0	0	0	0	0	2	0	0	0	0	0	AZ
BA	1	0	8	0	17	1	1	0	1	0	7	19	0	0	4	0	6	2	0	1	9	10	0	0	29	0	0	0	0	0	0	2	BA
BE	0	0	0	0	0	43	0	0	0	0	0	17	0	0	3	0	38	30	0	0	0	0	2	0	0	-0	0	0	2	0	0	0	BE
BG	2	0	4	0	2	1	80	1	1	0	4	14	0	0	2	0	4	2	0	26	2	7	0	0	9	0	1	0	0	0	2	1	BG
BY	0	0	5	0	1	6	3	84	1	0	13	67	9	2	3	4	11	17	0	3	2	7	1	0	8	0	1	16	1	6	4	0	BY
CH	0	0	2	0	0	2	0	0	46	0	0	16	0	0	6	0	35	5	0	0	0	0	0	0	23	0	0	0	0	0	0	0	CH
CY	0	0	0	0	0	0	0	0	0	4	0	0	0	0	0	0	0	0	0	1	0	0	0	0	0	0	0	0	0	0	0	0	CY
CZ	0	0	23	0	1	10	0	0	4	0	74	131	1	0	4	0	26	16	0	0	3	7	1	0	10	0	0	0	2	0	0	0	CZ
DE	0	0	30	0	0	109	0	1	30	0	34	935	10	0	25	1	245	199	0	0	1	4	12	0	21	0	0	1	16	0	0	0	DE
DK	0	0	1	0	0	5	0	0	0	0	2	38	23	0	1	0	8	29	0	0	0	0	2	0	1	0	0	0	0	0	0	0	DK
EE	0	0	1	0	0	1	0	3	0	0	1	13	3	9	1	7	3	5	0	0	0	1	0	0	1	0	0	4	0	5	0	0	EE
ES	0	0	1	0	0	2	0	0	1	0	1	6	0	0	635	0	33	7	0	0	0	0	1	0	11	0	0	0	0	0	0	0	ES
FI	0	0	2	0	0	4	0	8	1	0	4	38	9	10	2	99	9	21	0	0	0	2	1	0	1	0	0	6	0	6	0	0	FI
FR	0	0	5	0	0	37	0	0	14	0	4	83	1	0	178	0	774	140	0	0	1	1	12	0	44	0	0	0	6	0	0	0	FR
GB	0	0	1	0	0	12	0	0	0	0	1	28	1	0	13	0	40	415	0	0	0	0	44	0	1	0	0	0	1	0	0	0	GB
GE	0	5	0	15	0	0	0	0	0	0	0	1	0	0	0	0	0	0	36	1	0	0	0	0	0	0	1	0	0	0	0	0	GE
GL	-0	0	0	0	-0	0	0	0	0	0	0	1	0	0	0	0	0	1	0	0	-0	0	0	0	0	0	0	0	0	0	0	-0	GL
GR	5	0	2	0	1	1	19	1	0	0	2	7	0	0	3	0	4	1	0	150	1	3	0	0	15	-0	0	0	0	0	1	1	GR
HR	1	0	16	0	5	2	1	0	2	0	7	24	0	0	7	0	10	3	0	1	26	11	0	0	58	0	0	0	0	0	0	1	HR
HU	1	0	26	0	5	3	2	1	3	0	16	47	1	0	4	0	13	5	0	2	10	61	0	0	28	0	0	0	1	0	0	1	HU
IE	0	0	0	0	0	1	0	0	0	0	0	3	0	0	3	0	6	13	0	0	0	0	40	0	0	0	0	0	0	0	0	0	IE
IS	0	0	0	0	0	0	0	0	0	0	0	2	0	0	0	0	1	5	0	0	0	0	1	10	0	0	0	0	0	0	0	0	IS
IT	1	0	20	0	3	3	1	0	12	0	6	31	0	0	47	0	77	7	0	3	12	6	1	0	777	0	0	0	0	0	0	1	IT
KG	0	0	0	0	0	0	0	0	0	0	0	0	0	0	0	0	0	0	0	0	0	0	0	0	0	69	38	0	0	0	0	0	KG
KZ	0	7	2	25	0	2	2	10	1	0	3	20	2	1	5	4	7	6	7	3	1	2	1	0	6	43	910	2	0	2	2	0	KZ
LT	0	0	2	0	0	3	0	9	1	0	4	30	6	1	1	2	5	9	0	0	1	2	1	0	2	0	0	21	0	4	0	0	LT
LU	0	-0	0	0	0	1	0	0	0	-0	0	2	0	0	0	0	3	1	0	0	0	0	0	0	0	0	0	0	3	0	0	0	LU
LV	0	0	1	0	0	2	0	8	0	0	3	22	5	2	2	4	4	8	0	0	0	2	1	0	2	0	0	11	0	15	0	0	LV
MD	0	0	1	0	0	0	2	1	0	0	1	4	0	0	0	0	1	1	0	2	0	2	0	0	2	0	0	0	0	0	7	0	MD
ME	2	0	1	0	1	0	0	0	0	0	1	2	0	0	1	0	1	0	0	1	1	1	0	0	6	-0	0	0	0	0	0	7	ME
MK	2	0	1	0	1	0	3	0	0	0	1	2	0	0	1	0	1	0	0	14	0	1	0	0	3	0	0	0	0	0	0	0	MK
MT	0	0	0	0	0	0	0	0	0	0	0	0	0	0	0	0	0	0	0	0	0	0	0	0	0	0	0	0	0	0	0	0	MT
NL	0	0	0	0	0	21	0	0	0	0	1	25	1	0	3	0	24	52	0	0	0	0	3	0	0	0	0	0	1	0	0	0	NL
NO	0	0	1	0	0	5	0	2	0	0	2	30	12	1	3	5	9	49	0	0	0	1	4	1	0	0	0	2	0	1	0	0	NO
PL	0	0	22	0	2	31	1	12	4	0	77	380	26	1	7	2	49	73	0	1	5	23	5	0	17	0	0	5	3	2	1	0	PL
PT	0	0	0	0	0	0	0	0	0	0	0	1	0	0	42	0	3	1	0	0	0	0	0	0	1	0	0	0	0	0	0	0	PT
RO	3	0	16	1	5	4	29	4	3	0	14	53	1	0	6	0	12	8	0	18	6	33	0	0	27	0	1	1	1	0	7	3	RO
RS	3	0	9	0	8	2	7	1	1	0	9	26	0	0	3	0	6	3	0	9	6	20	0	0	20	0	0	0	0	0	1	5	RS
RU	2	8	20	45	4	22	18	169	7	1	35	227	36	47	19	125	53	83	21	25	6	25	6	1	40	5	717	47	2	39	15	2	RU
SE	0	0	2	0	0	12	0	5	1	0	6	85	40	3	6	26	22	62	0	0	0	2	4	0	2	0	0	5	1	4	0	0	SE
SI	0	0	12	0	0	1	0	0	1	0	2	9	0	0	2	0	4	1	0	0	5	2	0	0	26	-0	0	0	0	0	0	0	SI
SK	0	0	11	0	2	3	1	0	1	0	16	35	1	0	2	0	8	4	0	0	4	18	0	0	11	0	0	0	0	0	0	0	SK
TJ	0	0	0	0	0	0	0	0	0	0	0	0	0	0	0	0	0	0	0	0	0	0	0	0	0	3	5	0	0	0	0	0	TJ
TM	0	2	0	9	0	0	0	0	0	0	0	1	0	0	0	0	0	0	2	0	0	0	0	0	1	1	17	0	0	0	0	0	TM
TR	1	6	3	5	1	1	16	2	1	6	3	12	0	0	6	0	5	3	5	39	1	4	0	0	12	0	1	0	0	0	2	0	TR
UA	2	1	17	4	4	10	19	42	3	0	29	121	9	1	7	3	21	25	3	18	6	35	2	0	24	0	5	8	1	3	20	2	UA
UZ	0	1	0	5	0	0	0	0	0	0	0	1	0	0	0	0	0	0	1	0	0	0	0	0	1	13	29	0	0	0	0	0	UZ
ATL	0	0	8	0	0	47	1	10	4	0	12	187	24	5	379	40	230	422	0	1	1	3	114	38	12	0	9	5	4	4	0	0	ATL
BAS	0	0	7	0	0	23	0	13	2	0	17	197	55	10	8	39	37	88	0	0	1	5	5	0	5	0	0	14	1	11	0	0	BAS
BLS	1	1	6	5	2	3	30	8	1	1	7	32	2	0	3	1	7	7	17	23	2	10	1	0	12	0	3	1	0	1	10	1	BLS
MED	20	0	45	0	19	18	40	3	19	15	25	132	2	0	385	1	316	48	0	245	38	24	4	0	698	0	1	1	3	0	2	10	MED
NOS	0	0	5	0	0	61	0	4	2	0	11	214	42	1	36	3	143	703	0	0	0	2	51	2	3	0	0	2	3	1	0	0	NOS
AST	0	8	1	63	0	1	2	2	1	6	1	7	0	0	4	1	4	2	9	10	0	1	0	0	7	16	178	0	0	0	1	0	AST
NOA	1	0	4	0	1	2	3	0	2	0	3	15	0	0	108	0	36	6	0	15	2	2	1	0	55	0	0	0	0	0	0	1	NOA
SUM	67	59	441	244	88	525	284	407	187	34	475	3495	328	96	1986	368	2387	2598	115	622	160	346	321	54	2076	148	1922	155	54	107	78	39	SUM
EXC	44	49	365	175	66	370	209	368	155	12	399	2710	202	79	1063	284	1614	1324	88	327	115	298	146	14	1284	133	1731	131	43	89	63	28	EXC
EU	13	0	296	1	28	317	136	55	94	4	293	2156	132	26	1004	142	1454	1122	1	204	82	189	131	2	1098	0	3	55	37	37	13	8	EU
emis	77	61	440	240	93	536	313	436	186	44	497	3614	341	101	2249	395	2457	2718	115	775	167	363	336	69	2158	167	2300	163	56	114	86	43	emis
	AL	AM	AT	AZ	BA	BE	BG	BY	CH	CY	CZ	DE	DK	EE	ES	FI	FR	GB	GE	GR	HR	HU	IE	IS	IT	KG	KZ	LT	LU	LV	MD	ME	

Table C.2 Cont.: 2017 country-to-country blame matrices for **oxidised nitrogen** deposition.
Units: 100 Mg of N. **Emitters →, Receptors ↓.**

	MK	MT	NL	NO	PL	PT	RO	RS	RU	SE	SI	SK	TJ	TM	TR	UA	UZ	ATL	BAS	BLS	MED	NOS	AST	NOA	BIC	DMS	VOL	SUM	EXC	EU	
AL	3	0	0	0	1	0	1	7	0	0	0	0	-0	0	1	0	0	0	0	0	12	0	0	5	2	-0	-0	80	61	30	AL
AM	0	0	0	0	0	0	0	0	1	0	0	0	0	0	9	0	0	0	0	0	1	0	51	1	2	-0	0	87	32	1	AM
AT	0	0	7	0	10	1	2	2	0	0	7	2	0	0	0	1	0	2	1	0	6	9	0	3	3	-0	0	372	350	332	AT
AZ	0	0	0	0	0	0	0	0	10	0	0	0	0	1	9	1	0	0	0	0	1	0	134	1	3	-0	-0	241	100	2	AZ
BA	0	0	2	0	12	0	3	12	1	0	1	4	0	0	0	1	0	1	1	0	12	2	0	6	2	-0	-0	180	157	121	BA
BE	0	0	10	0	1	0	0	0	0	0	0	0	-0	0	0	0	0	4	0	0	1	25	0	0	4	0	-0	183	149	147	BE
BG	3	0	2	0	11	0	36	28	13	0	1	2	0	0	27	22	0	1	1	8	15	2	1	6	5	-0	0	349	310	207	BG
BY	1	0	11	4	156	0	16	6	64	7	1	6	0	0	6	62	0	3	24	2	5	19	1	2	4	-0	0	673	615	381	BY
CH	0	0	2	0	0	1	0	0	0	0	0	0	0	0	0	0	0	1	0	0	4	4	0	1	2	-0	0	152	139	93	CH
CY	0	0	0	0	0	0	0	0	0	0	0	0	0	0	5	0	0	0	0	0	4	0	4	1	1	-0	-0	20	11	5	CY
CZ	0	0	12	1	36	0	2	3	1	1	3	6	0	0	0	1	0	2	2	0	3	15	0	1	3	-0	0	407	380	369	CZ
DE	0	0	143	5	49	3	2	1	3	3	1	3	0	0	0	3	0	23	17	0	8	180	0	6	29	0	0	2156	1892	1847	DE
DK	0	0	12	2	10	0	0	0	2	2	0	0	0	0	0	1	0	3	13	0	0	32	0	0	2	-0	0	194	143	137	DK
EE	0	0	3	2	15	0	1	0	13	5	0	1	-0	0	0	2	0	1	20	0	0	6	0	0	1	-0	-0	126	98	77	EE
ES	0	0	1	0	1	50	0	0	0	0	0	0	0	0	0	0	0	67	0	0	116	5	0	69	46	-0	0	1056	754	752	ES
FI	0	0	9	12	41	0	2	1	71	27	0	2	0	0	1	5	0	6	62	0	1	22	0	0	10	-0	-0	496	395	297	FI
FR	0	0	23	1	4	13	0	1	1	1	1	0	0	0	0	0	0	80	1	0	74	109	0	31	43	-0	0	1686	1349	1330	FR
GB	0	0	17	2	4	3	0	0	1	1	0	0	0	0	0	1	0	58	2	0	2	76	0	2	28	0	0	755	587	582	GB
GE	0	0	0	0	1	0	1	0	7	0	0	0	0	0	29	2	0	0	0	4	1	0	53	1	5	-0	0	166	102	5	GE
GL	0	0	0	1	0	0	0	0	1	0	0	0	0	0	0	0	0	1	0	0	0	1	0	0	29	-0	-0	37	6	4	GL
GR	7	0	1	0	5	0	7	13	4	0	0	1	-0	0	29	7	0	1	0	3	67	1	1	18	9	-0	0	391	291	222	GR
HR	0	0	2	0	12	0	4	9	1	0	6	3	-0	0	0	1	0	1	1	0	24	3	0	7	3	-0	0	253	215	194	HR
HU	1	0	4	0	35	0	17	25	2	0	6	17	0	0	1	4	0	1	1	0	9	5	0	4	3	-0	0	367	343	300	HU
IE	0	0	1	0	0	1	0	0	0	0	0	0	-0	0	0	0	0	13	0	0	1	5	0	1	9	-0	0	99	70	69	IE
IS	0	0	1	1	0	0	0	0	0	0	0	0	0	0	0	0	0	4	0	0	0	2	0	0	12	-0	-0	40	22	11	IS
IT	1	0	3	0	10	3	3	6	1	0	12	2	0	0	1	2	0	6	1	0	176	5	0	54	22	-0	0	1318	1054	1025	IT
KG	0	0	0	0	0	0	0	0	3	0	0	0	4	7	2	0	107	0	0	0	0	0	116	0	12	-0	0	361	232	2	KG
KZ	1	0	3	3	25	1	8	2	674	3	0	1	3	42	47	98	130	3	8	6	6	6	1046	6	96	-0	0	3296	2119	113	KZ
LT	0	0	6	2	55	0	2	2	13	5	0	2	0	0	0	5	0	1	19	0	1	11	0	0	1	-0	0	232	197	165	LT
LU	0	0	0	0	0	0	0	0	0	0	0	0	-0	0	0	0	0	0	0	0	0	1	0	0	0	0	0	13	12	12	LU
LV	0	0	4	3	34	0	2	1	15	7	0	1	0	0	0	5	0	1	24	0	1	10	0	0	1	-0	-0	203	166	133	LV
MD	0	0	1	0	10	0	10	1	7	0	0	1	0	0	4	17	0	0	1	2	2	1	1	1	1	-0	0	86	77	38	MD
ME	0	0	0	0	1	0	0	3	0	0	0	0	-0	0	0	0	0	0	0	0	5	0	0	2	1	-0	-0	38	30	16	ME
MK	14	0	0	0	1	0	1	11	0	0	0	0	-0	0	2	1	0	0	0	0	3	0	0	2	1	-0	-0	69	62	31	MK
MT	0	0	0	0	0	0	0	0	0	0	0	0	0	0	0	0	0	0	0	0	0	0	0	0	0	0	0	1	0	0	MT
NL	0	0	61	1	1	0	0	0	0	0	0	0	0	0	0	0	0	6	0	0	1	48	0	0	6	0	-0	255	194	193	NL
NO	0	0	11	84	16	1	0	0	12	16	0	1	0	0	0	2	0	22	18	0	1	68	0	0	22	-0	-0	400	270	169	NO
PL	0	0	52	7	661	1	13	12	20	10	5	24	0	0	1	27	0	8	50	0	6	76	0	3	11	-0	-0	1737	1582	1495	PL
PT	0	0	0	0	0	89	0	0	0	0	0	0	-0	0	0	0	0	34	0	0	8	1	0	7	10	-0	-0	196	137	136	PT
RO	5	0	6	1	56	1	226	43	23	1	3	12	0	0	19	53	0	1	3	8	17	7	2	11	8	-0	0	763	705	534	RO
RS	6	0	3	0	20	0	18	94	3	0	2	6	0	0	3	5	0	1	1	1	9	3	0	5	3	-0	-0	323	299	170	RS
RU	4	0	39	39	335	2	68	21	6357	59	4	16	1	21	194	721	27	37	188	43	40	90	462	16	260	-1	0	10915	9779	1399	RU
SE	0	0	25	38	48	1	1	1	28	87	0	1	0	0	0	3	0	13	86	0	1	77	0	1	16	-0	0	716	523	446	SE
SI	0	0	1	0	2	0	1	1	0	0	19	1	-0	0	0	0	0	0	0	0	7	1	0	2	1	-0	-0	103	92	89	SI
SK	0	0	3	0	39	0	6	8	1	0	3	27	0	0	0	3	0	1	1	0	4	4	0	1	1	-0	0	222	209	193	SK
TJ	0	0	0	0	0	0	0	0	2	0	0	0	10	14	1	0	27	0	0	0	0	0	110	0	10	-0	0	184	63	1	TJ
TM	0	0	0	0	1	0	0	0	22	0	0	0	1	54	8	4	17	0	0	0	1	0	653	2	16	-0	-0	816	143	6	TM
TR	1	0	2	0	11	1	18	8	36	0	0	2	0	1	825	27	0	1	1	31	133	2	565	48	52	-0	0	1904	1071	147	TR
UA	3	0	17	4	257	1	91	25	207	6	4	20	0	1	79	474	0	4	22	28	26	26	17	11	17	-0	0	1783	1631	754	UA
UZ	0	0	0	0	1	0	0	0	25	0	0	0	4	31	8	4	125	0	0	0	1	0	420	1	18	-0	0	695	252	6	UZ
ATL	0	0	66	144	55	161	3	1	301	33	1	2	0	0	4	18	0	1170	51	1	96	249	5	98	1725	4	-0	5746	2348	1819	ATL
BAS	0	0	48	22	136	1	3	2	53	55	1	4	0	0	1	9	0	12	173	0	2	102	0	2	7	0	-0	1174	876	774	BAS
BLS	2	0	4	1	50	0	69	16	139	2	1	5	0	1	248	153	0	1	6	100	42	7	51	11	7	-0	0	1112	887	278	BLS
MED	11	11	18	2	49	18	31	45	21	1	17	10	-0	0	319	28	0	45	5	18	1723	37	193	750	106	1	3	5574	2693	2194	MED
NOS	0	0	106	71	49	6	2	1	12	15	0	2	0	0	0	6	0	103	38	0	6	443	0	4	53	2	0	2211	1560	1462	NOS
AST	0	0	1	1	6	0	4	1	117	1	0	1	5	66	168	27	47	1	2	4	56	2	8589	51	465	-0	0	9943	773	63	AST
NOA	1	1	3	0	4	16	3	4	2	0	1	1	0	0	13	3	0	55	0	1	234	4	16	965	173	-0	-0	1761	313	283	NOA
SUM	66	14	745	457	2339	379	680	418	8288	351	105	190	27	239	2064	1812	483	1799	845	261	2974	1804	12494	2223	3384	5	4	64716			SUM
EXC	51	2	500	216	1990	176	566	348	7644	243	84	167	22	173	1312	1568	435	412	571	138	814	960	3639	342	848	-2	1		29472	14790	EXC
EU	18	1	408	80	1140	169	328	157	214	150	70	109	0	0	85	146	0	333	307	20	551	734	9	230	277	-0	1		12208	11290	EU
emis	74	16	767	495	2446	484	705	449	9857	377	106	200	30	301	2388	1939	528	2352	874	275	3565	1855	22673	4419	0			78886	42873	22938	emis
	MK	MT	NL	NO	PL	PT	RO	RS	RU	SE	SI	SK	TJ	TM	TR	UA	UZ	ATL	BAS	BLS	MED	NOS	AST	NOA	BIC	DMS	VOL	SUM	EXC	EU	

Table C.3: 2017 country-to-country blame matrices for **reduced nitrogen** deposition.
Units: 100 Mg of N. **Emitters →, Receptors ↓.**

	AL	AM	AT	AZ	BA	BE	BG	BY	CH	CY	CZ	DE	DK	EE	ES	FI	FR	GB	GE	GR	HR	HU	IE	IS	IT	KG	KZ	LT	LU	LV	MD	ME	
AL	79	0	1	0	0	0	1	0	0	0	0	1	0	0	2	0	1	0	0	4	1	1	0	0	11	0	0	0	0	0	0	0	AL
AM	0	57	0	25	0	0	0	0	0	0	0	0	0	0	0	0	0	0	4	0	0	0	0	0	0	0	0	0	0	0	0	0	AM
AT	0	0	230	0	1	3	0	1	26	-0	18	157	0	0	10	0	38	5	0	0	4	7	1	0	48	-0	0	0	1	0	0	0	AT
AZ	0	18	0	311	0	0	0	0	0	0	0	0	0	0	0	0	0	0	11	0	0	0	0	0	0	0	1	0	0	0	0	0	AZ
BA	1	0	9	0	68	1	1	1	1	0	6	14	0	0	6	0	4	1	0	1	25	18	0	0	39	0	0	0	0	0	0	1	BA
BE	0	0	0	0	0	152	0	0	0	0	0	16	0	0	5	0	94	19	0	-0	0	0	3	0	1	-0	0	0	4	0	0	0	BE
BG	4	0	3	1	2	1	167	3	1	0	3	10	0	0	4	0	3	1	1	18	3	11	0	0	10	0	1	0	0	0	5	0	BG
BY	1	0	4	1	2	3	4	509	1	0	10	53	9	1	4	1	12	7	0	2	3	12	1	0	8	0	1	22	0	6	7	0	BY
CH	0	-0	2	-0	0	1	0	0	248	-0	0	21	0	0	12	0	44	2	-0	0	0	0	1	0	33	-0	0	0	0	0	0	0	CH
CY	0	0	0	0	0	0	0	0	0	10	0	0	0	0	0	0	0	0	0	0	0	0	0	0	0	-0	0	0	0	0	0	-0	CY
CZ	0	0	36	0	1	5	0	1	5	0	210	155	2	0	7	0	33	8	0	0	5	13	1	0	13	0	0	0	1	0	0	0	CZ
DE	0	0	32	0	0	95	0	2	63	-0	25	2818	17	0	44	0	378	108	0	0	1	4	16	0	29	-0	0	1	15	0	0	0	DE
DK	0	0	1	0	0	4	0	1	1	-0	2	75	174	0	2	0	12	16	0	0	0	1	2	0	1	-0	0	0	0	0	0	0	DK
EE	0	0	0	0	0	1	0	5	0	0	1	11	3	31	1	3	3	2	0	0	0	1	0	0	0	0	0	4	0	6	0	0	EE
ES	0	0	1	0	0	1	0	0	1	0	1	4	0	0	1853	0	46	3	0	0	0	0	1	0	15	0	0	0	0	0	0	0	ES
FI	0	0	1	0	0	2	0	10	1	0	3	32	9	5	2	126	10	11	0	0	1	2	1	0	1	0	0	5	0	4	0	0	FI
FR	0	0	4	0	0	35	0	0	30	0	2	53	1	0	350	0	2689	70	0	0	1	1	18	0	56	0	0	0	4	0	0	0	FR
GB	0	0	0	0	0	11	0	0	1	0	1	28	1	0	17	0	81	853	0	-0	0	0	114	0	1	0	0	0	0	0	0	0	GB
GE	0	14	0	45	0	0	0	0	0	0	0	1	0	0	1	0	0	0	131	0	0	0	0	0	1	0	1	0	0	0	0	0	GE
GL	0	0	0	0	0	0	0	0	0	0	0	1	0	0	0	0	0	0	0	0	0	0	0	0	0	0	0	0	0	0	0	0	GL
GR	11	0	2	0	1	0	18	1	1	0	1	5	0	0	5	0	3	0	0	162	2	4	0	0	15	0	0	0	0	0	1	0	GR
HR	1	0	16	0	11	1	1	1	2	0	6	20	0	0	11	0	8	1	0	0	99	24	0	0	76	-0	0	0	0	0	0	0	HR
HU	1	0	33	0	6	1	3	2	4	0	13	39	1	0	6	0	13	2	0	1	25	234	0	0	36	0	0	0	0	0	1	0	HU
IE	0	-0	0	-0	0	1	0	0	0	-0	0	2	0	0	4	0	11	15	-0	0	0	0	381	-0	0	-0	0	0	0	0	0	0	IE
IS	0	0	0	0	0	0	0	0	0	0	0	2	0	0	0	0	1	3	0	0	0	0	1	19	0	0	0	0	0	0	0	0	IS
IT	2	0	14	0	3	1	1	0	15	0	4	20	0	0	83	0	47	2	0	1	12	8	0	0	1705	0	0	0	0	0	0	0	IT
KG	0	0	0	1	0	0	0	0	0	0	0	0	0	0	0	0	0	0	0	0	0	0	0	0	0	289	26	0	0	0	0	0	KG
KZ	1	14	1	57	0	1	2	14	1	1	2	10	1	1	5	1	4	1	9	1	0	2	0	0	4	75	962	2	0	1	2	0	KZ
LT	0	0	2	0	0	2	0	27	1	0	3	26	7	0	2	1	5	5	0	0	1	4	1	0	2	0	0	91	0	6	0	0	LT
LU	0	0	0	0	0	2	0	0	0	0	0	3	0	0	0	0	10	1	0	0	0	0	0	0	0	0	0	0	8	0	0	0	LU
LV	0	0	1	0	0	1	0	19	0	0	2	18	6	2	2	2	5	4	0	0	1	2	1	0	1	0	0	20	0	54	0	0	LV
MD	0	0	1	0	0	0	2	2	0	0	1	3	0	0	1	0	1	0	0	1	0	3	0	0	2	0	0	0	0	0	40	0	MD
ME	3	0	0	0	2	0	0	0	0	0	0	1	0	0	1	0	1	0	0	0	1	1	0	0	7	0	0	0	0	0	0	5	ME
MK	7	0	1	0	0	0	3	0	0	0	1	2	0	0	1	0	1	0	0	7	1	2	0	0	3	0	0	0	0	0	0	0	MK
MT	0	0	0	0	0	0	0	0	0	-0	0	0	0	0	0	0	0	0	0	0	0	0	0	0	0	-0	0	0	0	0	0	-0	MT
NL	0	-0	0	0	0	49	-0	0	0	-0	0	65	1	0	4	0	45	35	-0	-0	0	0	5	0	0	-0	0	0	0	0	0	-0	NL
NO	0	0	1	0	0	3	0	3	0	0	2	30	13	0	4	2	11	27	0	0	0	1	5	0	0	0	0	1	0	1	0	0	NO
PL	0	0	25	0	3	17	1	33	5	0	70	398	34	0	13	1	58	36	0	0	10	39	5	0	20	0	0	6	2	1	2	0	PL
PT	0	0	0	0	0	0	0	0	0	0	0	1	0	0	76	0	3	0	0	0	0	0	0	-0	1	0	0	0	0	0	0	0	PT
RO	6	0	13	1	6	2	34	9	3	0	10	42	2	0	9	0	11	3	1	9	10	66	0	0	32	0	1	1	0	0	18	1	RO
RS	8	0	8	0	10	1	9	1	1	0	7	18	0	0	5	0	5	1	0	4	12	39	0	0	26	0	0	0	0	0	1	1	RS
RU	4	20	15	99	7	9	18	289	7	1	25	153	30	24	22	52	41	31	39	10	8	31	6	0	34	9	448	43	1	31	23	1	RU
SE	0	0	2	0	0	6	0	8	1	0	4	90	60	2	7	12	28	31	0	0	0	2	5	0	1	0	0	5	0	2	0	0	SE
SI	0	0	14	0	0	0	0	0	1	0	2	9	0	0	4	0	3	0	0	0	6	4	0	0	38	0	0	0	0	0	0	0	SI
SK	0	0	18	0	3	1	1	1	2	0	18	31	1	0	3	0	10	2	0	0	7	36	0	0	15	-0	0	0	0	0	0	0	SK
TJ	0	0	0	1	0	0	0	0	0	0	0	0	0	0	0	0	0	0	0	0	0	0	0	0	0	9	6	0	0	0	0	0	TJ
TM	0	2	0	16	0	0	0	0	0	0	0	0	0	0	0	0	0	0	2	0	0	0	0	0	0	1	13	0	0	0	0	-0	TM
TR	3	12	2	14	1	0	16	4	1	7	2	9	0	0	11	0	5	1	11	20	1	5	0	0	14	0	2	0	0	0	3	0	TR
UA	3	2	15	7	5	5	19	90	3	0	21	95	10	1	11	1	21	10	5	8	10	58	2	0	27	0	4	7	1	2	48	1	UA
UZ	0	2	0	10	0	0	0	1	0	0	0	0	0	0	0	0	0	0	1	0	0	0	0	-0	0	33	41	0	0	0	0	-0	UZ
ATL	0	0	5	1	0	27	1	10	5	0	8	131	16	2	528	13	462	300	0	0	1	3	301	21	16	0	8	3	2	2	0	0	ATL
BAS	0	0	6	0	1	12	0	21	3	0	12	296	130	9	11	30	44	41	0	0	1	6	6	0	4	0	0	17	1	12	0	0	BAS
BLS	2	3	4	12	2	1	27	13	2	1	4	20	2	0	5	0	5	2	35	10	2	11	0	0	15	0	3	1	0	0	18	0	BLS
MED	36	0	29	0	13	6	28	5	16	12	16	63	2	0	554	0	241	14	1	104	40	27	3	0	661	0	1	1	1	0	4	1	MED
NOS	0	0	4	0	0	68	0	4	3	0	7	319	81	0	49	1	323	565	0	0	0	2	73	1	3	0	0	2	2	1	0	0	NOS
AST	1	12	1	138	0	0	1	3	0	5	1	3	0	0	4	0	2	0	10	4	0	1	0	0	6	47	120	0	0	0	1	0	AST
NOA	2	0	3	0	2	1	2	0	2	0	2	8	0	0	115	0	26	2	0	5	3	2	0	0	47	-0	0	0	0	0	0	0	NOA
SUM	177	158	560	740	156	534	364	1094	459	39	527	5383	615	80	3881	247	4902	2245	263	374	298	692	957	41	3082	462	1641	235	46	132	177	13	SUM
EXC	137	142	508	589	137	418	304	1038	429	21	478	4542	384	68	2616	202	3799	1319	217	252	251	641	573	20	2330	415	1508	210	40	116	154	11	EXC
EU	26	1	450	2	40	395	229	123	165	11	400	4127	318	41	2528	145	3647	1234	2	193	188	466	557	0	2119	0	3	134	38	74	29	2	EU
emis	199	159	569	698	175	550	407	1135	454	53	552	5544	629	84	4267	256	4994	2332	255	459	310	722	976	43	3164	473	1924	243	48	136	187	17	emis
	AL	AM	AT	AZ	BA	BE	BG	BY	CH	CY	CZ	DE	DK	EE	ES	FI	FR	GB	GE	GR	HR	HU	IE	IS	IT	KG	KZ	LT	LU	LV	MD	ME	

Table C.3 Cont.: 2017 country-to-country blame matrices for **reduced nitrogen** deposition.
Units: 100 Mg of N. **Emitters →, Receptors ↓.**

	MK	MT	NL	NO	PL	PT	RO	RS	RU	SE	SI	SK	TJ	TM	TR	UA	UZ	ATL	BAS	BLS	MED	NOS	AST	NOA	BIC	DMS	VOL	SUM	EXC	EU	
AL	-0	0	0	0	1	0	1	4	0	0	0	0	0	0	1	0	0	0	0	0	-0	0	0	3	2	0	-0	117	113	27	AL
AM	0	0	0	0	0	0	0	0	1	0	0	0	0	0	47	0	0	0	0	0	0	0	41	1	2	0	0	181	136	1	AM
AT	0	0	5	0	6	1	2	1	0	0	11	2	-0	0	0	0	0	0	0	0	1	0	0	3	4	0	0	588	578	549	AT
AZ	0	0	0	0	0	0	0	0	21	0	0	0	0	2	33	1	2	0	0	0	0	0	98	2	3	0	0	506	403	2	AZ
BA	0	0	1	0	6	0	4	13	0	0	2	4	-0	0	1	2	0	0	0	0	0	0	0	4	2	0	0	237	230	142	BA
BE	0	0	21	0	0	0	0	0	0	0	0	0	0	0	0	0	0	-0	0	-0	0	-1	0	0	1	-0	0	317	317	316	BE
BG	6	0	1	0	6	0	69	17	12	0	1	2	0	0	41	21	0	0	0	0	1	0	1	4	4	0	0	440	429	315	BG
BY	1	0	6	1	130	0	28	8	43	6	1	5	0	0	12	106	0	0	-0	0	1	1	1	2	7	0	1	1046	1033	339	BY
CH	0	0	2	0	0	1	0	0	0	0	0	0	-0	-0	0	0	-0	0	0	-0	0	0	0	2	3	0	-0	373	367	119	CH
CY	0	0	0	0	0	0	0	0	0	0	0	0	-0	0	5	0	0	0	0	0	-0	0	1	2	0	-0	-0	21	17	11	CY
CZ	0	0	9	0	16	0	3	3	0	0	5	7	0	0	0	1	0	0	0	0	1	0	0	2	4	0	0	552	544	532	CZ
DE	0	0	253	1	33	3	2	1	1	2	1	2	-0	0	0	2	0	2	-1	-0	1	-9	0	6	18	1	0	3970	3953	3882	DE
DK	0	0	13	1	9	0	0	0	1	2	0	0	-0	0	0	1	0	0	-1	0	0	-1	0	0	2	-0	0	320	319	315	DK
EE	0	0	2	1	11	0	1	1	5	5	0	0	0	0	1	3	0	0	-0	0	0	0	0	0	1	0	0	104	102	87	EE
ES	0	0	1	0	0	47	0	0	0	0	0	0	0	0	0	0	0	-3	-0	-0	-7	0	-0	50	21	-1	-0	2036	1977	1975	ES
FI	0	0	6	4	30	0	2	1	54	19	0	1	0	0	2	5	0	0	1	0	0	1	0	0	8	-0	0	363	352	275	FI
FR	0	0	14	0	2	13	0	1	0	0	1	0	0	0	0	0	0	-4	0	-0	3	-8	0	24	27	-3	-0	3387	3348	3315	FR
GB	0	0	16	0	3	2	0	0	0	0	0	0	0	0	0	0	0	-5	-0	-0	0	-3	0	2	15	-3	0	1138	1132	1130	GB
GE	0	0	0	0	1	0	1	0	11	0	0	0	0	1	95	3	1	0	0	0	0	0	38	2	3	0	0	351	307	5	GE
GL	0	0	0	0	0	0	0	0	0	0	0	0	0	0	0	0	0	0	0	0	0	0	0	0	22	0	0	26	4	3	GL
GR	8	0	1	0	3	0	10	9	4	0	0	1	0	0	32	7	0	0	0	0	-1	0	1	8	6	-0	-1	323	311	234	GR
HR	0	0	1	0	4	0	5	9	0	0	13	3	0	0	0	1	0	0	0	0	1	0	0	6	3	0	0	326	316	289	HR
HU	1	0	2	0	10	0	30	27	2	0	9	23	0	0	2	7	0	0	0	0	1	0	0	4	3	0	0	542	534	483	HU
IE	0	0	1	0	0	1	0	0	0	0	0	0	-0	-0	0	0	-0	-2	-0	-0	0	-0	0	1	5	-3	0	419	417	417	IE
IS	0	0	1	0	0	0	0	0	0	0	0	0	0	0	0	0	0	0	0	0	0	0	0	0	9	-0	0	37	28	9	IS
IT	0	0	2	0	5	4	3	3	1	0	10	2	0	0	1	1	0	1	0	0	-3	0	0	35	14	0	-4	1996	1953	1925	IT
KG	0	0	0	0	0	0	0	0	4	0	0	0	50	4	6	1	184	0	0	0	0	0	254	1	9	0	-0	830	567	1	KG
KZ	0	0	1	0	13	0	10	2	536	1	0	1	32	63	121	54	398	0	0	0	1	0	1752	8	47	0	0	4218	2410	67	KZ
LT	0	0	4	1	66	0	3	2	11	5	1	2	0	0	0	9	0	0	-0	0	0	0	0	0	2	0	0	294	291	239	LT
LU	0	0	0	0	0	0	0	0	0	0	0	0	0	0	0	0	0	0	0	-0	0	-0	0	0	0	0	0	25	25	25	LU
LV	0	0	3	1	30	0	2	2	8	7	0	1	0	0	1	7	0	0	-0	0	0	0	0	0	2	0	0	208	204	165	LV
MD	0	0	0	0	4	0	23	1	5	0	0	1	0	0	7	25	0	0	-0	-0	0	0	1	1	1	0	0	127	125	43	MD
ME	0	0	0	0	1	0	1	3	0	0	0	0	0	0	1	0	0	0	0	0	0	0	0	1	1	0	0	34	31	16	ME
MK	26	0	0	0	1	0	2	8	1	0	0	0	0	0	3	1	0	0	0	0	0	0	0	1	1	0	-0	74	72	25	MK
MT	0	0	0	0	0	0	0	0	0	0	0	0	-0	0	0	0	0	0	0	-0	-0	0	0	0	0	-0	-0	1	1	1	MT
NL	-0	0	342	0	1	0	0	0	-0	0	0	0	-0	-0	-0	0	0	-0	-0	-0	0	-4	-0	0	1	-0	-0	546	549	548	NL
NO	0	0	8	138	14	0	1	0	8	13	0	1	0	0	0	3	0	0	0	0	0	1	0	0	18	0	0	311	290	138	NO
PL	0	0	38	2	1253	1	22	10	14	9	6	22	0	0	2	45	0	1	-1	0	1	2	0	3	13	1	1	2227	2205	2087	PL
PT	-0	0	0	0	0	136	0	0	0	0	0	0	0	0	0	0	0	-2	0	-0	-0	0	-0	4	5	-1	-0	225	218	218	PT
RO	4	0	3	0	24	1	606	39	23	1	3	11	0	0	32	72	1	0	0	-0	1	0	2	9	9	0	1	1133	1111	894	RO
RS	5	0	2	0	9	0	29	191	2	0	2	6	0	0	6	5	0	0	0	0	1	0	0	3	3	0	-0	423	415	184	RS
RU	3	0	19	9	242	1	92	28	6173	35	4	12	6	32	400	547	115	2	3	2	4	4	781	15	241	5	4	10313	9251	989	RU
SE	0	0	17	19	38	1	1	1	11	209	0	1	0	0	0	4	0	1	-1	0	0	1	0	1	12	0	0	584	570	525	SE
SI	0	0	0	0	1	0	1	1	0	0	54	1	0	0	0	0	0	0	0	0	0	0	0	2	1	0	0	145	142	138	SI
SK	0	0	2	0	14	0	10	8	1	0	4	67	-0	0	0	5	0	0	0	0	0	0	0	1	2	0	0	265	260	240	SK
TJ	0	0	0	0	0	0	0	0	2	0	0	0	222	8	3	0	103	0	0	0	0	0	136	1	6	0	0	498	355	0	TJ
TM	0	0	0	0	0	0	0	0	19	0	0	0	6	158	20	1	136	0	0	0	0	0	407	3	10	0	-0	798	377	3	TM
TR	2	0	1	0	7	1	24	5	40	0	0	1	0	1	3116	27	2	0	0	-1	-3	0	346	55	37	0	-4	3803	3372	129	TR
UA	2	0	10	1	159	1	165	25	166	4	4	16	0	1	129	1019	3	1	0	-0	2	1	15	9	19	1	2	2246	2196	681	UA
UZ	0	0	0	0	1	0	0	0	20	0	0	0	53	38	19	1	790	0	0	0	0	0	287	2	9	0	-0	1310	1012	3	UZ
ATL	0	0	40	43	32	145	3	2	1373	13	1	1	0	0	7	13	2	-25	2	0	2	3	8	57	1327	-20	0	4897	3542	2056	ATL
BAS	0	0	38	8	134	1	4	3	24	82	1	3	0	0	1	10	0	1	-6	0	0	-2	0	1	12	-2	0	979	975	903	BAS
BLS	2	0	2	0	25	0	97	13	121	1	1	3	0	1	424	138	2	0	0	-6	1	0	37	9	13	0	1	1088	1032	242	BLS
MED	7	5	8	0	20	15	34	26	16	1	13	7	0	0	358	24	0	1	0	-0	-50	2	97	473	92	-8	-5	3014	2411	1904	MED
NOS	0	0	173	42	34	5	2	1	6	13	0	1	0	0	0	6	0	-1	-1	0	1	-13	0	3	45	-4	0	1823	1792	1729	NOS
AST	0	0	0	0	3	0	3	1	149	0	0	0	64	86	233	13	188	0	0	0	-1	0	21692	118	290	-0	-5	23197	1102	35	AST
NOA	1	0	1	0	2	11	3	3	1	0	1	1	-0	0	11	2	0	-3	0	-0	-13	0	4	1392	86	-3	-9	1714	259	234	NOA
SUM	70	7	1070	275	2406	394	1300	475	8894	431	150	209	434	396	5171	2197	1929	-31	-6	-4	-51	-19	26002	2336	2507	-36	-17	87063			SUM
EXC	61	1	808	181	2155	217	1155	427	7203	321	133	193	370	309	4137	1991	1738	-4	-1	2	8	-11	4163	281	644	1	0		45269	24056	EXC
EU	21	1	756	30	1565	212	774	137	150	261	119	147	0	1	119	193	2	-9	-4	0	1	-19	6	166	188	-7	-2		22174	21128	EU
emis	84	9	1088	275	2533	474	1353	535	9913	439	153	219	434	504	6092	2355	2094	0	0	0	0	0	40269	5163	0			106000	60568	32564	emis
	MK	MT	NL	NO	PL	PT	RO	RS	RU	SE	SI	SK	TJ	TM	TR	UA	UZ	ATL	BAS	BLS	MED	NOS	AST	NOA	BIC	DMS	VOL	SUM	EXC	EU	

Table C.4: 2017 country-to-country blame matrices for $\mathbf{AOT40}_f^{\mathbf{uc}}$.
Units: ppb.h per 15% emis. red. of NO_x. **Emitters →, Receptors ↓.**

	AL	AM	AT	AZ	BA	BE	BG	BY	CH	CY	CZ	DE	DK	EE	ES	FI	FR	GB	GE	GR	HR	HU	IE	IS	IT	KG	KZ	LT	LU	LV	MD	
AL	515	0	38	0	57	2	58	13	9	0	29	68	4	1	72	3	80	13	0	144	56	55	4	1	267	0	1	3	1	1	6	AL
AM	1	427	2	420	1	0	6	5	1	4	3	9	1	1	16	2	9	3	115	12	1	4	1	0	12	0	26	2	0	1	3	AM
AT	0	0	317	0	4	3	1	3	85	0	64	338	5	1	83	5	290	20	0	1	26	27	9	1	231	0	0	3	3	2	1	AT
AZ	1	43	3	570	1	0	5	10	1	1	3	10	2	1	14	5	9	4	89	7	1	4	1	0	9	0	70	3	0	2	3	AZ
BA	9	0	97	0	369	3	12	13	13	0	70	153	6	1	84	5	103	19	0	13	192	106	6	1	276	0	1	4	2	2	1	BA
BE	0	0	1	0	0	-341	0	2	4	0	2	9	3	1	44	5	261	12	0	0	0	0	20	2	8	-0	0	1	10	1	0	BE
BG	13	0	35	2	18	3	527	25	4	0	33	82	4	2	33	7	46	15	2	115	21	68	4	1	55	0	7	6	1	3	28	BG
BY	1	0	6	0	2	4	5	162	2	0	17	74	14	9	11	26	31	33	1	3	3	12	8	1	10	0	3	39	1	19	5	BY
CH	0	0	23	0	1	-1	0	1	357	0	4	40	2	0	133	4	606	11	0	0	5	2	8	1	297	0	0	2	1	1	0	CH
CY	7	1	10	2	5	1	39	8	3	310	7	24	1	1	36	2	36	6	3	215	6	14	2	0	71	0	4	2	0	1	5	CY
CZ	0	0	108	0	6	6	2	6	15	0	208	406	10	1	48	7	205	45	0	1	19	47	13	2	45	0	0	4	6	2	1	CZ
DE	0	0	21	0	0	-2	0	3	23	0	25	121	7	1	44	8	245	46	0	0	1	4	17	2	20	0	0	2	7	1	0	DE
DK	0	0	1	0	0	-3	0	5	1	0	7	42	-58	3	6	17	34	117	0	0	0	2	32	4	1	0	1	8	1	5	0	DK
EE	0	0	1	0	0	1	0	18	0	0	6	40	18	35	3	55	15	39	0	0	0	2	7	1	2	0	0	19	0	27	0	EE
ES	0	0	5	0	1	1	0	1	3	0	2	12	1	0	1200	1	119	12	0	0	2	1	6	1	35	0	0	0	0	0	0	ES
FI	0	0	0	0	0	0	0	3	0	0	2	10	6	6	1	40	4	14	0	0	0	1	3	1	0	0	1	4	0	4	0	FI
FR	0	0	7	0	0	-4	0	1	14	0	3	29	2	0	187	3	703	21	0	0	2	1	15	1	57	0	0	1	1	1	0	FR
GB	0	0	0	0	0	-7	0	2	1	0	1	0	6	1	11	5	37	-130	0	0	0	0	33	2	1	0	0	2	0	2	0	GB
GE	1	60	3	287	1	1	11	10	1	1	4	15	2	1	16	3	11	5	467	10	2	6	1	0	12	0	29	4	0	1	7	GE
GL	0	-0	0	-0	0	0	0	0	0	-0	0	0	0	0	0	0	0	0	0	0	0	0	0	0	0	0	0	0	0	0	0	GL
GR	63	0	27	1	22	2	248	18	6	0	20	55	3	1	50	5	63	12	2	670	22	37	3	1	144	0	5	4	0	2	16	GR
HR	4	0	153	0	101	4	7	11	16	0	76	199	7	1	82	5	143	22	0	5	360	134	7	1	352	0	1	4	2	2	1	HR
HU	2	0	124	0	31	4	19	18	11	0	101	236	9	2	48	7	121	29	0	5	81	319	10	2	106	0	1	5	3	3	4	HU
IE	0	0	0	0	0	-0	0	2	0	0	0	4	5	1	6	5	28	26	0	0	0	0	30	2	1	0	0	2	0	2	0	IE
IS	0	0	0	0	0	0	0	0	0	0	0	4	3	0	1	1	3	26	0	0	0	0	6	8	0	0	0	1	0	0	0	IS
IT	3	0	79	0	16	3	6	4	37	0	29	104	4	1	136	4	294	16	0	9	52	26	6	1	814	0	0	2	1	1	1	IT
KG	1	3	3	9	1	1	2	3	2	0	2	8	1	1	21	2	12	3	5	4	1	3	1	0	12	603	253	1	0	1	1	KG
KZ	1	2	3	6	1	1	2	14	1	0	3	14	3	3	13	12	13	10	3	3	1	3	2	1	9	14	320	4	0	3	2	KZ
LT	0	0	5	0	1	3	1	68	1	0	12	75	24	9	8	30	30	54	0	0	2	8	13	2	5	0	1	86	1	24	1	LT
LU	0	0	3	0	0	20	0	2	7	0	4	108	2	0	56	5	391	29	0	0	0	0	14	2	12	0	0	1	-281	1	0	LU
LV	0	0	3	0	1	3	1	43	1	0	8	53	20	13	5	36	22	49	0	0	1	4	10	2	3	0	0	53	1	50	1	LV
MD	2	1	15	2	5	3	37	53	2	0	26	77	8	4	21	13	33	22	4	11	8	49	5	1	23	0	9	10	1	5	152	MD
ME	64	0	52	0	162	3	26	13	11	0	47	100	6	1	81	4	86	16	0	40	83	79	5	1	244	0	1	3	1	1	3	ME
MK	132	0	39	0	39	2	162	15	7	0	32	84	4	1	60	4	67	13	1	276	32	71	4	1	128	0	2	3	1	2	9	MK
MT	9	0	28	0	20	3	14	5	7	0	19	52	2	1	97	2	209	16	0	50	24	16	6	1	366	0	1	2	1	1	1	MT
NL	0	0	1	0	0	-49	0	3	1	0	3	-55	4	1	18	7	79	29	0	0	0	1	25	2	3	0	0	2	2	2	0	NL
NO	0	0	0	0	0	0	0	1	0	0	1	11	7	1	2	8	7	38	0	0	0	0	10	1	0	0	0	2	0	1	0	NO
PL	0	0	19	0	5	6	2	27	3	0	61	202	26	4	20	15	76	52	0	1	10	39	14	2	20	0	0	12	3	5	2	PL
PT	0	0	1	0	0	0	0	0	1	0	1	6	0	0	600	1	49	8	0	0	0	0	4	1	9	0	0	0	0	0	0	PT
RO	6	0	30	1	13	3	92	32	4	0	41	100	6	3	30	9	47	19	2	21	20	98	5	1	47	0	6	7	1	4	29	RO
RS	32	0	69	0	75	3	80	16	8	0	63	141	6	2	56	5	80	18	0	37	62	144	6	1	122	0	1	4	2	2	8	RS
RU	0	1	1	5	0	1	1	13	0	0	2	9	2	3	4	11	6	6	3	1	0	2	1	0	2	0	37	4	0	3	1	RU
SE	0	0	0	0	0	0	0	4	0	0	2	19	16	2	2	17	10	41	0	0	0	1	10	1	0	0	0	4	0	3	0	SE
SI	1	0	281	0	11	4	2	5	26	0	58	229	5	1	67	5	176	20	0	1	189	62	7	1	395	0	1	3	3	2	1	SI
SK	1	0	71	0	17	5	9	15	10	0	156	238	12	2	38	8	118	34	0	3	38	214	11	2	71	0	0	5	3	3	4	SK
TJ	0	3	2	7	1	0	1	2	1	0	2	7	0	0	20	1	11	2	3	3	1	2	1	0	10	62	85	1	0	0	1	TJ
TM	1	6	3	26	1	1	3	9	1	0	3	11	1	1	18	6	13	6	9	4	1	4	2	0	12	3	156	2	0	2	2	TM
TR	4	16	9	19	3	1	38	13	3	9	8	27	2	1	27	3	24	6	23	53	4	16	2	0	32	0	7	3	0	2	8	TR
UA	1	1	11	3	3	3	14	73	2	0	22	70	10	5	18	18	32	24	4	6	6	31	6	1	18	0	15	15	1	8	24	UA
UZ	1	4	3	12	1	1	2	9	1	0	2	10	2	1	15	6	11	6	6	4	1	3	1	0	10	32	210	2	0	2	2	UZ
ATL	0	0	0	0	0	-0	0	0	0	0	0	0	0	0	1	0	1	0	0	0	0	0	0	0	0	0	0	0	0	0	0	ATL
BAS	0	0	1	0	0	-0	0	4	0	0	2	17	7	4	1	12	9	26	0	0	0	1	7	1	0	0	0	5	0	4	0	BAS
BLS	0	1	1	3	0	0	8	7	0	0	2	6	1	1	2	2	3	2	8	2	1	3	1	0	2	0	3	2	0	1	5	BLS
MED	3	0	6	0	4	0	14	2	1	1	4	11	1	0	21	1	32	3	0	32	8	5	1	0	48	0	1	1	0	0	1	MED
NOS	0	0	0	0	0	-2	0	0	0	0	0	-0	1	0	2	1	7	3	0	0	0	0	4	0	0	0	0	0	0	0	0	NOS
AST	1	3	2	11	1	0	3	2	1	4	1	5	0	0	13	1	8	2	3	8	1	2	0	0	9	13	66	1	0	0	1	AST
NOA	3	0	6	0	4	1	8	2	2	1	4	12	1	0	118	1	49	5	0	27	5	4	2	0	72	0	0	0	0	0	1	NOA
EXC	2	3	9	9	4	0	10	15	4	1	9	30	4	3	55	10	52	11	5	11	6	11	4	1	30	10	76	5	0	3	3	EXC
EU	3	0	28	0	6	-2	28	9	10	1	24	76	7	2	199	11	178	19	0	26	16	26	12	1	94	0	1	6	1	3	3	EU
	AL	AM	AT	AZ	BA	BE	BG	BY	CH	CY	CZ	DE	DK	EE	ES	FI	FR	GB	GE	GR	HR	HU	IE	IS	IT	KG	KZ	LT	LU	LV	MD	

Table C.4 Cont.: 2017 country-to-country blame matrices for $\mathbf{AOT40}_f^{\mathbf{uc}}$.
Units: ppb.h per 15% emis. red. of NO_x. **Emitters →, Receptors ↓.**

	ME	MK	MT	NL	NO	PL	PT	RO	RS	RU	SE	SI	SK	TJ	TM	TR	UA	UZ	ATL	BAS	BLS	MED	NOS	AST	NOA	BIC	DMS	VOL	EXC	EU	
AL	85	113	1	1	6	68	6	84	298	45	5	7	21	0	0	10	47	0	23	8	6	259	12	1	67	274	0	0	2297	1093	AL
AM	1	1	0	0	3	20	2	17	4	148	3	0	2	0	20	309	41	8	6	4	26	26	3	1004	32	249	0	0	1669	134	AM
AT	0	0	0	-5	9	38	11	11	6	15	7	56	7	0	0	1	6	0	45	10	0	46	19	0	22	230	0	0	1688	1554	AT
AZ	0	1	0	0	5	24	2	19	3	378	5	1	2	0	40	101	62	17	7	6	24	13	4	537	17	200	0	0	1531	135	AZ
BA	34	3	0	1	10	104	9	42	90	32	9	27	39	0	0	2	25	0	29	12	1	118	16	0	52	250	0	0	1988	1385	BA
BE	0	0	0	-96	13	7	7	1	0	10	7	0	0	0	0	0	2	0	65	6	0	7	-72	0	6	181	0	0	-1	-35	BE
BG	8	17	0	2	9	93	4	325	142	144	9	6	23	0	1	45	172	0	19	14	49	40	14	5	33	234	0	0	2162	1522	BG
BY	1	1	0	4	22	172	2	22	6	224	29	1	10	0	0	3	87	0	28	52	3	5	28	1	3	162	0	0	1085	564	BY
CH	0	0	0	-13	8	10	14	1	1	8	5	6	1	0	0	0	2	0	54	5	0	54	17	0	32	251	0	0	1541	1161	CH
CY	3	7	0	1	3	26	5	50	24	79	3	2	6	0	1	789	50	0	11	4	36	746	5	81	94	296	0	0	1869	876	CY
CZ	0	0	0	-6	14	69	7	19	15	23	13	15	39	0	0	1	10	0	50	17	0	16	27	0	10	225	0	0	1433	1339	CZ
DE	0	0	0	-35	15	24	7	3	1	15	9	2	3	0	0	0	3	0	60	8	0	9	4	0	7	203	0	0	644	580	DE
DK	0	0	0	-18	43	41	1	2	0	37	26	0	1	0	0	0	5	0	72	-7	0	0	52	0	0	194	0	0	366	270	DK
EE	0	0	0	3	24	57	0	2	1	81	59	0	2	0	0	0	7	0	27	95	0	1	31	0	0	109	0	0	528	395	EE
ES	0	0	0	0	3	5	170	1	1	5	2	1	1	0	0	0	1	0	139	2	0	161	8	0	146	401	0	0	1595	1578	ES
FI	0	0	0	1	12	15	0	0	0	43	26	0	1	0	0	0	1	0	13	32	0	0	11	0	0	50	0	0	198	138	FI
FR	0	0	0	-10	10	6	17	1	1	8	5	2	1	0	0	0	1	0	97	5	0	66	16	0	27	231	0	0	1090	1052	FR
GB	0	0	0	-16	20	7	2	0	0	11	12	0	0	0	0	0	1	0	67	11	0	1	-7	0	1	145	0	0	8	-29	GB
GE	1	1	0	1	4	36	3	34	6	299	4	1	4	0	21	233	82	9	7	6	105	18	5	287	20	217	0	0	1710	191	GE
GL	0	0	0	0	1	0	0	0	0	1	0	0	0	0	0	0	0	0	1	0	0	0	0	0	0	20	0	0	4	2	GL
GR	13	57	1	2	7	64	5	129	114	114	6	5	14	0	0	105	122	0	20	10	37	288	11	4	69	271	0	0	2260	1593	GR
HR	8	1	0	1	10	107	8	32	54	29	10	65	37	0	0	1	21	0	34	14	1	175	19	0	36	226	0	0	2086	1826	HR
HU	3	2	0	3	12	196	7	138	101	40	12	28	114	0	0	2	41	0	34	21	1	41	25	1	22	225	0	0	1998	1728	HU
IE	0	0	0	-3	11	4	2	0	0	8	7	0	0	0	0	0	1	0	61	7	0	1	9	0	1	126	0	0	147	122	IE
IS	0	0	0	-0	15	3	0	0	0	3	5	0	0	0	0	0	0	0	29	4	0	0	15	0	0	63	0	0	80	54	IS
IT	4	2	1	1	8	46	10	16	17	19	6	31	11	0	0	3	12	0	42	7	1	349	17	0	84	247	0	0	1839	1709	IT
KG	1	1	0	0	2	8	3	7	3	111	2	1	1	47	53	34	16	481	5	3	3	9	2	610	21	328	0	0	1728	100	KG
KZ	0	1	0	1	10	20	2	9	3	660	9	1	2	1	12	17	43	24	14	13	4	6	8	97	8	272	0	0	1277	146	KZ
LT	0	0	0	5	33	152	1	9	3	116	50	1	7	0	0	0	26	0	37	88	0	2	47	0	1	160	0	0	867	614	LT
LU	0	0	0	-30	10	5	8	1	0	9	5	0	0	0	0	0	2	0	57	4	0	9	0	0	8	185	0	0	389	356	LU
LV	0	0	0	4	27	88	1	5	2	103	53	0	4	0	0	0	15	0	31	94	0	1	38	0	1	132	0	0	686	491	LV
MD	2	2	0	3	15	206	3	250	21	230	15	3	23	0	0	34	355	0	22	24	43	14	19	3	12	229	0	0	1764	874	MD
ME	407	10	0	1	8	88	8	78	191	38	7	12	34	0	0	6	35	0	25	9	3	176	13	1	68	281	0	0	2055	1105	ME
MK	24	320	0	2	6	82	7	115	359	61	6	8	23	0	0	26	65	0	21	9	10	90	12	2	64	278	0	0	2297	1227	MK
MT	8	6	-673	1	6	31	7	15	25	22	4	6	8	0	0	14	13	0	41	5	4	339	15	0	123	219	0	0	446	309	MT
NL	0	0	0	-538	18	9	5	1	0	13	10	0	1	0	0	0	2	0	63	6	0	3	-137	0	3	166	0	0	-399	-439	NL
NO	0	0	0	1	62	6	0	0	0	17	21	0	0	0	0	0	1	0	33	14	0	0	34	0	0	95	0	0	202	118	NO
PL	1	0	0	1	23	238	3	28	15	58	26	4	32	0	0	1	32	0	43	49	0	7	42	0	5	193	0	0	1085	914	PL
PT	0	0	0	0	3	2	739	1	0	4	1	0	0	0	0	0	1	0	254	1	0	54	6	0	82	389	0	0	1436	1425	PT
RO	5	6	0	3	11	161	4	689	70	128	10	6	36	0	0	18	173	0	21	18	23	23	16	3	23	221	0	0	1999	1493	RO
RS	37	21	0	2	9	124	7	187	369	51	8	15	45	0	0	6	58	0	25	13	4	57	16	1	46	246	0	0	1985	1290	RS
RU	0	0	0	1	6	16	1	5	1	404	7	0	1	0	2	5	31	1	8	11	4	2	5	10	2	90	0	0	599	89	RU
SE	0	0	0	1	36	20	0	1	0	28	48	0	1	0	0	0	2	0	31	35	0	0	32	0	0	99	0	0	271	199	SE
SI	1	0	0	-1	9	66	6	21	11	22	8	261	16	0	0	1	12	0	37	11	1	131	18	0	27	197	0	0	1989	1887	SI
SK	2	1	0	2	14	237	5	91	56	38	14	17	217	0	0	2	35	0	35	27	1	27	29	0	13	223	0	0	1817	1621	SK
TJ	0	0	0	0	1	6	2	5	2	75	1	0	1	237	179	32	11	304	4	2	2	7	1	676	19	350	0	0	1092	83	TJ
TM	1	1	0	1	5	17	2	10	3	346	5	1	2	4	136	36	46	113	8	7	7	9	4	404	15	291	0	0	1036	130	TM
TR	2	4	0	1	4	41	4	65	18	185	4	2	7	0	3	869	94	1	10	7	78	112	6	314	57	331	0	0	1669	393	TR
UA	1	1	0	2	17	194	3	93	14	416	18	3	18	0	2	16	339	1	23	33	29	10	21	5	9	223	0	0	1585	650	UA
UZ	0	1	0	1	6	15	2	8	3	355	5	1	2	23	68	28	39	242	9	7	4	8	5	246	13	279	0	0	1159	119	UZ
ATL	0	0	0	-0	0	0	1	0	0	0	0	0	0	0	0	0	0	0	3	0	0	0	0	0	1	3	0	0	6	5	ATL
BAS	0	0	0	-2	13	23	0	1	0	23	23	0	1	0	0	0	2	0	17	3	0	0	18	0	0	53	0	0	185	142	BAS
BLS	0	0	0	0	2	19	0	21	2	104	3	0	2	0	1	20	63	0	3	4	53	2	3	3	2	34	0	0	306	86	BLS
MED	2	2	-0	0	1	10	2	12	8	16	1	2	2	0	0	29	15	0	9	2	7	118	3	-3	20	48	0	0	303	218	MED
NOS	0	0	0	-7	5	2	0	0	0	3	3	0	0	0	0	0	0	0	15	2	0	0	-13	0	0	26	0	0	26	17	NOS
AST	0	1	0	0	1	6	2	5	2	76	1	0	1	5	44	80	12	36	3	2	3	27	1	1355	20	322	0	0	436	78	AST
NOA	2	2	1	0	1	8	24	8	8	9	1	1	2	0	0	19	8	0	57	1	2	180	3	-1	683	270	0	0	420	359	NOA
EXC	1	2	0	-2	10	35	11	26	10	311	10	2	5	3	10	48	44	21	23	14	8	26	10	65	15	177	0	0	943	352	EXC
EU	1	3	0	-10	15	55	40	59	18	37	16	8	13	0	0	8	24	0	62	19	4	71	16	1	35	211	0	0	1074	935	EU
	ME	MK	MT	NL	NO	PL	PT	RO	RS	RU	SE	SI	SK	TJ	TM	TR	UA	UZ	ATL	BAS	BLS	MED	NOS	AST	NOA	BIC	DMS	VOL	EXC	EU	

Table C.5: 2017 country-to-country blame matrices for $\mathbf{AOT40}_f^{\mathbf{uc}}$.
Units: ppb.h per 15% emis. red. of VOC. **Emitters →, Receptors ↓.**

	AL	AM	AT	AZ	BA	BE	BG	BY	CH	CY	CZ	DE	DK	EE	ES	FI	FR	GB	GE	GR	HR	HU	IE	IS	IT	KG	KZ	LT	LU	LV	MD	
AL	70	0	8	0	5	4	4	4	5	0	15	64	3	0	13	1	29	26	0	14	8	9	2	0	103	0	0	1	0	1	1	AL
AM	0	115	1	31	0	1	1	2	1	1	3	13	1	0	4	1	6	7	15	3	1	2	0	0	10	0	1	0	0	0	1	AM
AT	0	0	61	0	0	11	0	1	30	0	24	167	2	0	14	1	66	49	0	0	4	5	3	0	98	0	0	1	1	1	0	AT
AZ	0	9	1	65	0	1	1	4	1	0	4	16	1	0	3	1	6	9	14	2	1	2	1	0	8	0	3	1	0	1	1	AZ
BA	2	0	12	0	15	6	1	3	7	0	20	87	3	0	13	1	34	35	0	1	11	9	2	0	103	0	0	1	1	1	0	BA
BE	0	0	1	0	0	69	0	2	2	0	2	94	2	0	8	1	70	101	0	0	0	0	5	0	5	0	0	0	3	0	0	BE
BG	2	0	7	1	2	5	28	5	3	0	16	66	3	0	7	1	22	26	0	17	4	11	2	0	29	0	0	1	1	1	3	BG
BY	0	0	1	0	0	3	0	17	1	0	6	38	3	0	2	2	12	24	0	1	1	2	2	0	5	0	0	2	0	1	1	BY
CH	0	0	6	0	0	9	0	1	150	0	4	108	1	0	19	1	109	38	0	0	2	1	2	0	159	0	0	0	1	0	0	CH
CY	3	0	5	1	2	3	8	5	3	37	10	40	2	0	11	1	22	18	1	33	3	8	1	0	52	0	0	1	0	1	3	CY
CZ	0	0	18	0	1	14	0	3	9	0	87	176	4	0	9	1	52	68	0	0	3	8	4	0	24	0	0	1	2	1	1	CZ
DE	0	0	7	0	0	20	0	2	14	0	12	249	4	0	8	1	65	85	0	0	0	2	5	0	13	0	0	0	2	0	0	DE
DK	0	0	1	0	0	7	0	1	0	0	4	74	25	0	1	1	16	97	0	0	0	1	5	0	1	0	0	1	0	1	0	DK
EE	0	0	0	0	0	3	0	2	0	0	3	23	3	2	1	4	7	27	0	0	0	1	1	0	1	0	0	1	0	2	0	EE
ES	0	0	1	0	0	2	0	0	1	0	2	13	0	0	151	0	27	15	0	0	1	1	1	0	19	0	0	0	0	0	0	ES
FI	0	0	0	0	0	1	0	0	0	0	1	7	1	0	0	3	2	10	0	0	0	0	1	0	0	0	0	0	0	0	0	FI
FR	0	0	1	0	0	9	0	1	6	0	2	44	1	0	30	1	106	50	0	0	1	1	3	0	30	0	0	0	1	0	0	FR
GB	0	0	0	0	0	7	0	1	0	0	1	26	2	0	3	0	17	122	0	0	0	0	6	0	1	0	0	0	0	0	0	GB
GE	0	12	1	28	0	1	2	3	1	0	4	18	1	0	3	1	7	10	47	3	1	3	1	0	9	0	1	1	0	1	1	GE
GL	0	0	0	0	0	0	0	0	0	-0	0	0	0	0	0	0	0	0	0	0	0	0	0	0	0	0	0	0	0	0	0	GL
GR	10	0	7	0	3	4	12	5	4	0	15	63	3	0	11	1	28	25	0	122	5	10	2	0	66	0	0	1	1	1	3	GR
HR	1	0	18	0	6	8	1	3	9	0	23	112	4	0	16	1	46	44	0	1	30	11	3	0	175	0	0	1	1	1	0	HR
HU	1	0	20	0	2	9	2	4	7	0	30	121	4	0	9	1	40	49	0	1	9	41	3	0	57	0	0	1	1	1	1	HU
IE	0	0	0	0	0	3	0	0	0	0	0	8	1	0	1	0	9	41	0	0	0	0	11	0	0	0	0	0	0	0	0	IE
IS	0	0	0	0	0	0	0	0	0	0	0	5	1	0	0	0	1	12	0	0	0	0	1	0	0	0	0	0	0	0	0	IS
IT	1	0	12	0	2	7	1	2	14	0	15	89	3	0	28	1	74	41	0	2	9	5	2	0	568	0	0	1	1	1	1	IT
KG	0	1	1	2	0	1	0	2	1	0	2	9	1	0	3	1	5	5	1	1	0	1	0	0	7	98	20	0	0	0	0	KG
KZ	0	0	1	1	0	1	0	3	1	0	2	14	1	0	2	1	6	11	1	1	0	1	1	0	6	5	13	1	0	1	0	KZ
LT	0	0	1	0	0	4	0	7	1	0	5	38	5	1	2	2	13	33	0	0	0	2	3	0	3	0	0	6	0	2	0	LT
LU	0	0	1	0	0	33	0	1	4	0	3	132	2	0	9	1	81	68	0	0	0	0	4	0	9	0	0	0	23	0	0	LU
LV	0	0	1	0	0	3	0	4	1	0	3	29	4	1	1	2	9	29	0	0	0	1	2	0	2	0	0	3	0	5	0	LV
MD	0	0	4	0	1	4	3	6	2	0	13	54	3	0	4	2	15	26	1	3	2	8	2	0	12	0	0	1	0	1	13	MD
ME	11	0	7	0	8	5	2	3	5	0	15	67	3	0	12	1	28	28	0	5	8	9	2	0	87	0	0	1	1	1	1	ME
MK	12	0	7	0	3	4	7	4	4	0	15	63	3	0	10	1	25	24	0	33	5	10	2	0	50	0	0	1	1	0	2	MK
MT	3	0	8	0	4	6	2	3	5	0	16	70	2	0	28	1	58	38	0	12	7	7	3	0	204	0	0	1	1	1	1	MT
NL	0	0	1	0	0	33	0	1	1	0	3	103	2	0	4	1	45	122	0	0	0	0	6	0	3	0	0	0	1	0	0	NL
NO	0	0	0	0	0	1	0	0	0	0	1	8	2	0	0	0	3	18	0	0	0	0	1	0	0	0	0	0	0	0	0	NO
PL	0	0	4	0	1	9	0	5	3	0	21	106	6	0	4	2	29	53	0	0	2	7	3	0	10	0	0	1	1	1	1	PL
PT	0	0	0	0	0	1	0	0	0	0	1	7	0	0	70	0	16	9	0	0	0	0	1	0	6	0	0	0	0	0	0	PT
RO	1	0	7	0	2	5	6	5	3	0	16	68	3	0	6	1	20	28	0	4	3	13	2	0	26	0	0	1	1	1	3	RO
RS	5	0	12	0	6	6	4	4	5	0	23	89	4	0	10	1	30	34	0	6	8	18	2	0	53	0	0	1	1	1	1	RS
RU	0	0	0	1	0	1	0	2	0	0	1	7	1	0	1	1	3	6	0	0	0	0	0	0	2	0	1	0	0	0	0	RU
SE	0	0	0	0	0	2	0	1	0	0	1	14	4	0	0	1	4	23	0	0	0	0	1	0	0	0	0	0	0	0	0	SE
SI	0	0	35	0	1	9	0	2	14	0	21	130	3	0	14	1	55	47	0	0	22	8	3	0	267	0	0	1	1	1	0	SI
SK	0	0	12	0	2	9	1	3	6	0	37	110	4	0	7	1	35	49	0	1	5	24	3	0	34	0	0	1	1	1	1	SK
TJ	0	1	1	2	0	1	0	1	1	0	1	8	0	0	3	0	4	4	1	1	0	1	0	0	6	15	7	0	0	0	0	TJ
TM	0	2	1	5	0	1	1	3	1	0	3	14	1	0	4	1	6	10	2	1	1	1	1	0	9	2	5	1	0	1	1	TM
TR	1	4	3	3	1	2	4	4	2	1	7	31	1	0	6	1	13	12	3	10	1	5	1	0	21	0	0	1	0	1	2	TR
UA	0	0	3	1	0	3	1	8	2	0	10	46	3	1	4	2	14	26	1	1	1	5	2	0	9	0	1	1	0	1	2	UA
UZ	0	1	1	3	0	1	1	3	1	0	2	12	1	0	3	1	6	9	1	1	0	1	1	0	7	18	9	1	0	1	1	UZ
ATL	0	0	0	0	0	0	0	0	0	0	0	0	0	0	0	0	0	1	0	0	0	0	0	0	0	0	0	0	0	0	0	ATL
BAS	0	0	0	0	0	2	0	1	0	0	1	18	5	0	0	1	4	21	0	0	0	0	1	0	0	0	0	1	0	1	0	BAS
BLS	0	0	0	1	0	1	1	1	0	0	2	7	1	0	1	0	2	4	1	1	0	1	0	0	2	0	0	0	0	0	1	BLS
MED	1	0	1	0	1	1	1	1	1	0	3	13	1	0	7	0	10	7	0	11	1	1	0	0	30	0	0	0	0	0	0	MED
NOS	0	0	0	0	0	1	0	0	0	0	0	6	1	0	0	0	4	16	0	0	0	0	1	0	0	0	0	0	0	0	0	NOS
AST	0	1	1	3	0	1	1	1	1	1	2	8	0	0	3	0	4	4	1	2	0	1	0	0	7	3	4	0	0	0	0	AST
NOA	1	0	2	0	1	1	1	1	1	0	3	16	1	0	20	0	16	10	0	5	1	2	1	0	31	0	0	0	0	0	0	NOA
EXC	0	1	2	1	0	3	1	3	2	0	4	27	1	0	8	1	13	17	1	2	1	2	1	0	18	2	3	1	0	0	1	EXC
EU	1	0	5	0	1	7	2	2	5	0	10	68	3	0	28	1	39	44	0	5	2	4	3	0	59	0	0	1	1	1	1	EU
	AL	AM	AT	AZ	BA	BE	BG	BY	CH	CY	CZ	DE	DK	EE	ES	FI	FR	GB	GE	GR	HR	HU	IE	IS	IT	KG	KZ	LT	LU	LV	MD	

Table C.5 Cont.: 2017 country-to-country blame matrices for $\mathbf{AOT40}_f^{\mathbf{uc}}$.
Units: ppb.h per 15% emis. red. of VOC. **Emitters →, Receptors ↓.**

	ME	MK	MT	NL	NO	PL	PT	RO	RS	RU	SE	SI	SK	TJ	TM	TR	UA	UZ	ATL	BAS	BLS	MED	NOS	AST	NOA	BIC	DMS	VOL	EXC	EU	
AL	7	9	0	9	3	30	2	11	36	19	2	2	5	0	0	3	13	0	0	0	0	1	0	1	18	265	0	0	543	367	AL
AM	0	0	0	2	1	12	1	4	2	51	1	0	1	0	1	30	13	1	0	0	0	0	0	408	7	200	0	0	341	76	AM
AT	0	0	0	19	3	24	2	2	2	7	2	9	4	0	0	0	3	0	0	0	0	0	1	0	6	211	0	0	618	570	AT
AZ	0	0	0	3	2	16	1	5	2	103	2	0	2	0	2	17	20	1	0	0	0	0	0	250	5	250	0	0	332	88	AZ
BA	1	0	0	13	3	39	2	6	12	12	3	4	6	0	0	1	7	0	0	0	0	0	0	0	13	224	0	0	477	413	BA
BE	0	0	0	54	3	8	2	0	0	5	2	0	0	0	0	0	1	0	0	0	0	0	2	0	2	188	0	0	441	428	BE
BG	0	2	0	9	3	34	1	27	21	44	3	2	6	0	0	25	31	0	0	0	0	0	0	5	8	239	0	0	470	327	BG
BY	0	0	0	8	3	33	0	3	1	50	3	0	2	0	0	1	12	0	0	0	0	0	0	0	1	112	0	0	243	156	BY
CH	0	0	0	17	3	9	2	0	0	4	1	2	1	0	0	0	1	0	0	0	0	0	0	0	8	188	0	0	654	494	CH
CY	1	2	0	5	2	25	2	16	10	52	2	1	5	0	0	216	25	0	0	0	0	2	0	79	24	421	0	0	637	311	CY
CZ	0	0	0	25	4	65	2	4	3	11	3	3	8	0	0	0	5	0	0	0	0	0	1	0	3	228	0	0	618	582	CZ
DE	0	0	0	41	3	20	2	1	0	7	2	0	1	0	0	0	2	0	0	0	0	0	1	0	2	213	0	0	571	542	DE
DK	0	0	0	26	7	25	0	1	0	10	5	0	1	0	0	0	2	0	0	1	0	0	2	0	0	161	0	0	314	293	DK
EE	0	0	0	7	2	18	0	0	0	22	4	0	1	0	0	0	2	0	0	0	0	0	0	0	0	67	0	0	139	110	EE
ES	0	0	0	3	1	4	19	0	0	2	0	0	0	0	0	0	1	0	0	0	0	1	0	0	36	201	0	0	267	261	ES
FI	0	0	0	2	1	6	0	0	0	9	2	0	0	0	0	0	0	0	0	0	0	0	0	0	0	21	0	0	49	38	FI
FR	0	0	0	12	3	6	3	0	0	4	1	1	0	0	0	0	1	0	0	0	0	0	1	0	8	162	0	0	319	305	FR
GB	0	0	0	15	3	5	1	0	0	4	1	0	0	0	0	0	1	0	0	0	0	0	1	0	0	93	0	0	215	207	GB
GE	0	0	0	3	2	19	1	7	2	91	2	0	2	0	1	23	22	1	0	0	0	0	0	146	5	205	0	0	337	100	GE
GL	0	0	0	0	0	0	0	0	0	0	0	0	0	0	0	0	0	0	0	0	0	0	0	0	0	-5	0	0	1	1	GL
GR	1	8	0	9	3	34	2	17	22	41	3	2	6	0	0	36	27	0	0	0	0	1	0	3	17	314	0	0	613	448	GR
HR	1	0	0	17	4	43	2	6	10	13	3	10	6	0	0	1	7	0	0	0	0	1	0	0	12	269	0	0	636	581	HR
HU	0	0	0	17	4	71	2	17	18	16	3	5	17	0	0	1	12	0	0	0	0	0	1	1	6	248	0	0	597	530	HU
IE	0	0	0	5	1	2	0	0	0	2	1	0	0	0	0	0	0	0	0	0	0	0	0	0	0	46	0	0	90	86	IE
IS	0	0	0	1	2	2	0	0	0	0	0	0	0	0	0	0	0	0	0	0	0	0	0	0	0	8	0	0	27	25	IS
IT	0	1	0	13	4	29	3	5	5	12	3	9	3	0	0	1	6	0	0	0	0	2	0	0	27	323	0	0	975	925	IT
KG	0	0	0	2	1	6	1	2	1	36	1	0	1	5	2	6	6	90	0	0	0	0	0	208	4	163	0	0	321	49	KG
KZ	0	0	0	3	2	10	0	2	1	96	2	0	1	0	1	4	11	4	0	0	0	0	0	49	2	170	0	0	212	68	KZ
LT	0	0	0	10	3	37	0	1	1	27	4	0	1	0	0	0	5	0	0	0	0	0	0	0	1	105	0	0	220	175	LT
LU	0	0	0	23	3	7	2	0	0	5	2	0	0	0	0	0	1	0	0	0	0	0	1	0	2	171	0	0	415	401	LU
LV	0	0	0	8	3	24	0	1	1	24	4	0	1	0	0	0	3	0	0	0	0	0	0	0	0	80	0	0	171	135	LV
MD	0	0	0	8	3	54	1	25	4	59	3	1	5	0	0	10	47	0	0	0	0	0	0	2	4	204	0	0	402	254	MD
ME	22	2	0	10	3	34	2	9	19	15	2	2	6	0	0	2	10	0	0	0	0	0	0	0	16	223	0	0	447	346	ME
MK	1	47	0	8	3	30	2	12	42	21	2	2	5	0	0	10	14	0	0	0	0	0	0	1	14	222	0	0	485	320	MK
MT	1	2	59	10	4	28	3	6	8	17	2	3	5	0	0	7	9	0	0	0	0	6	0	0	44	368	0	0	644	579	MT
NL	0	0	0	116	4	9	2	0	0	5	2	0	0	0	0	0	1	0	0	0	0	0	2	0	1	190	0	0	467	454	NL
NO	0	0	0	3	10	3	0	0	0	3	1	0	0	0	0	0	0	0	0	0	0	0	0	0	0	23	0	0	56	43	NO
PL	0	0	0	20	4	138	1	5	3	18	4	1	6	0	0	0	11	0	0	0	0	0	1	0	2	192	0	0	482	435	PL
PT	0	0	0	2	1	2	127	0	0	1	0	0	0	0	0	0	0	0	1	0	0	0	0	0	17	178	0	0	250	246	PT
RO	0	1	0	10	3	46	1	59	13	36	3	2	7	0	0	7	31	0	0	0	0	0	0	3	6	215	0	0	444	337	RO
RS	2	5	0	12	3	47	2	18	71	18	3	3	9	0	0	2	14	0	0	0	0	0	0	1	10	237	0	0	530	394	RS
RU	0	0	0	1	1	6	0	1	0	64	1	0	0	0	0	1	6	0	0	0	0	0	0	5	1	56	0	0	111	34	RU
SE	0	0	0	5	3	8	0	0	0	5	4	0	0	0	0	0	1	0	0	0	0	0	0	0	0	38	0	0	79	69	SE
SI	0	0	0	18	4	31	2	4	3	11	3	61	4	0	0	0	5	0	0	0	0	1	1	0	9	264	0	0	782	741	SI
SK	0	0	0	17	4	99	1	12	10	14	3	3	32	0	0	1	10	0	0	0	0	0	1	1	4	218	0	0	554	503	SK
TJ	0	0	0	1	1	5	1	1	1	29	1	0	1	13	4	6	5	41	0	0	0	0	0	215	4	145	0	0	169	41	TJ
TM	0	0	0	3	2	11	1	3	1	86	2	0	1	1	9	10	15	8	0	0	0	0	0	226	5	255	0	0	229	76	TM
TR	0	1	0	4	2	22	1	10	5	58	2	1	3	0	0	149	22	0	0	0	0	1	0	135	12	233	0	0	423	166	TR
UA	0	0	0	8	3	46	1	11	3	92	3	1	4	0	0	4	59	0	0	0	0	0	0	3	3	190	0	0	382	205	UA
UZ	0	0	0	2	2	9	1	2	1	77	2	0	1	3	4	7	12	53	0	0	0	0	0	136	4	221	0	0	260	66	UZ
ATL	0	0	0	0	0	0	0	0	0	0	0	0	0	0	0	0	0	0	0	0	0	0	0	0	0	2	0	0	3	2	ATL
BAS	0	0	0	6	2	12	0	0	0	8	4	0	0	0	0	0	1	0	0	0	0	0	0	0	0	46	0	0	90	78	BAS
BLS	0	0	0	1	1	7	0	3	1	30	1	0	1	0	0	11	13	0	0	0	0	0	0	3	1	49	0	0	97	37	BLS
MED	0	0	0	2	1	6	1	2	2	7	1	1	1	0	0	15	4	0	0	0	0	1	0	4	14	76	0	0	137	103	MED
NOS	0	0	0	4	2	1	0	0	0	1	0	0	0	0	0	0	0	0	0	0	0	0	0	0	0	19	0	0	40	36	NOS
AST	0	0	0	1	1	5	1	2	1	26	1	0	1	0	2	19	6	4	0	0	0	0	0	735	6	191	0	0	119	46	AST
NOA	0	0	0	2	1	7	6	2	3	6	1	1	1	0	0	6	3	0	0	0	0	1	0	3	118	180	0	0	155	132	NOA
EXC	0	0	0	5	2	14	2	3	2	54	2	1	1	0	1	9	10	3	0	0	0	0	0	31	4	125	0	0	226	132	EXC
EU	0	0	0	14	3	27	6	6	3	11	2	2	3	0	0	3	6	0	0	0	0	0	0	1	9	169	0	0	377	341	EU
	ME	MK	MT	NL	NO	PL	PT	RO	RS	RU	SE	SI	SK	TJ	TM	TR	UA	UZ	ATL	BAS	BLS	MED	NOS	AST	NOA	BIC	DMS	VOL	EXC	EU	

Table C.6: 2017 country-to-country blame matrices for **SOMO35**.
Units: ppb.d per 15% emis. red. of NO_x. **Emitters →, Receptors ↓.**

	AL	AM	AT	AZ	BA	BE	BG	BY	CH	CY	CZ	DE	DK	EE	ES	FI	FR	GB	GE	GR	HR	HU	IE	IS	IT	KG	KZ	LT	LU	LV	MD	
AL	43	0	3	0	5	-0	5	1	1	0	2	4	0	0	7	0	7	0	0	15	5	5	0	0	24	0	0	0	0	0	0	AL
AM	0	19	0	34	0	0	1	0	0	0	0	1	0	0	1	0	1	0	10	1	0	0	0	0	1	0	2	0	0	0	0	AM
AT	0	0	17	0	0	-0	0	0	6	0	6	25	0	0	7	0	22	0	0	0	2	2	1	0	18	0	0	0	0	0	0	AT
AZ	0	4	0	52	0	0	1	1	0	0	0	1	0	0	1	0	1	0	8	1	0	0	0	0	1	0	7	0	0	0	0	AZ
BA	1	0	8	0	30	0	2	1	1	0	5	10	0	0	8	0	10	1	0	3	17	10	1	0	26	0	0	0	0	0	0	BA
BE	0	0	0	0	0	-51	0	0	0	0	0	-4	0	0	5	0	18	-4	0	0	0	0	2	0	1	0	0	0	0	0	0	BE
BG	1	0	3	0	2	0	43	2	0	0	2	5	0	0	3	1	4	1	0	12	2	5	0	0	5	0	1	0	0	0	2	BG
BY	0	0	0	0	0	0	1	11	0	0	1	4	1	1	1	2	2	2	0	0	0	1	1	0	1	0	1	3	0	2	0	BY
CH	0	0	2	0	0	-0	0	0	16	0	0	1	0	0	11	0	47	-0	0	0	1	0	1	0	24	0	0	0	0	0	0	CH
CY	1	0	1	0	1	0	3	1	0	32	1	2	0	0	3	0	3	0	0	19	1	1	0	0	7	0	0	0	0	0	0	CY
CZ	0	0	9	0	0	-0	0	0	1	0	10	26	1	0	4	1	15	2	0	0	1	3	1	0	4	0	0	0	0	0	0	CZ
DE	0	0	1	0	0	-1	0	0	1	0	2	-9	0	0	4	1	19	1	0	0	0	0	1	0	2	0	0	0	0	0	0	DE
DK	0	0	0	0	0	-0	0	0	0	0	1	2	-16	0	1	1	3	6	0	0	0	0	2	0	0	0	0	1	0	0	0	DK
EE	0	0	0	0	0	-0	0	2	0	0	1	2	1	-0	0	5	1	3	0	0	0	0	1	0	0	0	0	2	0	2	0	EE
ES	0	0	0	0	0	-0	0	0	0	0	0	1	0	0	105	0	10	1	0	0	0	0	1	0	3	0	0	0	0	0	0	ES
FI	0	0	0	0	0	-0	0	0	0	0	0	1	1	1	0	3	0	1	0	0	0	0	0	0	0	0	0	1	0	1	0	FI
FR	0	0	1	0	0	-1	0	0	1	0	0	1	0	0	18	0	53	-0	0	0	0	0	1	0	5	0	0	0	0	0	0	FR
GB	0	0	0	0	0	-1	0	0	0	0	0	-1	0	0	2	0	3	-34	0	0	0	0	3	0	0	0	0	0	0	0	0	GB
GE	0	6	0	25	0	0	1	1	0	0	0	1	0	0	2	0	1	0	42	2	0	1	0	0	1	0	3	0	0	0	1	GE
GL	0	0	0	0	0	-0	0	0	0	0	0	-0	0	0	0	0	0	0	0	0	0	0	0	0	0	0	0	0	-0	0	0	GL
GR	6	0	2	0	2	0	21	1	1	0	1	4	0	0	5	0	5	0	0	58	2	3	0	0	13	0	0	0	0	0	1	GR
HR	1	0	13	0	9	0	1	1	1	0	5	12	0	0	7	0	12	1	0	1	27	12	1	0	30	0	0	0	0	0	0	HR
HU	0	0	10	0	3	0	2	1	1	0	8	15	1	0	4	1	10	2	0	1	8	25	1	0	9	0	0	0	0	0	0	HU
IE	0	0	-0	0	0	-0	0	0	0	0	-0	-1	0	0	2	0	3	1	0	0	0	0	-9	0	0	0	0	0	0	0	0	IE
IS	0	0	0	0	0	-0	0	0	0	0	0	1	0	0	0	0	1	4	0	0	0	0	1	0	0	0	0	0	0	0	0	IS
IT	0	0	6	0	2	0	1	0	3	0	2	7	0	0	12	0	24	0	0	2	5	2	0	0	52	0	0	0	0	0	0	IT
KG	0	0	0	1	0	0	0	0	0	0	0	1	0	0	2	0	1	0	0	0	0	0	0	0	1	47	22	0	0	0	0	KG
KZ	0	0	0	1	0	0	0	1	0	0	0	1	0	0	1	1	1	1	0	0	0	0	0	0	1	1	32	0	0	0	0	KZ
LT	0	0	0	0	0	0	0	6	0	0	1	4	1	1	1	3	2	3	0	0	0	1	1	0	1	0	0	3	0	2	0	LT
LU	0	0	0	0	0	-5	0	0	1	0	0	1	0	0	6	0	30	-1	0	0	0	0	1	0	1	0	0	0	-40	0	0	LU
LV	0	0	0	0	0	0	0	3	0	0	1	3	1	1	1	4	2	3	0	0	0	0	1	0	0	0	0	4	0	1	0	LV
MD	0	0	1	0	0	0	3	4	0	0	2	5	1	0	2	1	3	1	1	1	1	4	0	0	2	0	1	1	0	0	11	MD
ME	6	0	4	0	13	-0	3	1	1	0	3	6	0	0	8	0	7	0	0	6	7	6	0	0	23	0	0	0	0	0	0	ME
MK	13	0	3	0	3	-0	14	1	1	0	2	5	0	0	6	0	6	0	0	26	2	5	0	0	12	0	0	0	0	0	1	MK
MT	1	0	2	0	2	0	2	0	1	0	1	3	0	0	11	0	20	0	0	5	2	2	1	0	41	0	0	0	0	0	0	MT
NL	0	0	0	0	0	-6	0	0	0	0	0	-8	0	0	2	1	7	-1	0	0	0	0	2	0	0	0	0	0	0	0	0	NL
NO	0	0	0	0	0	-0	0	0	0	0	0	0	1	0	0	2	1	3	0	0	0	0	1	0	0	0	0	0	0	0	0	NO
PL	0	0	1	0	0	0	0	2	0	0	4	12	2	0	2	1	6	3	0	0	1	3	1	0	2	0	0	1	0	0	0	PL
PT	0	0	0	0	0	-0	0	0	0	0	0	0	0	0	59	0	4	0	0	0	0	0	0	0	1	0	0	0	0	0	0	PT
RO	1	0	2	0	1	0	8	3	0	0	3	6	0	0	3	1	4	1	0	2	2	9	0	0	5	0	1	1	0	0	3	RO
RS	3	0	6	0	7	-0	7	1	1	0	4	9	0	0	5	0	7	1	0	4	5	12	0	0	12	0	0	0	0	0	1	RS
RU	0	0	0	1	0	-0	0	1	0	0	0	0	0	0	0	1	1	0	0	0	0	0	0	0	0	0	4	0	0	0	0	RU
SE	0	0	0	0	0	-0	0	0	0	0	0	1	1	0	0	3	1	3	0	0	0	0	1	0	0	0	0	0	0	0	0	SE
SI	0	0	23	0	1	-0	0	0	2	0	4	13	0	0	6	0	15	1	0	0	16	5	1	0	27	0	0	0	0	0	0	SI
SK	0	0	6	0	2	0	1	1	1	0	12	15	1	0	4	1	10	2	0	0	4	18	1	0	6	0	0	0	0	0	0	SK
TJ	0	0	0	1	0	0	0	0	0	0	0	1	0	0	2	0	1	0	0	0	0	0	0	0	1	5	7	0	0	0	0	TJ
TM	0	1	0	4	0	0	0	1	0	0	0	1	0	0	2	1	2	1	1	1	0	0	0	0	2	0	19	0	0	0	0	TM
TR	0	1	1	1	0	0	3	1	0	1	1	2	0	0	2	0	2	0	2	5	0	1	0	0	3	0	1	0	0	0	1	TR
UA	0	0	1	0	0	0	1	6	0	0	2	4	1	0	2	1	3	1	0	1	1	3	0	0	2	0	2	1	0	1	2	UA
UZ	0	1	0	2	0	0	0	1	0	0	0	1	0	0	2	1	1	1	1	0	0	0	0	0	1	2	24	0	0	0	0	UZ
ATL	0	0	0	0	0	-0	0	0	0	0	-0	-0	0	0	4	0	2	1	0	0	0	0	1	0	0	0	0	0	0	0	0	ATL
BAS	0	0	0	0	0	-1	0	1	0	0	1	2	1	1	1	5	2	5	0	0	0	0	2	0	0	0	0	2	0	2	0	BAS
BLS	0	1	1	2	0	-0	5	4	0	0	1	2	0	0	2	1	2	1	6	2	0	2	0	0	2	0	2	1	0	1	3	BLS
MED	1	0	3	0	2	0	5	1	1	1	2	4	0	0	14	0	19	0	0	16	3	2	0	0	31	0	0	0	0	0	0	MED
NOS	0	0	-0	0	0	-2	0	0	0	0	-0	-3	1	0	2	1	2	-2	0	0	0	0	4	1	0	0	0	0	0	0	0	NOS
AST	0	0	0	2	0	0	0	0	0	0	0	0	0	0	1	0	1	0	0	1	0	0	0	0	1	1	7	0	0	0	0	AST
NOA	1	0	1	0	1	0	1	0	0	0	0	1	0	0	16	0	6	0	0	5	1	1	0	0	11	0	0	0	0	0	0	NOA
EXC	0	0	1	1	0	-0	1	1	0	0	1	2	0	0	5	1	4	0	1	1	1	1	0	0	2	1	8	0	0	0	0	EXC
EU	0	0	2	0	1	-1	2	1	1	0	2	3	0	0	18	1	14	-1	0	2	1	2	1	0	7	0	0	0	0	0	0	EU
	AL	AM	AT	AZ	BA	BE	BG	BY	CH	CY	CZ	DE	DK	EE	ES	FI	FR	GB	GE	GR	HR	HU	IE	IS	IT	KG	KZ	LT	LU	LV	MD	

Table C.6 Cont.: 2017 country-to-country blame matrices for **SOMO35**.
Units: ppb.d per 15% emis. red. of NO_x. **Emitters →, Receptors ↓.**

	ME	MK	MT	NL	NO	PL	PT	RO	RS	RU	SE	SI	SK	TJ	TM	TR	UA	UZ	ATL	BAS	BLS	MED	NOS	AST	NOA	BIC	DMS	VOL	EXC	EU	
AL	8	10	0	-0	0	5	1	7	26	4	0	1	2	0	0	2	4	0	3	1	1	29	1	0	7	28	0	0	198	94	AL
AM	0	0	0	0	0	2	0	2	0	13	0	0	0	0	1	36	4	1	1	0	3	4	0	81	3	26	0	0	133	12	AM
AT	0	0	0	-1	1	3	1	1	0	1	1	5	1	0	0	0	0	0	4	1	0	5	1	0	3	23	0	0	123	112	AT
AZ	0	0	0	0	0	2	0	2	0	36	0	0	0	0	4	14	6	2	1	1	3	2	0	46	2	21	0	0	148	13	AZ
BA	3	0	0	-0	1	8	1	4	8	3	1	2	3	0	0	1	2	0	3	1	0	14	1	0	6	26	0	0	171	119	BA
BE	0	0	0	-12	1	0	1	0	0	1	1	0	0	0	0	0	0	0	7	0	0	1	-10	0	1	20	0	0	-38	-41	BE
BG	1	2	0	0	1	7	0	30	13	12	1	1	2	0	0	5	14	0	2	1	4	6	1	1	4	24	0	0	185	128	BG
BY	0	0	0	-0	2	12	0	2	1	21	2	0	1	0	0	0	8	0	3	4	0	1	2	0	1	16	0	0	87	42	BY
CH	0	0	0	-2	1	1	1	0	0	1	0	1	0	0	0	0	0	0	5	0	0	6	1	0	4	26	0	0	108	90	CH
CY	0	1	0	0	0	2	0	4	2	7	0	0	0	0	0	70	4	0	1	0	3	72	0	5	8	29	0	0	169	81	CY
CZ	0	0	0	-2	1	4	1	2	1	2	1	1	3	0	0	0	1	0	5	1	0	2	1	0	1	22	0	0	95	88	CZ
DE	0	0	0	-5	1	1	1	0	0	1	1	0	0	0	0	0	0	0	6	0	0	1	-2	0	1	21	0	0	26	21	DE
DK	0	0	0	-3	4	3	0	0	0	4	3	0	0	0	0	0	1	0	7	-3	0	0	1	0	0	20	0	0	14	4	DK
EE	0	0	0	-0	3	4	0	0	0	9	6	0	0	0	0	0	1	0	3	7	0	0	3	0	0	13	0	0	45	30	EE
ES	0	0	0	-0	0	0	16	0	0	0	0	0	0	0	0	0	0	0	14	0	0	13	0	0	13	39	0	0	138	137	ES
FI	0	0	0	-0	2	1	0	0	0	8	4	0	0	0	0	0	0	0	3	3	0	0	1	0	0	10	0	0	25	14	FI
FR	0	0	0	-1	1	0	2	0	0	1	0	0	0	0	0	0	0	0	10	0	0	7	0	0	3	25	0	0	84	81	FR
GB	0	0	0	-2	2	0	1	0	0	1	1	0	0	0	0	0	0	0	8	1	0	0	-3	0	0	19	0	0	-23	-26	GB
GE	0	0	0	0	0	3	0	3	1	29	0	0	0	0	2	28	8	1	1	0	10	3	0	27	3	24	0	0	164	19	GE
GL	0	0	0	-0	0	0	0	0	0	1	0	0	0	0	0	0	0	0	0	0	0	0	0	0	0	6	0	0	2	1	GL
GR	1	5	0	-0	0	4	1	11	10	9	0	0	1	0	0	10	9	0	2	1	3	32	1	1	8	26	0	0	191	135	GR
HR	1	0	0	-0	1	8	1	3	5	3	1	5	3	0	0	0	2	0	4	1	0	18	1	0	4	23	0	0	168	145	HR
HU	0	0	0	-0	1	15	1	12	9	4	1	2	10	0	0	0	4	0	3	2	0	4	1	0	2	22	0	0	160	136	HU
IE	0	0	0	-1	1	-0	1	0	0	1	1	0	0	0	0	0	-0	0	10	0	0	0	0	0	0	19	0	0	-2	-3	IE
IS	0	0	0	-0	2	0	0	0	0	2	1	0	0	0	0	0	0	0	6	1	0	0	2	0	0	19	0	0	14	9	IS
IT	0	0	0	-0	1	3	1	1	2	2	0	2	1	0	0	1	1	0	4	0	0	33	1	0	9	25	0	0	134	123	IT
KG	0	0	0	0	0	1	0	1	0	9	0	0	0	5	5	4	1	39	1	0	0	1	0	72	2	32	0	0	143	9	KG
KZ	0	0	0	0	1	2	0	1	0	63	1	0	0	0	2	2	4	3	1	1	1	1	1	11	1	28	0	0	126	13	KZ
LT	0	0	0	-0	3	11	0	1	0	10	4	0	1	0	0	0	2	0	4	6	0	1	3	0	0	15	0	0	64	42	LT
LU	0	0	0	-6	1	0	1	0	0	1	0	0	0	0	0	0	0	0	6	0	0	1	-3	0	1	20	0	0	-7	-10	LU
LV	0	0	0	-0	3	7	0	0	0	10	5	0	0	0	0	0	1	0	3	7	0	0	3	0	0	14	0	0	54	36	LV
MD	0	0	0	-0	1	13	0	23	2	19	1	0	2	0	0	3	31	0	2	2	4	2	1	1	1	21	0	0	144	69	MD
ME	31	1	0	-0	1	6	1	7	18	3	0	1	2	0	0	2	3	0	3	1	0	21	1	0	8	29	0	0	172	91	ME
MK	2	27	0	-0	0	6	1	10	32	5	0	1	2	0	0	3	5	0	2	1	1	12	1	1	7	28	0	0	197	102	MK
MT	1	1	-87	-0	0	2	1	1	2	2	0	1	1	0	0	1	1	0	4	0	0	22	1	0	25	25	0	0	24	11	MT
NL	0	0	0	-71	2	0	1	0	0	1	1	0	0	0	0	0	0	0	6	1	0	0	-19	0	0	18	0	0	-68	-71	NL
NO	0	0	0	-0	6	0	0	0	0	5	4	0	0	0	0	0	0	0	5	2	0	0	3	0	0	17	0	0	25	13	NO
PL	0	0	0	-1	2	7	0	2	1	5	2	0	2	0	0	0	3	0	4	3	0	1	2	0	1	18	0	0	69	54	PL
PT	0	0	0	-0	0	0	68	0	0	0	0	0	0	0	0	0	0	0	28	0	0	5	0	0	8	41	0	0	135	134	PT
RO	0	1	0	-0	1	12	0	57	6	11	1	1	3	0	0	2	15	0	2	1	2	4	1	1	3	22	0	0	168	122	RO
RS	3	2	0	-0	1	9	1	16	28	5	1	1	3	0	0	1	5	0	3	1	0	7	1	0	5	25	0	0	163	105	RS
RU	0	0	0	-0	1	1	0	1	0	40	1	0	0	0	0	1	3	0	1	1	0	0	0	2	0	11	0	0	61	8	RU
SE	0	0	0	-0	5	2	0	0	0	5	4	0	0	0	0	0	0	0	4	3	0	0	3	0	0	14	0	0	29	18	SE
SI	0	0	0	-1	1	4	1	2	1	2	1	13	1	0	0	0	1	0	4	1	0	12	1	0	4	21	0	0	142	134	SI
SK	0	0	0	-0	1	15	0	8	5	4	1	2	10	0	0	0	3	0	4	2	0	3	2	0	2	22	0	0	135	117	SK
TJ	0	0	0	0	0	0	0	0	0	7	0	0	0	22	16	3	1	24	1	0	0	1	0	83	2	35	0	0	95	7	TJ
TM	0	0	0	0	1	2	0	1	0	40	1	0	0	1	20	6	5	14	1	1	1	2	0	55	2	36	0	0	129	15	TM
TR	0	0	0	0	0	3	0	5	2	14	0	0	1	0	0	76	8	0	1	0	6	13	0	27	5	32	0	0	141	32	TR
UA	0	0	0	-0	1	14	0	8	1	34	1	0	1	0	0	2	28	0	2	2	3	1	1	1	1	20	0	0	128	49	UA
UZ	0	0	0	0	1	2	0	1	0	43	1	0	0	2	8	4	5	22	1	1	1	1	0	33	2	32	0	0	131	13	UZ
ATL	0	0	0	-0	2	0	2	0	0	3	1	0	0	0	0	0	0	0	19	0	0	1	1	0	1	27	0	0	17	12	ATL
BAS	0	0	0	-1	6	5	0	0	0	12	9	0	0	0	0	0	1	0	7	-5	0	0	4	0	0	23	0	0	59	38	BAS
BLS	0	0	0	-0	1	9	0	14	1	62	1	0	1	0	0	9	37	0	2	2	42	3	1	4	2	23	0	0	178	49	BLS
MED	1	1	0	-0	1	3	2	4	3	5	0	1	1	0	0	14	4	0	6	0	2	95	1	-1	16	29	0	0	146	111	MED
NOS	0	0	0	-5	5	0	1	0	0	3	2	0	0	0	0	0	0	0	16	1	0	1	-19	0	1	33	0	0	12	3	NOS
AST	0	0	0	0	0	1	0	1	0	11	0	0	0	1	4	8	2	3	0	0	1	3	0	131	2	34	0	0	49	8	AST
NOA	0	0	0	-0	0	1	3	1	1	1	0	0	0	0	0	3	1	0	7	0	0	26	0	-0	95	42	0	0	58	49	NOA
EXC	0	0	0	-0	1	2	1	2	1	31	1	0	0	0	1	5	4	2	3	1	1	3	1	8	2	20	0	0	86	28	EXC
EU	0	0	0	-2	2	3	4	5	2	4	2	1	1	0	0	1	2	0	7	1	0	7	0	0	4	22	0	0	83	69	EU
	ME	MK	MT	NL	NO	PL	PT	RO	RS	RU	SE	SI	SK	TJ	TM	TR	UA	UZ	ATL	BAS	BLS	MED	NOS	AST	NOA	BIC	DMS	VOL	EXC	EU	

Table C.7: 2017 country-to-country blame matrices for **SOMO35**.
Units: ppb.d per 15% emis. red. of VOC. **Emitters →, Receptors ↓.**

	AL	AM	AT	AZ	BA	BE	BG	BY	CH	CY	CZ	DE	DK	EE	ES	FI	FR	GB	GE	GR	HR	HU	IE	IS	IT	KG	KZ	LT	LU	LV	MD	
AL	10	0	1	0	1	0	1	0	1	0	2	7	0	0	1	0	3	3	0	2	1	1	0	0	12	0	0	0	0	0	0	AL
AM	0	28	0	4	0	0	0	0	0	0	0	2	0	0	0	0	1	1	2	0	0	0	0	0	1	0	0	0	0	0	0	AM
AT	0	0	7	0	0	1	0	0	3	0	3	18	0	0	1	0	7	5	0	0	1	1	0	0	13	0	0	0	0	0	0	AT
AZ	0	2	0	9	0	0	0	0	0	0	0	2	0	0	0	0	1	1	3	0	0	0	0	0	1	0	0	0	0	0	0	AZ
BA	0	0	1	0	3	1	0	0	1	0	3	9	0	0	2	0	4	4	0	0	2	2	0	0	14	0	0	0	0	0	0	BA
BE	0	0	0	0	0	7	0	0	0	0	0	10	0	0	1	0	8	12	0	0	0	0	1	0	1	0	0	0	0	0	0	BE
BG	0	0	1	0	0	0	5	0	0	0	2	6	0	0	1	0	3	3	0	3	0	2	0	0	4	0	0	0	0	0	0	BG
BY	0	0	0	0	0	0	0	2	0	0	1	4	0	0	0	0	1	3	0	0	0	0	0	0	1	0	0	0	0	0	0	BY
CH	0	0	1	0	0	1	0	0	19	0	1	13	0	0	2	0	13	4	0	0	0	0	0	0	24	0	0	0	0	0	0	CH
CY	0	0	1	0	0	0	1	0	0	4	1	4	0	0	1	0	2	2	0	3	0	1	0	0	5	0	0	0	0	0	0	CY
CZ	0	0	2	0	0	1	0	0	1	0	10	18	0	0	1	0	6	6	0	0	0	1	0	0	3	0	0	0	0	0	0	CZ
DE	0	0	1	0	0	2	0	0	2	0	2	26	0	0	1	0	7	9	0	0	0	0	0	0	2	0	0	0	0	0	0	DE
DK	0	0	0	0	0	1	0	0	0	0	0	8	3	0	0	0	2	10	0	0	0	0	1	0	0	0	0	0	0	0	0	DK
EE	0	0	0	0	0	0	0	0	0	0	0	2	0	0	0	1	1	3	0	0	0	0	0	0	0	0	0	0	0	0	0	EE
ES	0	0	0	0	0	0	0	0	0	0	0	1	0	0	17	0	3	1	0	0	0	0	0	0	2	0	0	0	0	0	0	ES
FI	0	0	0	0	0	0	0	0	0	0	0	1	0	0	0	1	0	1	0	0	0	0	0	0	0	0	0	0	0	0	0	FI
FR	0	0	0	0	0	1	0	0	1	0	0	5	0	0	4	0	13	5	0	0	0	0	0	0	4	0	0	0	0	0	0	FR
GB	0	0	0	0	0	1	0	0	0	0	0	3	0	0	1	0	2	13	0	0	0	0	1	0	0	0	0	0	0	0	0	GB
GE	0	2	0	3	0	0	0	0	0	0	1	2	0	0	0	0	1	1	8	0	0	0	0	0	1	0	0	0	0	0	0	GE
GL	0	0	0	0	0	0	0	0	0	0	0	0	0	0	0	0	0	0	0	0	0	0	0	0	0	0	0	0	0	0	0	GL
GR	1	0	1	0	0	0	2	0	0	0	2	6	0	0	1	0	3	3	0	15	1	1	0	0	8	0	0	0	0	0	0	GR
HR	0	0	2	0	1	1	0	0	1	0	3	12	0	0	2	0	5	4	0	0	4	2	0	0	22	0	0	0	0	0	0	HR
HU	0	0	2	0	0	1	0	0	1	0	4	12	0	0	1	0	4	5	0	0	1	6	0	0	8	0	0	0	0	0	0	HU
IE	0	0	0	0	0	0	0	0	0	0	0	1	0	0	1	0	2	4	0	0	0	0	1	0	0	0	0	0	0	0	0	IE
IS	0	0	0	0	0	0	0	0	0	0	0	1	0	0	0	0	1	2	0	0	0	0	0	0	0	0	0	0	0	0	0	IS
IT	0	0	2	0	0	1	0	0	2	0	2	9	0	0	3	0	8	4	0	0	1	1	0	0	71	0	0	0	0	0	0	IT
KG	0	0	0	0	0	0	0	0	0	0	0	1	0	0	0	0	1	1	0	0	0	0	0	0	1	17	2	0	0	0	0	KG
KZ	0	0	0	0	0	0	0	0	0	0	0	2	0	0	0	0	1	1	0	0	0	0	0	0	1	1	2	0	0	0	0	KZ
LT	0	0	0	0	0	0	0	1	0	0	1	4	1	0	0	0	1	3	0	0	0	0	0	0	1	0	0	1	0	0	0	LT
LU	0	0	0	0	0	4	0	0	0	0	1	15	0	0	1	0	9	8	0	0	0	0	0	0	1	0	0	0	2	0	0	LU
LV	0	0	0	0	0	0	0	0	0	0	1	3	0	0	0	0	1	3	0	0	0	0	0	0	0	0	0	0	0	1	0	LV
MD	0	0	1	0	0	0	1	1	0	0	2	6	0	0	1	0	2	2	0	1	0	1	0	0	2	0	0	0	0	0	2	MD
ME	2	0	1	0	1	1	1	0	1	0	2	7	0	0	1	0	3	3	0	1	1	2	0	0	12	0	0	0	0	0	0	ME
MK	2	0	1	0	0	0	1	0	1	0	2	6	0	0	1	0	3	3	0	6	1	2	0	0	7	0	0	0	0	0	0	MK
MT	1	0	1	0	0	1	0	0	1	0	2	7	0	0	4	0	7	4	0	1	1	1	0	0	24	0	0	0	0	0	0	MT
NL	0	0	0	0	0	3	0	0	0	0	0	10	0	0	1	0	5	13	0	0	0	0	1	0	0	0	0	0	0	0	0	NL
NO	0	0	0	0	0	0	0	0	0	0	0	1	0	0	0	0	1	3	0	0	0	0	0	0	0	0	0	0	0	0	0	NO
PL	0	0	1	0	0	1	0	1	0	0	3	11	1	0	1	0	3	5	0	0	0	1	0	0	1	0	0	0	0	0	0	PL
PT	0	0	0	0	0	0	0	0	0	0	0	1	0	0	9	0	2	1	0	0	0	0	0	0	1	0	0	0	0	0	0	PT
RO	0	0	1	0	0	1	1	1	0	0	2	7	0	0	1	0	3	3	0	1	0	2	0	0	4	0	0	0	0	0	0	RO
RS	1	0	1	0	1	1	1	0	1	0	3	9	0	0	1	0	4	3	0	1	1	3	0	0	7	0	0	0	0	0	0	RS
RU	0	0	0	0	0	0	0	0	0	0	0	1	0	0	0	0	0	1	0	0	0	0	0	0	0	0	0	0	0	0	0	RU
SE	0	0	0	0	0	0	0	0	0	0	0	2	0	0	0	0	1	3	0	0	0	0	0	0	0	0	0	0	0	0	0	SE
SI	0	0	4	0	0	1	0	0	2	0	3	14	0	0	2	0	6	5	0	0	3	1	0	0	35	0	0	0	0	0	0	SI
SK	0	0	2	0	0	1	0	0	1	0	5	11	0	0	1	0	4	4	0	0	1	4	0	0	4	0	0	0	0	0	0	SK
TJ	0	0	0	0	0	0	0	0	0	0	0	1	0	0	0	0	0	0	0	0	0	0	0	0	1	2	1	0	0	0	0	TJ
TM	0	0	0	1	0	0	0	0	0	0	0	2	0	0	0	0	1	1	0	0	0	0	0	0	1	0	1	0	0	0	0	TM
TR	0	0	0	0	0	0	0	0	0	0	1	3	0	0	1	0	1	1	0	1	0	1	0	0	2	0	0	0	0	0	0	TR
UA	0	0	0	0	0	0	0	1	0	0	1	5	0	0	0	0	2	2	0	0	0	1	0	0	2	0	0	0	0	0	0	UA
UZ	0	0	0	0	0	0	0	0	0	0	0	2	0	0	0	0	1	1	0	0	0	0	0	0	1	3	1	0	0	0	0	UZ
ATL	0	0	0	0	0	0	0	0	0	0	0	1	0	0	1	0	1	2	0	0	0	0	0	0	0	0	0	0	0	0	0	ATL
BAS	0	0	0	0	0	1	0	0	0	0	1	6	2	0	0	1	2	7	0	0	0	0	0	0	0	0	0	0	0	0	0	BAS
BLS	0	0	1	1	0	0	1	1	0	0	2	6	0	0	1	0	2	3	2	1	0	1	0	0	2	0	0	0	0	0	1	BLS
MED	1	0	1	0	0	1	1	0	1	0	2	8	0	0	5	0	8	4	0	5	1	1	0	0	21	0	0	0	0	0	0	MED
NOS	0	0	0	0	0	1	0	0	0	0	1	5	1	0	1	0	3	18	0	0	0	0	1	0	0	0	0	0	0	0	0	NOS
AST	0	0	0	1	0	0	0	0	0	0	0	1	0	0	0	0	1	1	0	0	0	0	0	0	1	0	1	0	0	0	0	AST
NOA	0	0	0	0	0	0	0	0	0	0	1	3	0	0	3	0	3	2	0	1	0	0	0	0	5	0	0	0	0	0	0	NOA
EXC	0	0	0	0	0	0	0	0	0	0	1	3	0	0	1	0	2	2	0	0	0	0	0	0	2	0	0	0	0	0	0	EXC
EU	0	0	1	0	0	1	0	0	1	0	1	7	0	0	3	0	5	5	0	1	0	1	0	0	8	0	0	0	0	0	0	EU
	AL	AM	AT	AZ	BA	BE	BG	BY	CH	CY	CZ	DE	DK	EE	ES	FI	FR	GB	GE	GR	HR	HU	IE	IS	IT	KG	KZ	LT	LU	LV	MD	

Table C.7 Cont.: 2017 country-to-country blame matrices for **SOMO35**.
Units: ppb.d per 15% emis. red. of VOC. **Emitters →, Receptors ↓.**

	ME	MK	MT	NL	NO	PL	PT	RO	RS	RU	SE	SI	SK	TJ	TM	TR	UA	UZ	ATL	BAS	BLS	MED	NOS	AST	NOA	BIC	DMS	VOL	EXC	EU	
AL	1	2	0	1	0	4	0	2	5	3	0	0	1	0	0	1	2	0	0	0	0	0	0	1	3	28	0	0	69	45	AL
AM	0	0	0	0	0	1	0	1	0	6	0	0	0	0	0	8	2	0	0	0	0	0	0	69	1	23	0	0	60	10	AM
AT	0	0	0	2	0	3	0	1	0	1	0	1	1	0	0	0	1	0	0	0	0	0	0	0	1	23	0	0	72	65	AT
AZ	0	0	0	0	0	2	0	1	0	12	0	0	0	0	0	3	2	0	0	0	0	0	0	41	1	26	0	0	44	11	AZ
BA	0	0	0	1	0	5	0	1	2	2	0	0	1	0	0	0	1	0	0	0	0	0	0	0	2	25	0	0	63	52	BA
BE	0	0	0	5	0	1	0	0	0	1	0	0	0	0	0	0	0	0	0	0	0	0	0	0	0	21	0	0	50	48	BE
BG	0	0	0	1	0	4	0	4	3	6	0	0	1	0	0	4	3	0	0	0	0	0	0	1	1	25	0	0	59	41	BG
BY	0	0	0	1	0	4	0	1	0	6	0	0	0	0	0	0	2	0	0	0	0	0	0	0	0	12	0	0	30	19	BY
CH	0	0	0	2	0	1	0	0	0	1	0	0	0	0	0	0	0	0	0	0	0	0	0	0	1	22	0	0	85	64	CH
CY	0	0	0	1	0	3	0	2	1	5	0	0	1	0	0	22	2	0	0	0	0	0	0	20	3	42	0	0	65	33	CY
CZ	0	0	0	2	0	7	0	1	1	2	0	0	1	0	0	0	1	0	0	0	0	0	0	0	0	24	0	0	69	64	CZ
DE	0	0	0	4	0	2	0	0	0	1	0	0	0	0	0	0	0	0	0	0	0	0	0	0	0	23	0	0	62	58	DE
DK	0	0	0	3	1	3	0	0	0	2	1	0	0	0	0	0	1	0	0	0	0	0	0	0	0	17	0	0	35	32	DK
EE	0	0	0	1	0	2	0	0	0	4	1	0	0	0	0	0	0	0	0	0	0	0	0	0	0	8	0	0	19	14	EE
ES	0	0	0	0	0	1	2	0	0	0	0	0	0	0	0	0	0	0	0	0	0	0	0	0	4	20	0	0	31	30	ES
FI	0	0	0	0	0	1	0	0	0	2	0	0	0	0	0	0	0	0	0	0	0	0	0	0	0	2	0	0	8	6	FI
FR	0	0	0	1	0	1	0	0	0	1	0	0	0	0	0	0	0	0	0	0	0	0	0	0	1	18	0	0	39	37	FR
GB	0	0	0	1	0	1	0	0	0	1	0	0	0	0	0	0	0	0	0	0	0	0	0	0	0	11	0	0	26	24	GB
GE	0	0	0	0	0	2	0	1	0	10	0	0	0	0	0	5	3	0	0	0	0	0	0	23	1	22	0	0	45	12	GE
GL	0	0	0	0	0	0	0	0	0	0	0	0	0	0	0	0	0	0	0	0	0	0	0	0	0	-1	0	0	1	1	GL
GR	0	1	0	1	0	4	0	2	2	5	0	0	1	0	0	5	3	0	0	0	0	0	0	1	3	31	0	0	70	51	GR
HR	0	0	0	2	0	5	0	1	2	2	0	1	1	0	0	0	1	0	0	0	0	0	0	0	2	29	0	0	78	69	HR
HU	0	0	0	2	0	8	0	3	2	2	0	1	3	0	0	0	2	0	0	0	0	0	0	0	1	26	0	0	70	62	HU
IE	0	0	0	1	0	1	0	0	0	1	0	0	0	0	0	0	0	0	0	0	0	0	0	0	0	7	0	0	14	13	IE
IS	0	0	0	0	0	1	0	0	0	1	0	0	0	0	0	0	0	0	0	0	0	0	0	0	0	2	0	0	8	7	IS
IT	0	0	0	1	0	3	0	1	1	2	0	1	1	0	0	0	1	0	0	0	0	0	0	0	4	34	0	0	118	111	IT
KG	0	0	0	0	0	1	0	0	0	4	0	0	0	1	0	1	1	11	0	0	0	0	0	35	1	16	0	0	42	5	KG
KZ	0	0	0	0	0	1	0	0	0	11	0	0	0	0	0	1	1	1	0	0	0	0	0	12	0	17	0	0	26	8	KZ
LT	0	0	0	1	0	5	0	0	0	4	1	0	0	0	0	0	1	0	0	0	0	0	0	0	0	12	0	0	28	21	LT
LU	0	0	0	3	0	1	0	0	0	1	0	0	0	0	0	0	0	0	0	0	0	0	0	0	0	20	0	0	49	47	LU
LV	0	0	0	1	0	3	0	0	0	4	1	0	0	0	0	0	1	0	0	0	0	0	0	0	0	9	0	0	22	16	LV
MD	0	0	0	1	0	6	0	4	1	7	0	0	1	0	0	1	5	0	0	0	0	0	0	1	1	20	0	0	49	31	MD
ME	3	0	0	1	0	4	0	2	3	2	0	0	1	0	0	1	1	0	0	0	0	0	0	0	3	24	0	0	59	44	ME
MK	0	7	0	1	0	4	0	2	5	3	0	0	1	0	0	2	2	0	0	0	0	0	0	1	2	23	0	0	65	42	MK
MT	0	0	5	1	0	3	0	1	1	2	0	0	1	0	0	1	1	0	0	0	0	1	0	0	9	41	0	0	76	67	MT
NL	0	0	0	11	0	1	0	0	0	1	0	0	0	0	0	0	0	0	0	0	0	0	0	0	0	20	0	0	48	46	NL
NO	0	0	0	0	1	1	0	0	0	1	0	0	0	0	0	0	0	0	0	0	0	0	0	0	0	2	0	0	10	7	NO
PL	0	0	0	2	0	14	0	1	0	2	0	0	1	0	0	0	1	0	0	0	0	0	0	0	0	20	0	0	52	46	PL
PT	0	0	0	0	0	0	15	0	0	0	0	0	0	0	0	0	0	0	0	0	0	0	0	0	2	19	0	0	31	30	PT
RO	0	0	0	1	0	5	0	9	2	5	0	0	1	0	0	1	4	0	0	0	0	0	0	1	1	23	0	0	57	43	RO
RS	0	1	0	1	0	5	0	3	9	3	0	0	1	0	0	1	2	0	0	0	0	0	0	0	1	25	0	0	66	47	RS
RU	0	0	0	0	0	1	0	0	0	9	0	0	0	0	0	0	1	0	0	0	0	0	0	2	0	6	0	0	17	5	RU
SE	0	0	0	1	0	1	0	0	0	1	1	0	0	0	0	0	0	0	0	0	0	0	0	0	0	4	0	0	12	9	SE
SI	0	0	0	2	0	4	0	1	1	2	0	7	1	0	0	0	1	0	0	0	0	0	0	0	2	29	0	0	98	91	SI
SK	0	0	0	2	0	12	0	2	1	2	0	0	6	0	0	0	2	0	0	0	0	0	0	0	1	24	0	0	69	61	SK
TJ	0	0	0	0	0	0	0	0	0	3	0	0	0	2	1	1	1	5	0	0	0	0	0	33	0	13	0	0	19	4	TJ
TM	0	0	0	0	0	2	0	0	0	11	0	0	0	0	2	2	2	1	0	0	0	0	0	50	1	31	0	0	33	11	TM
TR	0	0	0	0	0	2	0	1	1	6	0	0	0	0	0	21	2	0	0	0	0	0	0	24	2	24	0	0	50	18	TR
UA	0	0	0	1	0	5	0	2	0	10	0	0	1	0	0	1	7	0	0	0	0	0	0	1	0	19	0	0	45	25	UA
UZ	0	0	0	0	0	1	0	0	0	10	0	0	0	0	1	1	2	7	0	0	0	0	0	24	0	25	0	0	36	9	UZ
ATL	0	0	0	0	0	0	1	0	0	1	0	0	0	0	0	0	0	0	0	0	0	0	0	0	1	4	0	0	9	8	ATL
BAS	0	0	0	2	1	5	0	0	0	5	2	0	0	0	0	0	1	0	0	0	0	0	0	0	0	17	0	0	37	30	BAS
BLS	0	0	0	1	1	5	0	3	1	23	0	0	1	0	0	11	9	0	0	0	0	0	0	6	1	35	0	0	80	32	BLS
MED	0	0	0	1	0	4	1	2	1	4	0	0	1	0	0	6	2	0	0	0	0	0	0	5	12	47	0	0	85	68	MED
NOS	0	0	0	3	2	2	0	0	0	2	0	0	0	0	0	0	1	0	0	0	0	0	0	0	0	19	0	0	43	38	NOS
AST	0	0	0	0	0	1	0	0	0	4	0	0	0	0	0	3	1	0	0	0	0	0	0	118	1	24	0	0	17	6	AST
NOA	0	0	0	0	0	1	1	0	0	1	0	0	0	0	0	1	1	0	0	0	0	0	0	1	17	26	0	0	26	22	NOA
EXC	0	0	0	1	0	2	0	1	0	7	0	0	0	0	0	1	1	1	0	0	0	0	0	6	1	13	0	0	29	16	EXC
EU	0	0	0	1	0	3	1	1	0	2	0	0	0	0	0	0	1	0	0	0	0	0	0	0	1	18	0	0	45	40	EU
	ME	MK	MT	NL	NO	PL	PT	RO	RS	RU	SE	SI	SK	TJ	TM	TR	UA	UZ	ATL	BAS	BLS	MED	NOS	AST	NOA	BIC	DMS	VOL	EXC	EU	

Table C.8: 2017 country-to-country blame matrices for **PM2.5**.
Units: ng/m^3 per 15% emis. red. of PPM. **Emitters →, Receptors ↓.**

	AL	AM	AT	AZ	BA	BE	BG	BY	CH	CY	CZ	DE	DK	EE	ES	FI	FR	GB	GE	GR	HR	HU	IE	IS	IT	KG	KZ	LT	LU	LV	MD	
AL	228	0	1	0	2	0	3	0	0	0	1	1	0	0	0	0	1	0	0	5	1	3	0	0	8	0	0	0	0	0	0	AL
AM	0	67	0	3	0	0	0	0	0	0	0	0	0	0	0	0	0	0	8	0	0	0	0	0	0	0	0	0	0	0	0	AM
AT	0	0	84	0	1	0	1	0	2	0	10	17	0	0	0	0	4	1	0	0	3	11	0	0	14	-0	0	0	0	0	0	AT
AZ	0	4	0	24	0	0	0	0	0	0	0	0	0	0	0	0	0	0	26	0	0	0	0	0	0	0	1	0	0	0	0	AZ
BA	1	0	2	0	126	0	2	0	0	0	4	3	0	0	0	0	2	0	0	0	17	10	0	0	10	-0	0	0	0	0	0	BA
BE	0	-0	1	-0	0	229	0	0	0	-0	2	26	0	0	1	0	58	22	-0	0	0	0	1	0	1	-0	-0	0	3	0	0	BE
BG	1	0	1	0	1	0	174	0	0	0	2	2	0	0	0	0	1	0	0	5	1	5	0	0	2	0	0	0	0	0	1	BG
BY	0	0	0	0	0	0	0	59	0	0	2	2	1	0	0	0	1	1	0	0	0	2	0	0	1	0	0	2	0	3	1	BY
CH	0	-0	3	-0	0	0	0	0	85	-0	1	16	0	0	1	0	26	1	-0	0	0	0	0	0	19	-0	-0	0	0	0	0	CH
CY	0	0	0	0	0	0	0	0	0	24	0	0	0	0	0	0	0	0	0	2	0	0	0	0	1	0	0	0	0	0	0	CY
CZ	0	0	8	0	1	1	1	0	1	0	219	26	0	0	0	0	7	2	0	0	2	15	0	0	3	-0	0	0	0	0	0	CZ
DE	0	-0	5	0	0	7	0	0	3	0	11	124	2	0	1	0	18	7	-0	0	0	2	0	0	2	-0	0	0	1	0	0	DE
DK	0	0	0	0	0	1	0	0	0	0	2	11	111	0	0	0	3	8	0	0	0	1	0	0	0	-0	0	0	0	0	0	DK
EE	0	0	0	0	0	0	0	2	0	0	1	1	1	42	0	4	1	1	0	0	0	1	0	0	0	-0	0	2	0	12	0	EE
ES	0	-0	0	-0	0	0	0	0	0	-0	0	0	0	0	99	0	6	0	-0	0	0	0	0	0	1	-0	-0	0	0	0	0	ES
FI	0	0	0	0	0	0	0	0	0	0	0	0	0	1	0	21	0	0	0	0	0	0	0	0	0	-0	0	0	0	1	0	FI
FR	0	-0	1	-0	0	4	0	0	2	-0	1	7	0	0	4	0	152	7	-0	0	0	0	0	0	3	-0	-0	0	1	0	0	FR
GB	0	0	0	0	0	2	0	0	0	0	1	2	0	0	1	0	6	136	-0	0	0	0	3	0	0	-0	0	0	0	0	0	GB
GE	0	3	0	2	0	0	0	0	0	0	0	0	0	0	0	0	0	0	133	0	0	0	0	0	0	0	0	0	0	0	0	GE
GL	0	0	0	0	0	0	0	0	0	0	0	0	0	0	0	0	0	0	0	0	0	0	0	0	0	0	0	0	0	0	0	GL
GR	6	0	0	0	1	0	6	0	0	0	1	1	0	0	0	0	1	0	0	70	1	2	0	0	4	0	0	0	0	0	0	GR
HR	1	0	5	0	28	0	2	0	0	0	6	5	0	0	1	0	3	1	0	0	126	26	0	0	27	-0	0	0	0	0	0	HR
HU	0	0	9	0	4	0	2	0	0	0	11	7	0	0	0	0	3	1	0	0	18	288	0	0	10	-0	0	0	0	0	1	HU
IE	0	-0	0	-0	0	1	0	0	0	-0	0	1	0	0	0	0	2	9	0	0	0	0	45	0	0	-0	-0	0	0	0	0	IE
IS	0	0	0	0	0	0	0	0	0	0	0	0	0	0	0	0	0	0	0	0	0	0	0	3	0	-0	0	0	0	0	0	IS
IT	0	0	2	0	1	0	1	0	1	-0	1	2	0	0	1	0	7	0	0	0	3	2	0	0	394	-0	0	0	0	0	0	IT
KG	0	0	0	0	0	0	0	0	0	0	0	0	0	0	0	0	0	0	0	0	0	0	0	0	0	48	8	0	0	0	0	KG
KZ	0	0	0	0	0	0	0	0	0	0	0	0	0	0	0	0	0	0	0	0	0	0	0	0	0	2	51	0	0	0	0	KZ
LT	0	0	0	0	0	0	0	13	0	0	1	3	2	1	0	1	1	1	0	0	0	2	0	0	1	-0	0	35	0	10	0	LT
LU	0	-0	1	-0	0	35	0	0	0	-0	4	42	0	0	1	0	63	10	-0	0	0	1	0	0	1	-0	-0	0	74	0	0	LU
LV	0	0	0	0	0	0	0	5	0	0	1	2	1	3	0	1	1	1	0	0	0	1	0	0	0	0	0	7	0	78	0	LV
MD	0	0	0	0	0	0	3	2	0	0	1	2	0	0	0	0	1	0	0	1	0	3	0	0	1	0	0	0	0	0	133	MD
ME	17	0	1	0	8	0	3	0	0	0	1	1	0	0	0	0	1	0	0	1	2	4	0	0	6	0	0	0	0	0	0	ME
MK	18	0	1	0	1	0	15	0	0	0	1	1	0	0	0	0	1	0	0	11	1	4	0	0	3	0	0	0	0	0	0	MK
MT	1	0	0	0	1	0	0	0	0	0	1	1	0	0	2	0	5	0	0	1	1	1	0	0	23	0	0	0	0	0	0	MT
NL	0	-0	0	-0	0	47	0	0	0	-0	2	38	1	0	1	0	19	24	-0	0	0	1	1	0	0	-0	0	0	0	0	0	NL
NO	0	0	0	0	0	0	0	0	0	0	0	0	0	0	0	0	0	1	0	0	0	0	0	0	0	0	0	0	0	0	0	NO
PL	0	0	1	0	0	1	0	3	0	0	15	12	2	0	0	0	3	2	0	0	1	7	0	0	1	-0	0	0	0	0	0	PL
PT	0	0	0	0	0	0	0	0	0	0	0	0	0	0	33	0	2	0	-0	0	0	0	0	0	1	0	-0	0	0	0	0	PT
RO	1	0	1	0	1	0	7	1	0	0	2	2	0	0	0	0	1	0	0	1	1	14	0	0	3	0	0	0	0	0	5	RO
RS	5	0	2	0	10	0	22	0	0	0	4	3	0	0	0	0	2	1	0	1	7	24	0	0	5	0	0	0	0	0	1	RS
RU	0	0	0	0	0	0	0	1	0	0	0	0	0	0	0	0	0	0	0	0	0	0	0	0	0	0	6	0	0	0	0	RU
SE	0	0	0	0	0	0	0	0	0	0	0	1	3	0	0	1	1	1	0	0	0	0	0	0	0	-0	0	0	0	0	0	SE
SI	0	0	19	0	2	0	1	0	0	0	4	5	0	0	1	0	3	0	0	0	34	11	0	0	57	-0	0	0	0	0	0	SI
SK	0	0	5	0	1	1	1	0	0	0	20	7	0	0	0	0	3	1	0	0	4	60	0	0	4	-0	0	0	0	0	0	SK
TJ	0	0	0	0	0	0	0	0	0	0	0	0	0	0	0	0	0	0	0	0	0	0	0	0	0	3	1	0	0	0	0	TJ
TM	0	0	0	0	0	0	0	0	0	0	0	0	0	0	0	0	0	0	0	0	0	0	0	0	0	0	5	0	0	0	0	TM
TR	0	1	0	0	0	0	1	0	0	0	0	0	0	0	0	0	0	0	0	1	0	0	0	0	0	0	0	0	0	0	0	TR
UA	0	0	0	0	0	0	1	3	0	0	1	2	0	0	0	0	1	0	0	0	0	3	0	0	1	0	0	0	0	0	5	UA
UZ	0	0	0	0	0	0	0	0	0	0	0	0	0	0	0	0	0	0	0	0	0	0	0	0	0	8	10	0	0	0	0	UZ
ATL	0	0	0	0	0	0	0	0	0	0	0	0	0	0	2	0	1	1	0	0	0	0	0	0	0	0	0	0	0	0	0	ATL
BAS	0	0	0	0	0	1	0	1	0	0	1	5	9	2	0	4	2	3	0	0	0	1	0	0	0	-0	0	1	0	3	0	BAS
BLS	0	0	0	0	0	0	2	1	0	0	0	1	0	0	0	0	0	0	9	1	0	1	0	0	0	0	0	0	0	0	2	BLS
MED	2	0	0	0	1	0	1	0	0	0	1	1	0	0	6	0	7	0	0	4	1	1	0	0	21	0	0	0	0	0	0	MED
NOS	0	0	0	0	0	3	0	0	0	0	1	4	2	0	1	0	7	22	0	0	0	0	1	0	0	-0	0	0	0	0	0	NOS
AST	0	0	0	0	0	0	0	0	0	0	0	0	0	0	0	0	0	0	0	0	0	0	0	0	0	0	2	0	0	0	0	AST
NOA	0	0	0	0	0	0	0	0	0	0	0	0	0	0	3	0	2	0	0	0	0	0	0	0	3	0	0	0	0	0	0	NOA
EXC	1	0	1	0	1	1	1	1	0	0	2	4	0	0	3	1	6	2	1	1	1	3	0	0	7	1	10	0	0	1	1	EXC
EU	0	0	3	0	1	3	5	1	1	0	7	14	2	1	13	2	24	10	0	2	3	10	1	0	29	0	0	1	0	2	0	EU
	AL	AM	AT	AZ	BA	BE	BG	BY	CH	CY	CZ	DE	DK	EE	ES	FI	FR	GB	GE	GR	HR	HU	IE	IS	IT	KG	KZ	LT	LU	LV	MD	

Table C.8 Cont.: 2017 country-to-country blame matrices for **PM2.5**.
Units: ng/m^3 per 15% emis. red. of PPM. **Emitters →, Receptors ↓.**

	ME	MK	MT	NL	NO	PL	PT	RO	RS	RU	SE	SI	SK	TJ	TM	TR	UA	UZ	ATL	BAS	BLS	MED	NOS	AST	NOA	BIC	DMS	VOL	EXC	EU	
AL	6	13	0	0	0	2	0	2	25	0	0	0	1	0	0	1	1	0	0	0	0	4	0	0	1	0	0	0	305	30	AL
AM	0	0	0	0	0	0	0	0	0	1	0	0	0	0	0	35	0	0	0	0	0	0	0	9	0	0	0	0	115	0	AM
AT	0	0	0	0	0	4	0	3	1	0	0	11	3	0	0	0	1	0	0	0	0	0	0	0	0	0	0	0	172	167	AT
AZ	0	0	0	0	0	0	0	0	0	3	0	0	0	0	1	9	1	0	0	0	0	0	0	10	0	0	0	0	70	1	AZ
BA	3	0	0	0	0	4	0	5	13	0	0	1	2	0	0	0	1	0	0	0	0	1	0	0	0	0	0	0	211	64	BA
BE	0	0	0	14	0	2	0	1	0	0	0	0	0	-0	-0	0	0	-0	1	0	0	0	13	0	0	0	0	0	361	360	BE
BG	0	2	0	0	0	3	0	28	13	2	0	0	1	0	0	10	6	0	0	0	1	1	0	0	0	0	0	0	263	225	BG
BY	0	0	0	0	0	20	0	5	1	8	1	0	1	0	0	1	11	0	0	0	0	0	0	0	0	0	0	0	125	44	BY
CH	0	0	0	0	0	0	0	0	0	0	0	0	0	-0	-0	-0	0	-0	0	0	0	0	0	-0	0	0	0	0	155	70	CH
CY	0	0	0	0	0	0	0	1	0	1	0	0	0	0	0	70	1	0	0	0	0	12	0	10	1	0	0	0	103	30	CY
CZ	0	0	0	1	0	25	0	6	2	0	0	2	9	0	0	0	1	0	0	0	0	0	1	0	0	0	0	0	335	329	CZ
DE	0	0	0	5	0	9	0	2	0	0	0	0	1	-0	0	0	1	0	0	0	0	0	3	0	0	0	0	0	202	197	DE
DK	0	0	0	2	3	7	0	1	0	1	2	0	0	-0	0	0	1	0	0	4	0	0	5	0	0	0	0	0	157	151	DK
EE	0	0	0	0	1	6	0	1	0	5	2	0	0	-0	0	0	1	0	0	3	0	0	0	0	0	0	0	0	86	77	EE
ES	0	0	0	0	0	0	7	0	0	0	0	0	0	0	-0	0	0	-0	2	0	0	5	0	-0	2	0	0	0	115	115	ES
FI	0	0	0	0	1	2	0	0	0	3	2	0	0	-0	0	0	0	0	0	1	0	0	0	0	0	0	0	0	34	29	FI
FR	0	0	0	1	0	1	0	0	0	0	0	0	0	-0	-0	-0	0	-0	1	0	0	2	2	-0	0	0	0	0	186	184	FR
GB	0	0	0	1	0	1	0	0	0	0	0	0	0	-0	-0	0	0	-0	3	0	0	0	3	0	0	0	0	0	154	153	GB
GE	0	0	0	0	0	0	0	0	0	2	0	0	0	0	0	17	1	0	0	0	0	0	0	2	0	0	0	0	159	1	GE
GL	0	0	0	0	0	0	0	0	0	0	0	0	0	0	0	0	0	0	0	0	0	0	0	0	0	0	0	0	0	0	GL
GR	0	6	0	0	0	1	0	4	5	1	0	0	0	0	0	14	2	0	0	0	0	10	0	0	1	0	0	0	129	92	GR
HR	1	0	0	0	0	6	0	8	14	0	0	16	3	-0	0	0	1	0	0	0	0	4	0	0	0	0	0	0	281	235	HR
HU	0	0	0	0	0	16	0	40	17	1	0	8	25	0	0	0	4	0	0	0	0	1	0	0	0	0	0	0	468	440	HU
IE	0	0	0	0	0	0	0	0	0	0	0	0	0	-0	-0	0	0	-0	2	0	0	0	0	0	0	0	0	0	59	59	IE
IS	0	0	0	0	0	0	0	0	0	0	0	0	0	-0	0	0	0	-0	1	0	0	0	0	0	0	0	0	0	4	1	IS
IT	0	0	0	0	0	1	0	1	1	0	0	5	0	-0	0	0	0	0	0	0	0	9	0	0	2	0	0	0	426	421	IT
KG	0	0	0	0	0	0	0	0	0	0	0	0	0	1	0	0	0	5	0	0	0	0	0	8	0	0	0	0	62	0	KG
KZ	0	0	0	0	0	0	0	0	0	9	0	0	0	0	0	0	1	1	0	0	0	0	0	9	0	0	0	0	66	1	KZ
LT	0	0	0	0	1	27	0	4	0	6	2	0	1	-0	0	0	3	0	0	2	0	0	0	0	0	0	0	0	118	93	LT
LU	0	0	0	3	0	2	0	1	0	0	0	0	0	0	-0	0	0	-0	1	0	0	0	2	0	0	0	0	0	239	238	LU
LV	0	0	0	0	1	12	0	3	0	5	2	0	1	0	0	0	2	0	0	2	0	0	0	0	0	0	0	0	130	117	LV
MD	0	0	0	0	0	10	0	91	1	5	0	0	1	0	0	5	40	0	0	0	1	0	0	0	0	0	0	0	303	116	MD
ME	97	2	0	0	0	2	0	3	18	0	0	0	1	0	0	0	1	0	0	0	0	3	0	0	0	0	0	0	170	27	ME
MK	1	154	0	0	0	2	0	4	35	0	0	0	1	0	0	2	1	0	0	0	0	1	0	0	0	0	0	0	261	47	MK
MT	0	0	39	0	0	1	0	0	1	0	0	0	0	0	0	1	0	0	0	0	0	78	0	0	10	0	0	0	78	75	MT
NL	0	0	0	101	0	4	0	1	0	0	0	0	0	-0	-0	0	0	-0	1	0	0	0	23	0	0	0	0	0	243	242	NL
NO	0	0	0	0	28	0	0	0	0	1	1	0	0	0	0	0	0	0	1	0	0	0	1	0	0	0	0	0	32	4	NO
PL	0	0	0	1	1	205	0	5	1	2	1	1	9	0	0	0	6	0	0	1	0	0	1	0	0	0	0	0	284	270	PL
PT	0	0	0	0	0	0	171	0	0	0	0	0	0	0	-0	-0	0	-0	6	0	0	2	0	-0	1	0	0	0	207	207	PT
RO	0	1	0	0	0	7	0	312	8	2	0	1	2	0	0	3	10	0	0	0	1	0	0	0	0	0	0	0	387	355	RO
RS	5	8	0	0	0	6	0	26	221	1	0	1	3	0	0	1	2	0	0	0	0	1	0	0	0	0	0	0	362	108	RS
RU	0	0	0	0	0	1	0	0	0	28	0	0	0	0	0	1	2	0	0	0	0	0	0	1	0	0	0	0	42	3	RU
SE	0	0	0	0	6	2	0	0	0	1	15	0	0	-0	0	0	0	0	0	1	0	0	1	0	0	0	0	0	34	27	SE
SI	0	0	0	0	0	4	0	4	3	0	0	251	1	0	0	0	1	0	0	0	0	3	0	0	0	0	0	0	404	396	SI
SK	0	0	0	0	0	35	0	17	4	1	0	3	163	0	0	0	4	0	0	0	0	0	0	0	0	0	0	0	337	325	SK
TJ	0	0	0	0	0	0	0	0	0	0	0	0	0	20	1	0	0	7	0	0	0	0	0	14	0	0	0	0	33	0	TJ
TM	0	0	0	0	0	0	0	0	0	2	0	0	0	0	22	1	1	6	0	0	0	0	0	9	0	0	0	0	39	0	TM
TR	0	0	0	0	0	0	0	2	0	1	0	0	0	0	0	247	1	0	0	0	1	3	0	7	0	0	0	0	257	5	TR
UA	0	0	0	0	0	12	0	18	1	11	0	0	1	0	0	5	98	0	0	0	1	0	0	0	0	0	0	0	169	44	UA
UZ	0	0	0	0	0	0	0	0	0	3	0	0	0	2	2	1	1	33	0	0	0	0	0	4	0	0	0	0	60	0	UZ
ATL	0	0	0	0	0	0	2	0	0	1	0	0	0	0	0	0	0	0	3	0	0	0	0	0	0	0	0	0	8	7	ATL
BAS	0	0	0	1	2	13	0	1	0	3	7	0	1	0	0	0	1	0	0	9	0	0	1	0	0	0	0	0	63	55	BAS
BLS	0	0	0	0	0	3	0	12	1	10	0	0	0	0	0	57	19	0	0	0	11	1	0	0	0	0	0	0	121	22	BLS
MED	0	0	0	0	0	1	0	1	1	0	0	1	0	0	0	18	1	0	0	0	0	32	0	3	8	0	0	0	72	47	MED
NOS	0	0	0	3	3	1	0	0	0	0	0	0	0	-0	0	0	0	0	1	0	0	0	11	0	0	0	0	0	49	46	NOS
AST	0	0	0	0	0	0	0	0	0	1	0	0	0	0	1	6	0	0	0	0	0	0	0	233	0	0	0	0	11	0	AST
NOA	0	0	0	0	0	0	1	0	0	0	0	0	0	-0	0	2	0	0	1	0	0	5	0	1	41	0	0	0	13	10	NOA
EXC	0	0	0	0	1	5	1	6	2	13	1	1	1	0	1	11	5	1	0	0	0	1	0	2	0	0	0	0	99	49	EXC
EU	0	0	0	2	1	19	5	20	2	1	2	2	4	0	0	1	2	0	1	0	0	2	1	0	0	0	0	0	194	185	EU
	ME	MK	MT	NL	NO	PL	PT	RO	RS	RU	SE	SI	SK	TJ	TM	TR	UA	UZ	ATL	BAS	BLS	MED	NOS	AST	NOA	BIC	DMS	VOL	EXC	EU	

Table C.9: 2017 country-to-country blame matrices for **PM2.5**.
Units: ng/m^3 per 15% emis. red. of SO_x. **Emitters →, Receptors ↓.**

	AL	AM	AT	AZ	BA	BE	BG	BY	CH	CY	CZ	DE	DK	EE	ES	FI	FR	GB	GE	GR	HR	HU	IE	IS	IT	KG	KZ	LT	LU	LV	MD	
AL	61	0	1	0	38	0	8	0	0	0	5	7	0	0	2	0	2	1	0	13	1	2	0	0	12	0	0	0	0	0	0	AL
AM	0	210	0	6	0	0	0	0	0	0	0	0	0	0	0	0	0	0	5	0	0	0	-0	0	0	0	5	0	0	0	0	AM
AT	0	0	20	0	5	1	1	0	2	0	15	41	0	0	2	0	6	2	0	0	2	3	0	0	6	-0	0	0	0	0	0	AT
AZ	0	25	0	26	0	0	0	0	0	0	0	0	0	0	0	0	0	0	9	0	0	0	0	0	0	0	13	0	0	0	0	AZ
BA	1	0	2	0	245	1	3	0	0	0	10	15	0	0	3	0	3	1	0	1	3	3	0	0	9	-0	0	0	0	0	0	BA
BE	0	-0	0	-0	0	77	0	0	0	0	2	42	0	0	6	0	52	32	-0	0	0	0	1	0	0	-0	-0	0	1	0	0	BE
BG	1	0	1	0	13	1	91	1	0	0	5	9	0	0	1	0	1	1	0	8	1	2	0	0	2	0	1	0	0	0	1	BG
BY	0	0	0	0	2	1	1	29	0	0	3	9	1	3	1	1	1	2	0	0	0	1	0	0	0	0	1	4	0	1	1	BY
CH	0	-0	2	-0	1	1	0	0	30	-0	3	24	0	0	5	0	19	2	-0	0	0	0	0	0	7	-0	-0	0	0	0	0	CH
CY	0	0	0	0	3	0	6	0	0	43	1	1	0	0	1	0	0	0	0	6	0	0	0	0	3	0	1	0	0	0	0	CY
CZ	0	0	4	0	5	3	1	0	1	0	88	72	0	0	2	0	8	6	0	0	1	5	0	0	1	-0	0	0	0	0	0	CZ
DE	0	0	2	0	1	9	0	0	2	0	12	129	1	0	3	0	18	14	0	0	0	1	1	0	1	-0	0	0	0	0	0	DE
DK	0	0	0	0	0	2	0	1	0	0	3	23	16	0	1	1	3	16	0	0	0	0	1	0	0	-0	0	0	0	0	0	DK
EE	0	0	0	0	1	1	0	2	0	0	1	5	1	14	0	9	1	3	0	0	0	0	0	0	0	-0	0	3	0	2	0	EE
ES	0	-0	0	-0	0	0	0	0	0	0	0	2	0	0	104	0	6	1	-0	0	0	0	0	0	2	-0	-0	0	0	0	0	ES
FI	0	0	0	0	0	0	0	1	0	0	0	2	0	3	0	17	0	1	0	0	0	0	0	0	0	0	0	0	0	0	0	FI
FR	0	-0	0	-0	1	5	0	0	1	0	2	12	0	0	17	0	59	12	-0	0	0	0	1	0	3	-0	-0	0	0	0	0	FR
GB	0	0	0	0	0	1	0	0	0	0	1	5	0	0	2	0	4	83	0	0	0	0	5	1	0	-0	0	0	0	0	0	GB
GE	0	21	0	8	0	0	0	0	0	0	0	0	0	0	0	0	0	0	34	0	0	0	0	0	0	0	4	0	0	0	0	GE
GL	0	0	0	0	0	0	0	0	0	0	0	0	0	0	0	0	0	0	0	0	0	0	0	0	0	0	0	0	0	0	0	GL
GR	4	0	1	0	16	0	29	1	0	0	3	6	0	0	1	0	1	0	0	38	1	1	0	0	8	0	1	0	0	0	1	GR
HR	1	0	4	0	73	1	3	0	0	0	15	23	0	0	4	0	5	2	0	1	17	6	0	0	15	-0	0	0	0	0	0	HR
HU	0	0	5	0	25	1	4	1	0	0	21	31	0	0	2	0	5	3	0	1	4	36	0	0	6	0	0	0	0	0	1	HU
IE	0	-0	0	-0	0	0	0	0	0	0	0	2	0	0	2	0	2	11	0	0	0	0	24	1	0	-0	0	0	0	0	0	IE
IS	0	0	0	0	0	0	0	0	0	0	0	1	0	0	0	0	0	1	0	0	0	0	0	33	0	0	0	0	0	0	0	IS
IT	0	0	2	0	12	0	1	0	1	0	5	8	0	0	7	0	11	1	0	1	3	1	0	0	67	-0	0	0	0	0	0	IT
KG	0	0	0	0	0	0	0	0	-0	0	0	0	0	0	0	0	0	-0	0	0	-0	0	-0	-0	0	63	26	0	0	0	0	KG
KZ	0	0	0	0	0	0	0	0	0	0	0	0	0	0	0	0	0	0	0	0	0	0	0	0	4	89	0	0	0	0	0	KZ
LT	0	0	0	0	2	1	0	9	0	0	2	10	1	2	1	2	1	4	0	0	0	1	0	0	0	0	0	17	0	2	0	LT
LU	0	-0	0	-0	0	30	0	0	0	0	4	55	0	0	6	0	51	21	-0	0	0	0	1	0	1	-0	-0	0	11	0	0	LU
LV	0	0	0	0	1	1	0	5	0	0	1	7	1	4	1	4	1	3	0	0	0	0	0	0	0	0	0	9	0	7	0	LV
MD	0	0	0	0	4	0	8	4	0	0	5	9	0	1	1	0	1	1	0	1	0	3	0	0	1	0	2	0	0	0	18	MD
ME	7	0	1	0	85	0	5	0	0	0	5	8	0	0	2	0	2	1	0	3	1	2	0	0	7	0	0	0	0	0	0	ME
MK	12	0	1	0	23	0	22	0	0	0	5	7	0	0	1	0	1	1	0	25	1	2	0	0	4	0	0	0	0	0	0	MK
MT	1	0	1	0	18	0	2	0	0	0	4	5	0	0	8	0	7	1	0	3	1	1	0	0	50	0	0	0	0	0	0	MT
NL	0	-0	0	-0	0	37	0	0	0	0	3	57	1	0	4	0	24	34	-0	0	0	0	1	0	0	-0	0	0	0	0	0	NL
NO	0	0	0	0	0	0	0	0	0	0	0	1	0	1	0	1	0	2	0	0	0	0	0	0	0	0	0	0	0	0	0	NO
PL	0	0	1	0	4	2	0	3	0	0	14	39	2	1	1	0	3	5	0	0	1	2	0	0	1	-0	0	1	0	0	0	PL
PT	0	-0	0	-0	0	0	0	0	0	0	0	1	0	0	64	0	3	1	-0	0	0	0	0	0	1	-0	-0	0	0	0	0	PT
RO	1	0	1	0	11	1	16	2	0	0	7	12	0	0	1	0	2	1	0	2	1	6	0	0	2	0	1	0	0	0	2	RO
RS	4	0	2	0	58	1	15	1	0	0	11	16	0	0	2	0	3	1	0	5	2	7	0	0	5	0	0	0	0	0	1	RS
RU	0	0	0	0	0	0	0	1	0	0	0	1	0	1	0	1	0	0	0	0	0	0	0	0	0	0	16	0	0	0	0	RU
SE	0	0	0	0	0	0	0	1	0	0	1	3	1	1	0	3	1	3	0	0	0	0	0	0	0	0	0	0	0	0	0	SE
SI	0	0	8	0	11	1	2	0	0	0	12	24	0	0	3	0	5	1	0	0	14	3	0	0	24	-0	0	0	0	0	0	SI
SK	0	0	3	0	11	1	1	1	0	0	26	30	0	0	1	0	4	3	0	0	2	15	0	0	3	-0	0	0	0	0	0	SK
TJ	0	0	0	0	0	0	0	0	0	0	0	0	0	0	0	0	0	0	0	0	0	0	-0	-0	0	8	12	0	0	0	0	TJ
TM	0	2	0	1	0	0	0	0	0	0	0	0	0	0	0	0	0	0	0	0	0	0	0	0	0	2	31	0	0	0	0	TM
TR	0	5	0	0	1	0	4	0	0	2	1	1	0	0	0	0	0	0	1	2	0	0	0	0	1	0	1	0	0	0	0	TR
UA	0	0	0	0	3	0	3	6	0	0	4	8	0	1	1	0	1	1	0	1	0	2	0	0	0	0	4	1	0	0	2	UA
UZ	0	1	0	0	0	0	0	0	0	0	0	0	0	0	0	0	0	0	0	0	0	0	0	0	0	13	50	0	0	0	0	UZ
ATL	0	0	0	0	0	0	0	0	0	0	0	1	0	0	5	0	1	1	0	0	0	0	0	1	0	0	0	0	0	0	0	ATL
BAS	0	0	0	0	1	1	0	1	0	0	2	12	3	2	1	6	2	6	0	0	0	0	0	0	0	-0	0	1	0	0	0	BAS
BLS	0	3	0	1	2	0	7	2	0	0	2	4	0	0	0	0	0	0	4	1	0	1	0	0	0	0	3	0	0	0	1	BLS
MED	1	0	1	0	14	0	6	0	0	1	3	5	0	0	13	0	8	1	0	6	1	1	0	0	25	0	0	0	0	0	0	MED
NOS	0	0	0	0	0	1	0	0	0	0	1	7	1	0	2	0	4	24	0	0	0	0	2	1	0	0	0	0	0	0	0	NOS
AST	0	1	0	1	0	0	0	0	0	1	0	0	0	0	0	0	0	0	0	0	0	0	0	0	0	1	9	0	0	0	0	AST
NOA	0	0	0	0	4	0	2	0	0	0	1	1	0	0	10	0	2	0	0	2	0	0	0	0	6	0	0	0	0	0	0	NOA
EXC	0	1	0	0	2	1	2	1	0	0	2	6	0	1	4	1	3	2	0	1	0	1	0	0	2	2	22	0	0	0	0	EXC
EU	0	0	1	0	5	3	4	1	0	0	6	22	1	1	17	2	12	10	0	2	1	2	1	0	6	0	0	1	0	0	0	EU
	AL	AM	AT	AZ	BA	BE	BG	BY	CH	CY	CZ	DE	DK	EE	ES	FI	FR	GB	GE	GR	HR	HU	IE	IS	IT	KG	KZ	LT	LU	LV	MD	

Table C.9 Cont.: 2017 country-to-country blame matrices for **PM2.5**.
Units: ng/m^3 per 15% emis. red. of SO_x. **Emitters →, Receptors ↓.**

	ME	MK	MT	NL	NO	PL	PT	RO	RS	RU	SE	SI	SK	TJ	TM	TR	UA	UZ	ATL	BAS	BLS	MED	NOS	AST	NOA	BIC	DMS	VOL	EXC	EU	
AL	26	41	0	0	0	11	0	5	89	2	0	0	1	0	0	8	9	0	0	0	0	27	0	1	13	9	5	42	349	74	AL
AM	0	0	0	0	0	1	0	0	1	5	0	0	0	0	1	95	5	0	0	0	0	1	0	201	3	9	0	7	334	3	AM
AT	0	0	0	1	0	16	0	3	13	1	0	2	2	-0	0	1	5	0	1	0	0	3	0	0	2	7	2	2	151	123	AT
AZ	0	0	0	0	0	2	0	0	1	19	0	0	0	0	1	46	14	0	0	0	1	0	0	184	1	7	0	4	160	3	AZ
BA	17	3	0	0	0	22	0	5	68	2	0	1	3	0	0	2	9	0	1	0	0	12	0	0	7	8	3	15	434	86	BA
BE	0	0	0	12	0	5	0	0	1	0	0	0	0	-0	-0	0	1	-0	9	0	0	2	6	0	2	10	15	1	237	234	BE
BG	4	8	0	0	0	18	0	25	105	12	0	0	2	0	0	41	49	0	0	0	5	7	0	1	6	9	2	12	408	168	BG
BY	0	0	0	0	0	54	0	4	8	29	1	0	1	0	0	5	28	0	1	1	0	1	0	0	0	5	4	1	193	89	BY
CH	0	0	0	1	0	4	0	0	1	0	0	0	0	-0	-0	0	1	-0	1	0	0	4	0	0	3	8	2	6	102	68	CH
CY	1	2	0	0	0	3	0	3	13	5	0	0	0	0	0	647	14	0	0	0	3	64	0	132	22	12	18	36	756	69	CY
CZ	0	0	0	2	0	45	0	4	17	2	0	1	4	0	0	1	7	0	2	0	0	1	1	0	1	7	5	1	283	249	CZ
DE	0	0	0	8	0	18	0	1	2	1	0	0	1	-0	0	0	3	0	4	0	0	1	3	0	1	8	10	1	229	219	DE
DK	0	0	0	3	1	15	0	0	1	4	1	0	0	-0	0	0	4	0	4	2	0	0	4	0	0	6	20	0	100	87	DK
EE	0	0	0	1	1	14	0	1	2	17	2	0	0	-0	0	0	3	0	1	2	0	0	0	0	0	4	6	0	83	57	EE
ES	0	0	0	0	0	1	7	0	0	0	0	0	0	-0	-0	0	0	-0	15	0	0	36	0	0	24	15	11	3	125	124	ES
FI	0	0	0	0	1	5	0	0	1	21	3	0	0	-0	0	0	1	0	1	1	0	0	0	0	0	4	10	0	59	34	FI
FR	0	0	0	2	0	3	1	0	1	0	0	0	0	-0	-0	0	0	-0	13	0	0	11	3	0	5	10	14	4	121	117	FR
GB	0	0	0	1	0	3	0	0	0	0	0	0	0	-0	0	0	1	-0	18	0	0	0	2	0	1	9	23	0	108	106	GB
GE	0	0	0	0	0	3	0	1	1	11	0	0	0	0	1	75	12	0	0	0	3	1	0	73	1	7	0	5	174	6	GE
GL	0	0	0	0	0	0	0	0	0	0	0	0	0	0	0	0	0	0	0	0	0	0	0	0	0	23	3	0	0	0	GL
GR	6	23	0	0	0	11	0	8	63	6	0	0	1	0	0	66	30	0	0	0	2	43	0	1	14	10	7	42	328	111	GR
HR	4	2	0	1	0	27	0	7	68	3	0	3	3	0	0	2	12	0	1	0	0	22	0	0	6	7	4	14	302	137	HR
HU	3	2	0	1	0	60	0	22	93	4	0	2	12	0	0	3	21	0	1	0	0	6	0	0	3	8	3	6	368	215	HU
IE	0	0	0	0	0	1	0	0	0	0	0	0	0	-0	-0	0	0	-0	15	0	0	0	1	0	1	11	30	0	45	43	IE
IS	0	0	0	0	0	1	0	0	0	0	0	0	0	0	0	0	0	0	2	0	0	0	0	0	0	9	15	0	37	3	IS
IT	2	1	0	0	0	9	0	2	17	1	0	1	1	-0	0	2	4	0	1	0	0	52	0	0	19	8	8	62	162	122	IT
KG	0	0	0	0	0	0	0	0	0	2	0	-0	0	5	0	5	1	13	0	0	0	0	-0	47	0	8	0	2	117	0	KG
KZ	0	0	0	0	0	2	0	0	1	46	0	0	0	0	1	4	13	1	0	0	0	0	0	35	0	9	0	1	164	3	KZ
LT	0	0	0	1	1	55	0	2	6	18	2	0	1	-0	0	1	9	0	1	1	0	0	1	0	0	5	7	0	151	106	LT
LU	0	0	0	8	0	5	0	0	1	1	0	0	0	-0	-0	0	1	-0	7	0	0	2	3	0	2	10	11	2	199	195	LU
LV	0	0	0	1	1	25	0	1	3	17	2	0	1	0	0	1	6	0	1	1	0	0	1	0	0	4	7	0	104	69	LV
MD	1	2	0	0	0	50	0	24	21	23	0	0	2	0	0	32	99	0	0	0	4	2	0	2	2	9	2	4	318	110	MD
ME	131	9	0	0	0	12	0	5	79	1	0	0	2	0	0	4	7	0	0	0	0	14	0	0	9	8	3	22	380	57	ME
MK	10	116	0	0	0	13	0	8	121	3	0	0	2	-0	0	20	15	0	0	0	1	10	0	1	9	9	2	21	415	93	MK
MT	5	3	7	0	0	6	0	1	14	0	0	0	1	0	0	8	2	0	1	0	0	205	0	0	77	11	24	183	150	98	MT
NL	0	0	0	41	0	10	0	0	1	1	0	0	0	-0	-0	0	1	-0	9	0	0	1	9	0	1	9	17	1	218	214	NL
NO	0	0	0	0	5	2	0	0	0	7	1	0	0	0	0	0	1	0	3	0	0	0	1	0	0	6	14	0	23	9	NO
PL	1	0	0	2	0	175	0	3	15	7	1	0	3	0	0	1	14	0	1	1	0	1	1	0	1	6	7	1	302	258	PL
PT	0	0	0	0	0	0	43	0	0	0	0	0	0	0	-0	0	0	-0	45	0	0	12	0	0	18	17	18	1	115	115	PT
RO	3	4	0	0	0	38	0	74	61	12	0	0	4	0	0	21	49	0	0	0	2	3	0	1	3	8	2	6	334	168	RO
RS	18	16	0	1	0	30	0	19	268	5	0	1	4	0	0	8	21	0	1	0	0	7	0	0	7	9	2	13	523	124	RS
RU	0	0	0	0	0	4	0	0	1	79	0	0	0	0	0	3	14	0	0	0	0	0	0	4	0	7	4	0	124	9	RU
SE	0	0	0	0	3	5	0	0	1	8	6	0	0	0	0	0	1	0	2	1	0	0	1	0	0	4	8	0	41	26	SE
SI	1	1	0	1	0	19	0	4	24	2	0	18	2	-0	0	1	10	0	1	0	0	18	0	0	4	6	3	5	190	140	SI
SK	1	1	0	1	0	80	0	11	49	3	0	1	30	0	0	1	15	0	1	0	0	3	0	0	2	7	3	3	297	214	SK
TJ	0	0	0	0	0	0	0	0	0	3	0	0	0	41	2	6	1	9	0	0	0	0	0	62	0	9	0	2	83	0	TJ
TM	0	0	0	0	0	1	0	0	0	21	0	0	0	2	12	14	12	4	0	0	0	0	0	130	1	10	0	3	105	2	TM
TR	1	1	0	0	0	4	0	3	11	7	0	0	0	0	0	535	19	0	0	0	4	13	0	113	8	12	2	15	602	20	TR
UA	1	1	0	0	0	43	0	8	12	35	0	0	2	0	0	20	126	0	0	0	3	1	0	3	1	8	2	2	290	79	UA
UZ	0	0	0	0	0	1	0	0	0	25	0	0	0	7	4	9	13	19	0	0	0	0	0	68	1	10	0	2	143	2	UZ
ATL	0	0	0	0	0	1	2	0	0	4	0	0	0	0	0	0	0	0	18	0	0	2	0	0	5	17	32	0	18	12	ATL
BAS	0	0	0	1	1	17	0	1	2	11	4	0	0	0	0	0	3	0	2	3	0	0	1	0	0	4	11	0	79	60	BAS
BLS	1	1	0	0	0	18	0	9	13	37	0	0	1	0	0	140	101	0	0	0	29	4	0	13	2	8	1	5	355	46	BLS
MED	5	4	0	0	0	7	1	3	23	3	0	0	1	0	0	121	12	0	3	0	1	139	0	25	57	11	22	108	267	84	MED
NOS	0	0	0	2	1	4	0	0	0	1	0	0	0	-0	0	0	1	0	10	0	0	0	4	0	0	7	25	0	54	49	NOS
AST	0	0	0	0	0	0	0	0	1	5	0	0	0	1	1	52	4	1	0	0	0	3	0	352	4	16	1	5	78	2	AST
NOA	2	1	0	0	0	2	1	1	7	1	0	0	0	-0	0	21	3	0	7	0	0	39	0	7	174	19	11	47	69	30	NOA
EXC	1	1	0	0	0	10	0	2	7	42	0	0	1	1	1	28	16	1	2	0	1	4	0	19	2	8	5	3	167	41	EXC
EU	1	1	0	2	0	24	2	6	15	5	1	0	1	0	0	6	8	0	7	0	0	12	1	0	6	8	10	8	172	129	EU
	ME	MK	MT	NL	NO	PL	PT	RO	RS	RU	SE	SI	SK	TJ	TM	TR	UA	UZ	ATL	BAS	BLS	MED	NOS	AST	NOA	BIC	DMS	VOL	EXC	EU	

Table C.10: 2017 country-to-country blame matrices for **PM2.5**.
Units: ng/m^3 per 15% emis. red. of NO_x. **Emitters →, Receptors ↓.**

	AL	AM	AT	AZ	BA	BE	BG	BY	CH	CY	CZ	DE	DK	EE	ES	FI	FR	GB	GE	GR	HR	HU	IE	IS	IT	KG	KZ	LT	LU	LV	MD	
AL	59	0	2	0	3	0	1	0	0	0	1	4	0	0	1	0	2	1	0	10	3	2	0	0	16	0	0	0	0	0	0	AL
AM	0	60	0	30	0	0	0	0	0	0	0	0	0	0	0	0	0	0	9	0	0	0	0	0	0	0	1	0	0	0	0	AM
AT	0	0	81	0	1	3	0	0	10	0	12	84	0	0	1	0	15	5	0	0	5	8	0	0	33	0	0	0	1	0	0	AT
AZ	0	9	0	116	0	0	0	0	0	0	0	0	0	0	0	0	0	0	21	0	0	0	0	0	0	0	3	0	0	0	0	AZ
BA	0	0	6	0	27	1	1	0	1	0	5	13	0	0	2	0	3	2	0	1	10	5	0	0	15	0	0	0	0	0	0	BA
BE	0	0	2	0	0	46	0	0	1	0	2	78	1	0	5	0	108	84	0	0	0	0	5	0	1	0	0	0	6	0	0	BE
BG	1	0	2	0	1	0	52	1	0	0	1	4	0	0	1	0	1	1	0	9	1	3	0	0	3	0	0	0	0	0	1	BG
BY	0	0	1	0	0	1	0	30	0	0	2	14	2	1	0	1	2	3	0	0	0	2	0	0	1	0	0	6	0	2	1	BY
CH	0	0	10	0	0	4	0	0	141	0	2	63	0	0	3	0	56	6	0	0	0	0	0	0	37	0	0	0	1	0	0	CH
CY	0	0	0	0	0	0	1	0	0	20	0	1	0	0	1	0	1	0	0	10	0	0	0	0	2	0	0	0	0	0	0	CY
CZ	0	0	26	0	1	4	0	0	4	0	61	100	1	0	2	0	18	8	0	0	3	13	1	0	5	0	0	0	1	0	0	CZ
DE	0	0	15	0	0	19	0	0	11	0	11	224	4	0	3	0	44	33	0	0	0	1	2	0	3	0	0	0	3	0	0	DE
DK	0	0	1	0	0	9	0	1	0	0	4	73	45	0	2	1	14	46	0	0	0	1	2	0	0	0	0	1	0	0	0	DK
EE	0	0	0	0	0	1	0	2	0	0	1	6	2	7	0	5	1	3	0	0	0	0	0	0	0	0	0	3	0	4	0	EE
ES	0	0	0	0	0	1	0	0	0	0	0	2	0	0	99	0	11	2	0	0	0	0	0	0	2	0	0	0	0	0	0	ES
FI	0	0	0	0	0	0	0	0	0	0	0	1	1	0	0	7	0	1	0	0	0	0	0	0	0	0	0	0	0	0	0	FI
FR	0	0	2	0	0	13	0	0	6	0	2	33	0	0	10	0	134	33	0	0	0	0	2	0	4	0	0	0	2	0	0	FR
GB	0	0	0	0	0	5	0	0	0	0	0	15	1	0	1	0	18	95	0	0	0	0	13	0	0	0	0	0	0	0	-0	GB
GE	0	7	0	22	0	0	0	0	0	0	0	0	0	0	0	0	0	0	42	0	0	0	0	0	0	0	1	0	0	0	0	GE
GL	0	0	0	0	0	0	0	0	0	0	0	0	0	0	0	0	0	0	0	0	0	0	0	0	0	0	0	0	0	0	0	GL
GR	3	0	1	0	1	0	9	0	0	0	0	1	0	0	1	0	1	0	0	39	0	1	0	0	6	0	0	0	0	0	0	GR
HR	0	0	19	0	11	2	1	0	1	0	9	30	0	0	2	0	7	3	0	1	41	15	0	0	47	0	0	0	0	0	0	HR
HU	0	0	34	0	6	2	2	1	2	0	18	46	0	0	1	0	10	5	0	1	22	100	0	0	27	0	0	0	0	0	1	HU
IE	0	0	0	0	0	2	0	0	0	0	0	7	1	0	1	0	7	33	0	0	0	0	43	0	0	0	0	0	0	0	-0	IE
IS	0	0	0	0	0	0	0	0	0	0	0	1	0	0	0	0	0	1	0	0	0	0	0	-0	0	0	0	0	0	0	-0	IS
IT	0	0	10	0	1	1	0	0	4	0	2	14	0	0	4	0	14	1	0	1	5	1	0	0	312	0	0	0	0	0	0	IT
KG	0	0	0	0	0	0	0	0	0	0	0	0	0	0	0	0	0	0	0	0	0	0	0	0	0	31	7	0	0	0	0	KG
KZ	0	0	0	0	0	0	0	0	0	0	0	0	0	0	0	0	0	0	0	0	0	0	0	0	0	2	26	0	0	0	0	KZ
LT	0	0	1	0	0	2	0	12	0	0	2	19	4	1	1	2	3	6	0	0	0	2	0	0	1	0	0	19	0	5	0	LT
LU	0	0	5	0	0	58	0	0	2	0	4	128	1	0	5	0	120	45	0	0	0	0	3	0	1	0	0	0	12	0	0	LU
LV	0	0	1	0	0	1	0	6	0	0	1	11	3	2	0	2	2	5	0	0	0	1	0	0	0	0	0	10	0	10	0	LV
MD	0	0	2	0	0	1	7	4	0	0	3	10	1	0	0	0	2	2	0	2	1	4	0	0	2	0	0	1	0	0	26	MD
ME	4	0	1	0	8	0	1	0	0	0	0	1	0	-0	1	0	1	0	0	2	2	0	0	0	9	0	0	0	0	-0	0	ME
MK	7	0	1	0	2	0	6	0	0	0	0	2	0	0	1	0	1	0	0	20	1	1	0	0	5	0	0	0	0	0	0	MK
MT	0	0	1	0	1	0	0	0	0	0	0	2	0	0	4	0	6	1	0	2	1	0	0	0	30	0	0	0	0	0	0	MT
NL	0	0	2	0	0	42	0	0	1	0	4	126	4	0	5	0	68	107	0	0	0	1	6	0	1	0	0	0	2	0	0	NL
NO	0	0	0	0	0	0	0	0	0	0	0	1	0	0	0	0	0	2	0	0	0	0	0	0	0	0	0	0	0	0	0	NO
PL	0	0	4	0	0	3	0	3	1	0	11	51	4	0	1	0	7	7	0	0	1	5	0	0	2	0	0	1	0	0	0	PL
PT	0	0	0	0	0	0	0	0	0	0	0	1	0	0	40	0	3	1	0	0	0	0	0	0	1	0	0	0	0	0	0	PT
RO	0	0	4	0	1	1	12	1	1	0	4	12	0	0	0	0	3	2	0	2	2	13	0	0	5	0	0	0	0	0	3	RO
RS	3	0	9	0	9	1	7	1	1	0	7	19	0	0	1	0	4	2	0	4	7	21	0	0	10	0	0	0	0	0	0	RS
RU	0	0	0	0	0	0	0	1	0	0	0	1	0	0	0	0	0	0	0	0	0	0	0	0	0	0	5	0	0	0	0	RU
SE	0	0	0	0	-0	1	0	0	0	0	0	5	4	0	0	1	1	4	0	0	0	-0	0	0	0	0	0	0	0	0	0	SE
SI	0	0	47	0	2	2	0	0	3	0	7	41	0	0	2	0	9	3	0	0	29	8	0	0	146	0	0	0	0	0	0	SI
SK	0	0	18	0	2	2	1	0	2	0	17	32	0	0	1	0	8	3	0	0	6	42	0	0	8	0	0	0	0	0	0	SK
TJ	0	0	0	0	0	0	0	0	0	0	0	0	0	0	0	0	0	0	0	0	0	0	0	0	0	4	3	0	0	0	0	TJ
TM	0	0	0	1	0	0	0	0	0	0	0	0	0	0	0	0	0	0	0	0	0	0	0	0	0	1	8	0	0	0	0	TM
TR	0	1	0	1	0	0	2	0	0	1	0	1	0	0	0	0	0	0	1	3	0	0	0	0	1	0	0	0	0	0	0	TR
UA	0	0	1	0	0	1	2	5	0	0	2	8	1	0	0	0	2	1	0	1	0	3	0	0	1	0	1	1	0	0	4	UA
UZ	0	0	0	0	0	0	0	0	0	0	0	0	0	0	0	0	0	0	0	0	0	0	0	0	0	9	17	0	0	0	0	UZ
ATL	0	0	0	0	0	0	0	0	0	0	0	1	0	0	2	0	2	2	0	0	0	0	1	0	0	0	0	0	0	0	0	ATL
BAS	0	0	0	0	0	3	-0	1	0	0	1	25	9	0	1	1	4	11	0	0	0	0	1	0	0	0	0	1	0	1	0	BAS
BLS	0	0	0	1	0	0	3	1	0	0	0	1	0	0	0	0	0	0	3	1	0	0	0	0	0	0	1	0	0	0	1	BLS
MED	1	0	1	0	1	0	1	0	0	0	0	2	0	0	6	0	6	0	0	5	1	0	0	0	23	0	0	0	0	0	0	MED
NOS	0	0	0	0	0	5	0	0	0	0	1	21	2	0	1	0	16	36	0	0	0	0	3	0	0	0	0	0	0	0	0	NOS
AST	0	0	0	1	0	0	0	0	0	0	0	0	0	0	0	0	0	0	0	0	0	0	0	0	0	0	3	0	0	0	0	AST
NOA	0	0	0	0	0	0	0	0	0	0	0	0	0	0	5	0	2	0	0	2	0	0	0	0	5	0	0	0	0	0	0	NOA
EXC	0	0	2	1	0	1	1	1	1	0	1	10	1	0	4	0	7	4	0	1	1	1	1	0	6	1	7	0	0	0	0	EXC
EU	0	0	6	0	1	5	2	1	2	0	5	38	2	0	14	1	27	17	0	2	2	5	2	0	26	0	0	1	1	0	0	EU
	AL	AM	AT	AZ	BA	BE	BG	BY	CH	CY	CZ	DE	DK	EE	ES	FI	FR	GB	GE	GR	HR	HU	IE	IS	IT	KG	KZ	LT	LU	LV	MD	

Table C.10 Cont.: 2017 country-to-country blame matrices for **PM2.5**.
Units: ng/m^3 per 15% emis. red. of NO_x. **Emitters →, Receptors ↓.**

	ME	MK	MT	NL	NO	PL	PT	RO	RS	RU	SE	SI	SK	TJ	TM	TR	UA	UZ	ATL	BAS	BLS	MED	NOS	AST	NOA	BIC	DMS	VOL	EXC	EU	
AL	6	8	0	1	0	2	0	2	19	1	0	0	1	0	0	1	1	0	0	0	0	17	1	0	3	6	0	0	146	48	AL
AM	0	0	0	0	0	0	0	0	0	3	0	0	0	0	1	32	1	0	0	0	0	1	0	88	1	5	0	0	139	3	AM
AT	0	0	0	5	0	8	0	2	3	0	0	11	4	0	0	0	1	0	1	1	0	3	4	0	1	5	0	0	294	278	AT
AZ	0	0	0	0	0	1	0	0	0	13	0	0	0	0	1	11	2	1	0	0	1	0	0	104	0	5	0	0	179	3	AZ
BA	3	0	0	1	0	5	0	1	5	0	0	1	2	0	0	0	1	0	0	0	0	6	1	0	1	5	0	0	112	75	BA
BE	0	0	0	41	1	2	1	0	0	1	1	0	0	0	0	0	0	0	10	2	0	1	60	0	1	15	0	0	388	385	BE
BG	0	1	0	0	0	4	0	20	14	5	0	0	1	0	0	8	9	0	0	0	4	3	1	0	1	5	0	0	145	103	BG
BY	0	0	0	2	1	35	0	4	1	23	2	0	1	0	0	1	15	0	1	6	0	0	3	0	0	3	0	0	156	84	BY
CH	0	0	0	5	0	1	0	0	0	0	0	0	0	0	0	0	0	0	1	0	0	3	5	0	1	7	0	0	332	190	CH
CY	0	0	0	0	0	1	0	1	1	2	0	0	0	0	0	48	2	0	0	0	1	39	0	13	4	9	0	0	92	39	CY
CZ	0	0	0	8	1	17	0	4	3	1	0	3	10	0	0	0	1	0	1	1	0	1	8	0	0	6	0	0	297	286	CZ
DE	0	0	0	39	1	12	0	1	0	1	1	0	1	0	0	0	0	0	4	6	0	1	40	0	1	10	0	0	433	418	DE
DK	0	0	0	26	6	16	0	0	0	3	5	0	1	0	0	0	1	0	4	31	0	0	67	0	0	7	0	0	259	247	DK
EE	0	0	0	2	1	7	0	0	0	5	3	0	0	0	0	0	0	0	1	13	0	0	4	0	0	2	0	0	54	45	EE
ES	0	0	0	1	0	0	6	0	0	0	0	0	0	0	0	0	0	0	6	0	0	16	2	0	6	7	0	0	125	125	ES
FI	0	0	0	0	1	1	0	-0	-0	3	2	0	0	0	0	0	0	0	0	3	0	0	1	0	0	1	0	0	18	14	FI
FR	0	0	0	8	0	1	1	0	0	0	0	0	0	0	0	0	0	0	8	1	0	4	26	0	1	7	0	0	254	247	FR
GB	0	0	0	9	1	2	0	0	0	0	0	0	0	0	0	0	0	0	12	1	0	0	28	0	0	8	0	0	163	161	GB
GE	0	0	0	0	0	1	0	0	0	5	0	0	0	0	1	14	1	0	0	0	2	0	0	17	0	4	0	0	96	3	GE
GL	0	0	0	0	0	0	0	0	0	0	0	0	0	0	0	0	0	0	0	0	0	0	0	0	0	5	0	0	0	0	GL
GR	1	4	0	0	0	1	0	3	5	2	0	0	0	0	0	9	3	0	0	0	1	16	0	0	3	6	0	0	90	63	GR
HR	1	0	0	3	0	9	0	5	13	1	0	10	4	0	0	0	1	0	1	0	0	13	3	0	1	5	0	0	236	207	HR
HU	1	0	0	3	0	26	0	36	29	2	0	11	24	0	0	0	8	0	1	1	0	5	4	0	1	6	0	0	419	369	HU
IE	0	0	0	4	0	1	0	0	0	0	0	0	0	0	0	0	0	0	11	1	0	0	10	0	0	5	0	0	100	99	IE
IS	0	0	0	0	0	0	0	0	0	0	0	0	0	0	0	0	-0	0	0	0	0	0	0	0	0	1	0	0	2	2	IS
IT	0	0	0	1	0	3	0	1	1	0	0	7	1	0	0	0	1	0	1	0	0	41	1	0	4	8	0	0	390	381	IT
KG	0	0	0	0	0	0	0	0	0	1	0	0	0	1	1	0	0	25	0	0	0	0	0	20	0	2	0	0	67	0	KG
KZ	0	0	0	0	0	0	0	0	0	15	0	0	0	0	1	0	1	3	0	0	0	0	0	28	0	3	0	0	49	2	KZ
LT	0	0	0	4	1	40	0	1	1	14	4	0	1	0	0	0	3	0	1	16	0	0	7	0	0	3	0	0	151	119	LT
LU	0	0	0	26	1	2	1	0	0	0	1	0	0	0	0	0	0	0	6	1	0	1	34	0	1	10	0	0	415	411	LU
LV	0	0	0	3	1	16	0	0	0	9	4	0	1	0	0	0	1	0	1	13	0	0	5	0	0	2	0	0	90	72	LV
MD	0	0	0	1	0	23	0	62	3	16	0	0	2	0	0	5	55	0	0	2	6	2	2	0	0	5	0	0	238	126	MD
ME	21	1	0	0	0	-1	0	1	7	0	0	0	0	0	0	0	1	0	0	0	0	7	0	0	2	4	0	0	63	21	ME
MK	1	19	0	0	0	1	0	2	19	1	0	0	0	0	0	2	1	0	0	0	0	5	0	0	2	5	0	0	96	43	MK
MT	0	0	-2	0	0	1	0	0	1	0	0	0	0	0	0	1	0	0	1	0	0	63	1	0	16	7	0	0	52	48	MT
NL	0	0	0	94	2	9	1	0	0	1	1	0	0	0	0	0	0	0	13	4	0	1	104	0	1	19	0	0	481	475	NL
NO	0	0	0	0	4	0	0	0	0	1	1	0	0	0	0	0	0	0	1	1	0	0	3	0	0	1	0	0	10	5	NO
PL	0	0	0	6	1	92	0	3	2	5	2	1	4	0	0	0	6	0	1	9	0	1	9	0	0	5	0	0	224	207	PL
PT	0	0	0	0	0	0	46	0	0	0	0	0	0	0	0	0	0	0	15	0	0	4	1	0	3	7	0	0	92	92	PT
RO	0	1	0	1	0	13	0	99	10	7	0	1	4	0	0	3	17	0	0	1	3	2	2	0	1	5	0	0	224	178	RO
RS	4	4	0	2	0	11	0	19	61	2	0	2	5	0	0	1	4	0	1	0	0	4	2	0	1	6	0	0	223	133	RS
RU	0	0	0	0	0	1	0	0	0	30	0	0	0	0	0	0	2	0	0	1	0	0	0	2	0	2	0	0	43	4	RU
SE	0	0	0	2	2	1	0	-0	-0	2	5	0	0	0	0	0	0	0	1	6	0	0	5	0	0	1	0	0	30	25	SE
SI	0	0	0	4	0	8	0	3	5	1	0	81	2	0	0	0	1	0	1	0	0	19	3	0	1	5	0	0	405	393	SI
SK	0	0	0	2	0	15	0	14	9	1	0	4	40	0	0	0	5	0	1	0	0	2	3	0	0	5	0	0	235	215	SK
TJ	0	0	0	0	0	0	0	0	0	1	0	0	0	8	5	0	0	22	0	0	0	0	0	16	0	3	0	0	43	0	TJ
TM	0	0	0	0	0	0	0	0	0	7	0	0	0	0	15	1	1	11	0	0	0	0	0	41	0	5	0	0	48	2	TM
TR	0	0	0	0	0	1	0	2	1	4	0	0	0	0	0	91	3	0	0	0	4	10	0	22	2	8	0	0	117	14	TR
UA	0	0	0	1	0	19	0	14	1	27	1	0	2	0	0	3	49	0	0	2	3	1	2	1	0	4	0	0	156	63	UA
UZ	0	0	0	0	0	0	0	0	0	10	0	0	0	2	7	1	1	46	0	0	0	0	0	20	0	4	0	0	95	2	UZ
ATL	0	0	0	0	0	0	1	0	0	0	0	0	0	0	0	0	0	0	4	0	0	0	1	0	1	3	0	0	9	9	ATL
BAS	0	-0	0	7	2	11	0	-0	0	3	4	0	0	0	0	0	0	0	1	16	0	0	14	0	0	3	0	0	87	81	BAS
BLS	0	0	0	0	0	2	0	7	1	16	0	0	0	0	0	17	12	0	0	0	17	2	0	1	0	4	0	0	71	17	BLS
MED	0	0	0	0	0	1	0	1	1	1	0	0	0	0	0	8	1	0	1	0	1	43	0	-1	8	6	0	0	63	50	MED
NOS	0	0	0	11	1	2	0	0	0	0	1	0	0	0	0	0	0	0	5	2	0	0	22	0	0	5	0	0	104	101	NOS
AST	0	0	0	0	0	0	0	0	0	2	0	0	0	0	1	5	0	1	0	0	0	2	0	168	1	7	0	0	17	2	AST
NOA	0	0	0	0	0	0	1	0	0	0	0	0	0	0	0	2	0	0	3	0	0	15	0	0	37	8	0	0	20	16	NOA
EXC	0	0	0	2	0	4	0	3	1	16	0	0	1	0	1	5	4	2	1	1	0	2	3	8	0	4	0	0	93	52	EXC
EU	0	0	0	7	1	12	2	7	2	2	1	2	2	0	0	1	2	0	4	3	0	7	13	0	1	6	0	0	202	189	EU
	ME	MK	MT	NL	NO	PL	PT	RO	RS	RU	SE	SI	SK	TJ	TM	TR	UA	UZ	ATL	BAS	BLS	MED	NOS	AST	NOA	BIC	DMS	VOL	EXC	EU	

Table C.11: 2017 country-to-country blame matrices for **PM2.5**.
Units: ng/m^3 per 15% emis. red. of NH_3. **Emitters →, Receptors ↓.**

	AL	AM	AT	AZ	BA	BE	BG	BY	CH	CY	CZ	DE	DK	EE	ES	FI	FR	GB	GE	GR	HR	HU	IE	IS	IT	KG	KZ	LT	LU	LV	MD	
AL	76	0	1	0	0	0	1	0	0	0	1	4	0	0	0	0	1	0	0	5	1	4	0	-0	6	0	-0	0	0	0	0	AL
AM	0	73	0	16	-0	0	0	-0	0	0	-0	0	0	-0	0	-0	0	0	2	0	0	0	-0	-0	0	-0	-0	-0	0	-0	0	AM
AT	0	-0	90	0	1	1	0	0	4	0	13	45	0	0	1	0	5	2	0	0	4	8	0	0	18	0	-0	0	0	0	0	AT
AZ	0	5	0	66	-0	-0	0	-0	0	0	-0	-0	0	-0	0	-0	0	-0	5	0	-0	-0	-0	-0	0	0	-0	-0	0	-0	0	AZ
BA	1	0	6	0	102	0	2	1	0	0	7	12	0	0	1	0	2	1	0	0	25	16	0	0	10	0	-0	0	0	0	0	BA
BE	0	-0	2	-0	0	172	0	0	1	-0	3	73	1	-0	2	0	60	50	-0	0	0	1	4	0	1	-0	-0	0	5	0	0	BE
BG	1	0	2	0	1	0	95	1	0	0	2	6	0	0	0	0	1	0	0	6	2	8	0	0	3	0	-0	0	0	0	1	BG
BY	0	0	1	0	0	1	0	75	0	0	3	14	1	0	1	0	2	1	0	0	1	2	0	0	2	0	0	4	0	1	1	BY
CH	-0	-0	3	-0	0	1	0	0	86	-0	1	27	0	0	1	0	16	2	-0	-0	0	0	0	0	20	-0	-0	0	0	0	0	CH
CY	0	0	0	0	-0	0	-0	0	0	50	0	0	0	-0	0	-0	0	0	0	1	0	0	0	-0	1	0	0	0	0	0	0	CY
CZ	0	0	16	0	1	4	0	1	2	0	172	102	1	0	1	0	13	6	0	0	3	17	1	0	4	0	-0	0	1	0	0	CZ
DE	0	-0	7	-0	0	16	0	1	4	0	12	254	2	0	2	0	27	18	0	0	1	2	2	0	1	-0	-0	0	1	0	0	DE
DK	0	0	1	0	0	4	0	1	0	0	4	62	82	0	2	0	11	27	0	0	0	2	3	0	0	-0	0	0	0	0	0	DK
EE	0	0	0	0	0	1	0	7	0	0	1	13	3	30	0	6	2	3	0	0	0	1	0	0	0	0	0	7	0	10	0	EE
ES	-0	-0	0	-0	-0	0	-0	0	0	-0	0	1	0	-0	76	-0	7	1	-0	-0	0	0	0	0	1	-0	-0	0	0	-0	0	ES
FI	0	0	0	0	0	0	0	1	0	0	0	3	1	1	0	18	1	1	0	0	0	0	0	-0	0	-0	-0	1	0	1	0	FI
FR	0	-0	2	-0	0	8	0	0	4	-0	2	23	0	0	6	0	111	14	-0	0	0	0	1	0	3	-0	-0	0	1	0	0	FR
GB	0	-0	1	-0	0	6	0	0	0	0	1	17	1	0	1	0	17	133	0	0	0	0	8	0	0	-0	0	0	0	0	0	GB
GE	0	4	0	11	-0	0	0	0	0	0	-0	0	0	-0	0	-0	0	-0	30	0	0	0	-0	-0	0	-0	-0	0	0	0	0	GE
GL	-0	-0	-0	-0	-0	-0	-0	-0	0	-0	-0	-0	0	-0	0	-0	-0	0	-0	-0	-0	-0	-0	-0	0	0	-0	0	0	0	-0	GL
GR	2	0	1	0	0	0	5	0	0	0	1	3	0	0	0	0	1	0	0	54	1	2	0	-0	2	0	-0	0	0	0	0	GR
HR	0	0	12	0	18	1	1	0	1	0	10	17	0	0	1	0	3	1	0	0	86	21	0	0	38	0	-0	0	0	0	0	HR
HU	0	0	16	0	2	1	1	1	1	0	16	29	1	0	0	0	5	2	0	0	11	123	0	0	16	0	-0	0	0	0	1	HU
IE	0	-0	0	-0	0	2	0	0	0	0	0	5	1	0	1	0	7	16	0	0	0	0	32	0	0	-0	-0	0	0	0	0	IE
IS	0	-0	0	-0	0	0	0	0	0	0	0	1	0	-0	0	-0	0	1	-0	0	0	0	0	3	0	-0	-0	0	0	0	0	IS
IT	0	-0	4	-0	1	0	0	0	3	-0	2	5	0	0	2	-0	5	0	0	0	3	2	0	-0	215	-0	-0	0	0	0	0	IT
KG	-0	0	0	0	-0	-0	-0	-0	0	-0	-0	-0	-0	-0	-0	-0	-0	-0	0	-0	-0	-0	-0	-0	0	20	2	-0	-0	-0	-0	KG
KZ	0	0	0	0	-0	0	0	0	0	-0	0	0	0	0	0	0	0	0	0	0	0	0	0	-0	0	1	40	0	0	0	0	KZ
LT	0	0	1	0	0	1	0	22	0	-0	2	24	5	0	1	1	4	3	0	0	1	3	0	0	1	0	-0	55	0	4	0	LT
LU	0	-0	3	-0	0	48	0	0	1	-0	4	106	1	0	2	0	58	24	0	0	0	1	2	0	1	-0	-0	0	57	0	0	LU
LV	0	0	1	0	0	1	0	16	0	0	2	18	3	2	1	1	3	3	0	0	0	2	0	0	1	0	-0	23	0	38	0	LV
MD	0	0	1	0	0	0	3	3	0	-0	2	7	1	0	0	0	1	0	0	1	0	4	0	0	1	0	0	0	0	0	61	MD
ME	10	0	2	0	9	0	1	1	0	0	3	7	0	0	0	0	1	0	0	1	4	9	0	0	6	0	0	0	0	0	0	ME
MK	11	0	2	0	1	0	6	1	0	0	2	5	0	0	0	0	1	0	0	13	2	8	0	0	3	-0	-0	0	0	0	0	MK
MT	0	0	1	0	0	0	0	0	0	0	1	2	0	0	3	-0	4	0	0	0	1	1	0	0	18	0	-0	0	0	0	0	MT
NL	0	-0	1	-0	0	40	0	0	0	0	3	82	1	0	2	0	31	66	0	0	0	1	5	0	0	-0	-0	0	1	0	0	NL
NO	0	0	0	0	0	0	0	0	0	0	0	2	1	0	0	0	1	1	0	0	0	0	0	-0	0	-0	-0	0	0	0	0	NO
PL	0	0	4	0	0	3	0	5	1	0	21	72	5	0	1	0	8	5	0	0	2	10	1	0	3	0	-0	1	0	0	1	PL
PT	-0	-0	0	-0	-0	0	-0	-0	0	-0	0	1	0	-0	27	-0	3	0	-0	-0	0	0	0	0	0	0	-0	-0	0	-0	0	PT
RO	0	0	3	0	1	0	6	1	0	0	3	9	0	0	0	0	2	1	0	1	2	14	0	0	4	0	-0	0	0	0	3	RO
RS	3	0	5	0	6	0	7	1	0	0	6	14	0	0	0	0	2	1	0	2	7	25	0	0	6	0	-0	0	0	0	1	RS
RU	0	0	0	0	0	0	0	2	0	-0	0	1	0	0	0	0	0	0	0	0	0	0	0	-0	0	0	5	0	0	0	0	RU
SE	0	0	0	0	0	1	0	1	0	0	1	8	5	0	0	1	2	3	0	0	0	0	0	-0	0	-0	0	0	0	0	0	SE
SI	0	0	29	0	2	1	1	0	2	0	7	19	0	0	1	0	4	1	0	0	24	9	0	0	110	-0	-0	0	0	0	0	SI
SK	0	0	11	0	1	2	1	2	1	0	30	37	1	0	1	0	6	2	0	0	4	40	0	0	7	0	-0	0	0	0	0	SK
TJ	-0	0	-0	0	-0	-0	-0	-0	0	-0	-0	-0	-0	-0	-0	-0	-0	-0	0	-0	-0	-0	-0	-0	0	1	-0	-0	-0	-0	-0	TJ
TM	-0	0	-0	1	-0	-0	-0	0	0	-0	-0	-0	-0	-0	-0	-0	0	-0	0	-0	-0	-0	-0	-0	0	0	1	0	-0	0	-0	TM
TR	0	0	0	0	0	0	1	0	0	0	0	1	0	0	0	-0	0	0	0	0	0	0	0	-0	0	0	-0	0	0	0	0	TR
UA	0	0	1	0	0	0	1	7	0	0	2	9	1	0	0	0	1	1	0	0	0	4	0	0	1	0	0	1	0	0	4	UA
UZ	-0	0	-0	0	-0	-0	-0	0	0	-0	-0	-0	-0	-0	-0	-0	-0	-0	0	-0	-0	-0	-0	-0	-0	3	5	0	-0	0	0	UZ
ATL	-0	-0	0	0	-0	0	0	0	0	0	0	1	0	0	3	-0	2	2	0	-0	0	0	1	-0	-0	0	-0	0	0	0	0	ATL
BAS	0	0	1	0	0	2	0	3	0	0	3	43	18	1	1	5	5	8	0	0	0	2	1	0	0	0	-0	2	0	2	0	BAS
BLS	0	0	0	1	0	0	5	1	0	0	1	2	0	0	0	0	0	0	4	1	0	1	0	-0	0	0	0	0	0	0	2	BLS
MED	1	0	1	0	0	0	0	0	0	0	0	2	0	0	6	-0	4	0	0	2	1	1	0	-0	7	0	0	0	0	0	0	MED
NOS	0	0	1	0	0	10	0	0	0	0	1	28	5	0	1	0	22	67	0	0	0	0	5	-0	0	-0	0	0	0	0	0	NOS
AST	0	0	0	1	-0	0	-0	0	0	0	-0	0	-0	-0	-0	-0	0	-0	0	0	-0	-0	-0	-0	0	0	0	0	0	0	0	AST
NOA	0	0	0	0	-0	0	0	0	0	0	0	0	0	-0	2	-0	1	0	0	0	0	0	0	-0	-0	0	0	0	0	0	0	NOA
EXC	0	0	1	1	0	1	1	2	1	0	2	10	1	0	3	0	5	3	0	1	1	2	0	0	4	1	8	1	0	0	0	EXC
EU	0	0	4	0	0	5	3	1	1	0	7	39	2	0	11	2	21	13	0	2	2	6	2	0	18	0	-0	1	0	1	0	EU
	AL	AM	AT	AZ	BA	BE	BG	BY	CH	CY	CZ	DE	DK	EE	ES	FI	FR	GB	GE	GR	HR	HU	IE	IS	IT	KG	KZ	LT	LU	LV	MD	

Table C.11 Cont.: 2017 country-to-country blame matrices for **PM2.5**.
Units: ng/m^3 per 15% emis. red. of NH_3. **Emitters →, Receptors ↓.**

	ME	MK	MT	NL	NO	PL	PT	RO	RS	RU	SE	SI	SK	TJ	TM	TR	UA	UZ	ATL	BAS	BLS	MED	NOS	AST	NOA	BIC	DMS	VOL	EXC	EU	
AL	1	3	0	0	0	1	-0	2	16	0	0	0	1	0	0	1	0	0	0	0	0	0	0	0	-0	0	0	0	130	31	AL
AM	0	0	-0	0	0	-0	0	0	0	-0	0	0	0	0	-0	34	-0	-0	0	0	0	0	0	39	0	1	0	0	125	0	AM
AT	0	0	-0	2	0	5	0	3	4	0	0	7	2	0	0	0	2	0	0	0	0	0	0	0	0	1	0	0	219	208	AT
AZ	0	0	-0	-0	0	-0	0	0	-0	2	0	0	-0	0	0	9	-0	0	0	0	0	0	0	31	0	0	0	0	87	-0	AZ
BA	2	0	0	1	0	7	0	7	32	1	0	1	3	0	0	1	2	0	0	0	0	0	0	0	0	0	0	0	242	100	BA
BE	0	0	-0	48	0	3	0	0	1	0	0	0	0	-0	-0	0	0	-0	0	0	0	0	0	0	-0	1	0	0	427	425	BE
BG	0	1	0	0	0	3	0	24	22	3	0	0	2	0	0	12	7	0	0	0	0	0	0	-0	0	1	0	0	205	157	BG
BY	0	0	0	2	0	47	0	4	1	10	1	0	1	0	0	1	22	0	0	0	0	0	0	0	0	0	0	0	200	90	BY
CH	0	0	-0	3	0	0	0	0	0	0	0	0	0	-0	-0	-0	0	-0	0	0	0	0	0	-0	0	1	0	0	161	75	CH
CY	-0	-0	-0	0	0	-0	-0	0	-0	0	0	0	-0	0	0	37	0	0	0	0	0	0	0	13	2	0	0	0	91	53	CY
CZ	0	0	-0	7	0	25	0	6	6	1	0	2	9	0	0	0	3	0	0	0	0	0	0	0	0	1	0	0	404	391	CZ
DE	0	0	-0	28	0	14	0	2	1	0	0	0	1	0	-0	0	2	-0	0	0	0	0	0	0	0	1	0	0	401	392	DE
DK	0	0	0	16	1	17	0	1	0	1	3	0	1	0	0	0	2	0	0	0	0	0	0	0	0	1	0	0	243	236	DK
EE	0	0	0	2	0	18	0	1	1	7	4	0	1	0	0	0	3	0	0	0	0	0	0	0	0	0	0	0	122	103	EE
ES	-0	-0	-0	0	0	0	1	0	-0	-0	0	0	0	-0	-0	-0	0	-0	0	0	0	0	0	-0	-0	0	0	0	89	89	ES
FI	0	0	0	1	0	5	0	0	0	3	3	0	0	0	0	0	0	0	0	0	0	0	0	-0	0	-0	0	0	40	35	FI
FR	0	0	0	5	0	1	0	0	0	0	0	0	0	-0	-0	-0	0	-0	0	0	0	0	0	-0	0	0	0	0	183	178	FR
GB	0	0	0	9	0	2	0	0	0	0	0	0	0	-0	0	0	0	0	0	0	0	0	0	0	0	1	0	0	198	197	GB
GE	0	0	-0	0	0	0	0	0	0	1	0	0	0	0	0	14	-0	0	0	0	0	0	0	5	0	0	0	0	60	0	GE
GL	-0	-0	-0	-0	-0	-0	-0	-0	-0	-0	-0	-0	-0	0	-0	-0	-0	-0	0	0	0	0	0	-0	-0	8	0	0	-0	-0	GL
GR	0	3	0	0	0	1	0	3	5	0	0	0	1	0	0	12	1	0	0	0	0	0	0	0	0	0	0	0	99	74	GR
HR	0	0	0	1	0	8	0	9	29	1	0	9	3	0	0	0	4	0	0	0	0	0	0	0	0	0	0	0	275	221	HR
HU	0	0	0	2	0	21	0	20	16	1	0	5	21	0	0	0	9	0	0	0	0	0	0	0	0	1	0	0	323	291	HU
IE	0	0	0	2	0	1	0	0	0	0	0	0	0	-0	-0	0	0	-0	0	0	0	0	0	0	0	1	0	0	66	66	IE
IS	0	0	-0	0	-0	0	0	0	0	-0	0	0	0	-0	-0	0	0	-0	0	0	0	0	0	-0	0	0	0	0	6	3	IS
IT	0	0	0	1	0	1	0	1	2	0	0	3	0	-0	-0	0	0	0	0	0	0	0	0	-0	1	1	0	0	252	246	IT
KG	-0	-0	-0	-0	-0	-0	-0	-0	-0	-0	-0	0	-0	1	0	0	-0	5	0	0	0	0	0	3	-0	0	0	0	29	-0	KG
KZ	0	0	-0	0	0	0	0	0	0	18	0	0	0	0	0	0	1	3	0	0	0	0	0	13	-0	0	0	0	65	0	KZ
LT	0	0	0	3	0	82	0	4	1	10	3	0	1	0	0	0	9	0	0	0	0	0	0	0	0	0	0	0	245	201	LT
LU	0	0	-0	20	0	3	0	1	1	0	0	0	0	-0	-0	0	0	-0	0	0	0	0	0	0	-0	1	0	0	334	331	LU
LV	0	0	0	2	0	38	0	3	1	7	4	0	1	0	0	0	7	0	0	0	0	0	0	0	0	0	0	0	180	147	LV
MD	0	0	0	1	0	15	0	35	2	7	0	0	1	0	0	5	59	0	0	0	0	0	0	0	0	1	0	0	213	76	MD
ME	30	1	-0	1	0	4	0	3	22	0	0	0	2	0	0	1	1	0	0	0	0	0	0	0	-0	0	0	0	120	45	ME
MK	0	50	0	0	0	3	0	5	32	1	0	0	2	0	0	2	1	0	0	0	0	0	0	0	0	1	0	0	150	52	MK
MT	0	0	101	0	0	0	0	0	-0	0	0	0	0	0	0	0	0	0	0	0	0	0	0	-0	3	0	0	0	135	134	MT
NL	0	0	-0	194	0	6	0	1	0	0	0	0	0	-0	-0	0	1	-0	0	0	0	0	0	0	0	1	0	0	438	435	NL
NO	0	0	0	0	6	1	0	0	0	-0	1	0	0	-0	0	0	0	0	0	0	0	0	0	-0	0	-0	0	0	14	7	NO
PL	0	0	0	6	0	238	0	6	3	2	2	1	7	0	0	0	13	0	0	0	0	0	0	0	0	1	0	0	422	396	PL
PT	-0	-0	-0	0	0	0	41	0	-0	-0	0	0	0	0	-0	-0	0	-0	0	0	0	0	0	-0	0	1	0	0	72	72	PT
RO	0	0	0	1	0	8	0	113	11	2	0	1	3	0	0	2	15	0	0	0	0	0	0	0	0	1	0	0	207	170	RO
RS	1	4	0	1	0	8	0	23	145	1	0	1	4	0	0	1	5	0	0	0	0	0	0	0	0	1	0	0	281	114	RS
RU	0	0	0	0	0	2	0	0	0	56	0	0	0	0	0	1	4	1	0	0	0	0	0	2	0	0	0	0	75	6	RU
SE	0	0	0	2	2	5	0	0	0	1	14	0	0	0	0	0	0	0	0	0	0	0	0	0	0	0	0	0	46	43	SE
SI	0	0	0	2	0	6	0	5	10	0	0	108	2	0	0	0	3	0	0	0	0	0	0	0	0	1	0	0	346	328	SI
SK	0	0	0	3	0	45	0	13	7	1	0	2	102	0	0	0	10	0	0	0	0	0	0	0	0	1	0	0	328	307	SK
TJ	-0	-0	-0	-0	-0	-0	-0	-0	-0	-0	-0	-0	-0	5	0	0	-0	4	0	0	0	0	0	2	-0	0	0	0	10	-0	TJ
TM	-0	-0	-0	-0	-0	-0	-0	-0	-0	1	-0	0	-0	0	9	0	-0	6	0	0	0	0	0	16	0	0	0	0	19	-0	TM
TR	0	0	0	0	0	0	0	2	0	1	0	0	0	0	0	147	1	0	0	0	0	0	0	10	0	1	0	0	155	5	TR
UA	0	0	0	1	0	20	0	11	1	22	0	0	1	0	0	7	129	0	0	0	0	0	0	0	0	1	0	0	230	58	UA
UZ	-0	-0	-0	-0	0	-0	-0	-0	-0	2	0	-0	-0	1	1	0	-0	21	0	0	0	0	0	4	-0	0	0	0	33	-0	UZ
ATL	-0	-0	-0	0	0	0	1	0	0	0	0	0	0	-0	-0	-0	0	-0	0	0	0	0	0	0	-0	-1	0	0	10	10	ATL
BAS	0	0	0	6	1	33	0	1	1	3	13	0	1	0	0	0	2	0	0	0	0	0	0	0	0	0	0	0	158	148	BAS
BLS	0	0	0	0	0	2	0	13	2	15	0	0	0	0	0	48	22	0	0	0	0	0	0	1	0	1	0	0	124	28	BLS
MED	0	0	-0	0	0	0	0	1	0	0	0	0	0	0	0	10	0	0	0	0	0	0	0	2	-0	-0	0	0	39	26	MED
NOS	0	0	0	23	1	3	0	0	0	0	1	0	0	-0	0	0	1	0	0	0	0	0	0	0	0	0	0	0	171	168	NOS
AST	-0	-0	0	0	-0	-0	-0	0	-0	1	0	0	-0	0	0	2	0	0	0	0	0	0	0	79	1	0	0	0	5	0	AST
NOA	-0	-0	-0	0	0	0	0	0	-0	0	0	0	0	0	0	1	0	0	0	0	0	0	0	1	21	1	0	0	4	4	NOA
EXC	0	0	0	2	0	8	0	3	2	26	1	0	1	0	0	7	7	1	0	0	0	0	0	4	0	1	0	0	108	51	EXC
EU	0	0	0	7	0	24	1	9	3	1	2	1	3	0	0	1	3	0	0	0	0	0	0	0	0	0	0	0	199	187	EU
	ME	MK	MT	NL	NO	PL	PT	RO	RS	RU	SE	SI	SK	TJ	TM	TR	UA	UZ	ATL	BAS	BLS	MED	NOS	AST	NOA	BIC	DMS	VOL	EXC	EU	

Table C.12: 2017 country-to-country blame matrices for **PM2.5**.
Units: ng/m^3 per 15% emis. red. of VOC. **Emitters →, Receptors ↓.**

	AL	AM	AT	AZ	BA	BE	BG	BY	CH	CY	CZ	DE	DK	EE	ES	FI	FR	GB	GE	GR	HR	HU	IE	IS	IT	KG	KZ	LT	LU	LV	MD	
AL	2	0	0	0	0	0	0	0	0	0	1	2	0	0	1	0	1	0	0	1	0	1	0	0	5	0	0	0	0	0	0	AL
AM	0	16	0	1	0	0	0	0	0	0	0	0	0	0	0	0	0	0	0	0	0	0	0	0	0	0	0	0	0	0	0	AM
AT	0	0	5	0	0	0	0	0	1	0	1	4	0	0	0	0	1	1	0	0	1	1	0	0	3	0	0	0	0	0	0	AT
AZ	0	1	0	2	0	0	0	0	0	0	0	0	0	0	0	0	0	0	1	0	0	0	0	0	0	0	0	0	0	0	0	AZ
BA	0	0	0	0	1	0	0	0	0	0	1	2	0	0	1	0	1	1	0	0	1	1	0	0	4	0	0	0	0	0	0	BA
BE	0	0	1	0	0	6	0	0	0	0	2	12	0	0	1	0	6	11	0	0	0	0	0	0	1	0	0	0	0	0	0	BE
BG	0	0	0	0	0	0	2	0	0	0	1	2	0	0	0	0	1	1	0	1	0	1	0	0	1	0	0	0	0	0	0	BG
BY	0	0	0	0	0	0	0	0	0	0	0	1	0	0	0	0	0	0	0	0	0	0	0	0	0	0	0	0	0	0	0	BY
CH	0	0	2	0	0	0	0	0	8	0	1	6	0	0	1	0	3	0	0	0	0	0	0	0	3	0	0	0	0	0	0	CH
CY	0	0	0	0	0	0	0	0	0	0	0	1	0	0	0	0	1	0	0	2	0	0	0	0	2	0	0	0	0	0	0	CY
CZ	0	0	2	0	0	0	0	0	1	0	9	7	0	0	0	0	2	2	0	0	0	2	0	0	2	0	0	0	0	0	0	CZ
DE	0	0	2	0	0	1	0	0	1	0	3	14	0	0	1	0	4	4	0	0	0	1	0	0	1	0	0	0	0	0	0	DE
DK	0	0	0	0	0	0	0	0	0	0	1	4	1	0	0	0	1	2	0	0	0	0	0	0	0	0	0	0	0	0	0	DK
EE	0	0	0	0	0	0	0	0	0	0	0	0	0	0	0	0	0	0	0	0	0	0	0	0	0	0	0	0	0	0	0	EE
ES	0	0	0	0	0	0	0	0	0	0	0	0	0	0	7	0	1	0	0	0	0	0	0	0	1	0	0	0	0	0	0	ES
FI	0	0	0	0	0	0	0	0	0	0	0	0	0	0	0	0	0	0	0	0	0	0	0	0	0	0	0	0	0	0	0	FI
FR	0	0	1	0	0	1	0	0	1	0	1	3	0	0	1	0	6	1	0	0	0	0	0	0	2	0	0	0	0	0	0	FR
GB	0	0	0	0	0	0	0	0	0	0	0	2	0	0	0	0	1	7	0	0	0	0	0	0	0	0	0	0	0	0	0	GB
GE	0	1	0	1	0	0	0	0	0	0	0	0	0	0	0	0	0	0	3	0	0	0	0	0	0	0	0	0	0	0	0	GE
GL	-0	0	0	0	-0	0	0	0	0	0	0	0	0	0	0	0	0	0	0	-0	0	0	0	0	-0	0	0	0	0	0	0	GL
GR	1	0	0	0	0	0	1	0	0	0	1	2	0	0	0	0	1	0	0	5	0	0	0	0	3	0	0	0	0	0	0	GR
HR	0	0	1	0	1	0	0	0	0	0	2	3	0	0	1	0	2	1	0	0	2	1	0	0	9	0	0	0	0	0	0	HR
HU	0	0	1	0	0	0	0	0	0	0	2	4	0	0	0	0	2	1	0	0	1	4	0	0	4	0	0	0	0	0	0	HU
IE	0	0	0	0	0	0	0	-0	0	0	0	0	0	0	0	0	0	1	0	0	0	0	1	0	0	0	0	0	0	0	0	IE
IS	0	0	0	0	0	0	0	0	0	0	0	0	0	0	0	0	0	0	0	0	0	0	0	0	0	0	0	0	0	0	0	IS
IT	0	0	1	0	0	0	0	0	1	0	1	3	0	0	2	0	4	2	0	0	1	1	0	0	62	0	0	0	0	0	0	IT
KG	0	0	0	0	0	0	0	0	0	0	0	0	0	0	0	0	0	0	0	0	0	0	0	0	0	6	1	0	0	0	0	KG
KZ	0	0	0	0	0	0	0	0	0	0	0	0	0	0	0	0	0	0	0	0	0	0	0	0	0	0	1	0	0	0	0	KZ
LT	0	0	0	0	0	0	0	0	0	0	0	1	0	0	0	0	0	1	0	0	0	0	0	0	0	0	0	0	0	0	0	LT
LU	0	0	1	0	0	2	0	0	0	0	3	10	0	0	1	0	6	4	0	0	0	0	0	0	1	0	0	0	1	0	0	LU
LV	0	0	0	0	0	0	0	0	0	0	0	1	0	0	0	0	0	0	0	0	0	0	0	0	0	0	0	0	0	0	0	LV
MD	0	0	0	0	0	0	0	0	0	0	0	1	0	0	0	0	0	0	0	0	0	0	0	0	0	0	0	0	0	0	1	MD
ME	1	0	0	0	0	0	0	0	0	0	1	2	0	0	0	0	1	1	0	0	0	1	0	0	4	0	0	0	0	0	0	ME
MK	1	0	0	0	0	0	1	0	0	0	1	2	0	0	0	0	1	0	0	2	0	1	0	0	2	0	0	0	0	0	0	MK
MT	0	0	0	0	0	0	0	0	0	0	1	2	0	0	2	0	3	1	0	1	0	0	0	0	12	0	0	0	0	0	0	MT
NL	0	0	1	0	0	5	0	0	0	0	2	13	0	0	1	0	7	14	0	0	0	0	1	0	1	0	0	0	0	0	0	NL
NO	0	0	0	0	0	0	0	0	0	0	0	0	0	0	0	0	0	0	0	0	0	0	0	0	0	0	0	0	0	0	0	NO
PL	0	0	0	0	0	0	0	0	0	0	2	4	0	0	0	0	1	1	0	0	0	1	0	0	1	0	0	0	0	0	0	PL
PT	0	0	0	0	0	0	0	0	0	0	0	0	0	0	4	0	1	0	0	0	0	0	0	0	0	0	0	0	0	0	0	PT
RO	0	0	0	0	0	0	0	0	0	0	1	2	0	0	0	0	1	1	0	0	0	1	0	0	1	0	0	0	0	0	0	RO
RS	0	0	1	0	0	0	0	0	0	0	1	3	0	0	0	0	1	1	0	0	1	2	0	0	2	0	0	0	0	0	0	RS
RU	0	0	0	0	0	0	0	0	0	0	0	0	0	0	0	0	0	0	0	0	0	0	0	0	0	0	0	0	0	0	0	RU
SE	0	0	0	0	0	0	0	0	0	0	0	0	0	0	0	0	0	0	0	0	0	0	0	0	0	0	0	0	0	0	0	SE
SI	0	0	2	0	0	0	0	0	0	0	1	3	0	0	1	0	2	1	0	0	2	1	0	0	15	0	0	0	0	0	0	SI
SK	0	0	1	0	0	0	0	0	0	0	2	4	0	0	0	0	1	1	0	0	0	3	0	0	2	0	0	0	0	0	0	SK
TJ	0	0	0	0	0	0	0	0	0	0	0	0	0	0	0	0	0	0	0	0	0	0	0	0	0	1	0	0	0	0	0	TJ
TM	0	0	0	0	0	0	0	0	0	0	0	0	0	0	0	0	0	0	0	0	0	0	0	0	0	0	0	0	0	0	0	TM
TR	0	0	0	0	0	0	0	0	0	0	0	1	0	0	0	0	0	0	0	0	0	0	0	0	1	0	0	0	0	0	0	TR
UA	0	0	0	0	0	0	0	0	0	0	0	1	0	0	0	0	0	0	0	0	0	0	0	0	0	0	0	0	0	0	0	UA
UZ	0	0	0	0	0	0	0	0	0	0	0	0	0	0	0	0	0	0	0	0	0	0	0	0	0	3	1	0	0	0	0	UZ
ATL	0	0	0	0	0	0	0	0	0	0	0	0	0	0	0	0	0	0	0	0	0	0	0	0	0	0	0	0	0	0	0	ATL
BAS	0	0	0	0	0	0	0	0	0	0	0	1	0	0	0	0	0	1	0	0	0	0	0	0	0	0	0	0	0	0	0	BAS
BLS	0	0	0	0	0	0	0	0	0	0	0	1	0	0	0	0	0	0	1	0	0	0	0	0	0	0	0	0	0	0	0	BLS
MED	0	0	0	0	0	0	0	0	0	0	1	2	0	0	2	0	2	1	0	2	0	0	0	0	8	0	0	0	0	0	0	MED
NOS	0	0	0	0	0	1	0	0	0	0	0	2	0	0	0	0	1	4	0	0	0	0	0	0	0	0	0	0	0	0	0	NOS
AST	0	0	0	0	0	0	0	0	0	0	0	0	0	0	0	0	0	0	0	0	0	0	0	0	0	0	0	0	0	0	0	AST
NOA	0	0	0	0	0	0	0	0	0	0	0	1	0	0	1	0	1	0	0	0	0	0	0	0	3	0	0	0	0	0	0	NOA
EXC	0	0	0	0	0	0	0	0	0	0	0	1	0	0	0	0	1	0	0	0	0	0	0	0	1	0	0	0	0	0	0	EXC
EU	0	0	1	0	0	0	0	0	0	0	1	3	0	0	1	0	2	2	0	0	0	0	0	0	5	0	0	0	0	0	0	EU
	AL	AM	AT	AZ	BA	BE	BG	BY	CH	CY	CZ	DE	DK	EE	ES	FI	FR	GB	GE	GR	HR	HU	IE	IS	IT	KG	KZ	LT	LU	LV	MD	

Table C.12 Cont.: 2017 country-to-country blame matrices for **PM2.5**.
Units: ng/m^3 per 15% emis. red. of VOC. **Emitters →, Receptors ↓**.

	ME	MK	MT	NL	NO	PL	PT	RO	RS	RU	SE	SI	SK	TJ	TM	TR	UA	UZ	ATL	BAS	BLS	MED	NOS	AST	NOA	BIC	DMS	VOL	EXC	EU	
AL	0	1	0	0	0	1	0	1	1	1	0	0	0	0	0	0	1	0	0	0	0	0	0	0	1	-4	0	0	21	14	AL
AM	0	0	0	0	0	0	0	0	0	2	0	0	0	0	0	1	0	0	0	0	0	0	0	24	0	-8	0	0	22	0	AM
AT	0	0	0	0	0	1	0	1	0	1	0	1	1	0	0	0	0	0	0	0	0	0	0	0	0	-5	0	0	24	21	AT
AZ	0	0	0	0	0	0	0	0	0	5	0	0	0	0	0	1	1	0	0	0	0	0	0	24	0	-5	0	0	13	1	AZ
BA	0	0	0	0	0	2	0	1	1	1	0	0	0	0	0	0	1	0	0	0	0	0	0	0	1	-4	0	0	21	16	BA
BE	0	0	0	6	0	2	0	0	0	2	0	0	0	0	0	0	1	0	0	0	0	0	0	0	0	3	0	0	53	50	BE
BG	0	0	0	0	0	1	0	2	1	3	0	0	0	0	0	2	2	0	0	0	0	0	0	0	0	-4	0	0	22	13	BG
BY	0	0	0	0	0	2	0	0	0	3	0	0	0	0	0	0	1	0	0	0	0	0	0	0	0	-4	0	0	11	6	BY
CH	0	0	0	0	0	0	0	0	0	0	0	0	0	0	0	0	0	0	0	0	0	0	0	0	0	-6	0	0	27	17	CH
CY	0	0	0	0	0	1	0	1	0	3	0	0	0	0	0	9	1	0	0	0	0	0	0	14	1	-4	0	0	23	9	CY
CZ	0	0	0	1	0	3	0	1	0	1	0	0	1	0	0	0	1	0	0	0	0	0	0	0	0	-4	0	0	36	33	CZ
DE	0	0	0	3	0	2	0	1	0	1	0	0	1	0	0	0	1	0	0	0	0	0	0	0	0	-2	0	0	42	39	DE
DK	0	0	0	1	0	1	0	0	0	1	0	0	0	0	0	0	0	0	0	0	0	0	0	0	0	-3	0	0	16	14	DK
EE	0	0	0	0	0	1	0	0	0	2	0	0	0	0	0	0	0	0	0	0	0	0	0	0	0	-2	0	0	6	4	EE
ES	0	0	0	0	0	0	1	0	0	0	0	0	0	0	0	0	0	0	0	0	0	0	0	0	2	-3	0	0	12	11	ES
FI	0	0	0	0	0	0	0	0	0	1	0	0	0	0	0	0	0	0	0	0	0	0	0	0	0	-1	0	0	3	1	FI
FR	0	0	0	0	0	1	0	0	0	0	0	0	0	0	0	0	0	0	0	0	0	0	0	0	0	-5	0	0	19	17	FR
GB	0	0	0	1	0	0	0	0	0	0	0	0	0	0	0	0	0	0	0	0	0	0	0	0	0	-1	0	0	15	14	GB
GE	0	0	0	0	0	0	0	0	0	3	0	0	0	0	0	1	1	0	0	0	0	0	0	8	0	-3	0	0	12	1	GE
GL	0	0	0	0	0	0	0	0	0	0	0	-0	0	0	0	0	0	0	0	0	0	0	0	0	0	0	0	0	0	0	GL
GR	0	0	0	0	0	1	0	1	1	2	0	0	0	0	0	1	2	0	0	0	0	0	0	0	1	-3	0	0	24	16	GR
HR	0	0	0	0	0	2	0	1	2	1	0	1	1	0	0	0	1	0	0	0	0	0	0	0	1	-4	0	0	33	27	HR
HU	0	0	0	0	0	3	0	2	1	1	0	1	2	0	0	0	1	0	0	0	0	0	0	0	0	-5	0	0	34	29	HU
IE	0	0	0	0	0	0	0	0	0	0	0	0	0	0	0	0	0	0	0	0	0	0	0	0	0	-4	0	0	2	2	IE
IS	0	0	0	0	0	0	0	0	0	0	0	0	0	0	0	0	0	0	0	0	0	0	0	0	0	-0	0	0	1	0	IS
IT	0	0	0	0	0	1	0	1	0	1	0	1	0	0	0	0	1	0	0	0	0	0	0	0	1	-1	0	0	85	81	IT
KG	0	0	0	0	0	0	0	0	0	1	0	0	0	0	0	0	0	2	0	0	0	0	0	3	0	-2	0	0	10	0	KG
KZ	0	0	0	0	0	0	0	0	0	4	0	0	0	0	0	0	0	0	0	0	0	0	0	3	0	-2	0	0	7	1	KZ
LT	0	0	0	0	0	2	0	0	0	2	0	0	0	0	0	0	0	0	0	0	0	0	0	0	0	-4	0	0	10	7	LT
LU	0	0	0	3	0	1	0	0	0	1	0	0	0	0	0	0	0	0	0	0	0	0	0	0	0	-1	0	0	37	35	LU
LV	0	0	0	0	0	1	0	0	0	2	0	0	0	0	0	0	0	0	0	0	0	0	0	0	0	-3	0	0	8	5	LV
MD	0	0	0	0	0	2	0	2	0	4	0	0	0	0	0	1	3	0	0	0	0	0	0	0	0	-6	0	0	18	9	MD
ME	1	0	0	0	0	1	0	1	1	1	0	0	0	0	0	0	1	0	0	0	0	0	0	0	1	-3	0	0	17	13	ME
MK	0	4	0	0	0	1	0	1	1	1	0	0	0	0	0	0	1	0	0	0	0	0	0	0	1	-4	0	0	22	13	MK
MT	0	0	4	0	0	1	0	0	0	0	0	0	0	0	0	0	0	0	0	0	0	1	0	0	2	-1	0	0	31	28	MT
NL	0	0	0	12	0	2	0	1	0	2	0	0	0	0	0	0	1	0	0	0	0	0	0	0	0	7	0	0	65	61	NL
NO	0	0	0	0	0	0	0	0	0	0	0	0	0	0	0	0	0	0	0	0	0	0	0	0	0	-0	0	0	1	1	NO
PL	0	0	0	1	0	8	0	1	0	2	0	0	1	0	0	0	1	0	0	0	0	0	0	0	0	-2	0	0	28	24	PL
PT	0	0	0	0	0	0	4	0	0	0	0	0	0	0	0	0	0	0	0	0	0	0	0	0	1	-1	0	0	11	11	PT
RO	0	0	0	0	0	2	0	5	1	3	0	0	0	0	0	1	2	0	0	0	0	0	0	0	0	-5	0	0	23	16	RO
RS	0	1	0	0	0	2	0	2	3	2	0	0	1	0	0	0	1	0	0	0	0	0	0	0	0	-4	0	0	27	19	RS
RU	0	0	0	0	0	0	0	0	0	5	0	0	0	0	0	0	0	0	0	0	0	0	0	0	0	-2	0	0	7	1	RU
SE	0	0	0	0	0	0	0	0	0	1	0	0	0	0	0	0	0	0	0	0	0	0	0	0	0	-1	0	0	3	2	SE
SI	0	0	0	0	0	1	0	1	1	1	0	4	0	0	0	0	1	0	0	0	0	0	0	0	0	-4	0	0	40	36	SI
SK	0	0	0	0	0	4	0	1	0	1	0	0	4	0	0	0	1	0	0	0	0	0	0	0	0	-3	0	0	29	26	SK
TJ	0	0	0	0	0	0	0	0	0	1	0	0	0	0	0	0	0	3	0	0	0	0	0	6	0	-1	0	0	6	0	TJ
TM	0	0	0	0	0	0	0	0	0	4	0	0	0	0	0	0	0	0	0	0	0	0	0	18	0	-2	0	0	7	1	TM
TR	0	0	0	0	0	1	0	0	0	3	0	0	0	0	0	8	1	0	0	0	0	0	0	10	0	-6	0	0	17	4	TR
UA	0	0	0	0	0	2	0	1	0	5	0	0	0	0	0	1	3	0	0	0	0	0	0	0	0	-4	0	0	17	7	UA
UZ	0	0	0	0	0	0	0	0	0	3	0	0	0	0	0	0	0	6	0	0	0	0	0	8	0	-2	0	0	14	1	UZ
ATL	0	0	0	0	0	0	0	0	0	0	0	0	0	0	0	0	0	0	0	0	0	0	0	0	0	-1	0	0	1	1	ATL
BAS	0	0	0	0	0	1	0	0	0	2	0	0	0	0	0	0	0	0	0	0	0	0	0	0	0	-1	0	0	10	7	BAS
BLS	0	0	0	0	0	1	0	1	0	10	0	0	0	0	0	5	4	0	0	0	0	0	0	2	0	-3	0	0	28	7	BLS
MED	0	0	0	0	0	1	0	0	0	1	0	0	0	0	0	2	1	0	0	0	0	0	0	4	3	-2	0	0	27	21	MED
NOS	0	0	0	1	0	0	0	0	0	0	0	0	0	0	0	0	0	0	0	0	0	0	0	0	0	-0	0	0	11	10	NOS
AST	0	0	0	0	0	0	0	0	0	1	0	0	0	0	0	1	0	0	0	0	0	0	0	45	0	-3	0	0	5	1	AST
NOA	0	0	0	0	0	0	0	0	0	0	0	0	0	0	0	0	0	0	0	0	0	0	0	1	5	-2	0	0	10	8	NOA
EXC	0	0	0	0	0	1	0	0	0	3	0	0	0	0	0	0	0	0	0	0	0	0	0	2	0	-2	0	0	12	6	EXC
EU	0	0	0	1	0	2	0	1	0	1	0	0	0	0	0	0	1	0	0	0	0	0	0	0	1	-2	0	0	23	21	EU
	ME	MK	MT	NL	NO	PL	PT	RO	RS	RU	SE	SI	SK	TJ	TM	TR	UA	UZ	ATL	BAS	BLS	MED	NOS	AST	NOA	BIC	DMS	VOL	EXC	EU	

Table C.13: 2017 country-to-country blame matrices for **PM2.5**.
Units: ng/m^3 per 15% emis. red. of PPM, SO_x, NO_x, NH_3 and VOC. **Emitters →, Receptors ↓.**

	AL	AM	AT	AZ	BA	BE	BG	BY	CH	CY	CZ	DE	DK	EE	ES	FI	FR	GB	GE	GR	HR	HU	IE	IS	IT	KG	KZ	LT	LU	LV	MD	
AL	426	0	5	0	44	1	14	1	1	0	8	18	0	0	5	0	7	2	0	35	7	11	0	0	47	0	0	0	0	0	0	AL
AM	0	426	0	56	0	0	1	0	0	0	0	1	0	0	0	0	0	0	24	0	0	0	0	0	0	0	6	0	0	0	0	AM
AT	0	0	279	0	7	6	2	1	19	0	51	192	1	0	5	0	33	11	0	0	14	29	1	0	73	0	0	0	1	0	1	AT
AZ	0	45	0	234	0	0	0	0	0	0	0	1	0	0	0	0	0	0	62	0	0	0	0	0	0	0	17	0	0	0	0	AZ
BA	4	0	16	0	500	2	8	1	2	0	26	45	1	0	6	0	11	4	0	3	56	36	0	0	48	0	0	0	0	0	1	BA
BE	0	0	6	0	0	530	1	1	3	0	12	230	3	0	15	1	285	199	0	0	0	2	11	0	3	0	0	0	14	0	0	BE
BG	4	0	6	0	16	1	414	3	1	0	11	23	1	0	2	0	5	3	1	29	4	19	0	0	11	0	2	0	0	0	5	BG
BY	0	0	2	0	3	2	2	193	1	0	10	40	5	4	2	3	7	7	0	1	1	7	1	0	4	0	2	16	0	7	4	BY
CH	0	0	21	0	1	7	0	0	350	0	8	136	0	0	10	0	119	11	0	0	1	1	1	0	85	0	0	0	1	0	0	CH
CY	1	0	1	0	3	0	7	1	0	138	1	3	0	0	2	0	2	1	0	20	0	1	0	0	9	0	1	0	0	0	1	CY
CZ	0	0	56	0	7	12	2	2	7	0	549	306	3	0	5	0	48	23	0	0	11	52	2	0	15	0	0	1	2	0	1	CZ
DE	0	0	30	0	1	52	1	1	21	0	50	745	9	0	9	1	111	76	0	0	1	7	5	0	9	0	0	0	6	0	0	DE
DK	0	0	3	0	0	17	0	3	1	0	14	172	254	1	6	1	32	98	0	0	1	4	6	1	1	0	0	2	1	1	0	DK
EE	0	0	1	0	1	2	0	13	0	0	3	26	6	93	1	24	5	10	0	0	0	3	1	0	1	0	0	14	0	27	0	EE
ES	0	0	1	0	0	2	0	0	1	0	1	5	0	0	385	0	32	5	0	0	0	0	1	0	7	0	0	0	0	0	0	ES
FI	0	0	0	0	0	1	0	2	0	0	1	7	2	5	0	63	1	4	0	0	0	1	0	0	0	0	0	2	0	2	0	FI
FR	0	0	5	0	1	31	0	0	13	0	7	79	1	0	39	0	462	66	0	0	1	1	5	0	15	0	0	0	3	0	0	FR
GB	0	0	1	0	0	14	0	0	1	0	3	40	2	0	6	0	46	454	0	0	0	1	30	1	1	0	0	0	1	0	0	GB
GE	0	35	0	44	0	0	1	0	0	0	0	1	0	0	0	0	0	0	242	0	0	0	0	0	0	0	5	0	0	0	0	GE
GL	0	0	0	0	0	0	0	0	0	0	0	0	0	0	0	0	0	0	0	0	0	0	0	0	0	0	0	0	0	0	0	GL
GR	16	0	2	0	17	1	49	1	1	0	6	12	0	0	3	0	5	2	0	205	2	7	0	0	23	0	1	0	0	0	2	GR
HR	2	0	41	0	130	4	8	1	3	0	41	78	1	0	7	0	19	7	0	2	272	69	0	0	136	0	0	0	0	0	1	HR
HU	1	0	64	0	38	6	9	3	5	0	68	117	2	0	4	0	24	11	0	2	55	551	1	0	63	0	0	1	1	0	2	HU
IE	0	0	0	0	0	5	0	0	0	0	1	14	2	0	3	0	17	70	0	0	0	0	144	1	0	0	0	0	0	0	0	IE
IS	0	0	0	0	0	0	0	0	0	0	1	3	0	0	0	0	0	3	0	0	0	0	0	39	0	0	0	0	0	0	0	IS
IT	1	0	20	0	15	2	2	0	10	0	11	33	0	0	17	0	42	4	0	2	15	7	0	0	1051	0	0	0	0	0	0	IT
KG	0	0	0	0	0	0	0	0	0	0	0	0	0	0	0	0	0	0	0	0	0	0	0	0	0	168	44	0	0	0	0	KG
KZ	0	0	0	1	0	0	0	1	0	0	0	1	0	0	0	0	0	0	0	0	0	0	0	0	0	8	207	0	0	0	0	KZ
LT	0	0	3	0	2	4	1	55	1	0	9	57	12	4	2	5	10	15	0	0	1	8	1	0	3	0	0	125	0	21	1	LT
LU	0	-0	11	0	0	173	1	0	5	0	19	342	2	0	15	0	298	105	0	0	0	2	6	0	4	0	0	0	154	0	0	LU
LV	0	0	2	0	1	3	1	33	1	0	5	38	9	11	2	9	7	13	0	0	1	5	1	0	2	0	0	49	0	134	1	LV
MD	1	1	4	1	5	2	22	13	1	0	11	29	2	1	1	1	5	4	1	5	2	14	0	0	5	0	3	1	0	1	238	MD
ME	39	0	5	0	109	1	10	1	1	0	10	19	0	0	4	0	6	2	0	6	10	15	0	0	32	0	0	0	0	0	0	ME
MK	49	0	4	0	27	1	49	1	1	0	9	17	0	0	3	0	5	2	0	71	5	16	0	0	17	0	0	0	0	0	1	MK
MT	2	0	3	0	21	1	2	1	1	0	6	12	0	0	18	0	24	3	0	6	4	3	0	0	133	0	0	0	0	0	0	MT
NL	0	0	4	0	0	170	1	1	2	0	15	316	7	0	13	1	148	245	0	0	0	3	14	0	3	0	0	0	4	0	0	NL
NO	0	0	0	0	0	0	0	1	0	0	1	4	2	1	0	2	1	5	0	0	0	0	0	0	0	0	0	0	0	0	0	NO
PL	0	0	10	0	5	9	1	13	2	0	63	179	13	1	4	1	23	21	0	0	4	25	2	0	8	0	0	3	1	1	1	PL
PT	0	0	0	0	0	1	0	0	0	0	0	3	0	0	168	0	12	2	0	0	0	0	0	0	3	0	0	0	0	0	0	PT
RO	2	0	9	0	14	2	42	5	1	0	17	38	1	0	2	0	8	5	0	5	6	47	0	0	14	0	2	1	0	0	14	RO
RS	15	0	18	0	83	3	51	2	2	0	30	55	1	0	4	0	12	6	0	12	24	79	0	0	28	0	0	1	0	0	2	RS
RU	0	0	0	1	0	0	0	5	0	0	1	3	0	2	0	2	1	1	0	0	0	0	0	0	0	0	33	1	0	1	0	RU
SE	0	0	0	0	0	2	0	2	0	0	2	18	13	2	1	5	4	11	0	0	0	1	1	0	0	0	0	1	0	1	0	SE
SI	0	0	106	0	17	4	4	1	6	0	31	92	1	0	7	0	23	7	0	1	103	32	0	0	351	0	0	0	1	0	1	SI
SK	0	0	39	0	15	5	4	3	4	0	95	110	3	0	3	0	23	10	0	1	15	160	1	0	23	0	0	1	1	0	1	SK
TJ	0	0	0	0	0	0	0	0	0	0	0	0	0	0	0	0	0	0	0	0	0	0	0	0	0	17	16	0	0	0	0	TJ
TM	0	3	0	4	0	0	0	0	0	0	0	1	0	0	0	0	0	0	1	0	0	0	0	0	0	3	45	0	0	0	0	TM
TR	0	7	1	1	2	0	8	1	0	3	1	4	0	0	1	0	1	1	2	6	0	1	0	0	3	0	1	0	0	0	1	TR
UA	0	1	3	1	3	2	8	22	1	0	10	28	2	1	1	1	5	4	1	2	2	13	0	0	4	0	5	2	0	1	16	UA
UZ	0	1	0	1	0	0	0	1	0	0	0	0	0	0	0	0	0	0	0	0	0	0	0	0	0	35	82	0	0	0	0	UZ
ATL	0	0	0	0	0	1	0	0	0	0	0	2	0	0	12	0	7	6	0	0	0	0	2	1	0	0	0	0	0	0	0	ATL
BAS	0	0	2	0	1	6	0	6	1	0	7	86	40	6	3	17	13	28	0	0	1	3	2	0	1	0	0	5	0	6	0	BAS
BLS	0	4	1	3	2	0	17	5	0	0	4	9	1	0	1	0	2	2	21	4	1	4	0	0	2	0	4	1	0	0	7	BLS
MED	4	0	3	0	16	1	9	1	1	2	5	12	0	0	33	0	27	3	0	18	5	3	0	0	84	0	0	0	0	0	1	MED
NOS	0	0	1	0	0	19	0	1	1	0	3	63	10	0	6	0	50	152	0	0	0	1	11	1	1	0	0	0	1	0	0	NOS
AST	0	1	0	3	0	0	0	0	0	1	0	0	0	0	0	0	0	0	1	1	0	0	0	0	1	2	15	0	0	0	0	AST
NOA	1	0	1	0	5	0	2	0	0	0	1	3	0	0	20	0	7	1	0	5	1	1	0	0	16	0	0	0	0	0	0	NOA
EXC	1	2	4	2	4	4	5	6	2	0	7	31	2	1	14	2	21	13	2	2	2	7	1	0	21	4	47	1	0	1	2	EXC
EU	1	0	15	0	6	17	15	4	5	0	27	117	7	2	56	6	86	51	0	8	8	23	6	0	85	0	0	3	1	3	1	EU
	AL	AM	AT	AZ	BA	BE	BG	BY	CH	CY	CZ	DE	DK	EE	ES	FI	FR	GB	GE	GR	HR	HU	IE	IS	IT	KG	KZ	LT	LU	LV	MD	

Table C.13 Cont.: 2017 country-to-country blame matrices for **PM2.5**.
Units: ng/m^3 per 15% emis. red. of PPM, SO_x, NO_x, NH_3 and VOC. **Emitters →, Receptors ↓.**

	ME	MK	MT	NL	NO	PL	PT	RO	RS	RU	SE	SI	SK	TJ	TM	TR	UA	UZ	ATL	BAS	BLS	MED	NOS	AST	NOA	BIC	DMS	VOL	EXC	EU	
AL	39	66	0	2	0	17	0	12	150	4	0	1	4	0	0	10	12	0	1	0	0	48	1	1	17	11	5	42	951	197	AL
AM	0	0	0	0	0	1	0	1	1	10	0	0	0	0	1	197	6	0	0	0	1	2	0	361	4	7	0	7	735	6	AM
AT	0	0	0	9	0	34	1	12	21	3	0	32	11	0	0	1	9	0	2	1	0	6	5	0	3	8	2	2	860	798	AT
AZ	0	0	0	0	0	3	0	1	1	42	0	0	0	0	4	76	17	2	0	0	1	1	0	352	2	7	0	4	508	8	AZ
BA	24	4	0	3	0	39	1	20	121	5	0	4	10	0	0	3	14	0	1	0	0	19	2	0	9	9	3	15	1021	342	BA
BE	0	0	0	122	2	14	2	2	2	3	1	0	1	0	0	0	2	0	20	2	0	3	80	0	3	28	15	1	1467	1454	BE
BG	5	13	0	1	0	28	0	98	154	25	0	2	6	0	0	73	73	0	1	0	10	11	1	2	8	11	2	12	1043	666	BG
BY	1	1	0	4	2	158	0	18	10	73	4	1	5	0	0	8	76	0	1	7	1	1	4	1	1	5	4	1	685	312	BY
CH	0	0	0	9	0	6	1	1	2	0	0	1	0	0	0	0	1	0	3	0	0	7	6	0	5	9	2	6	777	421	CH
CY	1	2	0	0	0	4	0	6	14	11	0	0	1	0	0	812	19	0	0	0	5	115	0	183	31	18	18	36	1065	199	CY
CZ	0	0	0	19	1	117	1	22	28	4	1	9	34	0	0	1	13	0	3	2	0	3	10	0	2	10	5	1	1356	1289	CZ
DE	0	0	0	83	2	56	1	5	4	4	2	1	4	0	0	1	6	0	8	7	0	2	47	0	2	16	10	1	1307	1265	DE
DK	0	0	0	48	11	56	1	2	2	10	12	0	2	0	0	0	9	0	8	36	0	1	76	0	1	11	20	0	775	736	DK
EE	0	0	0	4	3	45	0	4	3	37	13	0	2	0	0	1	8	0	2	18	0	0	4	0	0	4	6	0	351	285	EE
ES	0	0	0	1	0	1	22	0	0	0	0	0	0	0	0	0	0	0	23	0	0	57	2	0	33	20	11	3	466	463	ES
FI	0	0	0	1	3	13	0	1	1	31	10	0	0	0	0	0	2	0	2	5	0	0	2	0	0	4	10	0	154	114	FI
FR	0	0	0	16	0	7	2	1	1	1	0	1	0	0	0	0	1	0	23	1	0	17	30	0	7	13	14	4	762	744	FR
GB	0	0	0	20	1	8	1	1	1	1	1	0	0	0	0	0	1	0	33	1	0	1	33	0	1	16	23	0	637	630	GB
GE	0	0	0	0	0	4	0	2	1	23	0	0	0	0	1	122	14	0	0	0	6	1	0	106	2	8	0	5	502	11	GE
GL	0	0	-0	0	0	0	0	0	0	0	0	0	0	0	0	0	0	-0	0	0	0	0	0	0	0	36	3	0	0	0	GL
GR	7	36	0	1	0	15	0	19	78	12	0	1	3	0	0	103	38	0	1	0	4	69	0	2	19	12	7	42	669	357	GR
HR	6	2	0	5	1	52	1	30	125	5	0	38	14	0	0	3	20	0	1	1	0	39	3	0	8	8	4	14	1127	827	HR
HU	4	3	0	7	1	126	0	119	156	9	1	26	85	0	0	4	44	0	2	1	0	11	5	0	4	9	3	6	1614	1345	HU
IE	0	0	0	6	1	4	1	0	0	1	0	0	0	0	0	0	0	0	28	1	0	0	11	0	1	14	30	0	272	269	IE
IS	0	0	0	1	0	1	0	0	0	0	0	0	0	0	0	0	0	0	3	0	0	0	1	0	0	10	15	0	49	10	IS
IT	3	2	0	3	0	15	1	5	22	2	0	18	2	0	0	2	6	0	2	0	0	102	2	0	27	16	8	62	1315	1251	IT
KG	0	0	0	0	0	0	0	0	0	4	0	0	0	8	1	6	1	51	0	0	0	0	0	82	0	8	0	2	285	1	KG
KZ	0	0	0	0	0	2	0	1	1	92	0	0	0	1	2	5	16	9	0	0	0	0	0	87	0	10	0	1	352	7	KZ
LT	0	0	0	9	3	206	0	11	8	50	11	1	5	0	0	1	25	0	2	18	0	1	8	0	0	5	7	0	674	526	LT
LU	0	0	0	60	1	13	2	2	2	2	1	0	1	-0	0	1	2	0	13	2	0	4	39	0	4	19	11	2	1225	1211	LU
LV	0	0	0	6	3	91	0	7	5	39	12	1	3	0	0	1	17	0	2	16	0	0	6	0	0	4	7	0	512	410	LV
MD	1	3	0	2	1	99	0	216	28	53	1	1	7	0	0	48	255	0	1	2	11	4	2	3	2	8	2	4	1090	436	MD
ME	280	12	0	1	0	19	0	13	126	3	0	1	5	0	0	6	9	0	1	0	0	23	0	0	12	10	3	22	750	163	ME
MK	12	343	0	1	0	20	0	20	208	6	0	1	5	0	0	27	20	0	1	0	1	15	1	1	13	11	2	21	943	248	MK
MT	6	4	148	1	0	9	1	2	16	1	0	1	2	0	0	10	3	0	2	0	0	347	1	0	106	18	24	183	445	381	MT
NL	0	0	0	442	3	31	2	4	2	4	2	0	2	0	0	1	4	0	22	4	0	2	136	0	3	36	17	1	1445	1427	NL
NO	0	0	0	1	44	3	0	0	0	9	4	0	0	0	0	0	1	0	4	1	0	0	4	0	0	7	14	0	81	26	NO
PL	1	1	0	15	3	720	0	18	21	17	5	3	25	0	0	1	41	0	3	11	0	2	11	0	1	10	7	1	1261	1154	PL
PT	0	0	0	0	0	1	306	0	0	0	0	0	0	0	0	0	0	0	66	0	0	17	1	0	24	23	18	1	497	496	PT
RO	4	5	0	3	1	67	0	602	92	26	1	2	13	0	0	30	92	0	1	1	6	6	2	2	4	9	2	6	1175	887	RO
RS	28	32	0	4	1	58	0	88	697	10	0	4	17	0	0	10	34	0	1	1	1	11	3	1	9	11	2	13	1416	498	RS
RU	0	0	0	0	0	8	0	2	1	198	1	0	0	0	1	5	23	1	1	1	1	0	0	10	0	8	4	0	292	23	RU
SE	0	0	0	4	13	14	0	1	1	13	40	0	1	0	0	0	2	0	3	8	0	0	7	0	0	4	8	0	154	123	SE
SI	1	1	0	6	1	39	0	17	43	5	0	461	7	0	0	1	15	0	1	1	0	39	3	0	5	8	3	5	1385	1293	SI
SK	2	1	0	6	1	180	0	56	68	6	1	10	338	0	0	2	34	0	2	1	0	5	4	0	2	9	3	3	1226	1087	SK
TJ	0	0	0	0	0	0	0	0	0	4	0	0	0	74	8	7	2	45	0	0	0	0	0	100	0	11	0	2	175	1	TJ
TM	0	0	0	0	0	2	0	0	0	35	0	0	0	3	58	17	14	28	0	0	0	0	0	214	1	13	0	3	218	5	TM
TR	1	1	0	0	0	6	0	9	13	16	0	0	1	0	0	1028	25	0	0	0	9	26	0	162	11	14	2	15	1148	48	TR
UA	1	1	0	2	1	96	0	53	15	101	2	1	7	0	1	36	406	0	1	2	7	3	2	4	1	8	2	2	861	250	UA
UZ	0	0	0	0	0	2	0	0	0	43	0	0	0	11	15	10	15	124	0	0	0	0	0	105	1	12	0	2	345	5	UZ
ATL	0	0	0	1	1	1	5	0	0	5	0	0	0	0	0	0	0	0	25	0	0	3	1	0	6	18	32	0	47	39	ATL
BAS	0	0	0	15	6	76	0	3	3	22	29	0	2	0	0	0	7	0	3	28	0	0	16	0	0	6	11	0	397	351	BAS
BLS	1	1	0	1	0	27	0	42	16	88	1	0	2	0	0	267	158	0	0	0	57	7	0	17	3	9	1	5	699	120	BLS
MED	6	4	0	1	0	10	2	6	26	6	0	2	1	0	0	159	15	0	4	0	2	214	1	32	77	14	22	108	468	228	MED
NOS	0	0	0	40	7	11	1	1	1	3	2	0	0	0	0	0	2	0	16	2	0	1	38	0	1	12	25	0	389	374	NOS
AST	0	0	0	0	0	1	0	0	1	10	0	0	0	1	4	66	4	2	0	0	0	5	0	877	6	21	1	5	116	6	AST
NOA	2	2	0	0	0	3	4	1	8	1	0	0	0	0	0	26	4	0	11	0	0	59	0	10	278	26	11	47	116	68	NOA
EXC	1	1	0	5	2	28	2	14	11	101	2	2	3	1	3	52	32	6	3	1	1	6	4	36	3	10	5	3	479	198	EXC
EU	1	2	0	18	3	80	10	43	22	10	6	6	10	0	0	9	15	0	11	4	1	21	15	1	9	12	10	8	790	709	EU
	ME	MK	MT	NL	NO	PL	PT	RO	RS	RU	SE	SI	SK	TJ	TM	TR	UA	UZ	ATL	BAS	BLS	MED	NOS	AST	NOA	BIC	DMS	VOL	EXC	EU	

Table C.14: 2017 country-to-country blame matrices for **fine EC**.
Units: 0.1 ng/m^3 per 15% emis. red. of PPM. **Emitters →, Receptors ↓.**

	AL	AM	AT	AZ	BA	BE	BG	BY	CH	CY	CZ	DE	DK	EE	ES	FI	FR	GB	GE	GR	HR	HU	IE	IS	IT	KG	KZ	LT	LU	LV	MD	
AL	537	0	2	0	4	0	6	0	0	0	2	3	0	0	1	0	3	0	0	9	4	5	0	0	17	0	0	0	0	0	0	AL
AM	0	61	0	5	0	0	0	0	0	0	0	0	0	0	0	0	0	0	9	0	0	0	0	0	0	0	1	0	0	0	0	AM
AT	0	0	286	0	1	1	1	0	4	0	22	42	0	0	1	0	11	2	0	0	9	17	0	0	26	0	0	0	0	0	0	AT
AZ	0	4	0	39	0	0	0	0	0	0	0	0	0	0	0	0	0	0	23	0	0	0	0	0	0	0	2	0	0	0	0	AZ
BA	3	0	6	0	237	1	4	0	0	0	9	8	0	0	1	0	5	1	0	1	46	17	0	0	21	0	0	0	0	0	0	BA
BE	0	0	2	0	0	482	0	0	1	0	4	53	1	0	3	0	137	44	0	0	0	1	1	0	1	0	0	0	7	0	0	BE
BG	3	0	2	0	2	0	331	1	0	0	4	4	0	0	0	0	2	1	0	9	3	8	0	0	5	0	0	0	0	0	2	BG
BY	0	0	1	0	0	1	1	106	0	0	4	6	1	0	0	1	2	2	0	0	1	3	0	0	2	0	0	6	0	4	2	BY
CH	0	0	10	0	0	1	0	0	212	0	2	41	0	0	2	0	67	2	0	0	0	0	0	0	38	0	0	0	0	0	0	CH
CY	0	0	0	0	0	0	1	0	0	80	0	1	0	0	0	0	1	0	0	4	0	0	0	0	3	0	0	0	0	0	0	CY
CZ	0	0	24	0	1	3	1	0	2	0	505	63	1	0	1	0	16	5	0	0	6	25	0	0	5	0	0	0	0	0	0	CZ
DE	0	0	14	0	0	14	0	0	6	0	23	334	2	0	2	0	42	14	0	0	1	3	1	0	3	0	0	0	2	0	0	DE
DK	0	0	1	0	0	3	0	1	0	0	5	25	168	0	1	0	7	18	0	0	0	2	1	0	0	0	0	0	0	0	0	DK
EE	0	0	0	0	0	1	0	3	0	0	1	3	2	57	0	10	1	2	0	0	0	1	0	0	0	0	0	4	0	15	0	EE
ES	0	0	0	0	0	0	0	0	0	0	0	1	0	0	254	0	13	1	0	0	0	0	0	0	3	0	0	0	0	0	0	ES
FI	0	0	0	0	0	0	0	1	0	0	0	1	1	1	0	53	0	1	0	0	0	0	0	0	0	0	0	0	0	1	0	FI
FR	0	0	2	0	0	8	0	0	3	0	3	17	0	0	10	0	383	14	0	0	0	0	1	0	7	0	0	0	1	0	0	FR
GB	0	0	0	0	0	3	0	0	0	0	1	5	0	0	1	0	12	330	0	0	0	0	7	0	0	0	0	0	0	0	0	GB
GE	0	3	0	4	0	0	0	0	0	0	0	0	0	0	0	0	0	0	159	0	0	0	0	0	0	0	1	0	0	0	0	GE
GL	0	0	0	0	0	0	0	0	0	0	0	0	0	0	0	0	0	0	0	0	0	0	0	0	0	0	0	0	0	0	0	GL
GR	14	0	1	0	1	0	13	0	0	0	2	2	0	0	1	0	2	0	0	137	2	3	0	0	9	0	0	0	0	0	1	GR
HR	1	0	17	0	52	1	4	0	1	0	14	13	0	0	2	0	7	1	0	0	336	42	0	0	51	0	0	0	0	0	1	HR
HU	1	0	27	0	8	1	4	1	1	0	24	18	0	0	1	0	8	2	0	0	43	471	0	0	19	0	0	0	0	0	1	HU
IE	0	0	0	0	0	1	0	0	0	0	0	2	0	0	1	0	4	17	0	0	0	0	109	0	0	0	0	0	0	0	0	IE
IS	0	0	0	0	0	0	0	0	0	0	0	0	0	0	0	0	0	1	0	0	0	0	0	8	0	0	0	0	0	0	0	IS
IT	1	0	7	0	2	0	1	0	3	0	3	5	0	0	4	0	18	1	0	0	7	3	0	0	776	0	0	0	0	0	0	IT
KG	0	0	0	0	0	0	0	0	0	0	0	0	0	0	0	0	0	0	0	0	0	0	0	0	0	118	10	0	0	0	0	KG
KZ	0	0	0	0	0	0	0	0	0	0	0	0	0	0	0	0	0	0	0	0	0	0	0	0	0	3	74	0	0	0	0	KZ
LT	0	0	1	0	0	1	1	17	0	0	3	8	3	1	0	1	3	3	0	0	1	3	0	0	1	0	0	91	0	12	0	LT
LU	0	0	3	0	0	72	0	0	1	0	7	98	0	0	3	0	152	21	0	0	0	1	1	0	2	0	0	0	238	0	0	LU
LV	0	0	1	0	0	1	0	8	0	0	2	5	2	4	0	3	2	3	0	0	0	2	0	0	1	0	0	16	0	110	0	LV
MD	1	0	1	0	1	0	6	3	0	0	3	4	1	0	0	0	2	1	0	1	1	6	0	0	2	0	0	0	0	0	222	MD
ME	36	0	2	0	14	0	5	0	0	0	3	4	0	0	1	0	3	1	0	1	6	6	0	0	13	0	0	0	0	0	0	ME
MK	43	0	2	0	2	0	29	0	0	0	3	3	0	0	1	0	2	0	0	19	3	7	0	0	7	0	0	0	0	0	0	MK
MT	1	0	1	0	2	0	1	0	0	0	2	2	0	0	4	0	11	1	0	1	2	1	0	0	53	0	0	0	0	0	0	MT
NL	0	0	1	0	0	84	0	0	0	0	4	77	1	0	2	0	40	49	0	0	0	1	2	0	1	0	0	0	1	0	0	NL
NO	0	0	0	0	0	0	0	0	0	0	0	1	1	0	0	1	0	1	0	0	0	0	0	0	0	0	0	0	0	0	0	NO
PL	0	0	3	0	1	2	1	4	0	0	33	30	3	0	1	0	7	5	0	0	2	12	0	0	3	0	0	1	0	1	1	PL
PT	0	0	0	0	0	0	0	0	0	0	0	1	0	0	81	0	5	1	0	0	0	0	0	0	1	0	0	0	0	0	0	PT
RO	1	0	3	0	2	0	14	1	0	0	5	6	0	0	0	0	3	1	0	1	3	23	0	0	5	0	0	0	0	0	8	RO
RS	12	0	6	0	17	1	40	0	0	0	9	8	0	0	1	0	4	1	0	3	18	39	0	0	10	0	0	0	0	0	1	RS
RU	0	0	0	0	0	0	0	1	0	0	0	0	0	0	0	1	0	0	0	0	0	0	0	0	0	0	7	0	0	0	0	RU
SE	0	0	0	0	0	0	0	0	0	0	1	2	4	0	0	2	1	3	0	0	0	0	0	0	0	0	0	0	0	1	0	SE
SI	0	0	62	0	3	1	2	0	1	0	10	14	0	0	1	0	8	1	0	0	84	17	0	0	109	0	0	0	0	0	0	SI
SK	0	0	16	0	2	1	2	1	1	0	45	18	1	0	1	0	8	3	0	0	9	100	0	0	8	0	0	0	0	0	1	SK
TJ	0	0	0	0	0	0	0	0	0	0	0	0	0	0	0	0	0	0	0	0	0	0	0	0	0	8	2	0	0	0	0	TJ
TM	0	0	0	0	0	0	0	0	0	0	0	0	0	0	0	0	0	0	0	0	0	0	0	0	0	1	7	0	0	0	0	TM
TR	0	1	0	0	0	0	1	0	0	0	0	0	0	0	0	0	0	0	1	1	0	1	0	0	1	0	0	0	0	0	0	TR
UA	0	0	1	0	0	0	2	6	0	0	3	4	1	0	0	0	2	1	0	1	1	6	0	0	2	0	1	1	0	0	9	UA
UZ	0	0	0	0	0	0	0	0	0	0	0	0	0	0	0	0	0	0	0	0	0	0	0	0	0	17	16	0	0	0	0	UZ
ATL	0	0	0	0	0	0	0	0	0	0	0	0	0	0	5	0	3	2	0	0	0	0	1	0	0	0	0	0	0	0	0	ATL
BAS	0	0	1	0	0	1	0	2	0	0	3	12	14	2	0	10	4	6	0	0	0	2	0	0	0	0	0	2	0	4	0	BAS
BLS	0	0	0	0	0	0	5	1	0	0	1	2	0	0	0	0	1	0	11	1	0	2	0	0	1	0	1	0	0	0	3	BLS
MED	3	0	2	0	2	0	2	0	0	0	2	2	0	0	14	0	17	1	0	8	4	2	0	0	43	0	0	0	0	0	0	MED
NOS	0	0	0	0	0	5	0	0	0	0	1	9	3	0	1	0	15	48	0	0	0	0	2	0	0	0	0	0	0	0	0	NOS
AST	0	0	0	0	0	0	0	0	0	0	0	0	0	0	0	0	0	0	0	0	0	0	0	0	0	1	3	0	0	0	0	AST
NOA	0	0	0	0	0	0	0	0	0	0	0	1	0	0	7	0	4	0	0	1	0	0	0	0	6	0	0	0	0	0	0	NOA
EXC	1	0	2	0	1	2	3	2	1	0	4	9	1	0	8	1	14	6	1	1	2	4	1	0	14	2	14	1	0	1	1	EXC
EU	1	0	10	0	1	7	10	1	1	0	16	37	3	1	33	4	59	24	0	4	7	16	2	0	58	0	0	2	1	2	1	EU
	AL	AM	AT	AZ	BA	BE	BG	BY	CH	CY	CZ	DE	DK	EE	ES	FI	FR	GB	GE	GR	HR	HU	IE	IS	IT	KG	KZ	LT	LU	LV	MD	

Table C.14 Cont.: 2017 country-to-country blame matrices for **fine EC**.
Units: 0.1 ng/m^3 per 15% emis. red. of PPM. **Emitters →, Receptors ↓.**

	ME	MK	MT	NL	NO	PL	PT	RO	RS	RU	SE	SI	SK	TJ	TM	TR	UA	UZ	ATL	BAS	BLS	MED	NOS	AST	NOA	BIC	DMS	VOL	EXC	EU	
AL	11	24	0	0	0	3	0	4	51	0	0	1	1	0	0	1	1	0	0	0	0	10	0	0	2	0	0	0	692	63	AL
AM	0	0	0	0	0	0	0	0	0	1	0	0	0	0	0	60	0	0	0	0	0	0	0	19	0	0	0	0	137	1	AM
AT	0	0	0	1	0	8	0	5	2	0	0	17	4	0	0	0	1	0	0	0	0	1	1	0	0	0	0	0	463	454	AT
AZ	0	0	0	0	0	0	0	0	0	3	0	0	0	0	0	15	0	0	0	0	0	0	0	21	0	0	0	0	89	1	AZ
BA	4	1	0	0	0	9	0	9	26	0	0	2	3	0	0	0	1	0	0	0	0	4	0	0	1	0	0	0	417	143	BA
BE	0	0	0	29	0	3	0	1	0	0	0	0	0	0	0	0	0	0	2	0	0	0	30	0	0	0	0	0	773	772	BE
BG	0	4	0	0	0	6	0	49	25	2	0	1	2	0	0	10	5	0	0	0	3	3	0	0	1	0	0	0	481	427	BG
BY	0	0	0	0	0	43	0	9	1	9	1	0	1	0	0	1	10	0	0	1	0	0	1	0	0	0	0	0	219	88	BY
CH	0	0	0	1	0	1	0	0	0	0	0	0	0	0	0	0	0	0	0	0	0	1	0	0	0	0	0	0	380	168	CH
CY	0	0	0	0	0	1	0	2	1	1	0	0	0	0	0	75	1	0	0	0	1	29	0	21	3	0	0	0	172	93	CY
CZ	0	0	0	2	0	53	0	10	3	0	0	3	12	0	0	0	1	0	0	0	0	0	2	0	0	0	0	0	746	737	CZ
DE	0	0	0	13	0	18	0	3	0	0	1	0	1	0	0	0	0	0	1	1	0	0	8	0	0	0	0	0	499	491	DE
DK	0	0	0	5	3	14	0	1	0	1	3	0	1	0	0	0	1	0	1	9	0	0	11	0	0	0	0	0	262	256	DK
EE	0	0	0	1	1	12	0	2	0	6	5	0	1	0	0	0	1	0	0	7	0	0	1	0	0	0	0	0	133	121	EE
ES	0	0	0	0	0	0	11	0	0	0	0	0	0	0	0	0	0	0	4	0	0	12	0	0	4	0	0	0	285	284	ES
FI	0	0	0	0	1	4	0	1	0	3	4	0	0	0	0	0	0	0	0	2	0	0	0	0	0	0	0	0	73	68	FI
FR	0	0	0	2	0	1	1	0	0	0	0	0	0	0	0	0	0	0	3	0	0	4	4	0	1	0	0	0	454	450	FR
GB	0	0	0	2	0	2	0	1	0	0	0	0	0	0	0	0	0	0	7	0	0	0	8	0	0	0	0	0	368	367	GB
GE	0	0	0	0	0	1	0	1	0	2	0	0	0	0	0	29	1	0	0	0	1	0	0	5	0	0	0	0	201	2	GE
GL	0	0	0	0	0	0	0	0	0	0	0	0	0	0	0	0	0	0	0	0	0	0	0	0	0	0	0	0	0	0	GL
GR	1	10	0	0	0	3	0	7	11	1	0	0	1	0	0	13	2	0	0	0	1	23	0	0	2	0	0	0	238	184	GR
HR	1	0	0	1	0	11	0	14	26	0	0	24	4	0	0	0	1	0	0	0	0	9	0	0	1	0	0	0	626	542	HR
HU	0	1	0	1	0	32	0	65	30	1	0	12	32	0	0	0	4	0	0	0	0	2	1	0	0	0	0	0	808	760	HU
IE	0	0	0	1	0	1	0	0	0	0	0	0	0	0	0	0	0	0	6	0	0	0	1	0	0	0	0	0	137	137	IE
IS	0	0	0	0	0	0	0	0	0	0	0	0	0	0	0	0	0	0	1	0	0	0	0	0	0	0	0	0	10	2	IS
IT	0	0	0	0	0	2	0	2	2	0	0	7	1	0	0	0	0	0	0	0	0	23	0	0	4	0	0	0	846	837	IT
KG	0	0	0	0	0	0	0	0	0	0	0	0	0	1	0	1	0	6	0	0	0	0	0	16	0	0	0	0	137	0	KG
KZ	0	0	0	0	0	0	0	0	0	8	0	0	0	0	0	1	1	1	0	0	0	0	0	15	0	0	0	0	90	2	KZ
LT	0	0	0	1	1	59	0	6	1	12	4	0	2	0	0	0	3	0	0	4	0	0	1	0	0	0	0	0	240	205	LT
LU	0	0	0	7	0	3	0	1	0	0	0	0	0	0	0	0	0	0	1	0	0	1	6	0	0	0	0	0	612	610	LU
LV	0	0	0	1	1	25	0	4	1	7	4	0	1	0	0	0	2	0	0	5	0	0	1	0	0	0	0	0	208	189	LV
MD	0	1	0	0	0	21	0	146	3	4	0	0	2	0	0	5	39	0	0	0	2	1	0	0	0	0	0	0	476	198	MD
ME	180	2	0	0	0	5	0	5	36	0	0	1	1	0	0	0	0	0	0	0	0	6	0	0	1	0	0	0	328	58	ME
MK	1	300	0	0	0	4	0	7	67	0	0	0	1	0	0	2	1	0	0	0	0	3	0	0	1	0	0	0	510	91	MK
MT	0	0	145	0	0	1	0	1	2	0	0	1	0	0	0	1	0	0	0	0	0	191	0	0	22	0	0	0	235	228	MT
NL	0	0	0	287	0	7	0	2	0	0	0	0	0	0	0	0	0	0	2	0	0	0	51	0	0	0	0	0	563	561	NL
NO	0	0	0	0	27	1	0	0	0	1	2	0	0	0	0	0	0	0	2	0	0	0	2	0	0	0	0	0	36	8	NO
PL	0	0	0	2	1	456	0	9	2	5	1	1	11	0	0	0	6	0	0	2	0	0	2	0	0	0	0	0	604	584	PL
PT	0	0	0	0	0	0	292	0	0	0	0	0	0	0	0	0	0	0	16	0	0	4	0	0	3	0	0	0	382	382	PT
RO	0	1	0	0	0	14	0	522	16	2	0	1	3	0	0	3	10	0	0	0	1	1	0	0	0	0	0	0	653	607	RO
RS	7	13	0	0	0	12	0	44	433	1	0	2	4	0	0	1	2	0	0	0	0	2	0	0	1	0	0	0	692	204	RS
RU	0	0	0	0	0	2	0	1	0	32	0	0	0	0	0	1	2	0	0	0	0	0	0	1	0	0	0	0	49	6	RU
SE	0	0	0	0	5	4	0	0	0	1	36	0	0	0	0	0	0	0	1	3	0	0	1	0	0	0	0	0	65	58	SE
SI	0	0	0	1	0	8	0	7	5	0	0	405	2	0	0	0	1	0	0	0	0	7	0	0	1	0	0	0	746	734	SI
SK	0	0	0	1	0	72	0	27	8	1	0	4	216	0	0	0	5	0	0	0	0	1	1	0	0	0	0	0	549	531	SK
TJ	0	0	0	0	0	0	0	0	0	0	0	0	0	25	1	1	0	7	0	0	0	0	0	29	0	0	0	0	44	0	TJ
TM	0	0	0	0	0	0	0	0	0	2	0	0	0	0	20	2	0	6	0	0	0	0	0	18	0	0	0	0	41	1	TM
TR	0	0	0	0	0	1	0	3	1	1	0	0	0	0	0	379	1	0	0	0	2	7	0	14	1	0	0	0	395	11	TR
UA	0	0	0	0	0	25	0	29	2	10	0	0	2	0	0	6	83	0	0	0	2	1	0	0	0	0	0	0	198	81	UA
UZ	0	0	0	0	0	0	0	0	0	3	0	0	0	2	2	1	0	35	0	0	0	0	0	9	0	0	0	0	78	1	UZ
ATL	0	0	0	0	0	0	3	0	0	1	0	0	0	0	0	0	0	0	8	0	0	1	0	0	1	0	0	0	16	14	ATL
BAS	0	0	0	2	2	27	0	2	0	5	16	0	1	0	0	0	1	0	1	21	0	0	3	0	0	0	0	0	119	109	BAS
BLS	0	0	0	0	0	5	0	21	2	10	0	0	1	0	0	74	14	0	0	0	26	3	0	1	0	0	0	0	158	42	BLS
MED	1	1	0	0	0	2	1	2	3	0	0	1	0	0	0	18	1	0	1	0	1	77	0	6	20	0	0	0	133	104	MED
NOS	0	0	0	6	4	3	0	1	0	0	1	0	0	0	0	0	0	0	4	0	0	0	26	0	0	0	0	0	101	96	NOS
AST	0	0	0	0	0	0	0	0	0	1	0	0	0	0	1	9	0	0	0	0	0	1	0	457	1	0	0	0	16	1	AST
NOA	0	0	0	0	0	0	2	0	1	0	0	0	0	0	0	2	0	0	2	0	0	12	0	1	101	0	0	0	27	23	NOA
EXC	0	1	0	1	1	12	2	10	3	15	1	1	1	0	1	17	4	1	1	0	0	2	1	4	0	0	0	0	170	103	EXC
EU	0	1	0	4	1	41	8	33	3	1	4	4	5	0	0	1	2	0	2	1	0	5	3	0	1	0	0	0	409	395	EU
	ME	MK	MT	NL	NO	PL	PT	RO	RS	RU	SE	SI	SK	TJ	TM	TR	UA	UZ	ATL	BAS	BLS	MED	NOS	AST	NOA	BIC	DMS	VOL	EXC	EU	

Table C.15: 2017 country-to-country blame matrices for **coarse EC**.
Units: 0.1 ng/m^3 per 15% emis. red. of PPM. **Emitters →, Receptors ↓.**

	AL	AM	AT	AZ	BA	BE	BG	BY	CH	CY	CZ	DE	DK	EE	ES	FI	FR	GB	GE	GR	HR	HU	IE	IS	IT	KG	KZ	LT	LU	LV	MD	
AL	0	0	0	0	0	0	0	0	0	0	0	0	0	0	0	0	0	0	0	0	0	0	0	0	0	0	0	0	0	0	0	AL
AM	0	8	0	0	0	0	0	0	0	0	0	0	0	0	0	0	0	0	0	0	0	0	0	0	0	0	0	0	0	0	0	AM
AT	0	0	3	0	0	0	0	0	0	0	0	1	0	0	0	0	0	0	0	0	0	0	0	0	0	0	0	0	0	0	0	AT
AZ	0	0	0	1	0	0	0	0	0	0	0	0	0	0	0	0	0	0	0	0	0	0	0	0	0	0	0	0	0	0	0	AZ
BA	0	0	0	0	24	0	0	0	0	0	0	0	0	0	0	0	0	0	0	0	0	0	0	0	0	0	0	0	0	0	0	BA
BE	0	0	0	0	0	6	0	0	0	0	0	2	0	0	0	0	1	1	0	0	0	0	0	0	0	0	0	0	0	0	0	BE
BG	0	0	0	0	0	0	2	0	0	0	0	0	0	0	0	0	0	0	0	0	0	0	0	0	0	0	0	0	0	0	0	BG
BY	0	0	0	0	0	0	0	2	0	0	0	0	0	0	0	0	0	0	0	0	0	0	0	0	0	0	0	0	0	0	0	BY
CH	0	0	0	0	0	0	0	0	23	0	0	1	0	0	0	0	0	0	0	0	0	0	0	0	0	0	0	0	0	0	0	CH
CY	0	0	0	0	0	0	0	0	0	1	0	0	0	0	0	0	0	0	0	0	0	0	0	0	0	0	0	0	0	0	0	CY
CZ	0	0	0	0	0	0	0	0	0	0	7	2	0	0	0	0	0	0	0	0	0	0	0	0	0	0	0	0	0	0	0	CZ
DE	0	0	0	0	0	0	0	0	0	0	0	13	0	0	0	0	0	0	0	0	0	0	0	0	0	0	0	0	0	0	0	DE
DK	0	0	0	0	0	0	0	0	0	0	0	1	2	0	0	0	0	0	0	0	0	0	0	0	0	0	0	0	0	0	0	DK
EE	0	0	0	0	0	0	0	0	0	0	0	0	0	1	0	1	0	0	0	0	0	0	0	0	0	0	0	0	0	0	0	EE
ES	0	0	0	0	0	0	0	0	0	0	0	0	0	0	2	0	0	0	0	0	0	0	0	0	0	0	0	0	0	0	0	ES
FI	0	0	0	0	0	0	0	0	0	0	0	0	0	0	0	3	0	0	0	0	0	0	0	0	0	0	0	0	0	0	0	FI
FR	0	0	0	0	0	0	0	0	0	0	0	0	0	0	0	0	3	0	0	0	0	0	0	0	0	0	0	0	0	0	0	FR
GB	0	0	0	0	0	0	0	0	0	0	0	0	0	0	0	0	0	9	0	0	0	0	0	0	0	0	0	0	0	0	0	GB
GE	0	0	0	0	0	0	0	0	0	0	0	0	0	0	0	0	0	0	1	0	0	0	0	0	0	0	0	0	0	0	0	GE
GL	0	0	0	0	0	0	0	0	0	0	0	0	0	0	0	0	0	0	0	0	0	0	0	0	0	0	0	0	0	0	0	GL
GR	0	0	0	0	0	0	0	0	0	0	0	0	0	0	0	0	0	0	0	3	0	0	0	0	0	0	0	0	0	0	0	GR
HR	0	0	0	0	7	0	0	0	0	0	0	0	0	0	0	0	0	0	0	0	3	0	0	0	0	0	0	0	0	0	0	HR
HU	0	0	0	0	1	0	0	0	0	0	0	0	0	0	0	0	0	0	0	0	0	3	0	0	0	0	0	0	0	0	0	HU
IE	0	0	0	0	0	0	0	0	0	0	0	0	0	0	0	0	0	0	0	0	0	0	2	0	0	0	0	0	0	0	0	IE
IS	0	0	0	0	0	0	0	0	0	0	0	0	0	0	0	0	0	0	0	0	0	0	0	0	0	0	0	0	0	0	0	IS
IT	0	0	0	0	0	0	0	0	0	0	0	0	0	0	0	0	0	0	0	0	0	0	0	0	3	0	0	0	0	0	0	IT
KG	0	0	0	0	0	0	0	0	0	0	0	0	0	0	0	0	0	0	0	0	0	0	0	0	0	1	1	0	0	0	0	KG
KZ	0	0	0	0	0	0	0	0	0	0	0	0	0	0	0	0	0	0	0	0	0	0	0	0	0	0	2	0	0	0	0	KZ
LT	0	0	0	0	0	0	0	0	0	0	0	0	0	0	0	0	0	0	0	0	0	0	0	0	0	0	0	1	0	0	0	LT
LU	0	0	0	0	0	1	0	0	0	0	0	3	0	0	0	0	1	0	0	0	0	0	0	0	0	0	0	0	6	0	0	LU
LV	0	0	0	0	0	0	0	0	0	0	0	0	0	0	0	0	0	0	0	0	0	0	0	0	0	0	0	0	0	0	0	LV
MD	0	0	0	0	0	0	0	0	0	0	0	0	0	0	0	0	0	0	0	0	0	0	0	0	0	0	0	0	0	0	1	MD
ME	0	0	0	0	1	0	0	0	0	0	0	0	0	0	0	0	0	0	0	0	0	0	0	0	0	0	0	0	0	0	0	ME
MK	0	0	0	0	0	0	0	0	0	0	0	0	0	0	0	0	0	0	0	0	0	0	0	0	0	0	0	0	0	0	0	MK
MT	0	0	0	0	0	0	0	0	0	0	0	0	0	0	0	0	0	0	0	0	0	0	0	0	0	0	0	0	0	0	0	MT
NL	0	0	0	0	0	1	0	0	0	0	0	3	0	0	0	0	0	1	0	0	0	0	0	0	0	0	0	0	0	0	0	NL
NO	0	0	0	0	0	0	0	0	0	0	0	0	0	0	0	0	0	0	0	0	0	0	0	0	0	0	0	0	0	0	0	NO
PL	0	0	0	0	0	0	0	0	0	0	1	1	0	0	0	0	0	0	0	0	0	0	0	0	0	0	0	0	0	0	0	PL
PT	0	0	0	0	0	0	0	0	0	0	0	0	0	0	0	0	0	0	0	0	0	0	0	0	0	0	0	0	0	0	0	PT
RO	0	0	0	0	0	0	0	0	0	0	0	0	0	0	0	0	0	0	0	0	0	0	0	0	0	0	0	0	0	0	0	RO
RS	0	0	0	0	1	0	0	0	0	0	0	0	0	0	0	0	0	0	0	0	0	0	0	0	0	0	0	0	0	0	0	RS
RU	0	0	0	0	0	0	0	0	0	0	0	0	0	0	0	0	0	0	0	0	0	0	0	0	0	0	0	0	0	0	0	RU
SE	0	0	0	0	0	0	0	0	0	0	0	0	0	0	0	0	0	0	0	0	0	0	0	0	0	0	0	0	0	0	0	SE
SI	0	0	1	0	0	0	0	0	0	0	0	0	0	0	0	0	0	0	0	0	1	0	0	0	0	0	0	0	0	0	0	SI
SK	0	0	0	0	0	0	0	0	0	0	1	1	0	0	0	0	0	0	0	0	0	0	0	0	0	0	0	0	0	0	0	SK
TJ	0	0	0	0	0	0	0	0	0	0	0	0	0	0	0	0	0	0	0	0	0	0	0	0	0	0	0	0	0	0	0	TJ
TM	0	0	0	0	0	0	0	0	0	0	0	0	0	0	0	0	0	0	0	0	0	0	0	0	0	0	0	0	0	0	0	TM
TR	0	0	0	0	0	0	0	0	0	0	0	0	0	0	0	0	0	0	0	0	0	0	0	0	0	0	0	0	0	0	0	TR
UA	0	0	0	0	0	0	0	0	0	0	0	0	0	0	0	0	0	0	0	0	0	0	0	0	0	0	0	0	0	0	0	UA
UZ	0	0	0	0	0	0	0	0	0	0	0	0	0	0	0	0	0	0	0	0	0	0	0	0	0	0	0	0	0	0	0	UZ
ATL	0	0	0	0	0	0	0	0	0	0	0	0	0	0	0	0	0	0	0	0	0	0	0	0	0	0	0	0	0	0	0	ATL
BAS	0	0	0	0	0	0	0	0	0	0	0	0	0	0	0	1	0	0	0	0	0	0	0	0	0	0	0	0	0	0	0	BAS
BLS	0	0	0	0	0	0	0	0	0	0	0	0	0	0	0	0	0	0	0	0	0	0	0	0	0	0	0	0	0	0	0	BLS
MED	0	0	0	0	0	0	0	0	0	0	0	0	0	0	0	0	0	0	0	0	0	0	0	0	0	0	0	0	0	0	0	MED
NOS	0	0	0	0	0	0	0	0	0	0	0	0	0	0	0	0	0	1	0	0	0	0	0	0	0	0	0	0	0	0	0	NOS
AST	0	0	0	0	0	0	0	0	0	0	0	0	0	0	0	0	0	0	0	0	0	0	0	0	0	0	0	0	0	0	0	AST
NOA	0	0	0	0	0	0	0	0	0	0	0	0	0	0	0	0	0	0	0	0	0	0	0	0	0	0	0	0	0	0	0	NOA
EXC	0	0	0	0	0	0	0	0	0	0	0	0	0	0	0	0	0	0	0	0	0	0	0	0	0	0	0	0	0	0	0	EXC
EU	0	0	0	0	0	0	0	0	0	0	0	1	0	0	0	0	0	1	0	0	0	0	0	0	0	0	0	0	0	0	0	EU
	AL	AM	AT	AZ	BA	BE	BG	BY	CH	CY	CZ	DE	DK	EE	ES	FI	FR	GB	GE	GR	HR	HU	IE	IS	IT	KG	KZ	LT	LU	LV	MD	

Table C.15 Cont.: 2017 country-to-country blame matrices for **coarse EC**.
Units: 0.1 ng/m^3 per 15% emis. red. of PPM. **Emitters →, Receptors ↓.**

	ME	MK	MT	NL	NO	PL	PT	RO	RS	RU	SE	SI	SK	TJ	TM	TR	UA	UZ	ATL	BAS	BLS	MED	NOS	AST	NOA	BIC	DMS	VOL	EXC	EU	
AL	0	0	0	0	0	0	0	0	0	0	0	0	0	0	0	0	0	0	0	0	0	0	0	0	0	0	0	0	2	1	AL
AM	0	0	0	0	0	0	0	0	0	0	0	0	0	0	0	9	0	0	0	0	0	0	0	7	0	0	0	0	17	0	AM
AT	0	0	0	0	0	1	0	0	0	0	0	0	0	0	0	0	0	0	0	0	0	0	0	0	0	0	0	0	7	6	AT
AZ	0	0	0	0	0	0	0	0	0	0	0	0	0	0	0	2	0	0	0	0	0	0	0	9	0	0	0	0	4	0	AZ
BA	0	0	0	0	0	1	0	0	0	0	0	0	0	0	0	0	0	0	0	0	0	0	0	0	0	0	0	0	26	2	BA
BE	0	0	0	0	0	0	0	0	0	0	0	0	0	0	0	0	0	0	0	0	0	0	0	0	0	0	0	0	12	11	BE
BG	0	0	0	0	0	1	0	0	0	0	0	0	0	0	0	1	0	0	0	0	0	0	0	0	0	0	0	0	5	3	BG
BY	0	0	0	0	0	6	0	0	0	0	0	0	0	0	0	0	0	0	0	0	0	0	0	0	0	0	0	0	9	7	BY
CH	0	0	0	0	0	0	0	0	0	0	0	0	0	0	0	0	0	0	0	0	0	0	0	0	0	0	0	0	25	2	CH
CY	0	0	0	0	0	0	0	0	0	0	0	0	0	0	0	11	0	0	0	0	0	0	0	6	0	0	0	0	13	1	CY
CZ	0	0	0	0	0	10	0	0	0	0	0	0	0	0	0	0	0	0	0	0	0	0	0	0	0	0	0	0	21	20	CZ
DE	0	0	0	0	0	3	0	0	0	0	0	0	0	0	0	0	0	0	0	0	0	0	0	0	0	0	0	0	18	18	DE
DK	0	0	0	0	0	2	0	0	0	0	0	0	0	0	0	0	0	0	0	0	0	0	0	0	0	0	0	0	6	6	DK
EE	0	0	0	0	0	2	0	0	0	0	0	0	0	0	0	0	0	0	0	0	0	0	0	0	0	0	0	0	4	4	EE
ES	0	0	0	0	0	0	0	0	0	0	0	0	0	0	0	0	0	0	0	0	0	0	0	0	1	0	0	0	2	2	ES
FI	0	0	0	0	0	1	0	0	0	0	0	0	0	0	0	0	0	0	0	0	0	0	0	0	0	0	0	0	4	4	FI
FR	0	0	0	0	0	0	0	0	0	0	0	0	0	0	0	0	0	0	0	0	0	0	0	0	0	0	0	0	5	4	FR
GB	0	0	0	0	0	0	0	0	0	0	0	0	0	0	0	0	0	0	0	0	0	0	0	0	0	0	0	0	10	10	GB
GE	0	0	0	0	0	0	0	0	0	0	0	0	0	0	0	4	0	0	0	0	0	0	0	2	0	0	0	0	6	0	GE
GL	0	0	0	0	0	0	0	0	0	0	0	0	0	0	0	0	0	0	0	0	0	0	0	0	0	0	0	0	0	0	GL
GR	0	0	0	0	0	0	0	0	0	0	0	0	0	0	0	2	0	0	0	0	0	0	0	0	0	0	0	0	6	4	GR
HR	0	0	0	0	0	2	0	0	0	0	0	0	0	0	0	0	0	0	0	0	0	0	0	0	0	0	0	0	13	6	HR
HU	0	0	0	0	0	4	0	0	0	0	0	0	0	0	0	0	0	0	0	0	0	0	0	0	0	0	0	0	10	9	HU
IE	0	0	0	0	0	0	0	0	0	0	0	0	0	0	0	0	0	0	0	0	0	0	0	0	0	0	0	0	3	3	IE
IS	0	0	0	0	0	0	0	0	0	0	0	0	0	0	0	0	0	0	0	0	0	0	0	0	0	0	0	0	0	0	IS
IT	0	0	0	0	0	0	0	0	0	0	0	0	0	0	0	0	0	0	0	0	0	0	0	0	0	0	0	0	4	4	IT
KG	0	0	0	0	0	0	0	0	0	0	0	0	0	0	0	0	0	0	0	0	0	0	0	4	0	0	0	0	1	0	KG
KZ	0	0	0	0	0	0	0	0	0	1	0	0	0	0	0	0	0	0	0	0	0	0	0	5	0	0	0	0	3	0	KZ
LT	0	0	0	0	0	9	0	0	0	0	0	0	0	0	0	0	0	0	0	0	0	0	0	0	0	0	0	0	12	11	LT
LU	0	0	0	0	0	0	0	0	0	0	0	0	0	0	0	0	0	0	0	0	0	0	0	0	0	0	0	0	12	12	LU
LV	0	0	0	0	0	4	0	0	0	0	0	0	0	0	0	0	0	0	0	0	0	0	0	0	0	0	0	0	5	5	LV
MD	0	0	0	0	0	3	0	0	0	0	0	0	0	0	0	1	1	0	0	0	0	0	0	0	0	0	0	0	6	3	MD
ME	1	0	0	0	0	1	0	0	0	0	0	0	0	0	0	0	0	0	0	0	0	0	0	0	0	0	0	0	3	1	ME
MK	0	1	0	0	0	1	0	0	1	0	0	0	0	0	0	0	0	0	0	0	0	0	0	0	0	0	0	0	3	1	MK
MT	0	0	11	0	0	0	0	0	0	0	0	0	0	0	0	0	0	0	0	0	0	0	0	0	2	0	0	0	11	11	MT
NL	0	0	0	5	0	1	0	0	0	0	0	0	0	0	0	0	0	0	0	0	0	0	0	0	0	0	0	0	12	12	NL
NO	0	0	0	0	1	0	0	0	0	0	0	0	0	0	0	0	0	0	0	0	0	0	0	0	0	0	0	0	1	0	NO
PL	0	0	0	0	0	83	0	0	0	0	0	0	0	0	0	0	0	0	0	0	0	0	0	0	0	0	0	0	86	85	PL
PT	0	0	0	0	0	0	3	0	0	0	0	0	0	0	0	0	0	0	0	0	0	0	0	0	0	0	0	0	4	4	PT
RO	0	0	0	0	0	2	0	1	0	0	0	0	0	0	0	0	0	0	0	0	0	0	0	0	0	0	0	0	4	3	RO
RS	0	0	0	0	0	2	0	0	5	0	0	0	0	0	0	0	0	0	0	0	0	0	0	0	0	0	0	0	9	3	RS
RU	0	0	0	0	0	0	0	0	0	5	0	0	0	0	0	0	0	0	0	0	0	0	0	0	0	0	0	0	6	0	RU
SE	0	0	0	0	0	1	0	0	0	0	4	0	0	0	0	0	0	0	0	0	0	0	0	0	0	0	0	0	5	4	SE
SI	0	0	0	0	0	1	0	0	0	0	0	3	0	0	0	0	0	0	0	0	0	0	0	0	0	0	0	0	7	6	SI
SK	0	0	0	0	0	12	0	0	0	0	0	0	1	0	0	0	0	0	0	0	0	0	0	0	0	0	0	0	16	15	SK
TJ	0	0	0	0	0	0	0	0	0	0	0	0	0	2	0	0	0	0	0	0	0	0	0	7	0	0	0	0	2	0	TJ
TM	0	0	0	0	0	0	0	0	0	0	0	0	0	0	0	0	0	0	0	0	0	0	0	6	0	0	0	0	1	0	TM
TR	0	0	0	0	0	0	0	0	0	0	0	0	0	0	0	72	0	0	0	0	0	0	0	4	0	0	0	0	73	0	TR
UA	0	0	0	0	0	3	0	0	0	0	0	0	0	0	0	1	2	0	0	0	0	0	0	0	0	0	0	0	7	4	UA
UZ	0	0	0	0	0	0	0	0	0	0	0	0	0	0	0	0	0	0	0	0	0	0	0	2	0	0	0	0	1	0	UZ
ATL	0	0	0	0	0	0	0	0	0	0	0	0	0	0	0	0	0	0	0	0	0	0	0	0	0	0	0	0	0	0	ATL
BAS	0	0	0	0	0	4	0	0	0	0	2	0	0	0	0	0	0	0	0	0	0	0	0	0	0	0	0	0	7	7	BAS
BLS	0	0	0	0	0	1	0	0	0	0	0	0	0	0	0	12	0	0	0	0	0	0	0	0	0	0	0	0	13	1	BLS
MED	0	0	0	0	0	0	0	0	0	0	0	0	0	0	0	3	0	0	0	0	0	0	0	2	3	0	0	0	4	1	MED
NOS	0	0	0	0	0	0	0	0	0	0	0	0	0	0	0	0	0	0	0	0	0	0	0	0	0	0	0	0	2	2	NOS
AST	0	0	0	0	0	0	0	0	0	0	0	0	0	0	0	1	0	0	0	0	0	0	0	192	0	0	0	0	1	0	AST
NOA	0	0	0	0	0	0	0	0	0	0	0	0	0	0	0	0	0	0	0	0	0	0	0	0	19	0	0	0	0	0	NOA
EXC	0	0	0	0	0	2	0	0	0	2	0	0	0	0	0	3	0	0	0	0	0	0	0	1	0	0	0	0	9	3	EXC
EU	0	0	0	0	0	7	0	0	0	0	0	0	0	0	0	0	0	0	0	0	0	0	0	0	0	0	0	0	12	12	EU
	ME	MK	MT	NL	NO	PL	PT	RO	RS	RU	SE	SI	SK	TJ	TM	TR	UA	UZ	ATL	BAS	BLS	MED	NOS	AST	NOA	BIC	DMS	VOL	EXC	EU	

APPENDIX D

Explanatory note on country reports for 2017

The country reports issued by EMEP MSC-W focus on chemical species that are relevant to eutrophication, acidification and ground level ozone, but also information on particulate matter is given. More specifically, these country reports provide for each country:

- horizontal maps of emissions, and modelled air concentrations and depositions in 2017
- emission trends for the years 2000 to 2017
- modelled trends of air concentrations and depositions for the years 2000 to 2017
- maps and charts on transboundary air pollution in 2017, visualizing the effect of the country on its surroundings, and vice versa
- frequency analysis of air concentrations and depositions, based on measurements and model results for 2017, along with a statistical analysis of model performance
- scatter plots for different species, including available stations within the country
- maps on the risk of damage from ozone and particulate matter in 2017

EMEP MSC-W issues these country reports for 47 Parties to the Convention, and for Tajikistan, Turkmenistan and Uzbekistan. For the Russian Federation, the country report includes the territory of the Russian Federation, which is covered by the extended EMEP domain (see Figure 1.1).

All 50 country reports are written in English. For the 12 EECCA countries, the reports are made available also in Russian. All country reports can be downloaded in pdf format from the MSC-W report page on the EMEP website `http://emep.int/mscw/mscw_publications.html`

This year, the country reports are found under the header 'MSC-W Data Note 1/2019'. The reports for each country can be selected conveniently from a drop-down menu.

APPENDIX E

Model Evaluation

The EMEP MSC-W model is regularly evaluated against various kinds of measurements, including ground-based, airborne and satellite measurements. As the main application of the EMEP MSC-W model within the LRTAP Convention is to assess the status of air quality on regional scales and to quantify long-range transboundary air pollution, the focus of the evaluation performed for the EMEP status reports is on the EMEP measurement sites.

Only parts of this evaluation are included in the printed version of the EMEP status report. A more comprehensive collection of maps, graphs and statistical analyses, including a more detailed discussion of model performance, are freely available as supplementary material from the MSC-W report page on the EMEP website `http://emep.int/mscw/mscw_publications.html`

This year, the evaluation report is found under the link 'Supplementary material to EMEP Status Report 1/2019'. It contains a comprehensive evaluation of the EMEP MSC-W model for air concentrations and depositions in 2017. The report is divided into three chapters, dealing with pollutants responsible for eutrophication and acidification (Gauss et al. 2019b), ground level ozone and nitrogen dioxide (Gauss et al. 2019a), and particulate matter (Tsyro et al. 2019), respectively.

The agreement between model and measurements in 2017 is visualized as:

- scatter plots for the EMEP MSC-W model domain
- time series for individual EMEP stations
- horizontal maps combining model results and EMEP measurement data

Tables summarize common statistical measures of model score, such as bias, root mean square error, temporal and spatial correlations and the index of agreement (see Chapter 1).

This type of model evaluation is performed on an annual basis and can be downloaded from the same web page also for previous years.

References

Gauss, M., Hjellbrekke, A.-G., Aas, W., and Solberg, S.: Ozone, Supplementary material to EMEP Status Report 1/2019, available online at www.emep.int, The Norwegian Meteorological Institute, Oslo, Norway, 2019a.

Gauss, M., Tsyro, S., Fagerli, H., Hjellbrekke, A.-G., and Aas, W.: Acidifying and eutrophying components, Supplementary material to EMEP Status Report 1/2019, available online at www.emep.int, The Norwegian Meteorological Institute, Oslo, Norway, 2019b.

Tsyro, S., Gauss, M., Hjellbrekke, A.-G., and Aas, W.: PM10, PM2.5 and individual aerosol components, Supplementary material to EMEP Status Report 1/2019, available online at www.emep.int, The Norwegian Meteorological Institute, Oslo, Norway, 2019.

emep

Meteorological Synthesizing Centre – West
Norwegian Meteorological Institute
P.O.Box 43 – Blindern, NO-0313 Oslo, Norway

NILU

ccc
NILU
Norwegian Institute for Air Research
P.O. Box 100
NO-2027 Kjeller
Norway
Phone: +47 63 89 80 00
Fax: +47 63 89 80 50
E-mail: kjetil.torseth@nilu.no
Internet: www.nilu.no

IIASA

ciam
International Institute for
Applied Systems Analysis
(IIASA)
Schlossplatz 1
A-2361 Laxenburg
Austria
Phone: +43 2236 807 0
Fax: +43 2236 71 313
E-mail: amann@iiasa.ac.at
Internet: www.iiasa.ac.at

umweltbundesamt
ENVIRONMENT AGENCY AUSTRIA

ceip
Umweltbundesamt GmbH
Spittelauer Lände 5
1090 Vienna
Austria
Phone: +43-(0)1-313 04
Fax: +43-(0)1-313 04/5400
E-mail:
emep.emissions@umweltbundesamt.at
Internet:
http://www.umweltbundesamt.at/

MSC-E

msc-e
Meteorological Synthesizing
Centre-East
2nd Roshchinsky proezd,
8/5, room 207
115419 Moscow
Russia
Phone +7 926 906 91 78
Fax: +7 495 956 19 44
E-mail: msce@msceast.org
Internet: www.msceast.org

Norwegian
Meteorological
Institute

msc-w
Norwegian Meteorological
Institute (MET Norway)
P.O. Box 43 Blindern
NO-0313 OSLO
Norway
Phone: +47 22 96 30 00
Fax: +47 22 96 30 50
E-mail: emep.mscw@met.no
Internet: www.emep.int